

Tracers in Hydrology

Tracers in Hydrology

Christian Leibundgut

Institute of Hydrology

University of Freiburg, Freiburg, Germany

Piotr Maloszewski

Helmholtz Center Munich

German Research Center for Environmental Health

Institute of Groundwater Ecology

Neuherberg, Germany

Christoph Külls

Institute of Hydrology

University of Freiburg, Freiburg, Germany



WILEY-BLACKWELL

A John Wiley & Sons, Ltd., Publication

This edition first published 2009, © 2009 by John Wiley & Sons Ltd

Wiley-Blackwell is an imprint of John Wiley & Sons, formed by the merger of Wiley's global Scientific, Technical and Medical business with Blackwell Publishing.

Registered Office

John Wiley & Sons Ltd, The Atrium, Southern Gate, Chichester, West Sussex, PO19 8SQ, UK

Other Editorial Offices

9600 Garsington Road, Oxford, OX4 2DQ, UK

111 River Street, Hoboken, NJ 07030-5774, USA

For details of our global editorial offices, for customer services and for information about how to apply for permission to reuse the copyright material in this book please see our website at www.wiley.com/wiley-blackwell

The right of the author to be identified as the author of this work has been asserted in accordance with the Copyright, Designs and Patents Act 1988.

All rights reserved. No part of this publication may be reproduced, stored in a retrieval system, or transmitted, in any form or by any means, electronic, mechanical, photocopying, recording or otherwise, except as permitted by the UK Copyright, Designs and Patents Act 1988, without the prior permission of the publisher.

Wiley also publishes its books in a variety of electronic formats. Some content that appears in print may not be available in electronic books.

Designations used by companies to distinguish their products are often claimed as trademarks. All brand names and product names used in this book are trade names, service marks, trademarks or registered trademarks of their respective owners. The publisher is not associated with any product or vendor mentioned in this book. This publication is designed to provide accurate and authoritative information in regard to the subject matter covered. It is sold on the understanding that the publisher is not engaged in rendering professional services. If professional advice or other expert assistance is required, the services of a competent professional should be sought.

Library of Congress Cataloging-in-Publication Data

Leibundgut, Christian.

Tracers in hydrology / Christian Leibundgut, Piotr Maloszewski, Christoph Külls.
p. cm.

Includes bibliographical references and index.

ISBN 978-0-470-51885-4

1. Radioactive tracers in hydrogeology. 2. Groundwater tracers.

I. Maloszewski, Piotr. II. Külls, Christoph. III. Title.

GB1001.72.R34L45 2009

551.49028'4—dc22

2009009327

A catalogue record for this book is available from the British Library.

Typeset in 10.5/12.5pt Minion by Aptara Inc., New Delhi, India.

Printed in Singapore by Markono Print Media Pte Ltd.

First Impression 2009

To

*Fritz Gygax, University of Berne, Switzerland
for having introduced Christian Leibundgut into the field of Tracerhydrology*

*Andrzej Zuber, Institute of Nuclear Physics in Krakow, Poland
for having introduced Piotr Maloszewski into the fields of Mathematical
Modelling and Tracerhydrology*

*Josef Zötl, University of Graz, Austria
leading person within the Association of Tracer Hydrology (ATH) for promoting
Christian Leibundgut within this group*

*Vit Klemes, Canada and Uri Shamir, Israel, Presidents of IAHS 1987-91 and
1991-95, for supporting and conveying the establishment of the Commission on
Tracers (ICT) within IAHS at Vienna Assembly 1991*

*Friedhelm Beyersdorf and his team
for making sure that Christian Leibundgut overcame a
life-threatening medical crisis*

*Ingeborg Vonderstrass
A personal dedication to my wife for giving me the scope for research and for the
substantial support of my professional work
(Christian Leibundgut)*

Contents

| | |
|--|-------------|
| Preface | xiii |
| Acknowledgements | xv |
| 1 Introduction | 1 |
| 2 The Integrated Concept of Tracers in Hydrology | 5 |
| 2.1 System approach | 5 |
| 2.2 Definition of tracers | 7 |
| 2.3 Modelling in the context of integrated tracerhydrology | 9 |
| 2.4 Fields of application | 12 |
| 3 Environmental Tracers | 13 |
| 3.1 Introduction | 13 |
| 3.2 Stable isotopes of water | 15 |
| 3.2.1 Notation | 15 |
| 3.2.2 Fractionation | 17 |
| 3.2.3 The global distribution in rainfall | 22 |
| 3.2.3.1 Temperature effect | 23 |
| 3.2.3.2 Seasonal effect | 24 |
| 3.2.3.3 Altitude effect | 25 |
| 3.2.3.4 Continental effect | 27 |
| 3.2.3.5 Regionalization of isotopes in rainfall | 29 |
| 3.2.3.6 Evaporation | 30 |
| 3.3 Stable isotopes in soil | 35 |
| 3.3.1 Attenuation | 35 |
| 3.4 Stable isotopes in surface and groundwater | 38 |
| 3.4.1 Temporal variability of stable isotopes in runoff | 38 |
| 3.4.2 Temporal variability of stable isotopes in groundwater | 39 |
| 3.5 The use of environmental isotopes for hydrological system analysis | 40 |
| 3.6 Nitrogen isotopes and origin assignment | 42 |
| 3.7 Age dating | 43 |
| 3.7.1 Tritium | 43 |
| 3.7.2 Dating with gases (CFC, SF ₆) | 45 |

| | |
|---|-----------|
| 3.7.2.1 Dating with other noble gases | 50 |
| 3.7.2.2 ^{14}C -Dating | 50 |
| 4 Artificial Tracers | 57 |
| 4.1 Fluorescent tracers | 59 |
| 4.1.1 Basics of fluorescence | 61 |
| 4.1.1.1 Spectra | 63 |
| 4.1.2 Chemical and physical characteristics of dye tracers | 65 |
| 4.1.2.1 Solubility | 66 |
| 4.1.2.2 Fluorescence intensity – detection limit | 67 |
| 4.1.2.3 Effects of dependencies | 69 |
| 4.1.2.4 pH Dependence | 70 |
| 4.1.2.5 Temperature dependence | 72 |
| 4.1.2.6 Photolytic dependence | 72 |
| 4.1.2.7 Sorption processes | 76 |
| 4.1.2.8 Chemical and biological stability | 84 |
| 4.1.2.9 Toxicity and related environmental effects | 86 |
| 4.1.2.10 General assessment | 86 |
| 4.1.3 Measurement techniques | 88 |
| 4.1.3.1 Filter fluorometer | 88 |
| 4.1.3.2 Spectral fluorometer | 89 |
| 4.1.3.3 Synchronous scan technique | 89 |
| 4.1.3.4 Background signals and light scattering | 94 |
| 4.1.3.5 Fibre optic fluorometer (FOF) | 96 |
| 4.1.3.6 Field fluorometer for in situ measurements | 97 |
| 4.1.3.7 Laser measurement | 99 |
| 4.1.3.8 Advanced measurement techniques | 100 |
| 4.1.3.9 Long term sampling using active charcoal bags | 100 |
| 4.2 Salt tracers | 102 |
| 4.2.1 Chemical and physical characteristics of salts | 102 |
| 4.2.1.1 Sodium chloride (NaCl) | 105 |
| 4.2.1.2 Bromide (Br^-) | 105 |
| 4.2.1.3 Lithium | 106 |
| 4.2.1.4 Iodide | 106 |
| 4.2.2 Measurement techniques | 107 |
| 4.3 Drifting particles as tracers | 107 |
| 4.3.1 General characteristics of drifting particles | 108 |
| 4.3.1.1 Lycopodium spores | 109 |
| 4.3.1.2 Bacteria and bacteriophages (or phages) | 109 |
| 4.3.1.3 Fluorescent microspheres | 111 |
| 4.3.2 Measurement techniques and sampling of particle tracers | 111 |
| 4.3.2.1 Measurement | 111 |
| 4.3.2.2 Sampling | 112 |
| 4.4 Radioactive tracers | 112 |
| 4.4.1 Basics of radioactivity | 112 |
| 4.4.2 Characteristics of radioactive tracers | 114 |
| 4.4.2.1 Single-well technique | 115 |
| 4.5 Other tracers | 115 |
| 4.5.1 Fluorobenzoic acids (FBA) | 115 |
| 4.5.1.1 Suitability/potential applications | 116 |
| 4.5.2 Deuterium ^2H as an artificial tracer | 117 |

| | |
|---|------------|
| 4.5.3 Dissolved gas tracers | 118 |
| 4.5.3.1 Common gas tracers and tracer characteristics | 119 |
| 4.5.3.2 Gas-specific methods – technical equipment | 119 |
| 4.5.3.3 Applications | 120 |
| 4.5.4 Nonfluorescent dyes | 120 |
| 4.5.4.1 Brilliant blue | 122 |
| 5 Mathematical Modelling of Experimental Data | 123 |
| 5.1 Artificial tracer (ideal) under saturated flow conditions | 123 |
| 5.1.1 Transport equations | 123 |
| 5.1.1.1 3D equations | 123 |
| 5.1.1.2 2D equations | 126 |
| 5.1.1.3 1D equations | 127 |
| 5.1.2 Solutions to the transport equations | 127 |
| 5.1.2.1 2D solution | 128 |
| 5.1.2.2 1D solution | 130 |
| 5.1.3 Estimation of the transport parameters | 133 |
| 5.1.3.1 Combined least squares method (LSQM) | 133 |
| 5.1.3.2 Method of moments (MM) | 136 |
| 5.1.3.3 The cumulative curve method (CCM) | 137 |
| 5.1.4 Artificial tracer experiments in multi-flow systems | 140 |
| 5.1.5 Experiments in double-porosity aquifers | 144 |
| 5.1.6 Examples | 148 |
| 5.1.6.1 Column experiment | 148 |
| 5.1.6.2 Combined pumping-tracer test | 149 |
| 5.1.6.3 Experiment in multi-flow system | 151 |
| 5.1.6.4 Experiment in double-porosity (fissured) medium | 153 |
| 5.2 Tracer experiments under unsaturated flow conditions | 154 |
| 5.3 Tracer experiments in streams and rivers | 158 |
| 5.4 Environmental tracer data | 160 |
| 5.4.1 Introduction | 160 |
| 5.4.2 The basic concept of lumped-parameter models | 161 |
| 5.4.2.1 Combined piston-flow diffusion model (SPFM) | 165 |
| 5.4.3 Selection of the model | 166 |
| 5.4.4 Examples | 168 |
| 5.4.4.1 Application of stable isotopes to bank filtration | 168 |
| 5.4.4.2 Application of tritium measurements in catchment areas | 170 |
| 5.4.5 Multi-cell approach and concluding remarks | 172 |
| 5.5 The goodness-of-fit of a model | 174 |
| 6 Technical Instructions | 175 |
| 6.1 Planning and execution of a tracer study | 175 |
| 6.1.1 Data collection and evaluation, field reconnaissance and mapping | 176 |
| 6.1.2 Choice of tracers and estimation of tracer mass | 177 |
| 6.1.3 Planning of studies and experiment execution in detail – creation of a schedule | 178 |
| 6.1.4 Risk management | 179 |
| 6.1.5 Consultation with authorities and formal application (legal process) | 179 |
| 6.1.6 Practical suggestions for experiment execution | 180 |
| 6.1.7 Requirements for an adequate groundwater sampling | 181 |

| | | |
|----------|--|------------|
| 6.2 | Estimation of tracer injection mass | 182 |
| 6.3 | Gauging discharge | 187 |
| 6.3.1 | Approach of dilution method | 187 |
| 6.3.2 | Slug injection (integration method, gulp injection) | 188 |
| 6.3.3 | Constant rate injection | 190 |
| 6.3.4 | Requirements for tracers | 191 |
| 6.3.5 | Salt dilution technique | 193 |
| 6.3.6 | Characteristic example of a tracer dilution gauging in a brook (slug injection) | 194 |
| 6.4 | Chloride method for groundwater recharge estimation | 195 |
| 6.5 | Hydrograph separation using the end member mixing analysis (EMMA) | 198 |
| 7 | Case Studies | 201 |
| 7.1 | Groundwater | 202 |
| 7.1.1 | Case study: 'Estimation of groundwater origin, residence times, and recharge of Chad Aquifers in Nigeria' | 210 |
| 7.1.1.1 | Introduction and aim | 210 |
| 7.1.1.2 | Description of test site | 210 |
| 7.1.1.3 | Hydrogeology | 210 |
| 7.1.1.4 | Methodology | 212 |
| 7.1.1.5 | Results | 213 |
| 7.1.1.6 | Interpretation | 218 |
| 7.1.2 | Case study: 'Vulnerability of a spring capture zone' | 218 |
| 7.1.2.1 | Introduction and aim | 219 |
| 7.1.2.2 | Description of test site | 219 |
| 7.1.2.3 | Methodology | 219 |
| 7.1.2.4 | Results | 220 |
| 7.1.3 | Case study: 'Evaluation of aquifer parameters by single well techniques' | 221 |
| 7.1.3.1 | Single well experiment using radioactive isotope ^{82}Br | 223 |
| 7.1.3.2 | Single well experiment with fluorescent tracers using fibre optic sensor | 224 |
| 7.1.3.3 | Single well experiment with fluorescent tracers using online fluorometer | 226 |
| 7.2 | Case studies in the unsaturated zone and in soils | 229 |
| 7.2.1 | Specific aspects of using tracers in the unsaturated zone | 230 |
| 7.2.2 | Case study: 'Environmental deuterium transport through soils' | 232 |
| 7.2.2.1 | Introduction and aim | 232 |
| 7.2.2.2 | Description of test site | 233 |
| 7.2.2.3 | Modelling | 233 |
| 7.2.2.4 | Results and conclusions | 236 |
| 7.2.3 | Case study: 'Determining the filtration capacity of soil-aquifer systems by multi tracer experiments' | 239 |
| 7.2.3.1 | Introduction | 239 |
| 7.2.3.2 | Laboratory experiments | 240 |
| 7.2.3.3 | Field experiments | 242 |
| 7.2.3.4 | Assessment of results and methodology | 244 |
| 7.3 | Surface water | 246 |
| 7.3.1 | Lakes | 247 |
| 7.3.2 | Rivers | 248 |
| 7.3.3 | Specific aspects of using tracers in surface waters | 250 |

| | |
|--|-----|
| 7.3.4 Case study: 'Calibration of transport models using tracer techniques – River Rhine' | 252 |
| 7.3.4.1 Introduction | 252 |
| 7.3.4.2 Methods | 253 |
| 7.3.4.3 Model conception to be calibrated and validated | 255 |
| 7.3.4.4 Method of resolution for river sections | 256 |
| 7.3.4.5 Tracer experiments | 258 |
| 7.3.4.6 Assessment of the experiments | 272 |
| 7.3.5 Case study: 'On mixing of effluent inflow' | 273 |
| 7.3.5.1 Introduction and aim | 273 |
| 7.3.5.2 Methodology | 274 |
| 7.3.5.3 Results | 276 |
| 7.3.6 Case study: 'Estimation of hydrodynamics and transport parameters in Paiva Castro reservoir, Brazil' | 277 |
| 7.3.6.1 Introduction and aims | 277 |
| 7.3.6.2 Methodology | 278 |
| 7.3.6.3 Measurements | 278 |
| 7.3.6.4 Mathematical modelling | 279 |
| 7.3.6.5 Results | 279 |
| 7.3.6.6 Conclusions | 281 |
| 7.3.7 Case study: 'Investigation of internal dynamics and residence time in Lake Bled' | 282 |
| 7.3.7.1 Introduction | 282 |
| 7.3.7.2 Tracer experiments | 283 |
| 7.3.7.3 Interpretation of the experiments | 290 |
| 7.3.7.4 Modelling | 291 |
| 7.3.7.5 Second study 1988–1991 – determination of residence time | 292 |
| 7.3.7.6 General assessment | 299 |
| 7.3.8 Case study: 'Optimization of a sewage effluent into Lake Murten' | 299 |
| 7.4 Glaciers | 303 |
| 7.4.1 Specific techniques of tracer experiments in glaciers | 308 |
| 7.4.2 Injection | 308 |
| 7.4.3 Sampling | 309 |
| 7.4.4 Analyses | 310 |
| 7.4.5 Case study: 'Tracer experiments in temperate alpine glaciers – Findelen' | 310 |
| 7.4.5.1 Summer experiments 1982 | 312 |
| 7.4.5.2 Winter experiments 1984 | 318 |
| 7.5 Catchment scale | 321 |
| 7.5.1 Case study: 'Surface-groundwater interaction' | 325 |
| 7.5.1.1 Introduction and aim | 325 |
| 7.5.1.2 Methodology | 326 |
| 7.5.1.3 Water level monitoring | 326 |
| 7.5.1.4 Stable isotopes | 327 |
| 7.5.1.5 Artificial tracer, SF ₆ | 329 |
| 7.5.1.6 Fluorescent dyes | 330 |
| 7.5.1.7 Conclusions | 330 |
| 7.5.2 Case study: 'Runoff generation processes investigated using tracers' | 331 |
| 7.5.2.1 Introduction and aim | 331 |
| 7.5.2.2 Description of test site | 331 |
| 7.5.2.3 Methodology | 332 |

| | |
|--|-----|
| 7.5.2.4 Data | 335 |
| 7.5.2.5 Results and discussion | 336 |
| 7.5.2.6 Application of tracer results for model design and model validation | 340 |
| 7.5.2.7 Multi tracer experiments at hillslopes | 342 |

Colour Plate Section

| | |
|-------------------|------------|
| References | 349 |
|-------------------|------------|

| | |
|--------------|------------|
| Index | 399 |
|--------------|------------|

Preface

‘Tracers in Hydrology’ has a long history. In the 1950s the use of tracer techniques in hydrology began to be developed broadly. This development was possible, in particular because of the progress made in measurement techniques and by the digitalization of data processing. Simultaneously, the computer era began and opened up new possibilities for environmental modelling. During this fascinating phase of development of natural science and, in the case of Tracerhydrology, came the evolution of a holistic approach towards the use of tracers in hydrology.

Besides many other factors, three fortunate milestones marked this development. A powerful framework for realizing numerous ideas was created through the founding of the Association of Tracerhydrology (ATH). The ATH promoted the use of tracer techniques in Europe between the 1960s and the end of the twentieth century in many ways.

The second milestone was the establishment of the Isotope Hydrology Laboratory by the International Atomic Energy Agency (IAEA) in Vienna in 1961. It pushed the rapid development of the isotope techniques, beginning with environmental tritium, as a research tool for investigating the hydrological cycle worldwide.

The XXth General Assembly of the International Union of Geodesy and Geophysics in 1991 in Vienna can be considered to be the third milestone. The International Commission on Tracers (ICT) within the International Association of Hydrological Sciences (IAHS) was established at this assembly. Its aim was, amongst others, to bring together the experimental hydrologists with modellers for the integrated investigation of the hydrological system. This event is significant since at the zenith of the modelling phase in hydrology the establishment of a clearly experimentally oriented commission within the IAHS was not without opposition. The following years showed an increasing integration of the tracer methods into hydrological research and applied hydrology by the international community, which validated this structural development. Experimental hydrology, in particular the strongly emerging catchment hydrology, used tracer methods increasingly in order to assess hydrological processes and system functions. In particular the calibration and validation of mathematical models was based increasingly on tracerhydrological research.

The authors are looking forward to the further development of new applications of tracer techniques and, in particular, to an increasing combination of tracer techniques with other hydrometric and hydrological methods. In order to provide independent, experimentally based hydrological data for the reliable modelling of hydrological processes and systems, the further methodological development of tracer methods is expected.

Acknowledgements

We are grateful to:

Hannes Leistert and Irene Kohn for the outstanding editorial work and substantial support in developing the textbook. Jonas Zimmermann, Jürgen Strub, Gaby Dietze and Stefan Kryszon for technical assistance and research with the literature.

Stefan Pohl for his critical review of the textbook.

Hansruedi Wernli, Hanspeter Hodel, Albrecht Leis, Ralph Benischke, Paul Königer, Spela Remec – Rekar, Rudi Rajar and Stefan Uhlenbrook for their critical review of parts of the textbook. John Tipper for the proof reading of Chapter 5 ('Modelling.')

The dedicated teams (scientists, students) at the Universities of Berne (Switzerland) and Freiburg i.Br. (Germany) for having applied and further developed tracer methods during four decennia and numerous colleagues at the ATH and the ICT/IAHS for fruitful collaboration.

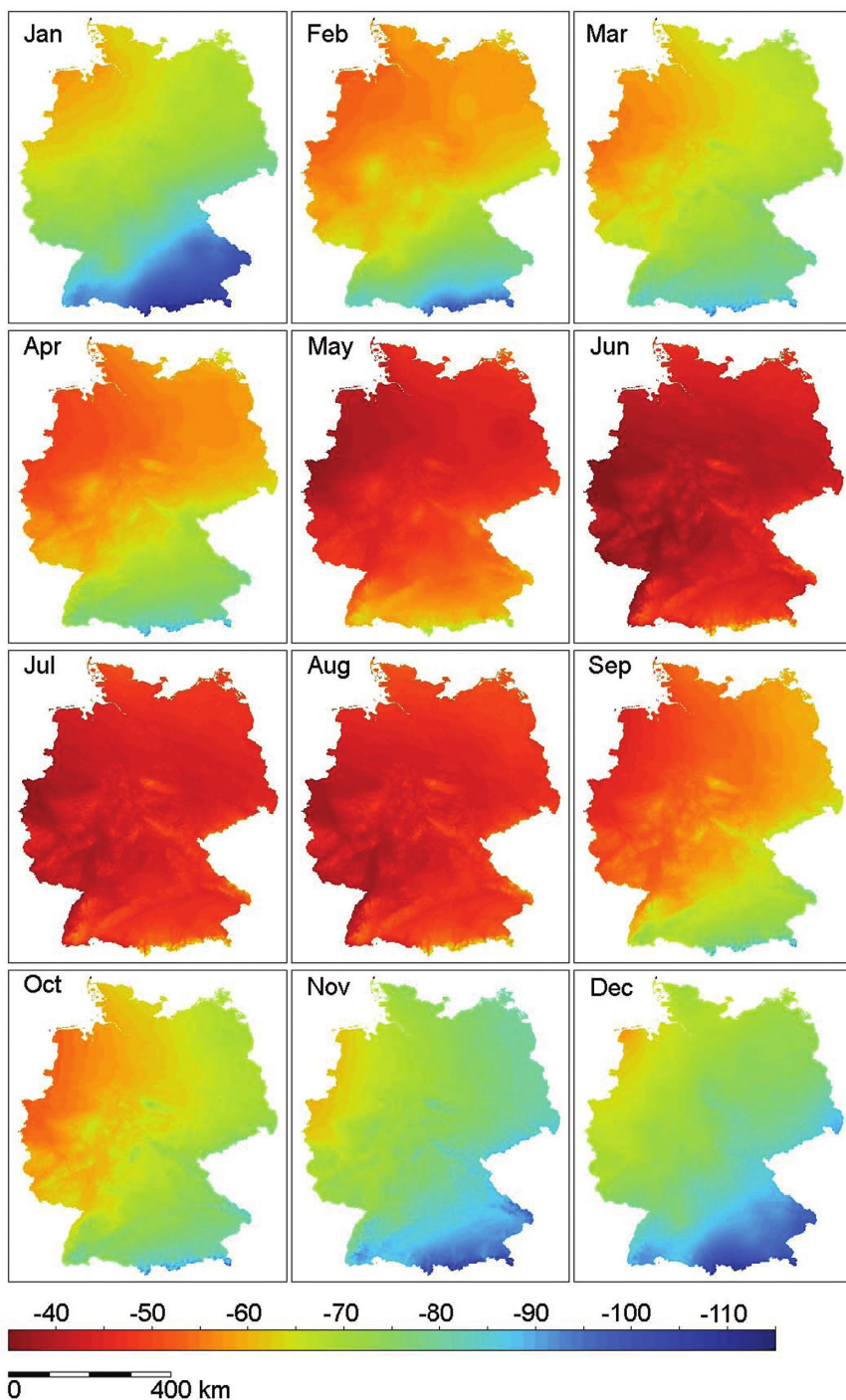


Plate 1: Map of the mean monthly composition of stable isotopes in rainfall in Germany ($\delta^2\text{H}$ V-SMOW in ‰) derived by regression from monthly data of 17 IAEA stations (Global Network of Isotopes in Precipitation), showing latitude, seasonal and altitude effects (modified after Schlotter, 2007)

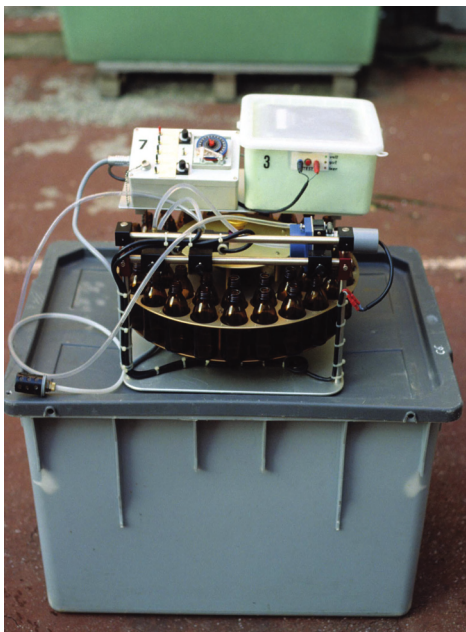
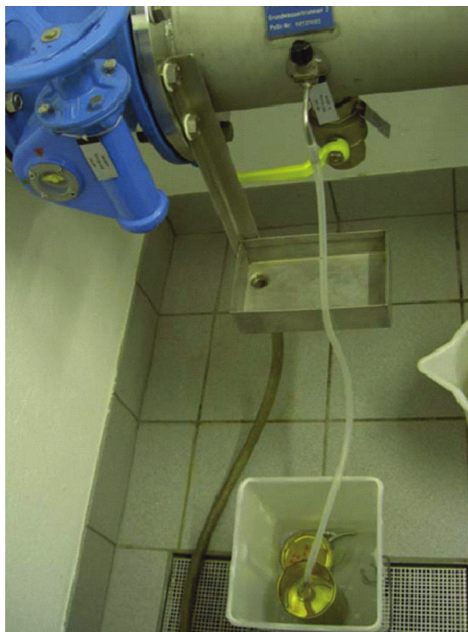


Plate 2: (*Upper left*) Sampling for CFCs and SF₆ by filling a glass bottle in a metal container with water through a continuous flow connection. (*Upper right*) autosampler for the sampling of stable isotopes (or geochemical and artificial tracers). (*Below*) Study area Andarax basin in Southern Spain, for which CFC, SF₆ data are presented in Box 3.1.

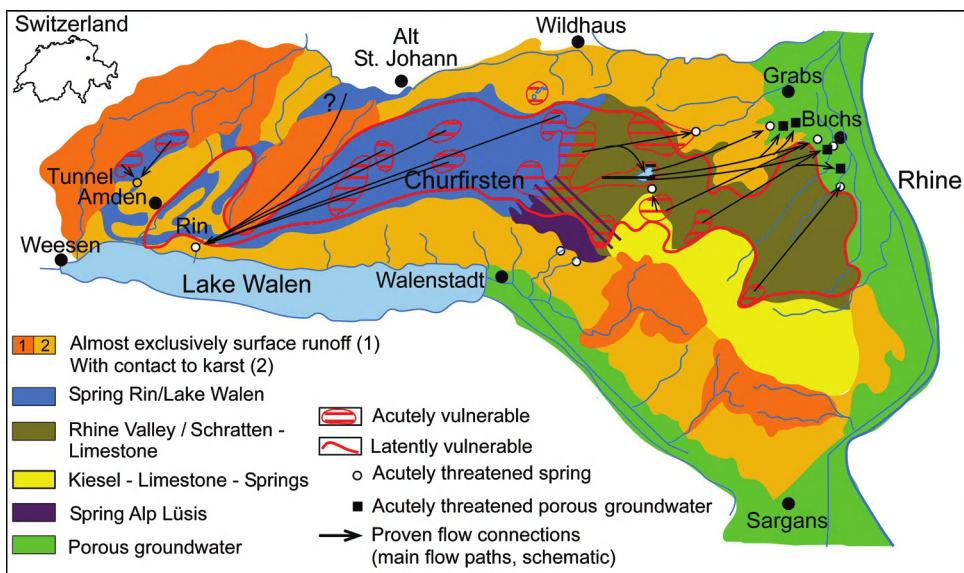


Plate 3a: Vulnerability map of the Churfürsten-Alvier Mountains, Swiss Alps. Delineation of the catchments and vulnerable zones and the hydrological system function respectively is strongly based on tracer methods.

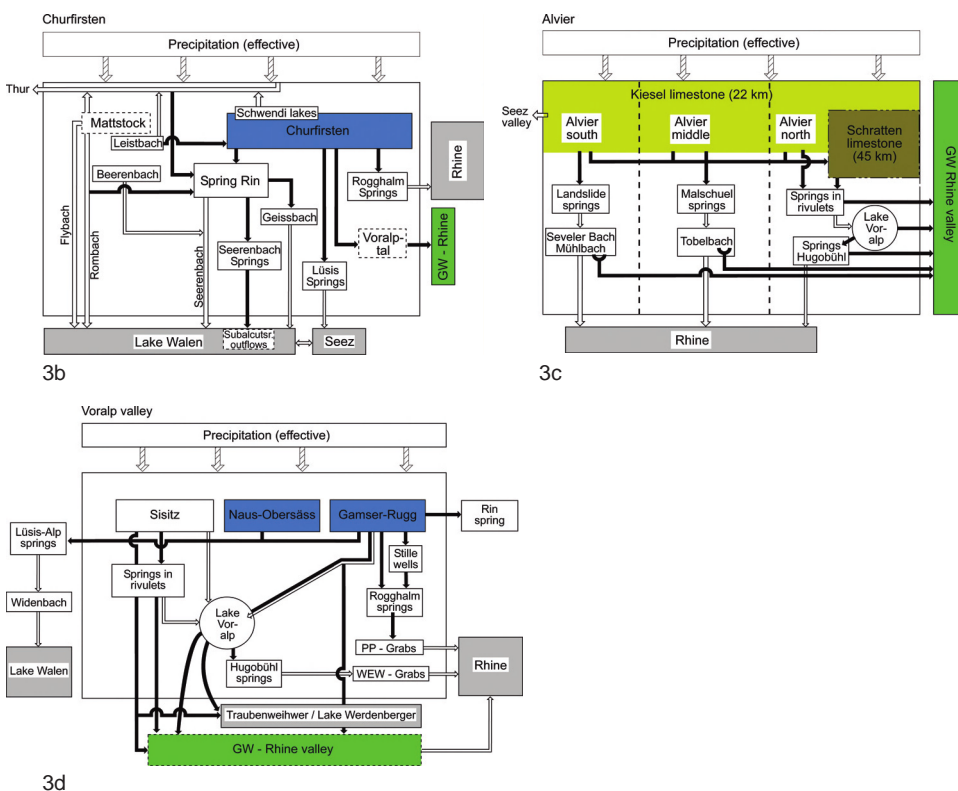


Plate 3b-d: Conceptual models (structure models) of complex hydrological systems (catchments) evaluated by tracer techniques serving as a base for further research and mathematical modelling.



Plate 4a: Typical sediment subcatchment in the recharge area of Churfirsten Mountains (CP3a). The loamy sediment-soil cover (barely vulnerable) drains the water by superficial channels discharging into karst ponors (sinkholes), thus leading to (very) a high vulnerability of the subcatchment.



Plate 4b: Typical karst subcatchment in the recharge area of Churfirsten Mountains (CP3a). The Doline covered karst catchment is highly permeable and of a high intrinsic vulnerability.



Plate 4c: The large drainage convergence of the Churfirsten mountains: Spring Rin (below) and Serenbach-Waterfall (above). The latter drains the remaining superficial water of the recharge area. Spring Rin ($Q_{\max} \text{ ca. } 50 \text{ m}^3/\text{s}$) drains the huge and complex karstic aquifers as overflow.

Plate 5 and 6: Tracer experiment to investigate the stratification of river water in a small alpine lake (Orbello, Switzerland) using Amidorhodamine G.



Plate 5a: Situation 10.23 a. m.: Injection of the small river. Start of stratification in the lake water body in the depth determined by the density.



Plate 5b: Situation 20.24 a. m.: The injection is completed; see the already clear water at the inflow of the river water. Distribution of the tracer cloud.



Plate 5c: Situation 10.25 a. m.: Formation of a right vortex due to the Coriolis force.



Plate 6a: Situation 10.27 a.m.: The portion of the traced water contained in the right vortex reaches the right bank leading to the start of the left rotation along the right bank.



Plate 6b: Situation 10.40 a.m.: The bay right hand of the injection is filled up with traced water (right vortex) and successively the traced water flows along the right bank and continues over into the left rotation.



Plate 6c: Situation 11.10 a.m.: Part of the tracer cloud in the left rotation which will pass the lake counter clockwise along the banks and end in a complete mixing within the lake due to complex vortices, diffusion and dispersion processes.

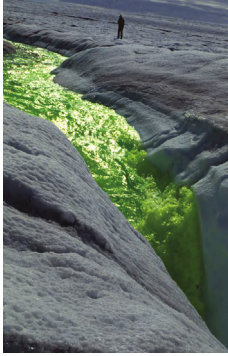
Plate 7: Bird's eye view of the distribution of the artificial tracer Uranine within the hypolimnion of Lake Bohini, Slovenia. Note: only the unique visibility depth of the pure water enables the recognition of the tracer cloud within the hypolimnion.



Plate 7a: Distribution of the tracer cloud approximately half a day after injection. Due to the high speed along the longitudinal axis the traced water reached the opposite bank quickly and turned into a left rotation. The right vortex movement is only recognisable at the right end of the tracer cloud. The injection took place in the River Sava Bohinska (small delta at mouth) at the left edge of the picture.



Plate 7b: Further development of the right vortex and extremel insight in the complex eddies of tracer mixing within the hypolimnion.



8a



8b



8c

Plate 8a: Tracing of the drainage system of the Greenland's ice shield (western ice edge). Injection of Uranine into a meltwater channel. The sampling took place in periglacial lakes and fjords at the ice border.

Plate 8b: Characteristic tracer experiment in an Alpine glacier (Gorner, Switzerland). Injection of Uranine in a meltwater channel which drains into the inter-subglacial drainage system.

Plate 8c: Tracer experiment aimed at determining the transmission losses through an high permeable debris cone using the fluorescent tracer Eosine. The sampling took place at springs at the base of the cone.

1

Introduction

‘Tracers in Hydrology’ defines the scientific field that aims at *understanding the hydrologic system* by making use of environmental and artificial tracers and modelling. Tracing of water provides unique methods for a direct insight into the dynamics of surface and subsurface water bodies. The relevance of tracer techniques in hydrological investigations and in applied hydrology ensues from the astounding complexity of water flow in natural systems. How much runoff in rivers really stems from rainstorms? How does water flow through a hill-slope or a glacier? How large is the storage of water resources in aquifers? Where, how and when was the water found in an aquifer formed? Tracer techniques are a useful tool in understanding the transport processes and quantifying their parameters. Tracers help to identify and quantify the phase changes (evaporation, condensation, sublimation), shed light on the origin of pollution and assist in the respective remediation processes. The natural tracers constitute a tool of prime importance in the reconstruction of the climate during the Holocene period when studying ice cores, old groundwater and the unsaturated zone in arid and semiarid regions. Tracer methods are also a major tool for calibration and validation both of strategies in modelling catchment hydrology and hydrological models of groundwater systems. Furthermore, tracer approaches are commonly used to address issues like surface water–groundwater interactions, paleohydrology, water movement in very low permeable rocks, calibrating and validating numerical flow and transport models and evaluating vulnerability of water resources. Finally for Integrated Water Resource Management, tracer techniques have great potential as tracers that provide integrated information and can be very efficient in characterising complex systems in remote areas.

The empirical observation of flow and transport processes with tracers and the theoretical formulation of flow and transport processes depend on each other and have resulted in a beneficial coevolution of both approaches if adequately combined. Tracers provide empirical data of real and often unexpected flow patterns – models provide tools for flow and transport predictions.

The term ‘*Tracerhydrology*’ is used as a short expression for the use of tracers in hydrology understood as an advanced method that allows for an integrative investigation

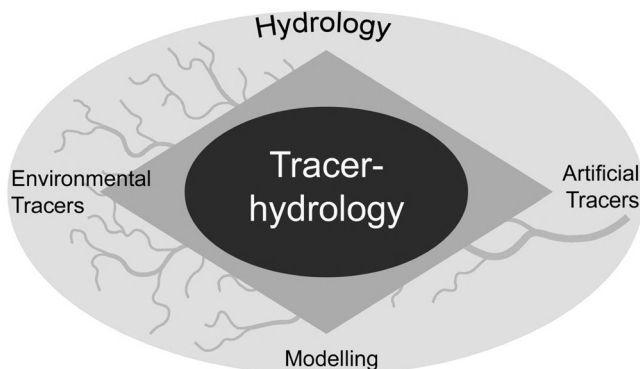


Figure 1.1 Tracerhydrology as a method of application tracers in water sciences understood as a holistic approach of hydrology and water research.

of the hydrologic system. It is not regarded merely as an isolated technique for solving particular problems of applied hydrology, although it certainly can be useful in those fields.

This book originated from the idea of interweaving knowledge from the fields of artificial and environmental tracers and of modelling, in order to present the options, opportunities and limits of tracers in hydrology to students, scientists, engineers and other users. In the following chapters the explanation of tracer and modelling basics builds a foundation for students and users to be able to understand the techniques, which are then applied to case studies of both specific applications and integrated studies. Herein, tracer techniques are described with regard to their relevance for advancing hydrological science and to their role in solving problems in applied hydrology. Students, scientists and consultants will find a wealth of information on tracers and modelling in order to introduce them to the field of tracerhydrology. A methodological chapter provides specific techniques such as the calculation of injection mass and the chloride method and also case studies dealing with the different approaches and problems of applied tracerhydrology (groundwater recharge).

Scientists can see the range of opportunities that tracer techniques offer through the variety of comprehensive case studies that are presented. Engineers and other users will find a large collection of work examples and may apply the methods described, for example tasks in integrated water resources management or the allocation of water supply protection zones, as well as many others. In this book the application of tracers in hydrology is understood basically as the integrated use of tracers in hydrology and therefore as a part of an integrated hydrological approach (Figure 1.1).

In Chapter 2 a detailed concept of tracerhydrology will be presented. The role of modelling in integrated tracerhydrology will be defined in a separate chapter. The combined application of tracerhydrology and modelling is presented by means of selected examples of applications in various hydrological compartments (glaciers, rivers, lakes, groundwater). The authors wish to present a textbook that starts from a simple and general overview and moves on to the more complex topics of tracerhydrology in

order to facilitate an easy understanding by the readers, be they students, water research scientists, engineers or applied hydrologists.

The application of tracers in hydrology has a long tradition among the geo- and water sciences. After what were at first somewhat ‘trial and error’ – based experiments about 150 years ago a fascinating development began. Artificial salt and fluorescence tracers have been used for decades. In the 1950s a wide variety of new artificial tracers were included in tests designed to trace water, mainly in karst aquifers. At the same time a compelling new direction in tracerhydrology based on the use of natural, mainly isotopic tracers began to develop. Most of the fundamental principles had been developed during this phase. Stable isotopes have provided a major input into the study of hydrological processes such as runoff generation and runoff component separation as well as recharge and groundwater flow and are still at the centre of defining the conceptual models of hydrological processes. The role of isotopes in the validation of circulation models and response of ecosystems to climate change is not yet fully explored.

In addition to an increasing number of papers on tracerhydrology published in international hydrological journals, there are many publications on the use of tracers for water research issued by international organizations, such as (i) the IAHS (International Association on Hydrological Sciences), (ii) the symposia proceedings of the IAEA (International Atomic Energy Agency), and (iii) the proceedings and project volumes of the ATH (International Association of Tracers). These publications are an excellent resource for all matters concerning the methodological aspects and application of tracers.

Comprehensive presentations of large combined tracerhydrological studies are given in the reports of the ATH (International Association of Tracers). The focus of these investigations was on groundwater systems but the approach was holistic within the respective river basins. Increasingly, investigations on runoff generation and catchment modelling have adopted an integrated tracerhydrological approach.

Innovations in analytical techniques will provide new tools for tracerhydrology. There are trends towards reducing sample volumes, increasing the number of samples analysed, reducing detection limits and identifying new natural and industrial substances that can be used for tracer studies. Certainly, natural remediation and reactive transport processes will be explored increasingly with tracers. For the advance of hydrological science, empirical data provided by tracer methods have and will continue to play an important role. Further integration of experimental and theoretical approaches leading to an integration of tracers into soil water atmosphere transfer schemes and catchment and groundwater models, will provide additional means of validating the hydrological concepts.

2

The Integrated Concept of Tracers in Hydrology

2.1 System approach

The system analysis of watersheds and aquifers draws key insights from artificial and environmental tracer data. Artificial tracers help to understand flow processes, to estimate main hydrological system parameters and to visualize the movement and mixing of otherwise indiscernible distinct water volumes. Hence, they provide a tool for understanding and characterizing complex flow through the soil, on surfaces, in channels, through and along hill-slopes, in aquifers or in artificial systems. Environmental tracers have become key tools for estimating water resources in the catchment areas, for the reconstruction of hydrological processes from the past, in ungauged basins or for the integration of hydrological processes that otherwise would be far beyond observation. Both environmental and artificial tracers have their own theoretical basis. This textbook will provide an introduction to both environmental and artificial tracer techniques along with their respective theoretical background and will demonstrate how both techniques can be modelled, combined and integrated into hydrological applications that work.

When trying to analyse hydrological systems' hydrometric data, hydro-chemical information and system characteristics need to be reconciled within a common system model (Dyck and Peschke, 1995). The aim of tracerhydrology is to develop, test and validate those representations of the hydrological system that best agree with the available data by making use of environmental and artificial tracers and modelling.

The general approach in system hydrology is based on the determination of:

- a known or measured input (volume, concentration, energy) as a function of time and space,

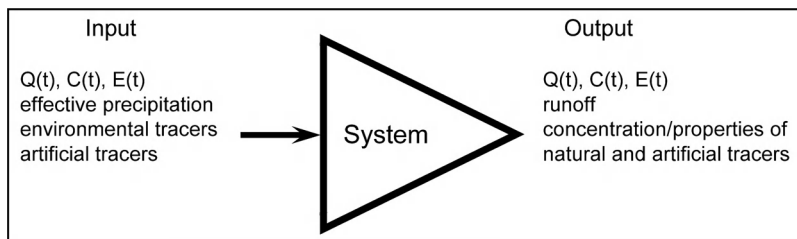


Figure 2.1 Hydrological system approach adapted to tracerhydrology by the convergence approach. Q: volume of water; C: concentration; E: energy.

- a function characterizing the system (e.g. catchment, spring. . .) by a set of equations describing the flow and/or transport processes at the atmosphere-surface boundary, in surface water or in subsurface-water,
- a known or measured output of the same parameters as a function of space and time (Figure 2.1).

Linking this to tracer techniques, the input will be the concentration of tracer in infiltrating water and effective precipitation (for environmental tracers) or the injection mass of artificial tracers. After flowing through the system the output will be characterized by the runoff volume, the environmental tracer concentrations (for isotopes and geochemical compounds) and/or artificial tracer concentrations. This concept has been described by Leibundgut (1987) and named the convergence approach. In other words tracerhydrology is based on decoding of information contained in the output parameters of a system. The simplest example is the system of a spring.

Both input and output parameters will be measured in order to understand the processes in a natural hydrological system be it a catchment, an aquifer or surface water. Besides the hydrological water balance parameters in particular, data of environmental and artificial tracers are measured. Models are simplified abstractions of nature that are used to obtain information from measured data about the system. The transfer function between input and output is identified from tracer data and can be used for predictions or system characterization. The modelling of both environmental tracers and artificial tracer experiments is a necessary tool for evaluating the application of tracers.

The application of the convergence approach in tracerhydrology can be used to derive concepts of hydrological systems (Figure 2.2). These conceptual models can be simple or more structured. They represent the principal functioning of the investigated hydrological system (Leibundgut, 1987; Attinger, 1988). Predictions derived from an existing, conceptual system model allow for an improved design of the experimental planning and the observation network.

The combined and simultaneous use of several independent methods and techniques in investigating a hydrological issue is considered as an axiom of tracerhydrology. This principle is applied using the different tracer techniques (natural, artificial tracers)

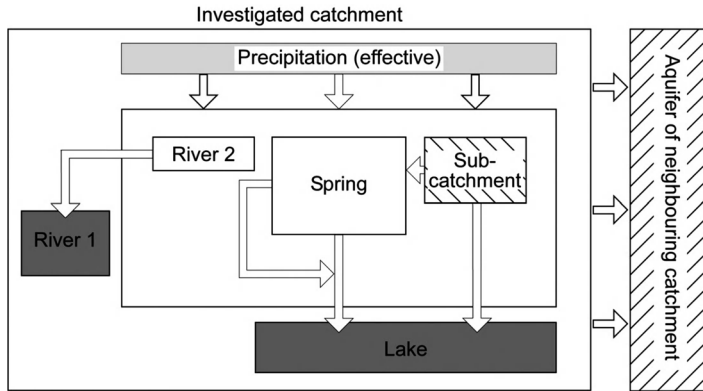


Figure 2.2 Conceptual model (Structure model) of a complex system (catchment) evaluated by tracer techniques serving as a base for further research and mathematical modelling (see colour plate section P3b-d).

in combination with independent hydrological methods. First, this means that several techniques should be combined in multi-tracer experiments, if possible. The combination of different tracers ensures that the specific limitations of single tracers or methods do not bias our understanding of the hydrological system. While it has become almost common practice to combine different artificial tracers, the combination of environmental *and* artificial tracers is the most promising approach. Furthermore, tracer methods should also be combined and integrated with other hydrological and scientific methods (hydrometry, geophysics, hydrochemistry, remote sensing, etc.).

The fascination of an integrated approach is the reconciliation of results obtained by different independent methods. If different methods provide consistent or concordant data, the scientific conclusion is more soundly based and validated. The fuzziness of individual methods can be overcome if different methods point in the same direction. Finally, contradictions between different methods can be very instructive and push for new experiments or research aimed at resolving the problem.

2.2 Definition of tracers

Environmental tracers are defined as inherent components of the water cycle. Sometimes, accidental injections can be used for hydrological studies. Global input functions have been created as the side effects of industrial or military activities (CFCs, $^{85}\text{Krypton}$ or bomb-tritium). Artificial tracers are defined by their active injection into the hydrologic system in the context of an experiment.

In nature tracers are widely used as markers, such as wildlife marking their territory or ants using pheromones for marking itineraries. Such markers are effective at extremely low concentrations (10^{-15}). All tracers carry discernable and preferably unique information. These two properties – carrying information that can be identified most effectively at low concentrations – categorize substances as trace elements.

Table 2.1 Systematic tracer classification, distinguished by their application. Pollution tracers originate from anthropogenic activities, however their input in the hydrological system can be similar to that of natural tracers

| Environmental tracers | Artificial tracers |
|---|--|
| <i>Utilization</i> | <i>Application</i> |
| Environmental isotopes | Chemicals |
| Hydrochemical substances | Biological substances |
| Pollution tracers | Drift substances |
| <i>Characteristics:</i> | <i>Characteristics:</i> |
| Spatial input via precipitation, geogenic sources | punctual input (injection), defined by time, place, hydrological situation |
| | Pollution tracers (e.g. Cl^- SF_6 CFCs) |

Hydrological tracers are dissolved, suspended or floating substances according to their purpose and field of application. Some natural and artificial substances which are suitable for scientific studies or can be applied for the investigation of hydrological systems and subsystems are given in Table 2.1 (Leibundgut, 1982). In principle, hydrological trace elements have to be detectable in solutions with mass ratios of water:tracer of $>10^9$.

Environmental tracers are inherent components of the water cycle, thus we speak of their *utilization*, while artificial tracers are brought actively into the hydrologic system, so that we refer to their *application*. Not belonging completely to either of the two groups, pollution tracers are substances introduced into the water cycle by anthropogenic activity, coming either from punctual contaminations such as waste deposits or brought in by accidents, or originating from the production of pollution gases released into the atmosphere. Consequently, they are not natural but feature the same input channels as environmental tracers.

The input of environmental tracers into the hydrologic system of surface, soil and ground water takes place by diffuse and continued processes via precipitation or the solution from minerals. An investigation with large scales of time and space is possible, and thus environmental tracers serve, in particular, to follow an integrated approach, for example not only catchment studies and water balances but also as a base for solving various applied problems. Often, the variability in time and space of the input function is hard to acquire, and the input 'signal' might be weak.

Artificial tracers are added to the system in well-defined hydrologic situations of time and space, by punctual injections; it is possible to label a specific component of the water cycle or investigated system, for example an inflow to the lake. The scales in time and space for application are limited, and it is only possible to gain insights into a part of the system during the time of the experiment. In general, artificial tracers are used in systems which have a residence time smaller than one year. Owing to this limitation it might happen that the hydrologic situation chosen for the experiment is not representative for the system. A list of available tracers in three groups is provided in Table 2.2.

Table 2.2 Currently available hydrological tracers.

| Environmental tracers | Artificial tracers | |
|---|---|---------------------------------------|
| | Solute tracers | Dissolved gas tracers |
| Stable isotopes | Fluorescence tracers | Helium |
| Deuterium (^2H) | Naphtionate | Neon |
| Oxygen-18 (^{18}O) | Pyranine | Krypton |
| Carbon-13 (^{13}C) | Uranine | Sulfur hexafluoride (SF_6) |
| Nitrogen-15 (^{15}N) | Eosine | |
| Sulphur-34 (^{34}S) | Rhodamines | |
| Radioactive isotopes | Non fluorescent dyes | |
| Tritium (^3H) (and Helium-3 (^3He)) | e.g. Brilliant Blue | Particulate tracers |
| Carbon-14 (^{14}C) | Salts | Lycopodium spores |
| Argon-39 (^{39}Ar) | Sodium/potassium chloride | Bacteria |
| Krypton-85 (^{85}Kr) | Sodium/potassium bromide | Viruses |
| Radon-222 (^{222}Rn) | Lithium chloride | Phages |
| Radium-226 (^{226}Ra) | Potassium iodide | DNA |
| Silicium-32 (^{32}Si) | Sodium borate (borax) | Synthetic microspheres |
| Chlorine-36 (^{36}Cl) | Fluorobenzoic acids | Phytoplankton |
| Noble gases | Deuterated Water (^2H) | |
| Geochemical compounds | Radionuclides | |
| e.g. Silicate, chloride, heavy metals | e.g. Tritium | |
| Physio-chemical parameters | Bromide-82 (^{82}Br) | |
| e.g. Electrical conductivity, Temperature | | |
| Pollution Tracers | | |
| e.g. CFCs, SF_6 , phosphate, boron, nitrate, radioactive compounds | | |

2.3 Modelling in the context of integrated tracerhydrology

Finding the parameters from the tracer experiment is only possible if an adequate mathematical model is used, meaning that the model is based on the proper concept of tracer transport and its behaviour in the system. In order to understand this, some definitions will be given below and the application of the mathematical models will be discussed (Maloszewski and Zuber, 1992a, b; 1993).

A *Conceptual model* is a qualitative description of a system and its representative factors (e.g. geometry, hydraulic connections, parameters, initial and boundary conditions) related to the intended use of the model. In practice, the conceptual model demonstrates the principal idea of water circulation in the system (Figure 2.2).

A *Mathematical model* is a mathematical description of a conceptual model, representing a hydrological, physical and/or hydro-chemical system, using functions designed to help in understanding and predicting the behaviour of the system under specified conditions. In tracerhydrology the mathematical model represents the solution to the mathematical equation(s) describing water and tracer transport for given boundary conditions.

Model calibration is a process in which the mathematical model assumptions and parameters are varied to fit the model to the experimental data. Calibration can be

carried out by a trial-and-error procedure, or by an automatic fit based on an objective function. The calibration of the model to experimental data solves the inverse problem by finding the right values for system parameters.

Model validation is a process of obtaining assurance that a model is a correct representation of the process or system for which it is intended. Ideally, validation is obtained when the parameters derived from the model agree with independently measured parameters (e.g. porosity) as described above.

The tracer method is usually applied to a system that is poorly known. As a consequence the mathematical model required to determine the system parameters must be as simple as possible. As mentioned earlier, mathematical modelling of experimental data in tracer hydrology can be separated into two different approaches, depending on the considered tracer method. The two approaches are i) deconvolution or inverse modelling of information provided by tracers and ii) mathematical modelling based on the transport equation.

In general, the tracer injection for artificial tracer experiments is reduced to a single point only (well, sinkhole, karst doline) or to a line (trench, river cross-section). Some pollution tracers also rather represent point sources (e.g. pollutants release by accident or from point sources). In this case mathematical models are used that are usually based on dispersion theory. Analytical solutions for advection-dispersion processes in one, two or three dimensions and different boundary conditions are available and described in detail in Chapter 5. For heterogeneous systems and complex boundary conditions, transport equations can be solved by numerical schemes.

For the modelling of environmental tracer data, a quite different approach is needed. In general, the 'injection' of tracer occurs naturally over an area and during a longer time either by precipitation or by solution of minerals from earth substrate. For instance, in the case of stable isotopes of water the tracer enters the hydrological system by precipitation that infiltrates. The environmental tracer concentration is observed in places where water discharges (e.g. in a river, at springs, at a pumping well).

Knowing both input and output concentrations as a function of time, one can consider the aquifer as a 'black-box'-system. Often this system can be described by mean parameters (volume of water, transit time and flow rate through the system). In this case, tracer transport between input and output (Figure 2.1) can be described by a lumped-parameter approach. Transport of tracer between input and output is characterized by the transit time distribution function, which needs to be defined for the investigated system (Maloszewski and Zuber, 1982, 1985). In mono-porous media, where the portion of stagnant water can be neglected, this type of modelling yields the mean transit time of water in the system as the main parameter. This parameter can be further used to estimate the volume of water in the system and thus the available water resources. In strongly heterogeneous (so called double-porous) media, for example fissured aquifers, which consist of mobile and stagnant water, application of the lumped-parameter approach to environmental tracer data yields the mean transit time of tracer instead of the mean transit time of water. The transit time of tracer describes both the transport of tracer by a mobile water component and the diffusive exchange of tracer between mobile and stagnant water. A detailed description of the lumped-parameter approach for mono- and double-porous media is given in Section 5.2. The transit time

Table 2.3 Main fields of applications in tracer hydrology

| | Atmospheric water | Surface water | Soil and unsaturated zone | Ground-water | Glacier and Snow | Catchment hydrology | Special application |
|---|----------------------|---------------|---------------------------------|--------------|---------------------|------------------------|------------------------|
| Global circulation | + | | | | | + | |
| Discharge measurement | | + | | + | + | + | |
| Delineation of hydrological units and protection zones | | | + | + | + | + | |
| Hydrologic/hydraulic connections | | | + | + | + | + | |
| Evaluation of flow paths | | | + | + | + | + | |
| Altitude of source areas | | | | + | + | + | |
| Age dating | | + | + | + | + | + | |
| Experimental hydrograph separation | | | | + | + | + | |
| Runoff generation processes | | | + | + | + | + | |
| Residence times | | + | + | + | + | + | |
| Flow and transport parameters | + | + | + | + | + | + | |
| Dispersion and diffusion processes | | + | + | + | + | + | + |
| Mixing processes | + | + | | + | | + | + |
| Permeabilities | | | + | + | + | + | |
| Infiltration processes | | | + | | | + | + |
| Infiltration/exfiltration processes | | + | + | + | + | + | + |
| Groundwater recharge | | + | + | + | + | + | |
| Interaction between surface and subsurface water | | + | + | + | | + | |
| Hyporheic exchange | | + | + | + | | | + |
| Filtration processes | | + | + | | | | + |
| Stratification of lakes | | + | | | | | |
| Circulation currents | | + | | | | | |
| Contaminant transport | + | + | + | + | | + | + |
| Engineering hydrology | | + | | + | | | + |

of water in double-porous systems can be derived if the porosity of the mobile and stagnant compartment are known. Both porosities can be only obtained by performing an artificial tracer experiment. The estimation of mean transit time of water can then be made based on these data (Maloszewski and Zuber, 1985, 1991).

2.4 Fields of application

Tracer methods provide direct insight into the dynamics of water in all compartments of the hydrologic cycle. The dynamics include the processes of motion, distribution and dissemination. Tracer techniques are experimental and independent and can thereby be applied to calibrate models. The fact that tracer methods allow for measurements of process- and system-parameters turns them into an effective tool for consultancies and legal authorities.

Regarding the general fields in hydrology where tracer techniques are applicable, experience was gained in all of the components of the water cycle. The possibilities of tracer techniques are vast and comprise, among many others, the investigation of processes such as groundwater recharge, runoff generation, water and solute transport and pollution assessment. A list of important questions that can be tackled by tracer techniques is given in Table 2.3. This list represents the most important components and is not conclusive or necessarily complete.

3

Environmental Tracers

3.1 Introduction

In this chapter, the fundamentals of applying environmental tracers will be introduced. The focus will be on applications for the characterization of hydrological systems. While qualitative interpretation will be introduced, quantitative environmental tracer hydrology will be described wherever possible. The useful combination of environmental and artificial tracer applications will be highlighted.

The most common environmental tracers are the isotopes of water $^{18}\text{O}/^{16}\text{O}$, $^2\text{H}/\text{H}$ and the isotopic ratios of dissolved constituents of water such as the $^{13}\text{C}/^{12}\text{C}$ ratio of dissolved inorganic carbon or $^{15}\text{N}/^{14}\text{N}$ of dissolved nitrate. With advances in mass spectrometry and with the advent of new measurement techniques (Inductively Coupled Plasma Mass Spectrometry, ICP-MS, Tunable Diode Laser Spectrography, TDLAS) environmental isotope methods move towards smaller sample amounts and the compound specific analysis of isotopes.

In the context of tracer hydrology, we define environmental tracers as the properties or constituents of water that have not been induced as a result of an intended experiment and which provide qualitative or quantitative information about the hydrological system. Part of environmental tracers that are being used in tracer hydrology result from anthropogenic releases to the atmosphere or to the hydrological cycle: nuclear bomb Tritium (^3H), $^{85}\text{Krypton}$, CFCs and SF_6 have been released into the atmosphere as a result of military activities and technical processes – not for the purpose of providing age dating methods for hydrologists. However, these environmental tracers – although environmental concerns or ethical principles might lead us to consider their restriction – have been used and can still be used for hydrological tracer studies, age dating or origin assignment. SF_6 , as will be shown, can also be used for artificial trace experiments, when the injection is intended in relation to a defined experiment. A series of pollution tracers, nitrate, organic pollutants, or remnants of past mining activities, can provide information about hydrologic processes. Besides anthropogenic environmental tracers, there are many natural environmental tracers. These include not only stable

and radioactive natural isotopes but also chemical compounds such as noble gases and trace elements associated with specific geologic units or lithologies.

The application of environmental tracers provides methods for the investigation of some major components of hydrological systems: environmental tracers have been used in studies on precipitation processes and origin assignment, open water evaporation, transpiration and stem flow, soil water dynamics, groundwater recharge, subsurface flow mechanisms, runoff components and groundwater studies. The major applications of environmental tracers are:

- *origin assignment of water and water constituents*: more specifically the assignment of recharge altitude and recharge amount or the discrimination of summer or winter recharge, detection of origin of nitrate or dissolved inorganic carbon;
- *hydrological process studies*: identification of runoff components, subsurface flow mechanisms, direct or indirect recharge mechanisms, water balance of lakes;
- *quantitative determination of flow components*: estimation of evaporation from open water surface, hydrograph separation;
- *determination of residence times*: age dating and transit time distribution.

The application of environmental tracers is limited by the availability of analytical techniques, knowledge and capacity on tracer methods and resources such as total cost of analysis, total effort of taking samples or time for analysis. The relevance of additional, independent and unique information that can be gained from the application of environmental tracers in relation to the uncertainty associated with these methods defines whether or not environmental isotopes will be useful. Uncertainty in perceptual and conceptual models of hydrological processes and uncertainty in hydrological modelling, especially in the field of subsurface flow processes, constitute fields of hydrological research where environmental tracers provide such unique and relevant additional information.

A major advantage of environmental isotopes is that the input function or the 'injection of tracer' into the hydrological system is provided by nature. Therefore, environmental isotopes can be used on different scales for local, regional and even global studies. If past input functions can be reproduced or reconstructed from data or known physical principles, environmental tracers can also be used for paleostudies or long time scales, for example for the analysis of rainfall origin or recharge in the Holocene or for groundwater flow in drylands. Another key characteristic of environmental isotopes is that they integrate over spatial and temporal scales. A sample taken for the analysis of environmental tracers represents a mixture of flow components characterized by different boundary and flow conditions. This requires another perspective and different methods of interpretation as compared to artificial tracers. The integration of boundary and flow conditions yields complementary information for artificial tracer experiments where only one (or few) points or injection areas in space are marked at one (or few) moments in time.

Therefore, the combination of environmental and artificial tracers can improve the success rate of tracer applications in hydrology significantly. Environmental tracers can be used in the initial phase of planning an artificial tracer test. Residence times and preliminary analyses of flow components may help significantly in reducing failures of artificial tracer tests. They can be used during an artificial tracer test as an additional method. Finally, environmental tracers can be used *a priori* as a backup strategy in the case of a negative tracer test when no breakthrough is received.

3.2 Stable isotopes of water

The most common stable isotopes used in hydrological studies are the stable and radioactive isotopes of water. As pointed out by Gat and Gonfiantini (1981) the fact that oxygen was used as unit mass for chemical weight until 1961 turned the early discovery of oxygen isotopes and of their variability in natural materials (Giauque and Johnston, 1929) into a metrist's nightmare. The resulting efforts in determining the abundance of oxygen isotopes in geological material and especially in water revealed most of the common isotope phenomena being used in modern isotope hydrology. The development and improvement of mass spectrometry techniques, especially the development of the double inlet spectrometer by McKinney *et al.* (1950) and Nier (1957) provided the analytical tools for the description of the variability of isotopes in the water cycle.

3.2.1 Notation

A substance containing the less abundant isotope species N_i and the more abundant isotope N has an isotopic abundance ratio R that is defined by:

$$R = \frac{N_i}{N} \quad (3.1)$$

For natural oxygen and hydrogen compounds N is much larger than N_i . The isotope species can also be expressed in terms of mole fractions $m = N/(N + N_i)$ and $m_i = N_i/(N + N_i)$. The standard mean ocean water (short SMOW) that has been defined by the International Atomic Energy Agency (IAEA) in Vienna as a common standard for expressing isotope ratios (the so-called Vienna SMOW or V-SMOW) has isotopic abundance ratios of (Baertschi, 1976; Hageman *et al.*, 1970):

$$R_{^{18}\text{O}/^{16}\text{O}} = \left(\frac{^{18}\text{O}}{^{16}\text{O}} \right)_{\text{VSMOW}} = 2005.2 \pm 0.45 \cdot 10^{-6} \quad (3.2)$$

$$R_{\text{D}/\text{H}} = \left(\frac{^2\text{H}}{^1\text{H}} \right)_{\text{VSMOW}} = 155.76 \pm 0.05 \cdot 10^{-6}$$

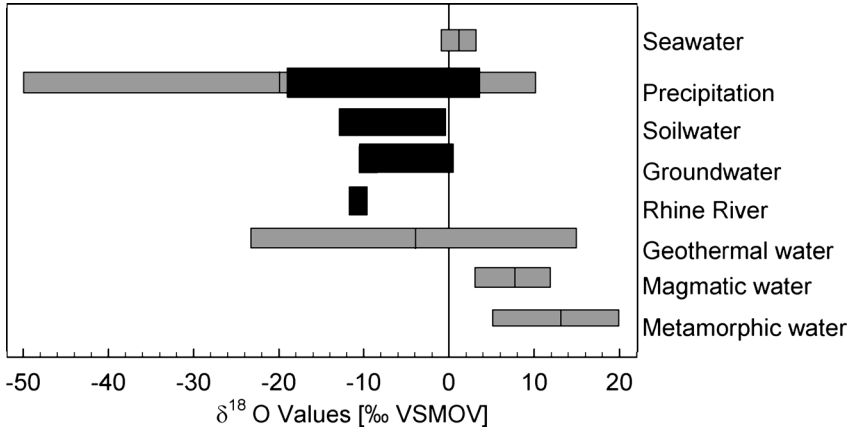


Figure 3.1 Range of isotopes in the water cycle (Königer, 2003 based on Clark and Fritz, 1997). Most common values are marked as black bars.

In general, the isotopic abundance ratio of a sample R_{sample} is given with respect to the internationally accepted standard V-SMOW with the isotopic abundance ratio R_{standard} .

$$\delta = \frac{R_{\text{sample}} - R_{\text{standard}}}{R_{\text{standard}}} \quad (3.3)$$

For water samples and many environmental isotopes it is convenient and common to multiply the $\delta^{18}\text{O}$ or $\delta^2\text{H}$ values by a factor of 1000 as ‰ difference from the standard being used. In δ notation, positive values indicate an enrichment of ^{18}O or ^2H compared to the standard being used whereas negative values signify a depletion of heavier isotopes in the sample. By definition, the ocean has a $\delta^{18}\text{O}$ value of $\approx 0\text{‰}$. The $\delta^{18}\text{O}$ of water in the hydrologic cycle ranges from about -50 and -25‰ in ice samples from cold, arctic regions to $+10\text{‰}$ in desiccating water bodies and terminal lakes in arid regions (Figure 3.1).

The precision of stable isotope measurements depends on the analytical technique, sampling and sample preparation. For $\delta^{18}\text{O}$ determined with double inlet mass spectrometry the error corresponds to about $\pm 0.1\text{‰}$, for deuterium ± 1.0 to 1.5‰ . The uncertainty is an important limit for the application of isotope techniques, which needs to be considered in mixing calculations and in origin assignments based on environmental isotopes. Tunable diode laser spectroscopy, an emerging technique for the measurement of stable isotopes, has a precision of about 0.3‰ for $\delta^{18}\text{O}$ and of about 1.0‰ for deuterium.

In order to express differences between isotopic ratios in δ notation simply, regardless of a genetic or thermodynamic link, the isotopic difference $\Delta_{A \leftrightarrow B}$ is also used, defined as $\Delta_{A \leftrightarrow B} = \delta_A - \delta_B$.

3.2.2 Fractionation

The isotopic composition changes due to fractionation processes. Fractionation occurs if – as a result of a physical or chemical process – the isotopic abundance ratio changes. Phase changes, evaporation, condensation, freezing, sublimation, melting and some chemical reactions are associated with an isotopic fractionation. In order to describe fractionation, a fractionation factor α is used, that is defined by:

$$\frac{dR}{R} = \left(\frac{dN_i}{dN} \right) / \left(\frac{N_i}{N} \right) = \alpha \quad (3.4)$$

According to a model suggested by Urey (1947), equilibrium fractionation arises from the exchange of isotopes between different phases (i.e. water and vapour) or chemical species at equilibrium conditions. For a specific reaction at full equilibrium, the degree of fractionation is then expressed by:

$$\alpha_{A \leftrightarrow B} = \frac{R_A}{R_B} \quad (3.5)$$

where R_A and R_B represent the isotopic ratios of the two phases A (water) and B (vapour). In ‰ notation also the enrichment factor $\varepsilon_{A \leftrightarrow B}$ is used. The enrichment factor is defined as:

$$\varepsilon_{A \leftrightarrow B} = \left(\frac{R_A}{R_B} - 1 \right) * 1000 = (\alpha_{A \leftrightarrow B} - 1) * 1000 \quad (3.6)$$

The approximate relation between the enrichment factor $\varepsilon_{A \leftrightarrow B}$ and the fractionation factor $\alpha_{A \leftrightarrow B}$ in the form $\varepsilon_{A \leftrightarrow B} \approx 10^3 \ln \alpha_{A \leftrightarrow B}$ only holds for small enrichment factors, because of the approximation $\ln \alpha \approx 1 - \alpha$ when $\alpha \approx 1$.

For the stable isotopes of water, ice \leftrightarrow water \leftrightarrow vapour phase transitions are of special importance. Fractionation between different phases of water results from differences in the physical properties of water molecules containing different isotopic species of oxygen and hydrogen. As an example, the water vapour pressures of the species $^1\text{H}_2^{16}\text{O}$ and $^1\text{H}_2^{18}\text{O}$ differ by about 1% at 20 °C (Szapiro and Steckel, 1967, Figure 3.2). This difference in physical properties causes a higher diffusion of $^1\text{H}_2^{16}\text{O}$ into the ambient air as compared to $^1\text{H}_2^{18}\text{O}$ during the evaporation process. Hence, there results a depletion of the heavier molecules of $^1\text{H}_2^{18}\text{O}$ in the gaseous phase.

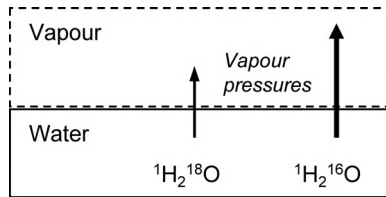


Figure 3.2 Differences in the vapour pressure for the two isotope species $^1\text{H}_2^{18}\text{O}$ and $^1\text{H}_2^{16}\text{O}$ during equilibrium exchange with water vapour.

For ^{18}O a fractionation factor of $\alpha_{\text{water} \leftrightarrow \text{vapour}}^{18}\text{O} = 1.0093$ was measured for equilibrium phase transitions between water and vapour at 25°C . The fractionation factor for ^2H during the same equilibrium phase transition is as high as $\alpha_{\text{water} \leftrightarrow \text{vapour}}^2\text{H} = 1.076$ (Majoube, 1971).

Isotope equilibrium fractionation is also a function of temperature. Szapiro and Steckel (1967) and Majoube (1971) found that the fractionation factor $\alpha_{A \leftrightarrow B}$ generally follows an equation of the type:

$$10^3 \ln \alpha_{A \leftrightarrow B} = 10^6 a/T^2 + 10^3 b/T + c \quad (3.7)$$

where T is the ambient water temperature in K and a , b , c are coefficients. Tabulated values for a , b and c for the most common thermodynamic reactions in hydrogeological systems are given in Clark and Fritz (1997). They also give data on their homepage at www.science.uottawa.ca/eih. More than 1100 fractionation equations are described at the site of the Department of Geology of the University Laval/Quebec in Canada (<http://www.ggl.ulaval.ca/cgi-bin/isotope/generisotope.cgi>).

For water \leftrightarrow vapour equilibrium exchange, the fractionation is higher at low than at high temperatures. The equilibrium fractionation as a function of temperature is shown in Figure 3.3. This dependence is the dominant process in many hydrological systems and contributes – together with other processes – to a series of macroscale effects described below such as the latitude effect, the altitude effect, the continental effect, the amount effect and the seasonal effect.

Often, the assumption of isotopic equilibrium is not met and so-called kinetic fractionation processes take place. This may be caused by rapid temperature changes or the removal or addition of the product or reactant during the reaction. Major nonequilibrium processes in hydrological systems are ‘diffusive fractionation’ and ‘Rayleigh distillation’.

Diffusive fractionation is the fractionation of isotopes caused by diffusion processes. In hydrological systems diffusive fractionation occurs, for example during the

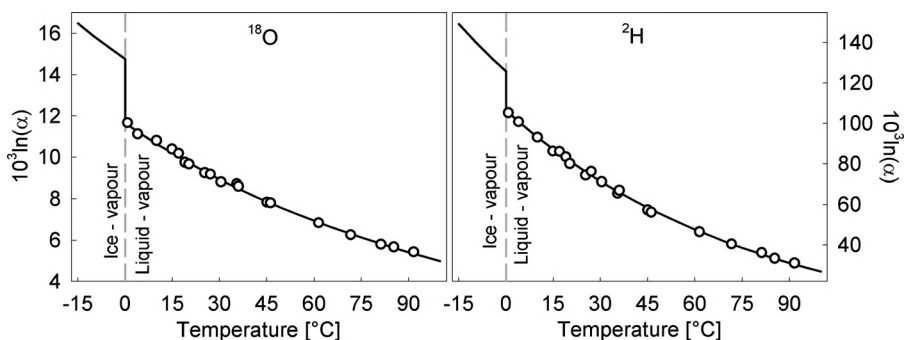


Figure 3.3 Temperature dependence of equilibrium fractionation, at 0°C the equilibrium is established for the ice-water phase assemblage (dashed line), causing a step in the temperature-equilibrium function (data are from Majoube, 1971).

evaporation process when water vapour diffuses into air. Diffusive fractionation results from the different molecular velocities of different isotopes. The molecular velocity depends on temperature (usually given in Kelvin) and on the mass of the atom or molecule according to statistical particle mechanics:

$$v = \sqrt{k * T / (2 * \pi * m)} \text{ [m/s]} \quad (3.8)$$

with the Boltzmann constant $k = 1.3806504 \cdot 10^{-23}$ J/K, the absolute temperature T in Kelvin, and the molar mass m in kg. As the unit of Joule corresponds to $[\text{kg} \cdot \text{m}^2 \cdot \text{s}^{-2}]$ with $m = \text{metres}$ and $s = \text{seconds}$ in SI units the resulting unit is $[\text{m/s}]$. From this equation, the diffusion of two isotopes of different masses in vacuum can be derived. From the molecular velocity of isotopes it can be shown that the diffusion rates for an ideal gas in a *vacuum* are just inversely proportional to the square root of the mass of its particles – the other constants and also temperature cancel out:

$$\alpha_{\text{diffusion (A-B)}} = \sqrt{\frac{m_B}{m_A}} \quad (3.9)$$

where m_A and m_B are the respective molecular weights of different substances. If this principle, known as Graham's Law of Effusion, is applied to dry air, the molecular mass of dry air needs to be taken into account. The molecular mass of dry air can be derived from the average gas composition and the molecular weights of its constituents and corresponds to about 28.8 g/mol (see also Clark and Fritz, 1997):

$$\alpha_{\text{diffusion air (A-B)}} = \sqrt{\frac{m_B * (m_A + 28.8)}{m_A * (m_B + 28.8)}} \quad (3.10)$$

The resulting fractionation factors can be derived and transformed into an isotope difference using Equation (3.6). The kinetic effect by diffusion $\varepsilon_{A \leftrightarrow B} = (\alpha_{A \leftrightarrow B} - 1)$ is 32.3‰ for $\text{H}_2^{18}\text{O}/\text{H}_2^{16}\text{O}$ and 16.6‰ for $^2\text{H}_2\text{O}/^1\text{H}_2\text{O}$. Hence, the fractionation by diffusion is stronger for oxygen isotopes than for deuterium isotopes. The above equation holds for dry air with a humidity of 0% only.

As we deal with real hydrological systems we need to include the effect of atmospheric humidity and turbulence. In a series of laboratory and field experiments the process of evaporation from an open water surface into an atmosphere with a relative humidity h in % has been studied. Gat (1970), Merlivat (1978) and Vogt (1976) report empirical values between 13 and 28.5‰ for $\text{H}_2^{18}\text{O}/\text{H}_2^{16}\text{O}$. In general isotopic differences resulting from kinetic fractionation in natural and turbulent systems are much smaller compared to diffusive fractionation only. Empirical values reported by Gonfiantini (1986) are commonly used stating that the kinetic fractionation factor given in ‰ is in proportion to $(1 - h)$ with $h = \text{relative humidity}$:

$$\Delta \varepsilon_{18\text{O}} = 14.2 * (1 - h) [\text{‰}] \quad (3.11)$$

$$\Delta \varepsilon_{2\text{H}} = 12.5 * (1 - h) [\text{‰}]$$

For deuterium also the theoretical approach yields a kinetic fractionation that is higher than for diffusion (16.6 to 12.5‰). Apparently for real and turbulent systems the ratio of diffusion coefficients scales to $(D_A/D_B)^n$ with a turbulence parameter n for which $0 \geq n \leq 1$. Many experimental data fit with $n = 0.5$ corresponding to the square-root of the diffusion coefficients $\sqrt{D_A/D_B}$.

As evaporation in real hydrologic systems differs from a pure diffusion process, it makes sense to define a kinetic fractionation by turbulent diffusion. While a water-vapour assemblage in a closed system would simply equilibrate according to Equation (3.11), in open systems there is an additional kinetic fractionation. For this process, resistance is in inverse proportion to the diffusion coefficients D_A and D_B or $\pi_i \sim 1/D_i$. Based on the concept of resistance controlling the flux of isotopes, it is stated that:

$$\varepsilon_{kinetic} (water - vapour) = (1 - h)^* \left(\frac{\rho_i}{\rho} - 1 \right) \quad (3.12)$$

It follows that the slope of an evaporation line depends on the humidity during evaporation. At high humidity (>85%) the slope is steeper approaching that of the meteoric water line and at low humidity the slope is dropping. In arid regions slopes of less than five can be observed.

The processes above are simplified and idealized representations of processes occurring in nature. Craig, Gordon and Horibe (1963) introduced the concept that evaporation results from a combination of several interconnected processes as summarized in Figure 3.4.

They propose that above an open water surface equilibrium fractionation takes place in a thin liquid-vapour interface layer that is vapour-saturated. The isotopic composition in this interface layer depends initially on temperature dependent equilibrium fractionation and on the initial isotopic composition of the liquid phase. In a second step vapour diffuses from this saturated interface layer. This process can be approximated by molecular diffusion, as described above. The diffusion process depends on the humidity in the diffusion layer and on the mass ratio of isotopes. The vapour finally enters the turbulent mixing zone of the atmospheric boundary layer and is mixed with the advected vapour of a given isotopic composition. In the turbulent boundary layer

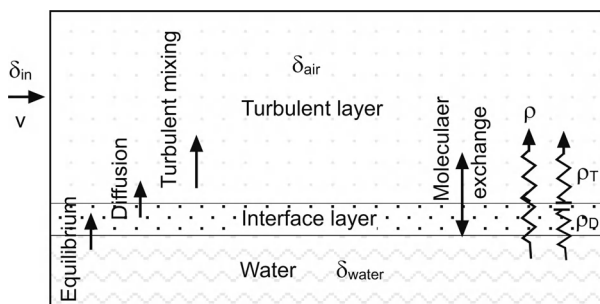


Figure 3.4 The concept of water-atmosphere exchange as a process in four steps: equilibrium-diffusion-mixing and re-equilibration.

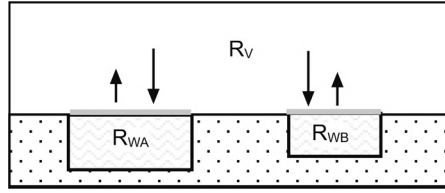


Figure 3.5 The exchange of isotope concentrations between two reservoirs by gas diffusion in a closed system.

no fractionation is assumed to take place. The mixed vapour then partially re-enters the diffusion layer and may re-precipitate at the surface of the liquid layer causing a molecular exchange. This equilibration may even result in an isotopic exchange between two fluid reservoirs that are connected with a common atmosphere in a closed system (Ingraham and Criss, 1993, Figure 3.5).

The advantage of this concept is that it allows a step-wise description of processes – the disadvantage is that the resulting integration of these processes is becoming quite complex:

$$E = (c_{liquid} - c_{air})^* \frac{1}{\rho} \quad \text{with} \quad h = \frac{c_{air}}{c_{liquid}} \quad \text{relative humidity} \quad (3.13)$$

$$E = (c_{liquid} - h^* c_{liquid})^* \frac{1}{\rho} = c_{liquid}^* (1 - h)^* \frac{1}{\rho}$$

where E is evaporation, h is the relative humidity and c_{liquid} the absolute moisture or vapour pressure above the open water surface, c_{air} the absolute moisture or vapour pressure in the atmospheric boundary layer and ρ the resistance coefficient for the flux of moisture. This equation is similar to turbulent diffusion equations widely used in meteorology for boundary layer physics. At this stage the isotopic ratios R , R_{liquid} and R_{air} can be introduced:

$$E = c_{liquid}^* \left(\frac{R}{\alpha} - h^* R_{air} \right)^* \frac{1}{\rho_i} \quad (3.14)$$

with ρ_i the specific resistant coefficient for an isotope. Gonfiantini (1986) discusses different aspects of this equation, notably the case in which the isotopic composition in the water column is not homogeneous. In a stratified lake c_{liquid} corresponds to the epilimnion. In the case of the uppermost part of the water column the isotopic composition is different. An additional resistance term needs to be specified because of incomplete mixing – however, in general this is not considered necessary.

Another important kinetic fractionation process is the Rayleigh distillation. It can be used to describe systems where the reactant is continuously being removed by, for example, rain-out from clouds or evaporation. The distillation equation states that the isotopic ratio R is a function of the initial ratio R_o , the fraction of water remaining in the reservoir f and the fractionation factor:

$$R = R_o f^{(\alpha-1)} \quad (3.15)$$

For Rayleigh distillation processes, the fractionation increases strongly when the residual water fraction approaches small values. The Rayleigh formula was developed for distillation processes. It is obtained from the differential equation relating the fractionation factor to the mass change. However, it is only valid if the fractionation factor is constant or can be approximated by a constant value. For condensation processes that cause altitude effects, the differential equation should be used and integrated with a variable temperature.

3.2.3 The global distribution in rainfall

A review of time series from a global survey of stable isotopes in rainfall (Rozanski, Araguás-Araguás and Gonfiantini, 1993) reveals patterns in their seasonal and geographic distribution. These patterns are the result of the fractionation processes described above that take place in the hydrologic cycle. The so called ‘*isotope effects*’ are the basis for the interpretation of isotope data in hydrogeological studies. Craig (1961) found that, at a global scale, $\delta^{18}\text{O}$ and $\delta^2\text{H}$ in surface waters are characterized by the correlation $\delta^2\text{H} = 8\delta^{18}\text{O} + 10\text{‰}$ (this equation was established for the SMOW reference, Standard Mean Ocean Water). The equation defines the *global meteoric water line*. The isotopic composition of precipitation in humid regions corresponds to this relationship for most continental stations (Figure 3.6).

At a regional scale deviations from this global correlation exist and specific regional meteoric water lines have been introduced, for example for the Mediterranean or some coastal regions. Meanwhile, a slightly modified relationship based on the data of the IAEA global network of isotopes in precipitation (GNIP) has been proposed by Rozanski, Araguás-Araguás and Gonfiantini (1993). This revised regression has a slope of $8.17 \pm 0.07\text{‰}$ and an intercept of $11.27 \pm 0.65\text{‰}$. It takes into account rainfall data from the IAEA only and is based on the VSMOW standard. In some cases, it is necessary to use other regional meteoric water lines or to define a local meteoric water line. However, this should be done only based on a regional analysis as local meteoric

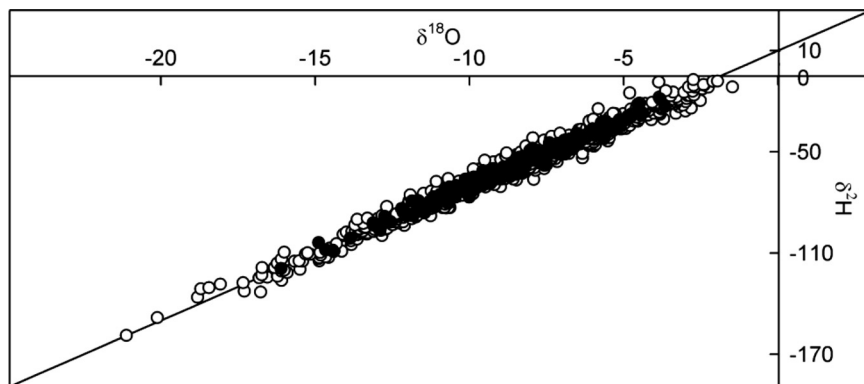


Figure 3.6 Isotopes in rainfall as such (open circles) and weighted with rainfall amount (full circles) for the Dreisam catchment, Germany (1998–2008).

water lines might be influenced by deficiencies of the sampling network or procedures and be therefore more misleading than an advantage. Especially in islands, coastal areas or tropical mountain areas, rainfall might deviate from the global meteoric water line.

3.2.3.1 Temperature effect

Fractionation factors depend on temperature. During water \leftrightarrow vapour phase transitions fractionation is more pronounced at low temperatures. As a result, the isotopic composition of rainfall in cold environments is more depleted compared to warm environments.

In Figure 3.7 the dependence between mean $\delta^{18}\text{O}$ values and mean annual temperature has been plotted for different regions. These dependencies exist for ^{18}O and for ^2H . Combining both, a general thermometer can be developed. The stable isotope thermometer reflects the ambient temperature of different sites (see the examples of Alaska, Switzerland, Greece, Namibia and Argentina). It can be used directly to estimate the temperature from stable isotope values. Dansgaard (1964) derived temperature effects of precipitation based on a theoretical treatment of cooling processes

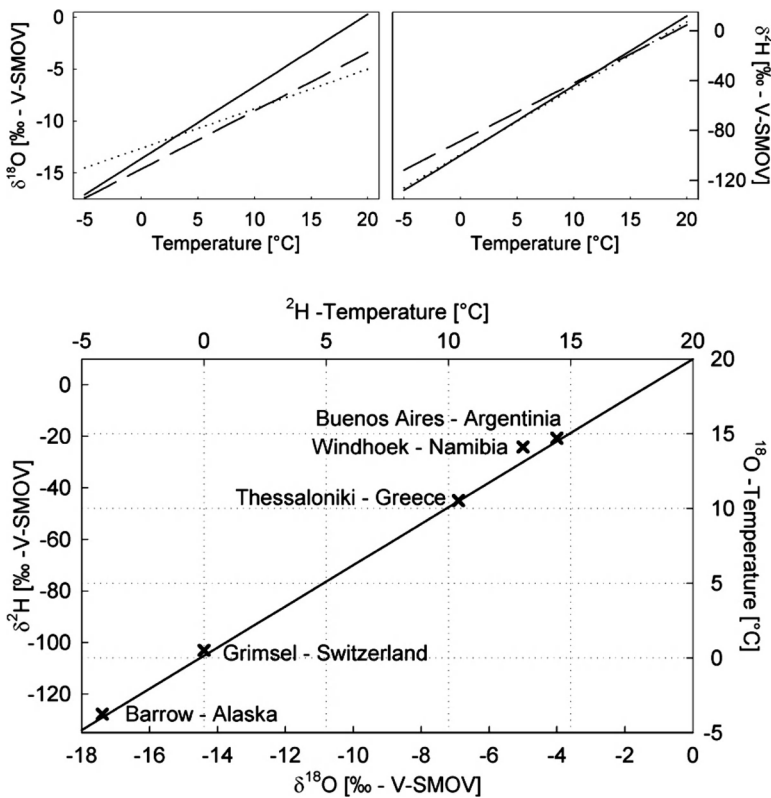


Figure 3.7 Upper graph: different observed regional temperature effects. Lower graph: The influence of mean annual temperature on the isotopic composition of ^{18}O and ^2H , Dansgaard (1961, 2004). Crosses mark values at -5 , 0 , 10 and 15 °C mean annual temperature.

at different boundary conditions (isobaric, isothermal). Based on measurements an isotope thermometer of about:

$$\delta^{18}\text{O} = -0.69 t_a - 13.6 \text{‰} \quad (3.16)$$

is given, where t_a is the mean annual air temperature in °C. For temperatures below 0 °C the temperature effect increases to about 0.95‰/°C at −20 °C. A major part of the temperature effect can be derived from the dependence of the fractionation factor on temperature and from the fractional distillation of water by cooling processes.

3.2.3.2 Seasonal effect

Often a seasonal fluctuation of stable isotope ratios is observed as a result of temperature effects, different trajectories of air masses and varying fractionation processes in the source area of atmospheric moisture.

The seasonal effect can be used and is important for input functions to the hydrological system. In general, the seasonal isotope effect of continental stations closely follows the temperature regime. In coastal areas, the seasonal effect is less pronounced. This is shown in Figure 3.8 (top) for the station Cuxhaven. Based on known principles of

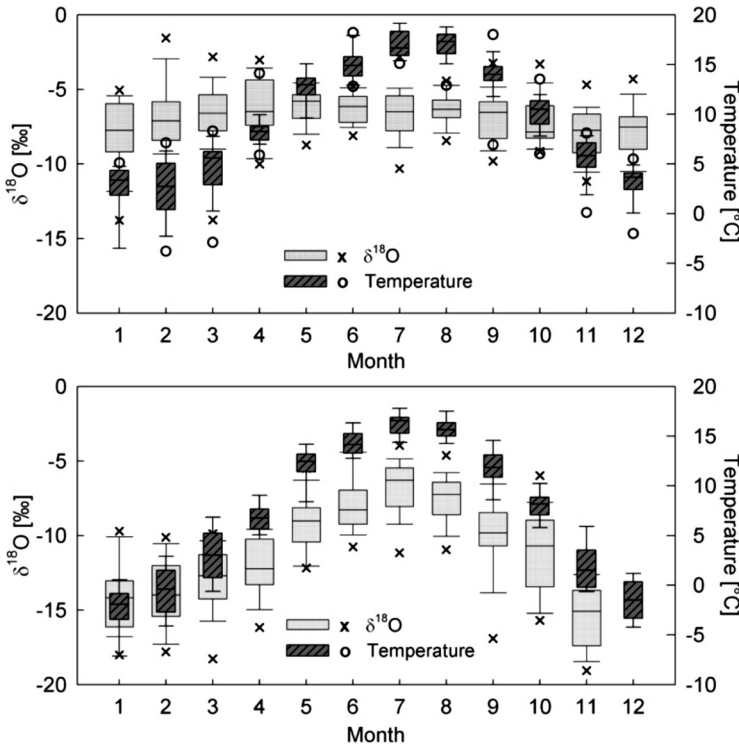


Figure 3.8 Box plots of seasonal effects – data isotopes in rainfall of Germany (Cuxhaven (top) – Garmisch (bottom): 1978–2002; Temperature in °C: 1984–2002).

fractionation and a conceptual model of the hydrological cycle there are several factors producing a seasonal effect:

- the temperature in the source region of atmospheric moisture will change the fractionation during evaporation,
- circulation of air masses and transport processes will cause advection of moisture from different origins and modify the original isotopic composition of moisture,
- and finally, the conditions during rainout (ambient temperature, absolute moisture and phases (snow, rain) will change.

If the seasonal variation of isotopes in precipitation is known, observations at different soil depths, in runoff and in groundwater time series can reveal the travel time and mean residence time of the system (see below).

3.2.3.3 Altitude effect

In general, precipitation is depleted increasingly at higher altitude. This is the combined result of temperature effect and moisture depletion by adiabatic cooling. Equilibrium fractionation increases with lower temperatures, making fractionation more efficient at higher altitudes. Repeated rainout during uplift of air masses causes a Rayleigh-type distillation process.

Altitude effects are often given only for annual mean rainfall. It also exists within different seasons (see Figure 3.9). The example of Cyprus shows that the variability of

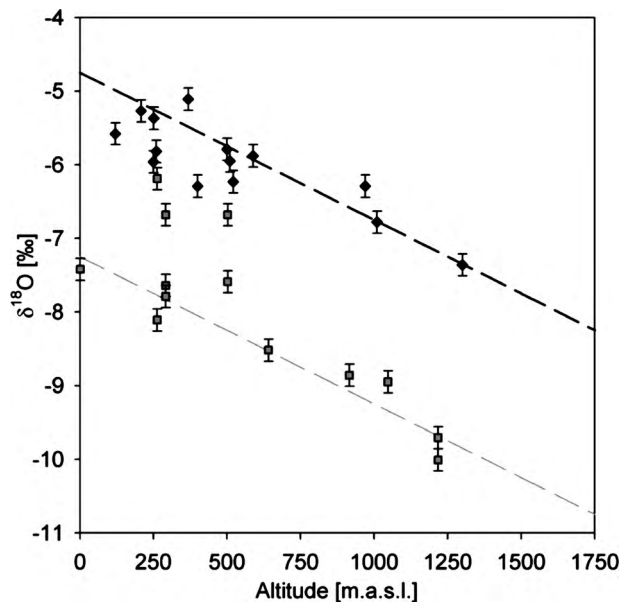


Figure 3.9 Altitude effect of winter (grey) and summer (black) precipitation (data from Cyprus).

rainfall is higher close to the coast, with increasing distance from the coast and therefore increasing altitude specific altitude effects develop in summer and in winter time.

A number of observed altitude effects exist. For $\delta^{18}\text{O}$ the range of observed altitude effects is between -0.1‰ and $-0.36\text{‰}/100\text{ m}$. Dansgaard (1964) presents a theoretical calculation of altitude effects and demonstrated that the altitude effect can be derived from the adiabatic cooling rate of air temperature in a straightforward way: the theoretical gradient is about $-0.36\text{‰}/100\text{ m}$ for $\delta^{18}\text{O}$. As Gat, Mook and Meijer (2000) point out, the altitude effect differs from the latitudinal effect because the decreasing pressure requires a higher temperature decrease to reach saturated water vapour pressure. As a result the change in moisture per change in temperature ($^{\circ}\text{C}$) is smaller than for isobaric condensation.

In some cases other factors also affect the composition of precipitation at different altitudes: different precipitation generation processes or mixing of air masses with different trajectories. Therefore, altitude effects need to be verified in each region in order to take into account these additional effects.

In remote areas especially the altitude effect is a key to hydrological studies. Recharge altitude, origin of water and conceptual models can be validated based on known altitude effects. The problem is that often data on local altitude effects are not available. Data from the IAEA GNIP network can be retrieved and used for a regional analysis with similar atmospheric circulation patterns. However, in many parts of the world, the network is not dense enough. Experimental isotope networks can be set up to provide such data. But these require at least a few years of measurement campaigns. There are two principle approaches to overcoming such problems. In principle, the altitude effect can be derived from a physical model of condensation and rainfall generation.

If the physics of water condensation and fractionation are taken into account, the relationship above between adiabatic cooling rate and isotopic composition can be derived. The adiabatic cooling rate can be retrieved from climatological network data. However, this estimate may be biased by specific local conditions and should be verified by an experimental approach.

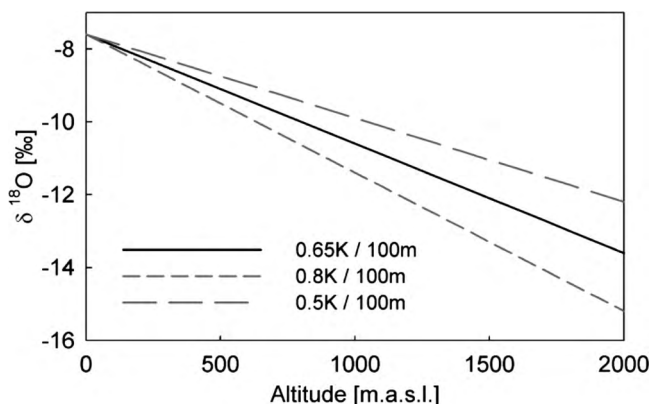


Figure 3.10 Altitude effect for different adiabatic cooling gradients.

A field method for verifying altitude effects consists of sampling shallow groundwater from very small watersheds with sufficiently long mean residence times to provide an average value of mean annual rainfall (>2 years) and sufficiently short flow distance from the recharge area to represent the conditions at the altitude of sampling. This practical approach uses the hydrological system as a natural integrator of rainfall samples. Based on a terrain analysis small catchments can be selected that represent an altitude range. Close to the watershed groundwater can be sampled from springs or shallow groundwater boreholes. These samples can be used to reconstruct the altitude effect. This altitude effect does not correspond to the weighted rainfall – it represents the weighted groundwater recharge. This, however, can be exactly what is needed for an origin assignment of groundwater recharge. Vogel, Lerman and Mook (1975) have adopted this approach to characterize the altitude effect of the Andes mountains. Together with modern GIS techniques this approach can be used to preselect sampling locations based on terrain analysis and an available borehole database.

It is interesting to note that the altitude effect and the analytic precision determine the accuracy of any determination of recharge altitude. In general, we assume $\pm 0.1\text{‰}$ for $\delta^{18}\text{O}$ and $\pm 1.0\text{‰}$ for $\delta^2\text{H}$. Therefore it is unrealistic to resolve the recharge altitude within less than the isotope altitude gradient divided by at least two times the analytical precision. Best results are obtained in mountain areas with distinct differences in recharge altitude well exceeding this uncertainty.

3.2.3.4 Continental effect

For large trajectories of air masses precipitation becomes more depleted with increasing distance from the coast. Since the vapour is mainly derived from oceans, water in clouds will become depleted in heavier isotopes with each rainfall event along the trajectory. This phenomenon is termed continental effect. Continental effects are relevant for characterizing the isotopic composition at continental or global scale.

The continental effect is caused by the gradual depletion of air masses by precipitation as they cross continents or move towards the interior of continents. Each condensation and precipitation event at a given temperature causes a fractionation. The accumulation of these effects leads finally to an isotopic depletion of air masses as they move from their source areas. This effect is reduced by transpiration and re-evaporation on the continent. As such the process can be modelled and quantified. Holtkamp (2008) developed a hydrological model of continental isotope effects:

$$R = R_o f^{(\alpha-1)} \quad \text{with} \quad f = \frac{Q_a - \int (P(\tau) dt + \int E(\tau) dt}{Q_a} \quad (3.17)$$

with R and R_o isotope ratios, f remaining fraction of water and α a temperature dependent fractionation factor. The fraction f is derived from a hydrological balance involving the inflow of moisture from the ocean Q_a and the hydrological balance $P(\tau) - E(\tau)$ that are here given as a function of trajectory length τ .

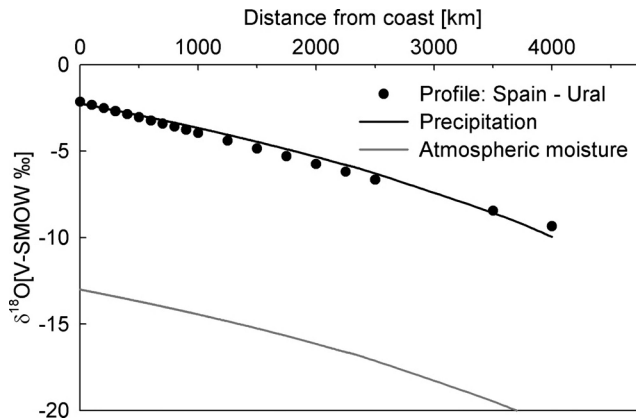


Figure 3.11 Continental effect for Europe modelled with a hydrological Rayleigh process.

The hydrological model of continental effects can be used to describe continental effects based on rainfall, evaporation (rainfall recycling), wind speed and moisture content (determining Q_a). It can be shown that the continental effect increases with rainfall amount and decreases with recycling of air masses by evaporation. Increased moisture flux (higher wind speed, absolute moisture) will reduce continental effects. Continental effects can be modelled as a result of these factors for different climatic conditions.

Different attempts have been made to integrate all atmospheric isotope effects into a general model. Dansgaard (1964) developed a conceptual model for isotopes in precipitation based on the assumption that the vapour mass moves from the oceanic origin to the condensation site without further mixing. Thus the isotopic composition of vapour and rain depends mainly on equilibrium fractionation and the fraction of vapour lost by the rainout process due to the temperature gradient between the source region and the precipitation site. This can be modelled by the Rayleigh distillation equation, which has been improved by incorporating the kinetic fractionation during evaporation from the ocean (Merlivat and Jouzel, 1979) or during the formation of ice crystals (Jouzel and Merlivat, 1984). Although these models predict high-latitude isotope – temperature dependence realistically, they are not able to describe the mixing of different air masses, the influence of evapotranspiration over continental surfaces or convective cloud processes (Sturm *et al.*, 2005).

While the isothermal Rayleigh fractionation formula is often used, adiabatic cooling in fact represents a nonisothermal process. This can be described by applying the differential form:

$$\frac{dR}{dN} = \frac{R}{N} (\alpha(T) - 1) \quad (3.18)$$

where R is the isotopic ratio of the stable isotope species, N the total mass and $\alpha(T)$ a temperature dependent fractionation factor. The difference between the integrated

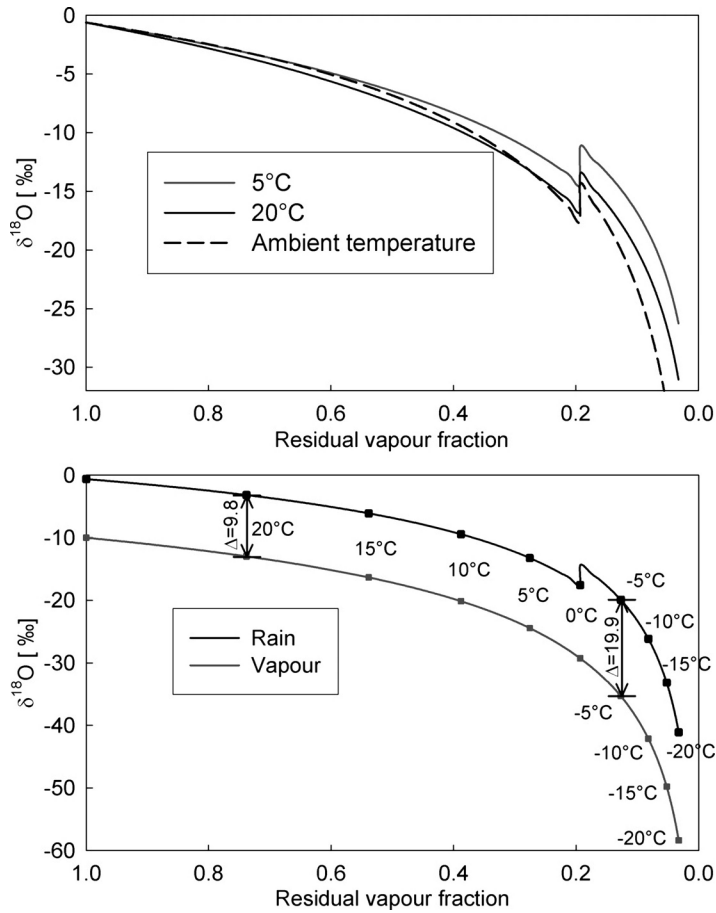


Figure 3.12 Isothermal and nonisothermal Rayleigh fractionation and resulting isotopic composition of vapour and rain.

and the differential equation is shown in Figure 3.12. For higher temperatures and fractions $f > 0.5$ the difference is small. For low temperatures and small fractions the difference increases and becomes relevant.

3.2.3.5 Regionalization of isotopes in rainfall

Regionalization of isotopes in rainfall is being used to define input functions for temporal and spatial distributions. Regional maps are very useful for origin assignment of water and for macroscale modelling of hydrological response by isotopes. Yurtsever and Gat (1981) found regional relationships between mean isotopic composition of precipitation and geographical and climatological parameters by performing multiple linear regression analyses on the GNIP database. Beginning the regressions with the parameters precipitation, latitude, altitude and temperature and then eliminating them one by

one, they found out that the use of precipitation, latitude and altitude besides temperature did not lead to a considerably better correlation between observed and predicted monthly mean ^{18}O values (for simple and for amount-weighted means). Temperature is the main parameter of importance. In a joint IAEA – University of Waterloo project Birks *et al.* (2002) re-evaluated and reconstructed GNIP station-based data to produce global and regional maps of the amount-weighted annual and monthly mean ^{18}O and ^2H values of precipitation. Bowen and Wilkinson (2002) empirically modelled relationships between amount-weighted annual mean ^{18}O values of modern precipitation and latitude and altitude using the third release of the GNIP database (IAEA/WMO, 2006). As the isotopic composition of precipitation is controlled by Rayleigh distillation, which in turn mainly depends on temperature, Bowen and Wilkinson (2002) argue that one has to include the geographic parameters that control temperature, that is latitude and altitude.

Looking at the spatial distribution of the residuals between observed and calculated values Bowen and Wilkinson (2002) concluded that the ^{18}O values of precipitation depend primarily on latitude and altitude dependent temperature variations. An example of regionalization of isotopes in rainfall is given in Figure 3.13 for Germany (see also colour plate section, Plate 1). The scale represents light (white) and heavy (dark) signature changing with time and in space. The precision of the map is $\pm 0.4\text{‰}$.

3.2.3.6 Evaporation

Evaporation from surface water causes an enrichment in the remaining water with a slope that is smaller than the slope of the meteoric water line in the $\delta^{18}\text{O}$ – $\delta^2\text{H}$ diagram. Typically, evaporation slopes are between 4 and 5.5.

Fractionation by evaporation from open surface water is obviously a key process in the generation of atmospheric moisture above the oceans. It is also known to characterize the isotopic composition of lakes and of temporary ponding of water in small surface depressions (Dody *et al.*, 1995).

For evaporation from open surface water, the slope depends on the atmospheric conditions during evaporation (Gonfiantini, 1986). In general, the slope of values in a $\delta^{18}\text{O}$ – $\delta^2\text{H}$ diagram increases with increasing humidity and decreases with lower humidity. Figure 3.14 shows evaporated water samples deviating from the global meteoric water line. While isotope data from different aquifers are often diffuse (top), samples characterized by similar meteorological conditions and stemming from the same source of water provide a characteristic evaporation line (Figure 3.14, bottom).

A characteristic evaporative enrichment of groundwater below dunes was found in arid and semiarid climate (Dinçer, al-Mugrin and Zimmermann, 1974; Allison, Stone and Hughes, 1985). The observed enrichment, with a small slope of about two in a $\delta^{18}\text{O}$ – $\delta^2\text{H}$ diagram, is seen as a result of vapour diffusion from soil moisture prior to recharge. Evaporation can remove moisture from a soil column by diffusion. Diffusive evaporation from a soil column results in a low-slope evaporation line in a $\delta^{18}\text{O}$ – $\delta^2\text{H}$ diagram (Dinçer, al-Mugrin and Zimmermann, 1974; Allison, Stone and Hughes, 1985; Gat, 1995).

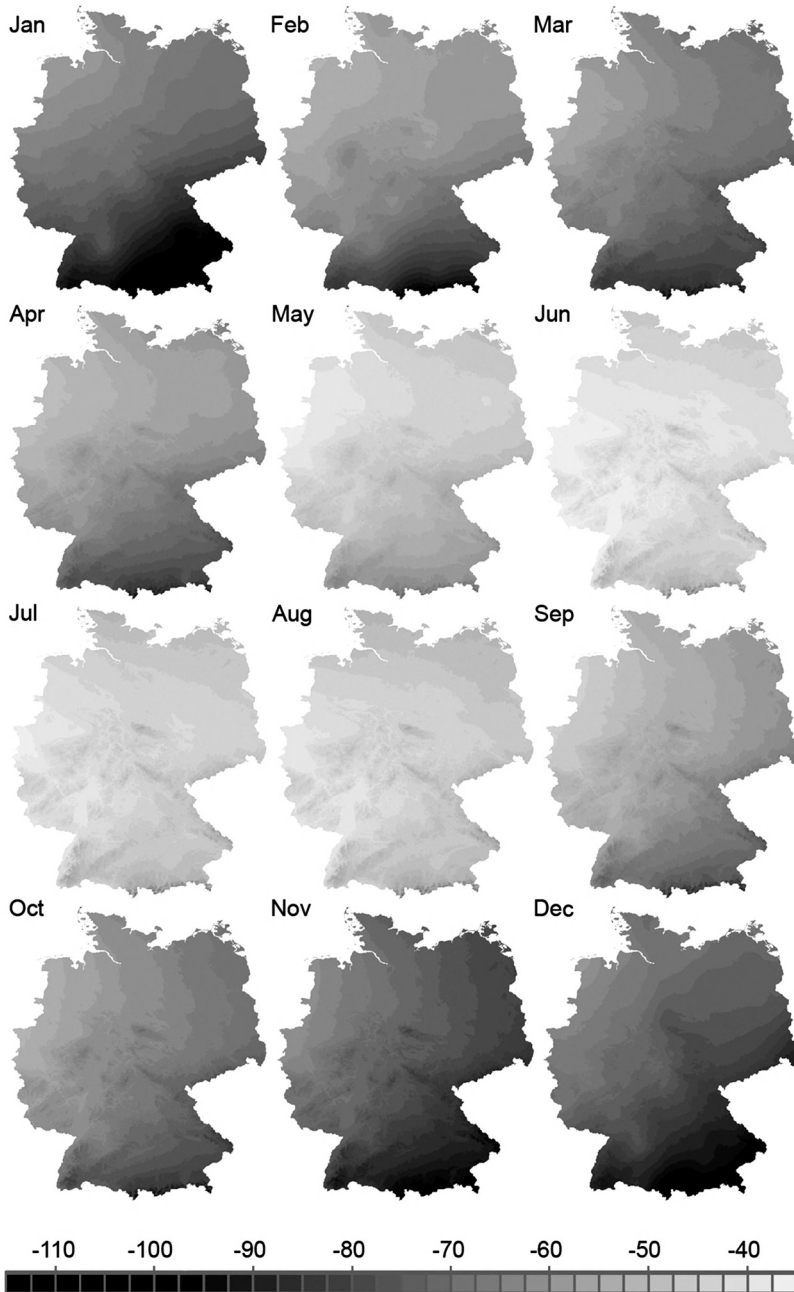


Figure 3.13 Map of the mean monthly composition of stable isotopes in rainfall in Germany ($\delta^2\text{H}$ V-SMOW in ‰) derived by regression from monthly data of 17 IAEA stations (Global Network of Isotopes in Precipitation), showing latitude, seasonal and altitude effects (modified after Schlotter, 2007). See also colour plate section, Plate 1.

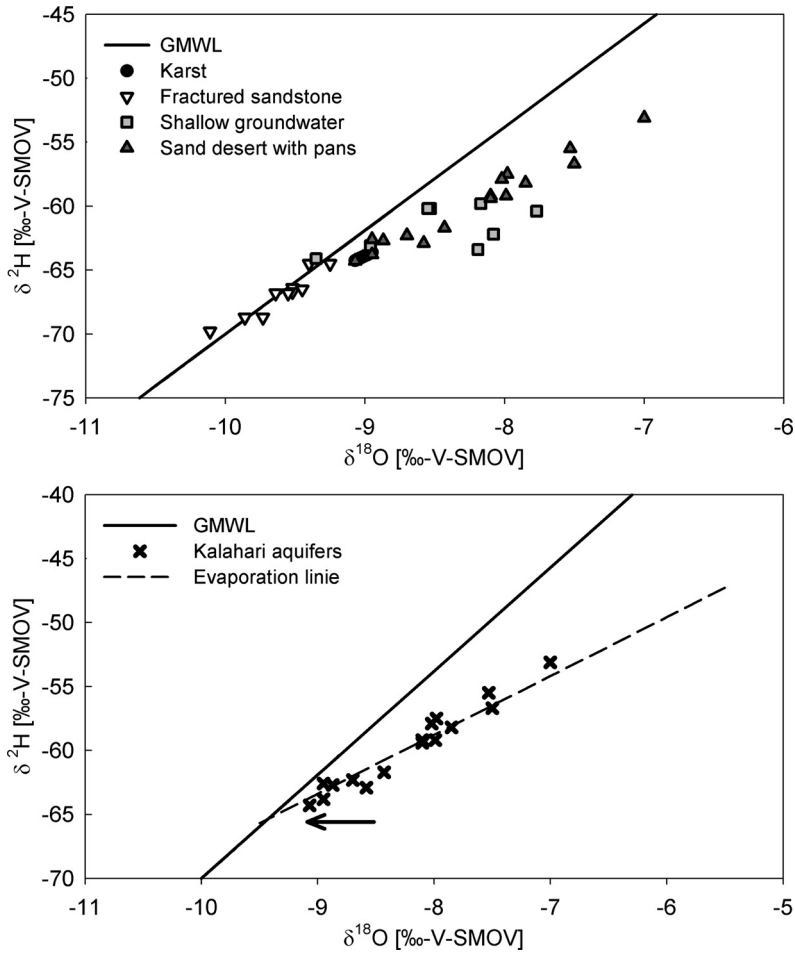


Figure 3.14 $\delta^{18}\text{O}$ – $\delta^2\text{H}$ diagrams of groundwater samples from the Kalahari. The continuous line represents the Global Meteoric Water Line, the dashed line the evaporation line fitted by linear regression. The arrow indicates the original isotopic composition of rainfall without evaporation.

A correction of $\delta^{18}\text{O}$ for evaporative enrichment according to Geyh and Ploethner (1997) can be applied. Corrected values indicate the isotopic composition without enrichment by evaporation. As the corrected value marks the intersection of the evaporation line with the Global Meteoric Water Line, it is defined by:

$$\delta^{18}\text{O}_{\text{corrected}} = \frac{\delta^2\text{H}_{\text{measured}} - e^* \delta^{18}\text{O}_{\text{measured}} - d}{8 - e} \quad (3.19)$$

where e corresponds to the slope of the evaporation line determined, for example, as 4.5, and d is the deuterium excess of global precipitation, with $d = +10\text{‰}$. Once the $\delta^{18}\text{O}$ has been corrected for evaporation, the corresponding deuterium value can be obtained by solving the equation for the global meteoric water line. This method is

extremely useful in studying flow paths of surface and groundwater that have been affected by evaporation. Once the evaporation effect has been corrected for, it can be analysed whether the original water type is prevailing or whether mixing with another source of water (resulting in different $\delta^{18}\text{O}$ values) takes place.

It is important to note that only conditions where (a) kinetic fractionation takes place and where (b) a reservoir is partially depleted result in evaporation effects. If a high number of small depressions are completely evaporated, no isotope effect results. Therefore complete evaporation from interception storage (leaves) leaves hardly any isotope signal. However, if small storages evaporate partially, significant isotope effects result. Detailed sequential sampling of rainstorms in the arid Negev Desert, Israel, revealed strong isotopic variations (-2‰ to -9‰ $\delta^{18}\text{O}$) between different rain spells within hours. Interestingly, a rain spell with low intensity but long duration was more depleted than preceding and following short, intensive spells (Dody *et al.*, 1995; Adar *et al.*, 1998). These data indicate, that partial depletion of water in surface depressions and subsequent flushing may result in high evaporative enrichment because this is a Rayleigh type process.

The evaporation of water from lakes can be estimated from water and isotope mass balances. Water and isotope mass balances have been used based on tritium data (Gat, 1970) and recently for water balances of large river systems (Königer *et al.*, 2008). The water balance of a lake is:

$$\frac{dV}{dt} = Q_{in} + P - Q_{out} - E \quad (3.20)$$

where V is the volume of the lake, Q_{in} and Q_{out} are in- and outflow, P precipitation and E evaporation. The general water and isotope balance approach is given by the equation below. Additional terms can be added for different types of inflow (surface, groundwater). The balance equation writes:

$$\frac{d(V^*\delta_V)}{dt} = Q_{in}^*\delta_{Q_{in}} + P^*\delta_P - Q_{out}^*\delta_{Q_{out}} - E^*\delta_E \quad (3.21)$$

where δ_i represent the respective isotopic composition of the hydrological component identified by the subscript i . Difficulties arise from the fact, that the lake volume is not fully mixed. The isotopic composition of the lake can be determined by adequate sampling. The isotopic composition of rainfall, inflow and outflow need to be determined in the field. The major difficulty is the determination of δ_E which depends on transport processes through the boundary layer and on atmospheric conditions such as wind speed and relative humidity. Different approaches were presented to use the balance equation for the estimation of evaporation flux and for lake water balances (Gat and Gonfiantini, 1981; Mook, 2001).

For well-mixed steady state systems Gibson *et al.* (1993) proposed an estimation based on a two-component mixing approach according to:

$$\frac{E}{P} = \frac{(\delta_P - \delta_V)}{(\delta_E - \delta_V)} \quad (3.22)$$

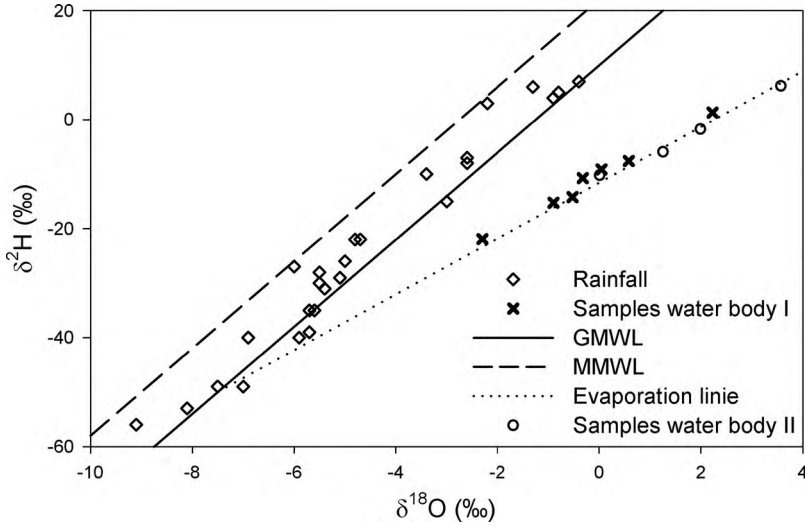


Figure 3.15 Evaporation from open surface water, example from Pantanal wetland/Brazil with local rainfall (squares), and two water bodies with different degrees of evaporation (modified from Schwerdtfeger, 2009).

where the subscripts P , V and E represent the mean weighted local isotopic composition of precipitation, lake water and evaporating moisture. While the isotopic composition of lake water and precipitation can be obtained by sampling, the isotopic composition of evaporating moisture needs to be determined by field experiments, for example with evaporation pan experiments or through calibration for lakes with known water balance or based on theoretical relationships. This approach works only for steady-state systems as long as evaporation does not affect the lake volume significantly.

If evaporation reduces the lake volume, the Rayleigh equation can be applied to estimate the evaporated volume for progressive evaporation in a simplified way based on:

$$\frac{E}{V} = 1 - \exp \frac{(\delta_V - \delta_i)}{\frac{1}{\alpha} - 1} \quad (3.23)$$

where δ_V is the isotopic composition of the well-mixed water body after evaporation E took place, δ_i the initial isotopic composition and α the fractionation factor. This approach only holds for idealized small and well-mixed water bodies (ephemeral pans with depths < 1 m) and does not take into account the exchange with atmospheric vapour.

A more accurate estimation of evaporation flux needs to take into account the fractionation processes between surface water, atmospheric moisture and the boundary layer forming between them. If the relative humidity is 100% an equilibrium between the liquid and the vapour phase will be established. This equilibrium fractionation depends

only on temperature and has been described above. Craig and Gordon (1965) have developed the principles of the conceptual model of isotopic exchange between surface water and an under saturated atmosphere (relative humidity <100%) for applications in oceanographic studies. They introduced a saturated layer between the liquid water and the turbulent atmosphere. Fractionation during evaporation therefore takes place as a result of (a) equilibrium fractionation between liquid water and the saturated layer of vapour at a given temperature and (b) kinetic fractionation between the saturated layer of vapour and the turbulent atmosphere.

3.3 Stable isotopes in soil

3.3.1 Attenuation

In the unsaturated zone an attenuation of seasonal variations of the isotopic composition of precipitation takes place. This is a result of hydrodynamic dispersion within the soil, where the infiltrating water travels at different velocities through pores with a range of different sizes and in some cases also through cracks, fissures or macropores (see modelling Chapter 5). In fine-grained soils the depth at which the seasonal signal is damped out tends to be less than in coarse soils. In fractured or karstified rocks attenuation is expected to be slow and depth of full attenuation relatively large. The depth at which the isotopic signal becomes stable was found to reach 3 to 5 m in fine-grained soils (Zimmermann, Münnich and Roether, 1967) and up to 9 m in gravel (Eichinger *et al.*, 1984). The isotopic composition of soil water is affected by several processes in the soil: firstly, the original input function is smoothed by dispersion. At the same time selective abstraction of soil water by plants may remove different fractions of infiltrated rainwater during summer and winter and thereby changing the average composition. The example in Figure 3.16 shows that heavy summer rainfall is removed selectively by

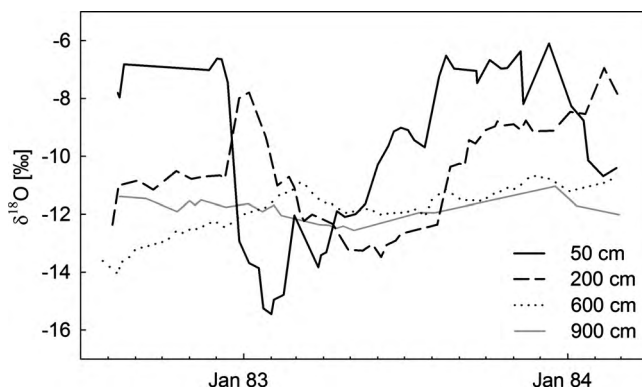


Figure 3.16 Isotopic composition of soil water at different depths in the gravel plain (Munich/Bavaria in Germany), graph redrawn with permission of Eichinger *et al.*, 1984).

plant transpiration. The weighted average of precipitation and percolating water can therefore differ.

The distribution of isotopes in soils can be used for estimating several aspects of soil water movement and vadose zone hydrology. The distribution with soil depth can be evaluated or time series of isotopes at different depths. The approach of Zimmermann *et al.* (1967) can be used as an approximation for saturated soils. For this approach the isotope profile in the soil is treated as an equilibrium state between the upward convection induced by soil evaporation and the downward diffusion of depleted water, resulting in:

$$E = D^* \frac{\ln\left(\frac{\delta}{\delta_g}\right)}{z} \quad (3.24)$$

where E represents evaporation, D the liquid diffusivity of isotopes δ the isotope content of liquid water, δ_g the isotopic composition of at greater depth and z depth, corresponding to a weighted mean of percolating water. This approach is only applicable for soil evaporation directly from the soil surface of a wet soil. It is not applicable for unsaturated zones and does not give information other than that on direct soil evaporation (e.g. total evapotranspiration).

If the percolating water reaches the water table before the seasonal signal has been fully attenuated, these fluctuations will also be found in the groundwater. Depth of attenuation is relevant as it determines whether seasonal fluctuations in the groundwater of the recharge area are to be expected. If seasonal fluctuations are damped out completely, samples can be taken to be representative for the location; otherwise time series sampling needs to be carried out.

If seasonal variations can be identified in the soil profile, the position of seasonal variations can be used to mark water of a specific year or event. The tritium-peak

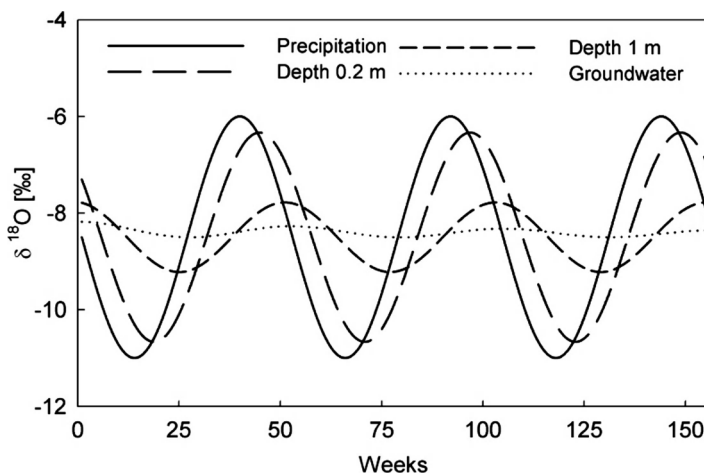


Figure 3.17 Modelled $\delta^{18}\text{O}-\delta^2\text{H}$ variability at different depths in the soil. With increasing depth the amplitude decreases and the peak shifts.

resulting from thermonuclear bomb tests has been used for this approach. In drylands with low recharge rates and in thick unsaturated zones, this approach can still provide recharge estimates. The recharge rate is defined by:

$$R = \frac{C_{total}}{\sum_{i=1}^n w_i * C_{pi} * e^{(-\lambda * t)}} \quad \text{with} \quad C_{total} = \int_0^{z_p} C(z) * \theta(z) * dz \quad (3.25)$$

where R is the mean annual recharge, w_i a weight transforming precipitation into effective precipitation, C_{pi} the tracer concentration of i years before present, n the years since the time series of the input function starts. C_{total} is calculated by integrating the tracer concentration $C(z)$ at different depths multiplied with the respective soil water content $\theta(z)$ along the whole soil profile. In humid areas and in most cases where the unsaturated zone is thinner, this peak has already passed through the unsaturated zone.

The use of stable isotopes is based on a similar approach. Instead of the tritium peak, the seasonal peaks of summer and winter rainfall are identified. The recharge rate R is then obtained simply by integrating the soil moisture down to an observed peak at the depth z_p and by dividing it by the time since the input into the soil zone t_{peak} .

$$R = \frac{\int_0^{z_p} \theta(z) * dz}{t_{peak}} \quad (3.26)$$

This method is limited by the dispersion of isotopic signals with depth. The attenuation of seasonal variation itself is the basis for another group of methods using stable isotope information in soils. For a time series of stable isotopes at a given point Maloszewski *et al.* (1983) have developed an approach for relating amplitude attenuation to residence time. The residence time would then be defined by:

$$T = \frac{\sqrt{\left[\frac{A_{precipitation}}{A_{flow}} \right]^2 - 1}}{\omega} \quad (3.27)$$

where ω is the transformed time period and $A_{precipitation}$ and A_{flow} are the respective amplitudes in rainfall (input) and flow (output). This method was developed for groundwater systems and applied to soil water. Stewart and McDonnell (1991) used this approach for soils and derived soil water residence times. Recently this approach was applied by Wenninger (2007).

Lysimeter studies were used by Maloszewski and Zuber (1982), Maciejewski *et al.* (2006) and Maloszewski *et al.* (2006a) to fit combined models of residence time distributions. A combination of an exponential model and a piston-flow model provided a good fit between modelled and measured isotope concentrations and allowed to derive flow velocities and mean residence times (see Section 7.2.2).

3.4 Stable isotopes in surface and groundwater

The isotopic input of precipitation is modified by fractionation processes during recharge. An excellent review of the isotope effects in the transition from rainfall to groundwater for semiarid and arid zones was prepared by Gat (1995). In this chapter an overview of evaporation, attenuation of seasonal variations, biases in the average isotopic composition and of mixing of groundwater is given. The influence of water-rock interactions on the stable isotopes ^{18}O and ^2H is only detectable in systems with specific conditions (hydrothermal springs, volcanic volatiles) and will not be dealt with. An introduction is given by Hoefs (1997). Weighted averages of the isotopic composition of precipitation and groundwater may differ and be biased. This happens if selective recharge occurs from precipitation events with a specific isotopic composition (Figure 3.18).

Recharge from flash floods has been observed to cause an isotopic depletion of the groundwater as compared to precipitation under arid conditions. This finding has been interpreted to result from selective activation of runoff and subsequent recharge by very intensive and exceptionally depleted precipitation (Levin, Gat and Issar, 1980). The effect of a bias between the average composition of precipitation and groundwater samples as well as of evaporation is shown below. On a secular time scale, a bias between the *actual* average isotopic composition of rainfall and groundwater may indicate that the groundwater was recharged during a period with a different isotopic signal in the precipitation.

3.4.1 Temporal variability of stable isotopes in runoff

As Frederickson and Criss (1999) have pointed out the isotopic variation of runoff is caused by the isotopic variation of runoff weighed by runoff rates. A simplified approach can be applied from the assumption that the isotopic input function is sinusoidal. Attenuation of the isotope signal and residence times can be determined

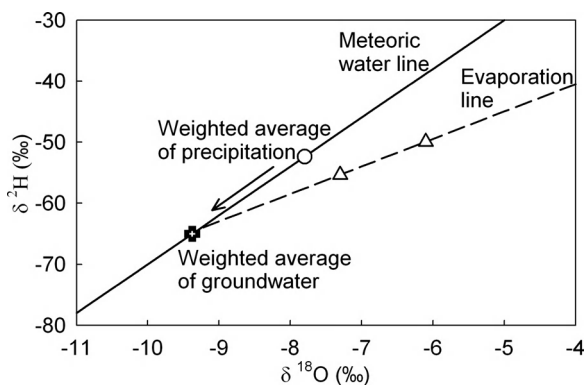


Figure 3.18 Weighted averages in the isotopic composition of precipitation (circle), of groundwater (cross) and partially evaporated surface water (triangles).

using Equation (3.27). Often a deviation from the ideal sinusoidal shape is observed. This bias is mainly caused by a superposition of the source strength of generated runoff and the isotopic signal. A good approximation of observed isotopic variation $\delta^{18}O_{river}$ in runoff can often be obtained by applying a weighing function that accounts for the variability of generated runoff. This weighing function can be approximated by using observed precipitation amounts P_i and isotope content δ_i at time intervals t_i . Equation (3.28) uses a time constant T_C .

$$\delta^{18}O_{river} = \frac{\sum \delta_i P_i \exp(-t_i/T_C)}{\sum P_i \exp(-t_i/T_C)} \quad (3.28)$$

Often T_C of the hydrologic response of the basin and of the isotopic signal is assumed to be equal. In fact, it can differ significantly. A further refinement – at the expense of an additional parameter – can be achieved by identifying individual time constants.

3.4.2 Temporal variability of stable isotopes in groundwater

Before a meaningful interpretation of the spatial distribution of stable isotopes can be made, the temporal variability of stable isotope data must be examined. Information on residence times and flow velocities can be derived from the temporal variability. On the other hand, if the seasonal variation is small or negligible as compared to spatial differences, a regional analysis can be carried out.

Temporal variations in groundwater occur where the isotopic variations in the precipitation are not attenuated in the unsaturated zone and then once more in the saturated zone, in other words where the depth to the groundwater table is smaller than the depth of attenuation. Variations in the isotopic composition of groundwater are most likely where depth to the groundwater table is small, reflecting isotopic variability in rainstorms and recharge.

Figure 3.19 shows the variability of rainfall and the response of a spring with high residence time (top). Springs with smaller residence times exhibit seasonal variations (bottom). The stability of groundwater values with time can be visualized in time series plots, in bi-plots or frequency distributions of re-sampling campaigns. Also, frequency distributions of deviations between $\delta^{18}O$ and δ^2H values can be considered in detail. Time series data show the influence of rivers or recharge events and can be used to identify and locate groundwater components with short residence times.

The analysis of temporal variation with time already presented above for soils was developed for aquifer systems. For the time series of stable isotopes at a given point Maloszewski *et al.* (1983) have developed an approach for relating amplitude attenuation to residence time in the case of a sinusoidal input function and an exponential distribution of residence time. The residence time T would then be defined by Equation (3.27).

This method has been used by Pearce, Stewart and Sklash (1986). Equation (3.28) can also be used when estimated recharge is used as a weighing function.

The models presented extensively in Chapter 5 can be used to ‘fold’ input functions and to produce a resulting time series of isotopes in groundwater.

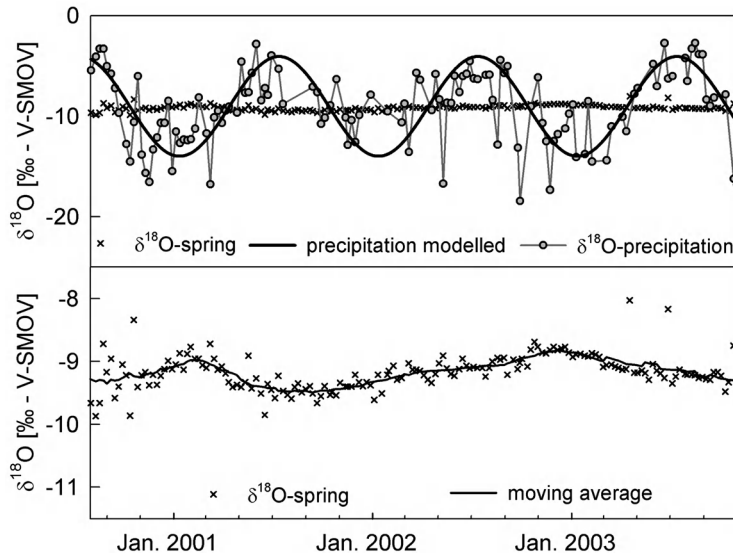


Figure 3.19 Time series of $\delta^{18}\text{O}$ indicating groundwater and rainfall time series.

The analysis of groundwater systems can also be based on a mass balance approach of water and of stable isotopes. The balance equation writes:

$$\frac{d(V^* \delta_V)}{dt} = \alpha^* P^* \delta_P - Q_{out}^* \delta_{Q_{out}} \quad (3.29)$$

where δ_i represent the respective isotopic composition of the hydrological component identified by the subscript i and where α is a weighting factor for effective precipitation.

3.5 The use of environmental isotopes for hydrological system analysis

A regional distribution of $\delta^{18}\text{O}$ can be used to identify the source of groundwater, mainly recharge altitude. When using oxygen isotopes it should be checked that evaporation effects do not occur or have been corrected for. In order to facilitate interpretation of data the expected mean $\delta^{18}\text{O}$ value of direct recharge at the local altitude can be plotted.

Stable isotopes have also been used to study hydrological systems and to identify flow components. Many applications are based on an end member mixing analysis (EMMA) and inverse modelling (IM) or on the analysis of dispersion of the seasonal variation. The end member mixing analysis is based mainly on measurements of water chemistry and isotopes assuming complete mixing between independent, distinct and conservative tracers. The mixing analysis provides an intrinsic integration of time and space for the examination of areas with scarce hydrologic information. EMMA includes various types of models using environmental tracer data and has been applied for runoff component separation (Sklash and Farvolden, 1979; Buttle, 1994).

Several environmental tracers have been used for end member analysis. In hydrological studies stable isotopes of water have been used ($\delta^{18}\text{O}$ or $\delta^2\text{H}$). Further studies have included Silica or for some applications quasi-conservative substances such as Cl^- .

The basis equation of EMMA can be derived from the mass balance of water and tracer. If we consider two flow components Q_1 and Q_2 , having respective concentrations c_1 and c_2 that mix completely in a flow Q_M with a resulting concentration c_M , it is evident from the conservation of mass of water and mass of tracer that:

$$Q_M = Q_1 + Q_2 \quad \text{and} \quad (3.30)$$

$$c_M Q_M = c_1 Q_1 + c_2 Q_2 \quad (3.31)$$

by rearranging, we get:

$$Q_1 = Q_M \frac{c_M - c_1}{c_1 - c_2} \quad \text{and} \quad Q_2 = Q_M - Q_1 \quad (3.32)$$

This method is based on some requirements regarding the environmental tracer data. A significant difference between end members must exist, the accuracy of the method is directly linked to the range between c_1 and c_2 divided by the analytical precision. The two end member mixing is based on the assumption that the system is in a steady state, that is that flow and concentrations do not change within the time period and system boundaries are considered. Finally, it is assumed that there are no other flow components contributing to the mass balance of water or tracer.

This approach can be extended to three or more flow components with independent and conservative environmental tracers (Uhlenbrook and Hoeg, 2003). The development of equations is always based on the initial equations of water and tracers. In Figure 3.20 a runoff component analysis is shown based on the end members precipitation and deep groundwater.

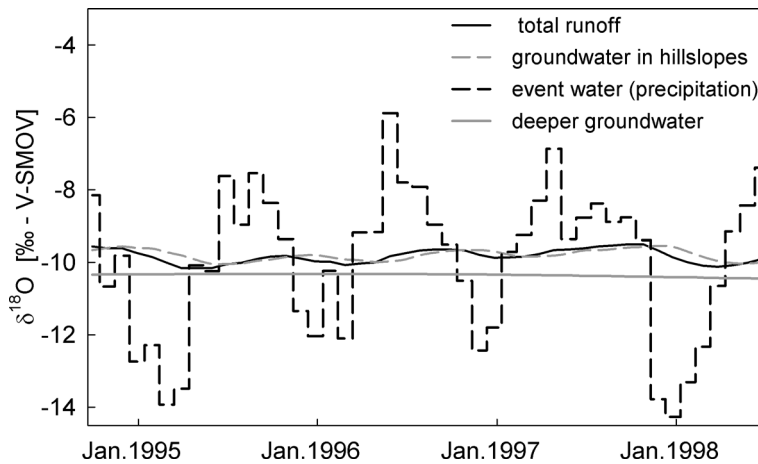


Figure 3.20 Variations of isotope ratios in different compartments of the hydrological system.

3.6 Nitrogen isotopes and origin assignment

Environmental tracers can be used to decipher the origin of solutes and pollutants. The combination with age dating information provides a straightforward approach for developing solutions for management problems. The origin analysis of nitrate shows how the nitrate entered the aquifer system. Stable isotopes of nitrate help to distinguish the possible sources: mineral fertilizers, organic fertilizers (manure) or mineralization of N-bearing substances in the soil and rainfall.

The origin of ammonium and nitrate in groundwater can be investigated by nitrate isotope analysis (Högberg, 1997). While earlier works have relied only on the $\delta^{15}\text{N}$ -nitrate fingerprint, advanced analytical methods also allow one to determine $\delta^{18}\text{O}$ -nitrate and to improve the reliability of nitrate origin assignment. The combination of $\delta^{15}\text{N}$ -nitrate and of $\delta^{18}\text{O}$ -nitrate is used to determine the isotopic composition of groundwater to that of the potential sources (Durka *et al.*, 1994).

Due to the large oxygen isotopic contrast between nitrates produced in the atmosphere and those produced by microbial processes in the soil (nitrification), the oxygen isotopes in nitrate are particularly useful for the identification of nitrates from fertilizer and atmospheric nitrates. The $\delta^{18}\text{O}$ of nitrates produced by nitrification varies regionally because one oxygen atom in the nitrate is derived from oxygen gas and two oxygen atoms are derived from soil water or groundwater.

The $\delta^{15}\text{N}$ -nitrate depends in part on that of the nitrogen source; however, this original signature may be modified by exchange with soil nitrogen and by ammonia volatilization and denitrification. The systematic shift in $\delta^{15}\text{N}$ -nitrate and $\delta^{18}\text{O}$ -nitrate

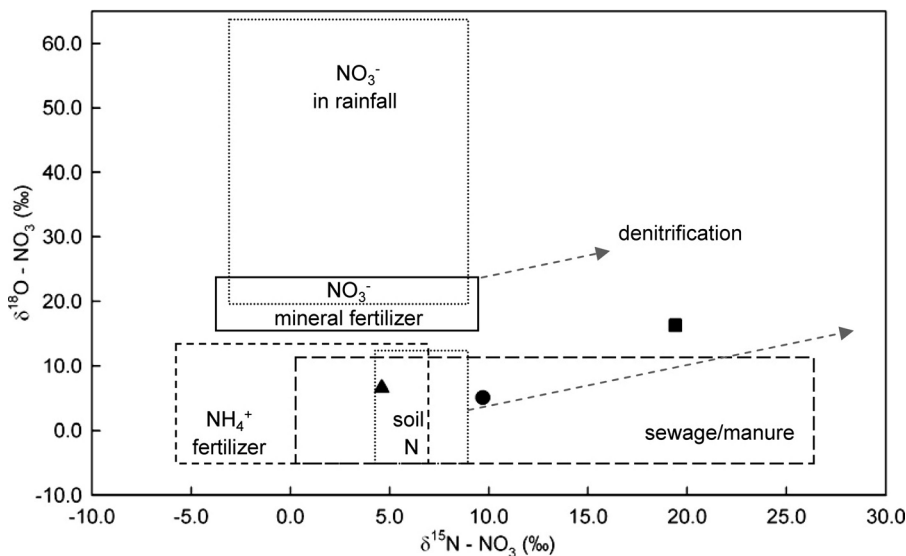


Figure 3.21 Results of nitrate isotope analysis.

allows for identifying denitrification processes that represent a natural remediation. The possible sources of nitrate are:

- nitrate from organic or mineral fertilizers (agriculture),
- ammonium/nitrate from sewage plants or losses from the sewage system,
- ammonium/nitrate from waste dumps.

Ammonium is synthesized technically by Haber-Bosch synthesis from ambient air. As a consequence the isotope ratios correspond to those of air $\delta^{15}\text{N}$ (-3 to 2‰). Mineral nitrate fertilizer is synthesized from ambient air nitrogen and oxygen. During the synthesis the $\delta^{15}\text{N}$ increases slightly – this results in $\delta^{15}\text{N}$ of -1 to 5‰ . Most of the oxygen in the nitrate fertilizer stems from ambient air oxygen with a $\delta^{18}\text{O}$ -nitrate value of about 23‰ V-SMOW. The measured $\delta^{18}\text{O}$ -nitrate values are in the range of 17 to 22‰ . Litter, nitrate stemming from soil nitrification and sewage/manure have similar $\delta^{18}\text{O}$ -nitrate values close to 0‰ but differ in the $\delta^{15}\text{N}$ signal.

The process of ammonia evaporation causes an enrichment of heavier nitrogen isotopes and hence increases the $\delta^{15}\text{N}$ value. Denitrification causes a characteristic increase of both the $\delta^{15}\text{N}$ and $\delta^{18}\text{O}$ -nitrate values in the remaining nitrate. Of course these changes of the isotopic composition should correlate with decreasing nitrate concentrations as nitrate is being transformed to nitrogen gas and removed from the system. It is important to check and validate whether the observed changes in the isotopic composition of the remaining nitrate correspond to a decrease of total dissolved nitrate in groundwater. This can be done by plotting $\delta^{15}\text{N}$ against a concentration scale e.g. $1/\text{NO}_3$ or $\ln(\text{NO}_3)$.

3.7 Age dating

3.7.1 Tritium

The radioactive isotope of hydrogen, ^3H (tritium), has a half life of 12.43 years. It decays to ^3He by β^- emission. Tritium levels are given as absolute concentrations in tritium units (TU). One tritium unit is defined as one ^3H atom per 10^{18} atoms of hydrogen, causing a radioactivity of 0.118 Bq per kg of water. Tritium is measured by liquid scintillation counting of β^- decays. Tritium is produced naturally in the upper atmosphere from nitrogen by neutron impacts of cosmic radiation. It enters the water cycle by precipitation with a seasonal and spatial variation in tritium fallout. Natural fallout is higher in higher geomagnetic latitudes. For northern mid-latitudes a natural level between 3.4 and 6.6 TU has been reconstructed from wines (Kaufmann and Libby, 1954). Thermonuclear bomb tests, starting in 1951, have overdriven this natural level for several decades.

Tritium levels in rainfall have exceeded the naturally occurring levels in the environment by several orders of magnitude. However, the impact of ^3H fallout has been

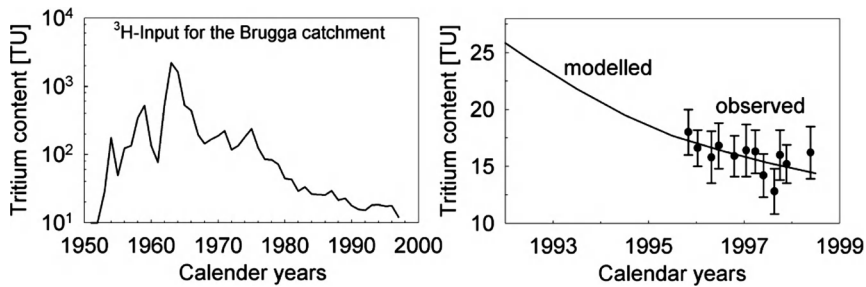


Figure 3.22 Input function for tritium, catchment response observed and modelled.

less pronounced in the southern hemisphere as compared to the northern hemisphere resulting from an asymmetric distribution of tritium emissions from bomb tests and an air mass circulation barrier along the equator. Due to low input levels of tritium in the southern hemisphere, natural attenuation by decay and mixing with pre-bomb groundwater with unique tritium levels can often be used for qualitative interpretation only. Repeated sampling of tritium (Figure 3.22) allows for a modelling of tritium decline and provides a more reliable mean of determining residence times.

Tritium decays to the noble gas ^3He . Since the absolute activity of ^3H has decreased and almost reached the level of natural input, the combined use of $^3\text{H}/^3\text{He}$ helps to define groundwater ages based on the ratio of both isotopes. The method has been proposed early by Tolstikhin and Kamensky (1969) and used in oceanography and limnology. Weise and Moser (1987), Schlosser *et al.* (1988) and Poreda, Cerling and Solomon (1988) have published applications in shallow aquifers. The application of this method requires adequate sampling techniques that allow one to preserve the concentration of the highly volatile noble gas. The method is based on the equation:

$$T = 1/\lambda^* \ln \left(\frac{{}^3\text{He}^*}{{}^3\text{He} + 1} \right) \quad (3.33)$$

with T a groundwater age, λ the decay constant for tritium. ${}^3\text{He}^*$ must correspond to the tritiogenic concentration, that is derived from the decay of tritium only. Other, atmospheric and geogenic sources of ${}^3\text{He}$ will bias results. The total helium measured in the groundwater sample is composed of dissolved atmospheric helium in equilibrium with the atmospheric partial pressure, excess helium entrapped in recharge water, helium released by emanations from the mantle of the earth and helium released by nuclear tests. The atmospheric dissolved ${}^3\text{He}$ can be determined from neon noble gas measurements. The correction for other sources can be carried out based on the measurement of ${}^3\text{He}/{}^4\text{He}$ ratios. Solomon and Cook (2000) suggest:

$$\begin{aligned} {}^3\text{He}^* = & 4\text{He}_m R_o - R_{sol} [{}^4\text{He}_{sol} + (N_{em} - N_{e_{sol}}) \alpha R_{He-Ne}] \\ & - R_{rad} [{}^4\text{He}_m - {}^4\text{He}_{sol} - (N_{em} - N_{e_{sol}}) R_{He-Ne}] \end{aligned} \quad (3.34)$$

where ${}^4\text{He}_m$ and Ne_m are the measured concentrations of ${}^4\text{He}$ and Ne , R_o is the measured ${}^3\text{He}/{}^4\text{He}$ ratio, R_{sol} is the ${}^3\text{He}/{}^4\text{He}$ ratio for water that is in isotopic equilibrium with the atmosphere, R_{rad} is the ratio of nucleogenic ${}^3\text{He}$ to radiogenic ${}^4\text{He}$ and $R_{\text{He-Ne}}$ is the Helium/Neon ratio in the atmosphere. The subscript in Ne_{sol} and ${}^4\text{He}_{\text{sol}}$ identifies the concentrations that correspond to the equilibrium solubility with the atmosphere, both depend on temperature. The fractionation factor α holds for the air-water isotope fractionation for Helium. This equation can be simplified to:

$${}^3\text{He}^* \approx 4\text{He}_m R_o - R_{\text{sol}} \quad (3.35)$$

for samples that do not contain radiogenic ${}^4\text{He}$ and for which excess air can be neglected. The development of the ${}^3\text{He}/{}^3\text{H}$ ratio as an age indicator starts only at the groundwater surface, once the system is closed. In the vadose zone helium is lost by gas diffusion. As Solomon and Cook (2000) point out, the method is less sensitive for older waters and requires precise determinations of excess air. The method also requires a good sampling as air bubble entrapment. Degassing and contamination need to be avoided. The presence of mantle helium close to major fault zones, geothermal fields or geologically young igneous rocks may prohibit the application of this method as the concentration of geogenic sources may exceed the ${}^3\text{He}$ derived from tritium decay by an order of magnitude.

3.7.2 Dating with gases (CFC, SF_6)

Chlorofluorocarbons (CFCs) are synthetic organic compounds and have been developed in the early 1930s. CFCs have marked the global atmospheric system and they have also entered and traced the hydrologic cycle. Data on concentrations of CFCs and sulfur hexafluoride (SF_6) can be used to trace the flow of young water (less than 50 years) (Busenberg and Plummer, 1993; Oster, Sonntag and Münnich, 1996). CFCs are not inflammable and not toxic. A recent review of their global impact on groundwater containing major references is given in Höhener *et al.* (2003). Several reviews exist on dissolved gases as environmental tracers in subsurface hydrology: Noble Gas Geochemistry (Ozima and Podozek, 1983), Dissolved Gases in Subsurface Hydrology (Solomon, Cook and Sanford 1998), Chemical and Isotopic Groundwater Hydrology (Mazor, 2004). A textbook on CFC application is available (IAEA, 2006).

For dating purposes three main substances are used that are abbreviated as CFC-11, CFC-12 and CFC-113. Their concentrations are measured and compared to the concentration curve of CFCs in rainwater of the last 50 years. In general, the absolute concentrations and the ratios of pairs of CFCs are used.

Chlorofluorocarbons (CFC-11, CFC-12, CFC-113) and sulfur hexafluoride represent an alternative method for dating subsurface water (Katz *et al.*, 1995; Beyerle *et al.*, 1999; Busenberg and Plummer, 2000). Unlike constant concentrations of noble gases, CFCs and SF_6 are released from anthropogenic sources. Air mixing ratios of CFCs show a monotone increase of concentrations through the 1970s and 1980s due to the comparatively high atmospheric lifetimes (approx. 45 years for CFC-11; 87 years for CFC-12;

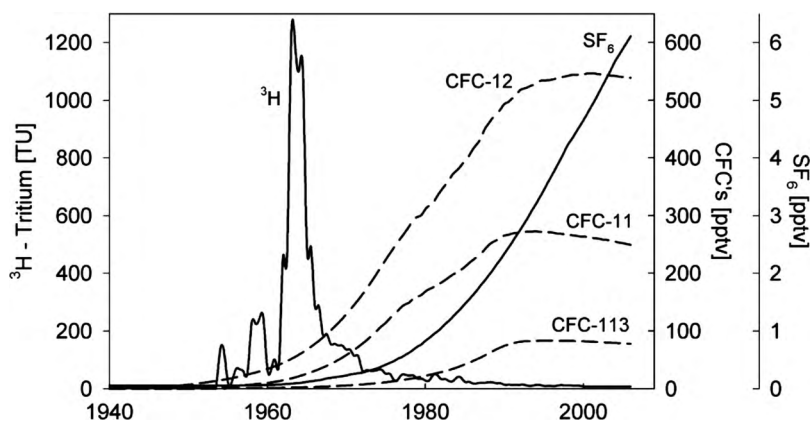


Figure 3.23 Input function for tritium and CFCs. Concentrations are given in parts per trillion volume.

100 years for CFC-113 (Volk *et al.*, 1997)). CFC-11 and CFC-113 peaked in 1993 and 1994, CFC-12 peaked in 1999, as a result of the limit to CFC release in 1987, SF₆ continues to increase. CFCs have been used in oceanic studies since the late 1970s as tracers of oceanic circulation and mixing processes. CFCs have then been introduced as environmental tracers to hydrologic and hydrogeologic studies (Busenberg and Plummer, 1992). Their applicability for very young groundwater (post 1995) is limited because the concentration in the atmosphere has stopped increasing and is actually decreasing.

Their concentration in the atmosphere – the input function – during the last 50 years has been reconstructed (Cunnold *et al.*, 1997). From chemical and physical studies their solubility and the influences of pressure and temperature on the solubility in water are known. Finally, analytical techniques have been developed to detect CFCs with sufficient precision. Dating with CFCs is based on the following principles:

- concentrations of CFCs in the atmosphere have been reconstructed and are known,
- the solubility under defined temperature and pressure conditions are known for specific CFCs,
- hence, the concentration of specific CFCs in rainwater can be calculated,
- rainwater recharging the aquifer carries the equilibrium CFCs concentration as a signal into the groundwater,
- the measurement of CFCs in groundwater is sufficiently precise to resolve the variations of dissolved CFCs in groundwater within the last 50 years.

The use of gases as environmental tracers is based on Henry's Law that means on the linear relationship between the partial pressure of a gas and its concentration as a

dissolved constituent of water. If the input function of the gas is known, the age can be derived from known concentrations. However, the validity of the approach is also based on the validity of Henry's Law. Temperature and pressure need to be known as they control the dissolution process. This is not as simple as it may seem, because the dissolution may take place under variable conditions. In addition, excess air – air in excess of the concentrations predicted by Henry's Law – have been observed. In order to reconstruct the partial pressure of the dissolving gas at the recharge altitude the total pressure p (Pa) is calculated for a given altitude h (m) (IAEA, 2006):

$$\ln p = -h/8300 \quad (3.36)$$

The dissolved concentration c_i (mol/l) of the gas is calculated according to Henry's Law as a function of partial pressure p_i (Pa) and of the Henry Constant k_{Hi} (mol/l*Pa)

$$c_i = k_{Hi}^* p_i \quad (3.37)$$

$$p_i = x_i(p - p_{H_2O}) \quad (3.38)$$

where x_i is the volumetric ratio of gas in air (pptv). A correction for atmospheric moisture p_{H_2O} (Pa) is taken into account. The dissolution constant k_{Hi} depends on temperature and for saline water also on salinity S (‰ mass ratio). The water temperature T (K) can be taken into account (IAEA, 2006) according to:

$$\ln k_H = a_1 + a_2 \left(\frac{100}{T} \right) + a_3 \ln \left(\frac{T}{100} \right) + S \left[b_1 + b_2 \left(\frac{T}{100} \right) + b_3 \left(\frac{T}{100} \right)^2 \right] \quad (3.39)$$

Tables for the coefficients a_1 , a_2 , a_3 , b_1 and b_2 are given in IAEA (2006). For the interpretation of data, measured concentrations are first converted to molar fractions per volume. These molar fractions c_i are used to calculate the initial gas concentration that can be compared to a known input function:

$$x_i = \frac{c_i}{k_H(p - p_{H_2O})} \quad (3.40)$$

The reconstructed concentration at recharge can exceed even present concentrations as a result of several factors. Excess air can be introduced into the groundwater system as a result of nonequilibrium conditions. It is assumed that air bubbles are transferred into the groundwater system by rapid rises of groundwater levels or by air entrapment in the soil or the aquifer. The air bubble may dissolve partially or completely if exposed to hydrostatic pressure. Excess air corrections can be taken into account based on quantitative gas analysis or on noble gas analysis (USGS, 2008; Aeschbach-Hertig *et al.*, 2000; Plummer and Busenberg, 2000; Bauer, Fulda and Schäfer, 2001).

In Figure 3.24 a typical analysis for CFCs is given. The input functions are given as volumetric ratios. Concentrations of CFCs in groundwater are measured with gas chromatography with electron capture detector (GC-ECD) and range from picomol/l (pmol/l) to femtomol/l (fmol/l). Based on Equations (3.36)–(3.40) these are converted to original volumetric ratios in the atmosphere and compared to the input functions.

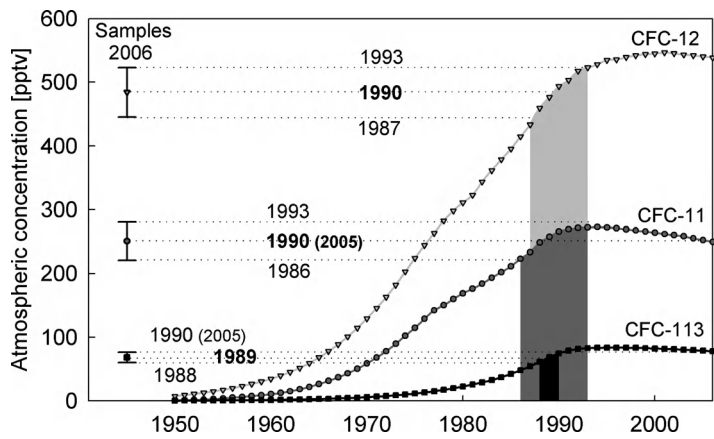


Figure 3.24 Input function of different CFCs (CFC-11, CFC-12, CFC-113) and measured concentrations.

The example below shows a good match of all three measured CFCs. Error ranges are given from ± 2 –4 years. In the case of CFC-11 and CFC-113 the result is not unique, two different recharge years are possible.

Bi-plots reduce the uncertainty and confirm whether CFC data are consistent. If the sample is located on the curve being defined by the pair of concentrations, residence times are concordant (Figure 3.25).

All of the graphs above are based on a piston flow model. Often it is useful to calculate the concentration resulting from an exponential model (see Chapter 5). This is done in Figure 3.26 (dashed line).

With only one exception (alluvium) samples are located on the line defined by the exponential model. This indicates that boreholes are located in a phreatic aquifer that is recharged on its entire length.

Local anomalies from the global atmospheric input function might exist at present or might have existed in the past (Oster, Sonntag and Münnich, 1996). In the northern hemisphere especially and close to highly industrialized areas such local effects have

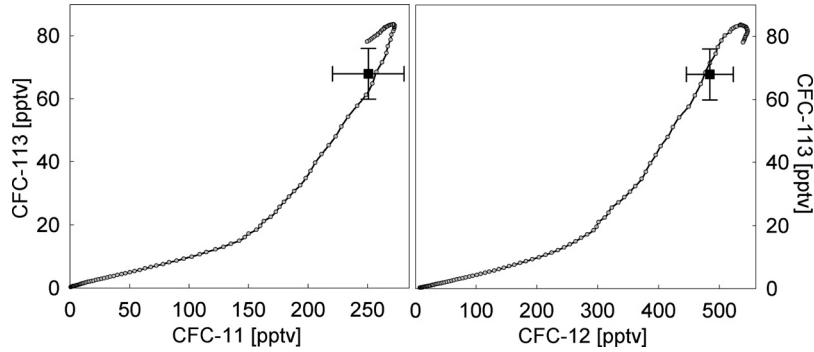


Figure 3.25 Bi-plot of concentrations of CFC-113 and CFC-11 (left) and of CFC-12 and CFC-113.

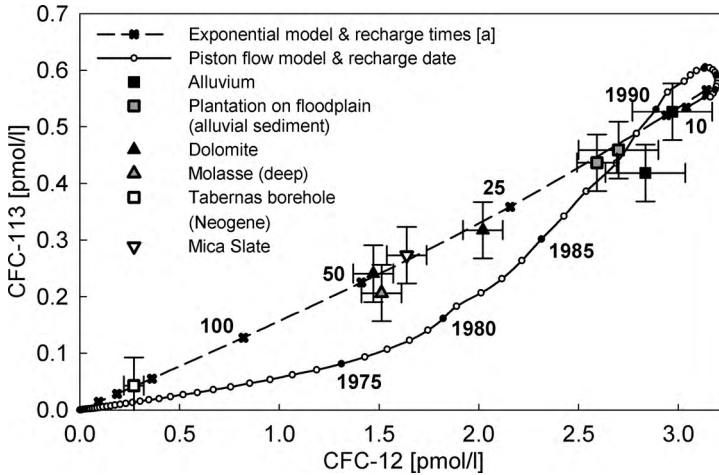


Figure 3.26 Concentrations of CFC-12 and CFC-113 in groundwater corresponding to original atmospheric concentrations for a piston-flow-model (continuous line) and for an exponential model (dashed).

been observed. Measurements of atmospheric samples can help to identify the local anomaly and apply corrections to the global atmospheric input function. In such cases at least a relative order of mean residence times can be established. In other cases local groundwater sources of CFCs exist. Uncontrolled municipal waste dumps (containing refrigerators) may release CFCs locally. In such cases dating with CFCs is often not feasible. The accuracy of the determined age depends on how conservative the transport of CFCs in water actually is. Especially, excess air, the influence of the soil atmosphere and degassing processes may affect the accuracy of CFC dating. Even if one or some of these limitations apply in a certain case, the presence of CFC is a marker for post 1950 influence. CFCs should be used after reconnaissance studies, based on hydrogeologic knowledge of the site conditions and together with other dating tools.

In recent years the role of SF_6 as a trace atmospheric gas has been recognized, mainly for dating post-1990s groundwater (Bauer, Fulda and Schäfer, 2001). SF_6 is produced since the 1960s, primarily as isolation in high voltage elements and as a cleaning agent, but also for shock (noise) absorption in windows. Unlike CFCs, atmospheric concentrations of SF_6 are expected to rise. Currently, the concentration of SF_6 is growing at a global scale because more substance is produced than the environment can destroy, absorb or store. The atmospheric lifetime of SF_6 is estimated to be at least 500 to 1000 years.

SF_6 is analysed with gas chromatography (ECD) (Oster, Sonntag and Münnich, 1996). Concentrations of down to 10^{-16} can be measured. SF_6 is a virtually conservative tracer with small known interactions and physical or chemical decay rates. CFCs enter the water cycle by dissolution in precipitation. Solution is controlled by known equilibria, temperature and pressure dependencies. Excess air, soil gas equilibria and degassing may affect the dating precision. It needs to be considered that SF_6 may also occur naturally in igneous rocks and in volcanic or igneous fluids. Also, the ratio of SF_6 to CFCs can be used as a dating tool.

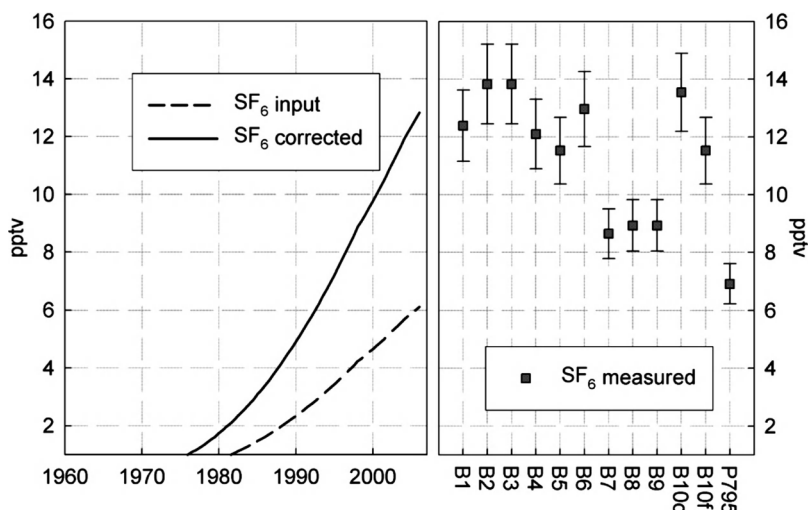


Figure 3.27 Application of gas dating with SF_6 .

3.7.2.1 Dating with other noble gases

Other gases have also been used for groundwater age dating. The application of ^{39}Ar (Loosli and Oeschger, 1968; Loosli, 1983; Loosli, Lehman and Balderer, 1989; Forster, 1983; Forster, Moser and Loosli, 1984) can fill the gap between tracers with short half-lives and ^{14}C . ^{85}Kr is an alternative for CFCs, SF_6 and tritium dating. It has a half-life of 10.75 years and atmospheric concentrations are increasing continuously. Dating of groundwater with ^{85}Kr has been developed by Salvamoser (1981) and a series of applications exist (Smethie *et al.*, 1992; Loosli, 1989; Cook and Solomon, 1997; Bauer, Fulda and Schäfer, 2001). Krypton in groundwater needs to be enriched from about 6000:1 in order to get sufficient accuracy for age dating. Enrichment is carried out in situ with a spray and strap method (see IAEA, 2006; USGS, 2008).

An interesting aspect of ^{85}Kr is the possibility to combine it with other tracers that have a significantly different input function. The ^{85}Kr -tritium harp combines both tracers and allows determining the residence time and the mixing with an old component (see Figure 3.28). The 'harp' is constructed by folding the input function with an exponential model (see Chapter 5). A dispersion or a piston-flow model or any combination of these can be used as well. The resulting line is mixed with a 0.0 component – a component containing no tritium and Krypton-85. Data plotted into this diagram indicated the residence time (intersection with the 100% line) and the amount in % of tracer-free groundwater as well.

3.7.2.2 ^{14}C -dating

Radiocarbon is produced in the upper atmosphere through cosmic radiation. Collision of a neutron with nitrogen produces ^{14}C and a proton. ^{14}C enters the troposphere as

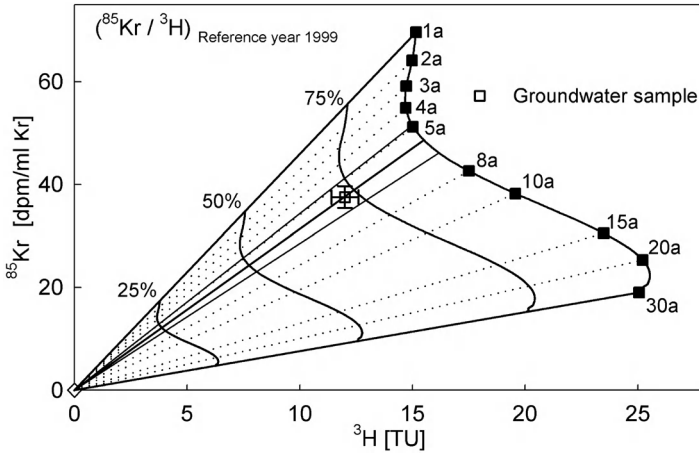


Figure 3.28 Krypton-85 and tritium harp.

CO₂ and participates in the hydrologic and biologic carbon cycles. It is radioactive and decays according to:

$$a_t = c^* a_0^* e^{-\lambda^* t} \quad \Rightarrow \quad t = -\frac{1}{\lambda}^* \ln \left(\frac{a_t}{c^* a_0} \right) \quad (3.41)$$

where $\lambda = 1.2097 \times 10^{-4}$ is the decay constant, c is a dilution factor, a_t is the ¹⁴C activity at time t and a_0 the initial ¹⁴C activity (Geyh and Schleicher, 1990). The half-life of ¹⁴C is 5730 years. Activities are expressed as percent of the standard 'modern carbon' abbreviated as 'pmC'. The standard is defined as 95% of the ¹⁴C activity in 1950 of a NBS oxalic acid standard. It corresponds to the activity of wood grown in 1890 before the combustion of fossil carbon. The actual ¹⁴C in the sample is measured by scintillation counting or with accelerator mass spectrometry. In some hydrogeological systems where groundwater is isolated from input of modern carbon sources containing ¹⁴C, radioactive decay of ¹⁴C in dissolved inorganic and organic carbon compounds may be used for dating. Time t since groundwater became isolated from the atmosphere and the soil can be derived from the ratio of actual and initial activities a_0 and a_t according to Equation (3.41).

Some difficulties arise for the estimation of the initial activity a_0 . The activity in living plants is about 100% pmC. However, the production of ¹⁴C in the upper atmosphere fluctuates with time. Calibration with oak tree dendrochronology (Stuiver and Kra, 1986; Stuiver and Reimer, 1993) and corals (Bard *et al.*, 1990) showed that initial ¹⁴C activity varied by about 10% during the Holocene. In addition anthropogenic effects have altered the natural regime. Combustion of fossil fuel has diluted the atmosphere with ¹⁴C-free CO₂. Nuclear weapons testing and power plants have released artificial ¹⁴C into the atmosphere.

An additional 'reservoir effect' needs to be taken into account for the application of ¹⁴C to groundwater systems (Geyh, 1995). Soil water equilibrates with soil CO₂ during infiltration. HCO₃⁻ concentrations increase and solution of available primary or secondary carbonates ensues (Munnich, 1968). The solution of ¹⁴C-free carbon

Table 3.1 Dilution factors for a preliminary estimation of initial ^{14}C activities at the groundwater surface for different environments (Vogel, 1970)

| Dilution factors | Recharge environment |
|------------------|--|
| 0.65–0.75 | For karst systems |
| 0.75–0.90 | For sediment with fine grained carbonate |
| 0.90–1.00 | For crystalline rocks |

reduces the initial activity of carbon compounds in deep percolation. Several correction methods have been proposed. Vogel (1970) derived initial activities using statistical analysis of measured activities in the recharge area. For different recharge environments the average factors provided in Table 3.1 were suggested.

The $^{13}\text{C}/^{12}\text{C}$ ratio has been proposed as a parameter for correcting ^{14}C initial activities (Pearson, 1965). Ratios of the stable carbon isotopes ^{13}C and ^{12}C are compared to the VPDB standard (Vienna Pee Dee Belemnite) and given in δ -notation. The correction method takes advantage of the large difference between $\delta^{13}\text{C}$ values of soil CO_2 and of marine limestone. C_3 plants reach $\sim -23\text{‰}$ VPDB, C_4 plant values range from ~ -10 to -16‰ (Vogel, 1993). Marine limestone is often close to zero. The correction is calculated with Equation (3.38):

$$c_{\text{Carbon-13}} = \frac{\delta^{13}\text{C}_{\text{DIC}} - \delta^{13}\text{C}_{\text{carbonate}}}{\delta^{13}\text{C}_{\text{soil}} - \delta^{13}\text{C}_{\text{carbonate}}} \quad (3.42)$$

where $c_{\text{Carbon-13}}$ is the dilution factor, $\delta^{13}\text{C}_{\text{DIC}}$ is the measured value in the dissolved inorganic carbon of groundwater, $\delta^{13}\text{C}_{\text{carbonate}}$ is that of the carbonate which is being dissolved and $\delta^{13}\text{C}_{\text{soil}}$ stands for the $\delta^{13}\text{C}$ value of the soil. Equation (3.42) holds only for closed system dissolution.

The chemical mass balance correction (CMB) is based on the ratio c_{CMB} between ^{14}C -active dissolved inorganic carbon ($m\text{DIC}_{\text{recharge}}$) from soil CO_2 and the total carbonate content at the time of sampling ($m\text{DIC}_{\text{final}}$). Different means of estimating $m\text{DIC}_{\text{recharge}}$ and $m\text{DIC}_{\text{final}}$ exist. The initial carbonate content during recharge can be estimated by assuming pH and pCO_2 and calculating the equilibrium concentrations of different carbonate species. The final carbonate content can either be measured (titrated) or calculated from chemical data as listed in Equation (3.43).

$$c_{\text{CMB}} = \frac{m\text{DIC}_{\text{recharge}}}{m\text{DIC}_{\text{final}}} \quad \text{with}$$

$$m\text{DIC}_{\text{final}} = m\text{DIC}_{\text{recharge}} + m\text{Ca}^{2+} + m\text{Mg}^{2+} - m\text{SO}_4^{2-} + \frac{1}{2} (m\text{Na}^+ + m\text{K}^+ - m\text{Cl}^-) \quad (3.43)$$

Finally the general hydrochemical correction by Fontes and Garnier (1979) is mentioned. This model combines measured $\delta^{13}\text{C}$ and major ion concentrations and also accounts for open system dissolution. This approach has not been used due to uncertain estimates of the strongly pH dependent enrichment factor $\varepsilon^{13}\text{C}_{\text{CO}_2 \leftrightarrow \text{CaCO}_3}$ that is required for this model.

Box 3.1 Example for Age Dating

Two groundwater samples were taken in a semiarid basin in southern Spain (Andarax catchment). The aquifers from which samples were taken are porous aquifers. One aquifer consists of alluvial sediments of about 20–30 m thickness, the second aquifer consists of tertiary alluvial and colluvial sediments.

The samples were taken from active production boreholes. Sampling was carried out after about 10 borehole volumes were pumped and in situ parameters were stable. Sample water was filled into an imerged glass bottle contained in a gas-tight container. Analysis of samples was made with GC-ECD (see colour plate section, Plate 2).

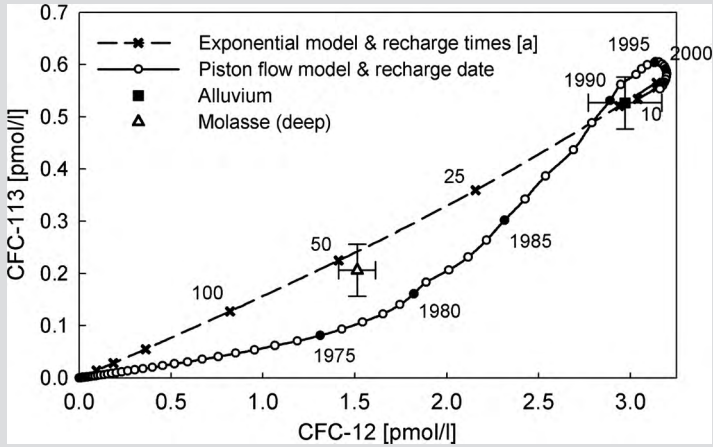
The laboratory report gives a concentration of dissolved gas in water as a concentration in picomol (pmol/l) or femtomol per litre (fmol/l). There are two ways of analysing data. The most common method consists of calculating the initial atmospheric volume ratio in pptv (=parts per trillion volume) from the concentration of the dissolved gas in water. The ambient temperature during dissolution of the gas and the atmospheric pressure need to be known for the application of Henry's Law. The atmospheric pressure is derived from the international barometric formulae based on the elevation. The reconstructed initial atmospheric pressure that was needed to produce the measured dissolved concentration at defined conditions of temperature and pressure is compared to the input function in pptv. The match indicates when recharge took place. In case of input functions that are not monotonous more than one recharge year can be obtained. This method has advantages as it allows one to compare values taken at different recharge conditions more easily.

The second method consists of calculating the concentrations that would result in groundwater for specific recharge temperature and a specific elevation or pressure. Then the laboratory values of dissolved trace gases in water are compared to the input function (as dissolved gas in water). This method has advantages if different water types are mixed with specific models (exponential model, dispersion model). Because mixing of groundwater containing specific concentrations of dissolved gases takes place the second approach should be applied if we intend to use dissolved concentrations for mixing or transport models. If dissolved concentrations of trace gases are to be compared in the same graph they need to be normalized to a standard elevation and standard temperature (e.g. 200 m and 8 °C). Then this allows the graphical presentation of different samples as dissolved concentrations in water in one graph as shown in the Figure Box 3.1 below. Both approaches are shown in this box.

The Calculation of Dissolved Input Concentration in Groundwater

The Henry Coefficient (k_H) for CFC-12 and CFC-113 for a given temperature and salinity is calculated using Equation (3.26) with a recharge temperature of

(continued)



Box Figure 3.1 Bi-plots for concentrations of CFC-12 and CFC-113 for a piston flow and for an exponential model.

8 °C (281.15 K), a salinity of 5 per mil (corresponds to the samples) and parameters a_i and b_i taken from IAEA (2006). For CFC-12 we get:

$$\begin{aligned} \ln k_H &= -124.44 + 185.43 \left(\frac{100}{281.15} \right) + 51.638 \ln \left(\frac{281.15}{100} \right) \\ &\quad + 5 \left[-0.149 + 0.095 \left(\frac{281.15}{100} \right) - 0.016 \left(\frac{281.15}{100} \right)^2 \right] \\ &= -5.1457 \Rightarrow k_H = 0.00576 \end{aligned}$$

and for CFC-113:

$$\begin{aligned} \ln k_H &= -136.129 + 206.475 \left(\frac{100}{288.15} \right) + 55.896 \ln \left(\frac{288.15}{100} \right) \\ &\quad + 5 \left[-0.028 + 0.006 \left(\frac{288.15}{100} \right) + 0 \left(\frac{288.15}{100} \right)^2 \right] \\ &= -4.962 \Rightarrow k_H = 0.007 \end{aligned}$$

The partial pressure is calculated according to Equations (3.23) and (3.25) for a recharge altitude of 200 m.a.s.l. as:

$$\begin{aligned} \ln(p) &= \left(\frac{-200}{8300} \right) = -0.0241 \Rightarrow p = 0.976 Pa \\ p_i &= xi(t)(0.976) \end{aligned}$$

We can then use the atmospheric input function of atmospheric concentrations and calculate the corresponding concentration in groundwater using x_i and $\ln k_H$. For CFC-12 and CFC-113 (data taken from http://cdiac.ornl.gov/oceans/new_atmCFC.html). Box Table 3.1 lists some of these values that represent the piston flow model respectively exponential mixing for different residence times (see Equations (5.114) and (5.115), Chapter 5) listed in Table Box 3.2 .

Box Table 3.1 Yearly values – Piston flow assumption

| Year | 2005 | 2000 | 1995 | 1990 | 1985 | 1980 | 1975 | 1970 | 1965 |
|-----------------|-------|-------|-------|-------|-------|-------|-------|-------|-------|
| CFC-12 [mol/l] | 3.185 | 3.19 | 3.129 | 2.888 | 2.314 | 1.812 | 1.311 | 0.757 | 0.397 |
| CFC-113 [mol/l] | 0.566 | 0.591 | 0.603 | 0.531 | 0.301 | 0.161 | 0.081 | 0.041 | 0.02 |

Box Table 3.2 Exponential mixing

| Residence time [a] | 2 | 5 | 10 | 25 | 50 | 100 | 250 | 1000 |
|--------------------|-------|-------|-------|-------|-------|-------|-------|-------|
| CFC-12 [mol/l] | 3.043 | 2.997 | 2.702 | 1.860 | 1.173 | 0.667 | 0.290 | 0.149 |
| CFC-113 [mol/l] | 0.623 | 0.590 | 0.484 | 0.288 | 0.168 | 0.091 | 0.038 | 0.019 |

The Calculation of Dissolved Concentrations in Groundwater for Standard Conditions

Sample no. 1 is taken at an altitude of 200 m.a.s.l. in the alluvium of the channel. The annual temperature averages 15 °C. Measurements result in a CFC-12 concentration of 2.2 pmol/l and CFC-113 concentration of 0.39 pmol/l. Sample no. 2 is taken at an altitude of 495 m.a.s.l. in the molasse. The CFC-12 concentration is 0.39 pmol/l and the CFC-113 concentration is 0.15 pmol/l. Here the average temperature is about 14.5 °C.

The concentrations are converted to a standard height of 200 m.a.s.l. and a temperature of 8 °C as follows. For CFC-12:

$$c_1(200m, 8^{\circ}C) = (1 + (15 - 8) \cdot 0.05) \cdot 2.2 \cdot \exp\left(\frac{200 - 200}{8000}\right) = 2.97 \text{ pmol/L}$$

$$c_2(200m, 8^{\circ}C) = (1 + (14.5 - 8) \cdot 0.05) \cdot 1.1 \cdot \exp\left(\frac{495 - 200}{8000}\right) = 1.51 \text{ pmol/L}$$

And for CFC-113:

$$c_1(200m, 8^{\circ}C) = (1 + (15 - 8) \cdot 0.05) \cdot 0.39 \cdot \exp\left(\frac{200 - 200}{8000}\right) = 0.53 \text{ pmol/L}$$

$$c_2(200m, 8^{\circ}C) = (1 + (14.5 - 8) \cdot 0.05) \cdot 0.15 \cdot \exp\left(\frac{495 - 200}{8000}\right) = 0.21 \text{ pmol/L}$$

(continued)

By comparison of these values and the calculated theoretical values it is possible to estimate a residence time and respectively a mean age of the groundwater. The upper curve represents values corresponding to an exponential model. The lower full line represents concentrations of dissolved gas in groundwater corresponding to a piston-flow model.

In this case the sample taken in the alluvium has a short residence time. It is not possible to distinguish whether it corresponds to a piston-flow or to an exponential distribution. In the case of piston-flow the samples were recharged in 1990 (15 years before sampling), in case of an exponential distribution the residence time is slightly above 10 years. The second sample plots close to the line derived for an exponential distribution. The corresponding mean residence time is about 50 years. The same concentration can also result from a binary mixing of various different end members.

4

Artificial Tracers

Artificial tracers are substances that offer additional information of value in the investigation of hydrological systems and subsystems. Artificial tracers must be introduced actively into the hydrological system under investigation. The scales of application are limited in both time and space. In general, artificial tracers are used in systems which have a residence time smaller than one year. However, it is possible to label a specific, well defined hydrological feature. Sometimes even the volume of water is defined. The general characteristics and the function of tracer hydrology were described in Chapter 2.

Typical fields of applications are: the detection of hydrological connections, flow paths and flow directions in catchments and aquifers, delineation of catchments and aquifers (qualitative), determination of flow velocities and further aquifer flow parameters based on the tracer breakthrough curves, hydrodynamic dispersion, runoff separation, residence time, infiltration and runoff generation processes, convection-diffusion processes in surface water, simulation of contaminant transport and discharge measurement applying dilution methods.

In principle, the guideline followed is that an ideal tracer represents the water flow, but nonideal tracers can also be useful for special applications. Six main groups of artificial tracers can be distinguished based on their chemical appearance (see Table 4.1). Up until the 1980s, during the pioneer phase of tracer hydrology, a wide spectrum of artificial tracers was being tested for their suitability. However, most did not exhibit the right combination of properties and, therefore were deemed to be ill suited to serve as water tracers. The tracers which are considered to be suitable water tracers are presented in Table 4.1, and only these substances will be dealt with in the remainder of this book. Of the six groups of artificial tracer listed in Table 4.1, fluorescence tracers are the most important and most often applied, followed by the salt and the advanced tracers. Drifting particles are tracers of a different physiochemical origin, and are used to assess special problems, such as the filtration capacity of unsaturated zones.

In order to perform experiments successfully in both the field and in the laboratory, a sound knowledge of the characteristics of the tracer substances and the respective measurement techniques is required. The publications prepared by the following international organizations dealing with tracer methods are an excellent resource for all

Table 4.1 Artificial tracers

| Artificial tracers | | | | | |
|--|--|--|--------------------------------------|--------------------------------|-----------------------|
| Dissolved (solute) Solute or in aqueous solution | | | | | |
| Fluorescence tracers | Salt tracers | Radioactive tracers | Activatable tracers (radioactive) | Advanced tracers | Solid |
| Naphthionate | Chlorid (Na^+Cl^- , K^+Cl^-) | Tritium ^3H | Bromide (^{80}Br) | Gases (e.g. SF_6) | Drifting particles |
| Pyranine | Lithium (Li^+Cl^-) | Chrome (^{51}Cr) | Indium ($^{116\text{m}}\text{In}$) | 'Heavy' water (^2H) | Lycopodium spores |
| Uranine | Bromid (K^+Br , Na^+Br^-) | Indium ($^{114\text{m}}\text{In}$, ^{114}In) | Manganese (^{56}Mn) | Fluorobenzoic acids | Fluorescent particles |
| Eosine | Iodide (K^+I^-) | Cobalt (^{58}Co , ^{60}Co) | Lanthanum (^{140}La) | Nonfluorescence dyes | Bacteria/viruses |
| Amidorhodamine G | | Bromide (^{82}Br) | Dysprosium (^{165}Dy) | Temperature | Phages |
| Rhodamines | | | | | DNA |

matters concerning the methodological aspects and the application of artificial tracers:¹ the International Association of Tracer Hydrology (ATH, 1967–2001), the International Commission on Tracers (ICT-IAHS, 1993–2000) and the International Atomic Energy Agency (IAEA, 1983–1991).

The objective of the application of tracers in hydrology is the investigation of water in all its various guises, behaviours and characteristics within the different media and substrates represented in the water cycle. Consequently, conservative tracers representing the flow of water are required. Conservativity exists if the tracer is physico-biochemically stable (nonreactive in natural water) and not sorptive. Good water solubility is also essential (see Section 4.1.2.1).

4.1 Fluorescent tracers

Fluorescent tracers are the most important of the artificial tracers. They are popular among tracer hydrologists because of their relatively easy handling, the seemingly simple analysis, the high sensitivity of the analysis, the low detection limit and, consequently, the small quantity of tracer needed in field experiments. Fluorescent tracers are also attractive because of the linearity of the calibration curve in the measuring scale, and their toxicity levels are very low compared to other tracer substances; some are entirely nontoxic.

Since the first known experiment using the fluorescent tracer Uranine more than one hundred years ago, much effort has been expended in the search for additional dye tracers. However, of the great number of potential fluorescent tracers only a few substances are truly suitable (Tables 4.1 and 4.2). The fundamental methodological basics have been discussed in publications by many authors.² As most of the research work in this area occurred prior to and during the 1980s, only a few papers dealing with the fundamentals of fluorescent tracers have been published in recent years.

Due to the need for toxicity tests, it is unlikely that the tracers currently available will be supplemented by new tracers. Research to find or to develop suitable substances has been largely unsuccessful. Viriot and André (1989) and Netter and Behrens (1992) suggested a few new tracers, none of which have received further application in the field. Hadi (1997) synthesized two new conservative dyes, succinylfluorescein disodium

¹ATH: Maurin and Zötl (1967), Käss (1972), Gospodaric and Habic (1977), Leibundgut and Weingartner (1982), Morfis and Paraskevopoulou (1986), Hötzl and Werner (1992), Kranjc (1997b), Seiler and Wohnlich (2001), ICT-IAHS: Peters *et al.* (1993), Leibundgut (1995), Adar and Leibundgut (1995), Pointet (1997), Peters and Coudrain-Ribstein (1997), Leibundgut, Gunn and Dassargues (1998), Leibundgut, Mc Donnell and Schultz (1999), Kovar *et al.* (1998), Dassargues (2000), IAEA: Drost (1983), Plata (1983), Rao (1983), Florkowski (1991), Mandel (1991), Margrita and Gaillard (1991), Navada (1991), Roldao (1991).

²Feuerstein and Selleck (1963), Käss (1964, 1967a, 1998), Moser and Sagl (1967), White (1967), Drew (1968), Wilson (1986), Gygax and Schwab (1969), Behrens (1971, 1973, 1982), Smart (1976), Smart and Smith (1976) and Smith and Laidlaw (1977), Leibundgut (1974, 1981a), André and Molinari (1976), Leibundgut and Hirsig (1977), Grisak and Pickens (1980), Behrens, Hötzl and Maurin (1981), Davis *et al.* (1985), Behrens (1986), Quinlan (1986), Benischke and Schmerlaib (1986), Leibundgut and Wernli (1986), Mull *et al.* (1988), Hadi *et al.* (1997), Wernli (2003), Flury and Wai (2003).

Table 4.2 The fluorescent tracers suitable for hydrological purposes, ordered according to the fluorescence emission maxima

| Commercial name | Ex/Em max nm | Compound class | Cl: generic name | CI number | Chemical name | Chemical formula | Molecular weight |
|---|------------------|-----------------------------------|---------------------|--------------|--|--|---------------------|
| Naphthionate <i>Naphtionate Sodium- salt</i> | 325/420 | Aminonaphthalen- sulfonic acid | | — | 4-Amino-1-naphtalensulfonic acid sodium salt | C ₁₀ H ₈ NNaO ₃ S | 245.23 |
| Pyranine <i>D&C Green 8</i> | Circa 460/510 | Anthraquinone | Solvent Green | 59040 | 1-Hydroxy-pyren-3,6,8-trisulfon- trisodium | C ₁₆ H ₇ Na ₃ O ₁₀ S ₃ | 524.39 |
| Uranine <i>Sodium-fluorescein, D&C Yellow 7</i> | 491/516 | Xanthene | Acid Yellow 73 | 45350 | Hydroxy-6-oxo-9-(2- carboxyphenyl)-xanthene | C ₂₀ H ₁₀ O ₅ Na ₂ | 332.31 |
| Eosine <i>Eosine Yellow D&C Red 22</i> | 515/540 | Xanthene | Acid Red 87 | 45380 | 3-Hydroxy-6-oxo-2,4,5,7- tetrabromine-9(-2'-caboxyphenyl)- xanthene-disodium | C ₂₀ H ₆ Br ₄ Na ₂ O ₅ | 691.88 |
| Amidorhodamine G <i>Sulforhodamine G</i> | Circa 530/555 | Xanthene | Acid Red 50 | 45220 | 3,6-Bis-ethylamino-2,7-dimethyl-9- 2',4'-disulfophenyl-sodium | C ₂₅ H ₂₅ N ₂ NaO ₇ S ₂ | 552.59 |
| Sulforhodamine B | Circa 560/585 | Xanthene | Acid Red 52 | 45100 | 3,6-Bis-diethylamino-9-(2',4'- disulfophenyl)-sodium | C ₂₇ H ₂₉ N ₂ NaO ₇ S ₂ | 580.65 |
| Rhodamine B | Circa 555/570 | Xanthene | BasicViolet 10 | 45170 | 3,6-Bis-diethylamino-9- (2'carbophenyl)-xanthylum-chloride | C ₂₈ H ₃₁ ClN ₂ O ₃ | 479.02 |
| Rhodamine WT | Circa 560/585 | Xanthene | Acid Red 388 | — | 3,6-Bis-diethylamino-9-(2',4'- dicarboxylphenyl)-xanthylum- sodium | C ₂₉ H ₂₉ N ₂ NaO ₅ | 480.55 |

salt (SF) and 5(6-)-carbocylfluorescein trisodium salt (CF), on the basis of xanthene structures, both of which may be used to extend the spectrum of fluorescent tracers used for special purposes. However, both are not a substitute for Uranine (Hadi *et al.*, 1997). Similarly, Einsiedl and Maloszewski (2005) developed a new fluorescent dye, pyrene-1, 3, 6, 8-tetra sulfonic acid (PTS), but its application is limited. Furthermore, as these new substances cannot yet be synthesized industrially they are very expensive. Rhodamine WTS (CI 555/580 nm) is a new fluorescent tracer that has recently been mentioned as a potential tracer for use in the investigation of drains. However, a detailed description outlining its suitability is not yet available.

The fluorescent tracers deemed suitable for hydrological purposes are presented in Table 4.2. The substance's common name is in bold font. Unfortunately, certain tracers have several commercial names. There are also examples of different tracers with the same name. The only way to overcome this problem is to identify the substances by the colour index (CI) name and number (Quinlan and Smart, 1977; Flury and Wai, 2003), also provided in Table 4.2. It is recommended that the colour index reference be cited in all scientific and applied communications. Other important specific characteristics such as the dye class and atomic weight provide an initial impression of each tracer substance.

Although Pyranine is listed in Table 4.2, and is indeed suitable for special applications, it is not a commonly used fluorescent tracer due to the fact that it is problematic from an analytical perspective and because it is quite expensive. Consequently, Pyranine has hardly been used in decades. It was applied successfully in a multi tracer test with Deuterium and Uranine in a fissured aquifer (Himmelsbach, Hötzl and Maloszewski, 1998). Smart and Smith (1976) reported on experiments using Pyranine in Jamaica, in which the tracer could be evaluated over distances of up to 3 km. Pyranine was used successfully to investigate macropore flow (Smart and Wilson, 1984).

The potential water tracer Rhodamine WTS is not listed. The reason for this is that not all of the relevant information (e.g. CI) is available for the substance, and references regarding hydrological experiments are also missing. However, Wernli (1996) has investigated carefully the substance's suitability as a hydrological tracer. Rhodamine WTS is characterized by an excitation/emission wavelength of 558/578 nm. Its solubility in water is high. Except for its low temperature dependence, the other relevant characteristics are similar to those of the Rhodamines generally. The substance is not available in highly concentrated form, which may be another limitation in terms of its broader application as a hydrological tracer.

4.1.1 Basics of fluorescence

Fluorescence is a luminescence that occurs where energy is supplied by electromagnetic radiation. The substances used for tracing purposes are situated within the small range of visible light between the higher ultraviolet and the infrared wavelengths (ca. 350–750 nm).

Fluorescence is one of the two luminescence phenomena, together with phosphorescence. Whereas phosphorescence takes energy from chemical processes and has an emission pulse of longer than 10^{-4} s, fluorescence has a very short pulse of 10^{-18} s. Fluorescence describes the ability of chemical compounds to emit an activating light impulse as longer-wave radiation. The excitation energy source kicks an electron of an atom from a lower energy state into an 'excited' higher energy state; the electron then releases the energy in the form of light (fluorescence) at which point it reverts to a lower energy state. The emission takes place just as long as the activation occurs, causing only transient fluorescence effects compared to longer-lived phosphorescence (Bandow, 1950; Eisenbrand, 1966).

The intensity of fluorescent emission follows a linear dependence involving the intensity of incident light and the tracer concentration:

$$I_e = A^* I_0^* \varepsilon(\lambda_{ex})^* \Phi(\lambda_{em})^* c^* d \quad (4.1)$$

I_e = fluorescence intensity

A = instrumental constant

I_0 = incident light intensity

$\varepsilon(\lambda_{ex})$ = molecular extinction coefficient at wavelength λ_{ex}

c = tracer concentration

$\Phi(\lambda_{em})$ = quantum yield

d = sample layer thickness

The extinction coefficient depends on excitation, while the quantum yield depends on emission wavelengths. Hence, an excitation scan reflects the properties of the extinction coefficient and an emission scan those of the quantum yield of the respective tracer.

For tracer concentrations in a certain range the intensity of emission is proportional to the tracer concentrations.

$$c \propto I_e \quad (4.2)$$

The linear correlation simplifies the finding of the relationship between intensity measurement and sample concentration, which is done by calibration (Figure 4.2 for Urarine). The upper boundary condition for this is that:

$$c < 1 / (2^* \varepsilon(\lambda)^* d) \quad (4.3)$$

and if not fulfilled, it leads to self-shadowing effects. If the concentration of the sample exceeds the upper boundary, the sample must be diluted to meet the linear range. The usual concentrations in tracer test samples are within the range 0.01–100 mg/m³. The chemical explanation for the fluorescent behaviour of a compound is the organic ring-structure with double bonds (Figure 4.1).

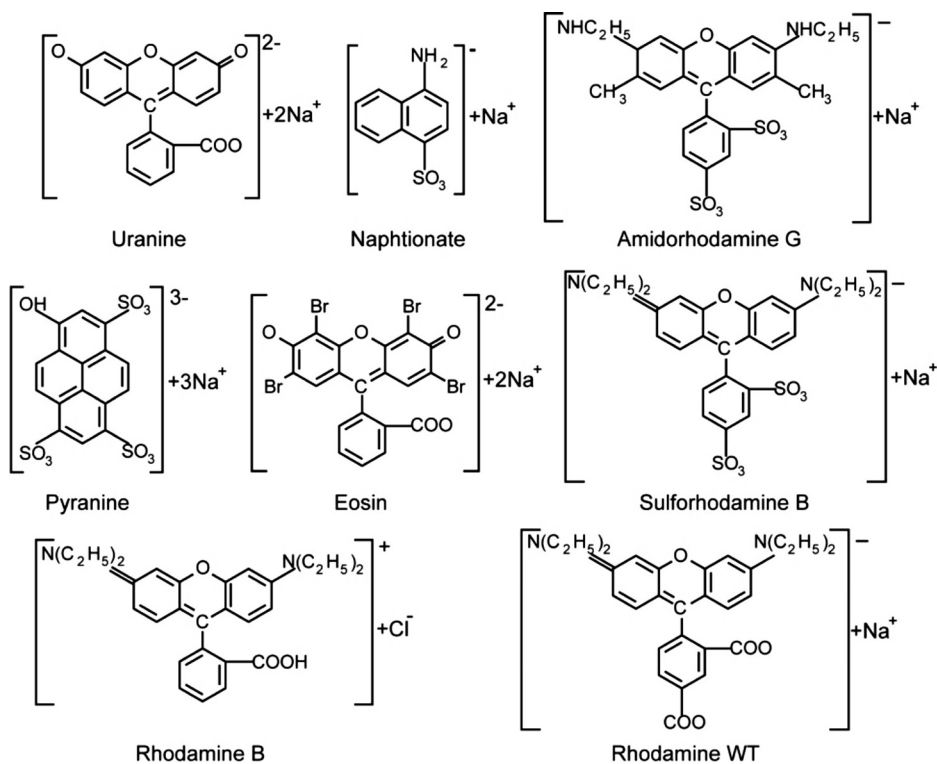


Figure 4.1 Structural formulae of the dyes listed in Table 4.2.

4.1.1.1 Spectra

The maxima of the spectra of fluorescent tracers are characteristic and constant. Having relatively small fluorescence ranges, tracers are well suited for application as hydrological tracers. When analysing fluorescent compounds two spectra, characteristic for each substance, are commonly processed: the excitation-spectrum and the emission-spectrum. They are inverted and their peaks stand apart at a specific wavelength-difference, referred to as 'Stokes shift' ($\Delta\lambda$). In the example below (Figure 4.2: Uranine), the two spectra of Uranine are indicated, with peaks at 491 and 516 nm. The characteristic $\Delta\lambda$ for Uranine is between 20 and 25 nm and is conventionally set to 25 nm to run synchronous scans. It is recommended, however, that the positions of the peaks be checked for each new charge of tracers, particularly in the event of a change of manufacturer.

The units of the spectral analysis are arbitrary. Therefore, in order to gain information about the concentration of the tracer, calibration curves must be produced by running spectral analyses of known tracer concentration samples, as presented in Section 4.1.2.2. The maximum intensity is realized with excitation and emission in the respective peaks of wavelength (Figure 4.2).

In order to avoid interferences between excitation and emission spectra using the classical spectral technique, the *synchronous scan* technique is widely used today

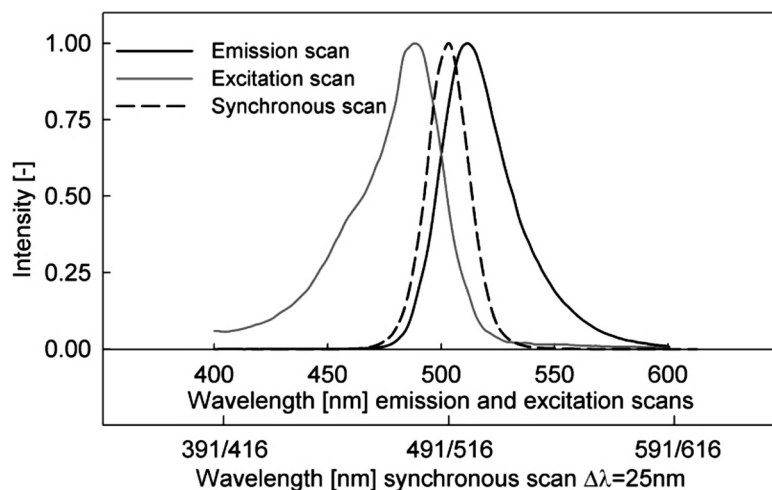


Figure 4.2 Excitation-spectrum (peak $\lambda = 491$ nm), emission-spectrum (peak $\lambda = 516$ nm) and synchronous scan spectrum of Uranine (normalized).

(Figure 4.2). Employing this technique, the two spectra (excitation and emission) are run synchronously with the characteristic $\Delta\lambda$ of the measured substance. The specific $\Delta\lambda$ for Uranine is depicted in Figure 4.2. The most important fluorescent tracers, namely Uranine, Eosine and the Rhodamines, all have the same $\Delta\lambda$ of approximately 25 nm. Although this method alternates the spectra it still possesses the advantages of narrowband spectra, with little light scattering and, therefore, no Raman scattering (see Section 4.1.3.3.1). It also allows for the measurement of multiple tracers in one scan.

A comparison between the Stokes shifts and relative fluorescence intensities of some commonly applied fluorescent tracers are shown in Figure 4.3. The dominant role of Uranine is clearly apparent, due to its much higher fluorescent intensity as compared to any of the other substances. This, and other beneficial properties associated with fluorescent tracers, makes Uranine the most suitable fluorescent tracer generally, and for groundwater in particular, as has been proven in a great number of tracer experiments.

Due to different ionic forms, the excitation and emission spectra of the fluorescent tracers might change. However, the problem can be solved using the synchronous scan technique and, if needed, the adjustment of the sample in the required pH range of the maximal intensity range. Only in the event of extraordinary analytical problems is there a need to consider this aspect carefully (Wolfbeis *et al.*, 1983; Behrens, 1986; Benischke and Schmerlaib, 1986).

4.1.2 Chemical and physical characteristics of dye tracers

The family of molecules that appears most suitable for use as water tracers features the basic structure of xanthene dye. The chemical explanation for the fluorescent behaviour of a compound is the organic ring-structure with double bonds (Bandow,

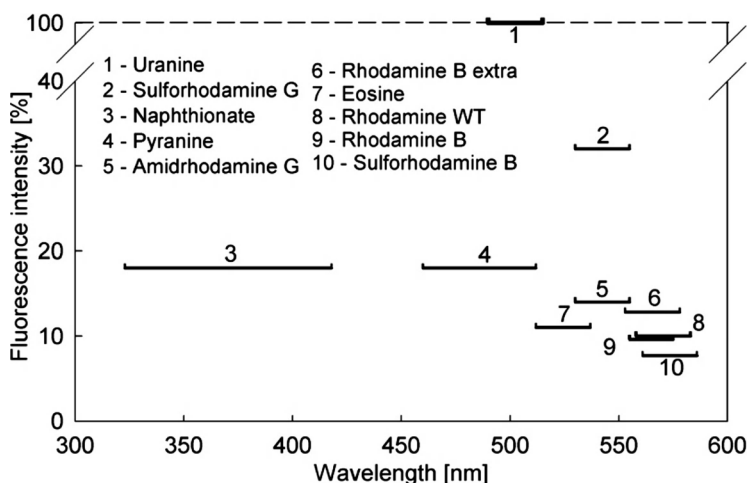


Figure 4.3 Fluorescent tracers: Stokes shifts (nm) and intensities (%) of different tracers. Note the break on the ordinate axis.

1950; Hadi *et al.*, 1997). Hence, the prime molecules suggested as hydrological tracers are the sulfonated xanthene derivatives, where the ring structure (R) is CH_3 , COOH or $\text{CH}_2\text{CH}_2\text{CO}_2\text{H}$ (see Figure 4.4).

The sulfonic acid functional groups, and their sodium salt derivatives, increase the solubility of the molecules. If the chemical structure is destroyed, the fluorescence is also lost. Deterioration may be caused by sunlight, chemical reaction or biological degradation.

A changing pH has the potential to change the electrical charge of the molecule from negative, through neutral to a positive value, and vice versa. If the medium reaches a certain degree of acidity, the protons will break up some of the double bonds, as a result of which the compounds lose their fluorescence until the proton concentration drops again (Figure 4.5). The process is discussed in detail in Hadi *et al.* (1997, p. 32) and Flury and Wai (2003, pp. 2–12).

The xanthenes include many commonly used dyes such as Uranine (sodium fluorescein), succinylfluorescein disodium salt and 5(6-)-carbocylfluorescein trisodium salt, Eosine and all the Rhodamines. Other chemical substances featuring fluorescence are,

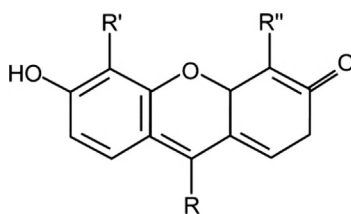


Figure 4.4 Crude sulfonated xanthene derivatives, with $\text{R} = \text{CH}_3$, COOH or $\text{CH}_2\text{CH}_2\text{CO}_2\text{H}$; $\text{R}' = \text{R}'' = \text{SO}_3\text{Na}$ or H (modified from Hadi *et al.*, 1997).

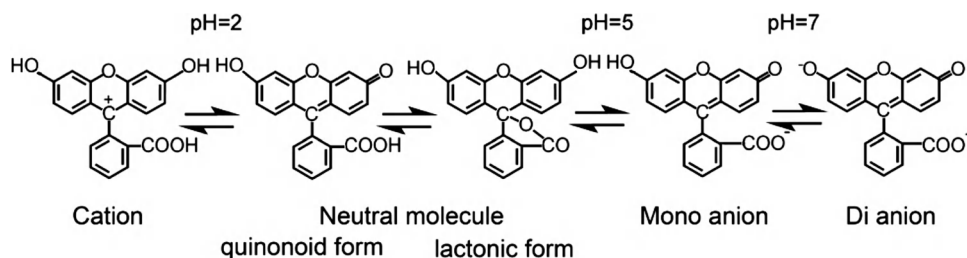


Figure 4.5 Change to the chemical structure and the net charge of Uranine as affected by pH (modified from Lindqvist, 1960; Behrens, 1986).

for example, Pyranine (anthraquinones) and Naphthionate (naphthylamine sulfonic acid). A more detailed summary of the chemical classes of dyes can be found in Käss (1998) and Flury and Wai (2003).

Each tracer application is individual and many things have to be taken into consideration. In addition to the most important property discussed above, conservativity, there are certain basic requirements that a tracer should meet. These requirements of tracers in general, and of artificial tracers in particular, are listed in Table 4.3.

4.1.2.1 Solubility

The solubility of tracers in water is a crucial requirement of tracers used to investigate water flows in the hydrological cycle as the tracer should be as close to the characteristics of water as possible. As fluorescent tracers are organic dyes, the solubility of nearly all is low, and some are even hydrophobic. The more soluble tracers include those listed in Table 4.2. Their solubility depends on both the temperature and the pH of the water.

Table 4.3 Required properties of artificial tracers in general and of fluorescent tracers in particular. The properties in bold are the main characteristics of conservative tracers

| Properties to be considered | Requirements of an ideal (conservative) tracer |
|---|--|
| 1. Solubility in water | High |
| 2. Fluorescence intensity | High |
| 3. Detection limit | Low |
| 4. pH dependence | Low |
| 5. Temperature dependence | Low |
| 6. Photolytic stability | High |
| 7. Sorption processes | Negligible |
| 8. Chemical and biological stability | High |
| 9. Toxicity and related environmental effects | None or minimal |
| 10. Costs and other practical aspects | Low or moderate |

The higher pH and temperature, the higher the compound's solubility. Thus, the more hydrophilic functional groups the molecule has, the higher its solubility in water. A substance's solubility is correlated inversely with adsorption (Bailey and White, 1970; Leibundgut and Wernli, 1986; Shiau, Sabatini and Harwell, 1992). The extent of the solubility of an organic compound in water depends upon its ability to form hydrogen bonds and van der Waals interactions.

The soluble tracer amounts (g/l) for pure water at a temperature of 20 °C are as follows: Pyranine (178), both Uranine and Eosine (300) and Naphthionate (240). They are characterized by good to very good solubility. By contrast, the solubility of the Rhodamines (3–20 g/l) is considerably lower (see Table 4.10). It is worth mentioning that, as a neutral molecule, fluorescein is poorly soluble in water, but as a charged molecule (from sodium fluorescein – Uranine) it has very good solubility (Hadi *et al.*, 1997; Flury and Wai, 2003).

The solubility of a substance can be increased by adding appropriate chemicals. However, each chemical added to water in nature represents a contamination. Therefore, chemicals should only be used in special situations, such as in the case of experiments in glaciers at low temperatures. In field experiments the dissolved amount of tracer can deviate from the solubility measured in the laboratory, due to the presence of salts or other materials, and factors such as pH and temperature.

4.1.2.2 Fluorescence intensity – detection limit

The fluorescence intensity of a trace substance depends on its physical properties, namely quantum yield, extinction coefficient and tracer concentration, as described in Section 4.1.1. This feature plays a crucial role insofar as the detection limit depends, on the one hand, on the fluorescence intensity to which it is positively correlated and, on the other, on the sample background. Due to higher scattering at wavelengths in the UV range (300–500 nm), the sample background concentration of those tracers is higher and, consequently, the detection limit lower. This mainly concerns Naphthionate and Pyranine. This becomes apparent in Table 4.4, where fluorescence intensity and

Table 4.4 Detection limits in pure natural water (groundwater) under optimal technical measuring conditions

| Dye | Relative fluorescence intensity [Uranine = 100%] | Detection limit [mg/m ³] | Excitation/emission [nm] |
|------------------|--|--------------------------------------|--------------------------|
| Naphthionate | 18 | 0.2 | 325/420 |
| Pyranine | 18 | 0.06 | 455/510 |
| Uranine | 100 | 0.001 | 491/516 |
| Eosine | 11.4 | 0.01 | 515/540 |
| Amidorhodamine G | 32 | 0.005 | 530/555 |
| Rhodamine B | 9.5 | 0.02 | 555/575 |
| Rhodamine WT | 10 | 0.02 | 560/585 |
| Sulforhodamine B | 7 | 0.03 | 561/586 |

detection limits are considered. The detection limit is clearly not the same for the different measurement devices. Using modern optical fluorometers the detection limits of fluorescent tracers in pure natural water are very low. The limits quoted in Table 4.4 are applicable for tracers measured in pure water by means of both optically and electronically optimal measurement sets. Using an optical fluorometer some of the lower detection limits stated are neither realistic nor reliable.

By the application of advanced techniques like HPTLC/AMD (Weiss *et al.*, 2008) lower detection limits are attainable. However, the costs and the time consuming analysis may restrict the operational use remarkably. Further information concerning advanced measurement techniques is discussed in Section 4.1.3.8.

When analysing surface water samples, or other nonoptically pure water, the background is relevant. Consequently, the detection limit may differ due to the scattering of light caused by the presence of suspended particles or green-blue fluorescents in natural water. The higher the background signal the lower the detection limit (Figure 4.6).

In order to improve the situation it is often sufficient to leave the sample to settle overnight so as to allow for the sedimentation of the suspended material. Should filtering be required, the use of membrane filters ($1\ \mu\text{m}$) or $0.45\ \mu\text{m}$ filters will suffice.

The intensity of fluorescence follows a function that is linear to the tracer concentration. This simplifies the measurement of fluorescence considerably. The shape of the curves is that of a straight line (Figure 4.7).

However, the linearity is only valid within a constricted concentration range of each tracer. According to Wilson (1968), linearity is given for up to several hundred mg/m^3 of the common tracers. Käss (1998) stated that Uranine, for example, exhibits a linear relationship, even up to approximately $1000\ \text{mg}/\text{m}^3$. Experience with modern devices indicates the range of linearity to be smaller. When measuring higher concentrations a self-shadowing effect occurs (concentration quenching), which prevents a direct measurement. The upper molecules may reduce the excitation beams of deeper molecules and, in the event of an overlap of excitation and emission spectra, the emitted light

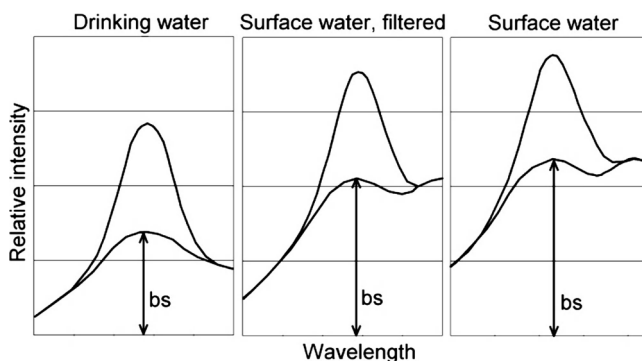


Figure 4.6 Spectral curves and background signals (bs) of Naphthionate ($1\ \text{mg}/\text{m}^3$) in different waters. The excitation and emission peaks lie at 325 and 420 nm, respectively. The relatively high background signals are caused by high scattering and the occurrence of blue fluorescents (Leibundgut and Wernli, 1986).

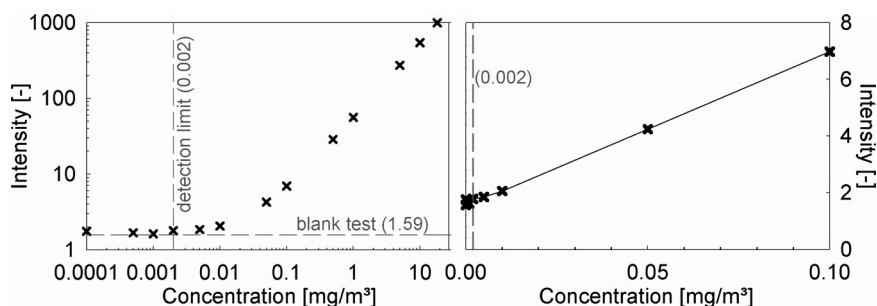


Figure 4.7 Calibration curve of Uranine in the range of linearity up to a fluorescence intensity of approximately 20 mg/m^3 ($y = 54.553x + 2.26213$; $R^2 = 0.99$) (for concentration $> 0.002 \text{ mg/m}^3$). Note the nonlinearity in the range of very low intensities around the detection limit.

may be reabsorbed (Rost, 1991). In this case the sample must either be diluted to an adequate concentration range, or grey filters or smaller slits must be attached to lower the excitation light.

The favourable linearity of the fluorescence over a wide spectrum is much lower due to the measurement range of the fluorometers. Usually, samples with a concentration $> 20 \text{ mg/m}^3$ have to be diluted. For practical purposes, it is recommended that the samples always be diluted to the measurement range quoted for the device used. The effect of this is to ensure that the nonlinearity of higher concentrations remains negligible and a modifying effect of the device and the layer thickness of the sample is avoided.

Near the origin the concentration/intensity curve is not strictly linear, which introduces an uncertainty for very low tracer concentrations around the detection limit. This is a fundamental problem and careful consideration is necessary. As the user becomes familiar with the calibration of the fluorometer it is normal that, once it has been established, the calibration remains valid for a long time, and the number of standards needed is reduced. However, occasional spot checks should be carried out. A recalibration is necessary whenever changes are made to a device; for example after removing the lamp.

Naphthionate, Eosine and the Rhodamines exhibit linearity similar to that of Uranine. The detection limit for Pyranine is more complicated, due to the high dependence upon the pH value, and the corresponding effect on the wavelength. A detailed description of Pyranine analysis was provided by Launay *et al.* (1980) and Benischke and Schmerlaib (1986). The analyses of tracer concentrations near the detection limit require careful consideration of all of the relevant dependencies – both the physical and the chemical – in order to avoid misinterpretation (Figure 4.7). Several repeat measurements of the samples are recommended, sometimes in combination with additional techniques, as described in Section 4.1.2.4.

4.1.2.3 Effects of dependencies

The properties presented in *italics* in Table 4.3 are the main characteristics defining conservative tracers, which are crucial particularly for quantitative investigations of

the water flow and hydrodynamic properties of groundwater and surface water. The dependence of fluorescence not only upon pH, temperature and light, but also upon chemical and microbiological effects (metabolism), can result in the degradation of the fluorescence in water samples and in natural water bodies. Consequently, when performing experiments using fluorescent tracers careful consideration of these aspects is required in both the planning of these experiments and in the analysis. Generally, the issue of pH dependence is of particular importance in experiments involving groundwater and soil water. Photolytic dependence, except in the case of surface water and temperature dependence, is usually not especially problematic.

However, the pH value and the photolytic effect can also be helpful in solving certain analytical problems such as, for example, the measurement of two or more tracers in the same sample (see Sections 4.1.2.4 and 4.1.2.6).

4.1.2.4 pH dependence

As was mentioned previously, a changing pH has the potential to change the net charge of the molecule from negative, through neutral to positive, and vice versa (see Figure 4.5). If the medium reaches a certain degree of acidity, the protons will break some of the double bonds, causing the compounds to lose their fluorescence until the proton concentration falls again. Variations in the pH value of the traced water have a twofold impact on fluorescent tracers: (i) on the analysis and (ii) on the degree of sorption affinity of the tracer.

4.1.2.4.1 Analytical problems Due to the different structures discussed above, the sensitivities of fluorescent tracers to pH vary, as illustrated in Figure 4.8.

Uranine and Pyranine react very sensitively to pH values below the range of most natural waters. Solutions in low mineralized water or in pure water must be alkalized before measuring. The fluorescence intensity of Pyranine in low buffered water may fluctuate strongly. Pyranine detection is more complicated due to the high dependence upon the pH value and the subsequent wavelength shift. A synchronous scan using a wavelength interval $\Delta\lambda = 25$ nm is optimal in the maximum of 445 nm. For alkaline solutions a $\Delta\lambda = 50$ nm is recommended, and for intermediate pH values (5–7) a $\Delta\lambda = 107$ nm (Benischke and Schmerlaib, 1986). A slightly different instruction is provided by Launay *et al.* (1980). Eosine and Naphthionate only react in a more acid environment, at pH values <5.5 . Therefore, they are usually easy to handle in the lab. The Rhodamines are less sensitive to pH and usually pose no analytical problems in natural waters.

As the pH dependence of dye tracers is reversible under natural conditions the problem of pH dependence can be managed quite simply. A sample showing a pH value below the critical boundary for a certain dye tracer (Figure 4.8) can be brought into the range of its maximum fluorescence intensity by means of adequate buffering. In principle, all solutions of the pH sensitive tracers should be buffered. In the case of highly alkaline solutions complexation is required to avoid the precipitation of alkaline earths.

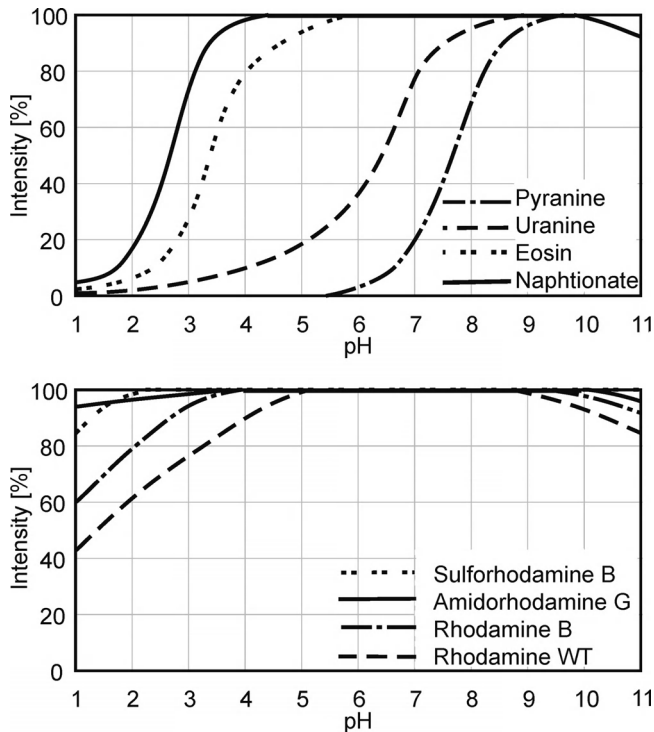


Figure 4.8 The pH dependencies of the fluorescence tracers measured in a synchronous scan at a wavelength interval of $\Delta\lambda = 25$ nm (modified and supplemented after Smart and Smith, 1976; Käss, 1998).

The reversibility of the pH dependence can also be advantageous in tracer analysis. Having conducted a multitracer test with two or more fluorescence tracers, the sample may contain a mixture of tracers. Due to the different pH dependencies, it is possible to separate them. The procedure will be described in Section 4.1.3.

The pH problem is more difficult to manage when performing in situ experiments, as here it is not possible to take advantage of the reversibility of pH dependence. pH should be measured during the online detection of fluorescence. However, using the curves presented in Figure 4.8, the necessary correction can be calculated when conditions within the medium are stable. The pH of natural waters is usually stable during measurement, except in low mineralized waters, which are poorly buffered (e.g. in crystalline catchments). Long term monitoring in the headwaters of catchments with differentiated geology, where there are changing pH values, may prove to be a serious problem.

4.1.2.4.2 Sorption problems The sorption affinity of the tracers also depends on the pH value. As was mentioned above, changing pH values have the potential to change the electrical charge of the molecule. This leads to the sorption effect of pH dependence. The higher the pH the lower the sorption. Fluorescent tracers are mostly organic molecules with various functional groups attached to the molecular kernel. In

addition, the functional groups protonate and deprotonate depending on pH, thereby changing the net charge of the molecule (Flury and Wai, 2003).

Consequently, certain tracers tend to be absorbed in different proportions within acidic media and substrates. In the case of experiments to be carried out in such media, it is necessary to consider carefully whether it is possible to use fluorescent tracers or not. Negative analyses caused by pH-induced absorption may lead to a complete misinterpretation of an experiment if the result is interpreted as an inexistent hydrological connection. The problem is discussed in Leibundgut (1974), Behrens, Oerter and Reinwarth (1982) and in the Section 7.5.2. In natural waters problems occur principally in acid soils, peat-bog and swamp regions, and generally in crystalline geological settings. Since these features are characteristic for the tropics and subtropics as well as the arctic, the use of fluorescent tracers is to be handled carefully in these regions. Typically only a few experiments are known to have been performed in these regions (Smart and Smith, 1976).

4.1.2.5 Temperature dependence

The temperature dependence of the fluorescent tracers is usually unproblematic. Fluorescence intensity and temperature are inversely proportional. For analytical purposes this dependence may be neglected during analysis and calibration, provided the laboratory temperature is 20 °C and measurement lasts no longer than 30 s (Feuerstein and Selleck, 1963; Leibundgut, 1974, 1978; Behrens and Demuth, 1992). The standardization of deviant temperatures can be made applying the equation resulting in the constants in Table 4.5 (Leibundgut, 1978):

$$F_s = F * \exp(h(T_s - T)) \quad (4.4)$$

F_s – fluorescence at temperature T_s

F – fluorescence at temperature T

h – tracer dependent coefficient (1/°C)

T_s – standard temperature (°C)

T – measurement temperature (°C)

Again, the products of different producers may exhibit a slightly different constant value (h). In order to be certain a controlling calibration is recommended.

Measurements made during in situ tests always require a standardized water temperature of 20 °C using the constants in Table 4.5. This may be difficult during tests in which there are rapid variations in temperature; for example in surface water tests (Leibundgut and Zupan, 1992). Further information on this subject is provided in Chapters 6 and 7.

4.1.2.6 Photolytic dependence

Unlike pH dependence, exposure to light has an irreversible effect on fluorescence. Therefore, the use of fluorescence in the study of surface waters is feasible only to a

Table 4.5 Fluorescent's tracer constants (h) of temperature dependence

| Tracer | Coefficient (h) |
|-------------------------------|-----------------|
| Naphthionate ^a | −0.0056 |
| Pyranine ^b | −0.0019 |
| Eosine ^c | 0.00036 |
| Uranine ^c | −0.0041 |
| Rhodamine B ^c | −0.0172 |
| Amidorhodamine G ^c | −0.0041 |

^aAnalysed at the tracer laboratory of the Institute of Hydrology, Freiburg, in 2008.

^bSmart and Smith (1976).

^cLeibundgut (1978).

limited extent. In soil and groundwater experiments photolytic decay is usually not a problem.

As neon light has a short wavelength the samples in the lab also undergo degradation during exposure. Therefore, only the sample currently being analysed should be handled in full light, whether neon or daylight. The other samples need to be covered. This applies in both the lab and out in the field.

The photolytic degradation of a substance is described by a first-order equation and depends on the energy of the excited state formed. The higher this energy and the longer the irradiation time (t), the greater the decomposition of the molecule of the excited substance. The smaller that (t) is, the less time the molecule has to react (Viriot and André, 1989):

$$I(t) = I_0^* \exp(-kt) \quad (4.5)$$

$I(t)$ = fluorescence after irradiation time t

I_0 = fluorescence at irradiation time t = 0

k = degradation coefficient

t = irradiation time

The decay rate is correlated inversely to the tracer concentration. The lower the concentration, the higher the decay rate. This is probably partly due to the filter role of the molecules at high concentrations. At high concentrations the molecules in the bulk of the solution are shielded from the incident light by the high absorption near the surface (quenching effect) and, therefore, fewer molecules degrade (Leibundgut, 1978). However, Feuerstein and Selleck (1963) claimed that the decay rates are independent of concentration in the range 1–100 mg/m³. Temperature is another factor involved in photochemical decay. However, as the temperature correction (Equation (4.4)) indicated, a difference of less than 2%, which is within the error deviation range (Behrens and Demuth, 1992), can be neglected.

Many of the researchers who have investigated the rapid photochemical decay of fluorescent tracers, mostly that of Uranine, did so under controlled conditions in the

Table 4.6 Benchmark values of the measured and the relative half-life values of dye tracers due to photolysis. The data are not strictly comparable due to different test conditions

| Fluorescence tracer | Measured half-life $T_{1/2}$ (h) | $T_{1/2}$ tracer/ $T_{1/2}$ Uranine |
|---------------------|-------------------------------------|--|
| Naphthionate | 41 | 3.7 |
| Pyranine | 47 | 4.3 |
| Uranine | 11 | 1 |
| Eosine | 6 | 0.5 |
| Amidorhodamine G | 550 | 50 |
| Rhodamine B | 790 | 71 |
| Rhodamine WT | 1300 | 118 |
| Sulforhodamine B | 820 | 75 |

lab (Leibundgut, 1974, 1978; Werthemann, 1980a, b; Behrens and Teichmann, 1982; Behrens and Demuth, 1992; Hadi, 1997). Even so, the results differ considerably. The boundary conditions of the lab experiment, such as radiation amount, wavelengths, temperature, type of bottle used and their radiation transmission, differ to the extent that only benchmark values can be provided (Table 4.6 and Figure 4.9).

Behrens and Teichmann (1982) discovered that for some dyes the process of photolytic decay does not necessarily follow a first-order equation as described above. As can be seen in Figure 4.9 (left), the rates of decay of Pyranine, Uranine, Eosine and Naphthionate follow straight lines, which contrasts with those of the Rhodamines (Figure 4.9, right). To the surprise of the investigators, however, when dissolved in pure water the Rhodamines also plotted as straight lines following a first-order equation.

Table 4.6 and Figure 4.9 clearly indicate two groups of tracers. The first are fluorescent tracers with excitation maxima below 520 nm (Eosine, Uranine, Pyranine, Naphthionate) and the second are those with maxima above 520 nm (Rhodamines). The latter are less sensitive to photochemical decay. The values given in Table 4.6 indicate the different sensitivities of tracers to light and should be consulted when planning the use

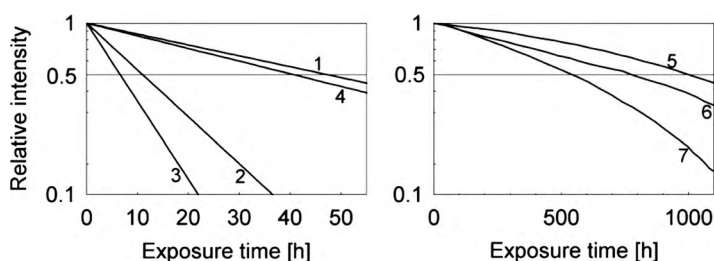


Figure 4.9 Photolytic decay of various fluorescence tracers caused by exposure to light. Left: tracer group with an excitation maximum below circa 520 nm (1: Pyranine, 2: Uranine, 3: Eosine, 4: Naphthionate). Right: tracer group with an excitation maximum above 520 nm (5: Rhodamine WT, 6: Sulforhodamine B, 7: Amidorhodamine G) Note the different time scales. [Source: Behrens and Teichmann, 1982; Wernli, 1986].

of fluorescent tracers in experiments. In principle, the two standard tracers, Uranine and Eosine, are not suitable for surface water experiments.

Under ideal laboratory conditions photolysis follows a strict law (Equation (4.5)), which is generally not applicable under field conditions. Here photolytic decay depends on the intensity of the radiation to which the tracer molecule is exposed. This intensity is not constant in space and time. It changes with different atmospheric conditions, the shading effects of trees and turbidity and/or turbulence effects (Hadi, 1997). The half-life lengths and decay rate values quoted in Table 4.6 and Figure 4.9 are, therefore, benchmark or guideline values to be referred to when planning field experiments. They allow for a rough estimation of photochemical decay under the conditions of a specific experiment. Consequently, they make an assessment of the suitability of a certain tracer for a particular experiment, and the calculation of the required tracer mass possible, but they do not allow for precise corrections. To be safe, the values should be considered to be minimum values as the decay rates under natural conditions may be higher rather than lower.

Experience shows that even the parallel measurement of radiation conditions during an experiment is problematic, due to the highly variable surrounding conditions described above, and also the water itself where turbulence and the varying layer depths result in further uncertainties (Petermann *et al.*, 1989). However, provided a successful determination of the photolytic decay during tracer experiments in rivers is achieved, a decay correction term can be introduced in the calculation of the flow parameters (Petermann *et al.*, 1989; Naturaqua, 1994). For further detail refer to Section 7.4.3.

Whereas no problems are to be expected in groundwater experiments, except where the sampling is effected in springs, it is readily apparent that tracer tests carried out in surface waters need to be rather of a relatively short duration. Great caution must be exercised when making quantitative measurements employing fluorescent tracers in rivers and lakes (see Section 7.3). In the case of surface waters the optimal time for tests using fluorescent tracers is at night. All in all, intelligent test arrangements may provide good solutions to this problem; for example, the use of the highly sensitive Uranine in a lake experiment carried out to determine the residence time of water in Lake Bled, Slovenia. The half-life time for Uranine of 11 h was used to calculate the decrease in the concentration and quantity of Uranine (Leibundgut and Zupan, 1992). Photolytic decay is crucial when using the tracer dilution method to determine runoff quantitatively. In this case, the problem can be eliminated or minimized only in experiments of very short duration carried out under adequate weather conditions (clouded), along shaded stretches of river or at night (see Chapters 6 and 7).

This dependence can also be useful, however. It is an effective way to eliminate specific tracers from a sample mixture (see Section 4.1.3.3). Photolytic decay can, in principle, also be turned into an advantage by using the relationship between irradiation and decay to measure the irradiation by assessing the decay of a known tracer substance over time. Leibundgut (1978) investigated this technique, developed the so-called fluorescence-actionometer (a bulb of special glass) and applied a number of them as free floating measuring points beneath the surface of a small lake. Field monitoring experiments lasting several weeks and requiring low maintenance are possible. The same approach was investigated systematically by Behrens and Demuth (1992).

4.1.2.7 Sorption processes

Sorption behaviour is the most important property relevant to the use of artificial tracers generally, and fluorescent tracers in particular. Sorption is a crucial process in the performance of experiments in the saturated and unsaturated zones. A first indication of the sorption behaviour of a tracer is provided by the solubility. The higher the solubility of a tracer substance, the lower its sorption (see Table 4.10). An exception is Amidorhodamine G, which has a low degree of solubility of approximately 3 g/l but possesses comparatively good sorption characteristics. Depending on their molecular make-up, fluorescent tracers exhibit widely contrasting reactions upon contact with different substrates. Generally anionic and neutral substances are less susceptible to sorption than cationic. Cationic tracers usually interact more strongly with the substrates, but both groups usually react in a way that is referred to as reversible sorption leading to retardation, the effect of which is chromatography (Leibundgut, 1981b).

The amphiphilic nature of fluorescent tracers and the fact that the electrical charge of the molecule is subject to change mean that their interaction with solid surfaces is complex. Sorption of dyes to solid surfaces involves one or a combination of the following interactions: hydrophobic, van der Waals, ion exchange, covalent bonding and hydrogen bonding (Zollinger, 1991; Schwarzenbach, Gschwend and Imboden, 1993; Flury and Wai, 2003). Rhodamine WT consists of two isomers with different sorption characteristics, which can lead to retardation (Shiau, Sabatini and Harwell, 1992; Sutton *et al.*, 2001; Hadi, 1997).

However, the averaged transport velocity of dissolved anionic tracers through sediments may be even greater compared to that of the water molecules due to anion exclusion (Gvirtzman and Gorelick, 1991). The electrostatic repulsion by negatively charged solid surfaces forces the tracer anions into the centre of the pores where the velocity is faster. The effect has been shown for Naphthionate in laboratory and field tests (Leibundgut and Wernli, 1986; Sansoni *et al.*, 1988).

The identification of sorption in a tracer experiment is quite difficult. The reason for this is that several processes, such as adsorption, absorption and so on, result in the 'sorption' of tracers. For tracer hydrological purposes, the phenomenon of the ratio of injected tracer mass captured by one or more of these processes is usually important. Leibundgut (1981b) proposed, therefore, that the definition of sorption in tracer hydrology be 'the total of the sorpted tracer caused by all or a part of the processes involved'. The fundamentals of the sorption processes themselves will not be discussed further here, but their impact on a tracer breakthrough will be presented in Figure 4.10.

The surfaces of soil and aquifer particles are usually negatively charged. The degree of sorption in these substrates rises from 0 to 100%. The latter number reflects an irreversible sorption, and a hydrological tracer which is consequently unusable.

The problem of reversible sorption is shown clearly in Figure 4.10. Curve A (ideal tracer) represents the breakthrough of water movement ($v_{\text{water}} = v_{\text{tracer}}$), the behaviour of the substance we wish to know more about. Curve B alternatively represents the breakthrough of a nonideal sorptive tracer ($t'_o = t_t - \text{mean transit time of tracer}$),

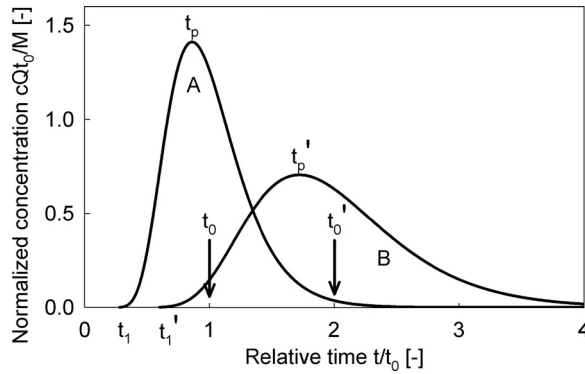


Figure 4.10 Effect of chromatography caused by reversible adsorption depicted in a tracer breakthrough curve. Curve A: ideal tracer breakthrough (t_0 – mean transit time of water); that is without any sorption effects. Curve B: reactive tracer breakthrough following a reversible reaction with an instantaneous equilibrium ($t'_0 = t_t$ – mean transit time of tracer). In both cases the recovery of the tracer is complete (100%).

resulting in lower flow velocities. The second tracer (curve B) follows reversible sorption with instantaneous equilibrium, which leads to a slower transport of the tracer relative to the flow of the water (see Equation (4.6)).

A precondition of the investigation of the flow dynamics of water is an ideal tracer representing the water flow, or at least a nearly ideal tracer. The mathematical description of the ideal tracer transport phenomenon is given in Chapter 5. However, not all of the available tracers are strictly conservative. Different mathematical models can be used to describe the reaction of a nonideal tracer with the matrix (e.g. Carnahan and Remer, 1984). Most tracer hydrologists, however, generally assume that a nonideal tracer reaction is followed by instantaneous equilibrium and a linear reaction isotherm, which is described by Equation (4.6). In this case, the transport of the nonideal tracer is slower than the flow of the water (curve B in Figure 4.10) by the retardation factor (R_d), described by Equations (4.7) and (4.8). This type of reaction is seldom observed in practice.

It is known from the literature that, in the case of nonideal tracers, two or even three reactions may often occur simultaneously. The conceptual outline of some of the types of reaction that occur between water (solute) and a porous matrix is provided in Figure 4.11. In the first-order reversible kinetic reaction model, the parameters k_1 and k_2 are the forward and backward reaction rate constant, respectively ($k_1 > 0$; $k_2 > 0$). The irreversible first-order reaction in which k_{irr} is the irreversible reaction rate constant (e.g. radioactive decay, biodegradation) is also incorporated in Figure 4.11. In the event that the first-order kinetic reaction becomes irreversible ($k_2 = 0$), the forward reaction rate is equal to k_{irr} . The parameter R_3 describes the retardation of pollutant movement relative to the flow of water in the case of an instantaneous equilibrium reaction. When both first-order kinetic (reversible or irreversible) and linear equilibrium reactions occur simultaneously the so-called two-site (or combined)

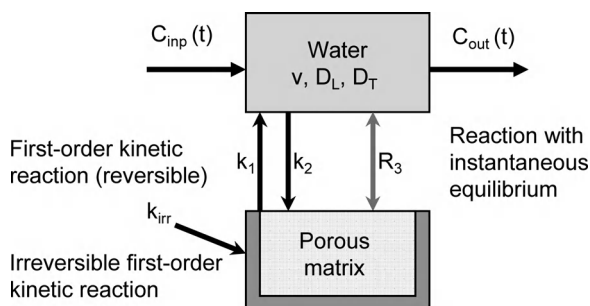


Figure 4.11 Dispersive transport in water (convection and dispersion). Presentation of some theoretical reactions between water (solute) and a porous matrix.

reaction model introduced by Cameron and Klute (1977) applies. This particular model combines two reactions: instantaneous equilibrium with a linear sorption isotherm and a first-order (reversible or nonreversible) kinetic reaction. Some typical tracer breakthrough curves yielded by the two-site reaction model are shown in Figure 4.12, where they are compared to the curve of an ideal tracer, which follows only convective-dispersive transport within flowing water.

In practice it is very important that tracer mass recovery be calculated according to Equation (5.40) in Chapter 5. The curve can help reveal the type of reaction that occurs between the matrix and the pollutant follows (Figure 4.13).

The analytical solution for convective-dispersive transport coupled with a combined (two-site) reaction model was developed by Klotz, Maloszewski and Moser (1988), and applied to evaluate the migration of two radioactive pollutants (strontium and europium). Hendry, Lawrence and Maloszewski (1997, 1999) used the same model

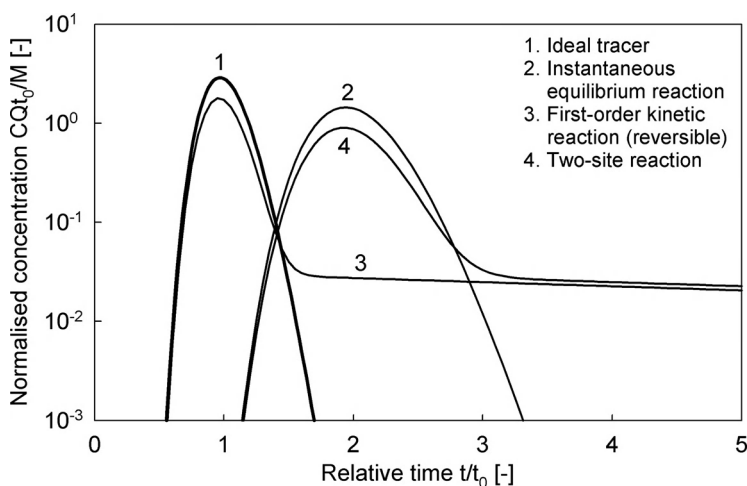


Figure 4.12 Tracer breakthrough curves observed after instantaneous injection of two tracers: ideal (1) and nonideal curves (2-4).

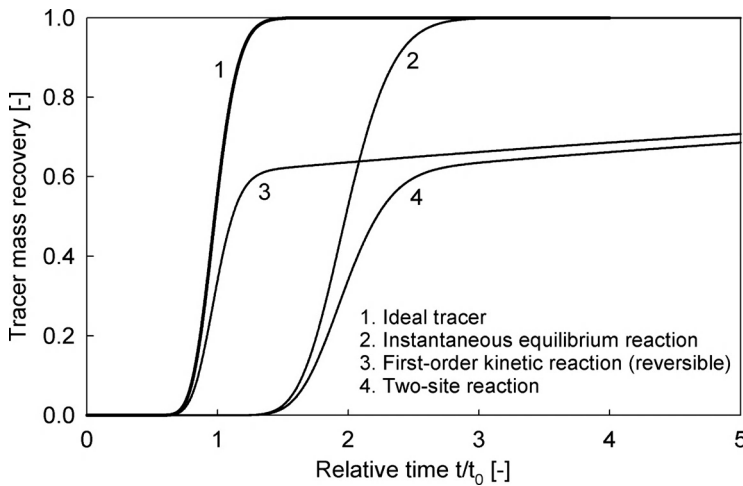


Figure 4.13 Tracer mass recovery curves calculated for the examples illustrated in Figure 4.12.

successfully to describe bacteria migration in a sand column, while Maloszewski *et al.* (2003) used it to describe herbicide transport in a porous aquifer. Maloszewski and Zuber (1990) also employed it in the interpretation of a multi-tracer test performed in fractured marls. The transport of nonideal tracers (contaminant transport) is not, however, the focus of this book. Some key publications are listed below for the benefit of the interested reader.³

The purpose of the following general considerations in relation to sorption is intended to illustrate the process. In general, tracer experiments in sandy substrates using suitable tracers (Table 4.2) allow for a complete, or nearly complete, recovery of the tracer, permitting a correct calculation of the aquifer parameters (Figure 4.14). Experiments in clayey material, however, usually result in incomplete recovery (Figure 4.15). The two Figures show two column experiments to investigate the tracer recovery of Uranine in a sandy (Figure 4.14) and in a clayey (Figure 4.15) substrate. Phase A_i represents the column transits by the tracer solution, including both saturation of column water and sorption processes, and phase B_i flushing transits with clear water and desorption. The simulation in the lab replicates the natural conditions present during a tracer experiment with an instant injection (Dirac impulse). In natural experiments the two processes occur simultaneously (Leibundgut, 1981b).

As well as aiding in the selection of tracers for field experiments and in the calculation of the amount of tracer to be injected, the two parameters K_d (distribution coefficient) and R_d (retardation coefficient) characterizing sorption processes are commonly used when the instantaneous equilibrium reaction with a linear sorption isotherm is applicable. The parameters are discussed in the following paragraphs.

³Cameron and Klute (1977), Carnahan and Remer (1984), Hendry, Lawrence and Maloszewski (1997, 1999), Klotz, Maloszewski and Moser (1988), Maloszewski and Zuber (1990), Maloszewski *et al.* (2003).

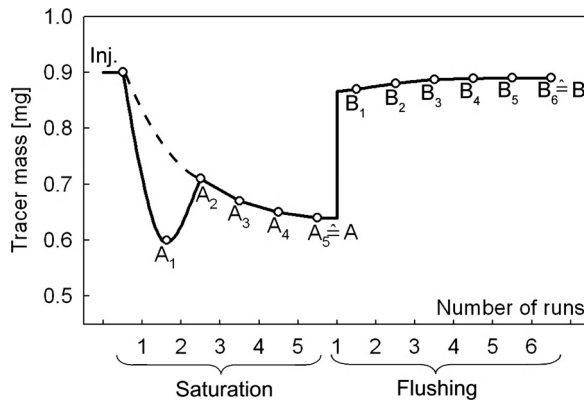


Figure 4.14 Tracer breakthrough curve of Uranine in a sandy substrate showing complete tracer recovery. Sorption during phase A is caused by saturation of the column water, whereas phase B represents the flushing effect.

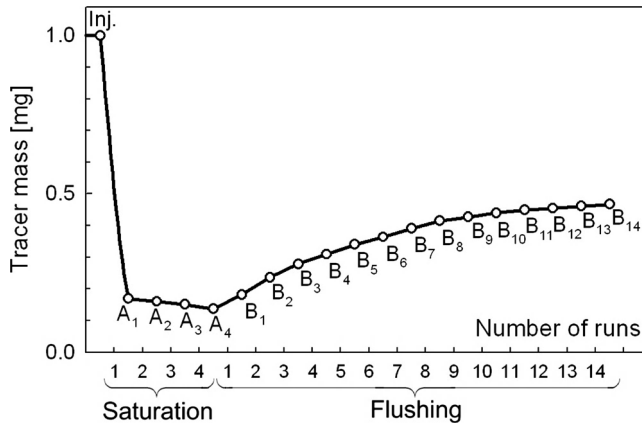


Figure 4.15 Tracer breakthrough curve of Uranine in a brown soil substrate showing incomplete tracer recovery with sorption of approximately 50% of the injected tracer mass.

4.1.2.7.1 The distribution coefficient K_d Distribution coefficients are commonly determined in batch experiments using the following equation:

$$K_d = V/m \cdot \frac{c_i - c_s}{c_s} [\text{cm}^3/\text{g}] \quad (4.6)$$

where

V = volume of the solution,

m = mass of the dry substrate,

c_i = initial tracer concentration and

c_s = dissolved tracer concentration (equilibrium solution).

K_d = depends on the ionic composition of the exchanger and the solution.

K_d represents the mobility of the tracers in groundwater, describing the thermodynamic equilibrium of the tracer between substrate and solution. Obviously, the tracer concentration has a strong impact on the sorption level of the tracer. The higher the K_d value, the higher the sorption. This process assumes the linear sorption isotherm with instantaneous equilibrium. One should take into account that most sorption/desorption processes follow a kinetic linear or nonlinear reaction. Hence, Equation (4.6) is not always applicable. For the batch experiment a short instruction is given in the box below.

The distribution coefficient K_d is determined by means of a batch test as follows:

Add 250 ml tracer solution (volume V with a concentration c_i) to a glass bottle containing 100 g of substrate (m) dried at a temperature of 105 °C. Shake for 24 h at a rate of 140 shakes per minute. After 24 h the tracer concentration in the equilibrium solution (c_s) is measured. K_d is calculated according to Equation (4.6).

Numerous sorption tests have been performed and further distribution coefficients can be found in the literature.⁴ In general, distribution coefficient values depend not only on the tracer properties, but also on the substrate (e.g. texture, material, grain size) and on the concentration, and so exhibit a high degree of variability (e.g. Ptak and Schmid, 1996; German-Heins and Flury, 2000). Values resulting from laboratory sorption experiments are maximum values considered to represent the upper boundary (Table 4.7). They facilitate the assessment of the suitability of a certain tracer for a given investigation, and the calculation of the required tracer mass. They cannot be used for linear corrections of field experiments.

4.1.2.7.2 The retardation coefficient The retardation coefficient can be calculated with:

$$R_d = \frac{v}{v_t} \quad (4.7)$$

where

v = mean flow velocity of water and ideal tracer respectively,

v_t = mean transport velocity of the tracer

or

$$R_d = 1 + \rho^* \frac{(1 - n_e)}{n_e} K_d \quad (4.8)$$

⁴For example, Feuerstein and Selleck (1963), Leibundgut (1974), Smart and Laidlaw (1977), Sabatini and Austin (1991), Leibundgut *et al.* (1992), Hadi *et al.* (1997), Allaire-Leung, Gupta and Moncrief (1999), Kasnavia, Vu and Sabatini (1999), Kranjc (1997) and others.

Table 4.7 Distribution coefficients (K_d) from batch experiments. The higher the K_d value, the higher the sorption

| Tracer | c_i [mg/m ³] | K_d [cm ³ /g] ^a | K_d [cm ³ /g] ^b | K_d [cm ³ /g] ^{c1} | K_d [cm ³ /g] ^{c2} | K_d [cm ³ /g] ^{c3} |
|------------------|-------------------------------|--|--|---|---|---|
| Naphthionate | 10 | 0 | 0.38 | — | — | — |
| | 100 | 0 | 0.28 | | | |
| Pyranine | 10 | 0.03 | | — | — | — |
| | 100 | 0.24 | | | | |
| Uranine | 10 | 0 | 0.4 | 0 | — | — |
| | 100 | 0 | 0.28 | 0 | 0 | 0 |
| Eosine | 10 | 0 | 5.51 | 0 | — | — |
| | 100 | 0.03 | 4.37 | 0.025 | 0.09 | 0.24 |
| Amidorhodamine G | 10 | 1.23 | — | 1.23 | — | — |
| | 100 | 0.92 | | 0.92 | 0.19 | 0.75 |
| Rhodamine B | 10 | 5.56 | — | 5.61 | — | — |
| | 100 | 4.75 | | 4.75 | 1.25 | 9.18 |
| Rhodamine WT | | — | — | — | — | — |
| Sulforhodamine B | 10 | — | 36.6 | — | — | — |
| | 100 | | 29.4 | | | |

^aWernli (1986), substrate: tertiary molasse sand; 250 ml tracer solution.

^bMägdefessel (1990), substrate: 79.6% sand, 18.1% silt, 2.3% clay; 250 ml tracer solution.

^cDervey (1985), substrate: (1) mica gneiss; (2) coarse lime sand; (3) fine lime sand.

Further distribution coefficients from batch experiments can be found in Klotz (1982a, b) and Sansoni *et al.* (1988).

where

ρ = dry density of substrate,

n_e = porosity of substrate and

K_d = distribution coefficient.

In order to provide the reader with an impression of the suitability of the fluorescent tracers in different soil and aquifer substrates, benchmark values obtained from batch and column experiments are listed in Tables 4.7 and 4.8. Two concentrations c_i (10 and 100 mg/m³) are selected in Table 4.7 to highlight the link between concentration and distribution coefficient. R_d describes the retardation of tracer transport caused by an instantaneous equilibrium reaction (Table 4.8). R_d values are obtained by means of column tests (e.g. Klotz, 1982a, b; Dervey, 1985).

Although the reference values obtained from lab experiments may not be transferred directly to field conditions, they provide a useful guideline for the estimation of the sorption losses of a given tracer and, consequently, the estimation of the tracer injection mass required. The formulae to estimate the tracer injection mass will be provided in Chapter 6. The following procedure is recommended for the preparation of an experiment:

1. Complete a batch test employing the tracers that may potentially be used in the substrates to be investigated.

Table 4.8 Retardation coefficients from column experiments

| Tracer | c_i [$\mu\text{g/l}$] | R_d^{a1} | R_d^{a2} | R_d^{a3} | c_i [$\mu\text{g/l}$] | R_d^{b1} | c_i [$\mu\text{g/l}$] | R_d^{b2} | c_i [$\mu\text{g/l}$] | R_d^{b3} |
|------------------|---------------------------|------------|------------|------------|---------------------------|------------|---------------------------|------------|---------------------------|------------|
| Pyranine | 20 | 1.18 | 1.22 | 1.04 | | | | | | |
| Uranine | 10 | 1.18 | 1.22 | 0.99 | 10 | 1 | 10 | 1 | 10 | 1 |
| Eosine | 20 | 1.69 | 1.55 | 1.12 | 90 | 1 | 90 | 1.9 | 90 | 1.1 |
| Amidorhodamine G | | | | | 30 | 2.7 | 30000 | 22.1 | 30 | 1.3 |
| | | | | | 80 | 2.3 | 80000 | 9.9 | | |
| Rhodamin B | 50 | >6 | >5 | >8 | 10 | 8.8 | 80000 | 40.3 | 80 | 2.4 |
| | | | | | 100 | 5.9 | | | | |

^aKlotz (1982a, b), substrate: (1) fluvio-glacial gravel; (2) drift and valley sand; (3) tertiary gravel sand.

^bDervey (1985), substrate: (1) mica gneiss; (2) molasse sandstone; (3) limestone.

2. Select the optimal tracer.

3. Estimate the tracer injection mass using a loss parameter for sorption.

As a result of the experience gained in many tests a general assessment of the tracer's suitability is listed in Table 4.9.

The use of artificial tracers in the vadose zone may involve additional criteria compared to the application in the saturated zone. In order to investigate macropore flow even sorptive tracers like Rhodamines and nonfluorescent dye tracers are needed to visualize the water flow. To simulate the leaching of compounds such as pesticides via macropores shortly after heavy precipitation events (strong) sorptive tracers, for example the Rhodamines, are suitable (Brandi-Dohrn *et al.*, 1995).

Tracer experiments, particularly in crystalline and in swampy areas, may be confronted with acidic water. In aqueous acidic solutions, some of the xanthene tracers may switch to a nonfluorescent form. Consequently, the tracer in the sample cannot be measured by means of a fluorescence analysis without readjusting the sample to an adequate pH range, as discussed in Section 4.1.2.4.

Furthermore in acidic environments some fluorescent tracers (e.g. Uranine) may change to a cationic state. This modifies the transport behaviour significantly. The positively charged molecule can be absorbed on the soil and aquifer matrix of which the tracer is lost entirely. Many tracer hydrologists know by experience that Uranine tracer tests have a higher failure rate in humic soils or acidic aquatic environments with low

Table 4.9 Suitability of tracers based on the sorption effect for different fields of application

| Hydrological compartment | Suitable tracer based on the sorption criteria |
|---------------------------|---|
| Porous groundwater | Uranine, Pyranine, Eosine, Naphthionate |
| Karst groundwater | Uranine, Pyranine, Naphthionate, Eosine, Rhodamines |
| Fissured rock groundwater | Uranine, Pyranine, Naphthionate, Eosine |
| Unsaturated (vadose) zone | Uranine, Eosine |
| Surface water | All fluorescent tracers |
| Glaciated areas | All fluorescent tracers, except Pyranine |

pH. In such cases, the application of Rhodamines represents an alternative due to their resistance to low pH values. However, the high sorption affinity of Rhodamines prohibits the use in aquifers, especially in soils and porous aquifers. For shorter distances, Bromide or Deuterium as an artificial tracer may represent alternatives.

4.1.2.8 Chemical and biological stability

Fluorescence quenching is used as an umbrella term for several processes causing a reduction or suppression of fluorescence intensity. Quencher molecules are molecules that are involved in these processes, and which either hinder molecules becoming excited or transfer the excited molecule radiation back to ground state. The latter can occur when excited fluorescent molecules and quenchers collide, and the energy is transformed into heat energy (dynamic Stern–Volmer relationship), or when the excitation energy is passed to the quencher due to resonance energy transfer (Förster resonance energy transfer). Complex building by fluorescent molecules and quenchers can limit or terminate the ability to fluoresce (static Stern–Volmer equation), or result in a colour change (Laitinen, 1960). A high energy state is more readily reactive than the base state.

Dye tracers may be readily quenched and/or decomposed as a consequence of oxidation and other chemical changes. However, oxidative processes affect the dye tracers to different degrees. Whereas the Rhodamines are more resistant, other dyes will be irreversibly quenched. Consequently, chlorinated water should not be used to prepare calibration solutions, nor should dye tracers be used in tests of water supply installations with chlorination or ozonization facilities if it is not possible to take samples prior to treatment (Wilson, 1968; Leibundgut, 1974; Käss, 1998).

Salinity may also affect fluorescence but generally to a much lesser degree than either pH or light. High concentrations of salt decrease the fluorescence signal, but do not change the spectrum itself (André and Molinari, 1976; Smart and Laidlaw, 1977; Flury and Wai, 2003). Magal *et al.* (2008) reported the same effect for sea water. In more saline sea water, the fluorescence signal is inversely proportional to the salinity, and the sorptivity increases. For example, in water from the Dead Sea the fluorescence intensity is 10–15% of that of pure water.

Chemical quenching may occur due to conversion of the dye to a nonfluorescent iodate derivate (Gaspar, 1987; Hadi *et al.*, 1997). Potentially more problematic is fluorescence quenching or metal complexation leading to reduced fluorescence, or even to a change in colour. A more detailed description of these processes can be found in the original literature published by Stern and Volmer (1919) and Förster (1952, 1982) and others.⁵

Another form of fluorescence quenching is concentration-quenching, which occurs at very high concentrations (see Section 4.1.2.2). The quenching is caused by a self-shadowing effect of the molecules, which reduce the fluorescent intensity. Photolytic decay, the chemical alteration of the fluorescent molecules brought about by exposure

⁵Williams and Bridges (1964), Gaspar (1987), Van Der Meer, Coker and Chen (1994), Flury and Wai (2003).

to light, is sometimes considered to be a form of fluorescence quenching, but unlike quenching processes it effects a change to the net charge of the molecule (pH). Photo bleaching is irreversible.

Microbial degradation of fluorescent tracers is also known to occur, in natural waters and in samples. However, no clear rules can be formulated to correct the measured concentration values of dyes (Zupan, 1982, 1989). Obviously, this kind of degradation can lead to misinterpretation of tracer experiments as shown by Goldscheider, Hötzel and Kottke (2001) for Naphtionate. It is noticeable the decay did not occur in the aquifer but in the samples stored at room temperature. Microbial decay of Uranine is widely described in the literature (Behrens, 1986; Behrens and Demuth, 1990; Behrens and Leibundgut, 1992; Hadi, 1997; Käss, 1998).

There are hints of metabolism of fluorescent tracers in contact with other chemicals and during long term experiments due to a shift of fluorescent maxima (see Section 4.1.2.4). Under special conditions, Sulforhodamine B appears to undergo the process of dealkylation quite quickly, which leads to a shift of the spectrum towards the emission peak of Eosine. Mägdefessel (1990) observed this phenomenon in a sample taken only eight months after injection in a porous aquifer. The analysis was performed by means of D,C-chromatography (Figure 4.16). Empirical data were provided by Weiss *et al.* (2008) based on reddish groundwater from an aquifer traced 30 years ago. In addition to the original tracer Sulforhodamine, its metabolites (amine derivatives) were also identified. However, studies of this nature require advanced analytical techniques (HPTL/AMD, Nano-Chip-LC/QTOF-MS) (see Section 4.1.3.4).

As demonstrated by the study above, fluorescent tracers appear to remain stable over very long periods of time in unpolluted groundwater aquifers. Other concurring examples have been reported by Bauer (1969) and Käss (1998). According to a personal communication by Wernli relating to an ongoing long term tracer experiment in the Swiss tertiary molasse (Wernli and Leibundgut, 1993), Eosine remained stable over a period of 24 years.

Samples of fluorescent tracer may remain stable for a long time provided the water is pure. Samples should be taken in brown glass bottles or, if using plastic,

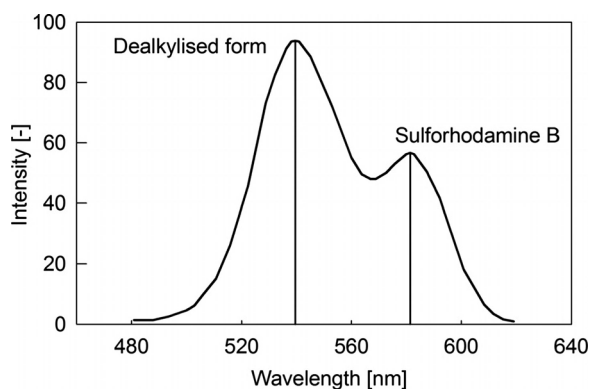


Figure 4.16 Shift of the emission peak of Sulforhodamine B brought about by a dealkylation process (Mägdefessel, 1990).

in polyethylene or polysulfone bottles. As the chemical compositions of plastic bottles differ, it is recommended to test the effects on sorption on all kind of bottles to be used.

In the case of field experiments dealing in particular with karst water, polluted water and sewage water, microbial decay must be considered carefully. It is recommended that the samples be analysed as quickly as possible in order to avoid the problem to the greatest degree possible.

4.1.2.9 Toxicity and related environmental effects

Each injection of artificial tracer in a hydrological system is in a sense a contamination of the water body in question. However, carefully planned and correctly prepared tracer experiments generally involve only minimal quantities of fluorescent tracer substances in the range of grams, or kilograms at most (cf. Section 6.1). Therefore, the 'contamination' is usually tolerable. When preparing a tracer experiment it is vitally important that national regulations pertaining to tracer experiments are consulted. It will be necessary to make a formal application in some cases.

The commonly used hydrological tracers have been investigated intensively in several studies.⁶ Summarizing the results in relation to human and eco-toxicological aspects the following can be stated: Uranine is harmless; Eosine, Pyranine and Naphthionate appear to be harmless. It is suspected that the Rhodamine group as a whole is toxic, except Amidorhodamine G and Sulforhodamine B which are less problematic (Table 4.10). When planning tracer experiments it must also be considered that problems may occur in future by metabolism of fluorescent tracers, as described in the previous chapter (Figure 4.16). A new study using the TDI approach (Tolerable Daily Intake) indicated a slightly different assessment for Uranine (Brüschweiler, 2007). All authors agree, however, that a correct evaluation of the injection mass of a tracer taking into consideration the expected tracer concentrations in the water used is required (cf. Section 6.2).

4.1.2.10 General assessment

Of practical interest is the price of tracer substances, which is not negligible. The comparative cost of the tracer required for an experiment can be calculated by multiplying the reciprocal relative fluorescence yield by the quantity (g) and the price. A comparative evaluation of the costs is not provided in Table 4.10 since the prices fluctuate considerably. An internet search is recommended in order to find the most reasonable current prices. In order to aid in the evaluation of tracer substances a summary assessment of the commonly used tracers is provided in Table 4.10.

⁶UBA (1996), Käss (1967a), Little and Lamb (1973), Nestmann, Kowbel and Ellenton (1980), Smart (1982), Hofstraat *et al.* (1991), Leibundgut and Hadi (1997), Käss (1998), Behrens *et al.* (2001).

Table 4.10 Summary of the characteristics of the fluorescent tracers

| Tracer | Ex/Em [nm] | Relative fluorescence yield | Detection limit [mg/m ³] | Toxicity | Solubility [g/l] (20 °C) | Light sensitivity | Sorption behaviour |
|------------------|----------------|--------------------------------|---|-----------------|-----------------------------|-------------------|--------------------|
| Naphthionate | 325/420 | 18 | 0.2 | Harmless | 240 | High | Very good |
| Pyranine | 455/510 | 18 | 0.06 | Harmless | 350 | High | Good |
| Uranine | 491/516 | 100 | 0.001 | Harmless | 300 | High | Very good |
| Eosine | 515/540 | 11.4 | 0.01 | Harmless | 300 | Very high | Good |
| Amidorhodamine G | 530/555 | 32 | 0.005 | Sufficient | 3 | Low | Sufficient |
| Rhodamine B | 555/575 | 9.5 | 0.02 | Toxic | 3–20 | Low | Insufficient |
| Rhodamine WT | 561/586 | 10 | 0.02 | Toxic | 3–20 | Very low | Insufficient |
| Sulforhodamine B | 564/583 | 7 | 0.03 | Sufficient | 10 (10 °C) | Low | Insufficient |

4.1.3 Measurement techniques

Fluorometry is by far the best of the techniques available for the measurement of fluorescent tracers. Depending on the wavelength ranges of the dye tracers, the analyses cover the visible and the near UV range of the electromagnetic spectrum. A high pressure xenon lamp used as a light emitting source covers a spectrum which includes the peak of most tracers, at wavelengths of approximately 400–550 nm. The emission intensity is used in the analysis of fluorescent tracers. Putting the physical laws to use, the measurement of fluorescence tracers dissolved in water is conducted nowadays by fluorometers. Several types of devices (filter and spectral fluorometer) are available.

Both techniques follow the general principle of fluorescence analysis using the fluorescence capacity of the tracer, and feature a light source that excites the sample and a detector that measures the emitted light. In order to analyse the characteristic wavelengths of the dyes (excitation, emission) filters or monochromators are used to extract from the wider wavelength range of the light source the excitation wavelengths, which is generally a narrow band. The excited solution scatters the light and fluorescence. A second set up of filters or monochromators separates the emitted scattered light from the fluorescence light, which is measured with a detector (photomultiplier). Usually the excitation light and the emission detector are arranged at right angles to one another to avoid distortion by the transmitted light (Figure 4.17). This way the strong transmission beam does not disturb the weak fluorescent light.

In order to avoid scattering light it is best to use narrow band filters or monochromators with a slit standard width of 10 nm. Overly narrow filters (<5 nm) are not useful as the drop in intensity is too great.

4.1.3.1 Filter fluorometer

Only one tracer can be measured at a time, which depends on the set of filters attached. Filter fluorometers are not entirely suitable for lab analyses as the fixed lamp/filter combination only allows for the detection of fluorescence intensity within a certain wavelength range as a sum of the background concentration plus the fluorescence

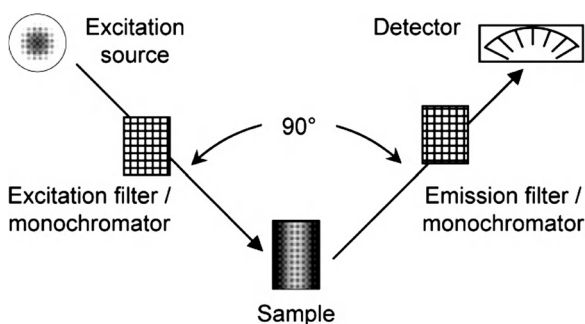


Figure 4.17 Basic fluorescence measurement set-up of a fluorometer.

signal. Therefore, it is impossible to state with certainty whether it is the fluorescence of the tracer applied or 'wild' fluorescence stemming from another substance. Therefore, a spectro-fluorometer is necessary.

However, in case of in situ measurements in field experiments, filter-fluorometers are the most appropriate device, in particular for monitoring purposes and in the case of discharge measurements using a known tracer. When performing multi-tracer experiments, each tracer applied necessitates one filter-fluorometer with the adequate light source/filter equipment. The filter required is a combination edge filter and double band interference filter.

4.1.3.2 Spectral fluorometer

Today the most common laboratory device is the spectral fluorometer. Its advantage derives from the two continuous adjustable monochromators, enabling it to run scans. To eliminate the fluctuation of the excitation energy a part of the excitation light is sidelined to a Rhodamine cell, which provides the needed reference signal. This method returns more precise qualitative and quantitative spectra. The fluorescence of the tracer and of the background at both ends of the spectrum can be identified, and separation of the background signal is possible. The measured fluorescence intensities are analysed directly by a software program. The repeatability of an analysis where a good device is set up optimally is $\pm 1\%$. The technical features of the spectral fluorometer are contained in the corresponding user manual.

4.1.3.3 Synchronous scan technique

The technique has been a feature of chemical analysis since it was presented by Lloyd (1971), and was introduced in the analysis of fluorescent tracers by Behrens (1971), Leibundgut (1973) and André *et al.* (1977). The application of qualitative fluorescent tracer analyses was only made possible by the development of the first spectrofluorometers for the analysis of fluorescence in water samples in the 1960s.

The synchronous scan technique is the most effective way to analyse fluorescence spectra (cf. Figure 4.2). All further information concerning measurement techniques relates to this technique. Instead of running separate scans of excitation and emission spectra, the synchronous scan runs through the spectrum with a constant wavelength distance $\Delta\lambda$, corresponding to the difference in the wavelength between the excitation and the emission spectrum. The optimal $\Delta\lambda$ is tracer specific and is between 20–25 nm for most of the xanthenes (Figure 4.18). However, the difference in intensity is negligible using $\Delta\lambda$ 25 nm instead of the absolutely specific $\Delta\lambda$ depicted in Figure 4.2. The spectrum of the synchronous scan (I_S) is the product of intensities of excitation (I_{Ex}) and emission (I_{Em}) scans: $(I_S) = (I_{Ex}) \times (I_{Em})$. For operational use a $\Delta\lambda$ of 25 nm is set.

As the scattering signals arise with a narrower $\Delta\lambda$, due to the overlapping of the transmission ranges of the monochromators, a $\Delta\lambda$ of 25 nm is the minimal distance. Pyranine and Naphthionate have a wider $\Delta\lambda$. The synchronous scan spectrum is

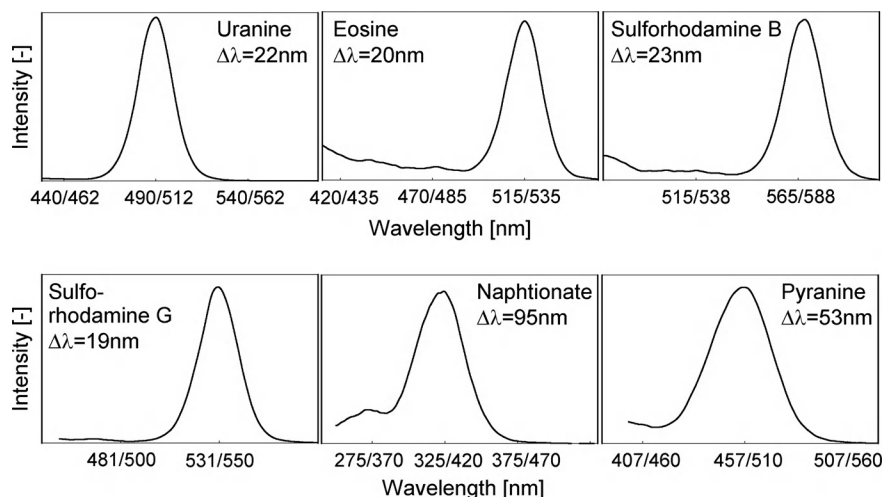


Figure 4.18 Synchronous scans of commonly applied fluorescent tracers. Rhodamine B and Rhodamine WT were omitted based on their similarity to Sulforhodamine B and Amidorhodamine G. 440/462 and so on: excitation/emission wavelength (nm).

considerably smaller than the emission spectrum of a fluorescent dye. It allows for a more precise qualitative identification of a substance.

The synchronous scan technique is essential when conducting multitracer tests. The technique allows for the separation of tracer mixtures in samples. Spectral analyses using synchronous scan provide a means to detect more than one tracer in a sample in only one run, provided the emission maxima of the respective tracers have approximately the same $\Delta\lambda$ and their fluorescence maxima lie in a minimum distance of about 50 nm from each other. Consequently, mixtures of Uranine/Rhodamines and Eosine/Rhodamines (except Amidorhodamine G) can be analysed elegantly in this way running the scan at $\Delta\lambda$ 25 nm (Figure 4.19).

Mixtures of Naphthionate and all other fluorescent tracers can also be detected by means of a synchronous scan. Although no further treatment is required, two runs are necessary; one at $\Delta\lambda = 95$ for the detection of Naphthionate and one at $\Delta\lambda = 25$ nm for the tracers with wavelengths higher than that of Eosine (Figure 4.20).

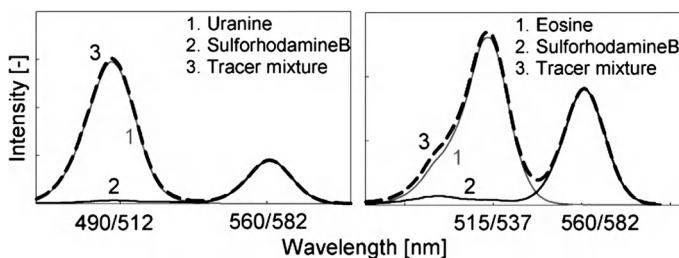


Figure 4.19 Fluorescence spectra of tracer mixtures measured with $\Delta\lambda$ 25 nm. Left: Uranine and Sulforhodamine B; right: Eosine and Sulforhodamine B.

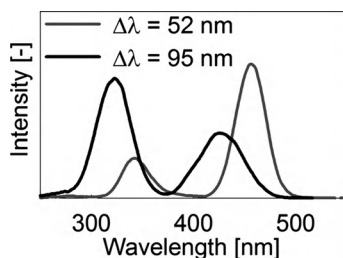


Figure 4.20 Synchronous scans of a Naphthionate-Pyranine tracer mixture require two scans ($\Delta\lambda = 95$ nm: Naphthionate; $\Delta\lambda = 52$ nm: Pyranine).

If the fluorescence maxima of the tracers in a mixed sample differ by $\Delta\lambda < 50$ nm, the (elegant) synchronous scan alone is not sufficient to separate the tracers. In Figure 4.21 the intensities of the two single tracers Uranine (1) and Eosine (2) are added on the mixture (3). Self-evident the spectra of the single tracers are covert within that of the mixture. In such situations further analytical techniques are needed to detect the individual tracers accurately.

Problems of overlapping spectra occur between Pyranine/Uranine, Uranine/Eosine and Eosine/Amidorhodamine G. Conveniently, the pH dependence proves helpful in solving at least part of the problem by bringing the pH to a value sufficient to quench one of the tracers (see Figure 4.8).

Uranine/Eosine mixture – detection of Eosine:

1. The combined signals of both tracers are measured in a synchronous scan.
2. The sample must be acidified to a pH value of five, which suppresses the fluorescence of Uranine to a large extent.
3. The excitation-emission scan provides the Eosine intensity at the fluorescence maximum for higher Uranine concentrations directly (the remaining Uranine does not affect the result). Where concentrations of both tracers are almost equal, a lower pH is required. As a consequence the Eosine level will also drop. Further calculation is necessary according to the instructions given in Figure 4.23.

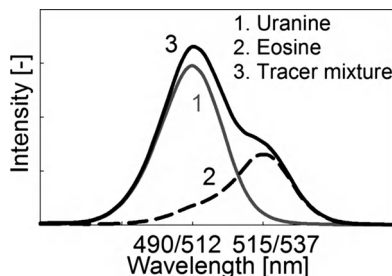


Figure 4.21 Fluorescence spectra of tracer mixtures: Uranine and Eosine.

Uranine/Eosine mixture – detection of Uranine.

A combination of pH dependence and photolysis is required:

1. The combined signals of both tracers are measured in a synchronous scan.
2. The sample must be acidified to a pH value of 4.3.
3. Expose the acidified sample to daylight for a number of hours. The result will be to destroy the fluorescence of Eosine but that of Uranine will not be affected.
4. An excitation-emission scan after (re)alkalinising reveals the Uranine fluorescence.

Pyranine can be determined in a Pyranine/Uranine mixture in an acid solution with a pH of 4.5 (Figure 4.22). When the concentrations of both tracers are equally low, the pH must be lowered to 3.0. Here Uranine has only a minimal fluorescence in the emission maximum of Pyranine at 405 nm. A synchronous scan at $\Delta\lambda = 25$ nm in the maximum of 445 nm is the best means to separate Pyranine from Uranine (Benischke and Schmerlaib, 1986).

Analysing Pyranine by suppressing Uranine fluorescence:

1. The combined signals of both tracers are measured in a synchronous scan ($\Delta\lambda = 25$ nm).
2. The sample must be acidified to a pH value of 4.5.

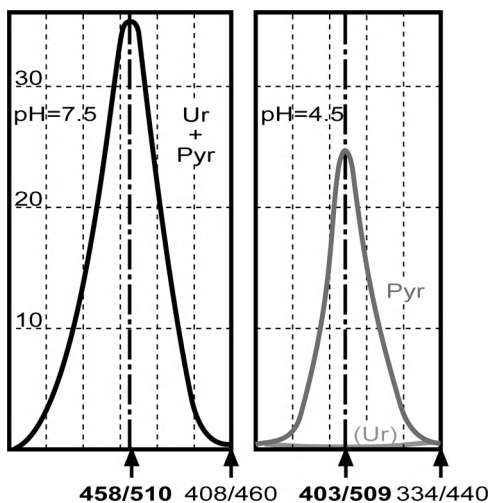


Figure 4.22 Pyranine detection by acidification of the Pyranine/Uranine tracer mixture. Measurement is at pH 4.5 ($\Delta\lambda = 106$ nm).

3. The excitation-emission scan provides the Pyranine intensity at the fluorescence maximum of Pyranine directly (Figure 4.22).

4. Bear in mind the shift in the wavelength due to acidification.

Pyranine/Eosine mixtures can be treated applying the same procedure at pH 1. Again, bear in mind the shift in the wavelength due to acidification.

A more rigorous option for the separation of a tracer mixture is to combine the pH and light dependence, acidifying the mixture and destroying the active tracer after measuring irradiation with a short-wave light, before then alkalinizing it to measure the second tracer.

Separation of fluorescence dyes using ratio calculation This method utilizes the fact that the ratio of two fluorescence intensities at two different wavelengths is independent of the tracer concentration. The technique is demonstrated for Uranine/Eosine below (Figure 4.23). In the example the broken line represents a mixture of Uranine and Eosine measured with $\Delta\lambda = 25$ nm. More information can be found in Käss (1998) and Wernli (2003).

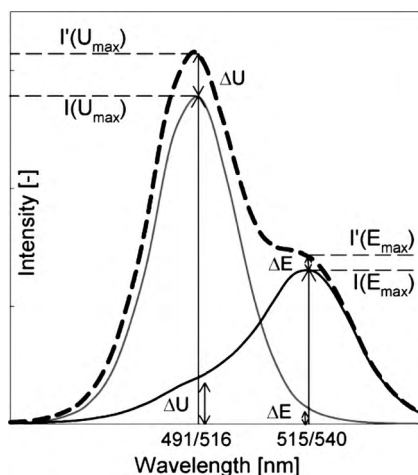


Figure 4.23 Separation of fluorescence dyes using ratio calculation. Broken line: mixture of Uranine and Eosine measured with $\Delta\lambda = 25$ nm. I: Intensity; U: Uranine; E: Eosine.

The synchronous technique with spectral fluorometers avoids another serious problem associated with fluorescence analysis. When changing the wavelength of only one monochromator, while keeping the other stable, as is done under the classical technique, three problems occur: (i) scattered light blurs the resulting spectrum, (ii) the signal gets too 'high' and, even more importantly, (iii) the *Raman effect*, as a form of scattering light, can fake fluorescence (Figure 4.24). The Raman effect is observed in all spectral ranges following excitation and is the result of the molecular oscillation of the water molecules. Its wavelength is as much higher as the oscillation frequency of water to that of the excitation light (Behrens, 1971; Harris and Bertolucci, 1989).

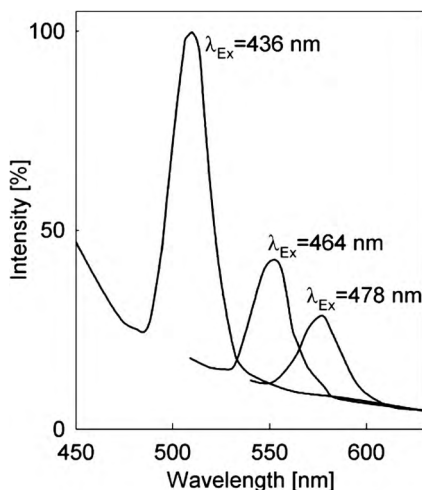


Figure 4.24 Raman scattering of water in the wavelength ranges of most fluorescence tracers (after Behrens, 1971).

4.1.3.4 Background signals and light scattering

Another advantage of synchronous scans is the masking of the blank value. Background signals (blank values) can be caused by high scattering and in the presence of the blue wavelengths, especially at low tracer concentrations (Figure 4.25).

These background signals are also caused by electronic noise, and may additionally be brought about or amplified by suspended material. When measuring fluorescence in pure water one expects the background fluorescence to be low. Where the correspondence between the amplification (gain) and the concentration is optimal, the background is equal to zero. Very low concentrations require a higher amplification in

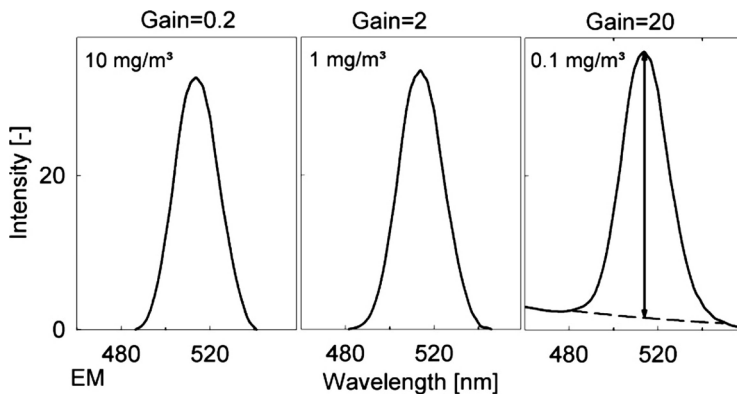


Figure 4.25 Spectral curves of Uranine in pure water revealed by a synchronous scan at $\Delta\lambda = 25$ nm. In the event of high amplification of the signal, the background signal has to be interpolated (see spectral curve to the right).

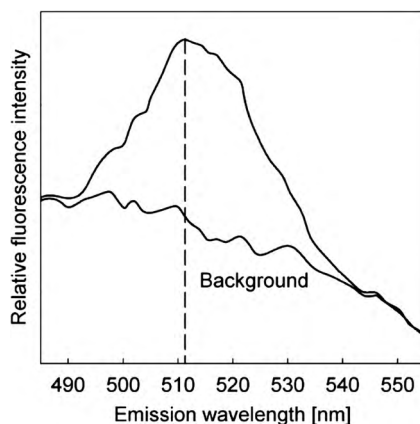


Figure 4.26 Uranine scan in turbid water. The turbidity distorts the spectral curve (modified from Wernli, 2003).

order to get a distinct signal (Figure 4.25). The example of 0.1 mg/m^3 in Figure 4.25 shows how to separate the background from the effective fluorescence signal. Additional problems may occur towards the end of the life of the energy source (xenon lamp). The stability of the fluorometer drops and consequently the background fluctuation rises.

Light is scattered in both pure and in unclear water. In pure water the background is nearly zero. Suspended material, colloids, humins and air or gas bubbles are common in samples of surface and karst water, and in samples from springs after heavy rainfall. The background signal then ranges from high to very high (Figure 4.26). The problem is more pronounced in the lower wavelength ranges (blue), particularly in the UV ranges. This is due to higher degrees of scattering. A very high background signal near the respective fluorescence peak may even result sometimes in a shift of the fluorescence peak.

The following procedure is recommended as a means to overcome the scattering problem:

1. Let the sample settle over night, allowing the suspended material to sink.
2. Filter the water ($1 \mu\text{m}$) if still unclear.
3. Alternatively, the sample can be centrifuged.

However, these measures are not effective where colloids are present in the sample.

In the future, very advanced multi-coupled analytical techniques such as HPTL/AMD (High Performance Thin Layer chromatography with Automated Multiple Development) and Nano-Chip-LC/QTOF-MS (Nanochip Liquid Chromatography/Quadruple Time-Of-Flight Mass Spectrometry) might become important instruments in fluorescent tracer analyses. The methods have been applied successfully to special problems measuring fluorescent tracers or their derivatives (Weiss *et al.*, 2008).

4.1.3.5 Fibre optic fluorometer (FOF)

Fibre optic fluorometers are used in the lab and in the field for in situ measurements and monitoring. The characteristics of the instruments available differ; that is the number of channels (multitracer measurements), detection limits, size, cable characteristics and applicability (surface waters, groundwater). There is a variety of suppliers and instruments on the market, which are easy to find on the internet. FOFs work according to the principles of the filter fluorometer. The light source used to stimulate fluorescence is either a halogen bulb or diodes (LED). Modern LEDs with a high spectral density are advantageous in terms of their robustness, reliability, maintenance and energy consumption. After passing through an excitation filter, the excitation signal is sent through a fibre optic cable (duplex fibre optic) to the probe head in the measuring volume (ca. 1 cm^3) introduced into the medium of interest. A part of the fluorescent light emitted isotropically by the tracer is collected by a second fibre optic cable and guided back to the photomultiplier with an emission filter and an I/U converter. The converted electrical signal is connected to the analogue output (Figure 4.27).

The excitation light can be selected according to the fluorescence range and irradiation density required for the tracer used. The detection limit for Uranine is in the range of 0.02 mg/m^3 . Provided the water is very pure, some devices with an optimal measuring set allow, from experience, a detection limit up to 0.002 mg/m^3 . Linearity between the FOF signal and tracer concentration is given up to the range of 10 mg/m^3 (Hodel and Stoller, 2000).

Fibre optics allow for continuous measurement with a high spatial and temporal resolution. The number of measurement channels varies from type to type, but usually up to six channels are available and allow the individual to choose the measurement interval (1 s to several hours). The most important fluorescent tracers (all xanthenes) can be measured. Several channels allow for the measurement of more than one tracer at

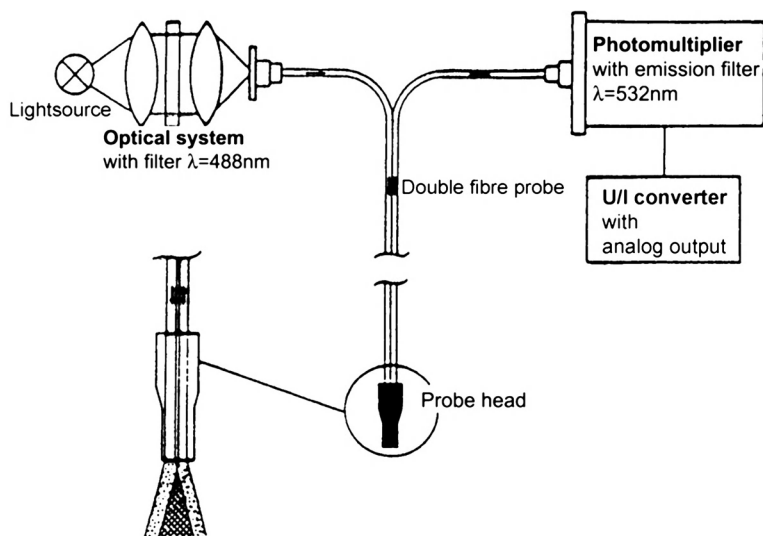


Figure 4.27 Fibre optic fluorometer set-up, schematic (Schmid and Barczewski, 1995).

a time at multiple sites. Due to this configuration, the technique is especially suitable for the measurement of fluorescent tracers within fractures, lakes or for (river) discharge measurements using dilution methods.

A weakness of the fibre optics approach, particularly in relation to surface water experiments, is the effect of ambient light on the probe head. In order to avoid disrupting the measurement signal as much as possible a phase sensitive detection (lock in technique) is used (Hodel and Stoller, 2000). However, the effect of ambient light cannot be entirely avoided when making measurements in surface waters. A protection tube around the probe head further reduces the influence of ambient light. A protection is recommended in surface water measurements generally to avoid damage to the probe. However, this precaution slightly slows the free water flow around the probe head, which is important for simultaneous in situ measurements. So, when a protection tube is used, its potential influence on the flow field needs to be taken into consideration. Further detailed technical information about fibre optics is provided in (Barczewski and Marschall, 1992; Benischke and Leitner, 1992; Schmid and Barczewski, 1995; Hodel and Stoller, 2000; Hodel, Stoller and Diem, 2004).

4.1.3.6 Field fluorometer for in situ measurements

Field experiments involve contrasting and more varied technical conditions than are found in the lab, but there are also advantages to the measurement of samples directly in the field. In situ measurements reduce the number of the required water samples drastically, with only control samples needed. Further advantages are less transport and the lack of a time lag between sampling and analysis. Thus, the risk of sample contamination and/or ageing with the associated potential negative consequences such as photolytic, biological and chemical degradation is eliminated. Furthermore, an immediate analysis and interpretation of the measurements means an onsite plausibility check is possible, and allows the researcher to extend or to shorten the measurement duration, or even to change the test arrangement and to repeat the experiment if necessary. With the development of low energy consuming diodes, the carrying of many or heavy batteries to the experimental site is no longer a problem.

However, unlike laboratory measurements, field experiments with in situ measurement require consideration of basic parameters such as water temperature and pH value. Variations in these parameters often result in fluorescence characteristics that are not consistent with the calibrations known from laboratory tests, as referred to previously. This may as a result lead to inaccurate results. Another factor that can affect and distort the measurement is turbidity (especially in surface water). Turbidity reduces excitation and emission radiation due to absorption and reflection of particles. Operators using the field fluorometer must accept that there is no possibility to prepare or to treat the sample so as to obtain better signals and results (e.g. adjusting pH value).

A much more successful approach than trying to correct the values measured in situ is, to calibrate the measurement directly in the field with the water to be measured in order to equalize the measurement conditions (e.g. calibration with 'shaken' river water) using the dilution method. However, this approach cannot be applied for all experiments. An example of a situation where this method does not work is in the case of

measurements made within lakes at the interface of epi- and hypolimnion, where there are quickly changing temperature conditions. The potential for calibration or instant calibration techniques varies considerably according to the type of field fluorometers.

Four types of device, each based on different principles, are applied in practice: the fibre-optic fluorometer, flow-through fluorometer, pocket fluorometer and in situ fluorometer (Variosens, others). So far applications of the spectral fluorometer have been limited to laboratories.

4.1.3.6.1 Fibre optic fluorometer (FOF) FOF measures the fluorescence applying a concept described in Section 4.1.3.6. FOFs are generally best suited for in situ measurements. They are especially suitable in field experiments investigating the unsaturated zone, fissured rock aquifers, the hyporheic interstitial and when measuring river runoff using the dilution method (Barczewski and Marschall, 1992; Schmid and Barczewski, 1995; Hodel, Stoller and Diem, 2004; Selker *et al.*, 2006). The use of FOFs is restricted by the limited cable length and problems with scattering light; for example in lake research.

4.1.3.6.2 Flow-through fluorometer The flow-through fluorometers take samples by pumping water into the device and sending the data to a data logger. The underwater or downhole fluorometers are a new type of flow-through-fluorometers. The data are logged into the device and are later transferred to a computer for evaluation. The detection limit is low, allowing the operator to take advantage of the advantages of fluorometry. However, suspended material causes problems when measuring directly in the field. The devices are simultaneously in situ fluorometers as they are watertight and can be placed in the water under investigation, such as rivers, lakes, groundwater boreholes and springs. An additional function of this device is the measurement of turbidity, enabling a correction for the fluorescence response. However, the correction is problematic and does not necessarily lead to absolutely correct values. When using the dilution method to measure runoff in rivers it is, therefore, also recommended that the 'instant calibration' be used. Further information pertaining to the devices, the measurement techniques and the application is provided in Schnegg and Kennedy (1998), Schnegg and Bossy (2001), Schnegg (2002), Flynn *et al.* (2005), Schegg and le Doucen (2006).

4.1.3.6.3 Pocket fluorometer Another means of measuring fluorescent tracers in field experiments is by using the pocket fluorometer. It is designed for Uranine and Rhodamines. As a handheld device it is very easy to transport to any site. However, the detection limit for Uranine (0.1 mg/m^3) is approximately 50 times higher than that of a spectro- and fibre optic fluorometer. Consequently, the pocket fluorometer is not suited to tracer hydrological investigations involving low tracer concentrations. On the other hand, it is very useful for discharge measurements using the dilution method, dealing with tracer concentrations in the range of $\geq 2 \text{ mg/m}^3$. A large effective range between approximately $0.1\text{--}200 \text{ mg/m}^3$ is sufficient for most experiments (Wernli, 2007).

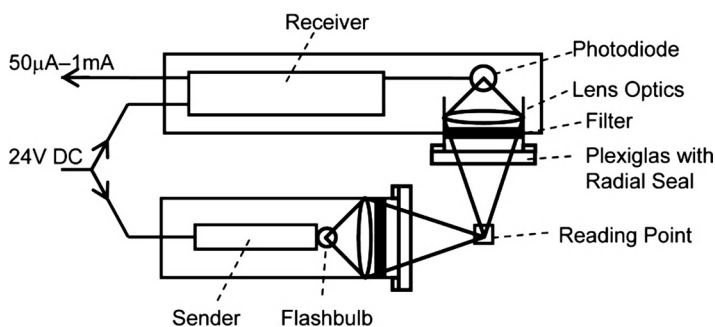


Figure 4.28 Set-up of the Variosens measurement device.

4.1.3.6.4 Variosens The in situ fluorometer 'Variosens' is based on a light pulse technique. Producing three decades' worth of concentration in just one second, it allows for the rapid measurement of fluorescence in the water body itself. The set-up is illustrated in Figure 4.28. The instrument covers a concentration range of four decades (0.01–100 ppb) by a linear current output of 0–1 mA. It operates with a power consumption of between 6 and 10 Watt. With a stainless steel housing (weight: 12 kg) it can be used for water depths of 0–1000 m, or 0–200 m with an aluminium housing (weight: 8 kg). Power is supplied to the device through an electrical cable extending from the boat from which the measurements are being made. The tracer is excited by a xenon flash bulb (frequency: 10 Hz) and the signal picked up by the receiver is transmitted to the boat where it is recorded continuously (Früngel, 1972, 1989; Früngel and Koch, 1974; Hirsig, Leibundgut and Nydegger, 1982). A similar device, 'Back Scat', is available for the applications in surface water (Goudsmit *et al.*, 1997).

Its application is known mainly from surface water experiments, particularly in oceanography where it was developed and used primarily for measuring chlorophyll (Herrmann, 1977). There have also been many studies carried out in lakes and rivers investigating diffusion and dispersion processes and other surface water specific processes, such as the horizontal and vertical distribution of river water in the epi- and hypolimnion of lakes and chlorophyll measurements respectively (e.g. Hirsig, Leibundgut and Nydegger, 1982; Stevens, Lawrence and Hamblin, 2004). Details of the practical application of the Variosens in field experiments will be presented in Chapter 6 and in the Lake Bled case study in Chapter 7.

4.1.3.7 Laser measurement

A laser (light amplification by stimulated emission of radiation) is a short wave radiation light source featuring various properties such as a narrow, low divergence beam with a well defined wavelength. These characteristics are used for 'laser spectroscopy'. The application of the laser technique to measure fluorescence is a promising area of measurement techniques in tracer hydrology. Essentially, three different laser-spectroscopy methods can be used for hydrological investigations, namely (i) absorption spectroscopy, (ii) laser Doppler velocimeter and (iii) laser-induced fluorescence. The

latter is directly related to the fluorescence characteristics of fluorescent dyes. Laser-spectroscopy is the experimental analysis of interactions between radiation (emitted by a laser) and matter (gas, fluid or solid). Due to the high radiation efficiency and the narrow spectral range, laser-spectrometry is very suitable for fluorescence measurements. However, there have only been a few applications in hydrology as of yet. Further information on laser-induced fluorescence techniques is provided by Brumley and Farley (2003) and Englert (2003).

4.1.3.8 Advanced measurement techniques

Where analytical problems are unsolvable using fluorometry, such as the separation of tracers in problematic mixtures and that of the separation of eluates of activated charcoal bags, recently advanced techniques are being offered increasingly.

High Performance Liquid Chromatography (HPCL) is a promising analytic for fluorescent tracers. The detection limits for Uranine (1.7 mg/m^3) and Sulforhodamine B (4.7 mg/m^3) are in the same order of magnitude as with optical fluorometers (Franke, Westerholm and Niessner, 1997). Recently advanced analytical techniques such as HPTL/AMD (High Performance Thin Layer chromatography with Automated Multiple Development) and Nano-Chip-LC/QTOF-MS (Nano-chip Liquid Chromatography/Quadruple Time-Of-Flight Mass Spectrometry) have been applied successfully to special problems with measuring fluorescent tracers or their derivatives (Weiss *et al.*, 2008). The detection limit is approximately ten times lower when using these techniques. Additionally, the tracers can be measured simultaneously. By enrichment of the tracers using solid-phase extraction (SPE), the detection limit can be further reduced by a factor of 10–100 compared to optical fluorometry. The opportunity to automatize the analyses using HPCL is an advantage over the conventional techniques. In future, the advantages of the (automated) advanced analytic may even compensate for the much higher costs for material and for time consuming preprocessing (oral information A. Leis, Graz).

4.1.3.9 Long term sampling using active charcoal bags

A completely different approach in the sampling of fluorescent tracers is the adsorption of the tracer substances by placing active charcoal bags (probe, fluocapteur) in the water under investigation, with the subsequent extraction of the tracer from the charcoal in the lab. As a solute, the elution is treated much like common samples and is measured using a fluorometer. As there is no strong correlation between the volume of water and adsorption in active charcoal, the technique provides qualitative, or perhaps semiquantitative results for the time period of exposure. Simultaneous monitoring of the concentration by both sampling and active charcoal gives reliable results for porous aquifers (Figure 4.29) and glaciers (Lang, Leibundgut and Festel, 1979; Leibundgut, 1981a; Behrens *et al.*, 1986). The active charcoal technique is successful in pure water, such as in springs and groundwater. The presence of organic matter may reduce the effectiveness of this technique when sampling in surface water, karst springs or in

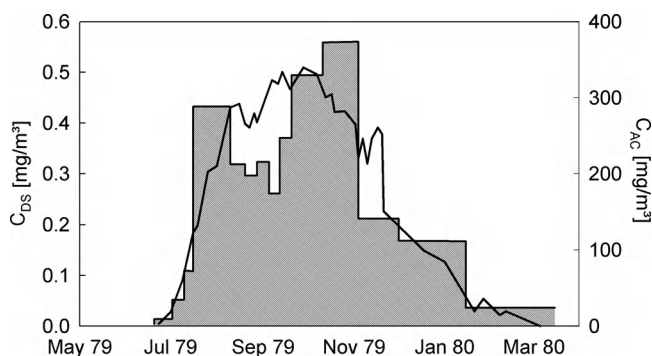


Figure 4.29 Comparative representation of a tracer breakthrough sampled by direct sampling (C_{DS} , line) and by active charcoal (C_{AC} , histogram, cumulative values) in a porous aquifer.

glaciated areas (Drew and Smith, 1969; Bauer, 1972; Brown and Ford, 1973; Smart and Smith, 1976; Perlega, 1977; Wernli, 2003).

The technique is used to sample at remote sampling points and where site access is difficult, such as in karst caves or glaciers (White, 1967; Hötzel, 1973; Lang, Leibundgut and Festel, 1979). Lange *et al.* (1998) described the usefulness of this technique in determining transmission losses during episodic flooding in small arid streams. Smart and Wilson (1984) utilized the activated charcoal technique to investigate the ephemeral nature of pipe flow (macropore). The ‘passive detector method,’ as so-called by the authors, proved to be an efficient technique for the definition of general network characteristics and function. Furthermore, tracer concentrations below the detection limit can be captured by collecting a high volume of water in the charcoal bag. Under ideal conditions, the concentration increases by up to 1000 times (cf. Figure 4.29). However, the progression in sensitivity will usually be limited due to the rise in background concentration. The detection limit may increase due to the presence of organic matter and the associated high background concentration. For tracer experiments related to drinking water supplies, charcoal bags offer the opportunity to monitor over long periods of time. In springs and boreholes also, where tracer breakthrough is not expected, charcoal bags can be used to make sure that no tracer passes unobserved. Suitable charcoal bags, ‘fluocapteurs,’ are described in Bauer (1972), Leibundgut (1981a) and Wernli (2003). Fluocapteurs must allow for sufficient water flow through the sample in order to ensure that the tracer can be adsorbed onto the active charcoal.

Analysis in the laboratory involves more steps than the ‘normal’ analysis. The general procedure is to extract the tracer from the active charcoal and to measure the fluorescence of the elution after a sedimentation phase. A solvent is needed to elute the tracer. For Uranine, methylamine 40% can be used. As methylamine degrades Rhodamine to a dye with a different fluorescence spectrum, it is not suitable to extract Rhodamine or mixtures of Uranine and Rhodamines. Other solvents are pure water, ethanol-caustic potash extraction mixture and ethanol-ammonia mixture. The latter is preferable as it does not turn yellowish during the sedimentation phase. Details of the different methods can be found in Perlega (1977) and Wernli (2003).

Independent of the extraction method, it is important to take into consideration a shift in the fluorescence maxima. For example, ethanol-ammonia mixture: an Uranine maximum lies at 526 nm; in dilutions of more than 1:4 the fluorescence wavelength drops to 516–518 nm (Wernli, 2003). In an ethanol-caustic potash mixture the Uranine maximum lies at 530 nm (Perlega, 1977).

4.2 Salt tracers

In hydrology, salts (i.e. their ions) represent environmental tracers as well as artificial tracers (Table 2.2). Salt tracers are used to investigate aspects of hydrological systems in the same way as other artificial tracers. They are widely used to measure smaller discharges in brooks and springs (cf. Section 6.3). Other specific fields of application are tracer tests in the saturated and the unsaturated zone (Singha and Gorelick, 2005), the combined use of salt tracers and geophysical methods to determine groundwater flow, or to investigate problems of leakage from rivers and sewage pipes (e.g. Armbruster *et al.*, 1992; Zellweger, 1994; Reeves, Henderson and Beven, 1998; Kollmann, Meyer and Supper, 1992; Hoffmann and Dietrich, 2004; Einsiedel, 2005). Furthermore, salt tracers are an alternative to fluorescent tracers in multi-tracer experiments.⁷

Prior to the 1960s, artificial salt tracers were used widely in experiments in karst hydrology (Gospodaric and Habic, 1977). In later years, fluorescent tracers gradually became the main tracers employed. Salt tracers are generally less sensitive than the fluorescent tracers, which limits their suitability and thus their application in recent times. For this reason, salt tracers will be discussed in the following, in order to provide readers with a basis upon which to make their own judgement about the potential use of salt tracers to meet their requirements. Out of the potentially numerous salts only a few are considered to be suitable water tracers (Table 4.11). A successful application of salt tracers is only feasible in small scale experiments, because relatively high tracer masses are needed. Salt tracers can be used for studies in soil profiles in the vicinity of springs or boreholes, and in small surface water bodies (creeks).

4.2.1 Chemical and physical characteristics of salts

Salts are inorganic compounds, which break up into cations and anions when dissolved in water. Ionic compounds in the solid salt form have a high melting point, a brittle consistency and are highly soluble in polar solvents. In solution, and when melted, their electrical conductivity is high due to the mobile ions. Their volatility is low due to strong binding energy (ionic bridges) in the ionic grid.

Again, sorptivity is a crucial property in applications of salt tracers in groundwater, in the unsaturated zone and in soils. Mineral and organic matrix particles with a large surface area (clay, iron oxides, humins) adsorb molecules and ions onto their surfaces.

⁷For example, Batsche *et al.* (1970), Gospodaric and Habic (1977), Müller and Zötl (1980), Leibundgut and Harum (1981), Behrens *et al.* (1992), De Carvalho-Dill *et al.* (1992); ATH (1992).

Table 4.11 The available salt tracers and their properties

| Salt | Molecular formula | Water solubility at 10 °C [g/l] | Ionic radius [Å] | Ionic potential (charge / radius) | Molecular weight [g/mol] | Analysis | |
|-----------------------------|---|---------------------------------|--|---|--------------------------|------------------------------------|----------------------------------|
| | | | | | | ion | method |
| Sodium chloride (mine salt) | NaCl | 357 | Na ⁺ : 1.02 Cl ⁻ : 1.81 | Na ⁺ 1.0 Cl ⁻ -0.6 | 58.44 | Na ⁺ Cl ⁻ | IC, AAS, AES EC, IC, ISE |
| Potassium chloride | KCl | 313 | K ⁺ : 1.38 Cl ⁻ : 1.81 | K ⁺ 0.7 Cl ⁻ -0.6 | 74.55 | K ⁺ Cl ⁻ | IC, ISE, AAS, AES EC, IC, ISE |
| Bromide | NaBr | 850 | Br ⁻ : 1.96 | Br ⁻ -0.5 | 102.89 | Br ⁻ | IC, ISE |
| Lithium | LiCl | 820 (20 °C) | Li ⁺ 0.76 | Li ⁺ 1.3 | 42.39 | Li ⁺ | AES |
| | LiCl 3H ₂ O | | | | 96.38 | | |
| Borax (sodium borat) | Na ₂ B ₄ O ₇ *10H ₂ O | 16.2 | — | — | | BO ₃ ⁻ | ICP-OES, Photometry |
| Iodide | NaI | 184 (25 °C) | I ⁻ 2.2 | I ⁻ -0.5 | 149.89 | I ⁻ | IC, ISE |

AAS: Atomic Absorption Spectroscopy, AES: Atomic Emission Spectroscopy, EC: Electrical Conductivity, IC: Ion Chromatography, ICP-EOS: Inductively Coupled Plasma Optical Emission Spectroscopy, ISE: Ion Selective Electrode.

Humins, for example, have a specific surface area of 800–1000 m²/g. Ionic adsorption is reversible and occurs only in an aqueous solution between the dissolved and solid phase. When tracers are applied to investigate processes in the unsaturated zone, that is in soils, one must bear in mind that the matrix surface of soils also constitutes an ion exchange capacity (Leditzky, 1978). The ions absorbed in the matrix tend to exchange with dissolved ions in the soil water, and therefore also with the tracing ions. Cations and anions exhibit different sorption behaviour. For many soils the cation exchange capacity is higher, and anions are generally characterized by low to very low sorption. In clays, soils containing (Fe, Al)-hydroxides and in soils with a high content of organic matter, however, anions can also be affected by significant sorption. The humic acids contained in such materials often lead to surface complexation, which appears as a sorption effect in a tracer breakthrough. As a result cations suffer a significant loss in passing the matrix due to the negative electrical potential of clays and humins. The nature of the ion exchange is dependent primarily upon the ionic potential (Table 4.11). The higher the potential, the smaller the exchange (Appelo and Postma, 2007). Ions with a higher charge especially exhibit a stronger tendency to sorption. Secondary effects depending on ion radius, concentration or specific affinity of ions, as in the example of potassium and illite, have also to be considered. The dynamics of ion exchange in soils are described, for example, in Scheffer and Schachtschabel (2008) or Appelo and Postma (2007).

In contrast to the sorption of ions is the so called anion exclusion, which may enhance the transport velocity of anions in porous media due to electrostatic repulsion by negatively charged solid surfaces (Gvirtzman and Gorelick, 1991).

Consequently, *salts possess only limited suitability as tracers*. The factors favouring the use of salt tracers are easy handling, availability and the potential for continuous recording. There are also, however, several attributes complicating the application of salt tracers. When using salts as tracers one is confronted, to differing degrees, with the following: high natural background and pollution, high detection limits, large injection masses, transport problems, relatively laborious analyses and the problem of sorption and ion exchange. Potassium cations and iodide anions are strongly affected by sorptive processes. In addition, the latter (I⁻) are unstable and tend to interact with other tracers or substances (e.g. S, Cd, Br, Cl). It also has an effect on water flavour and therefore should not be applied in potable water systems. Borax is limited to short distances in groundwater and the analysis of low concentrations is difficult. In summary, borax, iodide and potassium cations are poorly suited to applications in hydrological tracing. A summary is provided in Käss (1998).

Although salt tracers are of only limited suitability as tracers, there have been many salt experiments performed in the past.⁸ In the initial phase of tracer experiments in karst areas especially, salts served as important tracers alongside fluorescent tracers. The success of these experiments varied considerably. As the suitability of each of the few salt tracers available is quite different, the tracers will be characterized individually briefly in the following.

⁸For example, Verga and Zuppi (1986), Ramspacher *et al.* (1986), Dounas *et al.* (1982), Behrens (1981), Bögli, Leibundgut and Zojer (1981), Feyen *et al.* (1999), Maloszewski *et al.* (2006a, b), Deeks *et al.* (2008), Batsche *et al.* (1970), Gospodaric and Habic (1977), Müller and Zötl (1980), Leibundgut and Harum (1981), Behrens *et al.* (1992), De Carvalho-Dill *et al.* (1992).

4.2.1.1 Sodium chloride (NaCl)

Sodium chloride was the most widely applied artificial salt tracer in the past, due to its easy handling, good sensitivity, nontoxicity, low price and ubiquitous availability. When using this tracer detection is usually based on measurements of the chloride ion (Cl^-). It is assumed to be a chemically stable and conservative tracer with high geochemical mobility. Sorption is usually negligible. A widespread application of sodium chloride as a tracer is in the measurement of discharges in brooks up to several m^3/s using the dilution method. This approach is outlined in greater detail in Section 6.3. A disadvantage is the high natural background concentration of chloride generally, accentuated by pollution arising from activities such as road salting and fertilization. As a consequence, a large quantity of salt is needed. An elegant solution is the injection of brine by a tanker truck or some similar vehicle (Käss, 1972; Müller and Zötl, 1980; Leibundgut and Harum, 1981).

To estimate the tracer mass required for a particular field experiment the approximate ratio of sodium chloride to Uranine used is 10 000:1. This high tracer mass and the considerable transport costs negate the low price of the product itself. The large mass also means that instantaneous injection in a porous aquifer is not possible. An adequate input function has to be found (see Chapter 5). Furthermore, the large amounts needed may lead to a change in the hydraulic flow by changing the specific weight of the traced water mass and will probably cause stratification in the aquifer (e.g. Eissele, 1963). A typical example of this is a karst siphon, where stratification may occur due to the higher density of the traced water, often resulting in misinterpretation of the data. In porous aquifers also, the salt tracer plume may sink down towards the aquiclude. Furthermore, the mixing of the salt with the water requires a long time, which implies an adulteration of the water flow determined by the tracer breakthrough curve. Both phenomena were discussed by Leibundgut (1981a) in the context of a multi-tracer experiment in a fluvioglacial gravel aquifer.

The sorption potential of chloride is relatively low. In many cases it is even virtually an ideal tracer. Its suitability has been demonstrated particularly in karst experiments, but also in porous aquifers (summarized in Käss, 1998) and in the unsaturated zone (Scanlon, 1991; Flury and Wai, 2003; Ptak, Piepenbrink and Martac, 2004). The additional/simultaneous determination of the *Na-cations* in a tracer experiment may provide an interesting insight into the processes of ion exchange (Käss, 1967b; Batsche *et al.*, 1970). However, for technical reasons it is more or less impossible to monitor successfully the Na-cation using ion selective electrodes (Müller and Zötl, 1980).

4.2.1.2 Bromide (Br^-)

In natural hydrological systems Br^- usually occurs at a very low background concentration, usually below the detection limit. For this reason, and also because of its high solubility (ca. 850 g/l at 10 °C), it is easier to handle in the field than other salts. However, bromide also requires a high injection mass, due to its lower sensitivity, approximately 3000 times higher than that of Uranine.

Bromide is assumed to be chemically, biologically and photolytically stable, and due to its negative charge sorption is very low in mineral soils, where it acts mostly as an ideal, or nearly ideal, conservative tracer. Adsorption may occur in humic soils. Bromide is often used for tracer experiments in the vadose zone, and as a reference tracer for comparison purposes (e.g. Onodera and Kobayashi, 1995; Lennartz and Kamra, 1998; Sambale *et al.*, 2000; Ginn *et al.*, 2002; Stamm *et al.*, 2002; Parsons, Hayashi and Van Der Kamp, 2004; Gish *et al.*, 2004). Bromide may be an alternative in certain situations, particularly in problematic test areas with a pH range unsuited to Uranine (Didszun, 2004; Einsiedel, 2005; Hangen *et al.*, 2005; Leibundgut and Uhlenbrook, 2007).

In the case of multi-tracer tests potential interference with Eosine must be taken into consideration. Bromide metabolizes during the processes of chlorination and ozonation in water supply installations. Unlike sodium chloride, bromide can be monitored successfully using ion selective electrodes. However, the technical detection limit is quite high (50 $\mu\text{g/l}$).

Due to its relatively high charge density, Br^- transport generally occurs through the middle of pores, so that it passes through soil and groundwater systems faster than water molecules (Flury and Wai, 2003). As a consequence, the flow velocities measured using bromide do not correspond to those measured using other tracers like Uranine.

4.2.1.3 Lithium

The soft alkali metal lithium is employed as either lithium hydroxide (LiOH) or lithium chloride (LiCl) in hydrological investigations. Lithium cations rarely occur in natural soils and so the background concentrations are very low, or nonexistent. Of the cationic salt tracers, lithium has the lowest affinity for ion exchange.

It has been shown to be a suitable tracer in karst (e.g. Behrens *et al.*, 1992) as well as in porous aquifers (e.g. Käss, 1994; Vereecken *et al.*, 2000; Ptak, Piepenbrink and Martac, 2004). However, some authors reported problems in relation to the detection limit and ion exchange over longer distances; as stated by Käss *et al.* (1986), who detailed a tracer experiment carried out in the karst of Peloponnesus. In porous aquifers lithium is only a suitable tracer over short distances (<200 m).

Given its positive charge and that its retaining properties in the soil matrix are similar to those of metals, lithium is often used to investigate contaminant flow (e.g. heavy metals) in soils (e.g. Bencala, McKnight and Zellweger, 1990). Haase *et al.* (1996) injected lithium chloride into survey wells of different depths to investigate the rooting depth of semiarid vegetation (shrubs). Care needs to be taken when dissolving lithium since the dissolution reaction of, for example, LiBr or LiCl releases heat. To avoid this add sufficient water first and then add the tracer.

4.2.1.4 Iodide

Dissolved iodine occurs as iodide (I^-) or as iodate (IO_3^-) anions, depending on the reducing or oxidizing characteristics of the aquatic environment. The iodate anion is

more reactive and so is less suited to use as a hydrological tracer than iodide. This fact should be kept in mind when iodide is applied as a tracer in an environment with the potential to convert iodide to iodate or iodine. The use of iodine in medicinal products means that it can act as a pollution tracer. Iodide is chemically instable, as a result of which its use is limited to short distance experiments. In combination with starch, however, it forms a starch-iodide complex that can be used to illustrate flow paths in soils (van Ommen *et al.*, 1988; Lu and Wu, 2003). Tracers used for the purposes of visualization in the vadose zone are discussed in Section 4.5.4.

As a redox-sensitive element, iodine can exist in various forms, including iodide and iodate. In reducing environments, aqueous iodine usually occurs as the mobile iodide anion (I^-). Under more oxidizing conditions, iodine may be present as the more reactive iodate anion (IO_3^-), which is characterized by retarded transport due to the fact that iodate interacts with clays and organic matter (Couture and Seitz, 1983; Yoshida, Muramatsu and Uchida, 1992; Hu and Moran, 2005).

Of the halides, iodide is recommended for geothermal tracer studies; bromide and chloride are useful only when their natural background concentrations are low. However, iodide may not be an ideal tracer as it has a tendency to adsorb onto laboratory cores (Chrysikopoulos, 1993).

4.2.2 Measurement techniques

In the past, the analysis of salt tracers was quite complicated and involved several chemical methods. A thorough description of these is provided by Käss (1998). The current state of the art in the analysis of the salt tracers is ion chromatography (IC) and atomic spectroscopy methods. In the case of sodium chloride, electric conductivity can be used as a proxy value in small scale field experiments. There are ion selective electrodes available for the monitoring of chloride and bromide.

4.3 Drifting particles as tracers

Drifting particles, such as spores, phytoplankton, bacteria, viruses, phages and microspheres, constitute another group of artificial tracers, their most characteristic feature being that they are not in solution. Although applied mostly only in very specific situations, drifting particles have been shown to be good qualitative tracers for the investigation of flow paths and hydraulic connections. Traditionally they were widely applied in studies of karst systems. They also have considerable potential as tracers for special applications, particularly in the investigation of hygiene-related issues in the water supply. Nowadays they are being used to study and investigate the flow behaviour of micro-organisms and particles in saturated, unsaturated and surface water systems (Zötl, 1974; Leibundgut and Lüthi, 1977; Benischke *et al.*, 1980; Hötzl, Käss and Reichert, 1991; Sabir *et al.*, 1999; Auckenthaler, Raso and Huggenberger, 2002; Flury and Wai, 2003; Zvikelsky and Weisbrod, 2006; Göppert and Goldscheider, 2008).

4.3.1 General characteristics of drifting particles

Disregarding certain ‘exotic’ particles used in the past (such as chaff, etc.) that have proved to be unsuitable in modern hydrology, the *Lycopodium* spores (club moss spores) were the first particle tracers used successfully in karst systems to verify flowpaths and hydraulic connections. However, like all other particle tracers, they do not allow for an evaluation of the tracer breakthrough curve leading to correct flow parameters as sometimes presented without comment in publications. Other particle tracers include bacteria, phages, viruses and microspheres. The particle sizes limit the through flow of the tracers through larger pores, and so tracer breakthrough probably occurs earlier than is the case for ideal tracers. An accurate quantification of the traced water body is not possible using nonsolute tracers. Nevertheless, particle tracers have potential uses as tracers for special purposes, particularly in the investigation of the filtration capacity of the unsaturated zone and aquifers. They are also useful with respect to the infiltration of contaminants in sewage or irrigation water, and for all applications with hygiene implications, and impacts on water supply installations and water protection zones, subject to the principles outlined by Leibundgut and Lüthi (1977). The sizes of these particles range from 30 μm diameter in the case of *Lycopodium clavatum* to 0.01 μm for the Poliomyelitis virus and 0.001 μm for the DNA tracers (Figure 4.30).

The tracerhydrological suitability of the particle tracers is limited for several reasons:

- only qualitative, perhaps semi-quantitative evaluation is possible,
- all particles tend strongly to ‘adsorption’ onto the surfaces of solid particles,

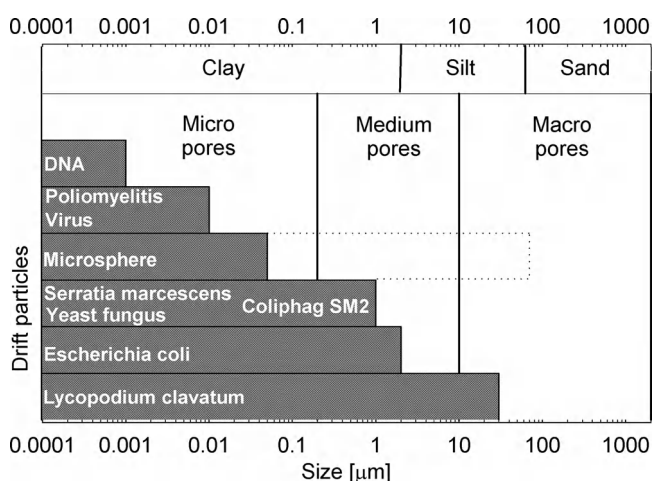


Figure 4.30 Comparison of drift particles (size plotted logarithmically) related to the pore size of substrate.

- the preparation and conducting of both the experiment and the analysis are labour intensive,
- analyses of viruses and bacteria can only be carried out in specialized laboratories,
- sampling bottles need to be uncontaminated and sterile.

Leibundgut and Lüthi (1977) provided a comparison of the application of soluble fluorescent tracers, the bacteria *Streptococcus* and *Lycopodium* spores, which is also presented as a case study in Section 7.2.2 of this book. The study deals with the determination of the filtration capacity of an aquifer and its unsaturated zone near a well.

4.3.1.1 *Lycopodium* spores

Clubmoss (*Lycopodium clavatum*) spores are so far the most commonly used particle tracers for hydrological studies. They have a tetrahedral form with convex surfaces and are almost spherical. They measure ca. 30 μm in diameter and possess a density similar to water (a little higher). The spores' surfaces are coated with a fine network (reticula), which serves to increase adhesion. Injection occurs as a suspension in water. It is necessary to add a detergent or ethyl alcohol as the spores are hydrophobic. One kilogram of spores amounts to between 100–300 billion individual spores. In order to analyse the samples, they must be processed using a caustic potash solution so as to eliminate detritus. After sedimentation the solid fraction is centrifuged and analysed with a microscope (100–200 \times magnification). The methods and analyses were outlined by Zötl (1967), Bauer (1967), Dechant (1967) Hötzl, Maurin and Zötl (1976), and discussed in detail by Zötl (1974).

In addition to the 'traditional' detection method, namely counting spores, it is also possible to add a fluorescent coloured dye (Käss, 1982; Dechant and Hacker, 1986; Käss and Reichert, 1986; Benischke, Goldscheider and Smart, 2007) and to subsequently measure applying fluorescence measurement techniques. The availability of multi-coloured spores allows for their application in combined or multi-tracer experiments.

4.3.1.2 *Bacteria and bacteriophages (or phages)*

Bacteria and bacteriophage tracers are used mainly to investigate the dissemination of germs in various systems, and especially to monitor pollution in potable water. Examples of the bacteria species employed include *Escherichia coli*, *Staphylococcus crus*, *Streptococcus faecalis* ATTC, *Serratia marcescens* and *Pseudomonas fluorescens* (e.g. Auckenthaler, Raso and Huggenberger, 2002; Silliman *et al.*, 2001; Gunn *et al.*, 1998; Sinton and Ching, 1987; Leibundgut and Lüthi, 1977). However, when applied in the unsaturated zone post-experimental treatment (e.g. with sodium hydroxide solution, as described

by Käss, 1998) is required due to the potential for proliferation. Bacteria and phages tend strongly to adsorption onto the surfaces of solid particles.

Bacteriophages (or phages) have been used as hydrological tracers in many studies in the past, and are still widely employed today, but apart from their low detection limit (1 phage per 1001) and the large range of possibilities for application, the obstacles to their widespread use still outweigh the advantages. The preparation and conducting of experiments is extensive, the sampling bottles must be uncontaminated and the analyses can only be carried out in specialized laboratories with electron microscopes. Bacteria and phages also tend to be adsorptive, even in karstic aquifers (Mallen *et al.*, 2005). Furthermore, their applicability as viable tracers depends very much on the environment. These particles have been used as hydrological tracers in many studies; in groundwater, in the vadose zone and in surface water. The methods of application have been described in great detail (Kinnunen, 1978; Aragno and Müller, 1982; Rossi, 1992, 1994; Rossi *et al.*, 1994; Bricelj and Sisko, 1992; Käss, 1982, 1998; Flynn *et al.*, 2006).

Bacteriophages can supplement the set of applicable tracers only where the flow paths in groundwater and surface water are of interest, and where no further quantitative and mathematical evaluation of the field experiments is required. Thus, tracer experiments with phages do not allow for an evaluation of the tracer breakthrough curve, needed to provide correct flow parameters according to the theoretical needs (cf. Chapter 5) as is sometimes claimed. For this reason, and due to the high adsorption affinity, phages are not suitable for state of the art experiments in aquifers and unsaturated zones. There is also no evidence to suggest that the phages continue to be the preferred tracers in lakes and seas (Käss, 1998). The potential benefits of stable isotope and fluorescent tracers are much greater, as will be discussed in Chapter 7.

In addition to the general restrictions mentioned above, the particular limitations with respect to the suitability of bacteria and bacteriophages are:

- deactivation as a result of rapid natural decay (loss of viable phages) following a first-order kinetic decrease (Bricelj and Sisko, 1992),
- phages have a strong tendency to adsorption onto the surfaces of solid particles,
- their applicability as viable tracers depends greatly on the environment (i.e. pH, chemistry, oxygen, organic matter and especially temperature),
- each type of phage reacts individually; not all react in the same way to physiochemical influencing factors such as pH, polarity and so on.

However, as mentioned above, the sensitivity of phages is high and they are potentially useful as tracers for special purposes, particularly in the investigation of the filtration effects of contaminants in sewage and irrigation water (Kinnunen, 1978), and for all studies concerning hygiene implications and impacts on water supply installations and

water protection zones (Leibundgut and Lüthi, 1977; Marti *et al.*, 1979; Auckenthaler, Raso and Huggenberger, 2002; Flury and Wai, 2003).

4.3.1.3 Fluorescent microspheres

Although fluorescent microspheres are applied widely in medical studies, they have only a limited recognized use as hydrological tracers. Microspheres are synthetic colloidal polystyrene latex particles. They are available in various sizes ranging from 0.05 to 90.0 μm , and may possess different surface characteristics. Mostly sizes $< 5 \mu\text{m}$ have been used for hydrological purposes as yet. Incorporated into the polystyrene latex beads are hydrophobic fluorescent dyes. Two types of beads are available: plain and carboxylated microspheres (Ward *et al.*, 1997). They can be supplied as an aqueous suspension in pure deionized water.

The analysis process is similar to that of fluorescent Lycopodium spores, involving epifluorescence microscopy of a membrane-filtered sample (see Section 4.3.1) and requiring no further preparation. Ward *et al.* (1997) developed the technique further by dissolving the microsphere matrix, which releases the fluorescent dye into a solution. The result is a much easier analysis. The costs are moderate and no interference with other tracers are known. The technical details and examples of several microsphere tracer tests were reported on by Harvey *et al.* (1989), Ward *et al.* (1997) and Käss (1998).

As with all of the other particle tracers, microspheres are only really suitable for special applications, such as the investigation of colloid or particulate transport processes and the simulation of the propagation of pathogenic bacteria. For the latter, a microsphere diameter of approximately 1 μm is recommended. Microspheres serve especially well in karst aquifers.

4.3.2 Measurement techniques and sampling of particle tracers

4.3.2.1 Measurement

The detection method is in the best case semi-quantitative but generally solely qualitative. In order to detect spores, bacteria and microspheres, the water from the investigated source is filtered, and the accumulated particles are counted under the microscope. The Lycopodium spores require further treatment before measurement (see Section 4.3.1.1). Bacteria and bacteriophages can be detected by cultivation. These methods require time and so are unsuitable for field measurements. However, a monitoring technique, similar to fluorescent tracers, has not been developed as yet.

In addition to the 'counting' method, it is also possible to measure fluorescent microspheres, and bacteria and spores dyed with fluorescent colours, employing fluorescence measurement techniques (Käss, 1982). Niehren and Kienzelbach (1998) presented an online microsphere counter with a detection limit of one microsphere (diameter: 1 μm)

per ml water. The availability of multi-coloured spores allows for their application in combined or multi-tracer experiments.

4.3.2.2 Sampling

The sampling of drift particles often proves difficult. Spores and microspheres must be sieved out. Naturally the pore size of the filter (plankton net/nylon net) must be smaller than that of the particles. A pore size of $25\ \mu\text{m}$ is recommended for spores (e.g. Käss, 1998; Hötzl, Maurin and Zötl, 1977). Microspheres with a smaller diameter require a smaller mesh size. To avoid clogging of the filter by other suspended materials, Wolkersdorfer (2001) recommended an upstream net with a larger mesh size.

4.4 Radioactive tracers

Radioactive tracers were used frequently to solve hydrological problems in the past, under the guidance of the International Atomic Energy Agency (IAEA).⁹ Nowadays radioactive substances may be applied to hydrological subsystems as artificial tracers only upon receipt of special permission from a local Atomic Energy Commission.

4.4.1 Basics of radioactivity

Every chemical element stands for various isotopes of nuclides, all of which have the same atomic number (i.e. number of protons), but different mass numbers (i.e. number of protons + neutrons). Some nuclides are stable, some are unstable; the latter being radioactive isotopes. The unit of radioactivity is the Becquerel (Bq), defined as decay per second. The old unit, Curie (Ci), is seldom used today ($1\text{Ci} = 3.7 \cdot 10^{10}\text{Bq}$). Essentially, radioactive decay can occur in three ways:

- α -Radiation: He-nuclides are emitted, resulting in a high ionization density. Thus, α -radiators are not used as tracers.
- β -Radiation: electrons are emitted, a medium ionization density allows for the use of a few substances as tracers.
- γ -Radiation: electromagnetic radiation takes place with a high diffusion capacity. γ -radiators are good tracers.

The decay is the basic behaviour of radioactive tracers. Decay is a first-order reaction, which means that the number of decaying atoms per unit of time is proportional to the

⁹For example, Moser and Rauert (1980), Drost (1983), Plata (1983, 1991), Rao (1983), Florkowski (1991), Mandel (1991), Margrita and Gaillard (1991), Navada (1991), Roldao (1991).

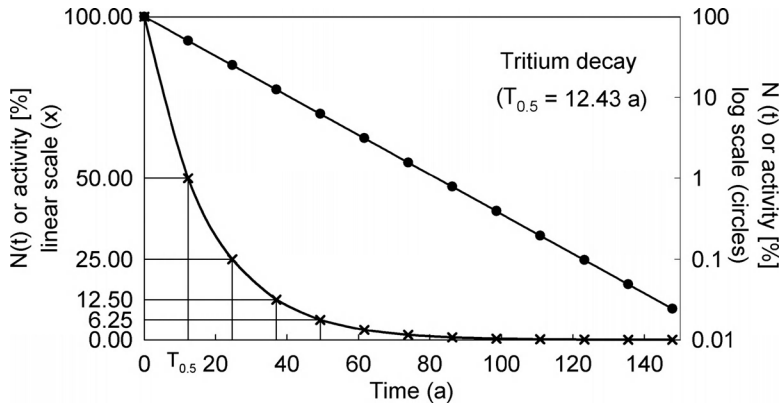


Figure 4.31 Decline of radionuclide activity with decay time; linear (left axis, x) and semilogarithmic (right axis, dots) graphs.

total number of atoms of the nuclide (where λ is the decay constant). After a certain time (t), from the initial N_0 atoms only $N(t)$ are left (Figure 4.31):

$$N(t) = N_0 \cdot \exp(-\lambda \cdot t) \quad (4.9)$$

A characteristic quantity is the time at which half of the original number of atoms has decayed, called a half-life time ($T_{1/2}$). It shows the following relationship:

$$N(t = T_{1/2}) = 0.5N_0 = N_0 \exp(-\lambda \cdot T_{1/2}) \quad (4.10)$$

So, the decay constant is related to the half-life by:

$$\lambda = \ln(2)/T_{1/2} = 0.693/T_{1/2} \quad (4.11)$$

Generally, the radiation and the decay per unit time are measured using counting devices such as the Geiger counter, semiconductor counter and scintillation counter. Depending on the device, these can be used to measure α , β or γ radiation.

The Geiger counter and similar devices record activity and decay. The output (count) is a summation of potentially more than one radioactive element, as the Geiger counter cannot distinguish between different nuclides. Due to the varying gamma quantum energies of different radionuclides, the semi-conductor and the scintillation counters can measure gamma spectra and so distinguish between different nuclides. Further information on the measurement of radioactivity can be found in Moser and Rauert (1980).

4.4.2 Characteristics of radioactive tracers

The potential health and environmental risks posed by radioactive substances mean that the use of artificially applied radioactive tracers is very limited nowadays. Those that still prevail are those with either low half-life times or low radiation energies, such as ^3H , ^{51}Cr , ^{114}In and ^{82}Br . Radioactive substances which have been used for water tracing are given in Table 4.12.

The advantages of radioactive tracers are that they are very sensitive and offer selective detection, the disappearance of the tracer from the system due to decay, and the ability to follow the flowpath of water and tracer using a Geiger counter. The disadvantages are the potential health risks of some tracers, the very high costs of measurement and materials, and the fact that it is unlikely that a permit will be granted for the tracer test. The disadvantages generally hinder the application of radioactive tracers in countries with modern environmental legal standards. Even so, they are very suitable for studies addressing specific problems and they disappear rapidly after their half-life period has expired.

Table 4.12 Radioactive substances used for water tracing (source: Moser and Rauert, 1980)

| Radioactive nuclide | $T_{1/2}$ | Chemical compound | Radiation | Characteristics |
|---------------------------|-----------|--|-----------|--|
| ^3H | 12.43 a | ^3HHO (Water) | β | Chemically identical to the labelled water |
| ^{51}Cr | 27.7 d | EDTE - chelat | γ | Low sorption |
| $^{114\text{m}}\text{In}$ | 50 d | EDTE - chelat | γ | Low sorption |
| ^{114}In | 72 s | EDTE - chelat | β | Low sorption |
| ^{58}Co | 70.8 d | $[\text{Co}(\text{CN})_6]^{3-}$ - chelat | γ | Low sorption |
| ^{60}Co | 5.3 a | $[\text{Co}(\text{CN})_6]^{3-}$ - chelat | γ | Low sorption |
| ^{82}Br | 36 h | Br^- - Anion | β | Very low sorption, chemically very stable |
| ^{131}I | 8.05 d | I^- - Anion | β | Chemically unstable, sorption by oxidation |
| ^{24}Na | 15.0 h | Na^+ - Kation | β | Sorption, can be used in channels |
| <i>Activation product</i> | | | | |
| ^{80}Br | 17.6 min | Br^- - Anion | γ | Low sorption |
| $^{116\text{m}}\text{In}$ | 54 min | EDTE - chelat | γ | Low sorption |
| Rare earth elements | | EDTE - chelat | γ | Low sorption |

Tritium (^3H) – tritiated water, as a constituent of the water molecule, is an ideal tracer. It can be used as an artificial tracer but only in applications that do not disturb measurements of environmental tritium. At the present time, tritium is mainly used in lysimeter and laboratory-column experiments, and in strongly contaminated sites, where the dye tracers are not suitable due to strong sorption processes. Tritium has declined in importance as an artificial tracer due to concerns over its toxicity and its relatively long half-life. An application is presented in Section 7.3.6.

$^{51}\text{Chromium}$ is still used in many tracer experiments; for example by Jonsson, Johansson and Wörman (2004) as a reactive radioactive tracer in the hyporheic interstitial. $^{114}\text{Indium}$ was used a lot more in the past than is the case today. It is a gamma-emitting radionuclide with a half-life of 49.5 days. It emits gamma-energies of 190, 558 and 725 MeV. To be suitable as a water tracer it must be used in the proper chemical form. The EDTA-complex has been proven to be perfect. Although the EDTA-complex provides a kind of negative shield around the indium-cation, sorption onto sediments can play a role when analysing the tracer quantitatively.

4.4.2.1 Single-well technique

One of the most important methods when using radioactive tracers is the single-well technique. The single-well technique makes use of radioactive isotopes artificially injected into the system under investigation in order to measure filter velocity and flow direction (Drost and Neumaier, 1974). Further information concerning the method and its application is contained in Section 7.1.3.

4.5 Other tracers

4.5.1 Fluorobenzoic acids (FBA)

A variety of fluorinated derivatives of benzoic acids (fluorobenzoates) have been proposed as tracers (Malcolm *et al.*, 1980; Stetzenbach, Jensen and Thompson, 1982; Bowman, 1984a; Bowman and Gibbens, 1992; McCarthy, Howard and McKay, 2000). Their use in hydrological applications has received considerable attention over the past 20 years. There are 16 FBA isomers or derivatives that exhibit similar physicochemical properties and environmental behaviour, due to the number and the position of the fluorine atom in the benzene ring (Hu and Moran, 2005). According to Juhler and Mortensen (2002), all of these can serve as tracers. FBAs typically chosen for hydrological studies are Difluoro-Benzoic Acids (DFBAs).

Fluorobenzoic acids do not occur naturally and are, therefore, suitable for use as hydrological tracers. Their pK_a values (acid dissociation constant) are relatively low. This indicates that FBA tracers are predominantly negatively charged under most environmental conditions. As anions they are readily soluble in water and are nonvolatile. In terms of their transport behaviour, Fluorobenzoic acids have often been compared

with the inorganic anion bromide (Bowman and Gibbens, 1992; Benson and Bowman, 1994; Jaynes, 1994; McCarthy *et al.*, 2000; Dahan and Ronen, 2001). FBAs are generally described as being conservative tracers with low levels of sorption and degradation under laboratory and field conditions. Recent investigations, however, reveal a more differentiated view. In substrates rich in clay or organic matter, both significant degradation and retardation are possible (Bowman and Gibbens, 1992; Jaynes, 1994). Seaman (1998) also observed the adsorption of FBAs to hydrous Fe-oxides. The suitability of FBAs as tracers for a specific material should, therefore, be evaluated prior to field experiments, especially in the presence of organic carbon, clay and Fe-oxides (Hu and Moran, 2005). Given the dependence upon pH conditions, low pH levels are generally problematic. Results from sorption and transport experiments presented by McCarthy *et al.* (2000) indicate that FBAs can be useful as nonreactive tracers as long as the pH is approximately 2 pH units above the FBA's specific pK_a . The stability of FBA isomers under strictly anaerobic conditions has yet to be investigated (Benson and Bowman, 1994). In summary, according to Flury and Wai (2003), benzoate and fluorobenzoates are useful tracers that migrate under most pH conditions found in soils and aquifers, similar to bromide. Under low pH conditions, mobility usually decreases. Sorption and transport of fluorobenzoates can be affected by the presence of organic carbon, clay and Fe-oxide. The behaviour of the tracer in the presence of these three compounds should be evaluated by means of sorption or column tests prior to conducting the experiment.

McCarthy *et al.* (2000) assessed the aquatic toxicity of four Fluorobenzoic acids tracers using a *Ceriodaphnia* 96-h acute toxicity test. The LD50 (lethal dose resulting in the mortality of $\geq 50\%$ of the test organisms) of the tested isomers was above 100 mg/l. The toxicity of FBAs for humans has not been established (Wright and Hull, 2004). FBAs should not be used as tracers where there is a risk of causing contamination to drinking water until more definite human toxicity information becomes available.

4.5.1.1 Suitability/potential applications

Fluorobenzoic acid tracers are applied in the investigation of water flow and solute transport in the unsaturated zone and in both porous and fractured aquifers (Dahan and Ronen, 2001). Recent studies have demonstrated that FBAs may not exhibit ideal conservative behaviour in certain experimental constellations. Nevertheless, FBAs were in the past often proposed as tracers for vadose zone hydrology because of the lack of background concentrations and the relatively good mobility properties. FBAs might be useful as alternative tracers where other common anionic tracers are not suitable. Unlike salts, most FBAs are quite expensive (Caldiga and Greibrokk, 1998; Turin *et al.*, 2002). As the aqueous diffusion coefficients of FBAs are about a third of those of the halides, diffusivity-tracer approaches using FBA and halide tracers simultaneously have also been employed to investigate solute dispersion and diffusive mass transfer between fast- and slow-moving flow regions (Hu and Moran, 2005 and references therein).

The greatest potential use of FBAs would appear to be in multi-tracer tests due to the wide variety of available isomers in this tracer family displaying similar characteristics (Dahan and Ronen, 2001; Juhler and Mortensen, 2002; Turin *et al.*, 2002; Wright

and Hull, 2004; Hu and Moran, 2005). Multiple FBA tracers can be applied either simultaneously or sequentially. This makes it possible to conduct several simultaneous leaching studies at the same location without tracer interference (e.g. Kung *et al.*, 2000; Gish *et al.*, 2004; Wright and Hull, 2004; Hu and Moran, 2005) and to tag individual injection boreholes (e.g. Turin *et al.*, 2002).

A systematic evaluation of the characteristics of FBAs as suitable tracers similar to that of fluorescent tracers taking into account the required properties for hydrological tracers is still needed (cf. Table 4.3).

Analytical methods and detection limits The detection limits of FBA tracers depend on the analysis method. In general, FBAs can be analysed using ion chromatography (Pearson, Comfort and Inskeep, 1992), high performance liquid chromatography (HPLC) with ultraviolet detection (Bowman, 1984b), HPLC combined with a reverse phased separation method (Dahan and Ronen, 2001), gas chromatography-mass spectrometry (GC-MS) analysis of derivatives (Caldiga and Greibrokk, 1998) and liquid chromatography-tandem mass spectrometry (LC-MS-MS) (Juhler and Mortensen, 2002). According to Hu and Moran (2005), the most widely used method for FBA analysis uses high-performance liquid chromatography (HPLC) with UV detection after separation by means of a strong anion exchange (SAX) column. For multi-tracer tests, the possibility of simultaneous analyses of multiple FBA isomers employing chromatography techniques is advantageous, and single run capacities might become crucial for cost efficiency (Hu and Moran, 2005).

4.5.2 Deuterium ^2H as an artificial tracer

The isotopes ^{18}O , ^2H and ^3H are essentially attractive hydrological tracers. The stable isotopes of water are the most commonly used environmental tracers. Being constituents of the water molecule themselves, they are considered to be those most capable of representing the true flow of water. Usually these isotopes are used as natural tracers, but the isotopes may potentially also be employed as artificial tracers. In both natural and artificial applications the physics and measurement techniques are identical (cf. Chapter 3).

In recent times the application of tritiated water (^3H) as an artificial tracer has become rather infrequent due to radiation risks and eco-toxicological concerns. Therefore, the most promising isotopes are the stable oxygen and hydrogen isotopes. Both deuterium (^2H) and oxygen 18 (^{18}O) are nontoxic, completely soluble, chemically and biologically stable and are not subject to photolytic decay.

As deuterated water, ^2H is available in concentrations of almost 100%. Double labelled water (^2H and ^{18}O enriched) can also be purchased and applied as a tracer. Experiments using environmental isotopes as a label (enriched or depleted) of the water in the system under investigation have also been reported. Such studies do not influence the environment and may be more affordable.

Successful applications of deuterated water have been reported in laboratory tests, lysimeter (cf. Section 7.2.2) and groundwater studies, and for investigations of solute

transport in the unsaturated zone and of water flow in the soil-vegetation system.¹⁰ The advanced application of deuterated water for the estimation of tree transpiration and the investigation of plant water uptake in the xylem flow has been discussed in several papers (Calder *et al.*, 1986; Calder, 1992; Kalma, Thorburn and Dunn, 1998; Maloszewski *et al.*, 2006).

Comparing deuterium with other groundwater tracers, Leis and Benischke (2004) found that deuterium and bromide showed the highest degree of conservativity. Consequently, deuterium is often regarded as a reference in multi-tracer tests. However, the diffusion rate of ^2HHO in water is high when compared with other conservative solute tracers. It is particularly important in experiments performed in the presence of immobile water zones (Becker and Coplen, 2001).

Deuterium can be purchased in concentrated form ($^2\text{H}_2\text{O}$), but because of the high costs only applications involving relatively small volumes of water are usually feasible. The sensitivity of the analytical equipment necessitates that special attention be paid to the determination of the injection amounts, to avoid an inappropriately 'heavy' signature of the water samples (Königer, 2003). This includes the conversion of the concentrations of the injected deuterated water to the δ notation used for sample analyses (cf. Chapter 3). In practice, a level of precision of 2‰ of the hydrogen-isotope analysis results in a minimum detectable concentration of about 0.1 mg/l above the background concentration (Becker and Coplen, 2001). However one should remember that deuterium has a high natural background of 155.76 mg/l.

The alteration of the natural isotope signature is another disadvantage of the use of deuterium as an artificial tracer in large scale experiments, as this may inhibit its usefulness as an environmental tracer. In spite of these restrictions, deuterium would appear to be an appropriate artificial tracer, particularly for investigations in the unsaturated zone. For this purpose the feasibility of analysing quite small sample volumes is also beneficial (Königer, 2003).

4.5.3 Dissolved gas tracers

The use of injected dissolved gas tracers was proposed by Carter *et al.* (1959). However, technical difficulties related to the injection, sampling and analysis of the gases have been obstacles to their widespread use as tracers. Many of these problems have been overcome in recent times and since the 1990s their application has increased (Solomon, Cook and Sanford, 1998). In addition to the naturally occurring noble gases, man made fluorinated compounds (SF_6 , CFCs, PFCs) display properties meeting the requirements for use as artificial tracers. In oceanography, sulfur hexafluoride (SF_6) has been applied in tracer experiments for many years (Watson and Ledwell, 2000), and its use in hydrological investigations seems to be increasing.

¹⁰García Gutiérrez *et al.* (1997), Himmelsbach, Hötzel and Maloszewski (1998), Schwinning *et al.* (2002), Stamm *et al.* (2002), Königer (2003), Benischke, Leis and Stadler (2004), Leis and Benischke (2004), Hangen *et al.* (2005), Cencur Curk, Bricelj and Stihler (2006), Mali, Urbanc and Leis (2007), Wenninger (2007), Stumpff (2008), Königer and Marshall (2008), Königer *et al.* (2009).

4.5.3.1 *Common gas tracers and tracer characteristics*

The most commonly used gas tracers include helium, neon and stable isotopes of krypton and sulfur hexafluoride. The favourable characteristics of noble gases are their inert and nontoxic nature in hydrological systems (Solomon, Cook and Sanford, 1998). Furthermore, concentrations of dissolved gas in many orders of magnitude greater than background concentrations can be obtained without any difficulty, even for large volumes of traced water. Argon is an exception due to the comparatively high natural background concentrations and for this reason is generally not used. Xenon gas is also rather expensive, which limits its practical application as a tracer substance (Solomon, Cook and Sanford, 1998).

Like the noble gases, fluorinated compounds are relatively inert in water, nontoxic and can be detected even at low levels (Solomon, Cook and Sanford, 1998). Significant degradation of CFCs is possible under highly reducing conditions (Busenberg and Plummer, 2000). Noble gases, CFCs and SF₆ have the potential to serve as environmental tracers for hydrological investigations (cf. Chapter 3). However, the choice of SF₆ as an artificial hydrological tracer should be considered carefully, given the high potential greenhouse gas effect of SF₆ gas (Busenberg and Plummer, 2000). In future its use may become subject to restrictions due to the potential for negative environmental impacts.

4.5.3.2 *Gas-specific methods – technical equipment*

Obviously dissolved gases differ from other tracers primarily on the basis of their volatile nature, with specific requirements in terms of tracer injection, sampling and analysis to prevent degassing.

Measures must also be taken at the time of injection to avoid the formation of air bubbles. Usually injection is by means of blowing the gaseous tracer directly into the water through diffusers, as described by Sanford, Shropshire and Solomon (1996). A near constant injection rate can be maintained during hours or days. A suitable injection porous pipe needs to be found through which gas diffuses slowly enough to be dissolved completely. In fact, the cost of the gas applied is the limiting factor for constant injection experiments. By contrast, gas tracers are less suited for instantaneous injection. Sugisaki and Aoki (1993), Gupta, Moravcik and Lau (1994), Uddin, Dowd and Wenner (1999) and Shapiro *et al.* (2008) provided examples of how a virtually instantaneous injection can be achieved in aquifers. This usually requires the prior preparation of a gas tracer solution. The methods and the equipment required for injection, sampling and the preparation of aqueous solutions of tracer gases were described in detail by, for example, Sanford, Shropshire and Solomon (1996), Sanford and Solomon (1998) and Wilson and McKay (1993, 1996).

Generally the analysis of gas tracers is carried out by means of gas chromatography, which is common to many laboratories (Sanford, Shropshire and Solomon, 1996). However, advanced methods using a gas chromatograph equipped with an electron capture detector (GC-ECD) improve sensitivity and yield an enlarged concentration range for tracer applications. For example, Law, Watson and Liddicoat (1994) reported a range up

to seven orders of magnitude greater for SF₆. There are commercial devices available for the detection of SF₆ based on spectrography with diode lasers. Although the detection is less accurate than with GC-ECD, these devices can be useful for online measurements.

4.5.3.3 Applications

The volatility requires that in field applications the gas tracers are used without the presence of a gas phase, if a quantitative evaluation is intended. Exchange with air entrained in unsaturated media and gradual losses from the solution through the air-water interface of shallow aquifers or surface water bodies reduce the validity of tracer tests (Wilson and McKay, 1993; Gupta, Moravcik and Lau, 1994; Engblom, Sanford and Stednick, 2004). However, by injecting a second nonreactive gas along with the tracer gas and monitoring the distributions of both gases, the gas transfer velocity can be quantified and the mass balance closed (Watson, Upstill-Goddard and Liss, 1991; Clark *et al.*, 1996). Gas tracers can also be useful for largely qualitative tracing of hydrological connections between surface waters and local aquifers (Engblom, Sanford and Stednick, 2004; Gamlin *et al.*, 2001; Avisar and Clark, 2005; Harden *et al.*, 2008). Several applications taking advantage of the volatile nature of gas tracers have been proposed; for example to delineate unsaturated zones (Upstill-Goddard and Wilkins, 1995) or use as a partitioning tracer to detect pools and residual zones of NAPLs in the subsurface (Wilson and McKay, 1995; Cirpka and Kitanidis, 2001; Divine, Sanford and McCray, 2003). Returning to the classical applications of artificial tracers, dissolved gases are regarded as being especially suitable for experiments involving large volumes of water (Solomon, Cook and Sanford, 1998; Gamlin *et al.*, 2001). This is attributed to the wide concentration range possible, which renders them cost effective. However, their potential can only be fully utilized if advanced analysis methods are available. One must also always take into consideration the laboratory costs. One may very well opt to use a dissolved gas in situations where other tracers are not applicable for certain reasons; for example in very sensitive environments.

4.5.4 Nonfluorescent dyes

Inevitably all dyes used for staining experiments make far from ideal tracers. Nonfluorescent dyes may be valuable tracers for transport studies but, particularly in terms of travel times and distances, they do not adequately represent the water itself. However, staining techniques have attracted remarkable interest as a tool for demonstrating the occurrence of preferential flow in soils.¹¹

In contrast to the classical idea of tracer applications, staining experiments rely on the usually problematic sorption effect of the tracer to a degree, ensuring its distinct visibility in the porous media. Thus, when choosing a tracer, two competing criteria

¹¹Van Stiphout *et al.* (1987), Van Ommen *et al.* (1988), Andreini and Steenhuis (1990), Ghodrati and Jury (1990), Hatano and Booltink (1992), Flury *et al.* (1994), Petersen, Hansen and Jensen (1997), Perillo *et al.* (1999), Öhrström *et al.* (2002), Weiler (2001), Weiler and Näf (2003), Morris and Mooney, (2004).

must be considered, namely visibility and mobility (Flury and Flühler, 1995). The major outcome of such tracer experiments are not breakthrough curves but stained profiles visualizing the spatial flow patterns of infiltrating water and solutes. Tracer visualization experiments can also be conducted by using iodide or bromide, if an indicator solution is applied in order to trigger a colour reaction (Van Ommen, 1985; Lu and Wu, 2003). A similar method using ammonium carbonate and pH indication was proposed by Wang *et al.* (2002).

A variety of tracers is available, fluorescent dyes included. Nonfluorescent dyes were tested for visualization purposes in soils by Corey (1968), Smettem and Trudgill (1983), Flury and Flühler (1995), Mon, Flury and Harsh (2006) and others. A comprehensive review of the application of dye tracers in the vadose zone was provided recently by Flury and Wai (2003). Most fluorescent and nonfluorescent dyes are organic molecules with varying functional groups. Apart from fluorescence itself, the chemical and physical principles relevant for tracing, discussed in Section 4.1.2, are also largely applicable to nonfluorescent dyes. The interaction of a dye with solid materials depends on its type of functional groups and the pH conditions. For instance, methylene blue (CI Basic Blue 9), which exhibits excellent visibility in most soils, has been used extensively for flow path visualization (e.g. Bouma and Dekker, 1978; Smettem and Collis-George, 1985; Van Stiphout *et al.*, 1987; Hatano *et al.*, 1992). However, due to its cationic form in aqueous solutions it adsorbs strongly onto most subsurface media and is not a good indicator of water movement. With respect to sorption behaviour in soils generally, acid dye tracers are preferable (Corey, 1968; Flury and Wai, 2003; Mon, Flury and Harsh, 2006). They are regarded as being relatively mobile and the best suited of the dyes for visualization experiments aimed at characterizing flow.

After dye-tracing conducted as part of a sprinkling experiment in an excavated soil section provides only one picture of the cumulative flow pattern, allowing at best for integral statements about major flow processes (Weiler, 2001). As the dye pattern does not match the infiltration pattern of water exactly, it must be interpreted with caution. The complex sorption mechanisms must be taken into account in order to avoid misinterpretations (Bouma and Dekker, 1978; Flury and Wai, 2003). The dye front is always retarded when compared to the wetting front and to conservative tracers. Furthermore, the pattern formed depends on the sorption characteristics of the dye, the varying chemical and physical conditions throughout the soil profile and the application rate and the resultant differences in contact time (Corey, 1968; Flury and Flühler, 1995; Perillo *et al.*, 1998; Ketelsen and Meyer-Windel, 1999; German-Heins and Flury, 2000; Kasteel, Vogel and Roth, 2002; Mon, Flury and Harsh, 2006).

Depending on the purpose behind the visualization and analysis of the spatial patterns, specific evaluation techniques are required for dye-tracing experiments if more than a qualitative illustration is intended. Usually this involves applying image analysis procedures to photographs taken from excavated stained soil sections after the tracer experiment.¹² The use of binary images revealing simply either the presence or absence

¹²Hatano *et al.* (1992), McBratney *et al.* (1992), Droogers *et al.* (1998), Ogawa *et al.* (1999), Forrer *et al.* (1999), Forrer *et al.* (2000), Weiler (2001), Vanderborght *et al.* (2002), Kulli *et al.* (2003), Weiler and Flühler (2004), Persson (2005), Schlather and Huwe (2005a), Mooney and Morris (2008), Bogner *et al.* (2008).

of the dye was common in the past. Recently considerable progress has been made in the development of methods enabling actual estimates of concentration.

4.5.4.1 *Brilliant blue*

Introduced to soil-hydrology by Flury and Flühler (1995), the food dye Brilliant Blue FCF (CI Acid Blue 9 also known as FD&C Blue 1/CI Food Blue 2) has become the most prominent tracer used in visualization experiments in the vadose zone. The bright greenish-blue colour of the dye provides a good contrast to most soils, and tracer fronts are likely to be very sharp. Another advantage is that as a food dye it possesses a relatively low toxicity, explaining its preferred use in field tracer experiments. Sorption behaviour is strongly nonlinear and generally complex, but it has been studied extensively in comparison with other potential dye tracers (German-Heins and Flury, 2000; Ketelsen and Meyer-Windel, 1999; Kasteel, Vogel and Roth, 2002; Stamm *et al.*, 2002). The costs are also reasonable. According to many authors, Brilliant Blue FCF is one of the best tracers currently available for visualization experiments in the vadose zone.¹³

¹³Flury and Flühler (1994), Flury *et al.* (1994), Flury and Flühler (1995), Perillo *et al.* (1998), Ketelsen and Meyer-Windel (1999), German-Heins and Flury (2000), Ketelsen and Meyer-Windel (1999), Kasteel, Vogel and Roth (2002), Flury and Wai (2003), Morris and Mooney (2004), Mon, Flury and Harsh (2006).

5

Mathematical Modelling of Experimental Data

Tracers are applied in hydrological systems mainly: (i) for the quantitative determination of rock and/or flow properties (e.g. water velocity, hydraulic conductivity, dispersivities, porosities, transit time, volume of water, flow rates); and (ii) for the calibration or validation of numerical flow and transport models. The estimation of parameter values from tracer experiments is only possible if an adequate mathematical model is used: the selected model must reflect the tracer transport and tracer behaviour in the system being studied. Some of problems related to model selection are discussed by, for instance, Maloszewski and Zuber (1992b, 1993). The definitions used here for tracer modelling are summarized in Chapter 2. The present chapter gives the mathematical description of artificial tracer transport in homogeneous and heterogeneous groundwater systems, in surface water (rivers and streams), as well as in double-porous media, such a fissured rocks, the unsaturated zone and rivers (streams) with stagnant water zones. Furthermore, the lumped-parameter approaches used for quantitative interpretation of environmental tracer data are discussed. Additionally, some examples of using those models are presented.

5.1 Artificial tracer (ideal) under saturated flow conditions

5.1.1 Transport equations

5.1.1.1 3D equations

In an aquifer containing only mobile water, the transport of nonreactive and non-decaying solutes in groundwater is described by a three-dimensional (3D) dispersion equation in which the dispersion has a tensor form and the water flow velocity a vector

form (Bear, 1961; Scheidegger, 1961). For an ideal tracer, this transport equation – here referred to as the general 3D transport equation – has the following form:

$$\begin{aligned}
 & \frac{\partial}{\partial x} \left(D_{xx} \frac{\partial C}{\partial x} + D_{xy} \frac{\partial C}{\partial y} + D_{xz} \frac{\partial C}{\partial z} - v_x C \right) \\
 & + \frac{\partial}{\partial y} \left(D_{yx} \frac{\partial C}{\partial x} + D_{yy} \frac{\partial C}{\partial y} + D_{yz} \frac{\partial C}{\partial z} - v_y C \right) \\
 & + \frac{\partial}{\partial z} \left(D_{zx} \frac{\partial C}{\partial x} + D_{zy} \frac{\partial C}{\partial y} + D_{zz} \frac{\partial C}{\partial z} - v_z C \right) = \frac{\partial C}{\partial t}
 \end{aligned} \tag{5.1}$$

where (x, y, z) is an arbitrarily chosen coordinate system; C is the concentration of solute in the water $[\text{ML}^{-3}]$; x, y, z are the flow distances $[\text{L}]$, in the directions (x, y, z) , respectively; t is time $[\text{T}]$; v_x, v_y, v_z $[\text{LT}^{-1}]$ are the x -, y -, z - components of the velocity vector (\vec{v}) , and D_{ij} $[\text{L}^2\text{T}^{-1}]$ (with $i, j = x, y, z$) are the components of the dispersion tensor (\vec{D}) :

$$D_{xx} = D_L \left(\frac{v_x^2}{v^2} \right) + D_T \left(\frac{v_y^2}{v^2} \right) + D_T \left(\frac{v_z^2}{v^2} \right) + \frac{D_m}{\tau} \tag{5.2}$$

$$D_{yy} = D_T \left(\frac{v_x^2}{v^2} \right) + D_L \left(\frac{v_y^2}{v^2} \right) + D_T \left(\frac{v_z^2}{v^2} \right) + \frac{D_m}{\tau} \tag{5.3}$$

$$D_{zz} = D_T \left(\frac{v_x^2}{v^2} \right) + D_T \left(\frac{v_y^2}{v^2} \right) + D_L \left(\frac{v_z^2}{v^2} \right) + \frac{D_m}{\tau} \tag{5.4}$$

$$D_{xy} = D_{yx} = (D_L - D_T) \left(\frac{v_x v_y}{v^2} \right) \tag{5.5}$$

$$D_{xz} = D_{zx} = (D_L - D_T) \left(\frac{v_x v_z}{v^2} \right) \tag{5.6}$$

$$D_{zy} = D_{yz} = (D_L - D_T) \left(\frac{v_z v_y}{v^2} \right) \tag{5.7}$$

where D_m is the molecular diffusion coefficient of tracer in free water $[\text{L}^2\text{T}^{-1}]$; τ is the tortuosity factor of the porosity matrix $[-]$; and D_L and D_T are the longitudinal and transverse dispersion coefficients $[\text{L}^2\text{T}^{-1}]$. D_L and D_T are equal to (Scheidegger, 1961):

$$D_L = \alpha_L v \tag{5.8}$$

$$D_T = \alpha_T v \tag{5.9}$$

where α_L and α_T are, respectively, the longitudinal and transverse dispersivities $[\text{L}]$ of the hydrodynamic dispersion, which characterize the heterogeneity of the porous

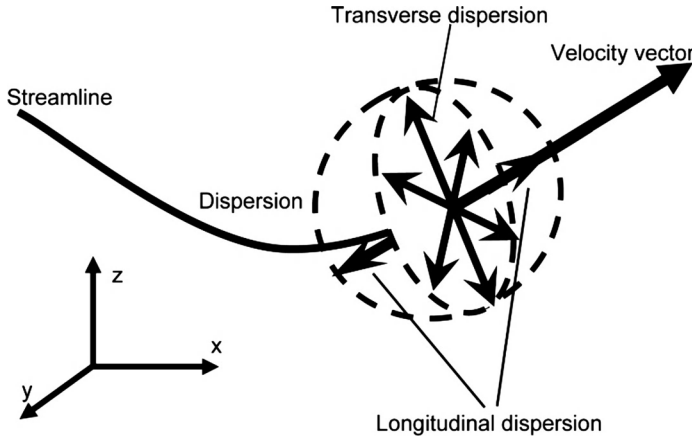


Figure 5.1 Schematic presentation of the two transport processes – convection and dispersion – in the 3D case. The dashed line shows the concentration distribution of an ideal tracer injected instantaneously into the groundwater at beginning of the stream line.

medium. The mean water velocity (v) is equal to:

$$v = \sqrt{v_x^2 + v_y^2 + v_z^2} \quad (5.10)$$

A schematic presentation of both possible transport processes – convection and dispersion, both longitudinal and transverse – is shown in Figure 5.1.

The solution to the general transport Equation (5.1) can only be found by applying numerical techniques. The solution obtained using finite difference methods (FDM) is used in the computer software MODFLOW, whereas that obtained using finite element methods (FEM) is used in, for instance, FEFLOW.

In a granular porous medium that is assumed to be homogeneous, the flow lines are parallel; the x-axis is then taken to be permanently parallel to the flow lines (Figure 5.2). In this situation the components of the velocity vector reduce to $v = v_x$, $v_y = v_z = 0$, and the dispersion tensor (5.2–5.7) is considerably simplified (5.12–5.14). The 3D transport Equation (5.1) then has following form for steady-state flow – this is here termed the specific 3D transport equation:

$$D_{xx} \frac{\partial^2 C}{\partial x^2} + D_{yy} \frac{\partial^2 C}{\partial y^2} + D_{zz} \frac{\partial^2 C}{\partial z^2} - v \frac{\partial C}{\partial x} = \frac{\partial C}{\partial t} \quad (5.11)$$

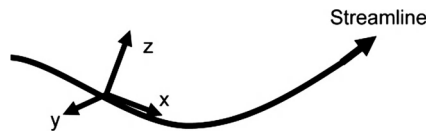


Figure 5.2 Schematic presentation of the coordinate system (x, y, z), with the x-axis parallel to the flow direction.

where D_{xx} , D_{yy} and D_{zz} are now given by:

$$D_{xx} = D_L + \frac{D_m}{\tau} \quad (5.12)$$

$$D_{yy} = D_T + \frac{D_m}{\tau} \quad (5.13)$$

$$D_{zz} = D_T + \frac{D_m}{\tau} \quad (5.14)$$

If the water flow velocity is greater than approx. 0.1 m/day, the molecular diffusion is negligibly small in comparison to the hydrodynamic dispersion; then (5.12–5.14) reduces to $D_{xx} = D_L$ and $D_{yy} = D_{zz} = D_T$.

5.1.1.2 2D equations

If a tracer is injected through the whole thickness of a homogeneous aquifer, for example into a fully penetrating well (Figure 5.3), then the tracer is already vertically well mixed in the injection well ($x = 0, y = 0$) and the vertical concentration gradient is equal to zero, that is

$$\frac{\partial C}{\partial z} = 0 \quad (5.15)$$

Taking (5.15) into account and assuming (i) that the x-axis is parallel to the flow direction and (ii) that the molecular diffusion is negligibly small, the transport Equation (5.11) can be reduced to the following specific two dimensional (2D) one:

$$D_L \frac{\partial^2 C}{\partial x^2} + D_T \frac{\partial^2 C}{\partial y^2} - v \frac{\partial C}{\partial x} = \frac{\partial C}{\partial t} \quad (5.16)$$

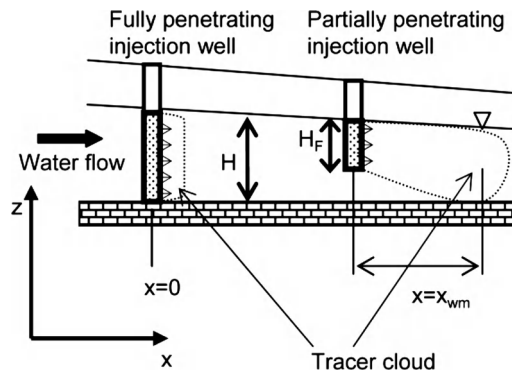


Figure 5.3 Schematic presentation of tracer injection performed into fully or partially penetrating wells.

Equation (5.16) describes tracer transport in the horizontal plane along the flow direction (x-axis) when the tracer is already completely mixed in the injection well through the vertical profile of the aquifer.

The situation is different when the tracer is injected into a partially penetrated well (Figure 5.3). Then it is necessary to estimate x_{wm} , the flow distance from the well within which the tracer will become vertically well mixed as the result of transverse dispersion. x_{wm} is given by following formula:

$$x_{wm} = \frac{(H - H_F)^2}{2\alpha_T} \quad (5.17)$$

where H [L] is the mean thickness of the aquifer and H_F is the length of the filter in the injection well. For flow distances larger than x_{wm} ($x > x_{wm}$), the 2D Equation (5.16) can be applied for parameter estimation.

5.1.1.3 1D equations

In some experiments, transverse dispersion can be neglected in both the y and z directions; an example is when the tracer is injected into the water flowing into a column throughout the whole cross-section of the column perpendicular to the flow direction. If the x-axis is taken along the column axis (flow direction), then the concentration gradients in the y and z directions both equal zero:

$$\frac{\partial C}{\partial y} = \frac{\partial C}{\partial z} = 0 \quad (5.18)$$

The same situation can be assumed for transport in streams or rivers, when the tracer is injected throughout the whole cross-section of the stream (cf. Section 7.3.5). When the x-axis is then taken parallel to the flow direction, Equation (5.16) is reduced to the 1D transport equation:

$$D_L \frac{\partial^2 C}{\partial x^2} - v \frac{\partial C}{\partial x} = \frac{\partial C}{\partial t} \quad (5.19)$$

Maloszewski and Zuber (1990) note that this equation can also be applied in radial-convergent flow (for instance, in a combined pumping and tracer experiment), provided that the dispersion parameter, $P_D = D_L/(vx) = \alpha_L/x$, is sufficiently small ($P_D < 0.2$).

5.1.2 Solutions to the transport equations

In most practical experiments, the injection of the tracer mass M into the water flux entering the system is performed instantaneously ($t_{inj} \approx 0$), which is mathematically described by the Dirac function $\delta(t)$. The 3D transport equation is in practice hardly ever applicable; for its theoretical solution, see Zuber (1970).

5.1.2.1 2D solution

The initial and boundary conditions for 2D transport in the horizontal (x, y) plane are as follows (Lenda and Zuber, 1970), assuming instantaneous injection in a fully penetrating well:

$$C(x = 0, y = 0, t) = \frac{M}{nH} \delta(t) \delta(x) \delta(y) \quad (5.20)$$

$$C(x, y, t = 0) = 0 \quad (5.21)$$

$$\lim_{(x, y) \rightarrow \infty} C(x, y, t) = 0 \quad (5.22)$$

where n is the effective water porosity $[-]$ and $\delta(x)$ and $\delta(y)$ are Dirac space functions $[1/L]$ in the x and y directions respectively.

The solution to Equation (5.16) with boundary and initial conditions (5.20–5.22) is (Lenda and Zuber, 1970):

$$C(x, y, t) = \frac{M}{nH} \frac{x}{4\pi vt^2 \sqrt{D_L D_T}} \exp \left[-\frac{(x - vt)^2}{4D_L t} - \frac{y^2}{4D_T t} \right] \quad (5.23)$$

This solution describes the horizontal transport of a tracer mass M that was injected instantaneously into a fully penetrating well situated at the origin $(0, 0)$ of the coordinate system (x, y) . Equation (5.23) has three parameters (v , D_L , D_T), the values of which need to be estimated. These parameters can only be found when the tracer experiment is performed in a test field which has observation wells situated perpendicular to the flow direction (Figure 5.4).

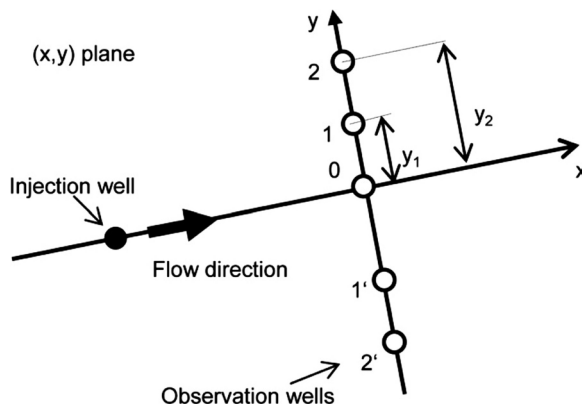


Figure 5.4 Test field in the horizontal plane (x, y) , with injection and observation wells situated perpendicular to the flow direction.

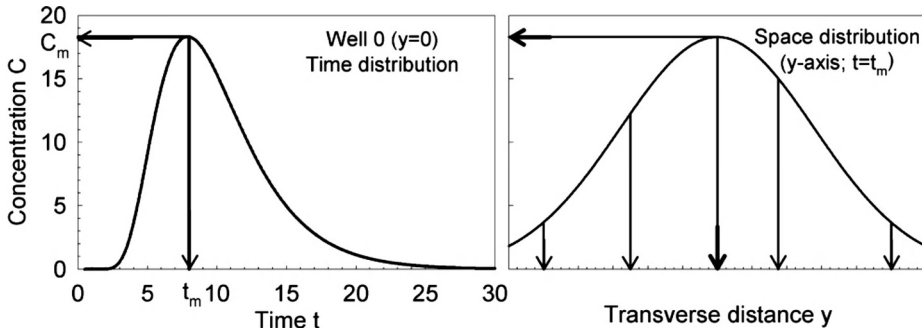


Figure 5.5 Left: Time distribution of tracer concentration $C(t)$, instantaneously injected, observed in well 0 (Figure 5.4). Right: Space (transverse) distribution of tracer concentration $C(y)$ observed in the wells: 2', 1', 0, 1, 2 (Figure 5.4) sited perpendicular to the flow direction (y -axis) measured at time $t = t_m$ after injection.

Consider first the tracer concentrations measured in the observation well 0 ($y = 0$) as a function of t , the time after injection (Figure 5.5, left). The so-called time distribution of the tracer concentration is derived from Equation (5.23) by using t_m and C_m (Figure 5.5, left) to be:

$$C(t) = C_m \left(\frac{t_m}{t} \right)^2 \exp \left[-\frac{(x - vt)^2}{4D_L t} + \frac{(x - vt_m)^2}{4D_L t_m} \right] \quad (5.24)$$

where C_m and t_m are the peak concentration and the time of the appearance of that concentration, taken from the tracer concentrations measured in well 0 (Figure 5.5, left).

Equation (5.24) has two parameters (v , D_L), the values of which can easily be calculated from experimental data obtained in well 0 (see Section 5.1.3). To calculate the transverse dispersion coefficient D_T , the tracer concentrations measured in the wells perpendicular to the flow direction (wells 2, 1, 0, 1', 2' in Figure 5.4) have to be measured at time $t = t_m$. Then the transverse distribution, the so-called space distribution, of the tracer concentration can be constructed as shown in Figure 5.5 (right). The transverse distribution of the tracer concentration $C(y)$ observed at the flow distance (x) at time e.g. $t = t_m$ after injection is described by following equation:

$$C(y) = C_m \exp \left[-\frac{y^2}{4D_T t_m} \right] \quad (5.25)$$

with the transverse dispersion coefficient (D_T) now being the only parameter that needs to be obtained.

The application of Equations (5.24) and (5.25) to the tracer concentrations measured in the observation wells shown in Figure 5.4 enables the three required parameters (v , D_L , D_T) to be determined under natural flow conditions.

5.1.2.2 1D solution

For tracer experiments performed in a column, or for combined pumping-tracer experiments (radial flow; Figure 5.6), the 1D transport Equation (5.19) is applicable. When the tracer is injected instantaneously, the initial and boundary conditions are as follows:

$$C(x = 0, t) = \frac{M}{Q} \delta(t) \quad (5.26)$$

$$C(x, t = 0) = 0 \quad (5.27)$$

$$\lim_{x \rightarrow \infty} C(x, t) = 0 \quad (5.28)$$

where M [M] is the mass of tracer injected and Q [L^3/T] is the volumetric flow rate through the column (or the pumping rate in a combined pumping-tracer experiment).

With these conditions, the solution to (5.19) is as follows (Lenda and Zuber, 1970; Kreft and Zuber, 1978):

$$C(x, t) = \frac{M}{Q} \frac{x}{\sqrt{4\pi D_L t^3}} \exp \left[-\frac{(x - vt)^2}{4D_L t} \right] \quad (5.29)$$

Here it is assumed that in a column experiment the tracer is injected at $x = 0$ into the water flowing into the column and measured in the water flowing out of the column (flux–flux mode, see Kreft and Zuber, 1978), and that in a combined pumping-tracer experiment the tracer is injected throughout the whole thickness of the aquifer (H) on the potential (vertical) line $0 \leq z \leq H$ and measured in the pumped water. Equation (5.29) has two parameters (v , D_L), the values of which can be calculated from experimental data obtained from the outflow (see Section 5.1.3).

One measure often used in tracer hydrology is the so-called mean transit time of water (t_0). This is defined as follows:

$$t_0 = \frac{x}{v} \quad (5.30)$$

which for 1D (closed) systems is equivalent to:

$$t_0 = \frac{V_m}{Q} \quad (5.31)$$

where V_m [L^3] is the volume of mobile water in the system.

By applying the mean transit time (5.30) and the dispersion parameter P_D :

$$P_D = \frac{D_L}{vx} = \frac{\alpha_L}{x} \quad (5.32)$$

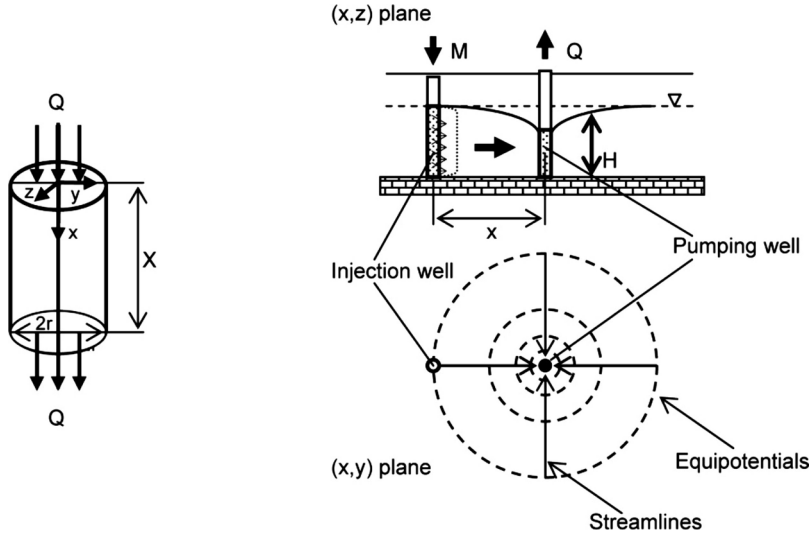


Figure 5.6 Practical applications of the 1D solution to the transport equation: column experiment (left); and combined pumping-tracer experiment (right). Q stands for the flow rate through the column (left), and for the pumping rate (right).

the solution (5.29) can be reformulated as the so-called normalized solution (Lenda and Zuber, 1970):

$$C(t) = \frac{M}{Q t_0} \frac{1}{\sqrt{4\pi P_D (t/t_0)^3}} \exp \left[-\frac{(1 - t/t_0)^2}{4P_D t/t_0} \right] \quad (5.33)$$

where $C(t)$ is the theoretical tracer concentration in the outflow from the closed system (a column or a pumping well). Equation (5.33) has two parameters P_D and t_0 , the second of which can be used to calculate the effective porosity (n) of the system. For the column experiment:

$$n = \frac{Q t_0}{\pi r^2 x} \quad (5.34)$$

and for a combined pumping-tracer (radial flow) experiment (Zuber, 1974; Kreft and Zuber, 1979):

$$n = \frac{Q t_0}{\pi x^2 H} \quad (5.35)$$

where x is the column length in (5.34) and the distance between the injection and pumping wells in (5.35), r is the column radius, and H is the mean aquifer thickness.

The value of t_0 obtained from a column experiment can be validated by comparing the value of the porosity calculated from (5.34) with the value otherwise obtained,

for instance by weighing the dry (m_d) and water saturated (m_s) column:

$$n = \frac{m_s - m_d}{\pi r^2 x} \quad (5.36)$$

For a combined pumping-tracer experiment, Equation (5.35) is the only way of determining the effective porosity.

Equation (5.33) written in dimensionless form – this can be termed with the $E(t/t_0)$ function – was given by Lenda and Zuber (1970):

$$E(t/t_0) = \frac{C(t)Q t_0}{M} = \frac{1}{\sqrt{4\pi P_D (t/t_0)^3}} \exp \left[-\frac{(1 - t/t_0)^2}{4P_D t/t_0} \right] \quad (5.37)$$

The form of the $E(t/t_0)$ function is shown in Figure 5.7, for various values of the dispersion parameter P_D . In this figure can be seen the influence of the system's heterogeneity on the shape of the tracer concentration curve: the time to reach the peak concentration (t_m/t_0) decreases with increasing of P_D values (increasing system heterogeneity). The position of the peak concentration on the time-axis (t_m/t_0) is related to the dispersion parameter P_D as follows:

$$\left(\frac{t_m}{t_0} \right) = \sqrt{1 + (3P_D)^2} - (3P_D) \quad (5.38)$$

(It is worth noting here that the time of appearance of the peak concentration in the 2D case (5.24) at the well situated on the x -axis ($y = 0$) is described by (5.38) with ' $4P_D$ ' replacing ' $3P_D$ '.)

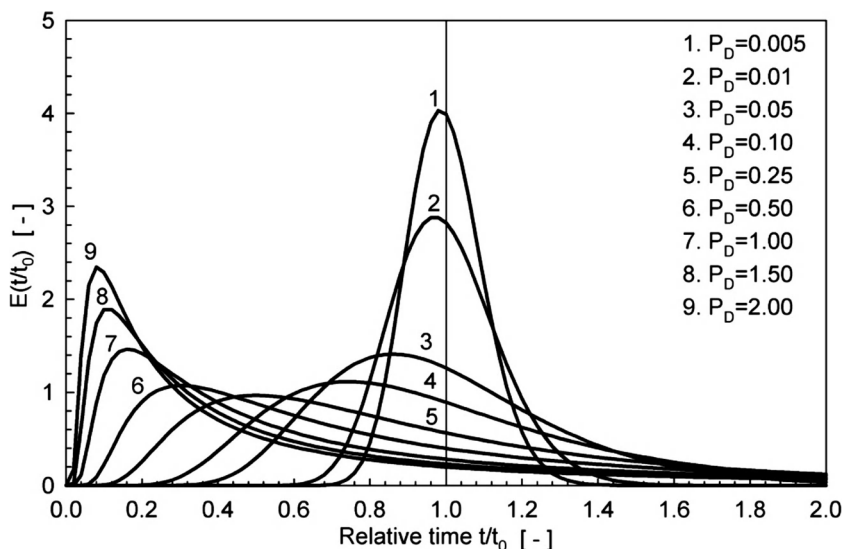


Figure 5.7 Graphical presentation of the solution to the 1D transport equation, Equation (5.37), given for the normalized time (t/t_0), for various values of the dispersion parameter P_D .

If the volume of water in the system ($V_W = Q \cdot t_0$) is known, and if the range of values of P_D can be estimated, then Figure 5.7 together with Equation (5.38) can be used to plan a tracer sampling campaign and to estimate the mass of tracer that needs to be injected. For the estimate of the mass it is also necessary to estimate the required peak tracer concentration $C_m = C(t_m)$. Generally, it is sufficient for C_m to be 10–20 times larger than the background concentration (C_B) measured in the groundwater in the area under investigation. In the worst case (the lowest $E(t)$ curve), this rule results in:

$$M = ca.(10 \text{ to } 20)C_B \times V_W \quad (5.39)$$

It was shown by Maloszewski and Zuber (1990) that in tracer experiments performed in closed systems (1D cases) the relative mass recovery RR can readily be calculated as a function of time (t):

$$RR(t) = Q \int_0^t C(t)dt/M \quad (5.40)$$

For the solution (5.33) found for the 1D case, $RR(t)$ is equal to the function $F(t/t_0)$ defined by Lenda and Zuber (1970) as:

$$RR(t) = F(t/t_0) = \frac{1}{2} \left[\operatorname{erfc} \left(\frac{1 - t/t_0}{\sqrt{4P_D t/t_0}} \right) + \exp \left(\frac{1}{P_D} \right) \operatorname{erfc} \left(\frac{1 + t/t_0}{\sqrt{4P_D t/t_0}} \right) \right] \quad (5.41)$$

with $\operatorname{erfc}(\omega) = 1 - \operatorname{erf}(\omega)$, where $\operatorname{erf}(\omega)$ is the error function defined as:

$$\operatorname{erf}(\omega) = \frac{2}{\sqrt{\pi}} \int_0^\omega e^{-\varepsilon^2} d\varepsilon \quad (5.42)$$

The form of the $F(t/t_0)$ function (5.40) is shown in Figure 5.8.

5.1.3 Estimation of the transport parameters

5.1.3.1 Combined least squares method (LSQM)

The solution of the inverse problem (i.e. the estimation of the transport parameters) can be obtained by fitting the appropriate theoretical solutions to experimental concentrations using a trial-and-error procedure. For 1D experiments the solution (5.33) is used; for 2D experiments the procedure starts by fitting (5.24) in the observation well on the x-axis ($y = 0$) and ends by fitting (5.25) to the transverse distribution of tracer concentrations.

Equations (5.24) and (5.33) can also be used in an automatic fitting procedure that combines the least squares method with Taylor series approximation of both solutions (Maloszewski, 1981). In both the 1D and 2D cases (in 2D, for $y = 0$), the solutions to

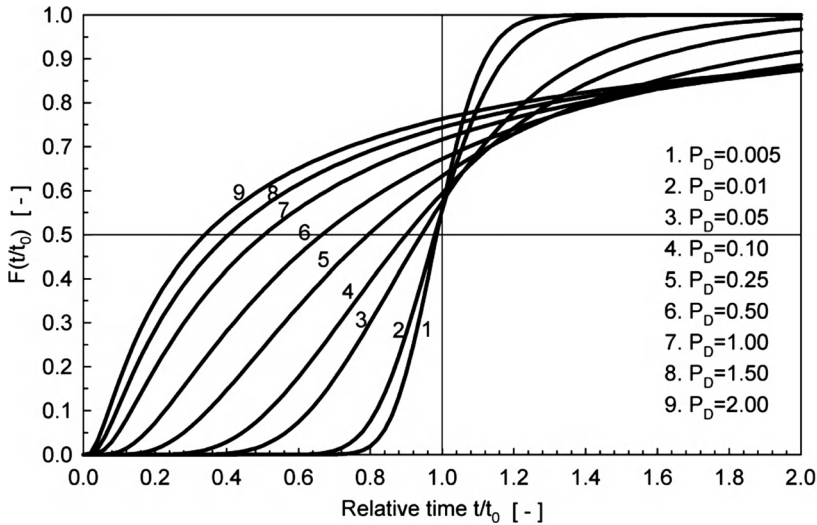


Figure 5.8 Graphical presentation of the solution of Eq. (5.41), the relative recovery curve for the 1D case (this is also the solution C/C_0 of the 1D transport equation for continuous injection of tracer C_0), given for the normalized time (t/t_0) , for various values of the dispersion parameter P_D .

the transport equations can be written using one common function $G(a, b, t)$, which has the following form:

$$G(a, b, t) = C_m \left(\frac{t_m}{t} \right)^k \exp \left[-\frac{(1 - t/b)^2}{4at/b} + \frac{(1 - t_m/b)^2}{4at_m/b} \right] \quad (5.43)$$

where $a = P_D$ and $b = t_0$ are the parameters to be estimated. In the 2D case (for $y = 0$), $k = 2$; in the 1D case, $k = 1.5$.

Assume that N values of the concentration C_i have been measured in an experiment for the times $t = t_i$ ($i = 1, N$). The fitting procedure assumes that the solution to the inverse problem ('best fit') is obtained when the values of parameters (a, b) yield the minimum value of the sum of the squared differences between the theoretical and observed concentrations:

$$\Phi = \sum_{i=1}^N [C_i - G(t_i, a, b)]^2 \quad (5.44)$$

Substitution of (5.43) into (5.44) yields a quadratic equation, which cannot be directly solved. To remedy this difficulty, (5.43) is first written as a Taylor series. Neglecting higher derivatives, this is:

$$G(a, b, t) \approx G(a_0, b_0, t) + \frac{\partial G}{\partial a} \Delta a + \frac{\partial G}{\partial b} \Delta b \quad (5.45)$$

Substitution of (5.45) into (5.44) now gives the following linear function:

$$\Phi = \sum_{i=1}^N [\varepsilon_i - (\beta_i \Delta a + \gamma_i \Delta b)]^2 \quad (5.46)$$

where:

$$\beta_i = \frac{\partial G}{\partial a} = -C_m \left(\frac{t_m}{t_i} \right)^k \left(b - \frac{t_m t_i}{b} \right) \left(\frac{1 - t_m/t_i}{4a^2 t_m} \right) \exp \left[\frac{1 - t_m/t_i}{4a t_m} \left(b - \frac{t_m t_i}{b} \right) \right] \quad (5.47)$$

$$\gamma_i = \frac{\partial G}{\partial b} = C_m \left(\frac{t_m}{t_i} \right)^k \left(1 + \frac{t_m t_i}{b^2} \right) \left(\frac{1 - t_m/t_i}{4a t_m} \right) \exp \left[\frac{1 - t_m/t_i}{4a t_m} \left(b - \frac{t_m t_i}{b} \right) \right] \quad (5.48)$$

$$\varepsilon_i = C_i - G(a, b, t_i) \quad (5.49)$$

Equation (5.46) has its minimum when:

$$\frac{\partial \Phi}{\partial (\Delta a)} = 0 \quad (5.50)$$

$$\frac{\partial \Phi}{\partial (\Delta b)} = 0 \quad (5.51)$$

Solving the above equations leads finally to:

$$\Delta a = \frac{- \left(\sum_{i=1}^N \gamma_i^2 \right) \left(\sum_{i=1}^N \beta_i \varepsilon_i \right) + \left(\sum_{i=1}^N \beta_i \gamma_i \right) \left(\sum_{i=1}^N \gamma_i \varepsilon_i \right)}{\left(\sum_{i=1}^N \beta_i \gamma_i \right)^2 - \left(\sum_{i=1}^N \beta_i^2 \right) \left(\sum_{i=1}^N \gamma_i^2 \right)} \quad (5.52)$$

$$\Delta b = \frac{- \left(\sum_{i=1}^N \beta_i^2 \right) \left(\sum_{i=1}^N \gamma_i \varepsilon_i \right) + \left(\sum_{i=1}^N \beta_i \gamma_i \right) \left(\sum_{i=1}^N \beta_i \varepsilon_i \right)}{\left(\sum_{i=1}^N \beta_i \gamma_i \right)^2 - \left(\sum_{i=1}^N \beta_i^2 \right) \left(\sum_{i=1}^N \gamma_i^2 \right)} \quad (5.53)$$

The solving of the inverse problem now requires only that the values of Δa and Δb be obtained. This is done iteratively, starting with calculation of all the N values of the functions (5.43) and (5.47–5.49) for the arbitrary initial values $a = a_0$ and $b = b_0$. After calculating Δa and Δb from (5.52) and (5.53), new values of a and b are calculated:

$$a = a_0 + \Delta a \quad (5.54)$$

and

$$b = b_0 + \Delta b \quad (5.55)$$

The following stopping condition is used for the iteration:

$$\left| \frac{\Delta a}{a} \right| \leq 0.005 \quad \text{and} \quad \left| \frac{\Delta b}{b} \right| \leq 0.005 \quad (5.56)$$

If condition (5.56) is not fulfilled, the iteration procedure continues with the values of (5.54) and (5.55) taken now as a_0 and b_0 . If condition (5.56) is fulfilled, the iteration procedure ends with last values of a , and b . This procedure allows the transport parameters P_D and t_0 to be estimated for any given set of data (t_i , C_i , for $i = 1, \dots, N$), with the best possible mathematical accuracy.

The estimation of parameters for the 1D or 2D ($y = 0$) cases using the combined least square method (*LSQM*) can be performed on a PC using the user-friendly software *FIELD*, which is available from one of the authors (Maloszewski).

5.1.3.2 Method of moments (MM)

Parameter estimation is often carried out using the well-known method of moments (Kreft and Zuber, 1978; Maloszewski and Zuber, 1985, 1992b; Maloszewski, 1994). Generally, the l^{th} moment M_l of the tracer curve $C(t)$ is defined as:

$$M_l = \int_0^{\infty} t^l C(t) dt \quad (5.57)$$

which, by applying the numerical (trapezoidal) method of integration (with $C_{i=0} = 0$), yields:

$$M_l = \frac{1}{2} \sum_{i=1}^{N+1} (C_{i-1} t_{i-1}^l + C_i t_i^l) (t_i - t_{i-1}) \quad (5.58)$$

In using the method of moments in tracer hydrology, two mathematical descriptors are always calculated: the centre of gravity \bar{t} , that is the mean tracer transit time (t_t):

$$\bar{t} = t_t = \frac{\int_0^{\infty} t C(t) dt}{\int_0^{\infty} C(t) dt} = \frac{M_1}{M_0} \quad (5.59)$$

and the variance of the tracer concentration curve:

$$\delta_t^2 = \frac{\int_0^{\infty} (t - \bar{t})^2 C(t) dt}{\int_0^{\infty} C(t) dt} = \frac{M_2 M_0 - M_1^2}{M_0^2} \quad (5.60)$$

The calculation of the integrals in (5.59) and (5.60) requires that the tracer concentration curve be obtained for a sufficiently long period – the upper limit of the integrals is $t \rightarrow \infty$. In practice this means that the tracer concentration has to be measured until its value tails off and reaches the background concentration in the water. Only in this situation can the values of the descriptors (5.59) and (5.60) be properly calculated. Even then there is a problem in deriving the transport parameters (t_0 and P_D or v and α_L) from these descriptors. Only in the 1D case –, that is only if Equations (5.29) or (5.33) are satisfied – are the following well-known relationships between the mathematical descriptors (5.59 and 5.60) and the transport parameters valid:

$$t_0 = \bar{t} \quad \text{or} \quad v = \frac{x}{\bar{t}} \quad (5.61)$$

$$P_D = \frac{1}{2} \left(\frac{\delta_t}{\bar{t}} \right)^2 \quad \text{or} \quad \alpha_L = \frac{x}{2} \left(\frac{\delta_t}{\bar{t}} \right)^2 \quad (5.62)$$

Unfortunately, (5.61) and (5.62) are often misused and wrongly applied in the 2D case. It must be remembered that, although the mathematical descriptors (5.59) and (5.60) can always be calculated when a tracer curve has been measured over a sufficiently long period, the Equations (5.61) and (5.62) are only applicable in 1D cases.

5.1.3.3 The cumulative curve method (CCM)

The cumulative curve method was developed by Fried and Combarous (1971), and has become very popular in German-speaking countries (Käss, 2004). However, the applicability of this method in practice is strongly limited. Fried and Combarous (1971) developed the cumulative curve method for the 1D case, using the relative tracer recovery curve, defined here by Equation (5.41). Generally, the experimental relative recovery $RR(t)$, called here the cumulative curve $S(t)$, is constructed using the following equation:

$$S(t) = RR(t) = \frac{\int_0^t C(t) dt}{\int_0^{\infty} C(t) dt} \quad (5.63)$$

where $\int_0^{\infty} C(t) dt$ is the area under the experimental curve (A).

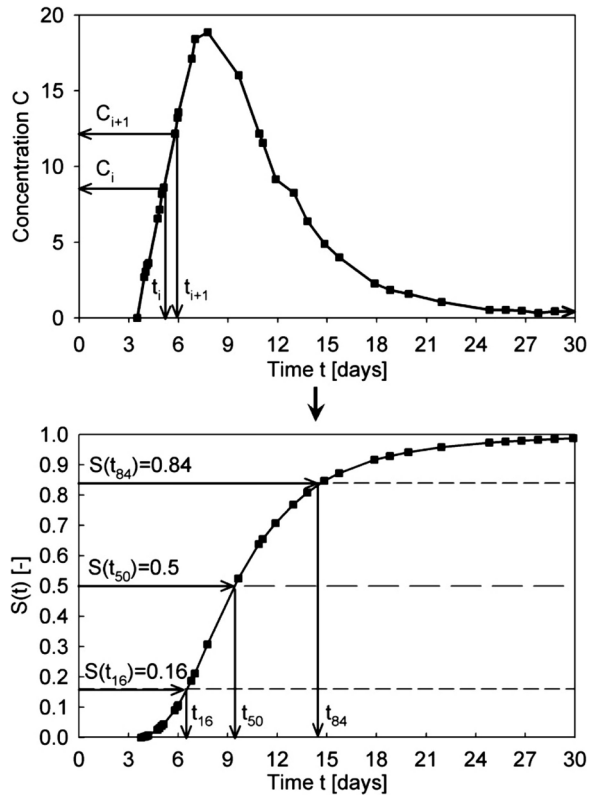


Figure 5.9 Presentation of the experimental tracer concentration curve¹⁾ C (top) and the constructed cumulative curve $S(t)$ (bottom), with the estimated times, t_{16} , t_{50} and t_{84} , needed for applying the method of the cumulative curve. ¹⁾Also called tracer breakthrough curve.

From that curve (5.63), the times $t = t_{16}$, $t = t_{50}$ and $t = t_{84}$ are read; these are the times for which $S(t)$ obtains the values 0.16, 0.50 and 0.84 (Figure 5.9). These times are then used to calculate the transport parameters using Equations (5.71) and (5.72). Unfortunately, these latter equations are very commonly misused (see Käss, 2004), simply because the ideas behind the development used by Fried and Combarous (1971) have been forgotten.

Fried and Combarous (1971) considered 1D cases (closed systems), and only in situations in which the second term in Equation (5.41) could be neglected:

$$\exp\left(\frac{1}{P_D}\right) \operatorname{erfc}\left(\frac{1+t/t_0}{\sqrt{4P_D t/t_0}}\right) \cong 0 \quad (5.64)$$

The above condition is satisfied with sufficient accuracy if

$$P_D \leq 0.005 \quad (5.65)$$

and only then can (5.41) and (5.63) be simplified to the following form:

$$S(t) = \frac{1}{2} \operatorname{erfc} \left(\frac{1 - t/t_0}{\sqrt{4P_D t/t_0}} \right) = \frac{1}{2} \operatorname{erfc} (\varepsilon(t)) \quad (5.66)$$

where $\varepsilon(t)$ is the argument of the erfc function:

$$\varepsilon(t) = \frac{1 - t/t_0}{\sqrt{4P_D t/t_0}} \quad (5.67)$$

To finally find the relationships between the parameters t_{16} , t_{84} and t_{50} of the $S(t)$ and the required transport parameters, the following properties of the $\operatorname{erfc}(\varepsilon)$ function have to be used. Function (5.66) obtains the values 0.16, 0.84 and 0.50 when the following equations are satisfied:

a) $S[\varepsilon(t_{16})] = 0.16$ for:

$$\varepsilon(t_{16}) = \frac{1 - t_{16}/t_0}{\sqrt{4P_D t_{16}/t_0}} = -\frac{1}{\sqrt{2}} \quad (5.68)$$

b) $S[\varepsilon(t_{84})] = 0.84$ for:

$$\varepsilon(t_{84}) = \frac{1 - t_{84}/t_0}{\sqrt{4P_D t_{84}/t_0}} = \frac{1}{\sqrt{2}} \quad (5.69)$$

c) $S[\varepsilon(t_{50})] = 0.5$ for:

$$\varepsilon(t_{50}) = \frac{1 - t_{50}/t_0}{\sqrt{4P_D t_{50}/t_0}} = 0 \quad (5.70)$$

Solving the above system of equations yields finally:

$$t_0 = t_{50} \quad (5.71)$$

and

$$P_D = \frac{1}{8t_{50}} \left(\frac{t_{50} - t_{84}}{\sqrt{t_{84}}} - \frac{t_{50} - t_{16}}{\sqrt{t_{16}}} \right)^2 \quad (5.72)$$

When $\sqrt{t_{50}} \approx \sqrt{t_{84}} \approx \sqrt{t_{16}}$ the above equation can be additionally simplified to:

$$P_D = \frac{1}{8} \left(\frac{t_{16} - t_{84}}{t_{50}} \right)^2 \quad (5.73)$$

The applicability of Equations (5.71) and (5.72) is limited to 1D cases characterized by very low values of the P_D parameter, which corresponds to very homogeneous systems. That condition is easy to detect from Figure 5.8, which shows the exact $S(t)$ -function. This figure demonstrates for different P_D values the difference between time t_{50} , which corresponds to the line $F = 0.5$ and the real mean transit time of water t_0 . For extremely heterogeneous media ($P_D = 2.0$), the cumulative curve method yields values of t_{50} about three times smaller than the real value of t_0 ; for less heterogeneous media ($P_D = 0.25$), it yields values of t_{50} about 1.33 times smaller than the real value of t_0 .

5.1.4 Artificial tracer experiments in multi-flow systems

It is sometimes seen that there are multiple peaks in the tracer concentration curve in the water flowing out of a system (Figure 5.10). This happens: (1) in karst aquifers, when the tracer is injected into a sinkhole and observed in the springs and (2) in heterogeneous multi-layered porous media, when the tracer is injected through the whole thickness of the aquifer and observed in a pumping well or spring. In aquifers such as these, the multiple peaks in the concentration curve result from tracer transport along several flow paths that have different water flow velocities (and therefore different transit times) and different dispersivities. The streamlines finally come together in the outflow from the system (Figure 5.11). Figure 5.12 presents a conceptual model of flow in those situations, which has been used to describe tracer transport in the multi-layered porous media of an artificial wetland (Maloszewski, Wachniew and Czuprynski, 2006) and to describe tracer transport between a sinkhole and a spring in a karst aquifer (Maloszewski, Harum and Benischke, 1992). The model assumes that the tracer transport through the system can be approximated by a combination of 1D dispersion-convection equations. Each

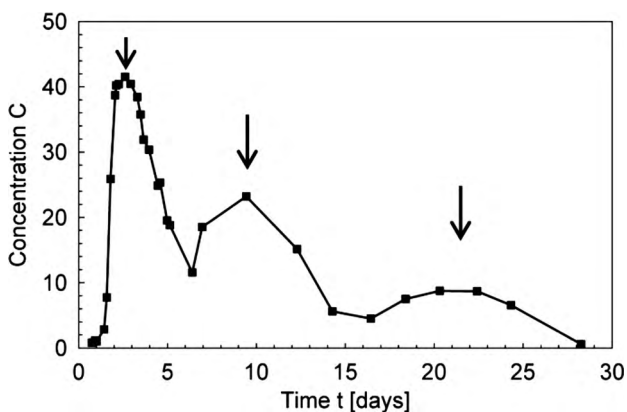


Figure 5.10 A multi-peak experimental concentration curve $C(t)$ resulting from tracer transport on different 'parallel' flow paths.

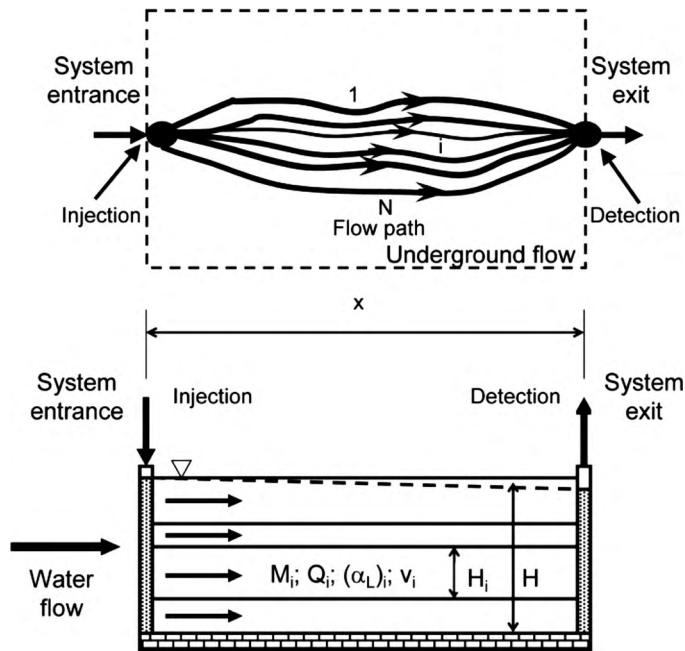


Figure 5.11 Schematic presentation of tracer transport in a multi-flow system, for a karst aquifer (top) and for a multi-layered porous medium (bottom).

flow path is characterized by a specific volumetric flow rate, mean transit time of water and dispersivity (or dispersion parameter). It is assumed (a) that the mass of tracer injected is divided into several flow paths proportional to the volumetric flow rates along those paths and (b) that there are no interactions between the flow paths.

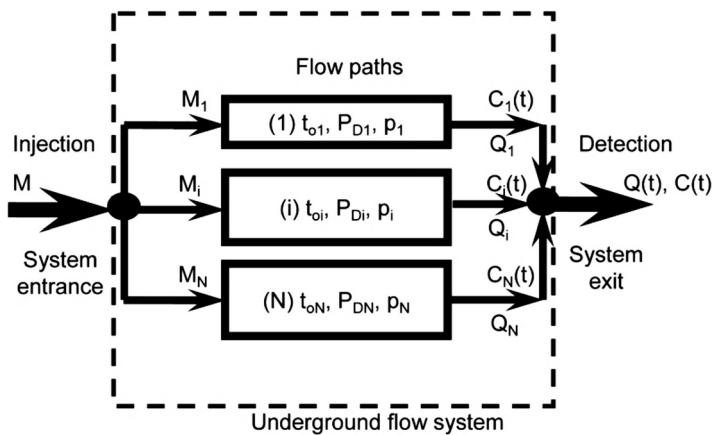


Figure 5.12 Conceptual model of tracer transport in multi-flow systems (multi-layered aquifer or karst aquifer).

The transport of an ideal tracer along the i^{th} flow path is described by the 1D dispersion equation:

$$\alpha_{Li} v_i \frac{\partial^2 C_i}{\partial x^2} - v_i \frac{\partial C_i}{\partial x} = \frac{\partial C_i}{\partial t} \quad (5.74)$$

where $C_i(t)$ is the concentration of tracer in the outflow from the i^{th} flow path (see Figure 5.12), and α_{Li} and v_i are, respectively, the longitudinal dispersivity and the mean water velocity for the i^{th} flow path. x is the length of the flow path and t is the time after injection.

For instantaneous injection of tracer, the solution to (5.74) reads as follows (Kreft and Zuber, 1978):

$$C_i(t) = \frac{M_i}{Q_i t_{oi} \sqrt{4\pi (P_D)_i (t/t_{oi})^3}} \exp \left[-\frac{(1 - t/t_{oi})^2}{4(P_D)_i (t/t_{oi})} \right] \quad (5.75)$$

where Q_i and M_i are the volumetric flow rate and the mass of tracer transported along the i^{th} flow path, respectively and

$$(P_D)_i = \alpha_{Li} / x_i \quad (5.76)$$

is the dispersion parameter, where x_i is the length of the i^{th} flow path.

$$t_{oi} = \frac{x_i}{v_i} = \frac{(V_m)_i}{Q_i} \quad (5.77)$$

is the mean transit time of water and $(V_m)_i$ is the mean volume of mobile water, in the i^{th} flow path. The model assumes that the whole injected tracer mass, M , is divided into N portions, which enter the N flow paths proportional to the volumetric flow rates Q_i :

$$M_i / Q_i = M / Q \quad (5.78)$$

where Q is the total flow rate through the system, that is the sum of the partial flow rates:

$$Q = \sum_{i=1}^N Q_i \quad (5.79)$$

The outflow tracer concentration $C(t)$ is the flux-weighted mean concentration for all flow paths observed in the outflow:

$$C(t) = \sum_{i=1}^N p_i C_i(t) \quad (5.80)$$

and

$$p_i = Q_i/Q = M_i/M = RR_i/RR = \frac{\int_0^{\infty} C_i(t) dt}{\int_0^{\infty} C(t) dt} \quad (5.81)$$

where p_i is the fraction of water flux in the i -th flow path, RR_i is the partial tracer recovery observed in the outflow of the i^{th} flow path and RR is the total recovery measured in the outflow.

The solution (5.80), combined with (5.75) and (5.81), is called here the Multi Flow Dispersion Model (MFDM). The parameters in the MFDM are: (1) the mean transit time t_{0i} , (2) the dispersion parameter $(P_D)_i$, (3) the fraction of water flux (p_i) for each flow path (i) and (4) the total number of flow paths N . It must be noted here that, due to the high number of unknowns, the calibration of the model to experimental data cannot be done in a straightforward way. The calibration is performed stepwise by fitting one-by-one the partial tracer concentration curves, each time subtracting the fitted (partial) curve from the total tracer concentration curve, beginning with the earliest peak (Maloszewski, Harum and Benischke, 1992; Maloszewski *et al.*, 1998, 2006). The number of flow paths N is then found automatically. After determining all the parameters and the partial volumetric flow rates (Q_i), the volume of water in each flow path $(V_m)_i$ can be easily calculated from (5.81) and (5.77) as: $Q_i = p_i \cdot Q$ and $(V_m)_i = Q_i \cdot t_{0i}$, assuming that all the water is mobile. Then the total volume of water in the system is given by:

$$V_m = \sum_{i=1}^N (V_m)_i \quad (5.82)$$

and the mean transit time of water through the whole system is given by:

$$t_0 = \frac{V_m}{Q} = \sum_{i=1}^N p_i t_{0i} \quad (5.83)$$

For the karst aquifer, the parameter estimation is limited to determining for each flow path the mean transport parameters (transit time and flow velocity, dispersion parameter and dispersivity, portion of tracer transported) and deriving from these the flow rate and volume of water for each flow path and the total volume of water in the system (between the injection and detection sites). The values obtained for the transit times, dispersion parameters, flow rates and volumes of water are real ones, whereas the values of water velocity and dispersivity calculated for each flow path using (5.77) and (5.76) are only approximations made assuming that the flow distance between injection and detection points is for each flow path (x_i) equal to the straight line distance (x) (Figure 5.11).

For the multi-layered porous medium, assuming that the porosities in each layer are similar and equal to n , and the hydraulic gradient is known, one can simply calculate the hydraulic conductivity for each layer (k_i) and the weighted mean (\bar{k}), by applying Darcy's law:

$$\bar{k} = \frac{x^2 n}{(\Delta H) t_0} \quad (5.84)$$

$$k_i = \frac{x^2 n}{(\Delta H) t_{0i}} \quad (5.85)$$

where $\Delta H/x$ is the hydraulic gradient between the injection and detection wells.

Finally, knowing the hydraulic conductivity for each layer (k_i), one can estimate the mean thickness of the layer (H_i) by combining (5.81) with (5.85):

$$H_i = \frac{p_i H \bar{k}}{k_i} = p_i H \frac{t_{0i}}{t_0} \quad (5.86)$$

Summarizing, in the multi-layered porous aquifer, the tracer experiment enables the estimation of the transport parameters and hydraulic properties of the individual layers. However, the relative position of the layers in the system stays unknown.

5.1.5 Experiments in double-porosity aquifers

Mathematical models used to estimate transport and rock parameters in fissured aquifers are well described in Maloszewski (1994). Those models assume that the aquifer can be approximated by a system of parallel, identical fissures, equally distributed in a microporous matrix (Sudicky and Frind, 1982). The fissures have aperture (2b) and include mobile water; in the matrix, which has the porosity (n_{im}), there is only stagnant (immobile) water. The ratio of fissure aperture (2b) to fissure spacing (L) is defined as fissure (effective and/or mobile) porosity (n_f). Tracer with mass (M) is injected into the water entering the aquifer, simultaneously into all the fissures, with flux Q. The tracer is transported in the fissures by convection (v) and dispersion (D) and there is, at the same time, a loss (sink term) due to diffusion through the fissure walls into the immobile water in the matrix. Figure 5.13 shows schematically an aquifer approximated with a system of parallel fissures, and also an aquifer consisting of a single fracture situated in an infinitely large matrix. Maloszewski and Zuber (1985) and Maloszewski *et al.* (2004) have shown that when a tracer experiment is performed over small distances, that is when the mean transit time of water through the fissures is sufficiently short, the tracer transport can be approximated using the single fissure approach. In practice, that assumption is realized when (Maloszewski, 1994):

$$t_o \leq \frac{L^2}{64D_p} \quad \text{or} \quad t_o \leq \frac{(2b)^2}{64n_f^2 D_p} \quad (5.87)$$

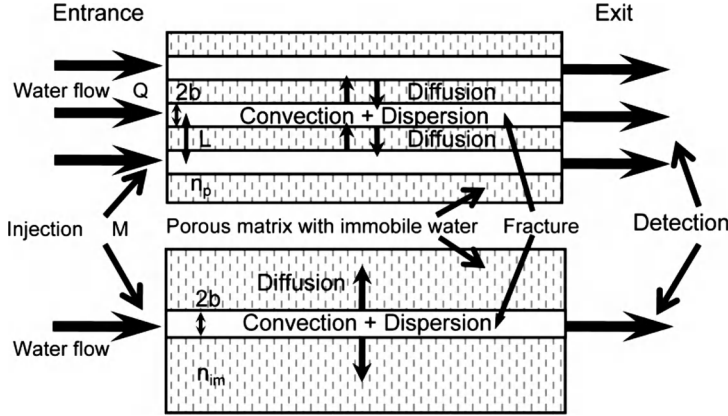


Figure 5.13 Conceptual model of tracer transport in a fissured aquifer consisting of parallel fractures (top), or a single fracture (bottom), with in each case a porous matrix with immobile water.

where D_p is the effective diffusion coefficient in the immobile water in the porous matrix and the fissure (mobile) porosity (n_f) is much smaller than 1.

If this is true, then the following equations describe the transport of an ideal tracer (Maloszewski and Zuber, 1985, 1990):

$$\frac{\partial C}{\partial t} + v \frac{\partial C}{\partial x} - D \frac{\partial^2 C}{\partial x^2} - \frac{n_{im} D_p}{2b} \frac{\partial C_{im}}{\partial y} \Big|_{y=b} = 0 \quad \text{for } 0 \leq y < b \quad (5.88)$$

$$\frac{\partial C_{im}}{\partial t} - D_p \frac{\partial^2 C_{im}}{\partial y^2} = 0 \quad \text{for } b \leq y < \infty \quad (5.89)$$

where $C(t)$ and $C_{im}(t)$ are the tracer concentrations in mobile and immobile water, respectively, D is the dispersion coefficient in the fissure, D_p is the effective diffusion coefficient of tracer in the immobile water, the x -axis of the coordinate system is parallel to the flow direction (fissure axis), y is the distance perpendicular to the flow axis, $2b$ and v are the fissure aperture and the mean water velocity in the fissure, respectively.

The solution to (5.88) and (5.89), for instantaneous tracer injection is given by Maloszewski and Zuber (1985, 1990):

$$C(t) = \frac{aM\sqrt{t_0}}{2\pi Q\sqrt{P_D}} \int_0^t \exp \left[-\frac{(t_0 - \xi)^2}{4\xi t_0 P_D} - \frac{a^2 \xi^2}{t - \xi} \right] \frac{d\xi}{\sqrt{\xi(t - \xi)^3}} \quad (5.90)$$

where ξ is the integration variable and a is a so-called diffusion parameter equal to:

$$a = \frac{n_{im}\sqrt{D_p}}{2b} \quad (5.91)$$

and t_0 is the mean transit time of water through the fissures

$$t_0 = \frac{V_m}{Q} \quad (5.92)$$

where V_m is the volume of mobile water in the whole system.

The solution (5.90) is termed by Maloszewski and Zuber (1985) the Single Fissure Dispersion Model (SFDM). It has three parameters: (1) the mean transit time of water (t_0), (2) the dispersion parameter (P_D) and (3) the diffusion parameter (a). Solution (5.90) is applicable when the tracer experiment is performed over small distances (5.87) in a fissured aquifer under natural flow conditions (e.g. detection in a spring or observation well), and also when it is performed in a radial-convergent (monopole) test (combined tracer and pumping experiment). The SFDM model can be applied for the interpretation of tracer experiments performed in aquifers that consist either of a fracture system or of a single fracture. Figure 5.14 shows the normalized (CQt_0/M) solution (5.90) calculated for constant values of the mean transit time of water (12 h) and the dispersion parameter (0.01), for different values of the diffusion parameter (a). The influence of tracer diffusion into the immobile water in the microporous matrix is easily seen there. Increases in the matrix diffusion (larger values of a) result in the concentration peak being delayed, in a stronger tailing effect and in a decrease of the relative tracer mass recovery.

Generally, the model parameters (t_0 , P_D , a) can be estimated relatively easily by fitting (5.90) to the experimental data using a trial-and-error procedure. After the values of those parameters have been found, it is possible to calculate values for other system properties, but this is done in different ways depending on the experimental conditions.

In combined tracer and pumping experiments (Figure 5.6), when the thickness of the aquifer (H) and the hydraulic conductivity (k) are known independently, the following properties can be given approximate values:

- mobile (effective, fissure) porosity (n_f);

$$n_f = \frac{Q t_0}{\pi x^2 H} \quad (5.93)$$

- mean fissure aperture ($2b$) for the fracture system (Maloszewski, 1994);

$$2b = 4.29 \tau_f \sqrt{\frac{k}{n_f}} \quad (5.94)$$

where ($2b$) in the above expression is expressed in [μm] and (k) in [m/d], and τ_f is the tortuosity factor – equal to about 1.5 for a network of tortuous fissures (Maloszewski and Zuber, 1985).

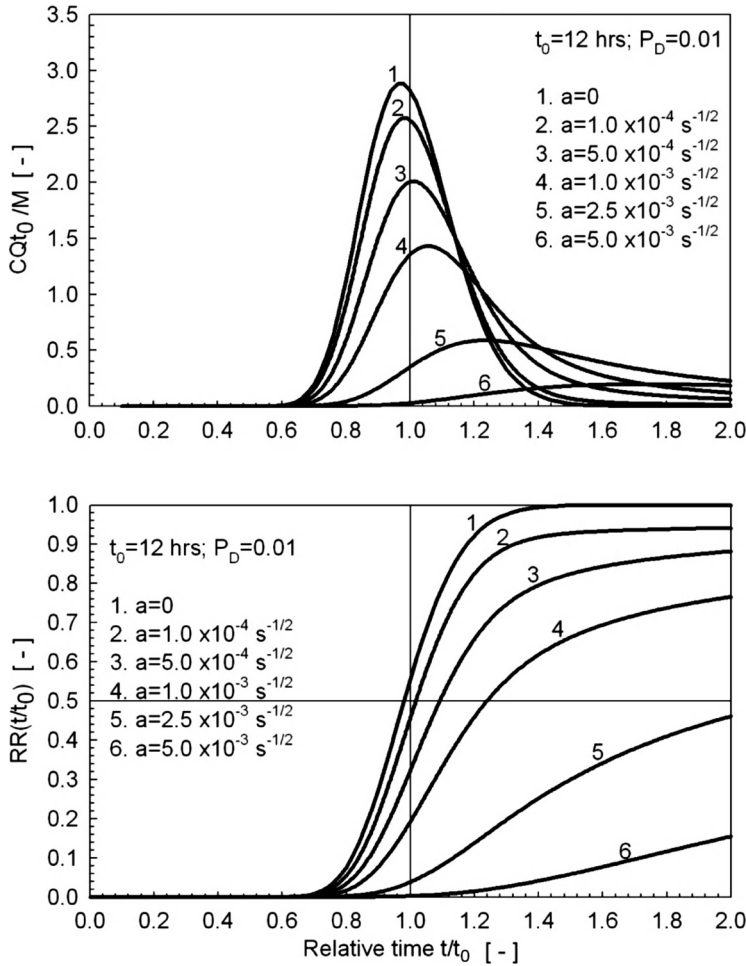


Figure 5.14 Theoretical normalized tracer concentration (top) and relative recovery (bottom) curves calculated by the SFDM for the mean transit time of water $t_0 = 12$ h and dispersion parameter $P_D = 0.01$, for different values of the diffusion parameter (a). This set of curves demonstrates the influence of matrix diffusion. Curves labelled '1' correspond to the situation of no diffusion of tracer into the immobile water ($a = 0$).

When the effective diffusion coefficient of tracer in the immobile water in the microporous matrix (D_p) is known or can be estimated (Neretnieks, 1980; Maloszewski, 1994), then, for a known fissure aperture (2b), the matrix porosity can be calculated from the formula:

$$n_{im} = \frac{(2b)a}{\sqrt{D_p}} \quad (5.95)$$

5.1.6 Examples

5.1.6.1 Column experiment

In a column ($L = 25$ cm, $2r = 5$ cm) filled with Quaternary gravels and a small proportion of clay, the volumetric flow rate was $Q = 6$ cm³/min (for the experimental setting see Figure 5.6). The tracer experiment was performed using Uranine (injected mass $M = 8.5$ mg), which was instantaneously injected through the whole column cross-section (Dirac impulse). The experimental tracer concentrations (in $\mu\text{g/mL}$) measured in the outflow from the column over nearly 40 min are shown in Figure 5.15 (top). The form of the tracer injection in this experiment allows the transport to be treated as one-dimensional, using Equations (5.29) or (5.33). The model has two parameters (t_0 and P_D), the values of which have to be found from the tracer curve. As mentioned in Section 5.1.3, the correct way to find these parameters is to use the

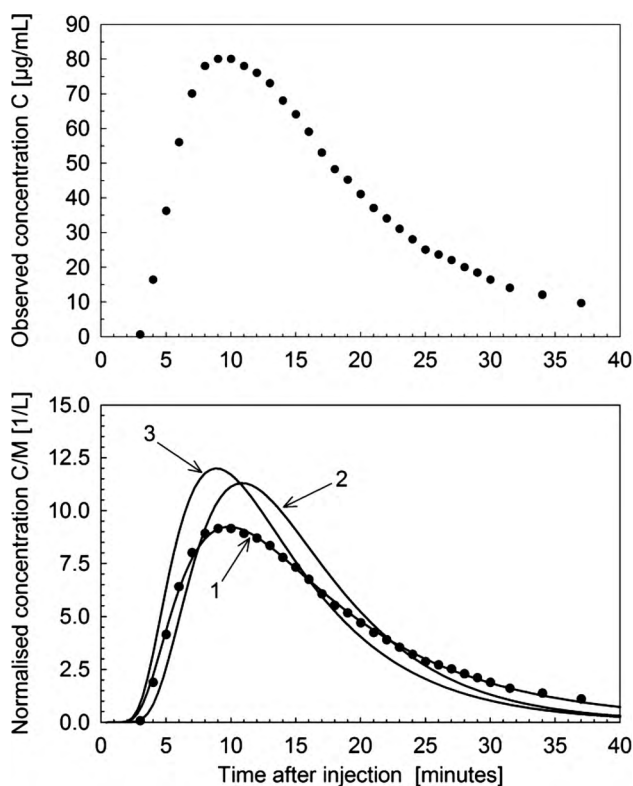


Figure 5.15 Tracer concentration observed in column experiment (top), and normalized C/M concentration curves observed (circles, bottom) and calculated (solid lines, bottom) using parameter values (t_0 and P_D) estimated from (1) least-squares fitting procedure (LSQM), (2) method of moments (MM) and (3) cumulative curve method (CCM). For parameter values see Table 5.1.

Table 5.1 Estimates of parameters (t_0 and P_D) and system properties (v , α_L , n) found from column experiment by different methods (LSQM, MM, CCM)

| Parameters | <i>Symbol</i> | <i>LSQM</i> | <i>MM</i> | <i>CCM</i> |
|-----------------------------------|----------------|-------------|-----------|------------|
| Mean transit time of water (5.31) | t_0 [min] | 17.6 | 15.6 | 14.0 |
| Dispersion parameter (5.32) | P_D [—] | 0.205 | 0.123 | 0.157 |
| Goodness-of-fit (5.132) | E [%] | 99.7 | 81.3 | 73.9 |
| <i>System properties</i> | | | | |
| Mean water velocity (5.30) | v [m/d] | 20.5 | 23.1 | 25.7 |
| Longitudinal dispersivity (5.32) | α_L [m] | 0.051 | 0.031 | 0.039 |
| Mean porosity (5.34) | n [%] | 21.5 | 19.1 | 17.1 |

proposed method of combined least squares (LSQM). Inspection of the tracer concentration curve (Figure 5.15, top) clearly demonstrates that the approximate methods (method of moments and cumulative curve method) cannot be used because the conditions for their application, discussed in Section 5.1.3, are not fulfilled (tracer recovery $RR \ll 100\%$). Despite this, the values of the parameters were also calculated using MM and CCM in this case, in order to appreciate better the disadvantages of these methods. The calculated parameter values (t_0 and P_D) and the values calculated from these for several system properties (mean water velocity, longitudinal dispersivity and porosity) are summarized in Table 5.1. The goodness-of-fit values are also shown there.

The theoretical concentration curves calculated using the parameter values summarized in Table 5.1 are shown in Figure 5.15 (bottom). The concentration curves are normalized to the mass of tracer injected – this is generally standard in the presentation of tracer data.

(C/M) are expressed in units [1/volume], and, especially in multi-tracer experiments, directly show the tracer behaviour in the system. From the goodness-of-fit values and from inspection of the curves shown in Figure 5.15 (bottom), it is clear that the approximate methods (MM and CCM) yield completely unsatisfactory results in this case. The worst results are yielded by the cumulative curve method (CCM).

5.1.6.2 Combined pumping-tracer test

A combined pumping and tracer test was performed for a flow distance of $x = 100$ m in an aquifer of Quaternary gravels, with an average thickness of $H = 8$ m (for experimental setting, see Figure 5.6, bottom). The aquifer was under steady-state flow conditions, with a constant pumping rate of $Q = 50$ m³/h. The mass of tracer (Uranine) instantaneously injected into the fully penetrating well was $M = 340$ g. The experimental tracer concentration (in mg/m³), shown in Figure 5.16 (top), was measured in the pumping well (used for drinking water production) over a period of 150 days. The flow is steady-state radial-convergent flow, therefore the tracer transport can be considered as

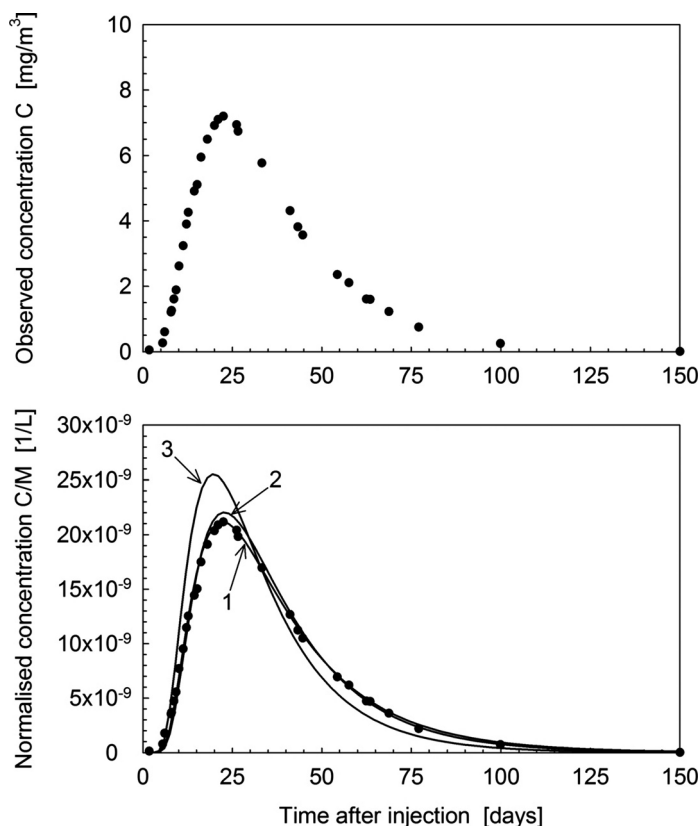


Figure 5.16 Tracer concentration observed in combined pumping-tracer experiment (top), and normalized C/M concentration curves observed (circles, bottom) and calculated (solid lines, bottom) using parameter values (t_0 and P_D) obtained from (1) least-squares fitting procedure (LSQM), (2) method of moments (MM) and (3) cumulative curve method (CCM). For parameter values see Table 5.2.

one-dimensional (5.19); the appropriate mathematical model is that given in Equation (5.35). The model has two unknown parameters (t_0 and P_D), the values of which have to be found. Because the mass recovery of tracer after 150 days was about $RR = 99\%$, it theoretically is possible to apply the approximate parameter estimation methods (see Section 5.1.3). The parameter values found using the least-squares procedure (LSQM) and the approximate methods (MM and CCM) are summarized in Table 5.2.

The sets of parameter values found with LSQM and MM are similar, as are the goodness-of-fitting values (99.5 and 98.5%, for LSQM and MM, respectively). The CCM yields again the worst results ($E = 75.4\%$), but it should be noted that the P_D value found in the experiment (0.173) is much larger than 0.005, which should exclude the application of CCM (see 5.65). The theoretical tracer concentration curves calculated using the t_0 and P_D values found by LSQM, MM and CCM (Table 5.2) are shown in Figure 5.16 (bottom).

Table 5.2 Estimates of parameters (t_0 and P_D) and system properties (v , α_L , n) found from combined pumping-tracer experiment by different methods (LSQM, MM, CCM)

| Parameters | Symbol | LSQM | MM | CCM |
|-----------------------------------|----------------|-------|-------|-------|
| Mean transit time of water (5.31) | t_0 [days] | 38.6 | 37.5 | 32.4 |
| Dispersion parameter (5.32) | P_D [—] | 0.193 | 0.174 | 0.173 |
| Goodness-of-fit (5.132) | E [%] | 99.5 | 98.5 | 75.4 |
| <i>System properties</i> | | | | |
| Mean water velocity (5.30) | v [m/d] | 2.59 | 2.67 | 3.09 |
| Longitudinal dispersivity (5.32) | α_L [m] | 19.3 | 17.4 | 17.3 |
| Mean porosity (5.35) | n [%] | 18.4 | 17.9 | 15.5 |

5.1.6.3 Experiment in multi-flow system

A tracer experiment was performed in one of the cells in the artificial wetland Nowa Slupia (Maloszewski, Wachniew and Czuprynski, 2006). The tracer concentration curve (in [g/L], see Figure 5.17, top) showed three peaks. This is due to the way the wetland was constructed: it consists of parallel porous layers with different hydraulic properties, similar to the system shown in Figure 5.11. The water flux through the wetland cell was relatively stable ($Q = 0.77$ l/s), and the hydraulic conditions could be assumed to be in a steady-state. Bromide ($M = 16.7$ kg) was injected through the whole cross-section perpendicular to the flow direction, and was measured in the outflow from the cell (which collected all of the water that flowed through that cell). The average flow distance was equal to $x = 25.1$ m. The experiment was analysed using the Multi-Flow Dispersion Model (MFDM) presented in Section 5.1.4. The parameters obtained for three single flow-paths found in the system are summarized in Table 5.3.

It must be stressed that estimation of transport parameters in multi-flow systems cannot be done using the approximate methods (MM, CCM); these are applicable only under the conditions mentioned earlier, in 1D and mono-flow systems. The parameter values found by applying the MM and CCM methods in this present experiment are shown here (Table 5.3) only to demonstrate how far those values are from reality. The corresponding theoretical concentration curves are additionally shown in Figure 5.17 (bottom). It is clear that the curves 2 and 3 (calculated with MM and CCM, respectively) do not follow the multi-peak concentration curve observed. The goodness-of-fit (E) of these two concentration curves is 47 and 50% (for MM and CCM, respectively). This contrasts with the value of $E = 99.5\%$ for MFDM. It should be noted that, when the relative recovery is close to $RR = 100\%$, the tracer mean transit time calculated by the method of moments (MM) in a multi-flow system can be used to estimate the total volume of water in the system ($V_m = Q \times \bar{t}$). The small difference between the volumes of water calculated here with MFDM and MM results from the fact that the tracer recovery was lower than 100% ($RR = 94.5\%$).

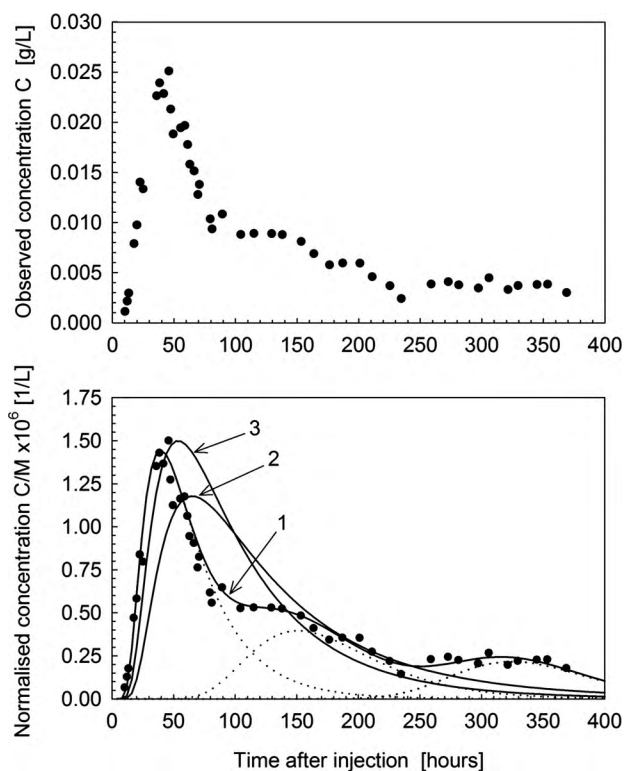


Figure 5.17 Tracer concentration observed in multi-layered porous medium experiment (top), and normalized C/M concentration curves observed (circles, bottom) and calculated (solid lines, bottom) using parameter values obtained from (1) multi-flow dispersion model (MFDM; dashed lines represent partial curves for the three flow-paths), (2) method of moments (MM) and (3) cumulative curve method (CCM). For parameter values see Table 5.3.

Table 5.3 Estimates of parameters and system properties found from multi-layered porous medium experiment (Maloszewski, Wachniew and Czuprynski, 2006) by different methods (MFDM, MM, CCM)

| Parameters | <i>Symbol</i> | <i>MFDM</i> | | | <i>MM</i> | <i>CCM</i> |
|-------------------------------------|-------------------------|-------------|------|------|-----------|------------|
| Partial transit times (5.77) | t_{0i} [h] | 66 | 179 | 346 | 133.4 | 104.8 |
| Partial dispersion parameter (5.76) | P_{Di} [—] | 0.18 | 0.06 | 0.01 | 0.26 | 0.24 |
| Portion of flow (5.81) | p_i | 0.53 | 0.29 | 0.18 | 1.0 | 1.0 |
| Goodness-of-fit (5.132) | E [%] | 99.5 | | | 47 | 50 |
| <i>System properties</i> | | | | | | |
| Mean transit time (5.83) | t_0 [h] | 149.2 | | | 133.4 | 104.8 |
| Volume of water (5.82) | V_m [m ³] | 400 | | | 370 | 290 |
| Mean porosity (V_m/V_{CELL}) | n [%] | 17.8 | | | 16.5 | 12.9 |

5.1.6.4 Experiment in double-porosity (fissured) medium

The tracer experiment described by Einsiedl and Maloszewski (2005) is used here as an example of parameter estimation in a double-porosity medium. The experiment was performed in the Lindau Rock Laboratory (Germany) in a highly permeable ore dike, with the flow distance between the B8 (injection) and BL10 (pumping) wells being in the distance of $x = 11.2$ m. The pumping rate was $Q = 0.23$ l/s. The thickness of the ore dike was approximately equal to $H = 2$ m, and the hydraulic conductivity approximately equal to $k = 2.07$ m/d. The test site is described in detail by Himmelsbach, Hötzl and Maloszewski (1998). A new fluorescent dye (pyrene-1, 3, 6, 8-tetra sulfonic acid, PTS) was used. The experiment was performed under radial-convergent flow conditions (Figure 5.6), and the SFDM model (5.90) was used for data interpretation. The best-fit concentration and recovery curves are shown in Figure 5.18 (top). The estimated parameter values, found by simultaneous fitting of the tracer concentration and recovery curves, as recommended by Maloszewski and Zuber (1990), were $t_0 = 2.4$ h, $P_D = 0.05$ and $a = 8.5 \times 10^{-3} \text{ s}^{-1/2}$; a is the diffusion parameter. The goodness-of-fit (E) was 98%. When combined with the known hydraulic properties of the system and the diffusion properties of the tracer, these estimates yield a fissure (mobile) porosity of 0.24%, a matrix (immobile) porosity of 5.0% and a mean fissure aperture of $188 \mu\text{m}$. The parameter values found using the SDFM model are summarized in Table 5.4, together with values found using the approximate methods (MM and CCM). Once again, these approximate methods cannot be applied to estimate transport parameters in double-porosity media, as is evident from the values of t_0 and P_D shown in Table 5.4. When these values are used to calculate the tracer concentration curves, the curves obtained are as shown in Figure 5.18 (bottom, curves 2 and 3). The goodness-of-fit (E) values for these curves are 13.9 and 1.5%, for MM and CCM respectively.

Table 5.4 Estimates of parameters and system properties found from fissured-aquifer experiment, using both the SFDM model and, wrongly, the approximate methods (MM, CCM)

| Parameters | Symbol | SFDM | MM | CCM |
|-----------------------------------|---------------------------|----------------------|------|------|
| Mean transit time of water (5.92) | t_0 [h] | 2.4 | 7.3 | 5.6 |
| Dispersion parameter (5.32) | P_D [—] | 0.05 | 0.26 | 0.33 |
| Diffusion parameter (5.91) | a [$\text{s}^{-1/2}$] | 8.5×10^{-3} | — | — |
| Goodness-of-fit (5.132) | E [%] | 97.5 | 13.9 | 1.5 |
| <i>System properties</i> | | | | |
| Dispersivity | α_L [m] | 0.56 | 2.94 | 3.70 |
| Mean fissure porosity (5.93) | n_m [%] | 0.24 | — | — |
| Mean fissure aperture (5.94) | $2b$ [μm] | 188 | — | — |
| Mean matrix porosity (5.95) | n_{im} [%] | 5.00 | — | — |

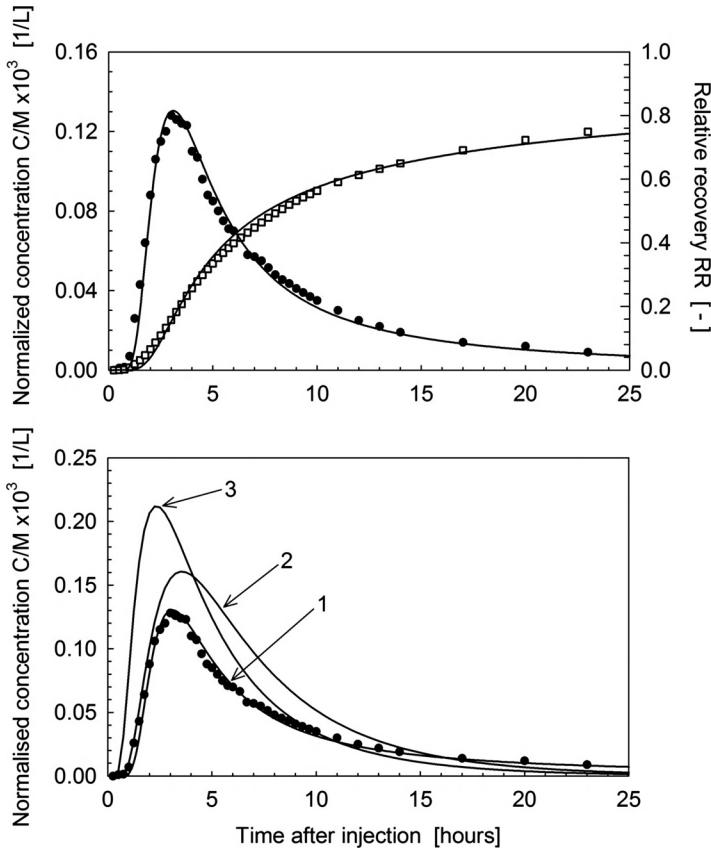


Figure 5.18 Normalized tracer concentration C/M (circles, top) and relative recovery (squares, top) observed in combined pumping and tracer test performed in fissured rock aquifer (Einsiedl and Maloszewski, 2005). Concentration and recovery curves (top) are those obtained by parameter estimation using SFDM (5.63). Bottom: observed concentration (C/M) compared with theoretical concentration curves (solid lines) calculated using parameter values obtained from (1) SFDM, (2) method of moments (MM) and (3) cumulative curve method (CCM). For parameter values see Table 5.4.

5.2 Tracer experiments under unsaturated flow conditions

Mathematical modelling of tracer (pollutant) transport in the unsaturated zone requires as a first step the determination of water flow through the soil, which is a function of time and space. The water flow is described by the Richards equation (Richards, 1931; Feddes *et al.*, 1988; Zaradny, 1993), which is a combination of the Darcy-Buckingham equation and the equation of continuity:

$$\frac{\partial \theta}{\partial t} = -\frac{\partial q}{\partial z} = \frac{\partial}{\partial z} \left[K(h) \frac{\partial h}{\partial z} - K(h) \right] \quad (5.96)$$

where z is the vertical coordinate, q is the water flux, t is the time, $K(h)$ is the soil hydraulic conductivity function, which depends on the pressure head h and the volumetric water content θ .

The solving of the above equation requires knowledge of the main hydraulic characteristics of the unsaturated soil, such as the relationship between the pressure head h and the hydraulic conductivity K , both of which depend on the soil water content θ . The relationship between $h(\theta)$ and $K(\theta)$ can be described using known laboratory and field methods, and also by many mathematical equations. For practical purposes, the hydraulic functions are defined by a number of closed-form analytical expressions, for example those due to Brooks and Corey (1964), Rijtema (1969), Mualem (1976) and Van Genuchten (1980). Forms for the water retention characteristic $\theta(h)$ and the conductivity function $K(h)$, for the unimodal case without a hysteresis effect, are given by Van Genuchten (1980), based on the Mualem approach (Mualem, 1979):

$$\begin{aligned}\theta(h) &= \theta_r + \frac{\theta_s - \theta_r}{[1 + (\alpha \cdot h)^n]^m} \quad \text{for } h < 0 \\ \theta(h) &= \theta_s \quad \text{for } h \geq 0\end{aligned}\tag{5.97}$$

$$K_r(h) = \frac{[1 - (\alpha \cdot h)^{n-1} \cdot [1 + (\alpha \cdot h)^n]^m]^2}{[1 + (\alpha \cdot h)^n]^{\frac{m}{2}}}\tag{5.98}$$

where θ_s and θ_r are the saturated and residual water content, respectively. α , n and m are empirical parameters describing the shape of the retention curves, where $m = 1 - 1/n$. $K_r(h)$ is the relative hydraulic conductivity function; this is the hydraulic conductivity function $K(h)$ divided by the saturated hydraulic conductivity K_s .

Traditionally, these highly nonlinear functions have been obtained in small-scale laboratory experiments using direct steady-state methods (e.g. Haws, Das and Rao, 2004; Kern, 1995; Vereecken, Maes and Feyen, 1990). Recently, however, experimental lysimeter methods have become more attractive (e.g. Kool and Parker, 1988; Kool, Parker and van Genuchten, 1985, 1987; Maciejewski *et al.*, 2006; Nützmann *et al.*, 1998); these methods are applied under transient-flow conditions, and are coupled with inverse modelling techniques. These methods require a special kind of experiment. During the experiments some auxiliary variables are measured, for example cumulative outflow, pressure head, water content or infiltration rate. Then the a priori unknown soil hydraulic parameters are determined by minimizing an objective function containing the deviations between observed and predicted quantities. An example of the characteristic found for sandy lysimeters by Maciejewski *et al.* (2006) is shown in Figure 5.19. Equations (5.96), with known soil characteristics, and (5.97) and (5.98), can be solved by finite-difference techniques using, for example, the computer programs SWATRE (Feddes *et al.*, 1978; Belmans, Wesseling and Feddes, 1983; Maciejewski, Zaradny and Klotz, 1992) or HYDRUS-1D (Simunek *et al.*, 2008).

Many investigators (e.g. Coats and Smith, 1964; Van Genuchten and Wierenga, 1977; Gaudet *et al.*, 1977; De Smedt and Wierenga, 1979) have shown that under unsaturated flow conditions only a part of the water in a REV (representative elementary

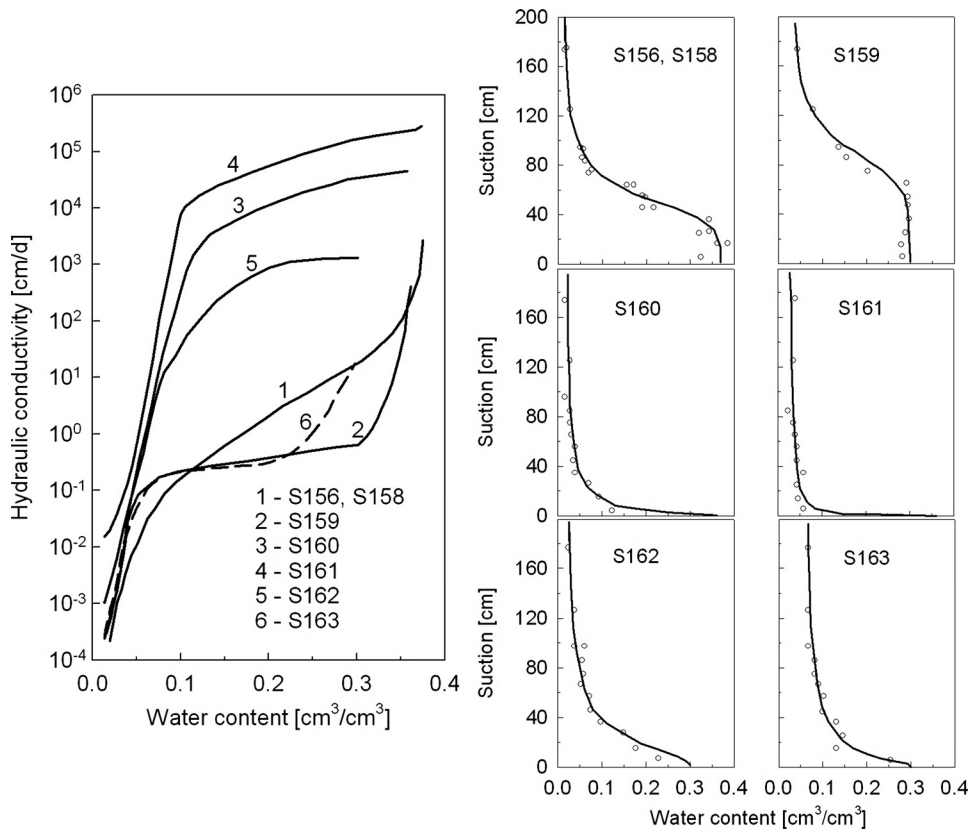


Figure 5.19 An example of soil characteristics: (left) $K(\theta)$; (right) water suction h as a function of water content after free drainage for typical Bavarian sands (after Maciejewski *et al.*, 2006) – circles show observed values, and solid line shows values obtained using van Genuchten Model.

volume; see Bear, 1972) takes part in motion; this is the so-called mobile water. As this the case, the unsaturated zone can be considered as a double-porosity medium with mobile and immobile water components. The transport of an ideal tracer in the mobile phase can be described by the dispersion-convection equation with a source/sink term that describes the tracer transfer between mobile and immobile water using in most cases the approximation introduced by Coats and Smith (1964). The tracer transfer is proportional to the difference between the tracer concentrations in the mobile and immobile water. The existence of immobile water in unsaturated soil is usually very difficult to document experimentally. But, given that there theoretically are two water phases, the mass balance equation for the double-porosity model is as follows (De Smedt, Wauters and Sevilla, 1986):

$$\frac{\partial(\theta_m C)}{\partial t} + \frac{\partial(\theta_{im} C_{im})}{\partial t} = \frac{\partial}{\partial z} \left(D \theta_m \frac{\partial C}{\partial z} \right) - \frac{\partial}{\partial z} (qC) \quad (5.99)$$

and

$$\frac{\partial}{\partial t} (\theta_{im} C_{im}) = \omega \cdot \theta_m \cdot (C - C_{im}) \quad (5.100)$$

where C and C_{im} are the tracer concentrations in the mobile and immobile water, respectively; θ_m and θ_{im} are the mobile and immobile water contents, respectively; ω is the transfer coefficient of the tracer exchange between the mobile and immobile water components; z and t are space and time variables, respectively.

In practice, it can be assumed that the ratio of immobile to total water content $f = \theta_{im}/\theta$ is constant, which reduces Equations (5.99–5.100) to:

$$(1 - f) \frac{\partial(\theta C)}{\partial t} + f \frac{\partial(\theta C_{im})}{\partial t} = (1 - f) \frac{\partial}{\partial z} \left(D \theta \frac{\partial C}{\partial z} \right) - \frac{\partial(qC)}{\partial z} \quad (5.101)$$

$$f \frac{\partial(\theta C_{im})}{\partial t} = \omega(1 - f) \theta (C - C_{im}) \quad (5.102)$$

where D is the dispersion coefficient given by:

$$D = \alpha_L \frac{q}{(1 - f)\theta} + D_d \quad (5.103)$$

α_L is the longitudinal dispersivity, D_d is the diffusion coefficient of tracer in the soil, given by $D_d = D_m/\tau$, where D_m is the molecular diffusion coefficient of tracer in free water and τ is the tortuosity.

Because θ and q depend on depth z and time t , Equations (5.99–5.100) or (5.101–5.102) are non-linear. They can only be solved numerically, for example using the method of moving coordinates (Maciejewski, 1993). This approach allows the convection term to be eliminated from the transport equation, which in the numerical solution strongly reduces the effect of numerical dispersion. The following variables are taken as known: the water flux $q(z, t)$, and the total water content $\theta(z, t)$, calculated with (5.96) and (5.97–5.98). The model of the tracer transport through the unsaturated zone (5.101–5.102) has three parameters: the longitudinal dispersivity (α_L), the tracer transfer coefficient between the mobile and immobile water (ω), and the ratio of immobile water to the total water content ($f = \theta_{im}/\theta$).

When all water takes is mobile, Equations (5.99–5.100) reduce to:

$$\frac{\partial(\theta C)}{\partial t} = \frac{\partial}{\partial z} \left(\theta D \frac{\partial C}{\partial z} \right) - \frac{\partial(qC)}{\partial z} \quad (5.104)$$

When this equation is applied to a tracer concentration curve measured in the unsaturated zone there is only one parameter to be estimated, the longitudinal dispersivity (α_L).

The modelling of tracer transport using the equations given above can be performed using software such as HYDRUS-1D (Simunek *et al.*, 2008), which includes different double-porosity models.

5.3 Tracer experiments in streams and rivers

The selection of a model to describe tracer transport in streams or rivers depends on the situation in which the tracer experiment is performed (Figure 5.20). Generally, one has to consider if there exist significant zones with immobile water between the injection and detection sites (e.g. Bencala and Walters, 1983; Choi, Harvey and Conklin, 2000; Kazezyılmaz-Alhan, 2008). When there are no such zones (or when those zones are of negligible importance), the tracer transport can be described by the 1D Equation (5.19) (see Section 5.1.1). This is especially true when the injection of the tracer is performed throughout the whole cross-section of the river; this is done by using several pipes situated at different points across the flow. The solution to (5.19), for the instantaneous injection (5.29 or 5.33), is given in Section 5.1.2. In most practical applications, hydrologists focus their attention on the estimation of the flow rate (Q) of the river. When the tracer concentration curve, $C(t)$, is fully measured at the observation site (see Figure 5.20, top), then the river flow rate, Q , can be easily calculated using Equation (5.40). After rearrangement, this reads as follows:

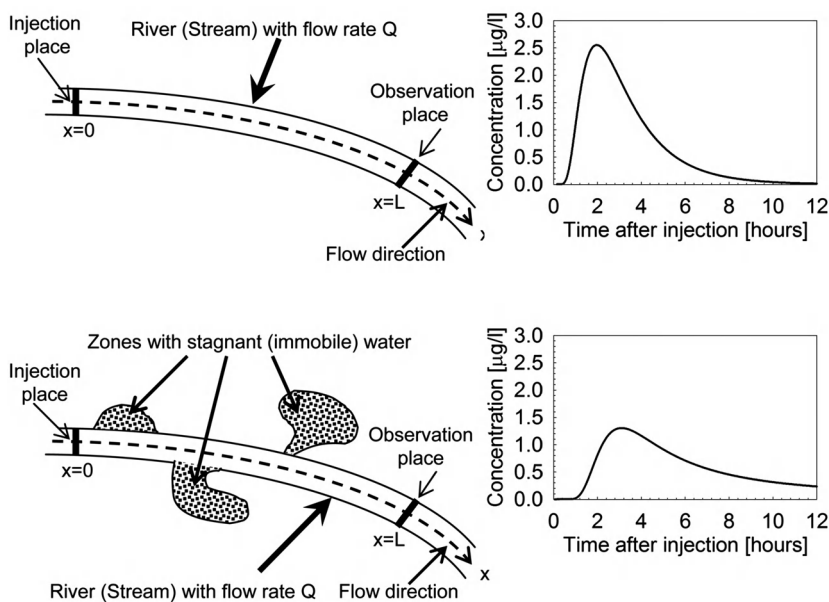


Figure 5.20 Schematic presentation of tracer experiments in rivers or streams where (top) there are no zones of immobile water and (bottom) zones of immobile water exist and the tracer transport is modelled using the concept of a double-porosity medium. The tracer concentration curves measured at the observation place in the former case (top) show no tailing effect; in the latter case (bottom), there is a strong tailing effect resulting from tracer diffusion into the immobile water.

$$Q = \frac{M}{\int_0^{\infty} C(t) dt} = \frac{M}{F} \quad (5.105)$$

where M is the mass of tracer injected (at $x = 0$) and F is the area under the tracer concentration curve, which can be calculated using the trapezoidal method of integration:

$$F = \frac{1}{2} \sum_{i=1}^N (C_{i-1} + C_i) \cdot (t_i - t_{i-1}) \quad (5.106)$$

where N is the number of points measured. For C_i and t_i , see Figure 5.9 (top).

Some flow fluorimeters perform the above calculation automatically during tracer detection in a river. Then one only has to give the mass of tracer injected (M) in order to obtain the flow rate (Q). To obtain the water flow velocity (v), the mean water transit time (t_o) or the longitudinal dispersivity (α_L), it is necessary to model the observed tracer concentration curve using (5.29) or (5.33). To find those parameters, one can use the LSQM method described in Section 5.1.3. Knowing the flow rate (Q) and the mean water transit time (t_o), the volume of water between the injection and detection sites can be estimated. This is also the volume of the mobile water, $V = V_m = Q \cdot t_o$. For a known flow length (L), the mean cross-sectional area of the river (S) is given by the ratio V_m/L .

When zones of stagnant water exist between the injection and detection sites (Figure 5.20, bottom), the exchange process (diffusion) of tracer between the mobile and immobile phases has to be included in the 1D transport equation. In most practical cases, the model of Coats and Smith (1964) is used, as mentioned in Section 5.2. The solution to (5.101–5.102) for a constant flow rate in the river ($q = Q$) and for instantaneous injection of tracer at $x = 0$ is (e.g. Herrmann, Maloszewski and Stichler, 1987):

$$C(t) = \frac{M}{Q\sqrt{4\pi P_D t^3/t_o}} \left\{ \exp \left[-\frac{(1 - t/t_o)^2}{4P_D t/t_o} - \omega t \right] + \omega t \sqrt{\beta} \exp(-\omega \beta t) \right. \\ \left. \times \int_0^1 I_1 \left(2\omega t \sqrt{\beta(1 - \xi)\xi} \right) \times \exp \left[-\frac{(1 - \xi t/t_o)^2}{4P_D \xi t/t_o} - \omega(1 - \beta)t\xi \right] \frac{d\xi}{\xi\sqrt{1 - \xi}} \right\} \quad (5.107)$$

where:

$$\beta = V_m/V_{im} \quad (5.108)$$

and $I_1(\eta)$ is the modified Bessel function of the first kind and first order of argument η , and ξ is the integration variable $[0, 1]$.

This model (5.107) has four parameters (t_o , P_D , ω , β), which are difficult to estimate because of their possible interplay. An alternative approach is to use the SFDM model (5.90), which was developed to describe convective-dispersive transport within mobile water with simultaneous diffusion into the zone with immobile water (see Section 5.1.5). This model has three parameters: t_o , P_D and the diffusion parameter a (5.91). Note that in this case, the fissure aperture (2b) is replaced by the mean river width (W),

and the diffusion parameter (a) reads as follows:

$$a = \frac{\sqrt{D_m}}{W(1 + \beta)} \quad (5.109)$$

where D_m is the molecular diffusion coefficient of tracer in free water.

If the discharge (Q) of the river is known (or can be estimated), then the volume of mobile water (V_m) can be easily calculated from the mean transit time parameter (t_0) of the SFDM model: $V = V_m = Q \cdot t_0$. Furthermore, if the mean width of the river (W) and the diffusion coefficient of tracer in free water (D_m) are known, the parameter β can be calculated from (5.109):

$$\beta = \frac{\sqrt{D_m}}{aW} - 1 \quad (5.110)$$

Finally, by using (5.108), the volume of immobile water is given by:

$$V_{im} = Q t_0 / \beta \quad (5.111)$$

5.4 Environmental tracer data

5.4.1 Introduction

The environmental isotopes, for example tritium and the stable isotopes ^{18}O or ^2H , are suitable for tracing the behaviour of water at different stages of the hydrological cycle because, among their other characteristics, they are constituents of the water molecule. When used as a supplement to conventional hydrological methods, these tracers may provide additional insight into problems such as the origin of water, the storage properties of catchments, water dynamics in groundwater systems and the interaction between surface and groundwater. The quantitative evaluation of the tracer data in these cases is most often based on the application of lumped-parameter models. The main advantage of these models is the fact that they require only the knowledge of the tracer concentration in the recharge area (input function) together with some records of tracer data at the observation site (output). In spite of their simplicity, lumped-parameter models yield useful information on zonal or regional values of some hydrologic parameters. Their applicability has been confirmed in a number of case studies, for example DeWalle *et al.* (1997), Kendall and McDonell (1998), Maloszewski and Zuber (1993, 1996), Maloszewski *et al.* (1983, 2002), McDonell, Rowe and Stewart (1999), McGuire, DeWalle and Gburek (2002), Stichler, Maloszewski and Moser (1986), Turner, Macpherson and Stokes (1987), Vitvar and Balderer (1997).

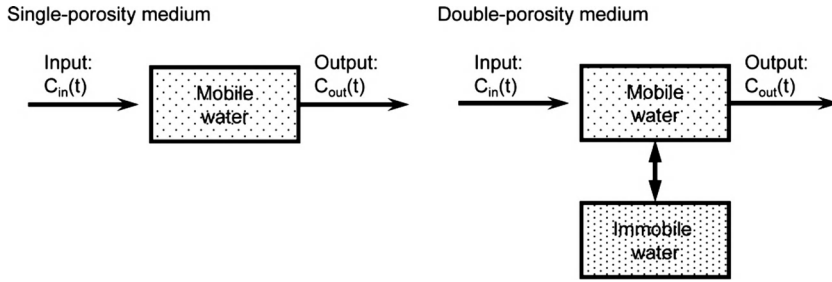


Figure 5.21 Conceptual models of the lumped-parameter approach in groundwater systems.

5.4.2 The basic concept of lumped-parameter models

The basic principles of lumped-parameter models (also called black-box models), together with details of their applicability, have been well described (e.g. Maloszewski and Zuber, 1982, 1996; Zuber and Maloszewski, 2001). Generally, it is presumed that the groundwater system can be considered as a closed system that (i) is sufficiently homogeneous, (ii) is in a steady state, (iii) has a defined input (recharge or infiltration area) and (iv) has a defined output in the form of pumping wells, springs or streams draining the system. The groundwater system can be considered as a single-porosity or double-porosity medium (Figure 5.21). For the single-porosity medium, it is assumed that all the water in the system is mobile, or that the volume of immobile water can be neglected.

Every lumped-parameter model is characterized by its own transit time distribution function. That function has either to be known, or to be assumed on the basis of hydrological information about the system being considered. In most cases, transit time distribution functions have one or two parameters, the values of which can be estimated by calibrating the model to the experimental data observed in the outflow from the system. The input concentration of the environmental tracer is either measured directly, or is calculated from known hydrological and isotope data (e.g. Maloszewski and Zuber, 1982, 1996; Grabczak *et al.*, 1984; McGuire, DeWalle and Gburek, 2002; Stichler *et al.*, 1986). The main parameter of all models for single-porosity media is the mean transit time of water (T) through the system, which is related to the mobile water volume (V_m) in the system and the volumetric flow rate (Q):

$$V_m = QT \quad (5.112)$$

This mean transit time represents the average of flow times along all of the individual streamlines in the aquifer, each weighted by the amount of flowing water. To determine the mean transit time of water (T), the temporal variation of the measured tracer input concentration, $C_{in}(t)$, is used to calculate the tracer output concentration, $C_{out}(t)$, which is then compared with the concentrations measured in the output from the system. The relationship between the input and output concentrations is given by the

convolution integral:

$$C_{out}(t) = \int_0^{\infty} C_{in}(t - \tau) g(\tau) \exp(-\lambda \tau) d\tau \quad (5.113)$$

where λ is the decay constant of the radioactive tracers and $g(\tau)$ is the transit time distribution function.

It should be remembered that the integral over the $g(\tau)$ for all possible transit times (τ), that is from zero to infinity, has to be equal to unity. For most of the models used for interpreting isotope data in single-porosity media, the mean value ($\bar{\tau}$) of the transit time distribution function $g(\tau)$ has to be equal to the mean transit time of water (T). The most common kinds of transit time distribution functions, $g(\tau)$, used for single-porosity media are:

Piston Flow Model (PFM)

$$g(\tau) = \delta(\tau - T) \quad (5.114)$$

Exponential Model (EM)

$$g(\tau) = \frac{1}{T} \exp\left(-\frac{\tau}{T}\right) \quad (5.115)$$

Combined Exponential Piston Flow Model (EPM)

$$\begin{aligned} g(\tau) &= \frac{\eta}{T} \exp\left(-\frac{\eta\tau}{T} + \eta - 1\right) \quad \text{for } \tau > (\eta - 1)T/\eta \\ g(\tau) &= 0 \quad \text{for } \tau \leq (\eta - 1)T/\eta \end{aligned} \quad (5.116)$$

Dispersion-Model (DM)

$$g(\tau) = \frac{1}{\tau\sqrt{4\pi P_D\tau/T}} \exp\left[-\frac{(1 - \tau/T)^2}{4P_D\tau/T}\right] \quad (5.117)$$

where P_D is the dispersion parameter and η is the ratio of the total water volume in the system to volume of that part of the water characterized by the exponential transit time distribution (V/V_{EM}).

The EPM model is a combination of the PFM and EM models in series; the order in which these models are applied is not important. A schematic representation of lumped-parameter models and their parameters is given in Figure 5.22, and examples of the transit time distribution functions (5.114)–(5.117) are shown in Figure 5.23. The use of the EPM yields the parameters (T) and (η), which are then used to determine the transit times (T_{PFM}) and (T_{EM}):

$$T_{EM} = \frac{T}{\eta} \quad (5.118)$$

$$T_{PFM} = \frac{1 - \eta}{\eta} T \quad (5.119)$$

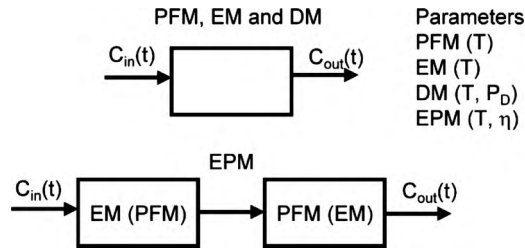


Figure 5.22 Schematic presentation of lumped-parameter models and their parameters.

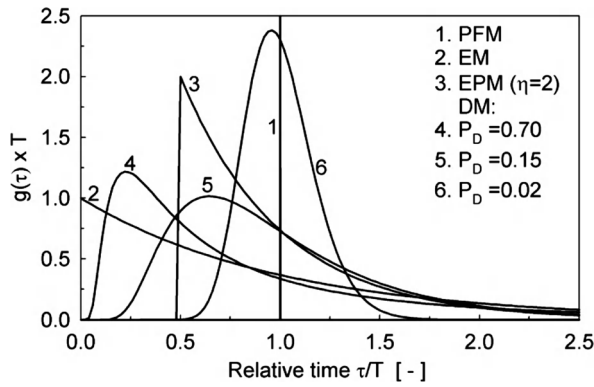


Figure 5.23 Examples of the transit time distribution function of tracer particles through a groundwater system calculated for different lumped-parameter models: PFM is the piston flow model, EM is the exponential model, EPM is the combined exponential-piston flow model and DM is the dispersion model.

and the volumes of water (V_{PFM}) and (V_{EM}):

$$V_{EM} = Q T_{EM} \quad (5.120)$$

$$V_{PFM} = Q T_{PFM} \quad (5.121)$$

in the parts of the system characterized by the exponential and the piston-flow transit time distributions, respectively. The sum of the water volumes in the parts with exponential and piston transit time distributions yields the volume of water in the whole system:

$$V = V_{EM} + V_{PFM} = QT \quad (5.122)$$

Different lumped-parameter models are required for double-porosity media characterized by systems of fractures (Figure 5.13, top) where there is both mobile water in the fractures and immobile water in the microporous matrix (e.g. Figure 5.13 top and 5.21 right). The transport of tracers within the mobile water (by convection and dispersion), with simultaneous diffusion into the immobile water, was described by

Maloszewski (1994) for a system of parallel fissures having the same aperture and spacing (Figure 5.13); this is referred to by Maloszewski and Zuber (1985) and Maloszewski (1994) as the Parallel Fissure Dispersion Model (PFDM). That model could also be used for the interpretation of environmental tracer data, but its transit time distribution function has four parameters that need to be estimated, which makes it inapplicable in practice in isotope hydrology. This difficulty can be avoided by noting, as did Maloszewski (1994), that after a sufficiently long time in a double-porosity system the transit time distribution function obtained from the PFDM model has the same shape as that obtained from the ordinary dispersion model (5.117). What happens physically is that after a sufficiently long time the tracer diffuses fully into the porous matrix holding the immobile water. Once that state is reached, the tracer observed in the output from the double-porosity system behaves as it would in a single-porosity system with a larger volume of water (porosity). It has been found possible in practice to use the ordinary dispersion model (5.117) to interpret tritium (^3H) or stable isotope (^{18}O and ^2H) data in double-porosity systems when the transit time of water (T) through the system is greater than 2–3 years (Maloszewski, 1994; Maloszewski, Stichler and Zuber, 2004); this applies to most applications of environmental tracers in fractured rocks. In applying the ordinary dispersion model (5.117) to a double-porosity medium, it must be noted that instead of the mean transit time of water (T) the apparent parameter T^* , referred to as the mean transit time of the tracer is yielded. T^* is given by:

$$T^* = \left(\frac{n_m + n_{im}}{n_m} \right) \times T = RT \quad (5.123)$$

where n_m is the mobile porosity defined as $2b/L$ (Figure 5.13) and R is the retardation factor resulting from the diffusion of tracer into the immobile water:

$$R = \left(\frac{n_m + n_{im}}{n_m} \right) = \frac{n_{total}}{n_m} \quad (5.124)$$

where n_{total} is the total porosity of the fissured rock ($n_{im} + n_m$).

In practice, the apparent parameter T^* can be used to calculate the total volume of water in the system (V), that is the sum of the mobile (V_m) and immobile (V_{im}) components:

$$QT^* = \left(\frac{n_m + n_{im}}{n_m} \right) \times TQ = RTQ = V_m + V_{im} = V \quad (5.125)$$

Accordingly, the total volume of water (V) in the groundwater system in a heterogeneous fissured aquifer is R times greater than the volume of mobile water (V_m), the volume that mostly is of interest. This fact has to be taken into account in interpreting environmental tracer data in fissured rocks, otherwise the volume of available water resources will be R -times overestimated.

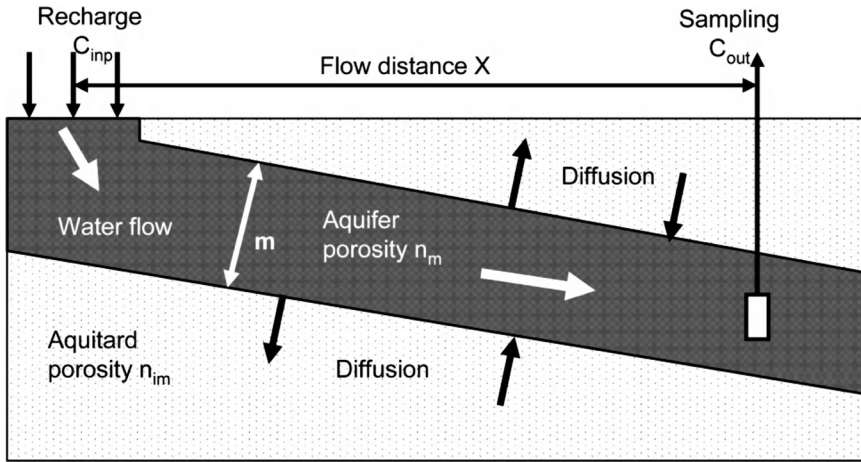


Figure 5.24 Schematic presentation of double-porosity system comprising an aquifer (with mobile water) and an aquitard with immobile water: m is the thickness of the aquifer, x is the distance from the recharge zone measured along the flow path.

The retardation factor R can be calculated when both the porosities n_m and n_{im} are known. These two porosities can be found only when a combined pumping test and tracer experiment is performed in the area under investigation (Maloszewski and Zuber, 1990, 1991). There are also tracer losses due to diffusion into regions with immobile water when aquifers are surrounded by large aquitards with immobile water (Figure 5.24). In this situation the tracer transport can be described by the SFDM (5.90) developed for artificial tracer experiments (Section 5.1.5). However, when the flow distance (x) is large and the thickness of the aquifer (H or m) is low, then for simplicity one can assume only convective flow in the aquifer. The analytical solution given by Maloszewski (1994), yields the transit time distribution function given by (5.126) and referred to as the Combined Piston Flow Diffusion Model (SPFM) (see Nolte *et al.*, 1991). However, one should note that the SPFM should not be considered as a classical lumped-parameter model due to irreversible losses of tracer in the infinitely large aquitard.

5.4.2.1 Combined piston-flow diffusion model (SPFM)

$$g(\tau) = \frac{n_{im}\sqrt{D_p}}{n_m m \sqrt{\pi T(\tau/T - 1)^3}} \exp\left(-\frac{n_{im}^2 D_p T}{n_m^2 m^2 (\tau/T - 1)}\right) \quad \text{for } \tau > T \quad (5.126)$$

$$g(\tau) = 0 \quad \text{for } \tau \leq T$$

This model can be used for the interpretation of environmental tracer data obtained from wells that are situated long distances away from the recharge area in comparison to the thickness of the aquifer ($x \gg m$). The transit time distribution functions calculated

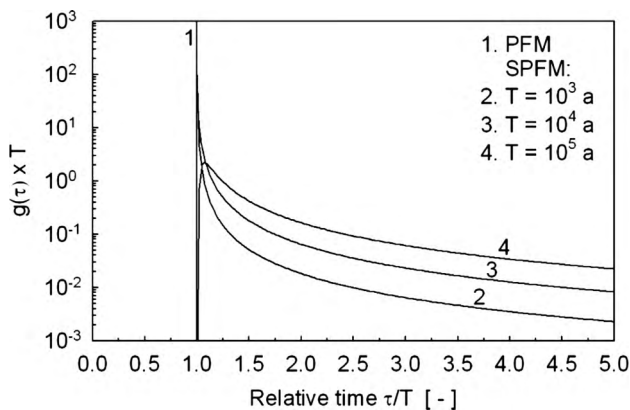


Figure 5.25 Examples of the transit time distribution function of tracer particles calculated for different models: PFM is piston-flow model; SPFM is combined piston-flow and diffusion model.

using (5.126) are shown in Figure 5.25. It can be seen there that for transit times of water greater than 1000a, the diffusion of the environmental tracer into the aquitard already plays a very important role. In such situations, the interpretation of environmental tracer data using the traditional PFM-model (radioactive water age) expressed by (5.114) will result in greatly underestimated values for the water transit time.

5.4.3 Selection of the model

Which model is selected for use in the groundwater system being considered depends on the hydrological conditions there. Generally, the dispersion and piston flow models are applicable for confined or partially confined aquifers; the exponential model can only be used for unconfined aquifers when the unsaturated zone is negligibly small. The hydrological situations in which different models can be applied are shown in Figure 5.26. The first example illustrated there (Figure 5.26, top) shows a confined aquifer with a narrow recharge zone and a sampling site far away from the recharge (similar to that shown in Figure 5.24). If the confined part of the aquifer has impermeable boundaries and there is negligible immobile water, then the Dispersion Model (5.117) can be applied. If the flow distance is very long (allowing the assumption that $P_D \approx 0$), then the PFM (5.114) can be applied; this is possible because if P_D has a very small value close to zero, then the dispersive transit time distribution becomes equivalent to the piston-flow distribution. However, that consideration and the application of the PFM model is no more generally valid. It is very well known that the confined part includes always stagnant water. Considering, for example measurements of ^{14}C ($D_p = 2.1 \cdot 10^{-2} \text{ m}^2/\text{a}$) in typical aquifer with a thickness of $m = 30 \text{ m}$ and an effective (mobile) porosity $n_m = 25\%$ located within an aquitard having a low porosity (stagnant) of about $n_{im} = 5\%$, the SPFM (5.126) has to be used for transit time of water $T \geq 1000$

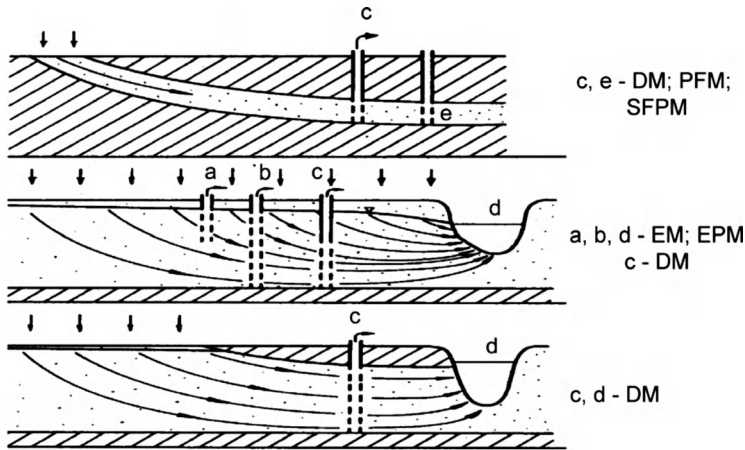


Figure 5.26 Presentation of hydrological situations in which particular models are applicable. Cases a, b, c and d correspond to sampling in out-flowing or abstracted water (in that form of sampling the water samples are automatically averaged by volumetric flow rates). Case e corresponds to samples taken separately at different depths (e.g. during drilling) (after Maloszewski and Zuber, 1982).

years. For tritium or stable isotopes ^{18}O and ^2H the influence of diffusion into aquitard is observed even for smaller transit times.

The second example illustrated in Figure 5.26 (centre) is an unconfined aquifer. If the unsaturated zone in that aquifer is negligibly small, then for sampling points a, b and d the Exponential Model (5.115) is applicable. If the unsaturated zone has to be taken into account, the combined Exponential-Piston Flow Model (5.116) can be used. In this situation, the piston-flow transit time distribution corresponds to tracer transport through the unsaturated zone, the exponential transit time distribution to tracer transport through the saturated zone. Modelling the tracer data with the EPM yields values of T and η . The application of Equations (5.118–5.119) yields $T_{\text{unsat}} = T_{\text{PFM}}$ and $T_{\text{sat}} = T_{\text{EM}}$. This enables the volume of water in the unsaturated $V_{\text{unsat}}(V_{\text{PFM}})$ and the saturated $V_{\text{sat}}(V_{\text{EM}})$ zones to be estimated using (5.120–5.121). If the water is sampled in a well that is screened in its lower part, the Dispersion Model (5.117) has to be used.

The third example illustrated in Figure 5.26 (bottom) shows a partially confined aquifer. In this case, the streamlines with transit times $\tau = 0$ do not exist, and only the Dispersion Model (5.117) can be applied.

As has been mentioned, each lumped-parameter model has one or two unknown parameters that can be found by solving Equation (5.113) with one of the transit time distribution functions (5.114–5.117) or (5.126). To find these model parameters, the user-friendly software FLOWPC can be used. This has been described in detail by Maloszewski (IAEA, 2002). This software is available free of charge from the Isotope Hydrology Section of the International Atomic Energy Agency (IAEA) in Vienna, or directly from the author (Maloszewski).

5.4.4 Examples

5.4.4.1 Application of stable isotopes to bank filtration

The example is taken from Stichler, Maloszewski and Moser (1986) and shows the typical application of stable isotope (^{18}O) measurements in a bank filtration problem. This project was performed (i) to determine the proportion of Danube River water in two pumping wells and (ii) to estimate the mean flow times between the river and the wells. Both wells are situated at a distance of about 150 m from the river bank. They produce drinking water for the city of Passau (Southeast Germany), with nearly constant pumping rates of about 105 l/s in total.

It is possible to use stable isotope data to determine the proportion of river water in a production well when (i) the mean $\delta^{18}\text{O}$ content in the river water is distinctly different from that in the local groundwater and (ii) when the data are collected over a sufficiently long time. To determine the flow time between the river and the well also requires that there be strong $\delta^{18}\text{O}$ variations in the river water (i.e. in the input function). The measurements in the Passau project, shown in Figure 5.27, were performed

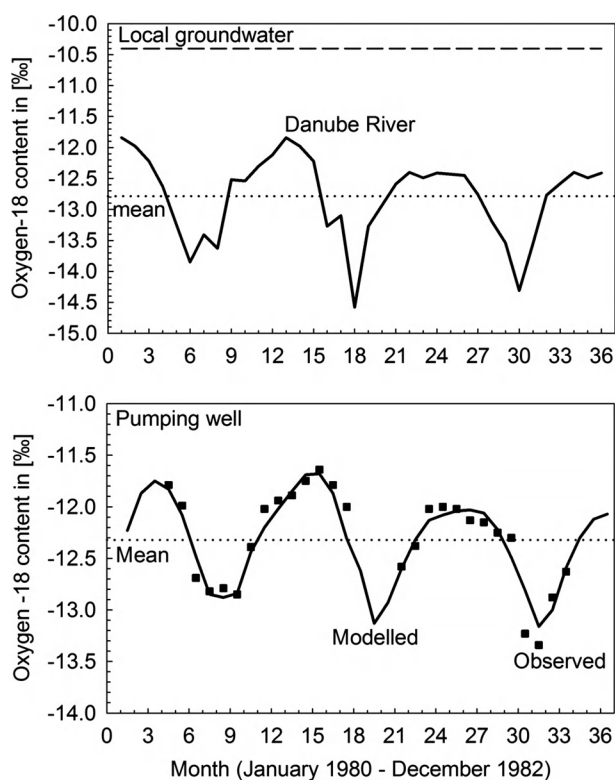


Figure 5.27 Stable isotope ($\delta^{18}\text{O}$) contents measured in the Danube River, in the local groundwater (top), and in the pumping well PSI (squares in lower figure) that produces drinking water for the city of Passau (after Stichler, Maloszewski and Moser, 1986).

twice-monthly over a period of three years. The measurements show that the mean $\delta^{18}\text{O}$ contents in both water components – the local groundwater and the Danube river water – are strongly different (-10.4 and -12.9‰ , respectively). Additionally, the $\delta^{18}\text{O}$ variations in the river water have an amplitude of more than 2.5‰ , whereas the local groundwater has practically no variation in $\delta^{18}\text{O}$ (Figure 5.27, top). In this situation, it is possible to use a very simple conceptual model of the water flow in the area under investigation (Figure 5.28).

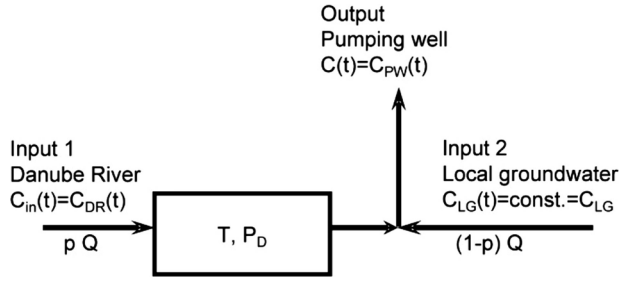


Figure 5.28 Conceptual model of water flow through the river bank to the drinking water supply of the city of Passau.

The mean proportion (p) of the Danube river water in the production well can be calculated using the following equation (Stichler, Maloszewski and Moser, 1986):

$$p = \frac{\bar{C}_{PW} - \bar{C}_{LG}}{\bar{C}_{DR} - \bar{C}_{LG}} \quad (5.127)$$

where \bar{C}_{PW} , \bar{C}_{DR} and \bar{C}_{LG} are mean $\delta^{18}\text{O}$ contents in the pumping well, the Danube River, and local groundwater, respectively.

The time-dependent concentration in the pumping well, that is the output concentration (Figure 5.28), $C(t)$, is given as follows:

$$C(t) = p \int_0^t C_{DR}(\tau) g(t - \tau) d\tau + (1 - p) \bar{C}_{LG} \quad (5.128)$$

where the dispersive transit time distribution function $g(t - \tau)$ is taken according to the hydrological situation (Figure 5.26) as:

$$g(t - \tau) = \frac{1}{(t - \tau) \sqrt{4\pi P_D(t - \tau)/T}} \exp \left[-\frac{\left(1 - \frac{t - \tau}{T}\right)^2}{4P_D \frac{t - \tau}{T}} \right] \quad (5.129)$$

where T and P_D are, respectively, the mean flow time and the dispersion parameter for the flow path between the Danube River and the production well.

The proportion of Danube river water (p) found for both production wells (PSI and PSII) was equal to 0.8. The best fit of Equation (5.128) to the $\delta^{18}\text{O}$ contents observed

in the pumping well PSI was given when the mean transit time was 60 days and P_D was equal to 0.12 (see Stichler, Maloszewski and Moser, 1986). The modelled $\delta^{18}\text{O}$ curve is shown for the well PSI in Figure 5.27 (solid line in lower part of figure).

The method presented for using isotope data in bank filtration can be applied in that form whenever the requirements for the isotope signals (mentioned above) are fulfilled. The tracer input function can be measured directly in the water infiltrating into the ground, that is in the river water, and therefore does not need to be calculated. The use of another input function obtained directly (in this case, measured in precipitation) is shown by Maloszewski *et al.* (2006); this was used for modelling deuterium ($\delta^2\text{H}$) transport through the unsaturated zone of unvegetated sandy soils, in lysimeter experiments.

5.4.4.2 Application of tritium measurements in catchment areas

Tritium (^3H) concentrations in atmospheric waters were constant and very low (5–10 TU) before the first hydrogen-bomb tests in the atmosphere, in 1954. After that, they increased until the years 1962–1963, when the highest concentrations (up to about 6000 TU) during the summer months in the northern hemisphere were reached. Since then, the atmospheric concentrations of tritium have decreased exponentially, reaching 15–20 TU in the late 1990s. The high tritium concentrations in precipitation during the early 1960s offer a unique opportunity for dating young groundwater systems having a relatively wide range of ages (up to approximately 250 years).

Seasonal variations in the tritium concentration in precipitation, coupled with variations in precipitation and infiltration rates, cause difficulties in the estimation of the input function, $C_{\text{in}}(t)$. For each calendar year the value of the input (C_{in}) can be expressed as:

$$C_{\text{in}} = \frac{\sum_{i=1}^{12} (C_i I_i)}{\sum_{i=1}^{12} I_i} = \frac{\sum_{i=1}^{12} (\alpha_i C_i P_i)}{\sum_{i=1}^{12} (\alpha_i P_i)} \quad (5.130)$$

where C_i , P_i and I_i are the tritium concentration in precipitation, the precipitation rate and the infiltration rate for the i^{th} month, respectively.

The infiltration coefficient ($\alpha_i = I_i/P_i$) for each of the 12 months represents the fraction of precipitation which enters the groundwater system in the i^{th} month; it is generally assumed to be the same each year. The record of C_{in} values, calculated for each year prior to the latest sampling date, represents the input function. For the interpretation of old tritium data, the record of C_{in} should include the constant C_{in} values prior to the beginning of the rise in 1954. In other cases, the calculation of the input function can be started in 1954. In most applications, it is assumed that the infiltration coefficient (α_i) in the summer months (α_s) of each year bears a constant

relationship to the infiltration coefficient in the winter months (α_w); this relationship is given by the infiltration constant ($\alpha = \alpha_s/\alpha_w$). Introducing α into Equation (5.130) results in (Grabczak *et al.*, 1984):

$$C_{in} = \frac{\alpha \sum_{i=4}^9 (C_i P_i)_s + \sum_{i=10}^3 (C_i P_i)_w}{\alpha \sum_{i=4}^9 (P_i)_s + \sum_{i=10}^3 (P_i)_w} \quad (5.131)$$

In the northern hemisphere, the summer months are from April to September (the fourth to the ninth month) and the winter months are from October to March (the tenth to the third month of the next calendar year). The monthly precipitation should be taken from the meteorological station and the tritium data should be taken from the nearest station of the IAEA network. However, for moderate and humid tropical climates, the α coefficient is usually within the range of 0.4–0.8, and experience shows that within this range the accuracy of modelling depends only slightly on the assumed α value, provided that the system is more than 10–20 years old.

In general, if the input function is not found independently, the α coefficient is either chosen arbitrarily by the modeller or is taken to be another parameter to be estimated. It is a common mistake to calculate the input function (5.131) assuming $\alpha = 0$ on the basis of conventional hydrological observations, which indicate the lack of net recharge in some areas during summer months, because it does not mean the lack of the summer tritium in recharging water.

Figure 5.29 (left) shows the tritium input function calculated for the Schneesalpe karst catchment. The Schneesalpe karst massif (Maloszewski *et al.*, 2002), of Triassic limestone and dolomites and with altitudes of up to 1800 m a.s.l., is located 100 km south-west of Vienna, in the northern Calcareous Alps. The aquifer there, underlain by impermeable strata, has a thickness of up to 900 m and is the main drinking water resource for Vienna. The mean precipitation is 1058 mm per year; the mean

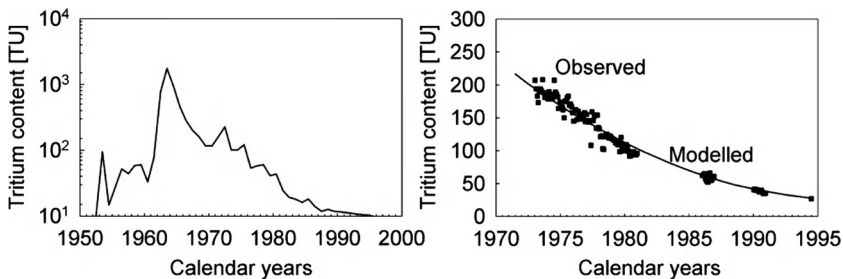


Figure 5.29 Tritium input function (left) calculated for the karst catchment of the Schneesalpe Massif (100 km SW of Vienna) and (right) the modelled tritium content (output function) for the spring at Wasseralm ($Q = 200$ l/s), calculated using the DM ($T = 26$ a, $P_0 = 0.8$, $\alpha = 0.4$) (after Maloszewski *et al.*, 2002).

evaporation is about 374 mm per year. The catchment area, about 23 km² in size (=F), is drained by two springs, the Wasseralmquelle and the Siebenquellen, situated on the northeastern and southwestern sides of the massif, respectively. The springs have mean discharge rates of about 200 and 310 l/s, respectively. The tritium concentrations during the base-flow were measured for nearly 25 years (1970–1995). The modelling of those data using the dispersion lumped-parameter model (5.113, together with 5.117) yielded mean transit times $T = 26$ years and $T = 14$ years for Wasseralm and Siebenquellen springs, respectively. The best fit of the DM to the experimental data for the Wasseralm spring is shown in Figure 5.29 (right). The transit times combined with the corresponding discharge rates give the volume of water (5.112) in the whole porous-fissured karst massif system as $V = 255 \times 10^6 \text{ m}^3$. Taking into account the surface of the catchment area, this volume corresponds to the water equivalent of about $h_{\text{eq}} = V/F = 11 \text{ m}$.

5.4.5 Multi-cell approach and concluding remarks

Some other modelling approaches are also used for the interpretation of isotope data, for instance, the compartmental (multi-cell or mixing cell) model. That approach was introduced by Campana (1975), Przewłocki and Yurtsever (1974), Simpson and Duckstein (1976) and has been further developed by combining it with a lumped-parameter approach (Amin and Campana, 1996). The mixing-cell approach is well described in Campana, Harrington and Tezcan (2001). The compartmental model represents the groundwater system as a network of interconnected cells or compartments through which water and one or more dissolved constituents (tracers) are transported. Within a given cell, perfect (complete) mixing of the tracer is assumed to occur. Some models however, relax this constraint. The rates of flow of water and tracer between cells can be calculated by:

- 1) the use of a flow model that solves the partial differential equations of groundwater flow,
- 2) calibration with observed tracer data,
- 3) a flow algorithm based on linear or nonlinear reservoir theory, or
- 4) some combination of these preceding possibilities.

Each cell in the model represents a region of the hydrogeological system. These regions are distinguished from each other on the basis of their hydrogeological uniformity, the availability of data, the degree of resolution desired and constraints imposed by numerical solutions. Compartment (mixing-cell) models have been applied to groundwater flow systems by a number of investigators. They have been used to estimate aquifer properties and recharge boundary conditions (e.g. Adar and Neuman 1988; Adar *et al.*,

1988; Adar and Sorek, 1989; Fontes *et al.*, 1991), to determine groundwater ages and residence times (Campana, 1987; Campana and Simpson, 1984; Campana and Mahin, 1985; Kirk and Campana, 1990; Love *et al.*, 1994) and to analyse tracer data and delineate groundwater dynamics (Yurtsever and Payne, 1985). Other investigators have used them as transport models (Van Ommen, 1985; Rao and Hathaway, 1989). One pioneering approach has used a compartmental model to constrain a finite-difference regional groundwater flow model (Harrington *et al.*, 1999).

When there is an unidimensional arrangement of the cells, the method can be regarded as a less versatile version of the lumped-parameter approach. For a single cell, the method is equivalent to the EM; for a very large number of cells, it approaches the DM or even the PFM. When more complicated configurations are used (e.g. different cell volumes, two- and three-dimensional cell arrangements), the number of parameters to be fitted increases and unique solutions are not attainable. Therefore, multi-cell models can be regarded as a distributed-parameter approach with lumping. When interrelated tracer data distributed in time and space are available, multi-cell modelling is definitely advantageous over the lumped-parameter approach. Unfortunately, there are many cases in which a single ^3H determination, or the mean value of several samples taken over a short period of time, have been interpreted either with the aid of the EM or with the aid of the multi-cell approach. These are examples of incorrect interpretation.

As mentioned above, lumped-parameter models are particularly useful when insufficient data exist to justify the use of multi-cell models, multi-tracer multi-cell models (Adar, 1996), or numerical solutions of the transport equation. They are also very useful in preliminary investigations of little-known systems. In the case when only separate sampling sites exist (e.g. a spring, or a withdrawal well), then the use of the lumped parameter models is sufficiently justified. Some investigators express the opinion that in the era of numerical models, the use of a lumped-parameter approach is out of date. However, as mentioned by Zuber and Maloszewski (2001) this opinion is comparable with trying to kill a fly with a cannon; neither effective nor economic. Experience shows that a number of representative hydrologic parameters can be obtained from the lumped-parameter approach to the interpretation of environmental tracer data in a cheap and effective way.

In conclusion, when estimating the parameters of a system, it should always be remembered that the lower the number of parameters to be estimated, the more reliable the result of the modelling usually is (Himmelblau and Bischoff, 1968). A better fit obtained with a larger number of parameters does not necessarily mean that a better model has been found. A modelling exercise should always start with the simplest available model. More sophisticated models with additional parameters should be introduced only if it is not possible to obtain a good fit with a simple model, or if other information excludes a simpler model. It should also be remembered that if a single-parameter model yields a good fit, an infinite number of two-parameter models also yield equally good fits. Therefore, in such situations, other available information should be used for final selection of the most appropriate model.

5.5 The goodness-of-fit of a model

Generally, the goodness of a calculation (model calibration/fitting procedure) can be calculated using the model efficiency (E) defined by Hornberger, Mills and Herman (1992):

$$E = \left\{ 1 - \frac{\sum_{i=1}^N (C_f^i - C_{obs}^i)^2}{\sum_{i=1}^N (C_f^i - C_{mean})^2} \right\} \times 100\% \quad (5.132)$$

where

$$C_{mean} = \sum_{i=1}^N C_{obs}^i / N \quad (5.133)$$

C_f^i and C_{obs}^i are, respectively, the fitted and observed concentrations at the time t_i and N is the number of observations.

A model efficiency $E = 100\%$ indicates an ideal fit of the model to the concentrations observed, while $E = 0$ indicates that the model fits the data no better than a horizontal line through the mean concentration observed. Equation (5.132) is mainly useful for testing breakthrough curves in artificial tracer tests and the periodic output functions as it is, for example in the case of stable isotopes.

6

Technical Instructions

This methodological oriented chapter provides specific methods and techniques of tracerhydrology. The planning and execution of a tracer study and, in particular, of a tracer experiment is described. This chapter is especially important for the field hydrologist and practitioner, facing decisions on how to organize tracer studies and tracer experiments.

6.1 Planning and execution of a tracer study

The success of an integrated tracer study as well as an artificial tracer experiment depends very much on careful planning. Tracer studies and experiments are always carried out as part of a hydrological or a water resources investigation. A flowchart may facilitate the process of planning and executing an experiment (Figure 6.1). In addition to a good theoretical and practical knowledge of tracers, as provided in the previous chapters, planning is also crucial to the success of any tracer experiment. The outcome of a hydrological study including a tracer experiment is only as good as the quality of the planning that went into it. The planning of any such experiment includes both the detailed planning of the tracer experiment itself, and the preliminary gathering and evaluation of the hydrological data and data regarding the pertinent boundary conditions. It is good practice to specify the necessary conditions explicitly (e.g. sufficient rainfall before the experiment) and to observe them. The sampling of water for artificial and environmental tracer studies may require significant manpower during the experiment and for days, weeks and months after. Good planning and coordination are important in order to be able to manage these efforts successfully.

The concept of a tracer study (Chapter 2) is understood as a hydrological study using any kind of hydrological tracers. A tracer study applying artificial tracers exclusively, which is the most efficient and the best-practice approach appropriate to the specific purpose of the investigation is called a tracer experiment. However, in general the combined use of all of the tracers adequate for the subject of the research is appropriate. Provided that enough time is available for sample collection and analysis prior to

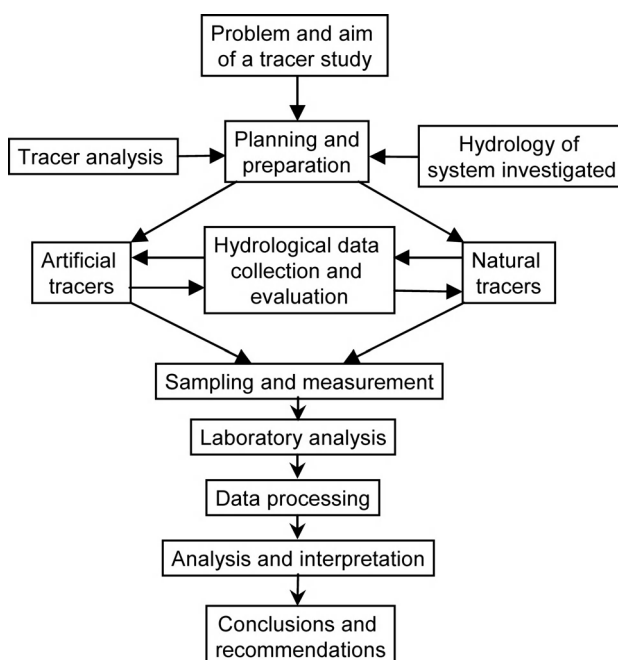


Figure 6.1 Flowchart illustrating the planning and execution of a tracer study and a tracer experiment.

a tracer experiment, it is often helpful to use environmental tracers to first gain an understanding of the system and the dominant processes.

Firstly, a clear idea of the aims of the experiment (e.g. delineation of protection zones) and of the influencing factors is fundamental. A major tracer study programme (master plan) must be established in advance, in order to minimize problems and inconsistencies. Included in this master plan is a map of the area indicating the experimental sites, a detailed schedule for the experiment, the names of the responsible persons and so on. It might be necessary to inform the owners of land and water bodies affected by the experiment. This plan can also serve as a basis for the cost analysis. The risks and possible reasons for failure should be considered in advance. It is recommended that a risk management procedure be put in place. This includes a back-up plan in case the experiment fails (before it fails).

6.1.1 Data collection and evaluation, field reconnaissance and mapping

All of the available general hydrological data pertaining to the study area are very useful for both the preparation and the interpretation of the results of a tracer experiment. Additional investigations carried out in preparation of tracer experiments should aim to provide an overview of the hydrological characteristics of the object of the research



Figure 6.2 Sampling to assess the levels of environmental tracers and to determine the background concentrations of the artificial tracers to be used.

and to identify difficulties and potential problems. This includes, for instance, clarifying whether there have been anthropogenic hydrological measures that might have major consequences for the interpretation of the results. Finally, the most appropriate sites for injection and sampling must be identified in the field and marked clearly. Without a good idea of the flow rates and water volumes (spring discharge, stream runoff, etc.), it is not possible to determine the adequate tracer injection mass. If not already available, basic hydrochemical parameters need to be acquired (Figure 6.2). The focus is not on a detailed analysis of these data, but on obtaining general information concerning the hydrochemical situation, the background concentrations in the system of the tracers being considered for use and the identification of abnormalities. When choosing certain tracers it is necessary to check, for example, the pH conditions in order to determine their suitability. All of these parameters must be sampled over a period that is long enough to cover possible temporal variation.

6.1.2 Choice of tracers and estimation of tracer mass

Part of the planning process is the proper justification of the choice of tracer with regard to multiple criteria central to tracer selection, as described in Chapters 3 and 4. One should also be aware of the different names of the artificial tracers available on the market (cf. Chapter 4).

The estimation of the necessary tracer mass must be made with great care, as it will affect all subsequent steps. The calculation of the injection amount must be described quantitatively and health and environmental risks must be minimized. The methods and further necessary information are provided in Section 6.2. A correct calculation of tracer mass is essential for the success of an experiment. Concentrations which are too high may impact upon drinking water supplies and ecosystems, whereas an underestimation may result in the failure of the experiment, and possible misinterpretation of the actual

situation. A second (alternative) tracer mass calculation is recommended, therefore, in order to verify the result of the first calculation.

6.1.3 Planning of studies and experiment execution in detail – creation of a schedule

The detailed planning of the specific study and of the experiment has to be done very thoroughly and usually results in a recorded schedule providing clear instructions for all those involved in the experiment. An expected tracer breakthrough curve indicating maximum concentrations based on the determined tracer mass is required for the optimization of the sampling design.

There should be the establishment of a sampling concept, with precise information concerning the sampling duration and frequencies (the sampling frequency is generally highest at the beginning of the expected tracer breakthrough and declines with time). The intervals and the required minimum duration of the sampling process should be estimated as precisely as possible in order to keep costs under control. The sampling intervals are determined by the characteristic breakthrough times in the investigated areas. An overly long sampling interval may have drastic effects upon the registration of the tracer breakthrough curve, as presented in Figure 6.3. In the example, the longer sampling interval lead to incorrect flow and transport parameters.

On site measurements to monitor the tracer breakthroughs are an elegant solution provided that the individual tracers to be measured as part of multi-tracer experiments can be isolated from the tracer mix in the sample. It is highly recommended that a few samples are extracted in case a validation of the findings is necessary.

No plan or schedule can be maintained if the necessary materials are missing. Great care must be taken, therefore, to ensure that all of the required materials are on hand at the specific experimental sites in time. Those responsible for the provision and preparation of the materials (such as sampling bottles, tracer substance, sample labels, instruments, protocol forms, etc.) should already have been identified at the planning stage.

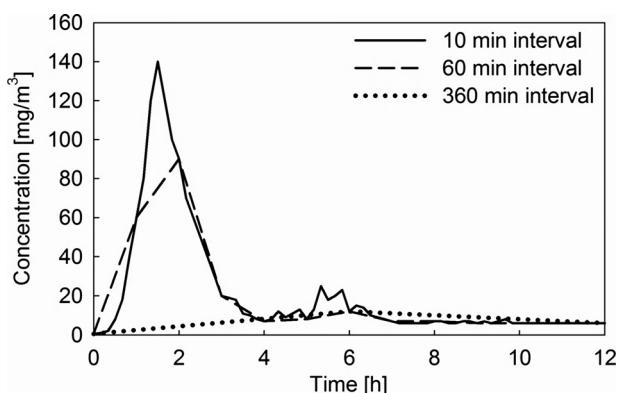


Figure 6.3 Influence of sampling interval on the shape of the observed tracer breakthrough curve.

It goes without saying that sufficient reliable and well-instructed personnel must be on hand to guarantee the professional execution of the experiment. The planning of the personnel requirements is particularly important in experiments with a longer duration.

6.1.4 Risk management

The potential risks, and the means to handle them should they occur, must be specified before the experiment begins. In general, experiments in or close to areas relevant for water supply are especially sensitive. A back-up water supply strategy should be agreed upon and prepared in case of contamination. Sometimes it is sufficient to store additional water. In other cases it might be reasonable to prepare a back-up chlorination unit to remove colouring caused by fluorescent dyes.

All of the people in the area under investigation need to be listed, whether they are involved directly in the experiment or are affected landowners (farmers). In most cases it will be necessary to inform the police, the relevant environmental authorities and health departments before the experiment commences. Environmental and health bodies need to be informed for obvious reasons; they must approve the experiment and verify that it is being carried out in accordance with existing laws and regulations. They will also check whether the experiment breaches the rights of any individuals or entities in any way. Informing the police and local stakeholders is important in order to avoid any potential negative reaction and possible interference during the experiment, or at least to allow for preparations to be made should any such reaction occur. Through information, public concerns in relation to environmental hazards and impacts upon ecosystems can be reduced or allayed altogether.

6.1.5 Consultation with authorities and formal application (legal process)

In addition to the possession of the necessary theoretical and practical scientific knowledge of tracers described in the previous chapters, planning and prior consultation with authorities are also mandatory. The legal modalities vary from country to country, but certain basic considerations are always necessary and should be included in the formal request for official permission to conduct a tracer experiment. Any alteration of the physical and chemical properties of the hydrological system under investigation should be minimized. A tracer experiment is considered to be an exceptional case, and therefore requires justification and careful planning. A formal request must address federal and/or state laws, and should correspond directly to the existing legislation. Accordingly, a formal application will generally include:

- the characteristics of the injection and sampling sites, including logistical considerations such as access (keys, permits, etc.);
- the necessary materials (tracer amount, bucket, funnel, tube, water for injection and/or flushing, water truck, keys for site access and to open wells, tools, instruments,

the number and material of sampling bottles, water proof labelling pens, boxes, instructions, paperwork);

- the expected tracer breakthrough curve and the maximum concentrations, and the corresponding sampling intervals;
- the sampling concept;
- the methods of analysis and interpretation;
- the potential risks and the contingency plans.

6.1.6 Practical suggestions for experiment execution

The preparation of a tracer solution must take place outside of the study catchment area. Those involved in injection should be excluded from subsequent sampling and analyses procedures. 'Contamination' can render an entire tracer experiment useless and must, therefore, be avoided at all costs. To prevent any contamination that could potentially affect sensitive areas within the research site, all personnel must wear protective clothing and the site must be carefully prepared (Figures 6.4 and 6.5).

The predefined *sampling* concept will generally envisage a higher sampling frequency at the beginning of the expected tracer breakthrough, and a decline with time. If possible, on site analysis techniques can be applied directly in order to facilitate a flexible reaction where necessary, and to optimize the sampling frequency in accordance with the real conditions influencing the tracer experiment. Automatic samplers are usually helpful as a means of obtaining an adequate determination of the breakthrough, and are perhaps even indispensable. Manual sampling requires that the timing be as exact as possible. Proper and consistent documentation of the experiment (at all experimental sites) is crucial to the success of the experiment and to the reliability of the results.



Figure 6.4 Preparation of a concentrated fluorescence tracer solution and the required precautionary measures.



Figure 6.5 Injection of a tracer into a well by means of a pump and a hose.

Samples should be taken in brown glass bottles or, if using plastic, in polyethylene or polysulfone bottles. As the chemical compositions of plastic bottles differ, it is recommended that the effects on sorption on all of the bottles be tested.

6.1.7 Requirements for an adequate groundwater sampling

Sampling within a groundwater system implies a mixing of groundwater samples. The geometry of aquifers, the distribution of aquifer depth, porosity and hydraulic conductivity and the extent, shape and distance of recharge zones control the type of mixing in aquifers. In springs, the sampling and mixing of different flow paths occurs naturally by convergence at the spring outlet. For springs, it is important to know whether the full or just a part of the depth of the aquifer is drained by the spring. In the latter case, environmental tracer data are only representative for the recharge area from which flow paths lead to and converge at the spring.

In boreholes, groundwater mixing depends on borehole penetration and on the length and position of filters. The quantitative interpretation of environmental tracer data and the identification of lumped parameter models depend strongly on these factors. For further information see Section 5.4.2, while detailed discussions of these issues are also given in Fritz and Fontes (1986) and more recently in Cook and Herczeg (1999).

It is indispensable to know the aquifer depth and the location and depths of filters when working with groundwater samples. For the application of environmental tracers it is often adequate to use boreholes that fully penetrate the aquifer and that have a complete filter (see Section 5.1). Even if this is the case the pump is always located at a certain depth and care should be taken that the pumped and sampled water corresponds to the flux of groundwater. For observation boreholes especially, there needs to be sufficient time to flush groundwater fully in the borehole itself several (at least two to three) times.

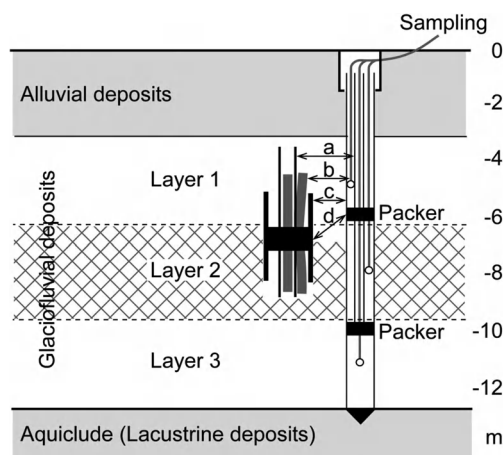


Figure 6.6 Sectional view of a sampling site in a multi layered aquifer and of a sampling system using packers with which each layer can be sampled individually.

Where depth-dependent sampling is intended, technical or hydrodynamic methods need to be used to sample groundwater at given depths. One method is the application of packers. The borehole is sealed above and below a sampling section by inflatable, extendable or even fixed vertical flow barriers. Samples are taken within (and if adequate, above and below) the packer. A series of packers may be used to provide a depth profile (Figure 6.6).

6.2 Estimation of tracer injection mass

The determination of the total tracer mass to be injected is the crucial point during the planning process of a tracer experiment. Principally, the considerations are always similar, but the specific boundary conditions are to be taken into account for each experiment. The basic idea is to trace an unknown water volume over an unknown time (travel time of tracer) to achieve an optimal tracer concentration (target concentration) at the measuring point. Thus, all parameters to be determined by the tracer experiment have to be pre-estimated. Success and failure of a tracer experiment depend strongly on a reliable estimation of the total tracer mass needed. Underestimating the tracer mass can result in misinterpretations, while the opposite, an overestimation, can lead to a much higher analytical effort as well as attracting unwanted attention. The target concentration should be as low as possible, due to environmental considerations, but high enough to provide a distinct signal beyond the range of uncertainty (Leibundgut and Wernli, 1982). Obviously, this boundary condition is dependent on the technical equipment available and the tracer used (see Chapter 4).

Since the beginnings of tracerhydrology many ideas formulated in equations have been developed to solve the problem of a reliable estimation. Field (2003) summarized more than 33 different approaches to the calculation of tracer masses. This summary is listed in Table 6.1 and may highlight the problem of tracer mass estimation. The decisive

Table 6.1 List of tracer mass equations (from Field, 2003).

| No. | Equation | Secondary reference | Primary Reference |
|-----|--|--|---|
| 1a | $M = 0.56 \left(\frac{Q C_p t_p}{1000} \right)^{0.91}$ | | Worthing, personal communication |
| 1b | $M = 0.56 \left(\frac{Q C_p L}{1000 v_p} \right)^{0.91}$ | | Worthing, personal communication |
| 2 | $M = 17 \left(\frac{Q C_p L}{3.6 \times 10^6} \right)^{0.93}$ | | Worthing, personal communication |
| 3 | $M = \frac{TC_1 L}{10}$ | Parriaux <i>et al.</i> (1988), p. 7 | UNESCO 1973–1983 |
| 4 | $M = T_{C_2} \left(\frac{QL}{8.64 \times 10^4 v} \right) + \frac{V}{5.0 \times 10^4}$ | Parriaux <i>et al.</i> (1988), p. 7 | UNESCO 1973–1983 |
| 5a | $M = \frac{T_{C_3} QL}{3600}$ | Parriaux <i>et al.</i> (1988), p. 7; Zötl (1974), p. 54; Käss (1998), p. 323 | Bendel (1948); Dienert (1913) |
| 5b | $M = \frac{T_{C_4} QL}{3600}$ | Milanovi (1981), p. 276 | Dienert ? ^b |
| 6 | $M = \frac{t_d C_p Q A_{d_1} s_f}{2000}$ | Parriaux <i>et al.</i> (1988), p. 8; Gaspar (1987), p. 49 | Leibundgut (1974); Leibundgut and Wernli (1982) |
| 7a | $M = \frac{bW[2L C_p + A_{d_2}(2L - W)]}{3731}$ | Parriaux <i>et al.</i> (1988), p. 8; Käss (1998), p. 326 | Leibundgut and Wernli (1982) |
| 7b | $M = \frac{bL\theta[2L C_p + A_{d_2}(2L - W)]}{2g}$ | Käss (1998), p. 325 | Leibundgut and Wernli (1982) |
| 8 | $M = \frac{QL}{3600}$ | Milanovi (1981), p. 276; Gaspar (1987), p. 49; Bögli (1980), p. 139 | Martel (1940) ^b ; Martel 1940 ^b ; Thuner, 1967 ^b |
| 9 | $M = \frac{T_{C_4} QL}{q}$ | Milanovi (1981), p. 276; Gaspar (1987), p. 49 | Guillard (1969) ^b ; Guillard (1969) ^b |
| 10 | $M = T_{C_5} L$ | Käss (1998), p. 325 | Siline-Bektchourine (1951) |
| 11 | $M = L T_{C_6} T_{C_7}$ | | Käss (1998), p. 327 |
| 12 | $M = L \left[\left(1 + \frac{Q}{1.8 \times 10^4} \right) + \frac{Q}{3600} \right]$ | Milanovi (1981), p. 276; Gaspar (1987), p. 49 | Stepinac (1969) ^b ; Stepinac (1969) ^b |
| 13 | $M = \left(\frac{Q^2 L}{3600 q} \right)$ | Gaspar (1987), p. 49 | Heys (1968) |
| 14 | $M = \frac{t_d Q P S_f}{8.64 \times 10^4}$ | | Gaspar (1987), p. 50 |
| 15 | $M = \frac{T_{M_1} Q}{3600}$ | Sweeting (1973), p. 228 | Jenko ? ^b |

(Continued)

Table 6.1 (Continued)

| No. | Equation | Secondary reference | Primary Reference |
|-----|---|------------------------------------|---|
| 16 | $M = \frac{T_{M_2} q}{3600}$ | Sweeting (1973), p. 228 | Jenko ? ^b |
| 17 | $M = \frac{QL}{40}$ | Davis <i>et al.</i> (1985), p. 101 | Drew and Smith (1969) |
| 18 | $M = \frac{C_p T_p QL}{2500v}$ | Aley and Fletcher (1976), p. 7 | Dunn (1968) |
| 19 | $M = 5.0Q$ | | Haas (1959) |
| 20 | $M = 9.5VL$ | | Haas (1959) |
| 21 | $M = \frac{QL}{366}$ | Aley and Fletcher (1976), p. 30 | Haas (1959) |
| 22 | $M = 1478 \sqrt{\frac{QL}{3.6 \times 10^6 v}}$ | | Aley and Fletcher (1976), p. 9 |
| 23 | $M = \frac{Q C_p t_p T_p}{3398}$ | | Rantz (1982), p. 237 |
| 24 | $M = \frac{Q C_p \bar{t}_p T_p}{747.23}$ | | Kilpatrick and Cobb (1985), p. 8 |
| 25 | $M = \frac{Q C_p T_p t_2}{1000}$ | | Rathbun (1979), p. 26; Rantz (1982), p. 236; Kilpatrick and Cobb (1985), p.17 |
| 26 | $M = \frac{Q C_p \bar{t}_p T_p}{498.15}$ | | Mull <i>et al.</i> (1988), p. 37 |
| 27 | $M = \frac{C_p T_p T_p}{2.94} \left(\frac{Q \bar{t}}{149.53} \right)^{0.94}$ | | Kilpatrick and Wilson (1989), p. 14 |
| 28 | $M = \frac{QL}{20}$ | | Käss (1998), p. 324 |
| 29 | $M = \frac{T_{M_3} L I A_{pp}}{1000}$ | | Alexander and Quinlan (1992), p. 19 |
| 30 | $M = S_m L$ | Käss (1998), p. 324 | Timeus (1926) ^b |
| 31 | $M = \frac{S_m V}{100}$ | Käss (1998), p. 324 | Timeus (1926) ^b |
| 32 | $M = \frac{V}{200}$ | | Kilpatrick (1993), p. 14 |
| 33 | $M_p = Q t_p P_h$ | Käss (1998), p. 327 | Kinnunen (1978) |

^aSome equations slightly modified for simplification and to allow consistency of units.^bPrimary reference not always properly identified or readily available. Secondary references do not always correctly reproduce the original equations.

quantities for mass estimates are the water volume (V_W) to be traced and the detection limit of the tracer. The basic ideas are explained clearly in Leibundgut and Wernli (1982). A robust and reliable method is proposed that was applied successfully by the authors in many tracer experiments. Generally, one can estimate the requested mass of tracer with the formula (5.39) given in Section 5.1.2 which can be written as follows:

$$M = 10 \times C_B \times V_W \quad (6.1)$$

where (V_W) is the water volume and C_B is the background concentration of the salt tracer or the detection limit for the radioactive tracer. While for the dye tracer C_B is equal to:

$$C_B = 0.01a \left[\frac{\mu g}{l} \right] \quad (6.2)$$

with (a) being a tracer dependent parameter according to its fluorescent intensity (see Chapter 4, Table 4.4):

- $a = 1$ for Uranine;
- $a = 3$ for Amidorhodamines;
- $a = 10$ for Eosine;
- $a = 5$ for Naphthionate; due to the high background of Naphthionate, a should be set to 20.

The volume of labelled water in the system (V_W) has to be estimated roughly depending on the type of experiment to be performed.

In the case of a *column experiment*:

$$V_W = \pi r^2 L n \quad (6.3)$$

where r and L are the radius and the length of the column, respectively, while n is the porosity of the material used in the experiment.

In the case of *combined pumping-tracer experiment* (monopole or dipole):

$$V_W = p \pi L^2 m n \quad (6.4)$$

where L is the distance between injection and pumping wells; m and n are the mean thickness and porosity of the aquifer, respectively; while $p = 1$ for monopole and $p = 3$ for dipole test.

In the case of a *field tracer experiment in the aquifer* being under natural flow conditions (test field):

$$V_W = 0.5 \times L^2 m n \quad (6.5)$$

where L is the flow distance between injection and the observation wells, while m and n are the thickness and the porosity of the aquifer, respectively.

In the case of a tracer experiment performed in the catchment area of a spring:

$$V_W = \pi L^2 m n \quad (6.6)$$

where L is the distance between injection well and the spring, while m and n are the thickness and the porosity of the aquifer, respectively.

In the case of a *tracer experiment in surface water* (discharge measurement) the volume of labelled water can be estimated from:

$$V_W = L \times A \quad (6.7)$$

where L is the flow distance between injection and detection sites and A is the mean cross-section of the stream (river).

The tracer mass estimation by formula (6.7) does not consider losses by photolytic decay or sorption. As both losses affect the targeted tracer breakthrough directly, formula (6.7) needs an additional term considering the experiment-specific conditions. Sorption and photolytic decay are specified in Chapter 4. Guideline values to estimate the loss term for sorption are given in Section 4.1.2.7.

Examples of estimations for different experimental sets:

1. Tracer experiment with Rhodamine in a semi-natural channel for the distance of $L = 1500$ m. The channel has a mean cross-section area $A = 10$ m²:
According to Equation (6.7) the labelled volume of water is equal to $V_W = 15 \times 10^6$ l, which, by applying Equations (6.1) and (6.2), yields the Rhodamine mass $M = 4.5$ g.
2. Monopole test in a gravel aquifer having the porosity of about $n = 0.25$. The distance between injection and pumping well is equal to $L = 50$ m, while the mean thickness of the water bearing layer is $m = 30$ m:
The labelled water volume is estimated with Equation (6.4) to be: $V_w = 58.9 \times 10^6$ l, which yields the required tracer mass (M) of about 6 g Uranine; 60 g Eosine or 120 g Naphthionate.
3. Field experiment under natural flow conditions for the distance of 150 m in the sandy aquifer having mean thickness of about $m = 30$ m and mean porosity of about $n = 0.33$:
The labelled volume of water estimated with Equation (6.5) is equal to $V_W = 111.38 \times 10^6$ l, which yields the required mass (M) of 11 g Uranine, 110 g of Eosine or 220 g of Naphthionate.

Another approach is to pre-model the system with a suitable model, for example dispersion model, where certain system parameters have to be assumed. These assumptions imply sources of errors that may lead to miscalculations. However, pre-modelling may also be used to validate the methods described above.

6.3 Gauging discharge

Discharge is certainly one of the most fundamental variables in river hydrology, as it stands in complex interaction. The tracer dilution method is widely used in order to determine discharge in small catchments, often in headwaters, and especially in poorly accessible regions. It is the only adequate technique for measuring discharge in *turbulent* rivers and springs where other techniques are not suitable. Consequently, in mountainous areas, the method is widely used. On the other hand, the technique is not suitable under non turbulent flow conditions due to insufficient mixing. Principles and practical instructions are given in Buchanan and Somers (1969), Kilpatrick and Cobb (1985), Spreafico and Gees (1997), Wernli (1996, 2003, 2007), Hodel (1992, 2009). Moore (2004a, b, 2005a, b) describes the procedure of stream flow measurement by the salt dilution method and its potential application in different kind of rivers.

6.3.1 Approach of dilution method

The approach of discharge measurement using artificial tracers (tracer dilution gauging) is based on the principle that the dilution of a known mass of tracer injected into the flow system is in proportion to discharge, if complete mixing of the tracer is ensured. The principle was discovered by a chemist in 1863. A known mass of Natriumchloride was injected into a pond. After mixing, the salt concentration was measured and the water volume was calculated.

For tracer dilution gauging, an artificial tracer is added to the surface water stream, and, after complete mixing, the concentration is measured downstream. The dilution is in proportion to the discharge. An indispensable prerequisite when applying the dilution method is a uniform, complete mixing of the tracer over the entire body of water at a cross-section of the measured watercourse in all three axes (Figure 6.7). Downstream of the point where full mixing is achieved, a measurement is possible at any point of the cross-section. Depending on the channel roughness, the required distance to achieve uniform mixing is considerably different. The correct estimation

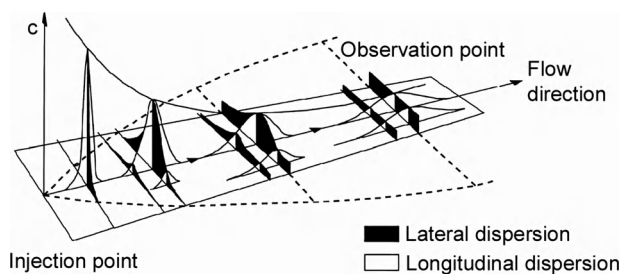


Figure 6.7 Schematic presentation of the mixing process after a tracer injection at an injection point. Vertical, lateral and longitudinal dispersion of concentration finally leads to complete mixing of the tracer over the whole cross section at observation point (after Hubbard *et al.*, 1982, modified).

of the distance requires some experience, which is the most valuable tool. Data from reference studies are only marginally helpful.

Formulae exist to estimate the minimum flow distances (Kilpatrick and Cobb, 1985; Hodel, 1993). In order to estimate the distances, it is assumed, in principle, that the higher the runoff, the longer the distance. Each meander of a river shortens the distance required. Furthermore, the higher the roughness of the rivers caused by coarse debris, the shorter the distance. As a general rule, the following distances can be taken as the minimum flow distance: for turbulent small channels approximately 50 m, for larger streams 200 m, and for rivers several kilometres. Within well-developed channels, such as the Upper Rhine, the distance increases to several tens of kilometres (cf. Section 7.3.1). However, often it is difficult or impossible to find an adequate river section without inflow and guaranteed complete mixing.

If there are outflow channels, notably after the tracer has reached complete mixing over the whole cross-section, the tracer concentration in the stream water does not change, thus the discharge measurement is not affected. Inflows, on the other hand, lead to a lower tracer concentration than before. However, this 'new discharge' can be measured if complete mixing of the total water is assured at the measured cross-section. Since the tracers are not all completely conservative, finding a mixing section which is as short as possible is recommended. However, even under very difficult conditions, solutions may be found. Take, for example, the gauging of the highly exposed karst spring 'Rin' in Switzerland (Rieg and Leibundgut, 1992).

Two methods with distinct technical differences are applied: the slug injection and the constant rate injection. The dry injection method (Moore, 2005a) is not recommended, since it is too difficult and risky to meet the required conditions of the dilution technique.

Sampling for background concentrations upstream of the injection site is required for both methods.

6.3.2 Slug injection (integration method, gulp injection)

A known mass of tracer (M) as concentrated solution is added in bulk into the system as a (quasi) instant impulse (mathematically handled as Dirac impulse). The tracer pulse spreads due to vertical, lateral and longitudinal dispersion as well as turbulent mixing (Figure 6.8). The longitudinal dispersion causes the 'typical' tracer breakthrough curve

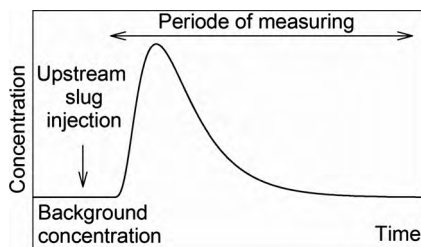


Figure 6.8 Schematic presentation of the tracer breakthrough curve after slug injection. At the downstream sampling point, after the mixing length, the tracer breakthrough curve is recorded.

(TBC) with a relatively steep increase from the background concentration to the peak, and a gradual decline (tailing) back to the background (Figure 6.8). Measurements and/or sampling are needed at the measuring cross-section during the entire passage of the tracer cloud downstream. Assuming 100% recovery of tracer at the sampling point (when there are no losses of the tracer mass, and the tracer breakthrough curve is measured until it reaches the background level (c_b)), the discharge (Q) can then be calculated as follows:

$$Q = \frac{M}{\int_0^{\infty} (c(t) - c_b) dt} \quad (6.8)$$

with M injected tracer mass (g)

$c(t)$ measured concentration at time, t
 c_b background concentration

The integral in Equation (6.8) is approximated commonly as summation and so Equation (6.8) results in:

$$Q = \frac{M}{\sum_i^N (c_i - c_b) \Delta t_i}; \quad i - \text{samples} \quad (6.9)$$

with c_i measured concentration at time, t_i
 $\Delta t_i = (t_{i+1} - t_i)$ time interval between two collected samples
 N amount of samples

Generally discharge (Q) can be calculated using Equations given in Section 5.3 where the influence of zones with stagnant water is also discussed. In addition to the estimation of the discharge (Q), the volume of water between injection and detection sites (V) can be found from the mean transit time of tracer, depending on the hydrological situation (see Figure 5.20 in Section 5.3).

Usually, the tracer is injected into the stream centre line. No special equipment for injection is needed when using the slug injection method provided that the tracer can be poured within the stream centre line, for example in small turbulent streams (Figure 6.9) or from a bridge in the case of wider streams. In the other cases, telescope stick equipment or grab sampler may be the solution.

Another approach, using fluorescent tracers with slug injection, is described by Wernli (2007). It consists of a pumping method in combination with a pocket fluorometer, whereby the entire measurement can be achieved by only one person. At the observation site stream water is pumped at a constant rate and over the whole tracer breakthrough into a bucket at the observation site, ensuring that the bucket always contains the mean concentration during the pumping time. After pumping, the concentration in the bucket is measured in situ by a pocket fluorometer. The cessation



Figure 6.9 Slug injection of a dye tracer into a turbulent flash flood of a small arid stream.

of pumping should occur when the tracer concentration converges to the background value. This can also be controlled with the pocket fluorometer.

6.3.3 Constant rate injection

The tracer solution is poured into the system at constant rate over a specific period of time (pulse injection with time duration of T_{pulse}). The quantity of solution and the tracer concentration have to be known exactly. A method that is used frequently is the application of a Mariotte bottle (Figure 6.10) in order to ensure a constant injection (Spreafico and Gees, 1997). Another possibility is the use of a precise peristaltic pump. Care should be taken to avoid solution residues from clogging or blocking the outlet pipe of the pump.



Figure 6.10 Constant rate tracer injection of a fluorescent tracer using a Mariotte bottle.

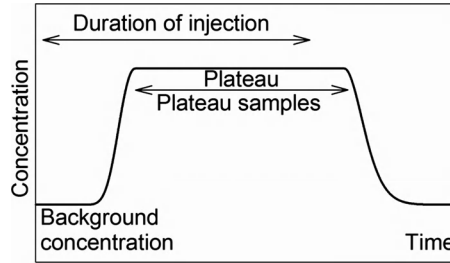


Figure 6.11 Schematic presentation of the tracer breakthrough after constant rate injection (e.g. via Mariotte bottle). At the downstream sampling point, the tracer concentration rises to a plateau value.

The resulting tracer breakthrough curve measured downstream arises typically from a background concentration to a constant value called the plateau concentration (Figure 6.11). Sampling is only permitted after the tracer has fully reached the constant plateau value at the end of the mixing section. One should remember that to obtain the plateau concentration downstream, the duration of pulse injection (T_{pulse}) has to be sufficiently long. The discharge is calculated as:

$$Q = \frac{q_{\text{in}} * (c_{\text{in}} - c_{\text{b}})}{(c_{\text{p}} - c_{\text{b}})} \quad (6.10)$$

with q_{in} tracer solution inflow rate (l/s)
 c_{in} tracer solution concentration (g/l)
 c_{p} measured sustained 'plateau' concentration (g/l)
 c_{b} background concentration (g/l)

Obviously, both techniques are characterized by specific advantages as well as problems. A short, comprehensive assessment is composed in Table 6.2. Although any good soluble chemical is a potential tracer for the dilution method, only the salt tracers (NaCl) and fluorescent tracers have been proven to be suitable, at least for operational purposes. When planning a dilution-gauging experiment several boundary conditions need to be considered. Table 6.2 provides a basis for decision making.

6.3.4 Requirements for tracers

Amongst the artificial tracers, two tracer groups, salts and fluorescent tracers, are commonly used. Theoretically, as mentioned above, all soluble artificial tracers are potentially suitable. However, for reasons of environmental protection, radioactive isotopes, for example, are no longer used in surface water. The salt tracer sodium chloride meets all of the requirements almost completely. However, a comparably high injection mass is necessary due to its high detection limit. As a general rule, 10 kg of sodium chloride per m^3 discharge are needed, depending on the background

Table 6.2 Comparative evaluation of the two measurement methods.

| | Advantage | Disadvantage |
|---------------------------------|---|---|
| <i>Using salt tracer</i> | | |
| Slug injection | <ul style="list-style-type: none"> – Short measuring time – Direct calculation in situ – May be also achieved with simple techniques – Rather cheap equipment | <ul style="list-style-type: none"> – Only small discharge measurable – High masses of tracer needed due to usually high background concentrations |
| Constant rate injection | not recommended for salt tracers | |
| <i>Using fluorescent tracer</i> | | |
| Slug injection | <ul style="list-style-type: none"> – High discharge measurable – Small amount of tracer – Short measuring time – High discharge measurable – High accuracy | <ul style="list-style-type: none"> – Accuracy may be affected by sorption effects on suspended load – Accuracy may be affected by sorption effects on suspended load – Analysis in the laboratory if no field fluorometer is available |
| Constant rate injection | <ul style="list-style-type: none"> – Validation possible by repeat sampling | <ul style="list-style-type: none"> – Photolytical decay of tracers – Long measuring time – More tracer needed – Higher effort required for preparation of experiment |

concentration. With fluorescent tracers, the injection mass is much smaller due to their very low detection limit (see Section 4.1.2.2).

The following should be considered when choosing a tracer for dilution discharge measurement. First of all, a tracer which does not undergo photolytic decay is required, since the solution to be measured is more or less completely exposed to daylight due to turbulence in rivers. Since all fluorescence tracers are at least slightly affected by the photolytic decay, the tracer experiment should be short (usually unproblematic) or scheduled for a night test using this type of tracer (cf. Section 7.3.1).

Furthermore, sorption into streambed materials should be negligibly low for the tracer used. Sorption leads to retention of the tracer cloud, thus the discharge estimation is incorrect. Finally, pH-independence, low detection limit and toxicological harmlessness are required. Detailed information concerning these characteristics is provided in Section 4.1.2.

The fluorescent tracer Amidorhodamine G (Sulforhodamine G) is the fluorescent tracer applied most often in dilution gauging. Other Rhodamines are also used. However, due to the strong sorption effects of the Rhodamines group, Uranine is used increasingly. Uranine may be used in short tests especially or in tests conducted at night in order to avoid photolytic decay. The background concentrations of fluorescent

tracers in most rivers are negligible. Hence, only small amounts of tracer are required, even for higher discharge, which is very convenient in contrast to salt tracers.

Robust portable fluorescent fibre optic fluorometers for in-situ measurement have been tested and described as useful and reliable (Hodel and Stoller, 2000, Hodel, Stoller and Diem, 2004). These instruments are operating according to the principle of a light conductor sensor. Through the light conductor, the emission signal enters the river water in the same way that the excitation signal arrives at the measuring instrument. The evaluated quantity is the intensity of the emission signal. As there is a linear correlation between fluorescence and the dye concentration, the fluorescence is used as measure for the dye concentrations.

Several sensors enable one to control the homogeneity of the mixing across the observation section. These instruments must be calibrated in the field, since only calibration with stream water results in an exact correlation between the measured signal and dye concentration. The calibration, as well as the measurement, has to be done with sufficient accuracy.

Calibration of the instruments with the river water to be measured is indispensable when using fluorescent tracers measured by in situ fluorometers. Hodel and Stoller (2000) describe the general linearity of the dependence between tracer concentration and fluorescent intensity of the water to be measured. Stream water is collected in a measuring cup, and the tracer concentration is increased gradually while the intensity of the fluorescence is measured. The background concentration, as well the whole calibration curve, needs to be specified correctly for any water to be measured.

6.3.5 Salt dilution technique

Sodium chloride was the first artificial tracer used in measuring discharge by dilution technique. Later, fluorescent tracers were substituted gradually for salt tracers (Fischer, 1982). However, new, advanced measurement sets, which allowed for an integrated simultaneous determination (measurement and calculation) of runoff, brought about a renaissance of the salt dilution technique. This was developed mainly to overcome two problems that arose frequently in field work: (i) often, runoff measurements had to be performed within a short time slot of optimal hydrological conditions by only one person and (ii) in wildlife areas, where some animals, such as bears, could be a threat to the people conducting the measurement. Again, a quick measurement providing calculated discharge data in situ is required for the plausibility and validation of the measurement.

The first salt measurement sets constructed in the late 1970s used microcomputers in combination with an electrical conductivity measuring instrument and independent electric power supply (Benischke and Harum, 1984; Leibundgut and Luder, 1986; Luder and Fritschi, 1990). A plotter prints the calculated tracer breakthrough directly after measuring. An integrated, magnetic tape recorder allows for the recording of all of the data on cassettes as the data storage medium.

Based on this principle, state-of-the-art measuring can be realized by complete solution systems with two sensors to record the tracer transit, which are stored in a

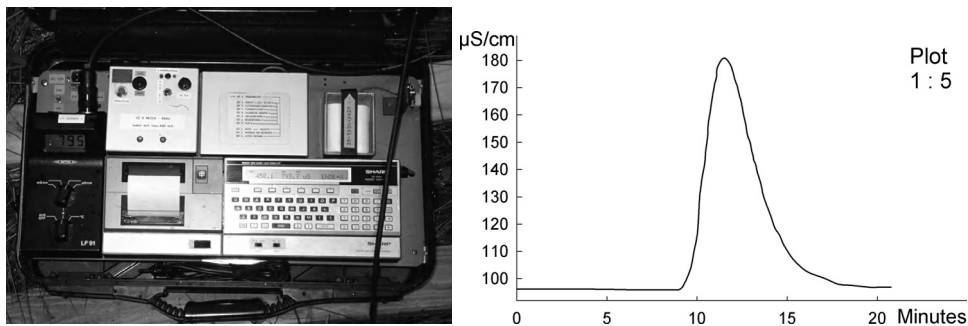


Figure 6.12 Measurement set for determining discharge by salt dilution based on electrical conductivity and a field computer with the plotted tracer breakthrough curve (right).

compact suitcase for transportation (Figure 6.12). The discharge is calculated directly and, with the two sensors, a plausibility check can be done directly. The calculation programme for slug injection is integrated.

The principle of the measurement is based on the relation between salt concentration and electrical conductivity, as there is a linear correlation between these parameters. Electrical conductivity, therefore, is a measure for the salt concentration in the water and can be measured easily. Natural electrical background conductivity, caused by the mineralization of the stream water, must be considered. Therefore, the required amounts of salts are usually relatively high in order to achieve a peak concentration which has an electrical conductivity of more than 100 $\mu\text{S}/\text{cm}$ above background. Therefore, under favourable measurement conditions, and a measuring duration of > 10 min, 30 $\mu\text{S}/\text{cm}$ is also acceptable. Calibration of the measuring instruments with stream water is essential in order to compensate for the natural background of the flow system and to consider the variability. The aim of the calibration is to estimate the specific correlation between salt concentration and the electrical conductivity of the water to be measured (Leibundgut and Luder, 1986; Hodel, 1992, 1993; Wernli, 2007).

6.3.6 Characteristic example of a tracer dilution gauging in a brook (slug injection)

The experiment was carried out in clear river water using Uranine. As expected, the background concentration (c_b) was zero, as Uranine is not part of chemical compositions of natural waters. The tracer breakthrough was sampled at constant time intervals of exactly $\Delta t = (t_{i+1} - t_i) = 20 \text{ s}$ and analysed in the laboratory (Figure 6.13).

The injected tracer mass was $M = 1 \text{ g}$ Uranine. Altogether 27 samples were taken. According to Equation (6.9), the discharge is calculated as follows:

$$Q = \frac{M}{\sum_i (c_i \times \Delta t)} = \frac{1000000 \mu\text{g}}{20\text{s} \times \sum_i c_i}$$

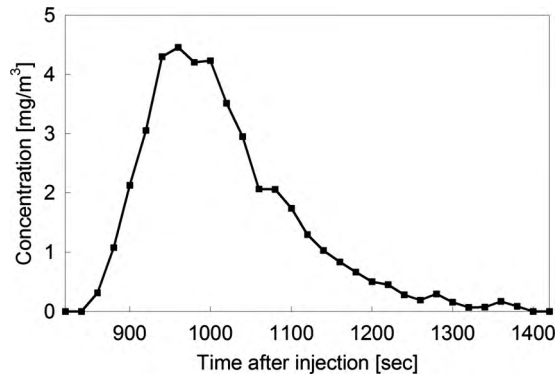


Figure 6.13 Observed tracer breakthrough curve for the gauging of a brook.

The sum of all products of measured concentrations ($\sum c_i \times \Delta t$) is $843.24 [\mu\text{g} \times \text{s/l}]$, which yields the discharge of:

$$Q = \frac{1000000 \mu\text{g}}{843.24 \mu\text{g/l/s}} = 1186 \text{ l/s} \approx 1.2 \text{ m}^3/\text{s}.$$

6.4 Chloride method for groundwater recharge estimation

The Chloride Mass-Balance Method (CMB) is used for estimating recharge fluxes in the saturated or unsaturated zone mainly in arid and semi-arid regions. The method is based on the mass balance of the chloride content of the input (precipitation) and the groundwater, respectively, in the vadose zone water. During evaporation the chloride concentration increases and this increase is a proxy of evaporation that is in inverse proportion to recharge, if a set of basic assumptions is met. The method is more precise with an increasing evaporation rate. The CMB was applied initially by Eriksson and Khunakasem (1969) to estimate groundwater recharge. Allison and Hughes (1978) were among the first to use the method in the unsaturated zone. The CMB covers only vertical flow processes and is limited in its applicability by the requirements of the method. Detailed descriptions of the method and the requirements that have to be met are given in the literature cited above and in reviews by Wood and Sanford (1995) and Wood (1999).

It must be assumed that:

- Only direct recharge takes place. That is recharge resulting from direct infiltration of precipitation without intermediate runoff generation.
- No additional internal source or lateral inflow of chloride exists.
- Chloride concentration in groundwater or in the vadose zone water experiences no increase or decrease by dissolution, plant uptake or other sink term.
- Precipitation amount and chloride concentration in precipitation are not correlated.

In this case the simplest form of the equation can be written as:

$$\bar{R} \approx \frac{\bar{P}^* \overline{Cl_{WP}}}{\overline{Cl_{GW}}} \quad (6.11)$$

where

R – recharge [mm/a]

P – Precipitation [mm/a]

Cl_{WP} – Weighted chloride concentration in wet and dry precipitation [mg/L]

Cl_{GW} – Chloride concentration in groundwater [mg/L]

Cl_{WP} – is calculated according to:

$$Cl_{WP} = \frac{\sum_i P_i^* Cl_i}{\sum_i P_i} \quad (6.12)$$

in order to use the average rainfall, the average recharge and the average chloride concentration, the correlation product $\Delta P^* \Delta Cl_{WP}$ needs to be close to zero.

In the following example (Wachtler, 2006), direct recharge from precipitation was determined with the soil water chloride balance and with the groundwater chloride balance method for the Buffelsriver catchment in South Africa. The chloride content in rainfall in the Buffelsriver catchment has been investigated in Adams, Titus and Xu (2004) and the weighted average of chloride concentrations of 2.4 mg/mm taken in that study is used as input concentration. The long-term average annual precipitation at each borehole site is taken from the mean annual precipitation grid of Dent, Lynch and Schulze (1989).

Soil profiles were dug in the catchment at sites characterized by different soil types. The soil water profiles 1–4 represent sites with different soil cover and vegetation (Figure 6.14, Table 6.3). At all of the profile sites soil samples at different depths were taken. Samples were weighed in the field on an electric weighing scale, with an accuracy of 0.1 g for about 250 g. After transport, the samples were weighed again in the laboratory, ensuring that no loss of moisture had occurred and that no material was lost from the bags. The samples were then dried at 105 °C for 24 h and weighed. After weighing the dried samples for water content calculation, 20 g of the samples were eluted with 200 ml deionized water for 24 h. The water-soil mixture was then filtered through a 0.45 µm filter. The filtrate was then analysed for chloride, nitrate and sulfate with an ion chromatograph. The density of each sample is calculated by measured wet weight divided by the defined volume of each sample. The absolute weight of the water content is calculated from the measured wet weight minus the measured dry weight, the absolute volumetric water content is then calculated as the product of the absolute weight of the water content and the density of water. The percentage volume water content is then the absolute volumetric water content divided by the volume of the sample. The results from the ion chromatograph are concentrations given in mg/L. As for elution, only 200 ml are taken to dissolve the chloride in 20 g of the soil sample; the concentrations are divided by five to get the mass of chloride per litre. The chloride mass of the

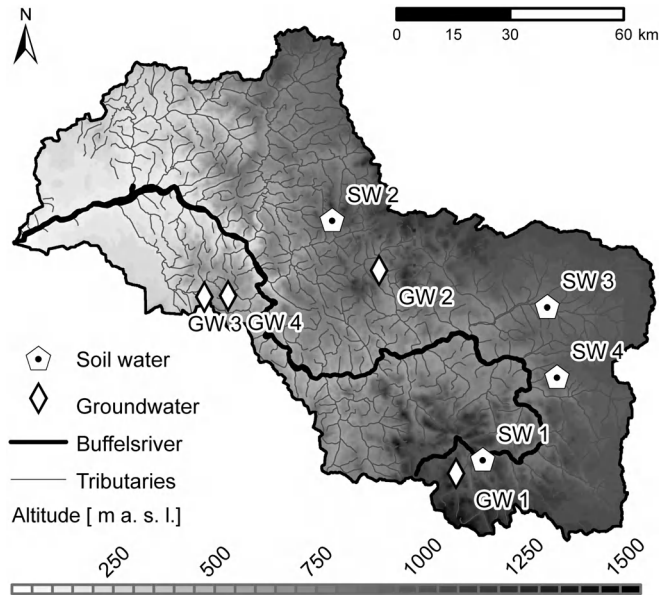


Figure 6.14 Buffelsriver catchment in South Africa with sampling sites of soil- and groundwater.

entire sample is then calculated to get the final concentration of chloride in the water contained in the soil sample.

In Table 6.3, the borehole positions, distance from the sea, water levels, chloride concentrations of the groundwater, the annual rainfall amount at the borehole sites and the calculated recharge rates are given. Rainfall amounts were derived from a regional map of mean annual recharge and correspond to the local rainfall conditions at the sampling site.

Table 6.3 Sampling site characteristics and groundwater recharge estimates for different sites.

| Sampling site | Sampling depth [m] | P [mm/a] | Cl_{wp} [mg/L] | Cl_{GW} [mg/L] | R [mm/a] |
|--------------------|--------------------|------------|------------------|------------------|------------|
| <i>Groundwater</i> | | | | | |
| GW1 | 11 | 231 | 2.42 | 114 | 4.9 |
| GW2 | 15 | 160 | 2.42 | 533 | 0.7 |
| GW3 | 26 | 135 | 2.42 | 317 | 1.0 |
| GW4 | 36 | 131 | 2.42 | 243 | 1.3 |
| <i>Soil water</i> | | | | | |
| SW1 | 0.195 | 180 | 2.42 | 331.51 | 2.4 |
| SW2 | 0.52 | 210 | 2.42 | 408 | 2.4 |
| SW3 | 0.575 | 110 | 2.42 | 904.97 | 0.3 |
| SW4 | 0.625 | 120 | 2.42 | 399.04 | 2.4 |

Groundwater recharge estimates by chloride concentrations from soil water ranged from 0.3 to 2.4 mm/a. If, instead of the average chloride concentration in soil water, the chloride concentration in groundwater is used, a recharge rate of 0.7 to 4.9 mm/a is obtained (Table 6.3). The sampling locations for the groundwater chloride method were chosen so as to be located in flat sandy areas close to the watershed or subbasin-watersheds where lateral subsurface flow could be minimized.

According to Bredenkamp *et al.* (1995) the chloride method is generally useful for estimating groundwater recharge in semiarid and arid regions, but only if a good spread of profiles over an area is obtained to depths of at least seven meters below the surface.

6.5 Hydrograph separation using the end member mixing analysis (EMMA)

Hydrograph separation is based on the assumption that water is composed of a set of well-mixed end members. These need to have distinct and independent isotopic or chemical signatures. Based on a known end member composition, different flow components can be separated. The mass balance equation for water and for water constituents is written and rearranged in order to get the flow rate or relative contribution of each end member. The details of this method are provided in Kendall and McDonnell (1998). In principle, this concept can be applied to two, three, or more end members. Due to error propagation and a limited availability of suitable, distinctly independent and conservative tracers for which the input function is known, it is applied mainly for two or three component separations. Here, an example is given to demonstrate how the most commonly used application – the separation of two temporal runoff components – works in practice.

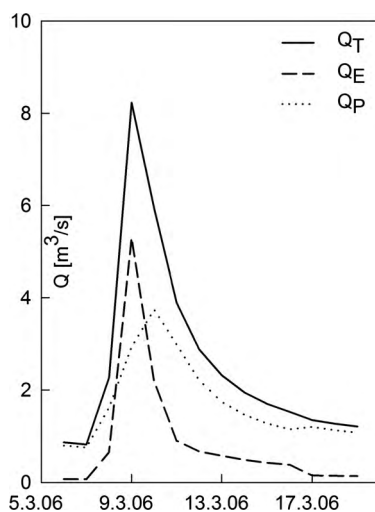
A separation of event and pre-event water is often used. This method is based on the assumption that a runoff event is composed of pre-event water with a stable isotopic composition and an event water, most often rainfall or, for example, snowmelt with an isotope composition sufficiently different from the pre-event signature. For both end members, their constant concentration needs to be known. Other applications can be devised for spatially distinct components related to known aquifers or storages, such as end members related to a fractured aquifer and to a shallow porous aquifer. Attention has to be paid to the fact that the spatial and temporal distributions of the tracers are often not well known. The initial concentrations cannot always be easily derived from available data. In the case of event and pre-event component separation, the transfer function from rainfall to channel inflow is not always sufficiently well defined by monitoring rainfall. Averaging of one or more components over time or space may result in significant errors. Recently, dispersion and systematic errors in conceptual models have also been discussed (see Renaud, Cloke and Weiler, 2007; Sudicky *et al.*, 2007). However, in spite of these issues, tracer-based separation of runoff components provides information on hydrological systems that is independent from modelling concepts and has played an important role in validating or rejecting modelling concepts (see Kirchner, 2003). Hydrograph separation tracers that are often used are deuterium and ^{18}O isotopes (e.g. Dinçer *et al.*, 1970; Sklash and Farvolden,

Table 6.4 Measured total discharge (Q_T) and isotope ratio (C_T) and calculated event (Q_E) and pre-event (Q_P) components.

| Date | Measured | | Calculated | |
|-----------|---------------------------|------------------|---------------------------|---------------------------|
| | Q_T [m ³ /s] | C_T [‰ V-SMOW] | Q_E [m ³ /s] | Q_P [m ³ /s] |
| 6/3/2006 | 0.87 | −9.78 | 0.05 | 0.82 |
| 7/3/2006 | 0.82 | −9.78 | 0.05 | 0.77 |
| 8/3/2006 | 2.27 | −10.07 | 0.60 | 1.67 |
| 9/3/2006 | 8.27 | −10.58 | 5.20 | 3.07 |
| 10/3/2006 | 5.93 | −10.19 | 2.08 | 3.85 |
| 11/3/2006 | 3.89 | −9.99 | 0.81 | 3.08 |
| 12/3/2006 | 2.88 | −9.99 | 0.60 | 2.28 |
| 13/3/2006 | 2.32 | −10.02 | 0.53 | 1.79 |
| 13/3/2006 | 1.95 | −10.02 | 0.45 | 1.50 |
| 15/3/2006 | 1.70 | −10.02 | 0.39 | 1.31 |
| 16/3/2006 | 1.53 | −10.02 | 0.35 | 1.18 |
| 17/3/2006 | 1.35 | −9.82 | 0.12 | 1.23 |
| 18/3/2006 | 1.27 | −9.82 | 0.11 | 1.16 |
| 19/3/2006 | 1.21 | −9.82 | 0.10 | 1.11 |

1979; McDonnell *et al.*, 1990), chloride (e.g. Neal *et al.*, 1988; Kirchner, 2003), radon-222 (e.g. Genereux, Hemond and Mulholland, 1993), and geochemical compounds that behave conservatively (e.g. Wels, Cornett and Lazerte, 1991; Uhlenbrook *et al.*, 2002).

The method has been demonstrated with ¹⁸O as a natural tracer to separate event and pre-event waters (Ehnes, 2006). These components do not correspond necessarily to spatial units such as aquifers. In the given example (Table 6.4 and Figure 6.15), the event

**Figure 6.15** Example for a hydrograph separation in event and pre-event water. Q = discharge and $C = \delta^{18}\text{O}$ content of E = Event water, P = Pre-event water.

occurred after a low water period during the wintertime in the Brugga catchment (Black Forest, Germany). The pre-event water concentration was defined as the concentration of the base-flow after a long low-flow period. The event water concentration was defined as the release of melt-water from a snow-pack of known isotopic composition. Fractionation processes for a slowly melting snow-pack and internal variability of the snow-cover have been described (Kuhn and Thurkauf, 1958; O'Neil, 1968; Craig and Hom, 1968; Suzuoki and Kumura, 1973). The isotope signature of the event water in this study, characterized by the isotopic composition of the mature snow-pack, showed little dependence on altitude. The total discharge, Q_T , and the isotopic composition of discharge were measured daily and every 8 h during the discharge peak.

Separation of total discharge in event and pre-event water: assumed event water input: $C_E = -11.1\text{‰}$, assumed pre-event water (after low-flow period): $C_P = -9.7\text{‰}$

$$Q_T = Q_E + Q_P \quad (6.13)$$

$$Q_T * C_T = Q_E * C_E + Q_P * C_P \quad (6.14)$$

$$\rightarrow Q_E = Q_T \frac{C_T - C_P}{C_E - C_P} \quad (6.15)$$

$$Q_P = Q_T - Q_E \quad (6.16)$$

The separation indicates that the event component (composed of melt water from the mature snowpack) and the pre-event component form two overlapping hydrographs with consecutive peaks. The event-component rises to more than 50%, corresponding to $5.3 \text{ m}^3/\text{s}$. The pre-event component, constituting initially all the discharge at the end of the low-flow period with temperatures below zero degrees, rises to about $3.9 \text{ m}^3/\text{s}$. The peak of the pre-event component is reached about a day after the peak of the event component. Within two weeks, the initial isotopic composition increases to the initial value, and the pre-event component dominates again. There are uncertainties in the concept and in the calculation. The average of the base-flow can be considered representative within 0.2‰ unless significant recharge takes place and modifies the initial end member concentration. This is unlikely, as after approximately 14 days the base-flow returns to the initial value. However, for a series of events or longer time periods this effect cannot be ignored. Then, the pre-event component should be sampled repeatedly. The highest uncertainty is related to the isotopic composition of the snow-melt component.

7

Case Studies

In the previous chapters this book has addressed different types of tracers, their characteristics, their potential application and the modelling of tracer data. The present chapter presents selected case studies of the use of artificial and natural tracers. The case studies are arranged according to the different components of the water cycle: groundwater, unsaturated zone, surface water, snow and glaciated areas. Finally, in a more integrated approach, examples of using tracers in catchment hydrology are given. Some of these case studies cover more than one component or relate to the interaction between two components, for example surface and groundwater. The tracer studies have also been selected in order to cover a range of different climatic conditions and geological settings. Although the selection of case studies must necessarily be incomplete and cannot cover the entire range of cases, this chapter tries to give an overview of major types of tracer applications in hydrology. The intention is to demonstrate tracer hydrology in practice through examples and to present the real problems that occur in such studies: that is the choice of tracer, the amount of artificial tracer applied, the injection method, the sampling protocol, data evaluation, modelling and interpretation, all of which have been discussed theoretically in the previous chapters. On these choices depends whether an application is successful or results in failure.

According to the concept of tracerhydrology as formulated in this book, an optimal experimental set-up uses a combined application of natural and artificial tracer. Not all of the case studies integrate artificial and environmental tracers. Some studies have been chosen because they present clearly an aspect of tracer application.

The cited references provide further reading on a certain issue. These reports are valuable as they give the benefit of experience of successful strategies and applications. The selection of references cannot be complete and cannot always represent a full selection of benchmark applications. However, in combination with the case studies they can be used as a practical guide. Thus, it is recommended that one reviews the available papers and reports related to the relevant chapter before putting a tracer experiment into practice.

Investigations of hydrological systems using tracer techniques are based on standard methods. Whereas tracer techniques for channel flow and groundwater investigation

are quite well developed, those related to other subsystems are still under development. A major part of any tracer experiment is practical knowledge. The application of tracers requires specific techniques for field procedures and for the evaluation of the data.

As described in the previous chapters, methods for conducting tracer experiments have been developed mainly for groundwater environments. In karst aquifers especially, many experiments have been carried out because of the obvious advantage of tracer applications. Later, artificial tracers were applied in porous aquifers. Based on this experience, applications for surface waters, in glaciers and snow, fissured rock, in soils and in the unsaturated zone were developed through the 1970s and 1980s (Leibundgut, 1995). Each hydrological subsystem has specific methodological peculiarities. Groundwater experiments, for example, need to deal with absorption while experiments in surface water need to take into account photolytic decay. A specific introduction to each group of case studies will address the specific issues of the application in different media.

Stable isotopes and dissolved gases have provided major input for the study of hydrological processes such as runoff generation, runoff component separation, recharge and groundwater flow and are still at the centre of defining conceptual models of hydrological processes (Sklash and Farvolden, 1979; Gonfiantini *et al.*, 1998; Solomon, Cook and Sanford, 1998; Kirchner, 2003). The application of isotopes for the study of evaporation processes (Fontes *et al.*, 1983; Gonfiantini, 1986) has become a valuable tool in studies on lake and surface water balances (Gibson, Prepas and McEachern, 2002). Recent developments have moved towards an integrated application of stable isotopes in catchment hydrology at different scales (McDonnell, Stewart and Owens, 1991) as well as component specific isotope analysis, especially in contaminant transport.

Comprehensive presentations of large combined tracerhydrological studies are given in the reports of the International Association of Tracers (ATH). The focus of investigation was mainly on groundwater systems but the approach was holistic within the respective river basins.¹ Recently the integrated tracerhydrological approach has been applied increasingly to catchment hydrology in order to investigate the water cycle and runoff generation in particular (Kendall and McDonnell, 1998; Leibundgut *et al.*, 2001; Leibundgut and Uhlenbrook, 2007).

7.1 Groundwater

The application of tracers in groundwater systems provides information on flow connections, on flow and transport mechanisms, and aquifer parameters (effective porosity, hydraulic conductivity, matrix and fissure porosities, etc.). The case studies presented here demonstrate selected applications and techniques related to the application of tracers in groundwater.

Tracer applications in groundwater comprise a very broad field of methods and techniques. Groundwater systems in karst areas have been studied extensively with

¹ Batsche *et al.* (1967, 1970), Gospodaric and Habic (1976), Müller and Zötl (1980), Leibundgut and Harum (1981), Bögli and Harum (1981), Morfis and Zojer (1986), ATH (1992), Kranjc (1997b).

artificial tracers and environmental isotopes (Criss *et al.*, 2007; Benischke, Goldscheider and Drew, 2007). It is difficult to derive and predict the groundwater flow connections of karst areas with methods other than tracers. The relevant references are listed in the introduction above.

Tracer methods have been applied successfully in porous and fissured aquifers (Leibundgut and Harum, 1981; De Carvalho-Dill *et al.*, 1992; Leibundgut *et al.*, 1992; Himmelsbach, Hötzl and Maloszewski, 1998; Maloszewski, Herrmann and Zuber, 1999; Herrmann *et al.*, 2001; Flynn *et al.*, 2006). As a rule of thumb, tracers are most commonly used in complex, remote and poorly known areas and for very slow or hardly predictable processes (Wernli and Leibundgut, 1993; Hötzl, 1991; Kosakowski, Berkowitz and Scher, 2000; Sinreich *et al.*, 2002; Maloszewski *et al.*, 2005; Einsiedl, Maloszewski and Stichler, 2005). Direct observation of interactions between karst and porous aquifers is impossible. Therefore, investigation by means of artificial and natural tracers (including modelling) is an adequate tool (Rieg *et al.*, 1993).

Tracer studies have contributed substantial information on the issue of *aquifer vulnerability*. As mentioned above, environmental tracers are used to study the entire system under investigation. In addition, artificial tracer experiments allow one to assess the dynamics of the fast conduit flow paths, which are crucial in the framework of vulnerability. The conduits, creating preferential flow, connect the most vulnerable areas, in particular within karst regions that are endangered by point source pollution (Leibundgut, 1984, 1998a, b; Rieg, 1994, 1995; Leibundgut *et al.*, 1995; Gunn *et al.*, 1998; Goldscheider, Hötzl and Kottke, 2001). A multilateral approach using natural and artificial tracers was applied by Herrmann *et al.* (2001) to assess the risk potentials of drinking water reservoirs in a fissured rock aquifer system. Three concepts of the vulnerability assessment of water resources using tracer methods are presented in Leibundgut (1998a): (i) hydroecological approach, (ii) intrinsic vulnerability approach and (iii) tracerhydrological approach. The concepts are presented in greater detail in the box at the end of the introduction.

For similar reasons, tracers play an important role in groundwater studies of arid and semiarid regions (Adar and Leibundgut, 1995; Külls *et al.*, 1995; Simmers, 1987; Lange and Leibundgut, 2003; Lange *et al.*, 2003). Large time scales involved in groundwater dynamics and the low intensity of recharge do not allow for efficient and meaningful direct monitoring. Therefore, environmental isotopes are often used for a first, and often the only feasible, general description of residence times or aquifer parameters. Groundwater systems are complex by nature. The validation of groundwater models and groundwater management plans requires adequate experimental data, for example for the delineation of wellhead protection zones. In karst aquifers vulnerable areas can be delineated (see colour plate section, Plate 3). The repeated application of artificial tracer experiments in karst areas provides a general picture of flow connections and can be summarized in vulnerability maps (Leibundgut, 1986, 1998a; Attinger, 1988; Rieg, 1995). In fractured aquifers, tracer studies have provided often unexpected and surprising data on spatial heterogeneity and flow velocities (Nativ *et al.*, 1992, 1995a, b; Bäumle *et al.*, 2001).

Environmental tracers can be applied in order to investigate tracer depth profiles at a given time, time series at given points (wells, streams, or springs) or the distribution

of environmental tracers along a flow path as a function of depth and of distance. Cook and Herczeg (2000) have pointed out the importance of understanding the physical principles of tracer movement and of the depth and longitudinal distribution of tracers when taking samples. How samples need to be taken so as to provide meaningful results depends, amongst other factors, on the specific groundwater system, the distribution of recharge and hydraulic conductivity and aquifer geometry. Analytical solutions for age profiles are given for different sets of boundary conditions.

Obviously, for both artificial and environmental tracer applications in groundwater, theoretical understanding and experimental setup or monitoring need to correspond closely. The application of adequate models helps to prepare a tracer experiment, the injection amount, the choice of adequate sampling boreholes and the estimation of the distance at which sampling will provide results within reasonable time. For environmental tracer studies a preliminary desk study or even modelling is also important in order to choose sampling points at the right distance and along expected flow paths and to decide whether a vertical, a horizontal or a combined distribution of samples is adequate.

Tracer injection into a single borehole (one-well test) and subsequent monitoring of the decline of tracer concentration in the same borehole is a rapid technique which will almost certainly provide results. It can therefore be combined with conventional tracer tests between boreholes. Additional techniques exist for the study of depth-dependent inflow to boreholes, flow direction and flow velocity in single boreholes.

Conventional multi-well artificial tracer tests and sampling in an aquifer are used to characterize the flow field between injection and sampling points during an experiment. For aquifer tests, the preparation of an injection point, and presaturation or flushing techniques are important. Decisions need to be made related to the timing of the experiment, preparation of trenches and pits, their depth, width and location, and the location and interval of sampling. Before an experiment or sampling is carried out, it is advisable to follow a scheme for the preparation of experiments based on the integration of different types of data on the groundwater flow system (cf. Section 6.1). Available hydrogeological and hydrodynamic information constraining groundwater flow needs to be reviewed first in order to identify major aquifers and hydraulic gradients that control the flow directions. It always needs to be kept in mind that groundwater systems are three-dimensional and that investigations only make sense within the same flow systems.

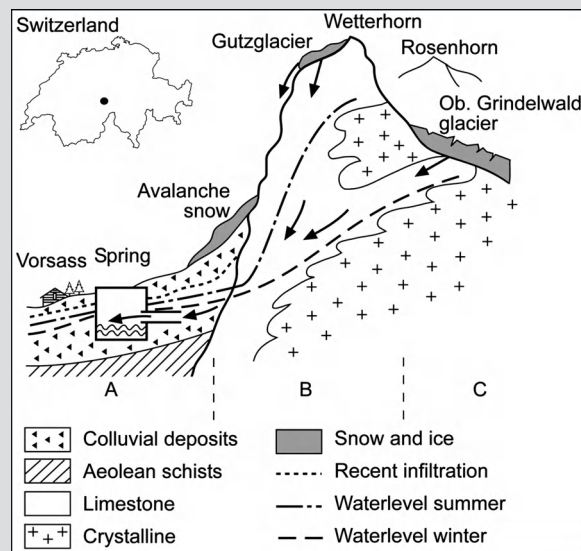
All available information on the geology and hydrogeology, on measured water levels and on the hydrochemistry of groundwater are needed for the design of tracer studies, sampling and modelling. It is important to identify aquifers and flow paths in order to choose the right locations for injection, sampling and in order to identify an adequate model for the interpretation of tracer data. Often, tracer experiments and environmental tracers will confirm the conceptual model and provide further, more detailed quantitative information on the hydrological system. On the other hand, tracers may modify and even refute some assumptions of the initial conceptual model.

Box 7.1 Assessment of Vulnerability of Groundwater Systems

A summary of each of the three approaches taken to evaluate vulnerability using tracer methods is given. With the presentation of the core steps of each method the user should be able to choose the one which is adequate for his purpose. Further information and literature are provided in Leibundgut (1998a).

The Ecohydrological Approach

The hydrological assessment follows the principle of convergence, as described in Chapter 2. All information from the entire catchment converges in the springs and must be disaggregated, in order to support conclusions concerning the system. Physical, chemical, biological and isotopic data can be monitored in the springs and will be interpreted with the help of geofactors such as geology and topography. Simultaneously, a conceptual model of the system structure of the catchment is established. Then the spatial information is combined with the point information at the springs (intrinsic vulnerability) resulting in a functional model of the karst system or even a mathematical model (see Box Figure 7.1)

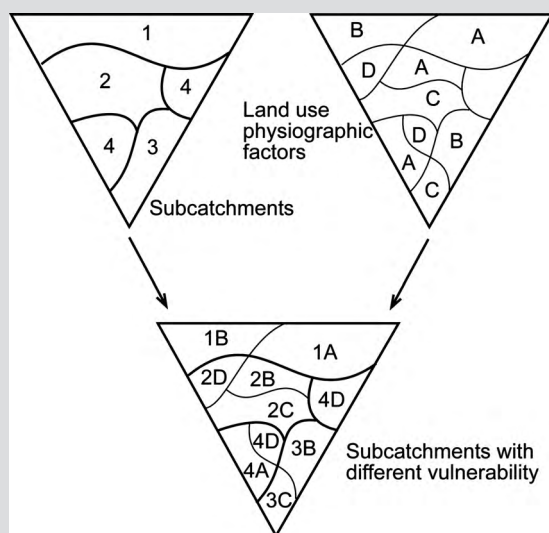


Box Figure 7.1 Conceptual model of a spring system with its catchment and subcatchments A, B, C.

The spatially differentiated evaluation of vulnerability can be assessed by an *overlay of spatial information*. The information from the hydrological investigation

(continued)

of subcatchments will be combined with the information on geofactors and land use (see Box Figure 7.2). Each resulting subsystem shows a characteristic response to a given input (specific vulnerability). The result is a set of subsystems with varying vulnerability, where adapted measures of protection can be planned. The example of the model of the spring illustrates the situation with three subcatchments A, B, C (see Box Figure 7.1).



Box Figure 7.2 Overlay of spatial information from Box Figure 7.1 and the assessment of the hydrological system characteristics by tracers.

The Intrinsic Vulnerability Approach

In the framework of a COST action 65, the vulnerability of karst aquifers in Europe has been investigated (further information is given by Hötzl (1995)). A distinction is made between intrinsic vulnerability associated with the aquifer system itself and specific vulnerability. Tracer hydrology provides methods for the investigation and characterization of intrinsic vulnerability, as summarized in Box Table 7.1 (cf. case study Section 7.1.2). The potential threats (specific vulnerability) for aquifers are imposed mainly by humans and are caused by infrastructural development, industrial activity, land use, aquifer overstress (e.g. pumping) and the long-term effects of air pollution.

Investigation methods in aquifers for the evaluation of intrinsic vulnerability using a multilateral approach including tracer techniques include the study of hydrodynamic parameters, water balance, origin assignment and modelling. In this context tracer techniques provide information on flow direction, velocity, residence times and transport parameters (e.g. dispersion).

Box Table 7.1 Investigation methods in karst for the evaluation of intrinsic vulnerability

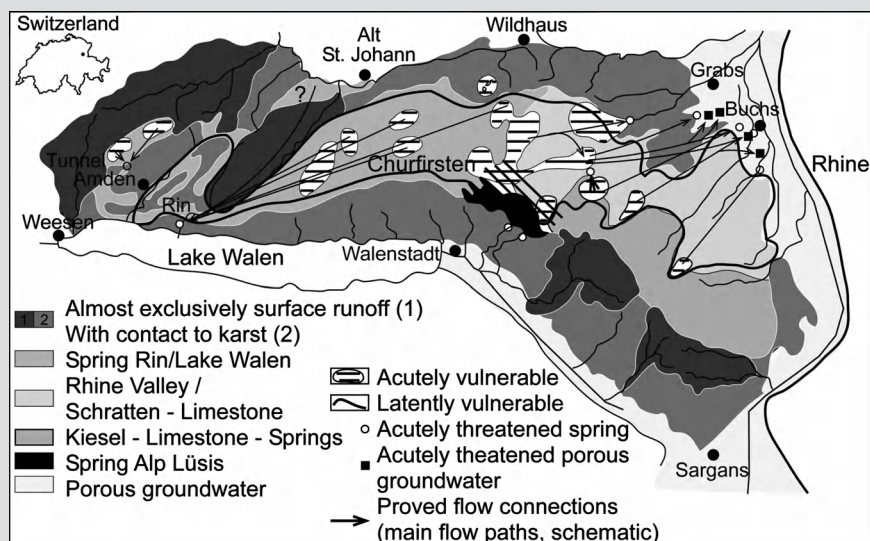
| Information on the karst medium: | | | | |
|---|---------------------------------|---|---|--------------------------------|
| Geology, geomorphology | | | Geophysics | |
| Structural and tectonic conditions, Hydraulically effective disturbance, Degree of karstification, Draining system | | | Spatial heterogeneities, Preferential flow paths, Draining system | |
| Information on the flow system and transport processes: | | | | |
| Hydrodynamics | Water balance | Hydrochemistry | <i>Tracer techniques</i> | Modelling |
| Hydrodynamic parameters, | Groundwater recharge, | Origin, | Flow direction | Flow and transport parameters, |
| Flow behaviour of the system | Available groundwater potential | Interactions with surrounding matrix, Mixing processes, Water quality | Flow velocity Residence times, Dispersion, Reaction parameters Determination of catchment | Calibration, Prediction |

Tracerhydrological Approach

The tracerhydrological approach is an assessment of intrinsic vulnerability. It will be determined by the extensive use of tracer methods. The approach follows the principles of convergence and conceptual system modelling of a catchment or aquifer, as discussed in Chapter 2. In fact, it is an integrated hydrological assessment comprising a complete hydrometric data collection and an extensive application of natural and artificial tracers. Of particular interest are the transfers of water between the single subcatchments which can be assessed by adequate mathematical modelling and the runoff generation processes.

The case of the Churfirten–Alvier study in the Swiss Alps provides an example where the vulnerability of a major karst aquifer system was studied using tracer techniques, mainly. As numerical modelling for a hydrodynamic characterization failed due to the complexity of the system, flow connections between springs and subcatchments had to be identified. A series of tracer experiments provided the base for the conceptual models and a list of flow connections based on which vulnerability zones and protection zones were identified and delineated (see colour plate section, Plate 3b–d). For each flow connection flow velocity and transport parameters could be assigned, as shown in Box Figure 7.3.

(continued)

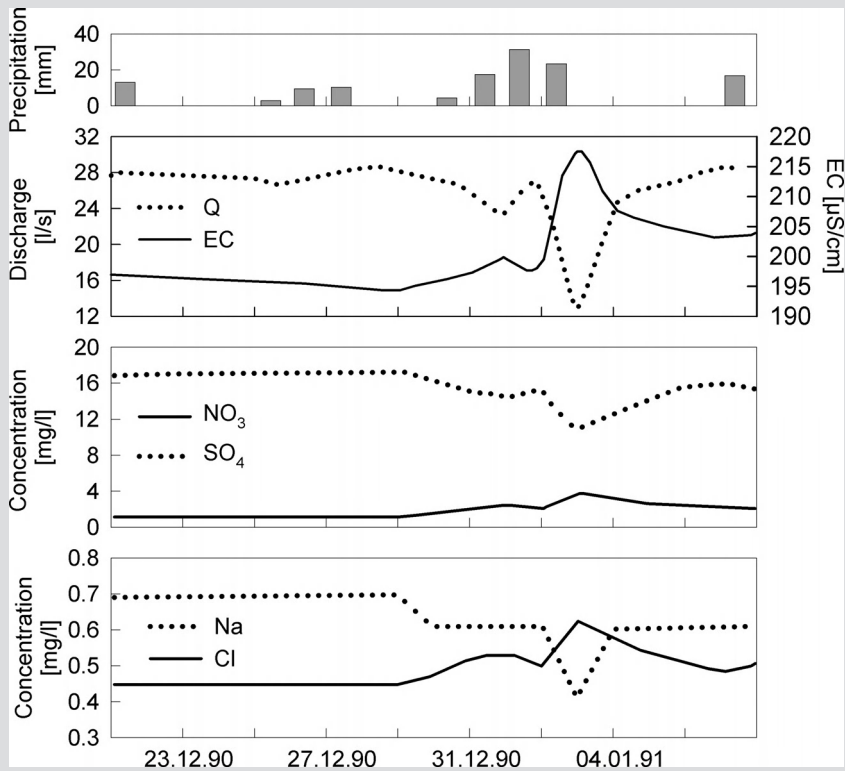


Box Figure 7.3 Vulnerability map of the Churfirsten-Alvier massif, Swiss Alps. Delineation of the catchments and vulnerable zones and the hydrological system function is strongly based on tracer methods (see colour plate section, Plates 3 and 4).

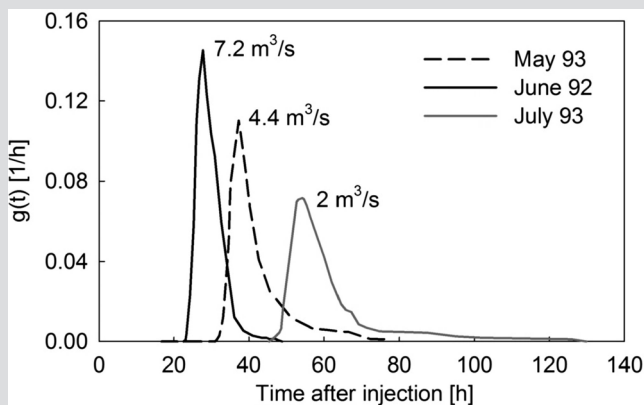
Monitoring of hydrochemical parameters in springs and of hydro-meteorologic conditions represents a first approach to the characterization of intrinsic vulnerability. Physico-chemical (pH, electric conductivity and temperature) and hydrochemical parameters (major ions) are important indicators for the quality and stability of shallow groundwater resources, especially spring catchments (Box Figure 7.4). The response of discharge and hydrochemistry to rainfall and runoff events can provide a framework for the type of system response. However, these observations are not conclusive without further artificial tracer tests or a quantitative evaluation of environmental tracer data based on adequate models.

An example of the results of one of these tests is provided in Box Figure 7.5. Tracer tests were repeated at different hydrological conditions (here spring discharge) in order to derive information on the variability of flow velocities for a specific flow connection. The use of tracer techniques in karst aquifers or in systems with complex hydrogeology may represent the only technique for providing empirical data.

The example of different system responses (Box Figure 7.5) shows that artificial tracer tests only represent hydrodynamic conditions during the experiment. In highly heterogeneous and dynamic systems only specific and extreme conditions might account for most of the vulnerability. Environmental tracer studies aiming at a characterization of residence times and of residence time distributions are needed in such cases.



Box Figure 7.4 Response of natural components (EC , SO_4^{2-}) that describe intrinsic vulnerability and anthropogenic components (NO_3^- , Cl^-) which are indicators of the specific vulnerability in a spring.



Box Figure 7.5 Breakthrough curves for a flow connection at three different system states characterized by different discharge conditions (source: Seifert, 1996).

7.1.1 Case study: 'Estimation of groundwater origin, residence times, and recharge of Chad Aquifers in Nigeria'

7.1.1.1 Introduction and aim

The case study is taken from Maduabuchi, Faye and Maloszewski (2006) and is representative of the Sahel zone and the semiarid climate in Central Africa. In this study, groundwater from the Quaternary and Continental Terminal Formations in the Nigeria sector of the *Chad Sedimentary Basin* (CSB) together with rain and surface waters were chemically and isotopically analysed in order to investigate the sources and ages of waters, possible modern renewal and mixing of the deep groundwaters, and to infer paleoclimate incidences.

This study, initiated in 2001, deals essentially with the investigation of the stable isotopes ^{18}O , ^2H and ^{13}C , and radioactive isotopes ^{14}C and ^3H , with less emphasis on chemical characteristics. The aim is to: (1) determine the chemical characteristics of the groundwaters; (2) investigate the origin and timing of recharge; (3) determine the relative residence times of the groundwater in the different layers (4) evaluate possible modern recharge and mixing of groundwaters.

7.1.1.2 Description of test site

The study area is located in the western part of the Chad Sedimentary Basin, which extends to Chad, Niger, Algeria, Libya, Sudan, Central Africa Republic and Cameroon (Figure 7.1). The basin is centred on Lake Chad, which is the main surface water body of the region. Inflow into the lake comes from the Chari Logone River (with its headwater located in the Central Africa Republic and Cameroon), the Komadugu-Yobi River and the Yedseram River (both located in Nigeria). These latter two rivers are ephemeral and account for about 10% of the total inflow to the lake. The surface elevation of the basin ranges from its highest point at 400 m a.m.s.l. to the lowest point, the Bodele Depression (located 300 km NE of the Lake), which lies more than 100 m below the lake level (281 m a.m.s.l.). The region has a continental, semiarid climate with a mean annual temperature of 30 °C, a low relative humidity (monthly averages ranging from 20 to 70%), a high potential evaporation exceeding 2000 mm/year and a mean annual precipitation of about 500 mm. The rainy season begins in May and ends in October, but 60% of the rainfall is concentrated in July and August.

7.1.1.3 Hydrogeology

The Chad Sedimentary Basin in the Nigeria sector shows the following depositional sequence from top to bottom: Quaternary, Early Pliocene, Continental Terminal, Gombe Sandstone, Fika Shale and Gongila, Yolde and Bima Sandstones Formations. The Bima Sandstone is the lateral equivalent of the regional Nubian Sandstone, which is the target aquifer unit in Niger, Chad, Sudan, Libya and Algeria. It is the deeper part of the aquifer

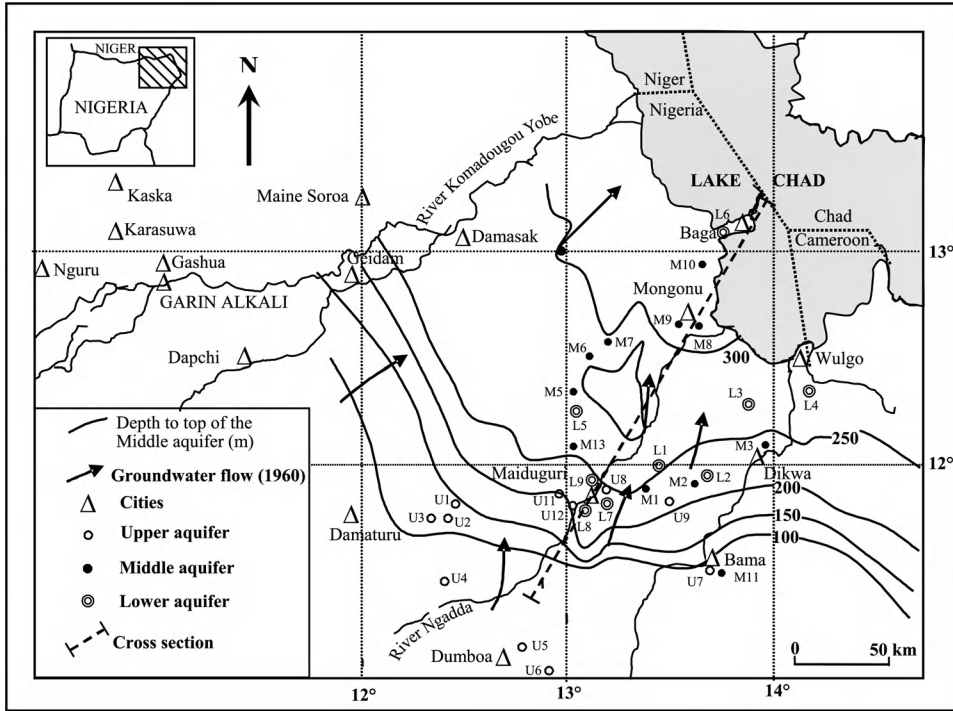


Figure 7.1 Study area location and sampling network.

series in the Nigeria sector of the basin. The thickness ranges from 300 to 2000 m and the depth between 2700 and 4600 m. The Plio-Pleistocene Chad Formation and the younger overlying Quaternary sediments are the main source of groundwater in the study area. Generally, in the Chad Sedimentary Basin, one can distinguish three water bearing layers, which are called the upper, middle and lower aquifer (see Figure 7.2).

The upper aquifer consists of Quaternary (lower Pleistocene) alluvial deposits of lake margin origin as well as alluvial fans or deltaic sediments that are related to sedimentation around Lake Chad. In many locations these sediments are covered by recent sand dunes. The transmissivity ranges from 0.6 to 8.3 m²/day. This aquifer is recharged from rainfall and runoff, and is mainly used for domestic water supply (hand dug wells and shallow boreholes), vegetable growing and livestock watering.

The middle aquifer is the most extensively encountered aquifer in the Nigeria sector of the Chad Sedimentary Basin. The average transmissivity is equal to 360 m²/day, while the hydraulic gradient is 0.015% (in the NE direction). The aquifer bears mineralized water comparable to the upper unit. About 70% of the wells are artesian (head pressure of up to 21 m above ground surface or the water table rises up to shallow depth due to pressure release). Abstraction from that aquifer is about 10⁶ m³/day, and free artesian discharge varies from 0.12 to 90 m³/h in some wells.

The lower aquifer consists of alternating Continental Terminal sands and clays. The transmissivity varies between 33 and 105 m²/day while the hydraulic gradient equals

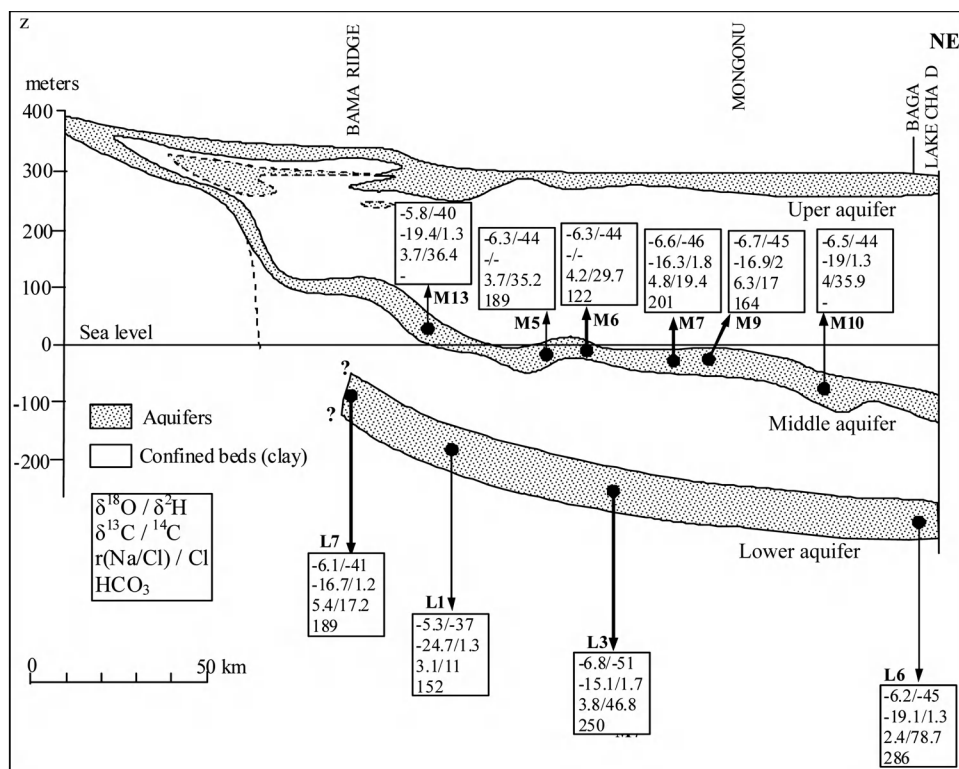


Figure 7.2 Hydrogeological layout, isotopic and chemical patterns along the axis Maiduguri-Chad Lake.

0.115% (in the N and NE direction). Free artesian flow varies from 7 to 17 m³/h, and the hydraulic heads may reach 3 to 6 m above the ground surface.

7.1.1.4 Methodology

In order to cover the sampling network in this large area, four campaigns were undertaken during 2001–2002. The network was comprised of 38 wells with 15, 14 and nine wells in the upper, middle and the lower aquifer, respectively (Figure 7.1). In addition to this network, 10 sampling wells were selected in the control zone (Figure 7.2) in order to compare data obtained from the individual layers. During the second sampling campaign, shallow groundwater from 47 dug wells (tapping the shallow aquifer), surface water from Lake Chad, rivers and Aludam reservoir, and rainwater from 28 storm events of the 2001 rainy season were sampled. Some of these wells were visited twice, and duplicate samples were collected for isotopes analyses. On site analysis included temperature, electrical conductivity (EC), total alkalinity (as HCO_3) by titration and pH. Filtered groundwater and surface water for chemical analyses were collected in 50 ml

bottles, and unfiltered samples for stable isotopes and tritium analyses were collected in one litre bottles, and then stored at 4 °C until samples were sent out for analyses.

Samples for ^{14}C analysis were taken by BaCO_3 precipitation, achieved by adding excess BaCl_2 to 100 l water previously brought to pH > 12 using NaOH. The major ions (Ca, Mg, K, Na, Cl, NO_3 and SO_4) were measured in filtered samples using a Dionex DX-100 Ion Chromatograph. An internal check on the quality of the chemical data was done by determining the ionic balance. Stable isotopes of oxygen and hydrogen were measured using mass spectrometry. The $\delta^{18}\text{O}$ values were measured via equilibration with CO_2 at 25 °C for 24 h, and $\delta^2\text{H}$ values were measured via reaction with Cr at 750 °C using an automatic Finnigan MAT H/device. Both $\delta^{18}\text{O}$ and $\delta^2\text{H}$ values were measured relative to internal standards that were calibrated using V-SMOW standard. The precision of the analytical measures is $\pm 0.1\text{‰}$ for $\delta^{18}\text{O}$ and $\pm 1\text{‰}$ for $\delta^2\text{H}$. Tritium samples were enriched electrolytically and analysed by the liquid scintillation counting method (Thatcher, Janzer and Edwards, 1977). Tritium contents are expressed in tritium units (TU), and the detection limit is 0.7 TU. Radiocarbon analyses were done using standard benzene synthesis (Pollack and Stipp, 1967) and liquid scintillation techniques. Radiocarbon activities are reported as the percent of the activity of modern carbon (pmc). The detection limit of measurement is 2 pmc, which corresponds to water age >32 thousand years BP. The $\delta^{13}\text{C}$ were measured using Finnigan Mat Delta E mass spectrometer.

7.1.1.5 Results

Hydrochemical characteristics The physical and chemical characteristics of the groundwater samples show important variations according to the progressive confinement from SW to NE, and from the geological facies variation of the aquifer system. The groundwater mineralization, expressed in electrical conductivity, EC ($\mu\text{S}/\text{cm}$), generally increases in the aquifers from the SW towards the NE. EC increases also with the aquifer depth. In the control zone sector, the groundwater is less mineralized (73–590 $\mu\text{S}/\text{cm}$), with a mean EC value of 283 $\mu\text{S}/\text{cm}$, while in the upper aquifer EC varied between 64 and 1167 $\mu\text{S}/\text{cm}$ with a mean of 340 $\mu\text{S}/\text{cm}$. The EC values of 708–856 $\mu\text{S}/\text{cm}$, found here, correspond mostly to the values measured in the middle and lower aquifer, which are already moderately mineralized. In the middle aquifer, EC gradually increases in the NE-SW direction from 530 to 1532 $\mu\text{S}/\text{cm}$, whereas in the lower aquifer the evolution trend from 355 to 1480 $\mu\text{S}/\text{cm}$ occurs in the opposite direction.

Groundwater typing based on the chemical composition varies widely in the upper, middle and lower aquifers. The Na- HCO_3 facies type dominates in the aquifer system accompanied with a Na/Ca- HCO_3 , Na- HCO_3/Cl , mixture- HCO_3 , and to a lesser extent with a Na-Cl, Ca/Cl, Na/ SO_4 and Na-mixture. This wide range of hydrochemical facies implies that the chemical processes also differ. Congruent dissolution, as well as incongruent dissolution, together with cation exchange reactions may control the ionic concentration and facies types of the groundwater.

The upper aquifer bears less mineralized water and is dominated by Na-HCO_3 . Some carbonate minerals dissolution may occur in this aquifer; this is indicated by a positive correlation between Ca and HCO_3 , an ionic ratio Ca/HCO_3 close to 0.5, and an increase in Ca and Mg concentrations. The Cl concentrations in the Na-HCO_3 groundwater are mostly low; plots of the Na/HCO_3 vs. Cl close to 1 and Na/Cl vs. Cl indicate strong water–rock interactions. While K and SO_4 concentrations may account for up to 20 to 30% of the total cations and anions, respectively, the NO_3 contents are below 10 mg/l.

Isotope composition of rainwater and surface waters Rainwater from 28 rain events during the period April to September 2001 with an amount varying from 2.5 to 54.9 mm was sampled at Maiduguri. Measured values of the stable isotopes $\delta^{18}\text{O}$ and $\delta^2\text{H}$ are extremely variable, ranging from -8.0‰ to $+3.7\text{‰}$ for $\delta^{18}\text{O}$, from -58‰ to $+31\text{‰}$ for $\delta^2\text{H}$, and from -0.6‰ to $+14.7\text{‰}$ for deuterium excess values. There is no discernable trend between the quantity of rainfall and the isotope signature; some small events (<5 mm) during May to July have low values while some bigger events have higher values. Thus, the extreme rainfall events (low or high) can produce isotopic signatures that are very different from typical rainfall values. This feature has been observed by Gat (1980), Joseph, Frangi and Aranyossy (1992), Mbonu and Travi (1994) and Taupin, Gallaire and Arnaud (1997).

Although the source of precipitation for the Sahara–Sahel, including Nigeria, is the Gulf of Guinea, re-evaporated water from the continent is certainly another important source of water vapour, as shown by the lack of continental effect and a large range in deuterium excess (-0.5‰ to $+14.7\text{‰}$) at beginning and end of the rainy season (Taupin, Gallaire and Arnaud, 1997; Taupin *et al.*, 2000). Thus, temperature, amount of rainfall, and relative humidity of the air column all act to control the isotope composition of rainfall. Goni, Fellman and Edmunds (2001) studying rainfall geochemistry for the period 1992–1997 in northern Nigeria at Kaska and Garin Alkali found a linear regression line ($\delta^2\text{H} = 6.33 \times \delta^{18}\text{O} + 9.9$). This trend is consistent with the Maiduguri station rainfall and other stations in the Sahel, which have slope and deuterium excess values less than those of the GWML (global water meteoric line), which perhaps indicates that much of the rainfall occurs at a mean humidity of less than 100% in the boundary layer. In fact, records of the humidity in the region show that values of only up to 70% occur during September then drop to their lowest values (12%) during March.

Despite the large variation in the rainfall isotope composition, the linear array formed by the data appears to be very close to the GMWL defined by Craig (1961) (Figure 7.3, top). The surface water collected from Lake Chad, local rivers and the Aludam reservoir plot on a linear regression of $\delta^2\text{H} = 5.2 \times \delta^{18}\text{O} + 2.1$ ($r^2 = 0.99$) (Figure 7.3, top) indicating an isotope enrichment typical for water that has been subject to open surface evaporation. Values range from -3.8‰ to $+5.3\text{‰}$ for $\delta^{18}\text{O}$ and from -23‰ to $+26\text{‰}$ for $\delta^2\text{H}$, with the Chad Lake and the Aludam reservoir waters being more enriched than river water samples. Despite the enrichment in stable isotopes composition in these waters, their EC values are very low: 299 and 174 $\mu\text{S/cm}$, respectively. This shows the sensitivity of stable isotopes to evaporation by kinetic fractionation in comparison

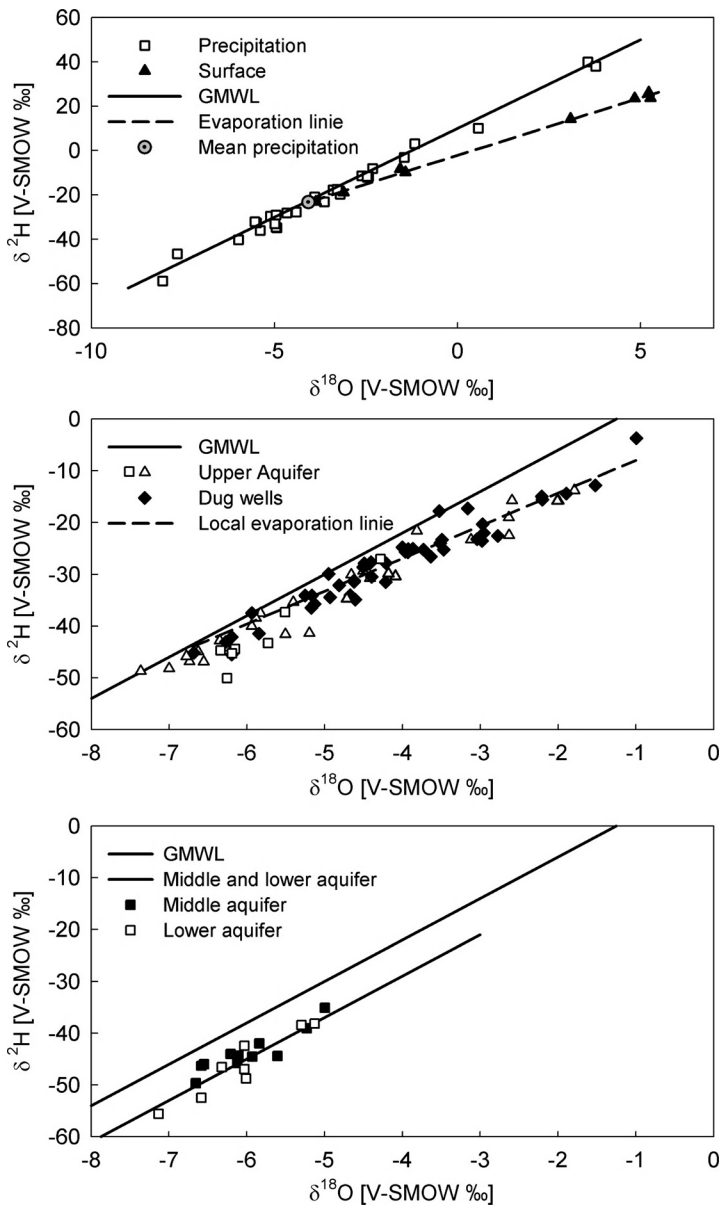


Figure 7.3 Isotope composition of precipitation, surface waters and groundwaters.

to ECs. The generally low tritium content of the surface water and groundwater is a reflection of the depleted tritium concentration in the northern hemisphere.

Groundwater isotope compositions In order to evaluate adequately the suitability of the isotopes for tracing recent and palaeorecharge in the NE Nigeria sector of CSB

subsystem, stable isotopes were analysed for each of these groundwater samples collected from wells in the unconfined shallow aquifer (exploited by shallow dug wells), from upper, middle and lower aquifer layers, as well as from control zone wells. Radiogenic isotope measurements were carried out on a few selected well samples of the middle, lower and control zone aquifers.

The shallow aquifer data (dug wells) plot along a trailing trend, which represents an evaporation line ($\delta^2\text{H} = 6.7 \times \delta^{18}\text{O} - 0.23$, $r^2 = 0.93$) that does not deviate significantly from the GMWL (see Figure 7.3, middle). This indicates that the groundwater has not been fractionated greatly by kinetic evaporation. Due to the fact that the rainwater isotope composition does not show a clear neither temporal nor amount effect, this wide range in the isotopic content of the shallow groundwater could be attributed to a heterogeneity of the recharge conditions and/or mixing of isotopically different rainfall events, which enter the system after being subject to evaporation at the ground surface and in the unsaturated zone. Tritium contents range from less than 1 to 6.5 TU; the higher values (from 4.6 to 6.5 TU) are measured in the shallow borehole waters which also exhibit enriched stable isotopes. The generally low (above background) tritium content of the groundwater indicates that the shallow groundwater is being recharged under modern climatic conditions.

The groundwater collected at greater depth in the upper aquifer unit (60 to 150 m below ground surface) contains very low tritium contents, which generally approach the detection limit, indicating an absence of modern post nuclear water recharge. The stable isotope values are more negative (between -7.3‰ and -5.2‰ for $\delta^{18}\text{O}$, and between -48‰ and -41‰ for $\delta^2\text{H}$) and plot to the right of the GMWL, presumably indicating a palaeo-recharge effect. The stable isotopes in the deep confined aquifers of the middle and lower units systems show a narrower range of isotope concentrations (Figure 7.3, bottom): -6.6‰ to -5.0‰ for $\delta^{18}\text{O}$ and -47‰ to -35‰ for $\delta^2\text{H}$ in the middle aquifer, and -7.1‰ to -5.1‰ for $\delta^{18}\text{O}$ and -55‰ to -38‰ for $\delta^2\text{H}$ in the lower aquifer. The lower aquifer exhibits lighter isotope values, and amplitudes of variation of 2 and 18‰ are found for the $\delta^{18}\text{O}$ and $\delta^2\text{H}$ respectively, which compares to amplitudes in present rainfall isotopic composition. Plotted against the GMWL, values shift to a more negative trend which has the same slope as the GMWL evidencing, therefore, palaeo-recharge water. This is confirmed by the low tritium content (less than 1.4 TU) and low ^{14}C activities (less than 2 pmc), the values of which are close to the detection limits. The depleted signatures in these aquifers are consistent with recharge during a more humid phase characterized by an increased frequency of heavy storm events and perhaps a lower surface air temperature than today's climate or a lower temperature at the site of condensation.

Carbon isotopes Much of the carbon (C) in groundwater derives from gaseous CO_2 in the vadose zone. However, this C, which contains high levels of the ^{14}C , is usually diluted by low ^{14}C activity in C dissolved from minerals during groundwater recharge. Therefore, for ^{14}C dating of groundwater, it is important to understand the geochemical processes in the unsaturated zone and in the aquifer after recharge. The dissolved inorganic carbon (DIC) and ^{13}C evolution provide an insight into these

processes. The concentration of HCO_3^- is controlled initially by variations in dissolved CO_2 present in the soil zone and then taken up by the reaction within the aquifers. There are differences in the $\delta^{13}\text{C}$ values obtained from the different CO_2 input which include marine limestone ($\delta^{13}\text{C} = 0\text{‰}$), organic carbon ($\delta^{13}\text{C} < 22\text{‰}$), mantle derived CO_2 ($-3\text{‰} < \delta^{13}\text{C} < -8\text{‰}$) (Hoefs, 1997), metamorphic processes producing CO_2 ($\delta^{13}\text{C} = 0\text{‰}$) and some primary biogenic carbon ($\delta^{13}\text{C} = -23\text{‰}$). It is possible to eliminate some of these CO_2 sources given the $\delta^{13}\text{C}$ values measured in the selected well groundwater samples. The $\delta^{13}\text{C}$ values of the CSB groundwater range from -13.8‰ to -27.0‰ in the lower aquifer, from -16.3‰ to -19.4‰ in the middle aquifer, and from -8.0‰ to -8.7‰ in the control zone. Two distinct populations can be depicted: an isotopically depleted $\delta^{13}\text{C}$ group (-13.8‰ to -27.3‰) which includes all the lower and middle aquifer water samples, and an isotopically enriched $\delta^{13}\text{C}$ group (-8‰) in the samples collected from the control zone.

From the wide range of $\delta^{13}\text{C}$ values measured in the deeper aquifers, it could be inferred that the sources of $\delta^{13}\text{C}$ are dissolved biogenic CO_2 and calcite dissolution. This hypothesis is consistent with the higher concentrations of HCO_3^- for the evolved water, which may be caused either by oxidation of organic matter, carbonate dissolution, and/or by incongruent reaction of the carbonate matrix. Biogenic CO_2 is inferred to emanate from plant respiration and soil zone through redox reactions. As this CO_2 charged water sinks through the soil zone and moves through the aquifer matrix, it dissolves present carbonates present in the soil. As the enriched inorganic $\delta^{13}\text{C}$ from the carbonate minerals mixes with the isotopically depleted biogenic $\delta^{13}\text{C}$, the water becomes isotopically enriched until the CO_2 is exhausted, the pH rises, and the dissolution of the carbonate minerals stops (Mook, Bommerson and Staverman, 1974; Salomons and Mook, 1986; Schofield and Jankowski, 2004). Through this process, the isotopic composition of the groundwaters evolves from biogenic carbon signature to inorganic carbonate influx, as ion exchange drives further calcite dissolution.

Groundwater age For calculations of the apparent ^{14}C ages of waters in siliceous aquifers, one of the simplest approaches can sometimes be used, that is the 'piston flow' model applicable to confined aquifers with the initial ^{14}C activity changed by dissolution of 'dead' carbonates in the soil zone (Ingerson and Pearson, 1964; Cook and Herczeg, 2000).

$$^{14}\text{C age [in thousand years (ka)]} = 8.267 * \ln [(100/C_{14}) * \delta^{13}\text{C}/-25] \quad (7.1)$$

where C_{14} is the ^{14}C activity measured in DIC expressed in pmc. In the model, the $\delta^{13}\text{C}$ value of the DIC produced by plants in moderate climates is taken as equal to -25‰ (Mook, 2000) and the $\delta^{13}\text{C}$ value of the marine carbonates as equal to 0‰ . We have assumed an initial input of 100 pmc in groundwater and 5730 years as the half life of the ^{14}C . The computed ^{14}C ages, which represent minimum values (given the low ^{14}C values approaching detection limit), are between 29 and 30 ka (thousand years) for the waters sampled in the control zone aquifer, and >37 ka for the waters sampled in the middle and lower aquifers. However, caution should be taken for the corrected middle

and lower aquifer waters since their measured ^{14}C activities are very low (<2 pmc), and ^{14}C dating is particularly uncertain when ^{14}C activities are close to zero and/or $\delta^{13}\text{C}$ values approach zero. Despite these facts, these results match with Edmunds *et al.* (1998, 1999) ^{14}C age range was found to be between 22 and 32 ka with values of ^{14}C activities between 2 and 8 pmc, and $\delta^{13}\text{C}$ values around 14‰.

7.1.1.6 Interpretation

Concerning recharge of the deep confined aquifers, the isotopic, geochemical and hydrogeological data show no systematic age differences related to flow direction over the 300 km distance area investigated that support piston flow movement towards the discharge (artesian) zone in the confined aquifers. Despite this fact, Oteze and Foyose (1988) suggested that the most likely recharge zone of the lower aquifer is outside of the Nigeria sector of Chad Sedimentary Basin at the Pays Bas (Chad) region where the Continental terminal outcrops, but also in southern Chad, Cameroon and east Niger. However, the mixing of waters between the two confined aquifer units by seepage of the upper one may occur as suggested by similar stable isotopic composition.

Based on the comparison of $\delta^{18}\text{O}$ and $\delta^2\text{H}$ values with the GWML (Craig, 1961), the deep formation waters (middle and lower aquifers) have a palaeometeoric origin in the Chad Basin of NE Nigeria. The depleted signatures of the stable isotopes in these groundwaters correspond better with a recharge during a wetter and cooler period than present day climatic conditions. The infiltration period deduced from ^{14}C range from at least 30 to 40 thousand years BP, which corresponds to a period prior to the Late Glacial Maximum (LGM). The low radiocarbon activities and tritium contents indicate that these waters are not being mixed with modern water in the Nigeria sector of the Chad Basin. In the upper aquifer and the control zone, isotope measurements indicate that recharge at shallower depths prevails under modern climatic conditions. At a depth of 100 m, the low ^3H content indicates recharge prior to nuclear tests. There is still the fundamental question about where the recharge takes place. There is some suggestion that the lower aquifer is recharged from the outcrop areas in the southern and north-central Chad (Barber, 1965; Barber and Jones, 1965), but the recharge zone for the middle aquifer is still unknown. As the deep aquifer water is being used, a proper monitoring of the artesian waters is needed for a viable long-term use of these resources.

7.1.2 Case study: 'Vulnerability of a spring capture zone'

7.1.2.1 Introduction and aim

In the following case study several artificial tracers were used in a shallow groundwater system that feeds into a spring. The spring was being used as a municipal drinking water

supply and suffered from occurrences of bacteria after strong rainfall events. The major spring had, in general, a regular and good water quality, and provided more than 150 l/s with only little variation in discharge. The site was investigated in order to identify the potential source of pollution. The multitracer experiment was conducted to investigate the groundwater system and to identify the potential pollution pathway. Based on the study, the protection area for the water supply had to be redefined.

7.1.2.2 Description of test site

The study site is located in the Bavarian alpine upland. The climate can be described as temperate, with about 950 mm of mean annual rainfall and a mean annual temperature of 7.5 °C. The geological setting consists of a porous gravel-aquifer with a permeability of $3\text{--}6 \times 10^{-3}$ m/s and a thickness of about 5 m. At the spring capture, the aquifer is overlain by a thick, loamy layer protecting the aquifer. The spring is captured by two infiltration galleries that had been renewed before the test. Several piezometers are located upstream.

7.1.2.3 Methodology

The chemical characteristics of the groundwater allowed the use of fluorescent tracers, due to low organic, salt and iron contents. Three boreholes (PN1, PN2 and PN3, Figure 7.4) were marked by different fluorescent tracers. The amount of tracer to be injected was calculated based on the desired concentration and aquifer geometry. The desired maximum concentration had to be 10–20 times above the detection limit, but also about well below visibility. The tracer's mass was obtained according to Equation (5.39) by multiplying the desired tracer concentration by the potentially traced volume V_W .

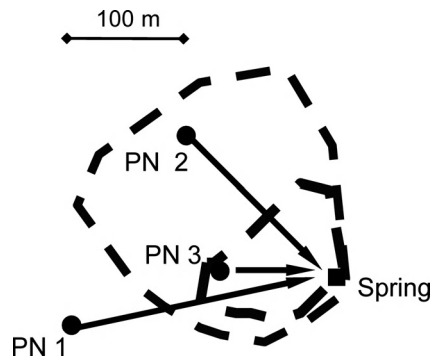


Figure 7.4 Location of injection sites (dashed lines: previously existent delineation of protection zones).

The traced water volume of a spring is estimated according to Equation (6.6). The calculated amount is a maximum value as the tracer plume will disperse mainly along its flow direction and not radially from the injection point as supposed by applying the formula. For borehole PN3, for example, the flow path length L is 50 m, the aquifer thickness m is 5 m and an effective porosity n of 0.15 was estimated. The tracer experiment was designed to reach a concentration of about 1 mg/m^3 , which is well below visibility and sufficiently high, enough to produce a well detectable breakthrough curve. In such a case the mass of tracer needed was estimated with Equation (6.6) to $M = 5.9 \text{ g}$.

Tracer mass for injection into borehole PN3 was set to 5 g of Uranine. Furthermore, 50 g of Eosine were injected into the newly installed piezometer PN2, and 3750 g of Naphthionate were injected into borehole PN1. All tracers were dissolved in the laboratory before the experiment. Before the injection, 1 m^3 was pumped from each borehole. The predissolved tracer was injected with a long pipe that was moved up and down within the borehole to reach a full distribution along the borehole filter. Of course, separate pipes were used for each borehole and tracer. After injection of the tracer, 1 m^3 of clean water was injected to flush the borehole. The injection took 5 min. An online fluorometer measured total fluorescence every 5 s. The online fluorimeter was installed to capture the very fast breakthrough curves in the initial phase of the test. An automatic sampling device took water samples with a sampling frequency of one in four minutes in the first 2 h, and one in 10 min afterwards.

7.1.2.4 Results

From all injection points, breakthrough curves could be measured (Figure 7.5). The first appearance of Eosine was measured 17.5 h after injection. The peak concentration

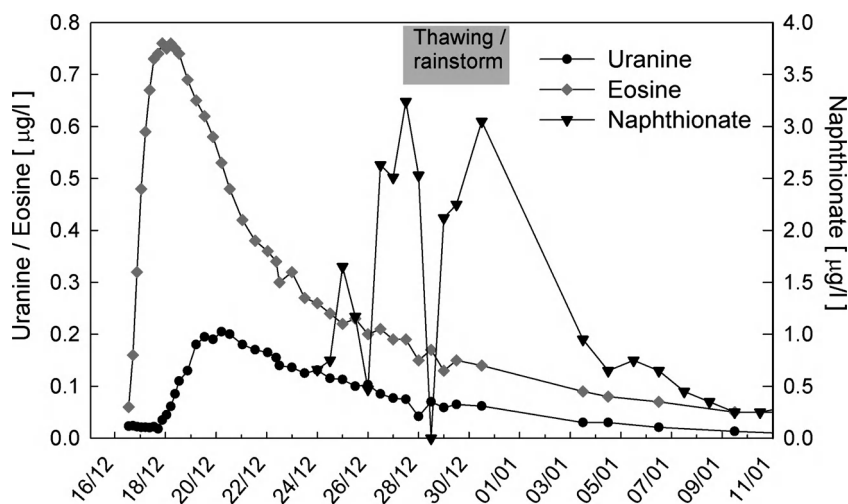


Figure 7.5 Breakthrough curves of Uranine, Eosine and Naphthionate.

(0.75 $\mu\text{g/l}$) was reached 61.5 h after injection. The first detection of Uranine was 53 h after injection. The peak (0.21 $\mu\text{g/l}$) was reached after 109 h. Naphthionate was first measured 9 days after injection. During the breakthrough Naphthionate concentrations fluctuated strongly. The highest concentrations with several peaks were measured after 12 days. Two weeks after injection, before sampling was stopped, Eosine and Naphthionate concentrations had declined to about 0.15 $\mu\text{g/l}$, and Uranine concentrations had declined to less than 0.1 $\mu\text{g/l}$.

The highly variable Naphthionate concentration was probably related to a strong rainfall event associated with snow melt during the tracer breakthrough of Naphthionate. Similar effects were less pronounced for the other breakthrough curves.

The experiment suggested that borehole PN1, while at the fringe of the capture zone, should be included in the protection zone because a fast flow connection obviously exists. The Naphthionate breakthrough curve showed that effective dilution occurred at only a short distance from the spring. Therefore, a source of fast infiltration and inflow was probably located along the flow line borehole PN1–spring.

The calculated maximum flow velocities for PN2 to the spring and PN3 to the spring were similar ($9 \cdot 10^{-4}$ m/s). The mean flow velocity for the flow line PN1–spring was $5 \cdot 10^{-4}$ m/s. Flow velocities along the flow lines PN2 and PN3 towards the spring are higher than flow velocities from PN1 towards the spring.

The hydrogeological setting, the availability of and the newly installed monitoring wells and their distances to the sampling location provided an ideal framework for the application of fluorescence dyes. Even though the spring water was not introduced into the public water supply system during the experiment, the applied amounts of tracer were not visible at any time. The source of fast infiltration – an old buried trench with coarse filling material – could be identified subsequently along the flow path PN1 towards the spring. The trench was refilled with fine material to block preferential flow paths. This measure was shown to be effective in eliminating the occurrence of bacteria after strong rainfall events.

7.1.3 Case study: 'Evaluation of aquifer parameters by single well techniques'

Single well techniques make use of tracers injected artificially into the system under investigation in order to estimate filter velocity or their vertical distribution in the aquifer (by applying packers in different depths). Additionally, by applying radioactive tracers the determination of water flow direction is possible. The technique was developed by Drost and Neumaier (1974) using radioactive isotopes. The measurement includes tracer dilution logs and direction logs. The tracer dilution logs lead to a quantitative determination of the groundwater discharge by measuring the decrease of the tracer concentration in the well (provided the groundwater flow is laminar). Direction logs determine the direction of the groundwater flow via a direction diagram measured by a collimated detector. The natural groundwater flow in porous aquifers consists mainly of a laminar movement relative to the hydraulic gradient (Darcy's Law). The filter

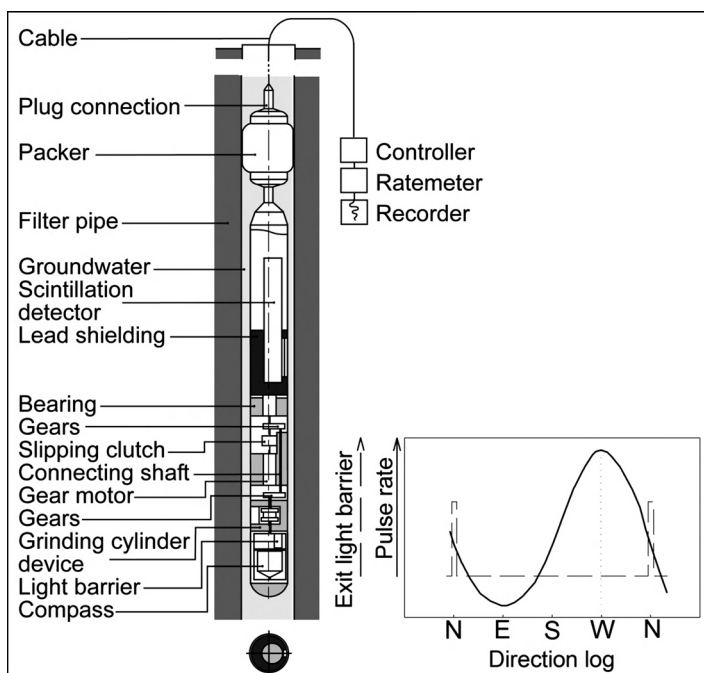


Figure 7.6 Single well tracer measuring tube to determine filtration velocity and groundwater flow direction (modified after Moser and Rauert, 1980).

velocity v_f is one of the parameters in Darcy's Law ($v_f = k \times i$), which relates to the true groundwater velocity v by $v = v_f \times n$, where n is the effective porosity of the aquifer. The application of this technique requires the complete vertical exploration of the aquifer or the investigated layer by well drilling. The well drilling needs to be constructed with a filter pipe and gravel, in order to provide for a sand-free groundwater movement through the well with low filter resistance (Drost, Klotz and Koch, 1968; Gaspar and Onescu, 1972; Moser and Rauert, 1980; Leibundgut, 1981a; Drost and Hoehn, 1989; Mairhofer, 1996).

The estimation of the filter velocity is carried out by measuring the dilution of tracer concentration $c(t)$ in the well, as a function of time (t). The tracer concentration is monitored continuously after the initial constant homogenous distribution of the injected tracer with the concentration c_0 ($t = 0$) is reached. The interpretation requires a stationary and horizontal groundwater flow through the filter pipe. These requirements are fulfilled for the tracer probe shown in Figure 7.6. The result of the measurement is a dilution log, in which the filter velocity v_f can be calculated from equation

$$v_f = \pi r \ln [c_0/c(t')]/(2\alpha t') \quad (7.2)$$

where

c_0 = tracer concentration at $t = 0$

$c(t')$ = tracer concentration at t'

r = inner radius of the filter pipe

α = correction factor (~ 1.5 – 2.0)

After finding the filter velocity and knowing the regional hydraulic gradient (i) one can also easily approximate the hydraulic conductivity (k) using Darcy's Law:

$$k = v_f / i \quad (7.3)$$

The probe can measure velocities of up to 50 m/d. Accuracy depends on the resolution of the dilution log and is usually better than 10%. At very low velocities (< 0.05 m/d) the dilution is outweighed by the diffusion of the tracer, at velocities > 50 m/d the laminar groundwater movement turns into a turbulent flow.

The concept of the direction log is connected to the measurement of filter velocity and consists of a direction-sensitive probe with which the radiation emitted by the radioactive tracer can be logged after having flown into the aquifer. Such a probe is shown in Figure 7.6 where a collimated radiation detector in the filter pipe rotates around its vertical axis. The collimator is a sliced lead shield. The orientation of the collimator is established by a compass. The result is a horizontal direction log documenting measured radiation during the 360° turn of the collimator. The maximum of the log gives the dominant flow direction of the groundwater. The accuracy is usually better than 20%. At filter velocities of less than 0.05 m/d the radial tracer diffusion influences the direction log, for high velocities no restrictions are given.

The two probes are combined so that the direction log is measured after the tracer has left the dilution probe.

As tracer, the radioactive element Bromide-82 is used in solution of NH_4Br . ^{82}Br is a rather short-lived element with a half life of 35.9 h which allows repeated experiments. The amount injected is less than 1 ml. ^{82}Br flows with the same velocity as water and is not absorbed in the filter pipe or gravel. The dose per sampling point depends on the filter pipe radius but does not exceed 2 to $8 \cdot 10^5$ Bq.

7.1.3.1 Single well experiment using radioactive isotope ^{82}Br

An informative study using this technique was carried out in order to investigate the impact of irrigation on the groundwater flow in a porous fluvioglacial aquifer. The filter velocities and the flow directions at several depths were determined. For both states before and after irrigation Figure 7.7 visualizes the flow direction in the wells at different depths compared to the general isohypses. The measurements after the irrigation show a strong impact on the gradients of groundwater level and consequently on the flow direction of the groundwater. In well G5 the irrigation induced groundwater ridge changed the local flow direction to three different directions in the distinct depths.

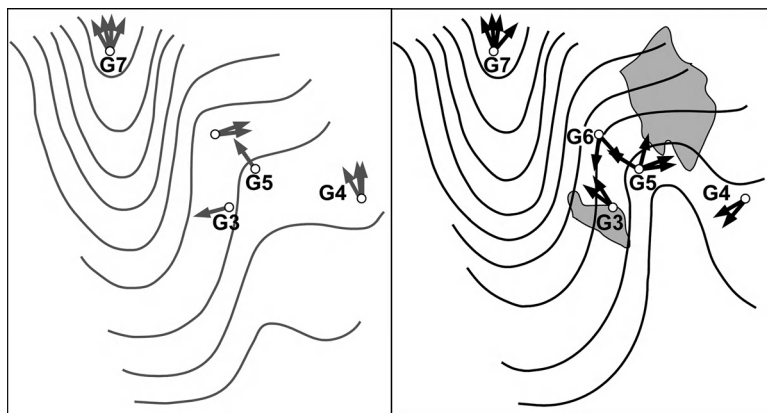


Figure 7.7 Single well measurements in a porous aquifer. The arrows represent the measured flow directions in different depths of groundwater. Left: stage before irrigation; right: stage after irrigation; shaded areas: irrigation fields.

Before the irrigation the filter velocity (v_f) was measured to be 1.6 to 2.2 m/d. The filter velocity increased considerably up to 5.3 m/d caused by the artificial infiltration. The measured depths are listed in Table 7.1. Remarkable changes in flow direction were measured in wells G3, G4 and G6, too.

Table 7.1 shows the potential of the single well technique by listing the obtained data (Leibundgut, 1981a). The specific measurement technique allows for the identification of complex flow behaviours in great detail. The measurement of a cluster of wells leads to an overall picture of the flow patterns that are representative for a distinct regional scale.

7.1.3.2 Single well experiment with fluorescent tracers using fibre optic sensor

While the single well technique was for a long time only feasible with radioactive isotopes, new developments in measuring technique now allow for the use of fluorescent tracers. However, with the fibre optic sensors direction logs cannot be provided. The technical features of FOF (fibre optics fluorometer) are reported in Section 4.1.3. The test arrangement is similar to that of radioactive tracers. In the frame of a multitracer experiment to investigate hydrogeological transport parameters in a large fissured sandstone aquifer, two single well tests were performed. The water in the wells was homogeneously traced over 11 and 15 m respectively in the filtration segment at depths of -245 and -218 m. The injection masses amounted to 1 and 5 g Uranine.

The measuring heads of FOF were positioned in the centre of the traced water column to measure concentration profiles (Figure 7.8, left). The profile measurements allow both, the fixing of optimal measurement point to determine the tracer concentration decrease and the control of homogenous mixing (Figure 7.8, right). The tracer injection occurred at a depth of -218 m.

Table 7.1 Data of a single well experiment with ^{82}Br in a fluvioglacial aquifer. R_i : direction

| Meas. point | Upper edge Above sea level | Date | Time | Groundwater level | | Meas. Depth | | v_f m/d | R_i N...E |
|-------------|-------------------------------|--------|-------------|-------------------|-----------------|----------------|--|--------------|----------------|
| | | | | m from Terrace | Above sea level | m from Terrace | | | |
| G2 | 497.25 | 28.11. | 15.00–18.00 | 4.29 | 492.96 | 4.7 | | 0.20 ± 0.1 | 170 ± 10 |
| | | 30.11. | 16.00–19.00 | 4.22 | 493.03 | 4.5 | | 0.30 ± 0.02 | 330 ± 20 |
| | | | | 4.22 | 493.03 | 5.0 | | 0.90 ± 0.05 | 200 ± 40 |
| G3 | 492.57 | 28.11. | 11.00–13.00 | 2.40 | 490.17 | 3.0 | | 4.60 ± 0.50 | 260 ± 50 |
| | | | | | | 3.5 | | 1.10 ± 0.20 | 260 ± 20 |
| | | 30.11. | 11.00–13.00 | 1.80 | 490.77 | 2.5 | | 9.90 ± 1.40 | 310 ± 40 |
| G4 | 494.03 | 28.11. | 14.00–18.00 | 1.80 | 490.77 | 3.5 | | 1.40 ± 0.40 | 330 ± 20 |
| | | | | 2.95 | 491.08 | 3.3 | | 0.90 ± 0.10 | 330 ± 60 |
| | | | | | | 4.0 | | 3.60 ± 1.00 | 360 ± 50 |
| G5 | 493.55 | 30.11. | 13.00–16.00 | 2.43 | 491.60 | 5.0 | | 0.10 ± 0.02 | 350 ± 60 |
| | | | | 2.40 | 491.63 | 3.0 | | 0.40 ± 0.10 | 230 ± 40 |
| | | 28.11. | 11.00–14.00 | | | 4.0 | | 1.70 ± 0.20 | 230 ± 20 |
| | | | | 3.10 | 490.45 | 5.0 | | 0.10 ± 0.04 | 240 ± 30 |
| | | | | | | 3.6 | | 12.60 ± 3.30 | 190 ± 30 |
| | | | | | | 4.2 | | 2.20 ± 1.40 | 320 ± 60 |
| | | | | | | 5.0 | | 1.60 ± 0.70 | 320 ± 10 |
| | | 30.11. | 10.30–15.00 | 1.51 | 492.04 | 2.5 | | 5.30 ± 1.10 | 300 ± 40 |
| | | | | 1.51 | 492.04 | 3.6 | | 3.60 ± 0.60 | 70 ± 60 |
| | | | | | | 4.2 | | 1.20 ± 0.10 | 60 ± 60 |
| G6 | 492.01 | 28.11. | 8.00–10.30 | 2.62 | 489.39 | 5.0 | | 1.20 ± 0.20 | 10 ± 60 |
| | | | | | | 3.4 | | 9.20 ± 1.60 | 70 ± 60 |
| | | | | | | 4.0 | | 13.80 ± 1.20 | 70 ± 50 |
| G7 | 489.60 | 30.11. | 8.00–10.00 | 2.51 | 489.50 | 4.5 | | 2.50 ± 0.60 | 80 ± 60 |
| | | | | 2.51 | 489.50 | 3.4 | | 23.00 ± 3.40 | 190 ± 10 |
| | | | | | | 4.0 | | 20.00 ± 5.00 | 140 ± 50 |
| | | 28.11 | 8.00–10.30 | 5.80 | 483.80 | 4.5 | | 4.20 ± 0.70 | 190 ± 10 |
| | | | | | | 6.3 | | 24.00 ± 5.00 | 20 ± 20 |
| | | | | | | 7.0 | | 4.70 ± 1.10 | 350 ± 40 |
| | | | | | | 8.0 | | 3.00 ± 0.20 | 340 ± 40 |
| | | | | | | 9.0 | | 6.40 ± 1.30 | 340 ± 40 |
| | | | | | | 10.0 | | 5.30 ± 1.00 | 330 ± 40 |
| | | 30.11 | 8.00– | 5.8 | 483.80 | 6.3 | | 35.00 ± 10 | 360 ± 30 |
| | | | | | | 7.0 | | 9.00 ± 2.00 | 340 ± 20 |
| | | | | | | 8.0 | | 3.50 ± 0.80 | 340 ± 30 |
| | | | | | | 9.0 | | 6.90 ± 1.40 | 40 ± 40 |
| | | | | | | 10.0 | | 5.70 ± 1.70 | 350 ± 40 |

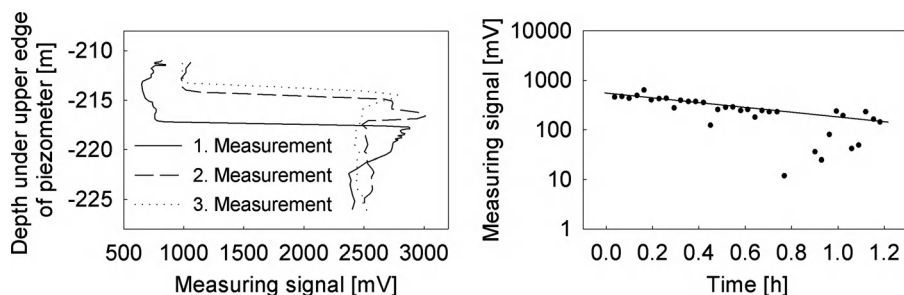


Figure 7.8 Left: Measured profiles of Uranine (–218 m) in a well showing low dilution, Profile 1: measured shortly after injection, profile 2: after 10 h, profile 3: after 23 h. Right: Measured and theoretical decrease of Uranine concentration value. Diffusion leads to homogenous mixing after 1.2 h.

The measuring signals in the profiles differ from the first to the second measurement and remain constant from the second to the third (Figure 7.8). This is due to inhomogeneous mixing shortly after injection. Beneath 217–226 m, the values of profile 1 are comparable to that of profile 2 and 3. It reflects a low perfusion of the well (Figure 7.8). The evaluation followed the nonsteady measurement at constant depths. Homogenous mixing is reached by diffusion after a given time. With $k_f = 2.05 \times 10^{-5}$ m/s and 6.25×10^{-5} m/s respectively ($i = 5\%$), the velocity v_f can be calculated. The values are in the range of those independently determined by slug- and bailer tests ($1.6 - 3.9 \times 10^{-5}$ m/s).

7.1.3.3 Single well experiment with fluorescent tracers using online fluorometer

Another case study is presented here, in which the depth of the groundwater inflow into a borehole and the respective hydrochemical composition (nitrate content) need to be known. Based on the depth distribution of inflow and the respective nitrate concentrations of inflow at different depths, a strategy for reducing the average nitrate concentration had to be derived.

For the application of this method an online fluorimeter needs to be available that can give high-resolution fluorescence data. An injection device is needed enabling the injection of a defined volume of tracer at different depths. This injection device needs to be precise as the same amount of tracer needs to be ejected at different depths and pressures. Usually, a remote-operated syringe with a small engine moving the piston gradually is used. The method can be used in production boreholes with a running pump. In observation boreholes an additional pump needs to be operated.

Along the depth-profile of the borehole, at each depth a given amount of groundwater is flowing into the borehole. Once it has reached the borehole it is drawn towards the pump. Within the boreholes the depth-dependent groundwater inflows mix. Injecting an artificial tracer at different depth enables the calculation of the percentage of inflow

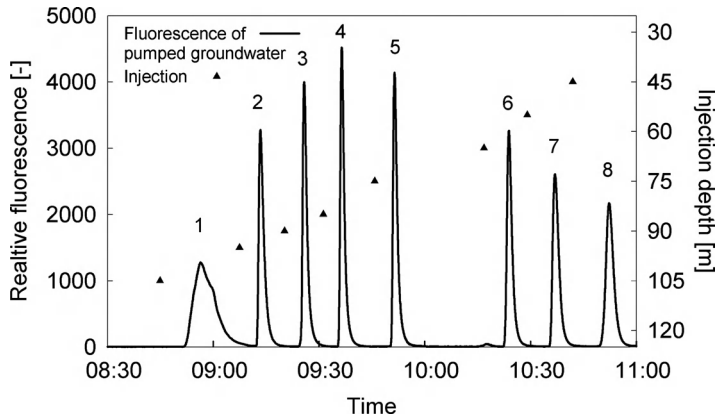


Figure 7.9 Breakthrough curves of tracer injection (the depth is marked by a triangle) measured at the borehole head.

above the injection point and between the injection point and the pump. By making multiple injections with increasing vertical distance from the pump, the increments of flow can be calculated. The graph shows all eight tracer injections and breakthroughs during the pumping tests (Figure 7.9). The absolute magnitude of the fluorescence is given on the left scale, the injection depth is shown on the right scale. Injections were made at 105, 95, 90, 85, 75, 65, 55 and 45 m depth. The time of each injection is shown. Shortly after each injection a breakthrough curve could be observed, the time between injection and observed breakthrough curve can be used to calculate the discharge marked with the injected tracer.

Figure 7.10 shows how the analysis is carried out for the first injection. The breakthrough is modelled with a 1D dispersion equation (see Section 5.1) and from the fitted breakthrough curve the mean velocity can be calculated. For the first injection,

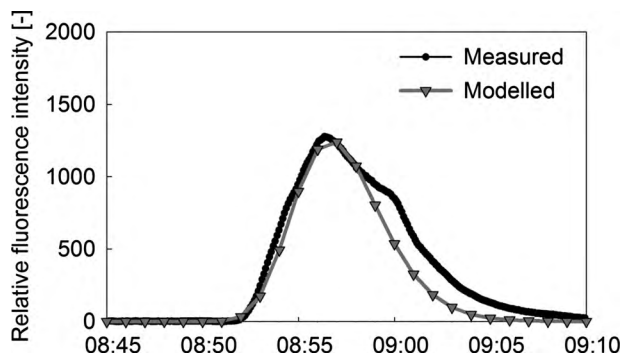


Figure 7.10 Single breakthrough – injection at 105 m (first injection in Figure 7.9), measured and modelled.

a nonideal breakthrough curve is observed due probably to the leaking of the syringe. The following breakthrough curves all show an almost ideal breakthrough.

From the cross-section area A of the borehole given by πr^2 (r = radius of the borehole), the travel time t' between injection and detection, and for the distance between the injection depth and the depth of the pump s , the discharge q can be calculated according to:

$$q = v_f A = \pi r^2 s / t' \tag{7.4}$$

The discharge calculated from the next injection corresponds to the sum of the discharge between the second injection depth and the first injection depth. By an incremental discharge measurement the increase of discharge can be derived section by section. The results of this analysis are shown in Figure 7.11.

The experiment proved that there were two distinct sections with groundwater inflow (bars in Figure 7.11). The upper section and the lower section were separated by a clay layer. The depth distribution of inflow can be useful for managing boreholes, especially if only certain sections are contaminated with nitrate or organic pollutants.

The fluorescent approach in single well technique is a reliable alternative to the radioactive technique, although it is not as powerful. On the other hand, the alternative technique is much easier to handle due to the absence of radiation protection problem.

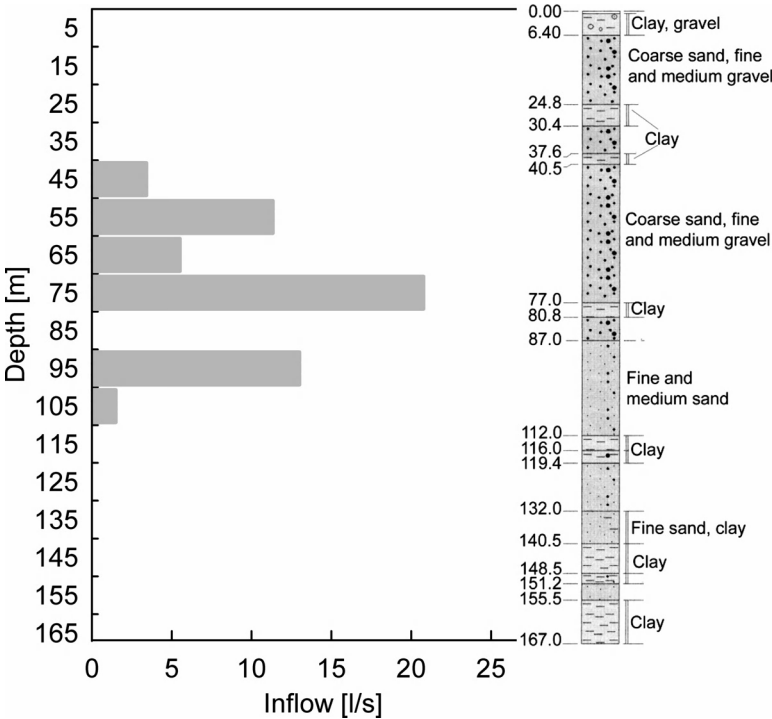


Figure 7.11 Depth distribution of lateral inflows obtained from tracer test to the borehole and lithological profile.

In addition, the new technique is cheaper in respect of hardware and in application. Furthermore, the high sensitivity of fluorescent tracers enables very small injection masses.

7.2 Case studies in the unsaturated zone and in soils

The vadose zone (soils and unsaturated zone) is a complex compartment of the hydrological cycle. The water flow parameters in unsaturated media are characterized by nonlinear behaviour and hysteresis. Chemical and physical properties change with water content and the variability of hydraulic and chemical parameters is high. Understanding hydrological processes in the unsaturated zone is of great importance for many hydrological applications and water resource uses, as well as agricultural and ecological management activities. Thus, processes of preferential flow, like fingering, have to be visualized. Tracers have provided evidence that the fastest flow velocities exceed expectations based on matrix flow. A review of tracer use in the vadose zone is provided by Flury and Wai (2003). The choice of tracer for the study of the unsaturated zone depends on the type of problem under investigation. Many key aspects of vadose zone hydrology, for example preferential flow and recharge mechanisms that are now common knowledge were discovered only by means of tracers.

Water flow and solute transport in the vadose zone have been investigated by tracer methods in the context of studies about runoff generation and the transportation of pollutants (Kendall and McDonell, 1998; Barnes and Turner, 1998). Artificial tracers were used to investigate preferential flow processes (Holden *et al.*, 1995; Mikovari, Peter and Leibundgut, 1995; Onodera and Kobayashi, 1995). A multi tracer experiment and its evaluation by a convolution integral was used to determine flow and transport parameters in the unsaturated zone (Mehlhorn, Leibundgut and Rogg, 1995).

Derby and Knighton (2001) applied potassium chloride (KCl) at the soil surface to investigate field scale water and solute transport through the unsaturated zone at a drained agricultural area. With respect to agricultural groundwater contamination, a tracer study showed that instances of high water input (snowmelt, large rain fall events) replenish the shallow aquifer. This recharge is also greater in small surface depressions. The high variability of solute fluxes, which depends on chemical characteristics and on the temporal variability of the moisture content of the vadose zone, is shown by Jaynes *et al.* (2001) through a multi tracer approach. They investigated the behaviour of artificially applied herbicides, pentafluorobenzoate, o-trifluoromethylbenzoate, difluorobenzoate and bromide over a period of 14 days on a drained 42.7×24.4 m field. An assessment of preferential flow processes in a forest-reclaimed lignitic mine soil using a tracer cocktail consisting of bromide, terbuthylazine and deuterium was performed by Hangen *et al.* (2005). In a multi tracer experiment (Br, Cl, HDO, fluorescent and non fluorescent dyes) to investigate the transport of fertilizers and agrochemicals in a loamy grassland, the tracers were added to the sprinkling water (Stamm *et al.*, 2002).

Tracer studies in the unsaturated zone can be combined with other experimental techniques such as geophysical methods (Uhlenbrook, Didszun and Leibundgut, 2005; Uhlenbrook, Didszun and Wenninger, 2008). Electrical resistivity tomography and transmission radar tomography in combination with NaCl in the vadose zone were

applied, for example by Singha and Gorelick (2005) and Binley *et al.* (2002). Ground-penetrating radar combined with artificial tracers has been used for nondestructive identification and mapping of soil pipes in blanket peat catchments by Holden (2004).

Zoellmann, Kinzelbach and Fulda (2001) used the environmental tracer ^3H (tritium) and SF_6 (sulfur hexafluoride) to calibrate a coupled model to address the unsaturated-saturated flow for nitrate pollution management. The model of the unsaturated zone was calibrated with ^3H , the model for the saturated zone with SF_6 . This approach is based on the fact that ^3H passes the vadose zone as a fluid (precipitation input), thus revealing information on the residence time in the unsaturated zone, while SF_6 passes the vadose zone as a gas (Cook and Solomon, 1997) and dissolves into the groundwater at the water table. The difference of both residence times can then be related to the travel time in the unsaturated zone. Natural tracers are in particular applied in arid zone hydrology to estimate water fluxes and ages in the unsaturated zone, chloride, water isotopes (tritium, deuterium, ^{18}O) (e.g. Allison and Barnes, 1983; Scanlon, 1991; Wood and Sanford, 1995; IAEA, 1985, 2001) are often used in these studies. Scanlon (2000) addresses the issue of uncertainties in water balance in a study in the Chihuahuan Desert of Texas where vadose zone water fluxes and ages were estimated with the chloride mass balance method. The uncertainties amounted to $\pm 38\%$ in water flux and -24 to 56% in water age.

All kind of tracers, in particular the combination of solute and particle tracers, are used to investigate the infiltration function of soils and unsaturated zone concerning the transport of contaminants and pathogenic germs. The relevant references regarding this issue are provided in Sections 4.3 and 7.2. Hydraulic characteristics and the bioremediation of a seminatural sewage plant have been investigated with fluorescent tracers. Residence time and distribution of the sewage water into the sand filter were determined (Schudel and Leibundgut, 1988). Recently, very interesting studies on tracer transport and water flow as well as on heterogeneity of the water fluxes were presented by Maciejewski *et al.* (2006), Maloszewski *et al.* (2006), Maloszewski, Wachniew and Czuprynski (2006) and Stumpp *et al.* (2007) who modelled environmental $\delta^2\text{H}$ data observed in precipitation and outflow from different soil lysimeters (Section 7.2.2).

Nonfluorescent dyes, such as Brilliant Blue, have been widely used in tracer experiments for the investigation, and especially for the visualization, of the infiltration process itself (e.g. Weiler and Naef, 2003; Stamm *et al.*, 2002; German-Heins and Flury, 2000). After applying the tracer and excavating soil profiles, it is possible to determine infiltration characteristics such as preferential flow paths (e.g. Weiler and Naef, 2003; Oehrstrom *et al.*, 2004). Image analysis methods enable the determination of the quantitative spatial distribution of the dye (e.g. Kasteel *et al.*, 2005; Weiler and Flühler, 2004; Forrer *et al.*, 2000; Schlather and Huwe, 2005b). This method can also be used to determine longitudinal and lateral dispersion (Forrer *et al.*, 1999) under given conditions.

7.2.1 Specific aspects of using tracers in the unsaturated zone

The principle of following the movement of water with tracers, of detecting breakthrough curves and of measuring the distribution of tracers along a flow path is the

same as for other components of the water cycle. However, in the unsaturated zone different phases (solid, fluid, gaseous) affect the movement of tracers. In addition to gravity, capillary forces must be accounted for. Sorption, ion exchange and variable hydrochemical conditions affect the movement of tracers in soil, and thus represent a complex mineralogical system. Since it is almost impossible to predict flow paths in advance, the calculation of injected mass is more difficult and sampling at the correct intervals is more demanding. Special methodological aspects must be considered.

If the injection is conducted on the surface of the soil, the problem of photolysis must be considered. A reliable estimation of the water volume required to cover the soil moisture deficit of the substrate is crucial. The injection of sufficient spill water is an indispensable requirement for the initiation of water flow. A reliable estimation of the tracer mass to be injected is difficult due to the wide spectrum of relevant possible parameters in soils and the unsaturated zone. In addition to the instructions given for groundwater experiments, the depth of the zone, the lateral losses and the losses by saturation of the traced substrate volume have to be taken into account. Of course, by using environmental tracers such as, for example, deuterium ($\delta^2\text{H}$), the problem of injected mass does not exist and the tracer is distributed with the recharging water through whole surface.

The most problematic part of a tracer investigation in the unsaturated zone is the issue of soil water sampling. Regardless of the sampling devices used, there is always the problem of ensuring good contact between probe and substrate. Adequate extraction of soil water from the substrate requires sophisticated techniques. Contributions to the issue of soil water sampling are provided, for example, by Grossmann, Bredemeier and Udluft (1990), Brandi-Dohrn *et al.* (1995, 1996), Gee *et al.* (2002), McGuire and Lowery (1994), Weihermüller (2005), Weihermüller *et al.* (2007), Figuera-Johnson, Tindall and Friedel (2007). Basically, there is a wide range of potential methods for the extraction of soil water with tracers, including techniques developed specifically for tracer hydrology and modifications of existing methods for soil water extraction only. Up to now none of them has proved to be superior to all of the others. There are constraints, advantages and disadvantages related to each method of extraction. The suitability of techniques depends on the soil water tension range, the resolution in space and time, cost and maintenance effort. In many cases destructive methods of soil water sampling 'a priori' are not considered appropriate. According to a comprehensive review by Weihermüller *et al.* (2007), relevant sampling devices for in situ soil water extraction are porous cups, porous plates, capillary wicks, resin boxes and lysimeters. Apart from rather practical constraints the representativeness of extracted soil water solution is a major problem. In general, data obtained from soil water sampling depend on the extraction technique (Weihermüller *et al.*, 2007). The presentation, interpretation and comparison of tracers in soil water should always be carried out in view of the applied extraction techniques. Finally, the exact definition of study objectives is crucial for identifying the most appropriate experimental design (Weihermüller *et al.*, 2007).

Other disadvantages are associated with the sampling techniques described above: (i) the determined concentrations may be biased by induced dispersion effects and delay of breakthrough, (ii) an online detection of the tracer breakthrough is not possible (iii) the costs are in proportion to the time it takes to achieve resolution of the measurements.

An advanced method of measuring tracer concentrations in the unsaturated zone is the use of a fibre optic fluorometer (FOF). It allows for an in situ measurement producing only a minimal disturbance of the substrate by very thin probe heads (cf. Section 4.1.3.5). In summary, this technique minimizes the disadvantages of the sampling methods described above (Barczewski and Flachowsky, 2003), Flachowsky *et al.* (2005). However, only fluorescent tracers can be measured and extraction water is not preserved for measuring other compounds.

7.2.2 Case study: 'Environmental deuterium transport through soils'

7.2.2.1 Introduction and aim

With the increasing efforts in protecting groundwater resources, more accurate simulation models to predict the pollutant migration under unsaturated and saturated water flow conditions are needed. The general approach requires, as a first step, the description of water flow conditions in the unsaturated zone and the identification of the chemical species transported through it. Normally, in such studies long-term experimental work is required in order to control all possible processes starting in the unsaturated zone. Several laboratory measurements on different soil materials have to be performed in order to obtain the hydraulic characteristics and parameters of the unsaturated soils. In most cases, these are carried out using small scale-column experiments performed in the laboratory. However, in practice, due to the high heterogeneity of the soil materials, measurements of crucial parameters performed in in situ lysimeters are more effective and accurate when undisturbed research soils are used. With this objective, infiltration experiments were conducted in the late 1980s at the HMGU-Institute of Groundwater Ecology (Munich-Neuherberg) using lysimeter columns in order to investigate the water flow and tracer transport through the unsaturated zone under natural atmospheric conditions.

This study was described in two papers: Maciejewski *et al.* (2006) and Maloszewski *et al.* (2006). The first presented the evaluation of soil hydraulic parameters for tested soils. The estimation of the physical soil characteristics, that is the relationship between water pressure head and water content $h(\theta)$, was performed by applying the van Genuchten model (see Section 5.2). To estimate the $k(\theta)$ characteristics, the inverse modelling technique was used for each lysimeter. The cumulative outflow curves $q(t)$ were fitted to the observed outflow data by a trial-and-error procedure using $k(\theta)$ as the fitting function. It was shown that this method of estimating the soil characteristics yields parameters which are closer to the true values as compared to those found in the small-scale column experiments. The soil characteristics obtained in that part of the study were further used for estimating environmental deuterium transport parameters (dispersion, water content and possible zones with stagnant water) through the soils (Maloszewski *et al.*, 2006).

This type of water flow modelling and tracer (pollutant) transport requires a great deal of data (mentioned above), which are difficult to estimate in practice without

intensive and costly experimental work. Additionally, exact modelling requires well developed numerical models in order to perform the calculations. By contrast, simple lumped-parameter approaches do not require such extensive information and data. They only need information about mean values of recharge and the measurements of stable isotope contents in water entering and flowing out from the soil. However, the lumped-parameter models were developed generally for steady-state flow conditions, which seldom exist in nature. The purpose of the work was: (1) the development of a simplified mathematical model which can describe mass transport through unsaturated water zone; (2) the application of this model to the environmental tracer data for quantitative estimation of model parameters and (3) the examination of the accuracy of these estimates by comparison with those obtained using more exact numerical models.

7.2.2.2 Description of test site

The seven lysimeters (length 2 m; diameter 0.39 m) were filled with different porous soil materials, ranging from quartz and tertiary sands to quartz and fluvioglacial gravels (see Table 7.2). Experiments were carried out in the soils without plants at the early stage of the research project over an eight year period (1984–1991) in the input–output mode. During that period the weekly water flow rates (precipitation amount and discharge) and the tracer contents (environmental deuterium) in the precipitation and in the outflow were observed in order to estimate the unsaturated hydraulic and transport parameters of the soils as previously there was only limited data available. Figure 7.12 presents the variation in the precipitation amount and the deuterium content in the precipitation during the total observation period of 417 weeks (eight years). The area under investigation was characterized by a mean annual precipitation of 1004 mm, whereas the average discharge from the lysimeters varied between 800 and 946 mm per year. The weighted mean deuterium contents in rainwater and in water flowing out of the lysimeters were nearly identical (see Maloszewski *et al.*, 2006). This indicates that, for these experiments, isotopic enrichment of deuterium due to evaporation or exchange with vapour could be neglected. In turn, this result permitted the use of directly measured deuterium contents as input and output functions.

7.2.2.3 Modelling

Two model approaches were used to describe deuterium transport. The first, the numerical solution of water flow and two-phase mass transport equations called Variable Flow Dispersion Model (VFDM), can simulate exactly the spatial and temporal distribution of flow and transport parameters. This model combines the numerical solution of the variable water flow in the unsaturated zone, described by the Richards and Darcy Equations (5.96–5.98, Section 5.2), with dispersive-convective transport in the double-porous medium (5.99–5.103). First, estimating the water flux $q(z, t)$ and water content $\theta(z, t)$ in the soils, the fitting parameters of VFDM are the soil characteristics

Table 7.2 Description of different soil materials used in lysimeter experiments and their parameters (d_{50} – median grain size; CU – coefficient of uniformity; ρ – dry density; K_{sat} – saturated hydraulic conductivity; θ_{sat} – saturated water content; θ_d – water content after free drainage)

| Lys. | Character of soil and grain size | d_{50} [mm] | CU (d_{60}/d_{10}) | ρ [g/cm ³] | K_{sat} [cm/day] | Mean water content | |
|------|------------------------------------|---------------|------------------------|-----------------------------|------------------------|--|--|
| | | | | | | θ_{sat} [cm ³ /cm ³] | θ_d [cm ³ /cm ³] |
| S156 | Quartz sand 0.1–0.4 mm | 0.22 | 1.78 | 1.75 ± 0.05 | 2.60 × 10 ³ | 0.374 | 0.112 |
| S158 | Quartz sand 0.1–0.4 mm | 0.22 | 1.78 | 1.75 ± 0.05 | 2.60 × 10 ³ | 0.391 | 0.121 |
| S159 | Quartz sand 0.06–0.2 mm | 0.11 | 1.47 | 1.75 ± 0.05 | 4.30 × 10 ² | 0.364 | 0.156 |
| S160 | Quartz sand 0.5–1.5 mm | 0.98 | 1.39 | 1.75 ± 0.05 | 4.32 × 10 ⁴ | 0.361 | 0.042 |
| S161 | Quartz gravel 2–3 mm | 2.75 | 1.31 | 1.75 ± 0.05 | 2.59 × 10 ⁵ | 0.380 | 0.033 |
| S162 | Fluvioglacial gravel 0.06–10 mm | 6.00 | 40 | 1.95 ± 0.05 | 1.36 × 10 ³ | 0.300 | 0.066 |
| S163 | Tertiary sand 0.06–0.6 mm | 0.32 | 1.74 | 1.95 ± 0.05 | 2.04 × 10 ¹ | 0.300 | 0.090 |

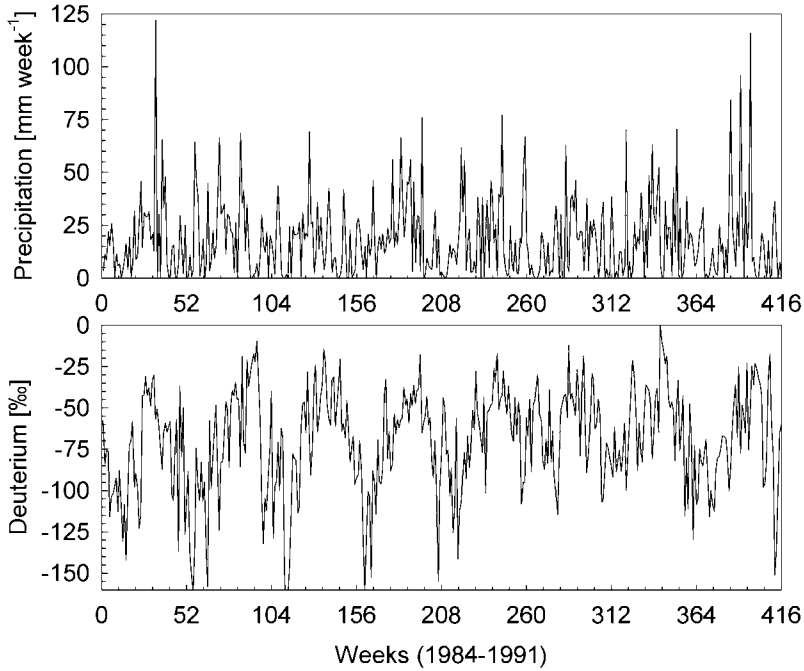


Figure 7.12 Weekly precipitation amounts (top) and deuterium content of weekly precipitation (bottom) for the rain gauge at the HMGU-Institute of Groundwater Ecology (Munich-Neuherberg).

$h(\theta)$ and $k(\theta)$. The soil characteristics found by Maciejewski *et al.* (2006) are shown in Figure 5.19 (Section 5.2). Resulting $q(z, t)$ and $\theta(z, t)$ are then taken as known parameters into the transport Equations (5.101–5.102, Section 5.2). Second, by the modelling of tracer transport, the fitting parameters of the VFDM were then reduced to those of the second model component, that is the longitudinal dispersivity (α_L), the tracer transfer coefficient between mobile and immobile water (ω), and the ratio of immobile water to the whole water content ($f = \theta_{im}/\theta$), which are assumed to have constant values (5.107 in Section 5.3). The boundary condition at the soil surface (at the top of lysimeters) is given as the known concentration function $C(0, t) = C_0(t)$ where $C_0(t)$ is the deuterium content measured directly as a weighted weekly mean in precipitation (input function $C_{in}(t)$, shown in Figure 7.12a). At the bottom of the lysimeters the complete mixing of tracer was assumed:

$$\frac{\partial C}{\partial z} = 0 \quad \text{for} \quad z = -L \quad (7.5)$$

where L is the length of the column.

Generally, the application of the VFDM for detailed water flow or tracer transport simulations requires a sufficient spatial and temporal database, which is often not

available. This is the reason why the applicability and the quality of the results of another, simpler model were tested. This model was the lumped-parameter steady state Dispersion Model (DM), as described by (5.113) with (5.117) in Section 5.4. That model assumes dispersive distribution of the transit time of tracer particles between input and output from the system and has two fitting parameters: the apparent dispersion constant, $(P_D)^*$ and the mean transit time of tracer, T^* , (5.123). It requires only the input and output concentrations of the tracer as a function of time. Both fitting parameters have a completely different definition for saturated and unsaturated porous media.

In the case of a saturated porous medium (water system with a negligible portion of immobile water), the model parameters are equal to $(P_D)^* = P_D$ and $T^* = T_0$ where, P_D is the dispersion parameter, while T_0 is the mean transit time of water through the system:

$$T_0 = L/\bar{v} = \frac{L\bar{\theta}_m}{\bar{q}} \quad (7.6)$$

where \bar{v} is the mean velocity of water through the system, defined in this case as: $\bar{q}/\bar{\theta}_m$, while \bar{q} is the mean water flux (equal to the recharge rate), and $\bar{\theta}_m$ is the mean mobile porosity, being in this case equal to the saturated porosity ($\bar{\theta}$).

In the case of an unsaturated porous medium the model parameters are equal to

$$(P_D^*) = P_D + \frac{f^2\bar{q}}{(1-f)\bar{\theta}\omega L} \quad (7.7)$$

and

$$T^* = T_t = \frac{\bar{\theta}}{\theta_m} T_0 = \frac{T_0}{1-f} \quad (7.8)$$

with T_t being so-called mean transit time of tracer.

7.2.2.4 Results and conclusions

The calibration of both models was carried out for the observation period of seven years (1985–1991) and separately for each year. Fitting and resulting parameters found for those observation periods are summarized in Tables 7.3 and 7.4, respectively. The best fit curves for three lysimeters (S159, S162 and S163) obtained with VFDM and DM models over the entire observation period are presented in Figure 7.13. Both models were calibrated to the experimental data with similar accuracy. Using VFDM, it was possible to fit output concentrations with the same accuracy, assuming that the entire volume of water takes part in the motion. The mean transit time of tracer found with the DM was used to estimate the average content of the entire volume of water in the

Table 7.3 Transport parameters and moisture content obtained over the entire observation period (1985–1991) by applying DM and VFDM models

| Lysimeter | VFDM: Fitted α_L/L | Calculated θ (cm ³ /cm ³) | DM: Fitted T^* (weeks) | Fitted (P_D)* | Calculated θ (cm ³ /cm ³) |
|-----------|------------------------------|--|-----------------------------|----------------------|--|
| S156 | 0.015 | 0.181 | 19.5 ± 1 | 0.015 | 0.168 ± 0.008 |
| S158 | 0.015 | 0.181 | 22.5 ± 1 | 0.015 | 0.173 ± 0.008 |
| S159 | 0.010 | 0.243 | 31.0 ± 1 | 0.010 | 0.265 ± 0.008 |
| S160 | 0.025 | 0.063 | 8.5 ± 0.5 | 0.020 | 0.075 ± 0.005 |
| S161 | 0.025 | 0.059 | 7.5 ± 0.5 | 0.020 | 0.068 ± 0.005 |
| S162 | 0.025 | 0.082 | 10.5 ± 1 | 0.020 | 0.089 ± 0.008 |
| S163 | 0.015 | 0.171 | 25.5 ± 1 | 0.020 | 0.214 ± 0.008 |

Table 7.4 Parameters of the lumped-parameter (DM) obtained by calibrating the model to the deuterium contents taken for each separate calendar year. The accuracy in determining of fitting parameters T^* and (P_D)* are ±0.5 week and ±0.005, respectively

| Lysimeter | Period of time: | 1985 | 1986 | 1987 | 1988 | 1989 | 1990 | 1991 |
|-----------|-----------------|------|------|------|------|------|------|------|
| S156 | T^* (weeks) | 18.5 | 19.5 | 17.5 | 18.5 | 21.5 | 19.5 | 21.5 |
| | (P_D)* | 0.02 | 0.02 | 0.02 | 0.02 | 0.02 | 0.02 | 0.02 |
| S158 | T^* (weeks) | 22.5 | 28.0 | 21.5 | 21.0 | 19.5 | 21.0 | 23.5 |
| | (P_D)* | 0.02 | 0.02 | 0.02 | 0.02 | 0.02 | 0.02 | 0.02 |
| S159 | T^* (weeks) | 28.0 | 30.0 | 32.0 | 32.0 | 33.0 | 31.5 | 33.0 |
| | (P_D)* | 0.01 | 0.01 | 0.01 | 0.01 | 0.01 | 0.01 | 0.01 |
| S160 | T^* (weeks) | 7.5 | 9.0 | 8.5 | 7.0 | 9.0 | 9.5 | 10.0 |
| | (P_D)* | 0.02 | 0.02 | 0.02 | 0.02 | 0.02 | 0.02 | 0.02 |
| S161 | T^* (weeks) | 6.5 | 7.5 | 7.0 | 7.0 | 8.0 | 8.5 | 9.0 |
| | (P_D)* | 0.02 | 0.02 | 0.02 | 0.02 | 0.02 | 0.02 | 0.02 |
| S162 | T^* (weeks) | 12.0 | 9.5 | 9.5 | 9.5 | 9.0 | 11.0 | 12.5 |
| | (P_D)* | 0.02 | 0.02 | 0.02 | 0.02 | 0.02 | 0.02 | 0.02 |
| S163 | T^* (weeks) | 28.0 | 26.5 | 23.5 | 23.5 | 26.5 | 28.0 | 29.0 |
| | (P_D)* | 0.02 | 0.02 | 0.02 | 0.02 | 0.02 | 0.02 | 0.02 |

lysimeter. Due to the fact that it was not possible to determine if the model parameter T^* corresponds to the mean transit time of water (when $f = 0$) or tracer (when $f > 0$), it was not possible to estimate the portions of mobile and immobile water. Average water contents found for different soil materials using the DM approach were very close to those obtained with the VFDM model (maximal relative difference of about 20%).

The water contents found by fitting the DM and the VFDM are summarized for all soil materials in Figure 7.14. This figure represents the general goodness of modelling results using the DM in comparison to modelling results obtained with the VFDM. The diagonal line in the figure represents the situation when both models yield exactly the same water contents. The regression line found for the modelling of the whole observation period is parallel to the diagonal and shifted by about 1.0 vol.-%. This

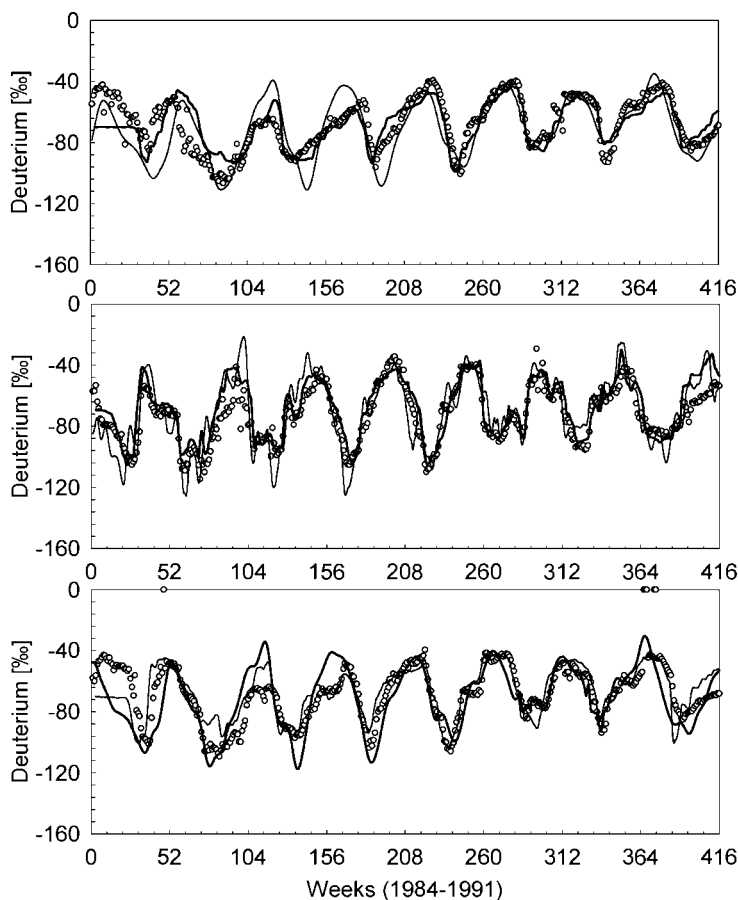


Figure 7.13 Deuterium contents in water flowing out from lysimeters filled with (top) Quaternary quartz sand (S159), (middle) fluvioglacial gravel (S162) and (bottom) Tertiary sand (S163): measured (circle) and calculated using the VFDM (bold line) and the DM (thin solid line) for the whole observation period. The accuracy of fitting with VFDM and DM is equal to $\delta = 0.55$ and 0.65% , respectively.

means that, for the overall long-term observation period, the DM yields water contents of that are on average about 1.0 vol.-% higher than those found with the VFDM. In the modelling of separate calendar years, the regression line found is also parallel to the diagonal and shifted by about 0.7 vol.-%. This means that, in that case, the DM generally yielded water contents that were about 0.7 vol.-% higher. The aforementioned accuracy ranges are astonishingly good when one takes into account the variability of hydraulic parameters that may have resulted from natural atmospheric conditions and/or inhomogeneities of soil materials.

The results obtained in this study show that environmental deuterium measured under natural flow conditions in precipitation and water flowing from the unsaturated

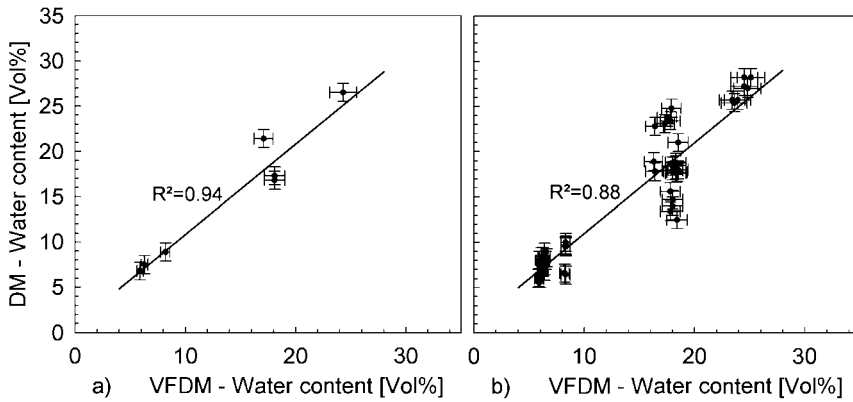


Figure 7.14 Comparison of estimating soil water content with the lumped-parameter approach (DM) to results obtained with the VFDM model, by fitting the models to the entire observation period of seven years (left) and to single calendar years (right).

zone, can be interpreted using a relatively simple modelling approach (DM). In the experiments considered herein, the DM, although it was designed primarily for steady flow, also performed very well under variable flow conditions. The output concentration curves for different soil materials, each with strongly different soil characteristics, fit the experimental data with almost the same accuracy as a more exact variable flow model. This shows that the DM can be applied successfully to describe tracer transport through the unsaturated water zone and might also be a suitable tool for the modelling of conservative pollutant transport. This is especially true for a long-term prognosis considering the time scale of several years: the longer the observation period, the better is the estimation of apparent parameters. The DM model cannot discern whether the system consists of both mobile and immobile water, or whether the entire volume of water takes part in the motion. The transit time, without defining whether it is transit time of water or transit time of tracer, estimates the mean water content in the considered soil materials to a good degree of accuracy. This indicates that the lumped-parameter DM can also produce satisfactorily accurate estimates of the average water contents (see Figure 7.14).

7.2.3 Case study: 'Determining the filtration capacity of soil-aquifer systems by multi tracer experiments'

7.2.3.1 Introduction

The increasing efforts toward the protection of groundwater resources require objective criteria in order to evaluate pollutant migration under unsaturated and saturated water flow conditions. Obviously, the filtration capacity of soils and aquifers plays a decisive

Table 7.5 Characteristics of tracers used

| Tracer | Sort | Abbreviation | Dimension |
|---------------------------|---|--------------|---------------|
| Uranine | Soluble dye | UR | $10^{-3} \mu$ |
| Sulforhodamine G extra | | SRG | $10^{-3} \mu$ |
| Bacteria | - Streptokokkus faecalis ATTC 19.433 - Coliforme germs out of drinking water | Bak | 1μ |
| Spores | Lycopodium spores coloured | Spo | 30μ |

role. The availability of experimentally proven data is important, especially in the delineation of protection zones for water supply installations.

The different characteristics of artificial tracers, both soluble and particle, which result in different flow behaviour, can be used to determine the filtration capacity of soils and aquifers. The filtration of specific tracers in a given substrate corresponds to its filtration capacity. It is defined as the ratio of tracer mass which moves through (mass injected–mass irreversible adsorbed) to the mass of tracer injected.

Therefore, a standard test arrangement for the combined application of four tracers was established: two soluble fluorescent tracers with different sorption potential and two drift substances: bacteria and spores. The working hypothesis is: the differently shaped tracers of different characteristics will pass the filtration layer to different degrees according to the filtration capacity of the substrate (Leibundgut and Lüthi, 1977). The filtration acts primarily by mechanical filtration, which will affect the passage of the drift substances, whereas solute tracers would merely pass through. The diameter magnitudes of the tracers are listed in Table 7.5. Other processes, like sorption, ion exchange and microbiological decomposition are effective in all of the tracers used and also considered part of the overall filtration process. Hence, the filtration can be regarded as a measurement of the total filtration capacity.

7.2.3.2 Laboratory experiments

To obtain an initial sense of the processes, laboratory experiments were conducted initially. Next, a proven test arrangement, as depicted in Figure 7.15, was used, thus allowing through-flow-measurement (Leibundgut 1981a).

Coevally, the laboratory experiments should determine whether they can replace the in situ experiments. Five different substrates were tested (Table 7.6) using the tracers listed in Table 7.5.

All of the soils reveal a consecutive increase of filtration capacity from the solute tracer to bacteria to spores (Figure 7.16). The idea behind the determination of the filtration capacity is already formulated above. The filtration capacity is expressed as 'filtration coefficient', calculated in a similar way as relative mass recovery of tracer

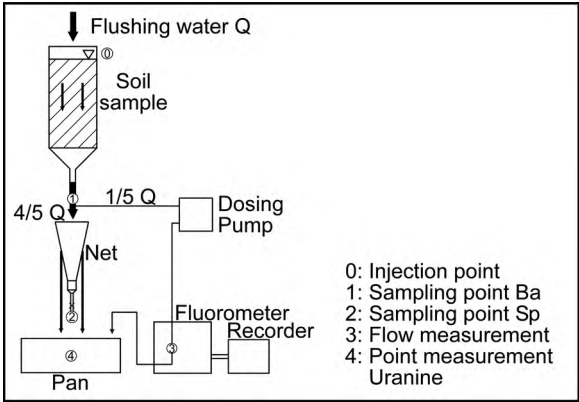


Figure 7.15 The laboratory test arrangement. Filtration cylinder is 30 cm in height, 400 cm² in diameter.

RR(t) defined by Equation (5.40) in Chapter 5. Here the RR(t) is calculated for the observation time corresponding to $t = \infty$, which theoretically reads as:

$$F_C = RR(t = \infty) = \frac{M_{recover}(t = \infty)}{M} \quad (7.9)$$

where

F_C = filtration coefficient

M = injected tracer mass

$M_{recover}$ = tracer mass recovered after sufficiently long time ($t = \infty$)

The value of $F_C = 1$ means no filtration effect; the total amount of injected tracer is recovered in sampling. The value of $F_C = 0$ stands for a complete filtration effect, proven by the complete irreversible retardation of the tracer in the system under investigation.

However, due to inconsistent data from laboratory tests, the direct transfer of the coefficients from lab to field was abandoned. The macropores found in natural settings increased the conductivity values over short vertical distances, as found in the laboratory test arrangement, in an unacceptable manner.

Table 7.6 Substrates tested in laboratory experiments

| Code | Depiction |
|------|---|
| B | Sand washed, grain size 0–4 mm crushed |
| Bg | Sand unwashed, grain size 0–4 mm uncrushed |
| Sch | Fluvio-glacial gravel, grain size 0–80 mm |
| H | Brown soil uncovered with vegetation, disturbed |
| Hb | Brown soil covered with vegetation, undisturbed |

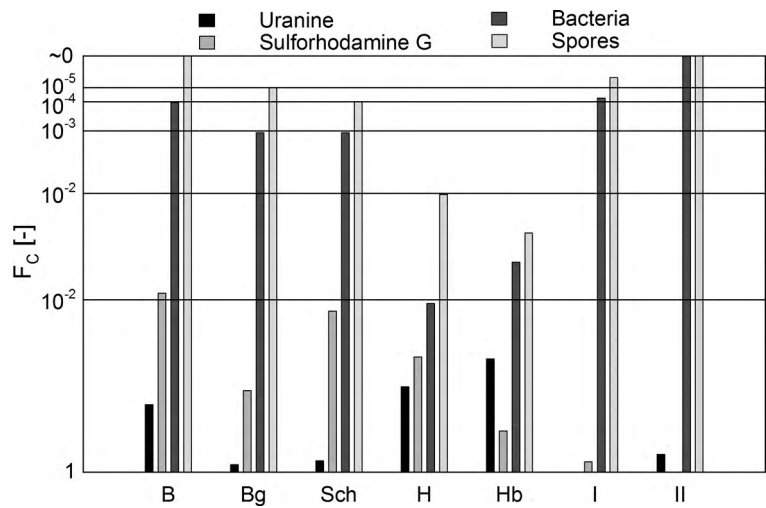


Figure 7.16 Filtration coefficients (F_c) of different tracers in different substrates B – Hb determined in laboratory test (see Table 7.6). Filtration coefficients determined in field experiments (I and II) are described below.

7.2.3.3 Field experiments

The filtration capacity of a water supply installation is usually determined first by assessing the vertical infiltration through the vadose zone, and secondly by testing the horizontal passage through the aquifer. Accordingly, these two filter test tracks with potentially different filtration capacities were chosen as subsets. To assure the comparability of the test results, both experiments were carried out at the same experimental station, which was situated in a fluvioglacial aquifer overlain by a thick brown soil (Figure 7.17).

The geological, hydrological and pedological boundary conditions in the test area are largely known (Leibundgut, 1975, 1981b). The horizontal groundwater flow direction goes from G 205 to G 101. The mean groundwater velocity in the aquifer is 7 m/d, and the maximum measures between 180 and 290 m/d. Like the aquifer, the soil cover

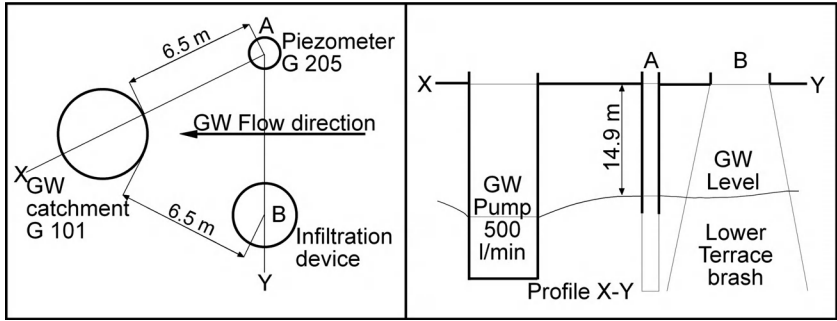


Figure 7.17 Schematic of the field test arrangement. Left: top view with axes of profiles. Right: cross section through aquifer.



Figure 7.18 Left: Injection equipment consisting of cone and fixed hose introduced in the 4 in.-well; right: Injection of concentrated Uranine solution in a filtration pool.

also shows a high conductivity due to the excessive occurrence of bio-macropores. Nevertheless, the thick brown soil layer has an excellent filtration potential (German and Beven, 1981).

In the first field experiment, the tracers were injected through a hose directly into the aquifer using a well (Figure 7.18). The head of the well is equipped with a hinged double board. It enables measurement, injection and sampling without removing the ground-water level monitoring device. The horizontal flow path with its high conductivity represents an aquifer with relatively low filtration capacity.

The injection during the second field experiment took place on top of the covering soil surface. According to the test arrangement scheme (Figure 7.17) the tracer solution infiltrated from within a percolation pool 80 cm in diameter (Figure 7.18, right).

The sampling was carried out in the pumping station by means of a bypass outlet (Figure 7.19, right). The fluorescent tracers were monitored by a through flow fluorometer, while bacteria and spores were collected by means of a plankton net (Figure 7.19, left) and were analysed in the field lab inside the pump station. The tracer injection masses listed in Table 7.7 were calculated according to the formula of Leibundgut and Wernli (1982) given in Section 6.1. The optimal target concentrations/number of particles is related to Uranine.

Table 7.7 Injection characteristics of the field experiments

| Tracer | Injection mass | Volume of flushing water |
|--------------|---|--------------------------|
| Experiment 1 | | |
| SRG | 10 g | 15 l |
| Bacteria | $15 \text{ l} = 7.5 \cdot 10^{10} \text{ CFU}$ | |
| Spores blue | $10 \text{ g} = 2 \cdot 10^{19}$ | |
| Experiment 2 | | |
| UR | 20 g | 750 l |
| Bacteria | $45 \text{ l} = 2.25 \cdot 10^{11} \text{ CFU}$ | |
| Spores red | 10 g | |

CFU: Colony Forming Units

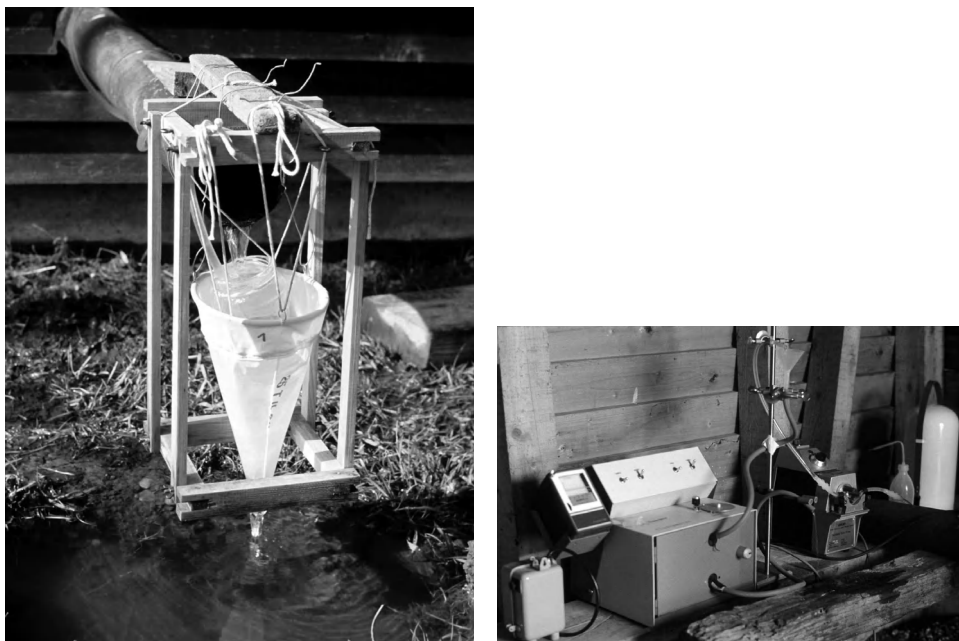


Figure 7.19 Left: Sampling of particle tracers by means of a plankton net; right: through-flow-measurement of the fluorescent tracer in the field lab within the pump station.

Whereas in field ‘Experiment 1’ (low filtration capacity) both the solute and the bacteria and spores tracer were able to pass (Figure 7.20), in field ‘Experiment 2’ (high filtration capacity) only the solute tracer was able to overbear the resistance (see Figure 7.16). The calculation of the Filtration coefficient (F_C) needs the transformation of the breakthroughs in normalized recovery masses according to the procedure given in Section 5.1.2. Uranine: Bacteria: Spores are at the ratios of = 1 g : 10 Mia : 2 g.

7.2.3.4 Assessment of results and methodology

Both, laboratory and field experiments show the suitability of combined applications of tracer use for the ascertainment of the filtration capacity of soils and groundwater aquifers. Following the hypothesis, tracers are filtered according to their size and sorption properties. The breakthrough of different tracers is related to the filtration capacity of the substrate (Table 7.8). Uranine simulates a soluble (penetration) tracer, bacteria simulate artificially injected (pathogenic) germs and clubmoss spores simulate finely dispersed suspended load, larger molecules and larger germs respectively. The solute tracer (Uranine) indicates if hydrological connections actually exist (reference tracer). The experiment is only valid when this connection is proven. The tracer Uranine is selected as the reference tracer due to its low adsorption and high mobility in various media (see Chapter 4).

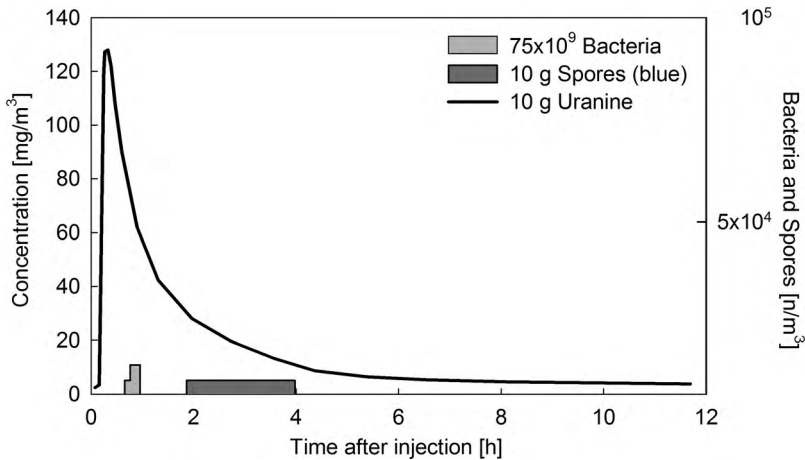


Figure 7.20 Tracer breakthrough in field experiment 1.

The delineation of groundwater protection zones requires the application of objective and comparable basics. The significance may not only be hydrological but juristic as well, since the experiments provide hard data. Thereby, modifications of the presented test arrangement for specific purposes are easily possible. To generalize, and to allow an objective evaluation of the filtration, coefficients are placed in a classification schedule (Table 7.8). The degree of filtration capacity is dependent on the number of the filtration coefficients given by the respective tracers. The investigated soil-aquifer system can be classified according to its filtration capacity.

To obtain comparable results, the following test arrangement is proposed: The injection shall be realized simultaneously on the unharmed surface of a groundwater aquifer in a percolation pool with a diameter ≥ 80 cm. The water level in the pool should not exceed 20 cm and should be kept constant. Before injection, the subsurface needs to be pre-flushed to saturate the filter layer, since the amount of the flushing water is a function of filter distance and pore volume. The volume of flushing water can be estimated according to the information given in Section 6.1. Its correct estimation is

Table 7.8 Appraisal of filtration capacity on the filtration coefficients (F_C) ascertained in the experiment

| Breakthrough of tracer | Filtration coefficient (F_C) | Degree of filtration capacity |
|------------------------|----------------------------------|----------------------------------|
| Uranine | Reference tracer | Proof of hydrological connection |
| Bacteria | $< 10^{-6}$ | high |
| | $10^{-5} - 10^{-6}$ | moderate |
| | $> 10^{-5}$ | low |
| Spores | $< 10^{-5}$ | moderate |
| | $10^{-5} - 10^{-4}$ | low |
| | $> 10^{-4}$ | very low |

crucial to record reliable values of filtration coefficients. The tracer masses to be injected are calculated as a function of the amount of flushing water, as well as being dependent on the discharge of the tested system. It is sufficient to calculate only the amount of the solute tracer and to subsequently deduce the amounts of the other tracers from this (see Chapter 4 and Section 6.1). According to experience, the relation of the injection mass between the different tracers is approximately:

$$\text{Uranine} : \text{Bacteria} : \text{Spores} = 1 \text{ g} : 10 \text{ Mia} : 2 \text{ g}$$

Comparable results always require a tracer injection in similar amounts.

Recent examples of multiple tracer studies using both solute and particle tracers are, for example: Vilks and Bachinsky (1996), Woessner *et al.* (2001), Mortensen *et al.* (2004), Pang *et al.* (2005) or Göppert and Goldscheider (2008). The case study 'Environmental deuterium transport through soils' (Section 7.2.1) is related to the topic discussed above (Maciejewski *et al.*, 2006; Maloszewski *et al.*, 2006; Van Genuchten and Wierenga, 1977).

7.3 Surface water

Surface water systems play an important role for humans and the biosphere. They serve as water supply, as natural flood retention reservoirs, fishing and recreation areas, and they provide habitats for flora and fauna. Surface waters are the dominant aquatic ecosystem on earth with a high ecological, economic and cultural significance. In addition, they are of crucial significance as transport pathways and are closely linked to settlements worldwide. The drainage system of the river basins also serves as a transport network for natural and anthropogenic solutes and sediments. Consequently, rivers are the most important global transport veins for sediments, minerals, nutrients and contaminants. The lakes as water systems with limited water movement are terrestrial sinks for all of these substances. Hence, an understanding of hydrological processes and characteristics of surface waters is of major interest for lake and river basin management activities. Again, tracer methods are a powerful tool for investigating system functioning and the often complex internal processes.

While water flows through a system of pores or fissures in groundwater aquifers, surface water bodies constitute the 'aquifer' itself. Consequently, the dynamic processes are different, as are the adequate tracer techniques. The applications mainly deal with transport processes in rivers and lakes. Investigation of interactions between surface waters and adjacent groundwater aquifers are also of particular interest for hydrological issues such as water supply.

Natural tracers are used frequently in surface water research for long-term investigations of the entire system, as well as for studies of seasonal variability. Furthermore, environmental tracers can be used to study nonpoint contamination due to their distributed input into the hydrological system.

In water courses and lakes of all scales the application of artificial tracers is focused mainly on issues related to point sources of contaminants which is, on the other

hand, the most typical problem to be solved by means of artificial tracers. Obviously, investigations with artificial tracers are restricted by scale. Only water bodies up to a certain size can be traced due to the targeted concentration and given detection limits of tracers. It is a specific advantage of artificial tracers that they are suited explicitly for the investigation of actual and specific hydrological conditions. On the other hand, strictly speaking, the results are also only valid for the respective hydrological condition.

In streams and lakes aerial photos can be used for evaluating the horizontal propagation of dye tracer clouds provided the visibility limit is exceeded. Aerial photos may supplement tracer measurements, yielding fast and general spatially distributed information. The evaluation of photos with the help of photo-densitometry through calibration of colour values with measured 'ground truth' concentrations enables a rough quantitative determination of tracer concentrations. However, this is restricted to a very thin surface layer only (Jäggi and Paris, 1978). Currents and river inflows into lakes can be detected with natural tracers by remote sensing techniques, for example by their chlorophyll and suspended sediment loads (e.g. Rainey *et al.*, 2003; Giardino and Gomarasca, 2006).

7.3.1 Lakes

In lake research and paleohydrological investigations of lake sediments natural tracers are used frequently to determine lake water balances, groundwater-lake exchange, lake water residence times, as well as stratification and mixing characteristics.

Lake mixing and internal flow processes induced by wind and tributaries from different catchments can be determined by means of water isotopes (Siegenthaler, 1982; Gibson *et al.*, 2002, 2005). Investigations of vertical exchange processes in lakes and quantification of transport mechanisms and gas diffusion coefficients are often carried out with natural tracers, for example tritium (Quay *et al.*, 1980). The vertical as well as the horizontal mixing of lakes was traced by SF₆ (Maiss *et al.*, 1994; Maiss, Ilmberger and Münnich, 1994; Schlatter, Wüst and Imboden, 1997; von Rohden and Ilmberger, 2001). Temperature and electric conductivity are also commonly used as tracers for the matter of lake mixing (e.g. Boehrer, Matzinger and Schimmele, 2000).

Albrecht, Goudsmit and Zeh (1999) used the radioactive isotope ⁶⁰Co, which was emitted by a nuclear power plant into the River Aare (Switzerland) some kilometres upstream of Lake Biel, as pollution tracer in combination with Uranine in order to track river water intrusion into the lake during different seasons. They found significant differences for Aare water residence times in the lake during summer stratification (6–7 d) and during winter circulation (up to four months), respectively.

A method used for the determination of lake water balance parameters based on isotopes is described, for example, by Gat (1970, 1981), Zuber (1983) Gonfiantini (1986) or Mook (2001). Gibson (2002a, b; Gibson, Prepas and McEachern, 2002; Gibson *et al.*, 2005) reviews several isotope approaches in Canadian lakes and describes different issues such as steady-state and nonsteady state formulations of stratified and nonstratified lakes. Furthermore, examples are provided on how to estimate through flows, residence times and runoffs of headwater lakes in Alberta, Canada.

Artificial tracers can be used in lakes to solve various different hydro-limnological problems. But above all, they are used to determine the current dynamics in lakes induced by wind and streams (see colour plate section, Plates 5–7). A classical example is described in the case study of Lake Bled (Section 7.3.4). The systematic investigation of lake currents with artificial tracers began in the 1970s (Nydegger, 1967, 1976; Leibundgut and Hirsig, 1977). Practical applications such as the spreading of sewage effluent in lakes or the impact of internal lake remediation measures such as deep water outlets are also investigated preferably with tracing tests (Leibundgut and Zupan, 1992; Env. Canada, 1993; Stevens, Lawrence and Hamblin, 2004). The use of artificial tracers allows the determination of convective, dispersive and diffusive processes (e.g. Werthemann, 1980a, b). In Lake Sempach, the impact of lake ventilation was investigated using tracers (Hirsig and Petermann, 1984). Up to now, calibration and validation of mathematical current models based on experimental tracer results have only rarely been applied, although this approach seems promising (Leibundgut *et al.*, 1983; Peeters, Wüest and Imboden, 1993; Peeters *et al.*, 1996; Goudsmit *et al.*, 1997; Rajar, Četina and Širca, 1997). Furthermore, artificial tracers can be applied to detect sublacustric and submarine water exchanges and to determine these flows quantitatively (Attinger and Leibundgut, 1986; Leibundgut and Attinger, 1988; Rieg and Leibundgut, 1992; Ross, Rieg and Leibundgut, 2001). Tracing techniques are suitable for investigating hydrological connections between lakes, ponds, or pools and the adjacent aquifers (Leibundgut and Adler, 1989).

Irradiation, important for photosynthesis and thus for primary production, can be determined integrally by injecting a light sensitive fluorescent tracer, as described in Section 4.1. It is also necessary in this case to correct the influence of the dispersion by using a second tracer that is not sensitive to light (Behrens and Demuth, 1992).

Carpenter (1968) described a test in Baltimore Harbour with Rhodamine B. The goal of the test was to investigate the exchange processes in the harbour, in order to determine the capacity of the harbour basin for industrial sewage. Costin (1963) reported about a similar test in the New York Bight. Joseph, Sendner and Weidemann (1964) described a carefully conducted test series with Rhodamine B in the North Sea. The distribution of sewage plumes in coastal water has been followed repeatedly with bacterial tracing tests. Robson (1956) and Pike, Bufton and Gould (1969) also used the isotope ^{32}P . To trace coastal water and also the open sea, perfluorochemicals can be applied. To do this, Wanninkhoff, Ledwell and Broecker (1985) and Watson, Liddicott and Ledwell (1987) used sulfurhexafluoride, the latter also used perfluorohydrocarbons. Roldao, Pegly and Leal (1997) reported about large-scale tests with fluorescent tracers where industrial and domestic sewage was labelled and introduced into the sea by submarine outfalls. This study was aimed at evaluating the effluent's dilution pattern in the sea water.

7.3.2 Rivers

In the investigation of a river's hydrodynamics artificial tracers are often applied. Seo, Baek and Jeon (2006) conducted tracer tests (slug tests) at several sites in tributaries of the Han River, Korea to analyse the transverse mixing of potential pollutants. To study

the potential effects of accidental leaks of nuclear power plants at two Spanish rivers Palancar *et al.* (2003) calculated dispersion coefficients using experimental tracer data and hydraulic parameters. A method employed to determine longitudinal dispersion coefficients in large rivers using SF₆ and ³He is presented in Clark *et al.* (1996).

In the case study (Section 7.3.2) a tracer experiment was conducted in order to investigate the influence of in-channel constructions on the dispersion and dilution dynamics of substances from anthropogenic sources. The hydrodynamical parameters such as mean flow velocity and dispersion can be used to describe pollutant propagation and dilution (e.g. Hubbard *et al.*, 1982; Kilpatrick and Wilson, 1989; Spreafico, Leibundgut and Kühne, 1989; Leibundgut, Speidel and Wiesner, 1993; van Mazijk, 1996). Case Study 7.3.1 describes an example where a warning system was developed, with the aid of a tracer calibrated matter propagation model, in order to predict the arrival time, the duration and the concentrations of the pollutant plumes.

Ho, Schlosser and Caplow (2002) injected SF₆ into the Hudson River to study advection, dispersion and air-water gas exchange, as these are major physical processes controlling the movement and modification of contaminant concentration in the river. The dispersion of treated sewage in rivers is a key problem in water protection. Reber and Weingartner (1986) quantified the amount of phosphorus that is released into a back water of a river by a treatment plant upstream. The fraction of sewage water flowing into the intake of the backwater was investigated by fluorescent tracers.

The investigation of stream erosion and sedimentation geomorphologic processes forms another broad field of research using tracer techniques but is not covered in this book. Knowledge of erosion and sedimentation rates plays a significant role in water engineering (e.g. bank or bridge pier stability) and as well as for ecological functions (e.g. habitat or biodiversity development). Different tracers, including particle tracers, are being used to investigate fluvial sediment movement. The book '*Tracers in fluvial geomorphology*' (Foster, 2000) describes sediment tracing methods such as radionuclide, geochemical and magnetic approaches. '*Tracing fluvial sediments*' (Hassan and Ergenzinger, 2003) also provides some case studies in different climates, providing a broad overview of the application in fluvial geomorphology. To cite just a few of the tracers used in these studies: exotic particles, painted particles, fluorescent paint, radioactive tracers, ferruginous tracers, magnetic tracers, active tracers including radio transmitters, suspended load and wash load are applied.

Physical parameters of water such as reaeration or irradiation can be determined with tracers indirectly. Reaeration is a key parameter for natural attenuation in rivers. For measurement of reaeration, a gas tracer (e.g. ⁸⁵Kr) can be injected undergoing gas exchange with the atmosphere. Since this process is controlled by the similar kinetics as reaeration, the reaeration coefficient can be determined directly from tracer concentrations. The simultaneous decrease of concentration due to dispersion can be corrected for by using a second conservative tracer (Günthert and Behrens, 1982; Kilpatrick and Wilson, 1989).

A fundamental and widely used application of artificial tracers is the measurement of discharge in highly turbulent rivers without a well-defined or accessible cross section. This method is described in detail in Chapter 6.

7.3.3 Specific aspects of using tracers in surface waters

Specific characteristics required for successful applications of tracers in surface water are good accessibility of the water bodies to be traced and their highly dynamic behaviour. In surface water a quickly spreading tracer plume needs to be measured. In addition, measurements at different water depths may be required to determine the three-dimensional tracer distribution as a function of time. As an exception, tracer distribution in rivers after complete mixing at steady state can often be approximated by a one-dimensional distribution (cf. Sections 7.3.2; 5.3).

The high dynamics of flow and transport processes in surface water require basically in situ measurements (Leibundgut and Hirsig, 1977; Leibundgut and Zupan, 1992; Peeters and Wüest, 1992; Peeters *et al.*, 1996; Goudsmit *et al.*, 1997). However, only a few natural or artificial tracers can be measured in situ with sufficient precision. Details on the possibilities, limitations and essential considerations for in situ measurements are described in the forthcoming chapters.

When artificial tracers are injected into surface water, the tracer needs to meet certain specific requirements. As described in detail in Chapter 4 many fluorescent tracers are subject to photochemical decay. This depends on irradiation and tracer specific sensibility to photochemical decay. Table 7.9 shows Uranine tracer losses at different depths and highlights the problem. According to the positive correlation of light absorption with depth, tracer loss decreases with depth. The slightly differing data are due to measurements at different locations but with similar experimental design. The differences highlight the sensitivity of in situ field measurements. Care needs to be taken when using such data for the correction of measured data. The effective measured loss at a cross section with complete mixing results from complex processes that are changing with depth. Photolytic decay in river water during an experiment that lasted several days shows that tracer loss is proportional to time. Loss in plain sunlight can give a reference. With the exception of the first two values, which are related to incomplete mixing, differences between day and night appear clearly (Figure 7.21).

Table 7.9 Photolytic decay of Uranine in different water depths measured in situ in river water (Naturaqua, 1989, 1994)

| Water depth [m] | Concentration [mg/m ³] | | |
|-----------------|------------------------------------|------------------|--------------------|
| | Before exposition | After exposition | Losses per day [%] |
| 0.1 | 10 | 1.66 | 83.4% |
| 0.2 | 10 | 2.3 | 77% |
| 0.5 | 10 | 3.43 | 65.8% |
| 1 | 10 | 4.89 | 50.9% |
| 1 | 10 | 4.0 | 60% |
| 2 | 10 | 6.75 | 32.5% |
| 2 | 10 | 6.0 | 40% |
| 0.2 above water | 10 | 0.1 | 99% |

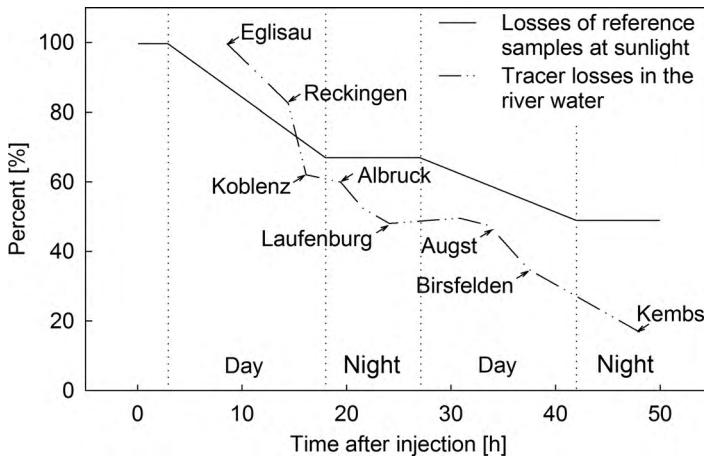


Figure 7.21 Losses (%) of fluorescent tracer (Uranine) due to photolytic decay along a river distance of 66.5 km lasting several days (see case study 7.3.1). Source: Naturaqua (1994).

Similar attention needs to be paid to higher biological activity and the higher biochemical decay present in surface water as compared to groundwater. Since only degradable tracers should be applied for environmental reasons, quantitative experiments should be restricted to short-term tests of several days at most. Since aquatic life comes into contact with the tracers used, ecotoxicological harmlessness is a further important requirement imposed on the tracers used in surface water. The attributes of artificial tracers needed for surface water experiments are documented in Chapter 4.

The hydrodynamic characteristics of lakes exhibit prominent differences to other hydrological system elements. Although there are similarities to streams in terms of tracer applications, which were outlined above, there are also particularities and differences in the case of tracer experiments in lakes that need to be considered and which necessitate specific approaches. Additional relevant information should be gathered beforehand to ensure the correct classification and interpretation of the results. These are the inflow and outflow relationships, wind and weather conditions, as well as air temperature and irradiation. The determination of temperature-depth profiles during the tracer experiment is indispensable. When necessary, electrical conductivity and oxygen distribution must also be determined. Hirsig, Leibundgut and Nydegger (1982) differentiate between external and internal artificial tracer injections in lakes. With an external injection, the water that enters the lake as a natural or artificial inflow is traced in order to observe its behaviour upon entering the lake and in the lake. In this case, a thorough mixing of the tracer solution must be guaranteed, that is a sufficiently long flow distance is necessary when using natural inflows. With an internal injection, the tracer is injected directly into the lake with a hose or a depth-injection device that injects the tracer at a specific depth (Werthemann, 1980a; Peeters *et al.*, 1996). It must be guaranteed that the dense tracer solution remains at the targeted stratification depth and does not sink. This can be assured by compensating for the density effect by tuning the temperature of the solution.

7.3.4 Case study: 'Calibration of transport models using tracer techniques – River Rhine'

7.3.4.1 Introduction

The case study presented in this section describes the investigation of flow and transport parameters in rivers by means of tracer experiments carried out in order to calibrate and verify transport models. The investigations of transport processes in the Rhine began in the aftermath of an accident at the Sandoz chemical plant in Switzerland in 1986. As a consequence of the accident, large quantities of chemicals were flushed into the River Rhine, causing considerable damage to the ecosystem. During the days and weeks that followed, the extraction of riverbank filtrated drinking water had to be stopped (Capel *et al.*, 1988; Mossman, Schnoor and Stumm, 1988).

In addition to general ongoing pollution of rivers by, for example treated sewage and diffuse inflow, accidental spills such as occurred in the Sandoz incident represent a major threat to the ecology of rivers and to the associated economies. In the event of accidental spills, downstream users need to be informed of the propagation of the pollutants and of their projected concentrations. The application of two- and three-dimensional transport models is not plausible in this context because of their complex, time consuming computations. To meet the required short warning time for the users downstream high speed computations are needed.

Consequently, the states abutting the Rhine initiated a project to develop a model and alarm system for the waterway within the framework of the Commission for the Hydrology of the Rhine (CHR). The system was expected to both explain transport processes and to warn the partners affected in the event of similar accidents. The warning system was required to ensure the minimization of economic damage and was expected to predict the arrival time and propagation of a pollutant plume in the River Rhine. It was also a prerequisite that the model developed be applicable operationally for real-time predictions, meaning that it had to be executable on a PC and use the data available. Therefore, a relatively simple one-dimensional (1D) dispersion model was developed (Griffioen, 1989) and further refined in several steps.

The entire Rhine downstream of the Rhine Falls, which has seen the introduction of many man-made changes for the purposes of flood control and is intensively used, was investigated in the study (Figure 7.22). The river plays a vital role in the regional economy, in trade and in transport between Basel and the North Sea. Many large water suppliers draw filtrated groundwater from adjacent aquifers. To improve flood control, the river bed has been modified and stabilized along a straight line, dams and canals have been constructed, the navigation channel has been deepened and the riverbanks have been stabilized. These changes all have major impacts upon the hydraulic parameters of the river, which as a result are particularly difficult to estimate. The trans-boundary basin (185 000 km²) of the Rhine (1–320 km) drains water from nine states, namely Switzerland, Germany, France, the Netherlands, Italy, Austria, Liechtenstein, Luxembourg and Belgium. The long term mean discharge at Rheinfelden-Basel is 1037 m³/s (1935–2007) and 2234 m³/s at Lobith (1931–2004).

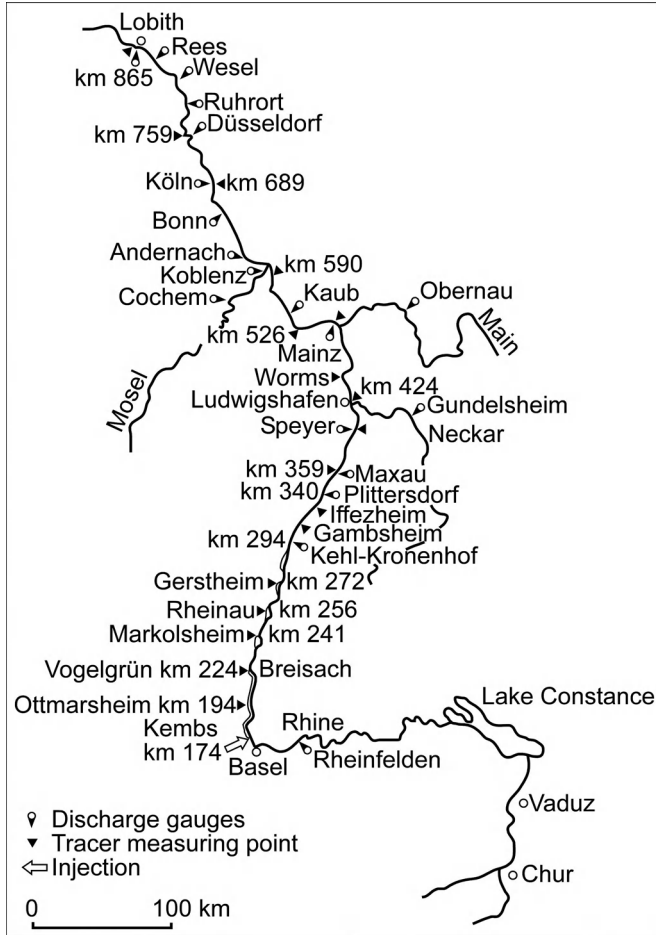


Figure 7.22 Tracer injection and observation points along the River Rhine between Switzerland and the Netherlands.

7.3.4.2 Methods

There are two methods that are used generally to estimate contaminant transport parameters in waterways. One method is based on river morphological data and hydraulic modelling – in the case of the Rhine this method is difficult to apply because of data limitations, extensive computational requirements and high levels of uncertainty. The second approach is based on transport modelling using a (1D) advection-dispersion model and employing calibration and validation procedures to estimate the parameters flow velocity (v) and dispersion coefficient (D). The important calibration/validation procedure is usually done using mathematical techniques. Their disadvantage is the limited control over natural conditions (Teuber and Wander, 1987; Kühne, 1988; Engel, Menzel and Wander, 1988). In both cases, tracer experiments are needed to

calibrate and verify the calculations. Given that exact morphological data are often unavailable, the parameter estimation technique is the more promising alternative. Tracer methods allow for model calibration and validation using field data. Such experiments, therefore, play a central role in model development of river transport models. Tracer experiments were conducted in the Rhine to collect the data necessary for the calibration and the validation of the contaminant simulation under different flow conditions and subject to the different morphological conditions prevailing along various segments of the river.

A 1D dispersion model was calibrated using the data obtained from the tracer experiments. The model incorporated longitudinal dispersion only and assumed a homogeneous distribution of the contaminant over the flow cross section. The model assumes stationary discharge relationships. The decay of contaminants was included based on a first-order term. Clearly, the error occurring over the course of the long flow distance between Basel and the North Sea (approx. 1000 km) is likely to be high. Three steps were taken to overcome this problem:

- (1) In order to take into account the differences in the morphology occurring along the Rhine, the river was subdivided into longitudinal sections (Figure 7.22). The model parameters provided by the tracer experiments were determined for each section, with the output values for a given section used as the input values for the following downstream section. Using this approach, uncertainties and errors arising from measurement errors and tracer losses could be avoided (Becker and Sosnowski, 1969).
- (2) A 1D advection-dispersion transport model (SAMF) adapted to the specific needs of the project was developed (Bremicker, 1989; Leibundgut, Bremicker and Wiesner, 1989).
- (3) The impacts of stagnant water zones on solute transport were incorporated in the 1D transport model.

Several tracer experiments were carried out in different river sections to simulate the propagation and dispersion of contaminants and to calibrate and validate the model. Model parameters were determined for individual river sections. The parameters were evaluated using the SAMF model, by fitting them with the different breakthrough curves (Leibundgut, Speidel and Wiesner, 1993). Subsequently, the parameters were applied in the calibration of the Rhine Alert Model. Stagnant water zones can have a considerable influence upon solute propagation. Their impact was studied in several sections by making *in situ* measurements from a boat equipped with a fluorometer (Variosens). The tracer breakthrough in stagnant zones was observed as a function of time and space and implemented in the model.

7.3.4.3 Model conception to be calibrated and validated

The principles underlying the theory of using (1D–3D) transport models were presented in Section 5.1. Generally, 3D dispersion models require a high storage capacity, long computing times and very detailed measurement data. Additionally, extensive mathematical numerical algorithms are necessary. The long computing times are limiting for an alert model. The transport of contaminants in the Rhine was simulated on the basis on the 1D approach (Equation (5.19), Section 5.1.1) deduced from the laws of conservation of mass, impulse and energy (Markofsky, 1980). This approach is valid when: (1) so-called conservative tracers and pollutants, which follow dispersion and advection processes only, are taken into consideration; (2) the concentrations in the river are considered after a mixing stage has been allowed for, after which the tracer (pollutant) is distributed homogeneously in the cross section perpendicular to the flow direction and (3) zones with stagnant water do not exist. The latter boundary condition is not met in the case of the River Rhine. However, by means of an adoption of the stagnant water effects into the calculations of the transport model a solution was found.

Equation (5.19) describes the change in concentration over time as a function of transport in the field of velocity and dispersion. Under natural conditions additional processes such as turbulence (time-dependent differences in velocity) and dispersion (spatial differences in velocity) also exert an influence. Under the 1D approach, and for the instantaneous injection of tracer into the river, the solution to the transport equation is provided by Equation (5.29) (Section 5.1.3). The solution provided by the equation is not wholly satisfactory, however, as it provides only mean transport parameters over the entire flow distance. Further theoretical approaches are required to account for the variability in flow conditions in the morphologically differing sections along the longitudinal profile of the river. A new approach is required to provide a theoretical solution to the shortcomings of the 1D transport (Equation (5.19)). Generally, under the 1D approach, the output concentration $C_{out}(t)$ for any type of input concentration $C_{inp}(t)$ is given by the convolution integral (5.113) provided in Section 5.4.2. For nonradioactive tracers, and after rearrangement, this reads as:

$$C_{out}(t) = \int_0^{\infty} C_{inp}(t - \tau)g(\tau) d\tau \quad (7.10)$$

where $g(\tau)$ is the normalized solution to the 1D transport Equation (5.29), which reads:

$$g(\tau) = \frac{x}{\sqrt{4\pi D\tau^3}} \exp \left\{ -\frac{[x - v\tau]^2}{4D\tau} \right\} \quad (7.11)$$

7.3.4.4 Method of resolution for river sections

To calculate the migration of a tracer in different river sections, with different flow velocities and dispersion coefficients, a method for calculating flood waves in river sections (differentiation of the St Venant equations) was translated (Becker and Sosnowski, 1969) in the same way as (7.10) and (7.11) described above. The Rhine was divided into $n = 71$ sections, for which a constant (mean) water velocity (v_n) and a constant dispersion coefficient (D_n) were assumed. The sections were differentiated according to gauging stations indicating existing water level–discharge relationships. The input concentration into each section (n), was assumed to be the corresponding output concentration from the previous section ($n - 1$). Each river section could be described on the basis of its characteristic system function, $g_n(t - \tau)$, with characteristic transport velocities and dispersion coefficients, so that the propagation of the tracer along the river could be followed:

$$C(x_n, t) = \int_0^t C(x_{n-1}, \tau) \cdot g_n(t - \tau) d\tau \quad (7.12)$$

where

$$g_n(t - \tau) = \frac{x_n - x_{n-1}}{\sqrt{4\pi D_n(t - \tau)^3}} \cdot \exp \left\{ -\frac{[(x_n - x_{n-1}) - v_n(t - \tau)]^2}{4D_n(t - \tau)} \right\} \quad (7.13)$$

with x_{n-1} and x_n the river distance markers (kilometres) at measurement points ($n - 1$) and (n), respectively; and v_n and D_n the mean water flow velocity and mean dispersion coefficient of the river section (n), respectively.

The input into the section n , $C(x_{n-1}, t)$, is indicated by the concentration identified as the outflow from section ($n - 1$). The output concentration, $C(x_n, t)$, is the concentration at the end of the river section considered, as indicated by the concentration curve (7.12). The output concentration of the first section ($n = 1$) is given by Equation (5.29), which, after rearrangement, reads as follows:

$$C(x_1, t) = \frac{M(x_1 - x_0)}{Q\sqrt{4\pi D_1 t^3}} \exp \left\{ -\frac{[(x_1 - x_0) - v_1 t]^2}{4D_1 t} \right\} \quad (7.14)$$

with M the mass of tracer injected instantaneously, Q the river discharge and x_0 the point along the river at which the injection took place.

This approach of applying the model to consecutive river segments provides a more accurate representation of tracer propagation along long river stretches, than if a bulk model would be used for the whole river (Taylor, 1954). Each stream section is characterized by different flow velocities and dispersion coefficients. The method facilitates the calculation of these sometimes very different parameters for individual sections of

the river, taking into account the varying combinations of flow velocities and dispersion coefficients. There is no averaging of these parameters over the whole flow distance.

The most effective feature of this type of calculation of tracer propagation within a river section is the use of the tracer breakthrough curves for a specific sampling point as inputs for the next downstream section of the river. This means that uncertainties and errors arising from measurement errors and tracer losses are limited to the individual river segments and the errors will not be propagated to the following downstream sections. Thus, the method of calculation facilitates an updating of tracer (and contaminant) propagation forecasts, as measured substance breakthroughs can be incorporated into the calculations by the model (Leibundgut, Bremicker and Wiesner, 1989; Bremicker, 1989). The two parameters used to calibrate the model were the mean transport velocity and the longitudinal dispersion coefficient calculated for different river sections. The deviation of the measured tracer curve from the modelled tracer curve was denoted by the standardized variation coefficient Err_n :

$$Err_n = \frac{\sqrt{\sum_{i=1}^N (C_S(x, t_i) - C_M(x, t_i))^2}}{\sum_{i=1}^N (C_S(x, t_i)/N) \cdot (N - \ell)} \quad (7.15)$$

where

N = number of measured concentrations in section n $C(t_i)$

ℓ = number of parameters in the model

$C_S(x, t_i)$ = measured concentration (profile x , time t_i)

$C_M(x, t_i)$ = modelled concentration (profile x , time t_i).

The normalized variation coefficient Err_n calculated for each section (n) representing the quality of the tracer breakthrough is a dimensionless parameter with values 0–1. It is, therefore, a suitable means of comparing the values modelled for the different profiles (sections). A normalized variation coefficient value of 0 indicates a perfect fit of the model (no differences between the measured and the calculated tracer breakthrough curve). A value of 1 means that there is no correlation between the values of the measured and the calculated tracer breakthrough curve. Values <0.25 represent a very good calibration, whereas values >0.50 indicate that the modelling of the measured tracer breakthrough is insufficient. Consequently, in this case and state the 1D approach was not suitable. The dispersion coefficient and transport velocity values determined were used as guideline values in the calibration of the actual Rhine Alert Model. For further information see e.g. Spreafico and van Mazijk (1993), van Mazijk (1996).

The first relatively simple version was developed in 1989 (Rhine Alert Model, RAM 1.0), based on a 1D advection-dispersion model. The influence of stagnant water zones (common in the River Rhine) was incorporated in version 2.0. Major tributaries were integrated in RAM 2.1 and finally, in 2000, the model was rebuilt in two dimensions, in order to calculate also the dispersion over the channel width, for example, downstream of tributaries.

7.3.4.5 Tracer experiments

Eight tracer experiments were carried out in total. Three tests investigating the river downstream of Basel (1989, 1990, 1991) and one (1988) upstream of Basel have been selected in order to present the case study. Fluorescence tracers were chosen for the purposes of the investigations. In Switzerland, Uranine was applied; in the German-Dutch experiments, Rhodamine WT was used. Given the longer flow distances, Uranine would have been subject to photolytic decay if applied in the downstream investigations.

The tracer input was assumed to occur as an instantaneous injection, although the actual injection time ranged between 1.5 and 6 min. Samples were generally taken using battery-powered, automatic sampling systems (APEG), which allowed for regular sampling at short time intervals. Real-time monitoring was not required in this instance and sampling was more reliable. Sampling was also carried out manually in part, particularly when measuring sections in situ using an underwater fluorometer (Variosens). Sampling intervals were chosen based on the results of model runs carried out prior to the test. The fluorometric analyses of the samples were carried out in the lab using a spectrofluorometer (see Chapter 4). There was no pre-treatment except for the sedimentation of suspended material in some of the samples. The HPCL analysis technique was used to determine the Rhodamine WT concentrations in the Netherlands, where tracer concentrations were low (Broer and Wijnstock, 1990). To measure the influence of stagnant water zones in the vicinity of groynes, direct measurements were made from a boat equipped with an in situ fluorometer (Variosens).

On the basis of the assumption that the tracer was distributed uniformly over the channel width, measurements could, in principle, be taken anywhere along the cross section (see Section 6.3, Figure 6.7). Nevertheless, an attempt was made to consistently sample along the river's centre line in order to minimize the influence of edge effects. Optimal sampling points can be found downstream of power plants, where mixing is assured. Insofar as it was possible, the sampling sites were located near river gauges in order to convert the measured concentrations to tracer loads. Other criteria applied in the selection of sampling sites were accessibility, and the avoidance of ships, amongst others.

The model allowed for the simulation of the solute transport for any runoff. The data for the calibration and validation by means of tracer experiments were collected for three runoff states: "low flow" ($712 \text{ m}^3/\text{s}$, 09/90), "mean flow" ($1170 \text{ m}^3/\text{s}$, 04/89) and "high flow" ($1820 \text{ m}^3/\text{s}$, 06/91).

The long term mean low flow (MNQ) at Rheinfelden is $770 \text{ m}^3/\text{s}$, the long term mean flow (MQ) is $1034 \text{ m}^3/\text{s}$ and the long term mean high flow (MHQ) is $1350 \text{ m}^3/\text{s}$. Whereas the low and mean flow experiments were close to the respective long-term means, the experiment in June 1991 deviated considerably from the long term high flow mean by occurring at a discharge of $1820 \text{ m}^3/\text{s}$. The quality of the three tests carried out in the Upper Rhine was good. A previous experiment in the Rhine upstream of Basel (1988) also served to provide an initial experience of the application of the method and insights into the processes involved.

7.3.4.5.1 Tracer experiment April 1989 The tracer experiment of April 1989 represented the mean runoff condition (discharge at Rheinfelden at the time of the



Figure 7.23 Tracer injection into the Rhine downstream of Basel.

experiment: $1169 \text{ m}^3/\text{s}$) of the River Rhine downstream of Basel (Leibundgut, Bremicker and Wiesner, 1989). Exactly at 8 a.m. on the 26th of April, 100 kg Rhodamine WT in solution were injected at Village-Neuf, downstream of Basel at the start of the Grand Canal d'Alsace (Upper Rhine channel), river distance marker 174.1 km. The injection was carried out from a ferry situated in the river's centre line (Figure 7.23). Five barrels, each containing 90 l of concentrated tracer solution, were discharged within a 5 min period. A stirring unit was applied to avoid the sedimentation of the highly concentrated tracer solution.

In order to plot the required high resolution temporal tracer breakthrough curves, eleven automatic samplers (APEG) were installed between Basel and Plittersdorf (see Figure 7.22). Where possible, sampling was done beneath power plant (PP) outlets to ensure a complete mixing of the tracers (Table 7.10).

The individual tracer breakthroughs measured at and modelled for the sampling points (Table 7.10) are depicted in Figure 7.24 and discussed in more detail in the following.

Description of the sections of Figure 7.24

Figure 7.24a: Village Neuf–Ottmarsheim river section (Rhine km 174.1–194.4).

The first appearance of the tracer at the Ottmarsheim PP occurred 4 h and 50 min after the injection 20.3 km upstream in Village Neuf. The shape of the measured tracer breakthrough curve was compact and the breakthrough time was approximately 2 h.

Table 7.10 Characteristics and results of tracer test 04/89 for the Upper Rhine

| | River section | Distance between sampling sites [km] | Rhine- kilometre $x_{n-1} - x_n$ [km] | Sampling interval $t_i - t_{i-1}$ [min] | Mean water velocity v_n [m/s] | Longitudinal dispersion coefficient D_n [m ² /s] | Normalized variation coefficient Err_n [—] |
|--------------|----------------------------|---|--|--|--|--|---|
| Village-Neuf | Ottmarsheim | 20.30 | 174–194 | 10 | 1.09 | 20 | 0.049 |
| Ottmarsheim | Neuenburg | 4.85 | 194–199 | 15 | 1.09 | 41 | 0.035 |
| Neuenburg | Fessenheim | 11.85 | 199–211 | 20 | 1.08 | 42 | 0.043 |
| Fessenheim | Vogelgrün | 13.80 | 211–224 | 30 | — | — | — |
| Fessenheim | Marckolsheim | 16.15 | 211–241 | 20 | 0.98 | 63 | 0.039 |
| Marckolsheim | Rheinau | 15.55 | 241–256 | 20 | 0.80 | 76 | 0.024 |
| Rheinau | Gerstheim | 15.95 | 256–272 | 20 | 0.68 | 19 | 0.015 |
| Gerstheim | Strasbourg | 15.65 | 272–288 | 30 | 0.96 | 112 | 0.016 |
| Strasbourg | Kehl | 5.95 | 288–294 | 30 | 0.87 | 294 | 0.023 |
| Kehl | Gambsheim | 16.35 | 294–311 | 30 (21h) 60 (+21h) | 0.65 | 841 | 0.063 |
| Gambsheim | Iffezheim | 23.50 | 311–334 | 30 (16h) 60 (+16h) | — | — | — |
| Gambsheim | Plittersdorf ferry dock | 6.30 | 311–340 | 30 (15h) 60 (+15h) | 0.74 | 396 | 0.019 |

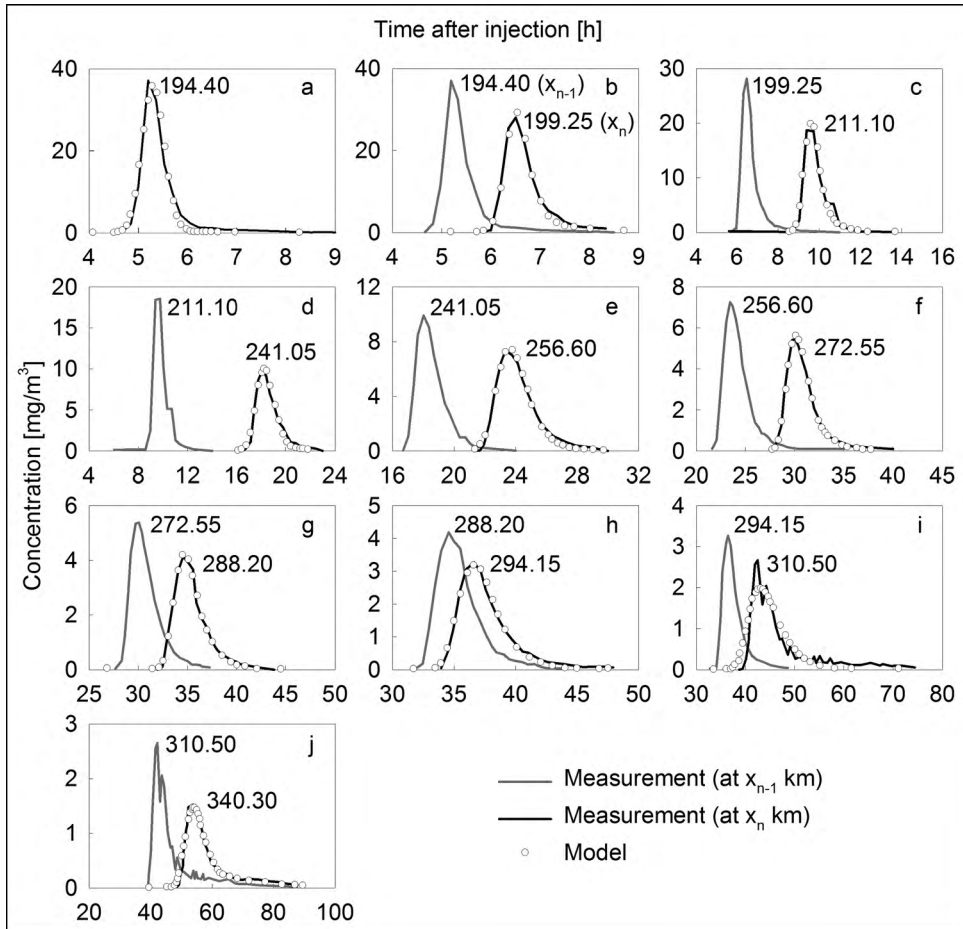


Figure 7.24 Experiment 04/89. Measured tracer breakthroughs at the following river sections (x_n): Ottmarsheim (km 194.4), Neuenburg (km 199.25), Fessenheim (km 211.1), Marckolsheim (km 241), Rheinau (km 256.6), Gerstheim (km 272.5), Strasbourg (km 288.2), Kehl (km 294.1), Gamsheim (km 310.5), Plittersdorf (km 350.3).

The obtained mean transport velocity of 1.09 m/s is typical for a dammed river section in the artificial channel of the 'Rheinseitenkanal'. A low longitudinal dispersion coefficient ($D = 20 \text{ m}^2/\text{s}$) resulted as a consequence (Table 7.10).

Figure 7.24b: Ottmarsheim PP–Neuenburg Bridge river section (Rhine km 194.4–199.25).

Three breakthroughs over the cross section (20, 60 and 100 m from the right bank) were monitored by hand from the bridge at the Neuenburg sampling site. The three curves were converted to a representative tracer concentration curve with a weighting of 20, 60 and 20%. The transport velocity was exactly the same as for the previous section of the river, whereas D was twice that of the upstream section.

Figure 7.24c: Neuendorf Bridge–Fessenheim PP river section (Rhine km 199.25–211.1).

The tracer cloud continued to flow through the Upper Rhine channel, maintaining a similar transport velocity (1.08 m/s) and dispersion coefficient ($D = 42 \text{ m}^2/\text{s}$). The tracer breakthrough measured at ‘Fessenheim’ (km 211) revealed the problem of incomplete mixing of the substance being measured (inhomogeneity in tailing). In spite of the relative short sampling interval, the maximum peak of concentration was presumably not measured. However, the peak could only have been insignificantly higher than the measured maximum of $26.1 \text{ mg}/\text{m}^3$. The ‘step’ in the tail of the curve can be explained by the operation of a lock located upstream, which seems to have released stored quantities of the tracer.

Figure 7.24d: Fessenheim PP –Marckolsheim PP river section (Rhine km 211.1–241.05).

Within this section, the Rhine first flows through the Upper Rhine channel and then through a section where the river’s meanders have been partially preserved (referred to as the meander section). The different morphology of the section is represented only slightly by the somewhat lower mean transport velocity of $v_n = 0.98 \text{ m/s}$, and a slightly higher dispersion coefficient ($D = 63 \text{ m}^2/\text{s}$).

Figure 7.24e: Marckolsheim PP–Rheinau PP river section (Rhine km 241.05–256.0).

This section is located entirely within the meander section of the river. The trend in the flow and transport parameters evidenced previously was amplified with a further reduction in transport velocity and an increase in the dispersion coefficient ($v_n = 0.80 \text{ m/s}$ and $D = 76 \text{ m}^2/\text{s}$).

Figure 7.24f: Rheinau PP–Gerstheim PP river section (Rhine km 256.0–272.55).

The evaluated transport parameters ascertained for this section, again located within the meander section of the Rhine, showed a considerably slower flow velocity ($v_n = 0.68 \text{ m/s}$) and a strong decrease in the dispersion coefficient ($D = 19 \text{ m}^2/\text{s}$). According to the control measurements made during the 1991 test, this was due to an incomplete mixing of the tracer and, consequently, an incorrect estimation of the parameters.

Figure 7.24g: Gerstheim PP–Strasbourg PP river section (Rhine km 272.55–288.2).

Sampling at Strasbourg took place above the power plant inlet. In this channelled section of the Rhine both transport parameters increased strongly. The flow velocity ($v_n = 0.96 \text{ m/s}$) returned to the values recorded for the sections upstream of Rheinau, whereas the dispersion coefficient $D = 112 \text{ m}^2/\text{s}$ revealed a much stronger dispersion of the tracer.

Figure 7.24h: Strasbourg PP–Kehl river section (Rhine km 288.2–294.15).

At Kehl sampling occurred from the landing. In this section of the Rhine the river morphology changes. The meandering section comes to an end and the Rhine begins to flow in a network of streams. Nevertheless, the mean flow velocity ($v_n = 0.87 \text{ m/s}$) was similar to that of the upstream section while D increased to $294 \text{ m}^2/\text{s}$.

Figure 7.24i: Kehl–Gambenheim PP river section (Rhine km 294.15–310.5).

The entire Kehl–Gambenheim section is channelled and barrage regulated. The flow velocity dropped down to $v_n = 0.65 \text{ m/s}$ and dispersion increased strongly ($D = 842 \text{ m}^2/\text{s}$). Due to the relatively high model error (Err_n) a second evaluation

was carried out. The second sampling provided only a small improvement, however, and confirmed the measured values.

Figure 7.24j: *Gambsheim PP–Plittersdorf river section (Rhine km 310.5–340.3).*

At Plittersdorf sampling was carried out from the landing. The transport parameters exhibited normal values.

The general picture revealed by the tracer transport experiment of 04/89 was as follows: as expected, the flow velocities of the Grand Canal d'Alsace were higher than those of the meandering and channelled sections. The calculated dispersion coefficients proved to be more informative than the flow velocities. The dispersion coefficients increased dramatically downstream of Rheinau (Rhine km 272). The measurement results from 'Vogelgrün' (Table 7.10) were not used in the calculation as the tracer breakthrough was only detected partially at this location. The measurement results from 'Iffezheim' were also discarded as the insignificant difference in the substance breakthrough between 'Iffezheim' and 'Plittersdorf' did not allow for a reliable calculation of the dispersion coefficient for this section.

The obtained mean transport velocity (v_n) and longitudinal dispersion coefficient (D) allowed the calibration of the model. The change of concentration at the end of each segment was modelled. Its accuracy and correspondence with the measured data are indicated by a normalized variation coefficient Err_n (Equation (7.15)).

The validation of the tracer experiments demonstrated the suitability of the calibrated model to predict the dispersion of tracers and pollution in the sections of the River Rhine investigated applying the approach given by Equation (7.12). The forecasts provided by the model approach used, can be adapted to simulate an ongoing event. Thus, deviations in the dammed sections of the river can be considered and eliminated, and their impact on the entire flow distance can be avoided (Figure 7.25).

A comparison between the measured and modelled tracer breakthrough curves revealed a general overestimation by the model, which decreased continuously with increasing distance. As the skewedness of the tracer breakthrough in natural river beds cannot be included in the model, differences between the modelled and the measured values existed particularly in the tails. However, the approach taken allowed for an improvement of the prediction by using the assessment of the tracer breakthrough upstream as an input function for the next section. Thus, Figure 7.25c shows a considerable improvement in the prediction compared to that contained in Figure 7.25a.

Another step in the improvement of the model approach was the incorporation of the flow characteristics of so-called 'stagnant zones' near the river bank. In order to understand the processes, and to obtain the necessary parameters, the hydrodynamics of some stagnant zones were measured in situ employing underwater fluorometry. The technique, results and evaluation are described below.

7.3.4.5.2 Tracer experiment September 1990 With a runoff of only 620 m³/s the experiment of September 1990 represented low flow conditions in the River Rhine. Once again 100 kg Rhodamine WT in solution was released within a 5 min period, at the same injection site as the tests of April 1989 (04/89) and June 1991 (06/91). The same injection technique was also used. As both the sites and the sampling techniques

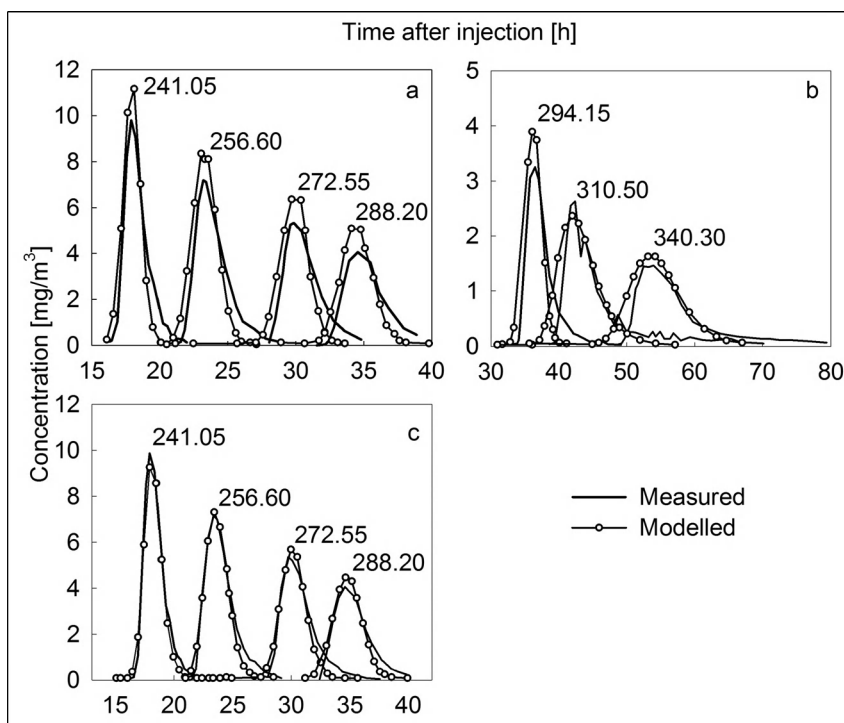


Figure 7.25 Validation of the Upper Rhine river sections: a) postmodelling, Rhine km 241.05–288; b) postmodelling, Rhine km 294.15–340.3; c) forecast improvement, Rhine km 241.05–288.2.

applied were the same as in the previous experiment, the outcome of this experiment will be discussed in the general assessment (Figure 7.34).

7.3.4.5.3 Tracer experiment June 1991 The flow conditions at the time of the June 1991 tracer experiment represented the mean high flow conditions ($1820 \text{ m}^3/\text{s}$, Rheinfelden) of the Rhine downstream of Basel (Leibundgut *et al.*, 1992). In fact, the actual mean flow velocity during the experiment was considerably higher than it would have been at the long-term mean high water level of $1350 \text{ m}^3/\text{s}$.

One hundred kilograms Rhodamine WT in solution were injected in a 6 min period, at the same site as the tracer test 04/89. Seven sampling sites with automatic sampling systems were installed along the Upper Rhine. Thirteen more sampling sites were established downstream, extending to the German border with the Netherlands (see Figure 7.22). After bifurcation of the Rhine in the Netherlands, additional concentration measurements were conducted in the rivers Waal, Nederrijn-Lek and IJssel.

A comparative assessment of the results obtained for the Upper Rhine River sections with those of the 04/89 experiment revealed differences in the boundary conditions. In contrast to the tracer test of 04/89, no flow regulation by the power plants was necessary due to the high flow conditions during this experiment. The higher runoff led to considerably higher mean flow velocities (v_n), in spite of the partial redirection of

Table 7.11 Transport parameters of tracer test 06/91 for the river sections from Basel to Bimmen. Sections from Village–Neuf to Karlsruhe belong to the Upper Rhine

| | River section | Rhine km | Mean velocity [m/s] | Longitudinal dispersion [m ² /s] | Normalized variation coefficient [-] |
|------------------|--------------------|---------------|---------------------|---|--------------------------------------|
| Village–Neuf | - PP Ottmarsheim | 174.00–194.00 | 1.36 | 41 | 0.064 |
| PP Ottmarsheim | - PP Vogelgrün | 194.00–224.90 | 1.50 | — | — |
| PP Ottmarsheim | - PP Markolsheim | 194.00–241.05 | — | 87 | 0.042 |
| PP Vogelgrün | - PP Markolsheim | 224.90–241.05 | 0.97 | — | — |
| PP Markolsheim | - PP Rheinau | 241.05–256.60 | 1.00 | — | — |
| PP Markolsheim | - PP Gerstheim | 241.05–272.55 | — | 108 | 0.033 |
| PP Rheinau | - PP Gerstheim | 256.60–272.55 | 1.03 | — | — |
| PP Gerstheim | - WSA Steiger Kehl | 272.55–294.15 | 1.12 | 301 | 0.038 |
| WSA Steiger Kehl | - Plittersdorf | 294.15–340.30 | 0.85 | — | — |
| WSA Steiger Kehl | - Karlsruhe | 294.15–359.20 | — | 1118 | 0.079 |
| Plittersdorf | - Karlsruhe | 340.30–359.20 | 1.58 | — | — |
| Karlsruhe | - Speyer | 359.20–400.00 | 1.45 | — | — |
| Karlsruhe | - Mannheim | 359.20–424.70 | — | 1105 | 0.019 |
| Speyer | - Mannheim | 400.00–424.70 | 1.52 | — | — |
| Mannheim | - Worms | 424.70–443.50 | 1.01 | — | — |
| Mannheim | - Mainz | 424.70–498.50 | — | 325 | 0.011 |
| Worms | - Mainz | 443.50–498.50 | 1.15 | — | — |
| Mainz | - Koblenz | 498.50–590.35 | 1.20 | 1115 | 0.020 |
| Koblenz | - Bad Honnef | 590.35–640.00 | 1.43 | — | — |
| Koblenz | - Köln | 590.35–689.50 | — | 627 | 0.013 |
| Bad Honnef | - Köln | 640.00–689.50 | 1.53 | — | — |
| Köln | - Bimmen | 689.50–865.02 | — | 1191 | 0.020 |
| Köln | - Düsseldorf | 689.50–759.60 | 1.47 | — | — |
| Düsseldorf | - Wesel | 759.60–814.00 | 1.24 | — | — |
| Wesel | - Bimmen | 814.00–865.02 | 1.29 | — | — |

water through the old river bed, which functioned as a flood discharge channel. Of the seven sections measured, five provided reliable data (Table 7.11). The values revealed the following tendency.

As in the 04/89 tracer test, the transport velocities in the sections of the Grand Canal d'Alsace (to river distance marker km 226) were higher and the dispersion coefficients lower than in the sections of the meandering part and the extended channel area (Table 7.11). The transport parameters were linked to the different velocity distributions, which were affected by the different roughnesses and shapes of the transverse and cross sections considered. The transport velocities for the river sections from Basel to Strasbourg were especially revealing. In this complex stretch, the prediction of flow velocities using hydraulic models is potentially very difficult due to the numerous bifurcations and barrages.

In the 04/89 tracer test, the threshold value of the normalized variation coefficient (0.25) was exceeded only in the Kehl–Gambshheim section. The other ten sections modelled exhibited a very good fit (<0.25). The standardized variation coefficients for

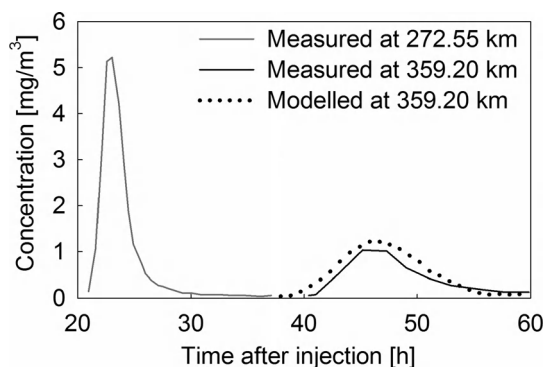


Figure 7.26 Post-modelling of the Gerstheim–Kehl river section.

the 06/91 tracer test were not as good as those obtained in the previous test (Table 7.11). None of the sections of the Upper Rhine region investigated exhibited a value lower than 3.3%, and two sections exceeded 5%. This was probably caused by both the high flow conditions and by the longer distances between the sampling sites. However, the transport velocity and the dispersion coefficient values were not as bad as the normalized variation coefficients suggested, especially in case of the tracer breakthrough curve for the Kehl–Karlsruhe section. The high value there can be attributed to the concave shape of the measured tracer curve.

Greater differences in transport parameters were obtained for the sections of the Rhine downstream of Karlsruhe. Particularly worthy of note are the sections Karlsruhe–Mannheim, Mainz–Koblenz and Köln–Bimmen, which were characterized by high dispersion. However, the normalized variation coefficients were below the threshold and indicated a good fit.

The application of the ‘routing approach’ (Equation (7.12)) is shown for the Gerstheim–Kehl section of the Rhine (Figure 7.26). The measured breakthrough at Gerstheim was used as the input function for the section beginning at Kehl. The deviations between the measured and the calculated travel times for the sections downstream of Speyer were a maximum of 4 h. This was a relatively good result for a forecast model covering approximately 950 km (Table 7.12). This range is nearly optimal for application in real situations; for example the regulation of water extraction by waterworks.

Incorporation of stagnant water zone effects The results of the first tracing tests (1988) revealed that it was necessary to enhance the model by including a stagnant water zone parameter in order to simulate tracer breakthrough satisfactorily. The 1D model was not a sufficiently accurate means to simulate tracer breakthrough. The reasons for this were the very different flow behaviour and flow velocities occurring in the streamline of a river compared to the stagnant water zones (Figure 7.27). Stagnant water zones are natural irregularities or artificial (groynes) dead pond areas where the water remains largely still. The overall transport of solutes is retarded due to the time that tracers and contaminants stay in stagnant water zones, in bank areas and on the

Table 7.12 Deviations between the measured and the calculated travel times experiment of June 1991) for the sampling sections situated furthest from the point of injection

| Observation point | Rhine - km | T_m [h] | T_c [h] | T_d [h] |
|-------------------|------------|-----------|-----------|-----------|
| Injection | 174.1 | | | |
| Speyer | 400.0 | 54.25 | 55.77 | -2.8 |
| Bad Honnef | 640 | 107.25 | 110.44 | -3.0 |
| Duesseldorf | 759.6 | 129.25 | 134.21 | -3.8 |
| Bimmen | 865.0 | 153.25 | 159.35 | -4.0 |
| Hagenstein | 946.5 | 185.25 | 191.96 | -3.3 |

T_m = measured travel time, T_c = calculated travel time, T_d = travel time deviation.

river bottom. The breakthrough curve, consequently, is characterized by a long tail, as shown in Figure 7.27. The theory of water flow in river sections with immobile water was discussed extensively in Section 5.3, where the pertinent Equations (5.107–5.110) were also provided.

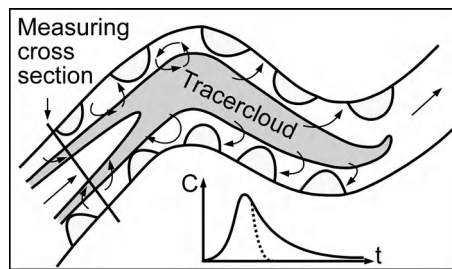


Figure 7.27 Schematic sketch of the impact of dead pond zones upon tracer breakthrough. Due to the impact of the stagnant water flow the resulting tracer breakthrough curve is positively skewed.

To improve the 1D Rhine model, van Mazijk (1996) introduced a lag coefficient, φ (Equation (7.16)), taking into account the effect of tracer diffusion (losses) into the stagnant water zone. This coefficient must be determined for the section of the river (n) in which these losses occur. Among other things, the immobile water zone parameter (φ) takes into account the impact of the stagnant water zones upon the mean apparent velocity of a conservative tracer $(v_t)_n$ and upon the mean real transport velocity of water in the river (v_n) :

$$(v_t)_n = \frac{v_n}{\varphi} = \frac{v_n}{1 + \beta} \quad (7.16)$$

where $\beta = A_{im}/A_m$ (see Figure 7.28).

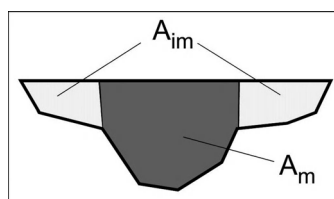


Figure 7.28 Flow in a cross section with stagnant zones. A_m = stream line area (mobile water), A_{im} = stagnant water zones.

However, for the proper interpretation of tracer experiments carried out in areas where there are stagnant zones, additional experimental information concerning the flow processes in these stagnant zones is required. This information can be provided by in situ measurements. In this study, these measurements were made from a boat equipped with an in situ fluorometer (VARIOSENS). The extraordinarily low dispersion coefficient observed in the Rheinau–Gerstheim river section during the experiment carried out in April 1989 was investigated during the June 1991 experiment (Figure 7.29). The impact of the dead pond zones became obvious. The low dispersion coefficient was explained by an incomplete mixing of the tracer in the Gerstheim section (cf. Table 7.10), which resulted in an incorrect calculation of the transport parameter.

7.3.4.5.4 Tracer experiment September 1988 The tracer experiment carried out in the Rhine in September 1988 was particularly interesting as it provided the experience necessary for the subsequent larger experiments carried out downstream from Basel. Furthermore, the contrasting morphology that characterizes this area of the River Rhine meant that it was reasonable to expect different transport parameter values from those observed downstream from Basel. The routing technique was not yet used as during

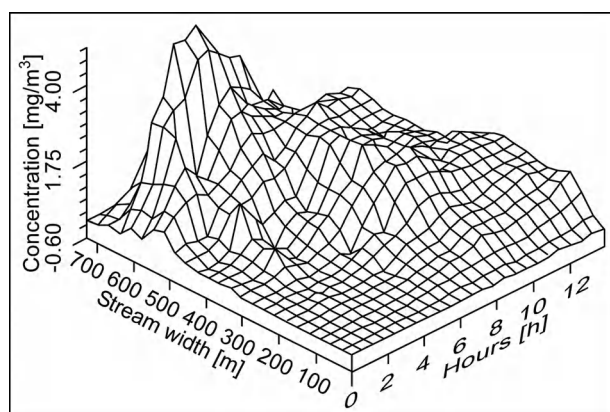


Figure 7.29 Tracer breakthrough in a river section influenced by stagnant water zones (Gerstheim, km 268.3).

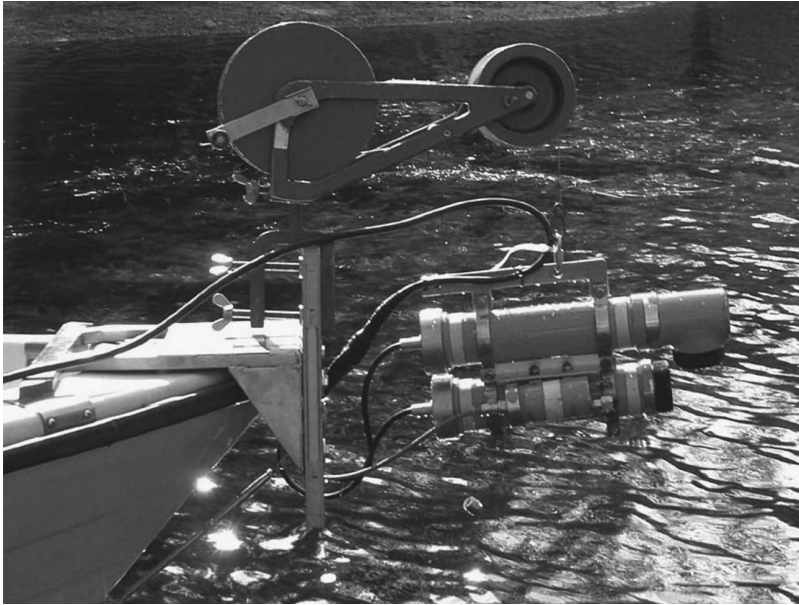


Figure 7.30 In situ measurement device (Variosens).

the following experiments. Helpful information concerning the processes of water flow in the dead pond areas was provided. The most important issue of this experiment was the direct comparison of the parameters estimated by a hydraulic routing model (Kühne, 1988) and those derived from the tracer experiments.

The experiment was carried out in the Rhine section between the confluence of the Aare/Rhein and Basel (Leibundgut, Petermann and Schudel, 1988). On the 27th of September 35 kg of Uranine, as concentrated solution, was injected into the Rhine over the course of a few minutes. The tracer cloud was measured at 17 downstream sampling sites and also directly from three boats using an in situ fluorometer (Figure 7.30). The discharge of the Rhine at Albbruck was $700 \text{ m}^3/\text{s}$ and stationary. The runoff situation was similar to that of the experiment carried out in the Upper Rhine in September 1990 and represented low flow conditions.

The stationary sampling provided the time distribution of the tracer transport. From this the flow velocity, travel times and the longitudinal dispersion could be calculated for the individual river sections. The tracer transport within inaccessible sections was determined by means of in situ measurements to calculate the lateral dispersion. The maximum travel times (frontline) are of particular interest in relation to the transport of pollutants. These increased proportionately to the distance from the place of injection.

The main parameter used to forecast pollutant distribution is the longitudinal dispersion coefficient D . It describes the velocity distribution in the longitudinal axis of a pollutant cloud (Figure 7.31). The dispersion coefficients increased progressively with

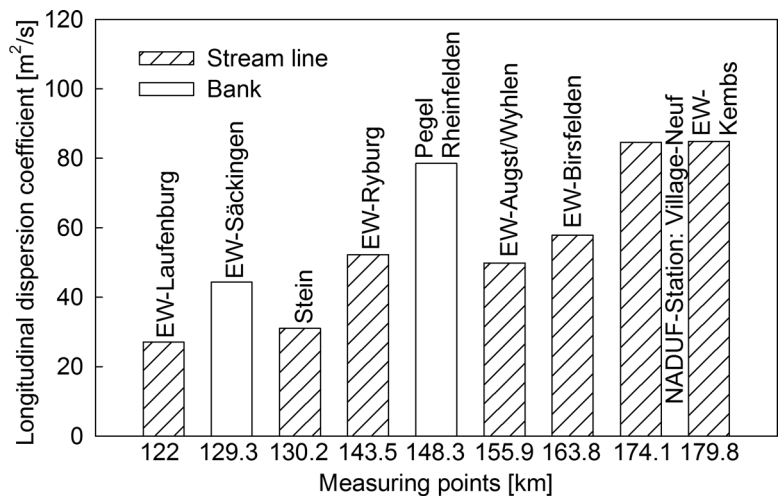


Figure 7.31 Longitudinal dispersion coefficient D . Injection point at km 113.5.

distance. The variability of the D values was high due to the different morphologies of the various river sections. For distances of less than 100 km the range of D values corresponded closely to known values.

The analysis of the individual river sections revealed a rapid decrease in the maximum concentrations with increasing distance from the tracer injection site (Figure 7.32).

The distribution of the tracer at the downstream sampling sections as a function of time must be observed in order to ensure the necessary homogenous distribution. The measurements at the stations Rheinfelden (4) and NADUF (7) were only partially

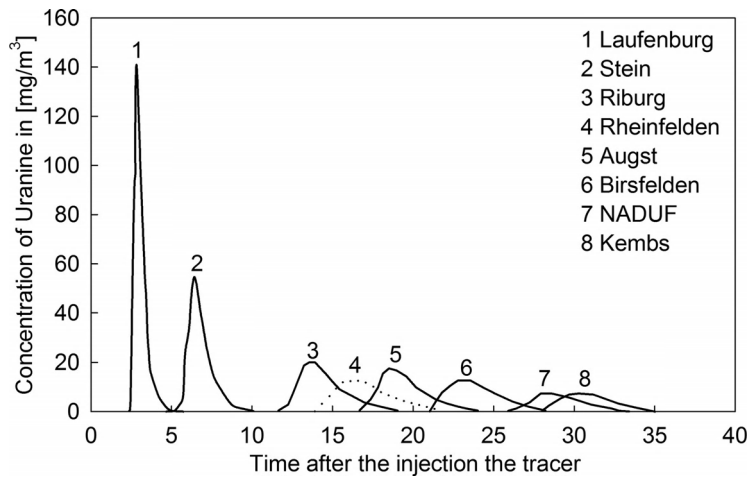


Figure 7.32 Decrease in tracer concentration as a function of time (hours).

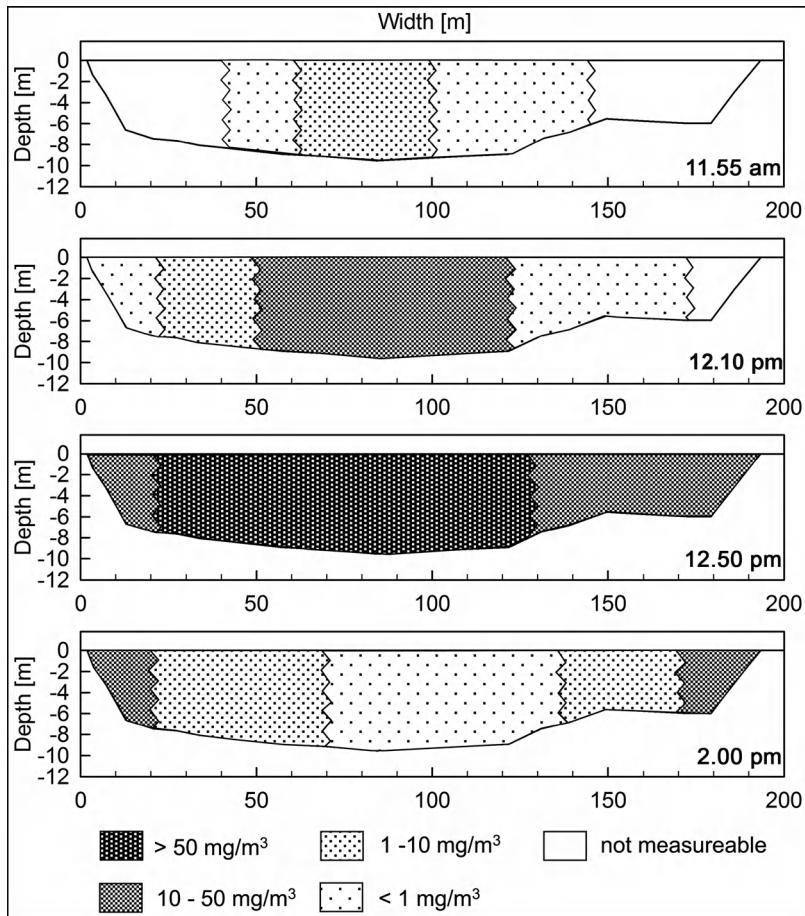


Figure 7.33 Distribution and concentration of a tracer cloud in a river section situated 15 km downstream of the injection point at different times.

representative, as the tracer concentration could not be ascertained in the channel line (Figure 7.32).

In the vertical direction (z) the tracer was well mixed over the whole depth after only a short distance from the injection point, which was situated almost directly in the channel line. In the transverse direction the situation was much more complex. The tracer cloud was first observed at the river streamline (11.55 h). After 1 h (12.50 h) the tracer cloud was distributed over the entire river section, but in very different concentrations (Figure 7.33).

Figure 7.33 illustrates the situation of transverse dispersion 15 km below the injection point. The tracer appears in the channel line first. A short time later the entire cross section (except the areas close to the river banks) was well mixed with tracer, with the highest concentration still evident in the channel line. One hour after the first appearance, at about 12.50 p.m., the peak concentration was spread over the entire

cross section. The concentration in the channel line subsequently began to decrease continuously. At 2.00 p.m., when the measurements at this section finished, the tracer concentration ratio of the channel line versus that of the river bank was approximately 1 : 6 (river bank: 25–50 mg/m³; channel line: 6 mg/m³). This discussion of the transverse dispersion illustrates the great importance of selecting multiple sampling points across the river cross section when investigating tracer and pollutant transport in rivers.

A comparison of the travel time values provided by the tracer experiment with those provided by the hydraulic model (Kühne, 1988; Spreafico, Leibundgut and Kühne, 1989) revealed a difference of less than 10%. Whereas tracer experiments provide hard data by means of the measurement or the calculation of all of the transport parameters, the 1D computer model FLORIS can only predict mean travel times. However, tracer experiments allow only for the investigation of momentary flow conditions. The transfer of these calibrations to other discharge conditions demands further treatment using suitable models.

7.3.4.6 Assessment of the experiments

The deviations between the measured and the calculated travel times differed for the three runoff situations. The best representation by the model ($\pm 2.5\%$) resulted for mean runoff (Figure 7.34). The travel time during low flow was underestimated by approximately 5%. The high flow velocities were overestimated and the low flow velocities underestimated by the same range.

This is a relatively good result for a forecast model covering a flow distance of approximately 950 km in length (Figure 7.34).

In general, it can be stated that the tracer techniques applied were adequate and represented a successful means for determining the transport parameters required for the

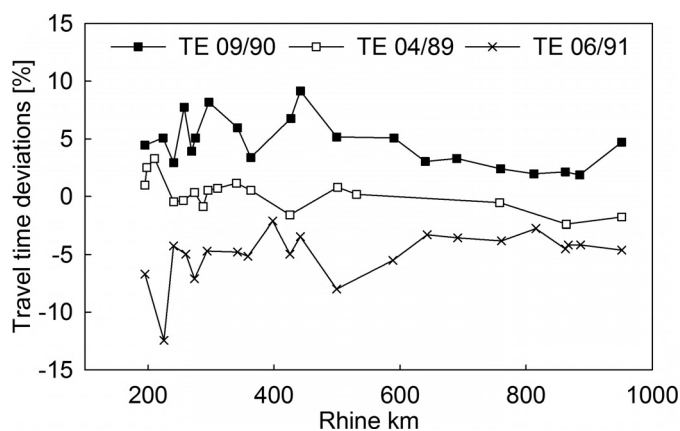


Figure 7.34 Deviation of travel times calculated for the three experiments described (Spreafico and van Mazijk, 1993).

models used. The comparison of the fluorescent tracers deployed – Uranine upstream and Rhodamine WT downstream of Basel – underlined the greater suitability of Rhodamine WT as a tracer in surface water applications. Due to its photolytic sensitivity, Uranine is only an option for investigations over short distances and for experiments carried out at night. Other effects on tracers that are potentially problematic in such experiments, such as sorption and degradation, were eliminated nearly completely by the introduction of the routing approach (see Equation (7.12)).

The 1D model approach supplemented with the stagnant water zone parameter provided satisfactory results and met the requirements of the Rhine Alert Model (RAM). On the whole, the tracer tests provided the parameters needed to calibrate the Rhine Alert Model (RAM). However, additional 3D in situ measurements in morphologically complex bank areas and river sections were indispensable for the provision of the necessary lag parameters for φ (Equation (7.16)).

Further information is given in other, not cited, publications of this project.²

7.3.5 Case study: 'On mixing of effluent inflow'

7.3.5.1 Introduction and aim

The aim of this artificial tracer study was to investigate the inflow and the transversal dilution of sewage water from a sewer channel in southern Germany near Munich. A continuous injection experiment was chosen to study transversal dilution in the river. An artificial tracer was injected continuously into the sewage water to trace the sewage and monitor dilution in river water downstream.

As a result of the tracer experiment with continuous injection, discharge at and discharge differences between different cross sections during the experiment could be determined. Based on the discharge differences the location of river reaches with lateral inflows and the amount of lateral inflow could be determined. Thus, the case study also presents the methodology of continuous tracer injection experiments as required for discharge measurements.

The study reach extends from the injection site to a bridge 5.8 km downstream. The tracer test was done at mean low flow conditions. At a gauging station upstream of the

²Beffa, Rutschmann and Trösch (1990), Bloss *et al.* (1987), Capel *et al.* (1988), Günneberg (1990), Hötzl and Werner (1992), Jäggi and Paris (1978), Kilpatrick and Wilson (1989), Kühne *et al.* (1991), Kuik (1994), Kuik and van Mazijk (1994), Landeshydrologie und -geologie (1991), Leibundgut and Bremicker (1989), Leibundgut (1991), Leibundgut, Speidel and Wiesner (1993), Leibundgut and van Mazijk (1996a, b), Markofsky (1980), van Mazijk and Verwoerd (1989), van Mazijk, van Mierlo and Wiesner (1991), van Mazijk *et al.* (1991), van Mazijk, Wiesner and Leibundgut (1992), van Mazijk and Leibundgut (1999), van Mazijk, van Gils and Weitbrecht (2000), Mendel (1988), van Mierlo (1993), Mugie (1990), Naturaqua and GIUB (1988, 1989), Naturaqua (1990, 1994), Neff (1995), Ossman, Schnoor and Stumm (1988), Speidel (1991), Spreafico, Leibundgut and Kühne (1989), Steinebach (1995), Wiesner (1989), Verboeket-Klavers and Sprokkereef (1994), Verwoerd (1990).

study reach a discharge of about $15.5 \text{ m}^3/\text{s}$ was recorded at the day of the experiment. During the experiment, no rainfall was recorded.

7.3.5.2 Methodology

For continuous injection, a high precision peristaltic pump is used to provide a homogenous tracer solution (Sulforhodamine G) injected at a constant rate. Care needs to be taken to stir the tracer solute and to avoid coagulation. Suspended solids, nondissolved or coagulated tracer could block the pump or modify the injection rate. A fine sieve is used to protect the pump inlet. The tracer was injected directly into the treated sewage water at an injection rate of 5 mg/s . At the moment the sewage water reached the channel, the sewage water was mixed completely with the tracer.

At any point in the stream downstream of the injection point, tracer concentration increases first and then reaches a plateau that will only diminish after the end of the continuous injection. After an initial time during which the plateau builds up, cross section profiles are measured in order to study the transverse dilution of tracer. It is assumed that during the plateau phase and at steady state longitudinal dispersion does not affect measurements. The injection was maintained for 5 h in order to establish a steady tracer concentration within the 5.8 km study reach. The advantage of a continuous injection in this case is that the cross section profiles can be measured repeatedly.

Background samples were taken prior to the injection. Stream profiles were sampled repeatedly for Sulforhodamine G at five cross sections at 10, 50, 1000, 1750 and 5800 m

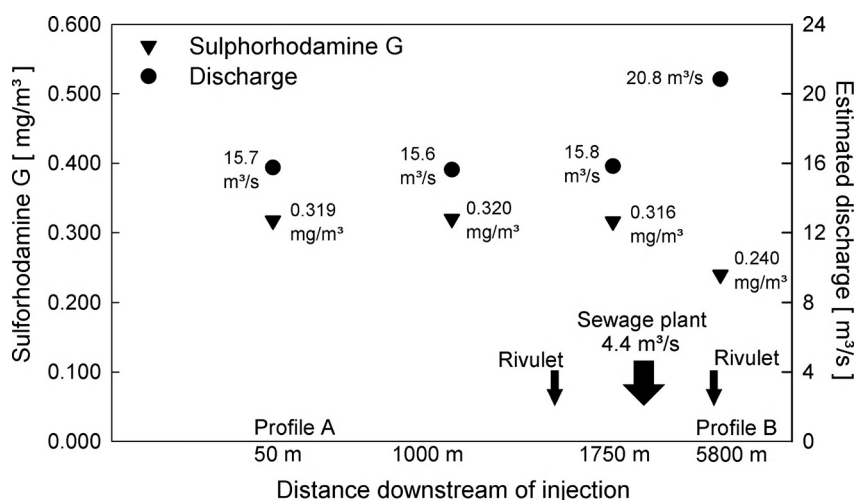


Figure 7.35 Profile along the study reach with concentrations of Sulforhodamine G and calculated discharge.

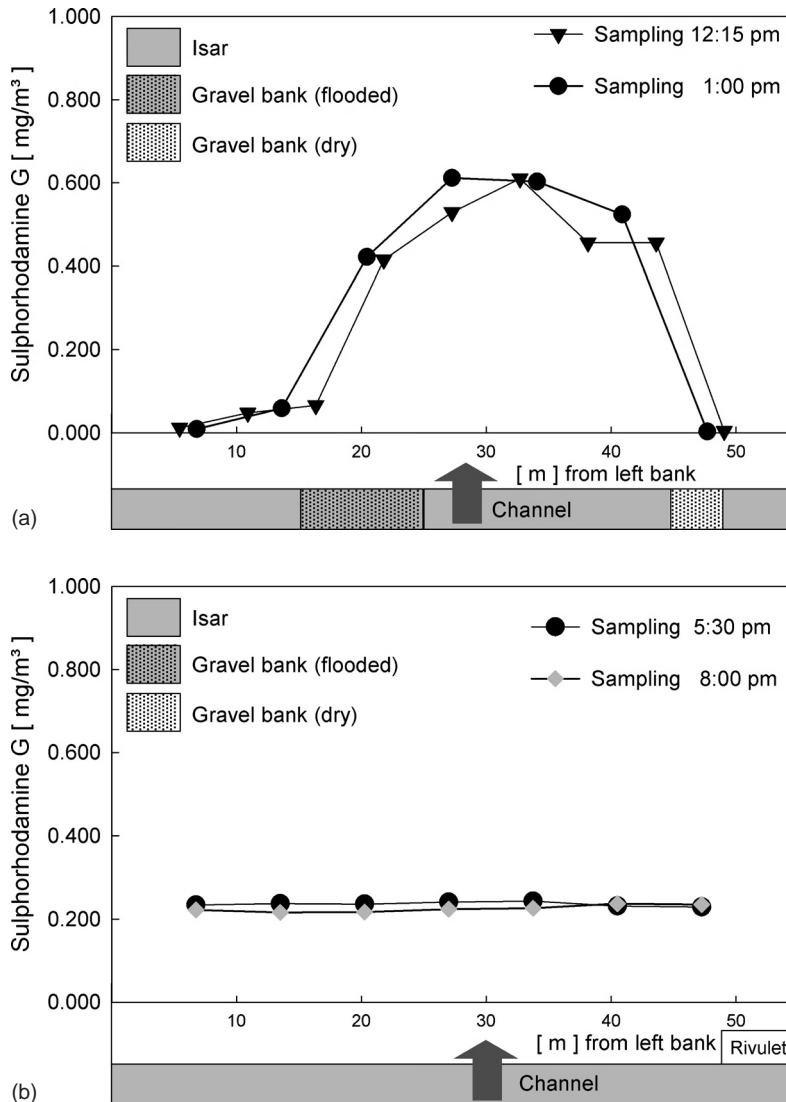


Figure 7.36 Transverse profiles of the river Isar at 50 m (top) and at 5800 m (bottom) downstream of injection (with repeated sampling at 12.15 and 1:00 p.m. and at 5:30 and 8:00 p.m.).

downstream of injection. Samples were taken with 50 ml brown glass bottles and analysed in the laboratory by a spectral fluorometer.

River discharge can be calculated from the tracer concentration during the plateau phase according to Equation (6.10) once lateral dilution has taken place and assuming that the inflow rate of the traced sewage water q_{in} is much smaller than Q . The peak concentration C_{peak} found in consecutive cross sections was found to decrease and

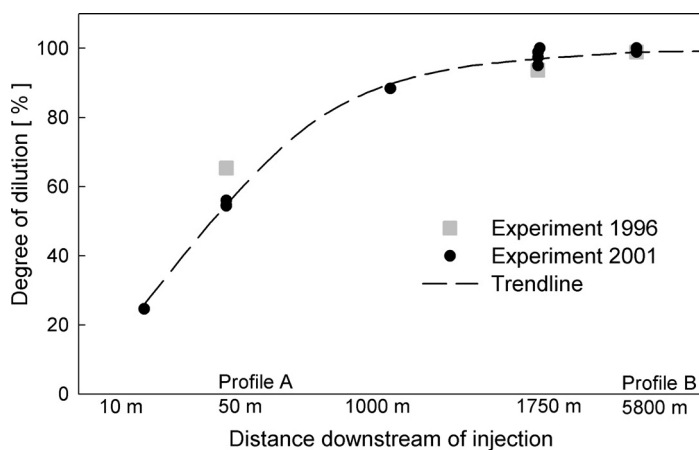


Figure 7.37 Degree of dilution along the river Isar for the experiment in 2001 and a previous experiment.

represents a rough measure of dilution of sewage water with the total discharge and a corresponding mean concentration C at steady state for a complete mixing.

$$f_D \approx C/C_{peak} \quad (7.17)$$

7.3.5.3 Results

The experiment provided a discharge measurement for the downstream sections where complete mixing was achieved. The discharge measurement helped to quantify the inflow from a sewage plant ($4.4 \text{ m}^3/\text{s}$).

The dilution of Sulforhodamine G was found to increase with flow distance (Figure 7.37) in profile 1, at a distance of 10 m from the injection point, the tracer had mixed with approximately 25% of the total discharge volume. At 50 m distance (Figure 7.36, top) maximum concentrations reached about 0.6 mg/m^3 indicating that the tracer had mixed with about 45% of river discharge. At 1 km the degree of dispersion reached more than 85% and maximum concentration was $0.358 \text{ } \mu\text{g/l}$. At 1750 m distance 95% of the total discharge volume was mixed with the tracer. Finally, at the most distant profile (Figure 7.36, bottom) >99% of tracer (and sewage) were mixed. The tracer experiment further indicates a diffuse inflow of about $5 \text{ m}^3/\text{s}$ (Figure 7.35).

The continuous injection used in this study was very helpful in demonstrating mixing dynamics: longitudinal mixing and the progression of mixing between treated wastewater and inflow from upstream reaches could be shown. The degree of dilution of sewage water reached almost 90% within 1000 m. Because of the photostability (half-life: 770 h) the usage of Sulforhodamine G during the day was acceptable. Retention was not a major issue as the amount of suspended sediment was low during low flow conditions. The experiment could have been carried out at night to improve the accuracy of the test. Stable isotope analysis along the river section could have been used to check whether subsurface inflow exists. However, discharge data indicate that this was not the case.

7.3.6 Case study: 'Estimation of hydrodynamics and transport parameters in the Paiva Castro reservoir, Brazil'

7.3.6.1 Introduction and aims

This case study is taken from Aoki, Bombonato and Maloszewski (1996). The Paiva Castro reservoir is used to supply about 12 million inhabitants of the Sao Paulo metropolitan region (Figure 7.38). This reservoir is one of the final steps in the hydraulic complex named 'the Cantareira System', which provides 67% of the water consumed in the metropolitan region of Sao Paulo. The main function of the Paiva Castro reservoir is to collect and store the water of the River Juqueri that flows through other reservoirs and finally to the Guarau water treatment station. The reservoir, with a length of 9.5 km, was constructed to store $32 \times 10^6 \text{ m}^3$ water. Its depth varies from 2 m at the inflow to 12 m at the outflow, and it has an average flow rate of about $30 \text{ m}^3/\text{s}$.

A tracer experiment with artificial tritium was performed to obtain information about:

- 1) The hydrodynamics of the Paiva Castro reservoir, including the determination of the mean transit time of water through the reservoir, the volume of water in the reservoir, and the detection of the main flow path within the reservoir.
- 2) Transport parameters, including the determination of flow velocity and dispersivity at the flow path between the entrance to the reservoir and the outflow to the pumping station as tools for predictions of nonreactive pollutant transport.

7.3.6.2 Methodology

The injection sites and all sampling points are shown in Figure 7.38. The injection of $M = 37 \times 10^{10} \text{ Bq}$ tritium was performed in August 1993. The volumetric flow rate of water through the reservoir was assumed to be $Q = 30 \text{ m}^3/\text{s}$. The tracer was divided into four 10 ml glass bottles and injected simultaneously in four places at a reservoir cross-section (see Figure 7.38: 'Injection'). It was assumed that this type of injection produces a homogeneous tracer distribution perpendicular to the flow direction. Initially, it was intended to inject the tracer directly into the River Juqueri at the entrance of the reservoir. However, due to the fact that there is a small pumping station for the city of Mairipora, the injection was performed 350 m downstream of the reservoir entrance.

Water samples were collected at three cross-sections located 1000 m (X1, peak: 25 h after injection), 4200 m (X2, peak: 75 h after injection) and 7100 m (X3, peak: 125 h after injection) downstream, to detect tracer distribution across the reservoir and to ensure its complete transversal mixing.

Furthermore, the tracer concentrations, as a function of time, were collected at the distance of 3200 m (Section 8), 6600 m (Section 9) and 7600 m (Section 7) downstream.

In each of those sections, 12 samples taken across a depth and a width profile (three and four, respectively) were mixed in order to obtain an integrated representative sample for the whole cross-section in each time interval.

7.3.6.3 Measurements

Generally, it is assumed that the mass of tracer transported along the different flow paths is directly proportional to the water velocities of these paths, and that the differences in the flow velocities are not too great. According to the measurements of tracer concentrations in Sections X1, X2 and X3, the greatest water flow velocity and the major tracer transport took place within the first 1000 m along the right hand bank. Equally distributed tracer concentrations across the flow cross-section were obtained after a flow distance of approximately 3 km. This effect was well observed in the Section X2 (4200 m downstream). The tracer concentrations were measured as a function of time at three distances from the injection site. The concentrations reached maximum values of 1620 TU, 461 TU and 305 TU at the flow distances of 3200 m (Section 8), 6600 m (Section 9) and 7600 m (Section 7), respectively. The natural background tritium content in the Paiva Castro reservoir was 10 TU. A complete tracer mass recovery (100%) was observed in Section 8 and 9 (3200 and 6600 m, respectively) while in Section 7 (outflow to the pumping station, see Figure 7.38) only 85% of the injected mass was recovered. Considering the construction of the reservoir, the loss of 15% tracer mass at the flow distance between Section 9 and Section 7 was attributable to transversal

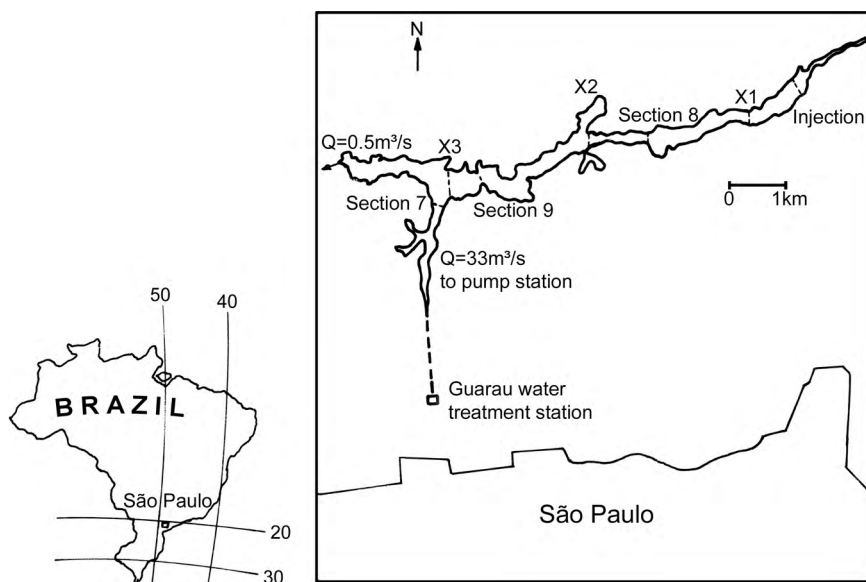


Figure 7.38 Map of the Paiva Castro reservoir with injection and detection sites and its location within Brazil. X1–X3: sampling sites.

dispersion and diffusion of tracer mass into the southwest part of the reservoir (see Figure 7.38).

7.3.6.4 *Mathematical modelling*

The dispersion model defined by Equation (5.33) described in Section 5.1.2 was used to find two parameters, mean flow time and the dispersion parameter (t_0 , P_D), from the tracer concentration curves measured in the Sections 8 and 9. For Section 7 where tracer losses were observed, the model defined by Equation (5.107) in Section 5.3 was applied. The calibration of that model was performed assuming that, for the tracer transport, the volume of immobile water in the southwest part of the reservoir (V_{im}) is infinitely large, which results in parameter β (Equation (5.108)) being equal 0. Then model (Equation (5.107)) has three parameters (t_0 , P_D , ω) which must be obtained by model calibration. From the known flow distance $x = L$, the mean water velocity in the reservoir (at the flow distance L) can be determined from t_0 and dispersivity α_L from P_D and L .

Additionally, the volume of water in the reservoir can be estimated from the known flow rate and the flow time ($V = Q \times t_0$). As was described in Section 5.3, the average depth of the reservoir, H_b , can be determined from the known volume of water and the surface area of the part of the reservoir located between the injection and detection sites, A , ($H_b = V/A$). Here, the depth of the reservoir was known, so the calculated parameter H_b was used to validate the model.

The relative tracer mass recovery RR (Equation (5.40)) could be calculated from the flow rate, the concentration curve measured and the tracer mass injected. RR ($t = \infty$) provides the necessary information about the tracer losses along the flow path between injection and detection sites.

Model parameters were obtained by applying a fitting procedure based on the least square method as described in Section 5.1.3. To verify the quality of fitting, these parameters were used to calculate the tracer recovery curves, which agreed very well with the experimental recoveries. The examples of the model calibration are shown in Figure 7.39 for Sections 9 and 7.

7.3.6.5 *Results*

The mean water velocities, dispersivities, volumes of water and the average depths of the reservoir were calculated from the fitting parameters and are summarized in Table 7.13. The water flow velocities decreased with flow distance. This was expected, as the cross-sectional area increased in the direction of the reservoir outflow. The dispersivity increased with flow distance. For that part of the reservoir between inflow and outflow to the pumping station (flow distance of 7600 m), the mean flow time was $t_0 = 130$ h and the dispersion parameter $P_D = 0.052$. This yielded a mean water velocity $v = 0.016$ m/s (1.4 km/d) and a mean dispersivity $\alpha_L = 395$ m (the model fit presented here was improved compared to the original study, so the parameter values

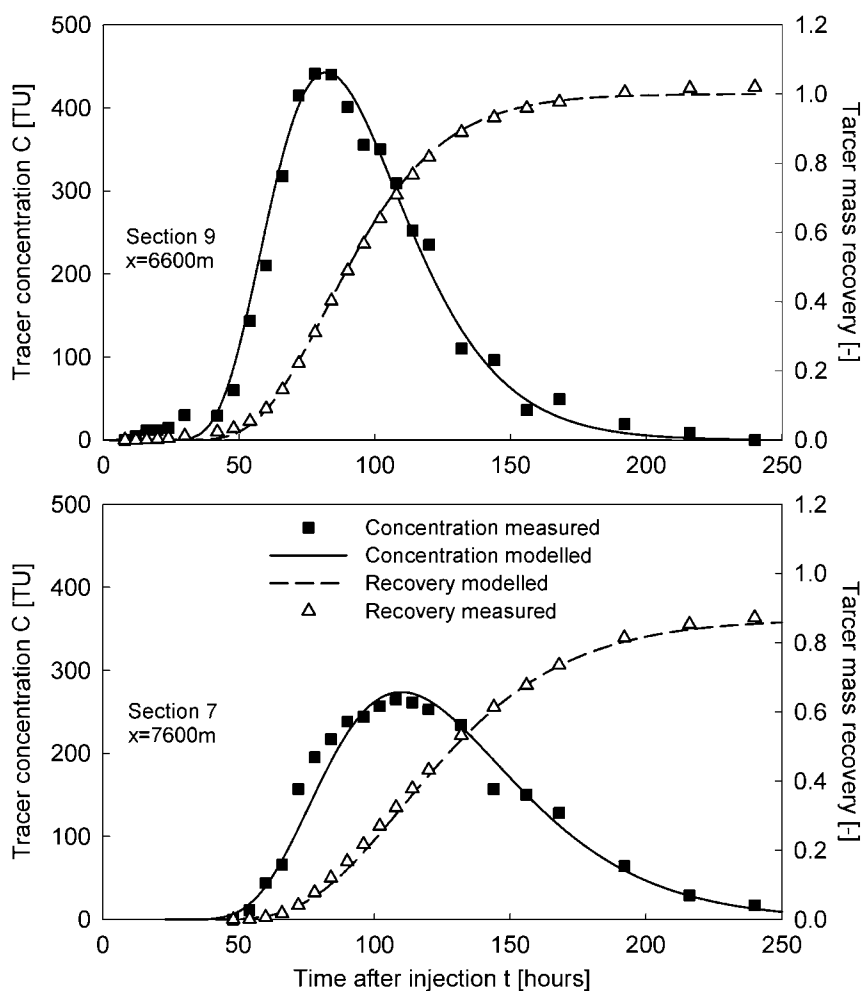


Figure 7.39 Best fit of the model to the tracer concentration and recovery curves obtained in Section 9 (top) and in Section 7 (bottom). For parameters see Table 7.13. (1 TU = 0.118 Bq/L).

differ slightly from those presented in Aoki, Bombonato and Maloszewski, 1996). The volume of water found for that part of the reservoir is approximately equal to $V = 13 \times 10^6 \text{ m}^3$. Knowing the surface of the corresponding area ($A = 1.71 \text{ km}^2$), a mean depth of the reservoir, $H_b = 7.6 \text{ m}$, was estimated, which agrees nearly perfectly with the average 7.5 m known from the hydraulic data. This validates the results obtained by the modelling.

The parameter ω , which describes the losses of tracer mass (see Equations (5.107) and (5.108)) between Sections 8 and 7, was found to be 0.0011 h^{-1} . That parameter (ω), taken together with the calculated mean transit time (T) and the dispersion parameter (P_D), can be used to predict the transport of nonreactive pollutants through

Table 7.13 Model and resulting parameters obtained by calibrating the mathematical model to the tritium concentrations measured in two Sections: 9 and 7. (T – Mean transit time of water, P_D – dispersion parameter; v – water flow velocity, α_L – longitudinal dispersivity, ω – transfer coefficient between mobile and immobile water, V – volume of water, H_b – mean reservoir depth)

| Sec. | Flow distance | Mean tr. time | Disp. Par. | Trans. coeffic. | Flow velocity | Long. disper. | Water volume | Reser. depth |
|------|---------------|---------------|------------|-----------------|---------------|----------------|-----------------------|--------------|
| | L [m] | t_o [hrs] | P_D [-] | ω [1/h] | v [m/s] | α_L [m] | V [m ³] | H_b [m] |
| 9 | 6600 | 94.5 | 0.047 | 0 | 0.019 | 310 | 9.5×10^6 | 6.1 |
| 7 | 7600 | 130.0 | 0.052 | 0.0011 | 0.016 | 395 | 13.1×10^6 | 7.6 |

the Paiva Castro reservoir at the same or similar flow rates, Q . By applying the convolution integral (Equations (5.113) and (5.117) in Section 5.4.2) with $\lambda = \omega$ to any initial concentration, $C_{inp}(t)$, the concentration of contaminant in the outflow to the pumping station can be calculated.

It is also interesting to consider the water balance of the reservoir. The volume of water in the channel between Section 7 and the pumping station is about 2.5×10^6 m³, while about 0.3×10^6 m³ are stored between the Jurqueri River inflow and the injection site. Together with the volume of water located in the part of reservoir between the injection and detection sites, this yields $V = (13 + 2.5 + 0.3) \times 10^6$ m³ $\approx 16 \times 10^6$ m³. As was mentioned, the reservoir was constructed for a total volume of water of about 32×10^6 m³. That difference suggests that about 16×10^6 m³ of water was stored in the west part of the reservoir (see Figure 7.38). This means that 50% of water in the reservoir can be considered to be inactive (quasi stagnant) under the hydraulic conditions that existed during the experiment.

7.3.6.6 Conclusions

The mathematical modelling of the experimental data yielded the transport and hydraulic parameters needed to assess the effects of nonreactive contaminants through the reservoir. The transport parameters and the model used can be applied to predict the movement of nonreactive contaminants through the Paiva Castro reservoir, thus providing the water authority with a much needed tool to prepare remedial measures and manage the water supply. The volume of water found to be active under the experimental conditions was about 50% of the total water stored in the reservoir. The loss of tracer mass by diffusion, transverse dispersion and a small volumetric flow rate ($Q = 0.5$ m³/s) into the stagnant zone situated in the west was relatively small (15%). The average calculated depths of the reservoir conformed well with direct measurement. These determinations validated the mathematical model of the system under the conditions investigated. It would not have been possible to obtain all this information without performing artificial tracer experiments.

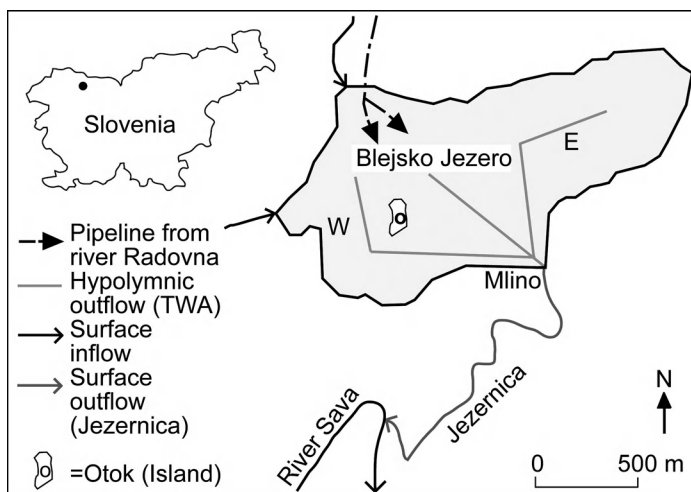


Figure 7.40 Lake Bled with natural and artificial in- and outflows. W: Western basin, E: Eastern basin.

7.3.7 Case study: 'Investigation of internal dynamics and residence time in Lake Bled'

7.3.7.1 Introduction

Lake Bled (Blejsko jezero) in Slovenia is one of the Earth's numerous alpine lakes. Usually these lakes are characterized by a high internal dynamic, be it inflow or wind determined. Tracer methods, both natural and artificial, are a useful tool for investigating the internal flow systems of lakes. Due to its natural characteristics and the technical installations, Lake Bled is suitable for showcasing the methodological features of such experiments.

Lake Bled is a small lake situated in Slovenia with an area of 1.44 km^2 , a maximum depth of 30 m, and located at 476 m a.s.l. (Figures 7.40 and 7.42 left). With an area of approximately 8.1 km^2 , its catchment is roughly five times greater than the lake area. Consequently, the total natural lake inflow by way of 13 small brooks is smaller than 350 l/s . The lake is drained by the stream 'Jezernica'. The lake's volume comes to $25.56 \times 10^6 \text{ m}^3$. The lake was eutrophic until the second remediation step in 1982, and afterwards became mesotrophic. Super saturation with nutrients has increased at a very high rate since the 1960s due to an uncompleted and broken sewage system, intensive agriculture and tourism concentrated in the borough of Bled. A phytoplankton overpopulation, especially by *Planktothrix rubescens* (*oscillatoria rubescens*), could be observed regularly (Rekar and Hindak, 2002).

A small island (Otok) situated on a reef of dolomite separates the lake into two basins: a smaller Western and a larger Eastern basin with maximum depths of 30

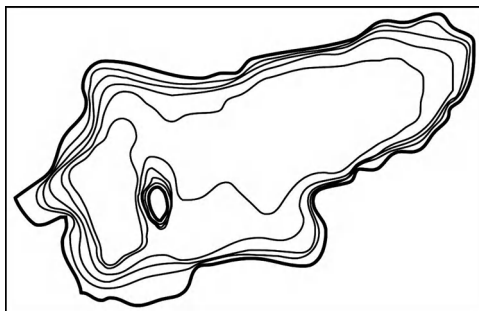


Figure 7.41 Isobathic patterns of Lake Bled showing the morphological features.

and 24 m, respectively. The Eastern basin shows a relatively flat bottom morphology (Figure 7.41). The mean depth of the lake is 17.5 m.

The lake is characterized by a position that provides shelter against wind influences. During the 1982 experiment wind speeds of 1–2 Beaufort, typical for Lake Bled, were measured. This causes stratification during spring, which changes very rapidly into a strong and stable summer stagnation. Extensive oxygen starvation due to organic overproduction could be observed in the hypolimnion. Lake Bled is hardly being streamed or drifted due to its small affluents and effluents, respectively. The lake's physical, chemical and biological parameters have been under regular observation since 1974 (Vrhovsek, Kosi and Zupan, 1981; Rekar and Hindak, 2002).

In order to increase the natural flow of water through the lake and to aerate the lake, oxygen rich water from the River Radovna was channeled by pipeline into the lake in 1964. The pipe has a length of 1097 m, a diameter of 40 cm and provides a maximum of 380 l/s driven by a hydraulic head of 40 m. It is bifurcated to supply both basins and its mouth is situated at a depth of –23.3 m at the SW edge of the lake (Figure 7.40). On the basis of a transport model (Imboden, 1973; Imboden *et al.*, 1983), a second sanitary measure was taken by means of a siphon installation ('Olsewski tube') for channelling off the anaerobic water from the bottom (hypolimnion) of the lake. The outlet (Natega) was installed as a supplementary preventive measure in 1981/82 (Figure 7.42 right). It diverts the highly concentrated water from the lake bottom by three drains (one in the Western and two in the Eastern basin) into the River Sava (Rismal, 1980). During high lake water levels epilimnic water is diverted supplementarily through the surface outflow Jezernica near Mlino; the maximal surface outflow rate is 380 l/s.

7.3.7.2 Tracer experiments

Two tracer studies were conducted. The aim of the first study (1982) was to investigate the efficiency of both the inflow and diversion measures by analysing the internal circulation, and to investigate the internal lake remediation measures. The current patterns were investigated under two different fresh water inflow and deep water outflow situations (Leibundgut *et al.*, 1983). The second study was a long lasting experiment



Figure 7.42 Left: Lake Bled with the island Otok; Right: Technical installation of the outlet (Natega).

(1988–1991) devoted to investigating experimentally the mean residence time of lake water (Leibundgut and Zupan, 1992; Nebel, 1992).

The first study, which consisted of two experiments at Lake Bled, can be considered as a characteristic example of a tracer experiment designed to investigate the internal dynamics and current patterns of lake water (Nydegger, 1967, 1976; Leibundgut and Hirsig, 1977; Hirsig, 1983; Peeters *et al.*, 1996). Further relevant references are provided in Section 7.3.5. Two experiments with different water inflow rates at the artificial hypolimnic inlet were conducted. The tracer input was carried out at the inflow pipe. Adequate mixing was ensured by means of overfall sills in the inlet pipe.

First experiment 1982 – investigation of internal lake dynamics – Rhodamine experiment The first experiment was carried out under the following hydrological conditions: a flow rate in the pipeline of 200 l/s and a water temperature of 8.3 °C. The artificial runoff through the diversion tube amounted to 100–350 l/s, depending on the water stage. The natural runoff over the spill varied correspondingly (0–200 l/s). During the experiments no wind-induced currents were measured and the lake was in a stagnant stadium with a thermocline at 4–10 m depth and in a stable stratification (Figure 7.43).

Since the temperature of the pipeline water from River Radovna had a daily amplitude of 7 to 12 °C, it was expected that the river water would move to the uppermost layer of the hypolimnion. On July 8th 8 kg Rhodamine B in concentrated solution were injected into the artificial inflow over a period of 18 min. The subsequent, and always necessary, flushing lasted 1 h. An hour later, the tracer front reached the intake of the lake. Tracer concentration was measured from a boat with the in situ Variosens technique, where vertical and horizontal profiles were measured and control samples were taken. Several horizontal profiles were taken at the longitudinal and transversal cross section. The position of the boat with the measuring equipment was determined by theodolite survey. A similar study would be much easier today, owing to the advanced technique

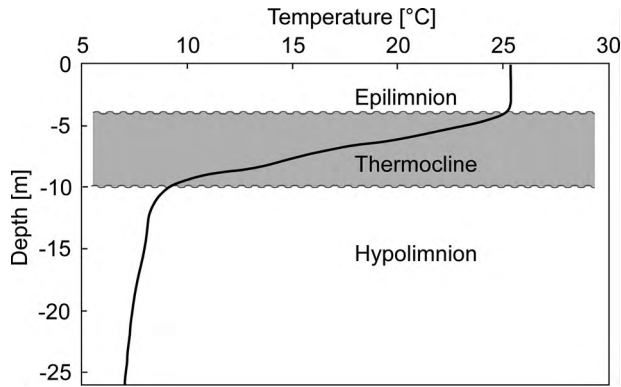


Figure 7.43 Stratification of Lake Bled caused by temperature, representative of the conditions during the experiments in 1982.

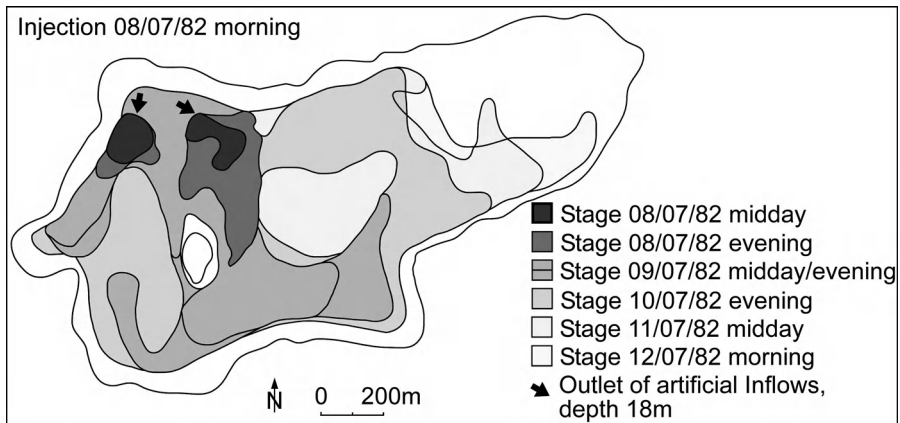


Figure 7.44 Internal flow dynamic of the hypolimnion, visualized by measured tracer concentration of the Rhodamine experiment.

of GPS. Since the two inlets of the pipeline produced two tracer clouds, both clouds had to be tracked. Two to four hours were needed for each. A comprehensive impression of the aerial view of the tracer distribution at different times, which reflects the internal dynamic into the hypolimnion, is presented in Figure 7.44. The exhibited general pattern corresponds to the theoretical expectations and experiences from similar experiments (Nydegger, 1976; Leibundgut and Hirsig, 1977; Hirsig, 1983).

According to the temperature of the inflowing water, the tracer cloud of Rhodamine B stratified underneath the thermocline, forming Coriolis force induced eddies to the right with secondary counter-vortexes, whereas the overall water movement follows a left-rotation caused by the secondary effect of the continuously pushing inflow

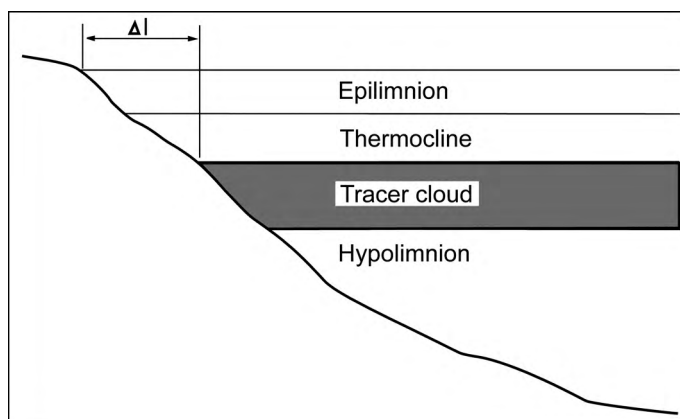


Figure 7.45 Schematic presentation of the tracer free fringe (ΔI) along the lake banks caused by the topography of the lake bottom and the thermal stratification.

water. This pattern is typical for inflow-driven currents of standing water bodies in the Northern hemisphere.

According to the measured tracer concentrations (Figure 7.44), the migration of tracer took its course more moderately in the Western basin, due probably to its smaller inlets and its comparatively higher ‘insularity,’ in relation to the Eastern basin. There, as a result of the larger inlet, the tracer-front bifurcated and spread more rapidly. After 24 h, the velocity of the tracer in the Western basin was approximately 20 m/h while about 30–40 m/h were observed in the Eastern basin. After two days, the tracer fan in the Eastern basin encountered the opposite bank and eluded laterally due to the pressure of the following water. The majority of the tracer followed the left-rotation and reached water that was already marked at the Northern bank by the end of the third day. In the middle of the Eastern basin, a “tracer-free eye” appeared, which was filled on the fourth and fifth day of experiment. The current velocity declined below 20 m/h in the Western basin and below 25 m/h in the Eastern basin at the end of 12th July. The peculiar fringe along the banks (Figures 7.44 and 7.45) was due to the stratification of the tracer cloud in the hypolimnion (ΔI).

Horizontal profiles of tracer concentration were taken, one along a longitudinal SW to NE direction (Figure 7.46), and two along cross sections, one in the Western basin (Figure 7.47) and one in the Eastern basin (Figure 7.48), roughly in a N—S direction. The longitudinal profile is particularly instructive. It can be seen that the compact propagation of the traced river water in the lake was especially pronounced during the first day while, later on, the influence of bottom morphology and day/night differences in inflow water temperature caused a greater *fluctuation* of the traced water layer.

According to the different volumes of water injected through the two inlets into both basins (West:East = 1 : 1.8), the depth of the traced water layer in the Eastern basin is twice as thick as in the Western basin (Figures 7.47 and 7.48).

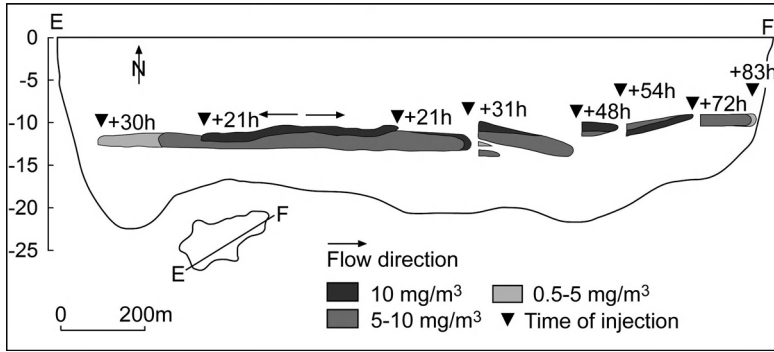


Figure 7.46 Rhodamine B experiment in Lake Bled. Longitudinal profile of tracer distribution (section E-F) in several time steps (h) after injection with phases of propagation (▼ + 21h = 21 hours after injection).

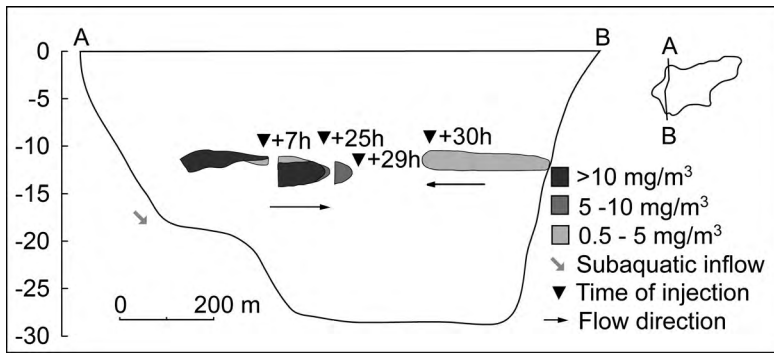


Figure 7.47 Rhodamine B experiment of 8 July 1982 in Lake Bled. Cross section (A-B) of tracer concentrations in the Western basin during the first and second day showing different phases of tracer propagation (▼ + 7h = 7 hours after injection). Layer thickness ≤ 2 m.

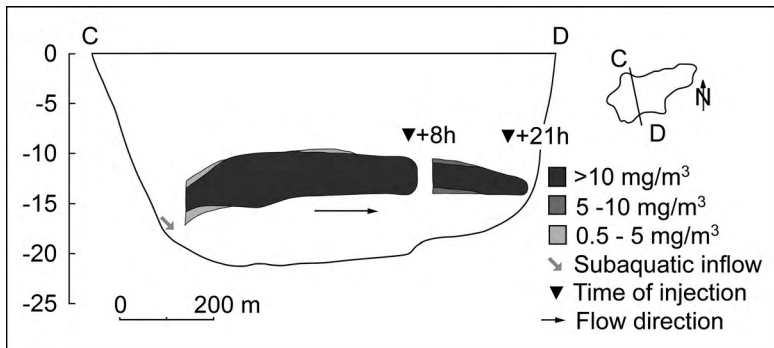


Figure 7.48 Rhodamine B experiment of 8 July 1982 in Lake Bled. Cross section (C-D) of tracer concentrations in the Eastern basin with different phases of tracer propagation (▼ + 8h = time after injection). Layer thickness ≤ 4 m.

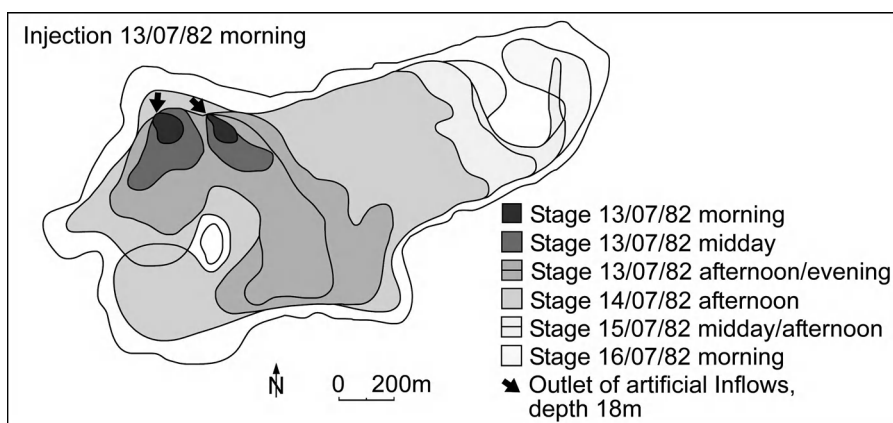


Figure 7.49 Internal dynamic of the hypolimnion visualized by measured tracer concentration of the Uranine experiment.

Second experiment 1982 – investigation of internal lake dynamics – Uranine experiment The experiment was carried out under similar thermic conditions with a stable stratification of the lake, a threefold inflow rate of 600 l/s through the pipeline, and a somewhat lower temperature of the utilized water from River Radovna of 7.3 °C. On July 13th, 6 kg Uranine in concentrated solution were injected into the artificial inflow. The decision to inject a considerably smaller injection mass compared to the first experiment was made due to the higher flow rate, which caused a shorter test duration. The subsequent flushing took 12 min. The higher solubility of Uranine allowed a much quicker injection compared to the Rhodamine B experiment. Again, several horizontal profiles were taken along longitudinal and transversal cross sections (Figures 7.50–7.52).

The mitigation of tracer cloud (front velocity) generally showed the same pattern as in the first experiment, but, due to the higher inflow rate, showed less distinctly shaped Coriolis force induced eddies to the right. This can be attributed to the faster propagation of the tracer cloud which inhibited the formation of such eddies (Figure 7.49). On the other hand, the left-rotation was more dominant than during the first experiment, which can be attributed to the stronger dynamic impulse of the successive water. However, the increment pattern of the general lake dynamic was less differentiated. At the end of the first day, the state of the second day in the first experiment was reached: the Western basin was completely filled with traced water, while simultaneously the velocity of the tracer cloud decreased.

Overall, tracer velocities were significantly higher than in the first experiment: in the Western basin, the inflow velocity was initially about 190 m/h with a subsequent rapid decrease to 50–60 m/h and finally to 10 m/h. In the Eastern basin, the initial inflow velocity was about 420 m/h, until the impact of the tracer cloud upon the Southern bank when it decreased to 100–150 m/h. On its way eastward, it further decelerated from 60 to 25 m/h and finally to a velocity of 12 m/h. The intensified flow dynamic was

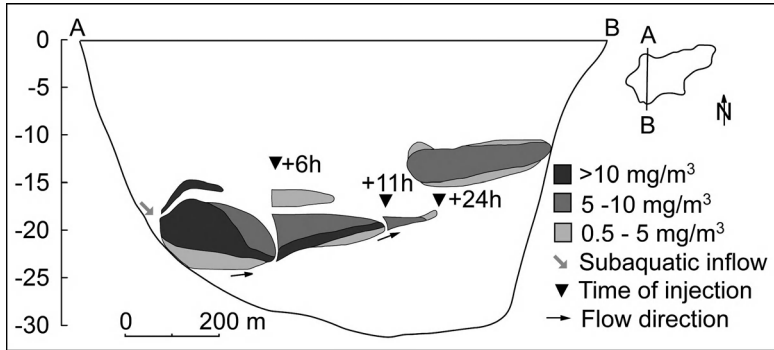


Figure 7.50 Uranine experiment of 13–16 July 1982 in Lake Bled. Section A–B with different phases of tracer propagation (▼ + 6 h = 6 h after injection).

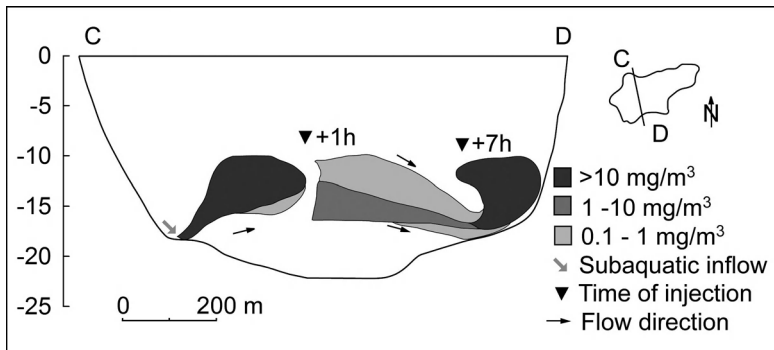


Figure 7.51 Uranine experiment of 13–16 July 1982 in Lake Bled. Section C–D with different phases of tracer propagation (▼ + 1 h = 1 h after injection).

manifold. The observed concentration differences within the traced water were much smaller. Compared with the first experiment, the layer formed by traced river water was distinctly thicker (approx. 8 m, see Figure 7.52).

An instructive picture of the flow dynamic is given in Figures 7.50 and 7.51. The stratifying according to the temperature dependent density, directly after entering the lake, is clearly represented. It was completed after one hour (Figure 7.51). After seven hours, the tracer cloud had already reached the opposite bank (Figure 7.51). Regarding the experiment's goal of keeping the freshwater beneath the thermocline, the effect of the turnover and the ascension was crucial. Had the freshwater penetrated the thermocline, the experiment would have failed due to the resulting exposition of the fluorescent tracer to the daylight. However, the stratification was strong enough to resist the dynamic forces, and confirmed the correct estimation and planning of the test.

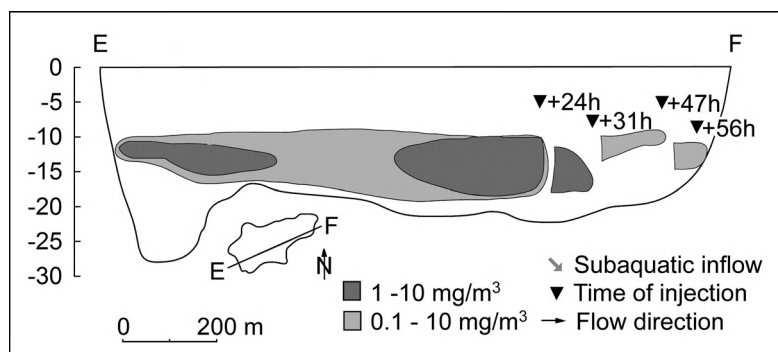


Figure 7.52 Uranine experiment of 13–16 July 1982 in Lake Bled. Section E–F with different phases of the propagation of the tracer cloud (▼ + 24 h = 24 h after injection).

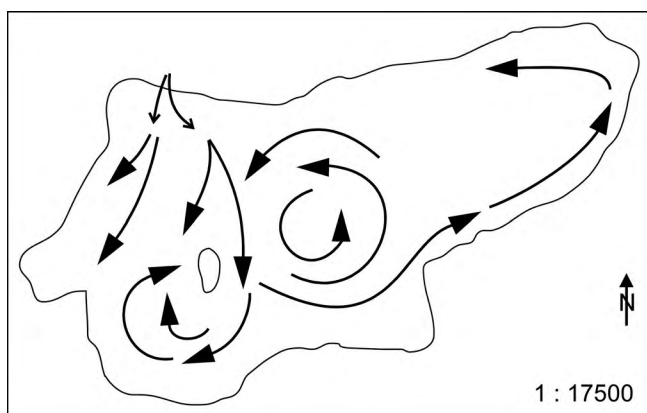


Figure 7.53 Schematic pattern of currents in Lake Bled, evaluated by tracer tests in summer 1982.

7.3.7.3 Interpretation of the experiments

Both experiments show the typical inflow-driven current characteristics of a lake in the Northern hemisphere caused by Coriolis forces: eddies of the inflowing water to the right within a general left hand rotation of the water masses. The individual impacts from lake topography, shape of lake, position of inlet and so on modify these circumstances for each lake (Figure 7.53).

The differences between the 200 l/s-experiment and the 600 l/s- experiment are to be found in the radius of the current turbulence and in the intensity of circulation. The differences in mitigation velocities are considerable. Accordingly, at an inflow rate of 600 l/s, the lake is supplied with fresh water at twice the speed (Table 7.14). With higher inflow and outflow rates, the fresh water spreads through the hypolimnion more quickly and more broadly and reaches the deep water outflow faster; therefore, the mean turnover time of the hypolimnion is clearly reduced under such conditions.

Table 7.14 Mitigation velocity of tracer clouds in the different experiments 1982, after Leibundgut *et al.* (1983)

| | Rhodamine B experiment (200 l/s) | | Uranine experiment (600 l/s) | |
|------------|----------------------------------|---------------|------------------------------|---------------|
| | Western basin | Eastern basin | Western basin | Eastern basin |
| 1/2 day | 28 m/h | 63 m/h | 50 m/h | 150 m/h |
| First day | 15 | 40 | 40 | 100 |
| Second day | 10 | 35 | 20 | 70 |
| Third day | — | 25 | — | 50 |
| Fourth day | — | 20 | — | 40 |

When looking at the decontamination of Lake Bled, one has to keep an eye on the long term effects of the experiments. In the 200 l/s experiment with Rhodamine B, the inflow rate was less than the maximum outflow rate of 380 l/s. Thus, there will be no rise in the water level, and the contaminant hypolimnion will be replaced from top to bottom, slowly, but successively. At an inflow rate of 600 l/s, the maximum outflow rate of the artificial outlet is exceeded, and the water level will rise, which by the overflowing of the spill causes a degradation of the epilimnion. However, the degradation is too small to initiate the breakup of the stratification.

With the lower boundary of the thermocline located at a depth of 12 m, the volume of hypolimnion in the summer of 1982 was about $10.3 \times 10^6 \text{ m}^3$, which can be considered to be characteristic for summer stagnation. Thus, the 200 l/s inflow rate resulted in a theoretical mean transit time of the lake water of 2 years and 200 days as calculated by comparing the inflow rate and volume of lake water. The Rhodamine B reached the lake bottom after 2 months while Uranine was detected in the diversion water after 40 days, and, in the overflow, after 50 days. Thus, the effect of restoration measures is higher at higher inflow rates. Stratification, at the most, will be shortened by a few days, but not disturbed. Nevertheless, to be safe, keep in mind the necessary stable stratification in order to avoid a breakthrough of hypolimnic water to the epilimnion.

The further development of the lake, concerning its trophic state, can be summarized briefly: In the years 1982–1985 a renovation of Bled's sewage system decreased the inflow of wastewater into the lake. Consequently, the primary nutrient charge decreased. Subsequently, due to the siphon installation and sewage system development carried out in 1982, nutrient concentrations had been decreasing gradually. This has been reflected in a lower total phytoplankton biomass, lower average chlorophyll concentration, and the increased higher average and maximum transparency of the lake. According to monitoring data, Lake Bled ranked among the eutrophic lakes in 1970s. Owing to its effective antipollution treatment, Lake Bled has now once again joined the rank of the moderately polluted mesotrophic lakes.

7.3.7.4 Modelling

Lake dynamics models are the principal tool in state of the art investigations. At Lake Bled, no transport model was available at the time of the first experiment in 1982. For once, the tracer experiment was not a tool of model validation, but provided the

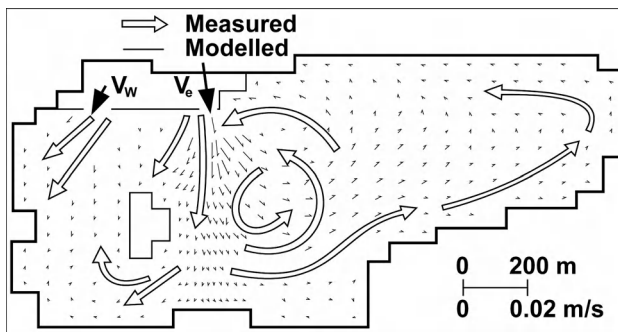


Figure 7.54 Comparison of measured and modelled velocities and general circulation patterns in Lake Bled (from Rajar, 1989, modified).

definition of the boundary conditions in the mathematical model. The system to be modelled is regarded as two-dimensional, because the inflowing water only moves in the stratified layer with temperatures ranging from 8 to 11 °C between the epi- and the hypolimnion. The basic equations applied in the modelling approach are the continuity and two-dimensional dynamic equation. Additionally, a finite difference numerical method (hybrid scheme) was used to solve them (Patankar, 1980). It was later further developed by Rajar, Četina and Širca (1997).

Since the control volumes of the numerical grid were relatively large, the boundary had to be displaced into the interior of the lake. Conservation of momentum was taken into account for the measured velocities in the tracer experiment for those boundaries. In the model, it is assumed that the inflow water of the pipeline replaces the hypolimnic water approximately uniformly towards the bottom, as ascertained experimentally in the second tracer study. In every control volume lateral as well as vertical flow is assumed. The volume ($\Delta x = 70$ m, $\Delta y = 50$ m) is calculated with a four times smaller Δx near the Eastern inflow jet. The Coriolis effect, as shown in Figure 7.53, is taken into account for the model. The calculation was done for a 1 m deep layer. The model was fully elliptic (Rajar, 1989). The measured magnitude of velocity was in the order of 1×10^{-3} m/s, except in the Eastern edge of the lake, where it was smaller (Figure 7.54).

Considering the rather poorly defined boundary conditions, the computed values and patterns matched the measured ones satisfactorily. The model depicts nicely the situation in the Western basin where the downward flow towards the siphon is not uniform, but is concentrated west of the island, as shown in the currents in Figure 7.54. The difference in the centre of the vortex in the Eastern basin is probably due to the assumed constant coefficient of effective viscosity.

7.3.7.5 Second study 1988–1991 – determination of residence time

While mean residence times of lakes are usually determined by natural tracers, such as tritium or geogenic compounds (Mori, 1978; Ozretisch, 1975; Gat, 1981; Gonfiantini, 1986; Gibson, 2002a), the capacities and limits of a fluorescent tracer were investigated in the study presented here.

The tracer experiment in 1988 was aimed at calculating the mean transit time of lake water using the knowledge of the internal dynamics gained from the 1982 test (Leibundgut and Zupan, 1992). At 5 p.m. on the 10th of August, 20.57 kg of the fluorescent tracer Uranine were injected into the intake of the Radovna pipeline. The injection of the tracer was completed within 10 s. Rinsing the containers took 5 min and cleaning the water basin of tracer took another 15 min. The discharge was 1000 l/s. Water samples were taken at the following sampling sites (see Figure 7.40):

- Lake: in the centres of the Western and Eastern basin vertical profiles, samples were taken every 2 m down to the bottom, at 24 m or 30 m depth respectively, from the 15th of August until February 1991. Samples were taken two to three times a month in August, September and October 1988, and once a month in 1989 until February 1991.
- In the natural outflow 'Jezernica' at Mlino samples were taken from 10th of August 1988 until February 1991. Samples were taken at 6 a.m. and 6 p.m., almost daily in the month after injection, and less frequently later on.
- At the artificial hypolimnic outflow Natega samples were taken from 10th of August 1988 until October 1990. Samples were also taken at 6 a.m. and 6 p.m., almost daily in 1989 and at less regular intervals later on.

Further tracer samples were collected on a monthly basis for the duration of more than two years after the injection in the Western and Eastern basin of Lake Bled. Additional samples were collected at the outflows of Lake Bled almost daily in 1988 and 1989, but just monthly later on. Discharge data for the artificial inflow of Radovna water and the hypolimnic outflow (Natega, TWA) were recorded. The measurements were carried out by the Limnological Station Bled. Data for daily discharge of the natural outflow Jezernica were taken from the stream flow record of the Jezernica and compiled by the Environmental Agency of Slovenia. Additionally, in the Eastern basin, profiles of temperature, oxygen and ammonium were taken monthly at 2 m intervals (from the surface to the bottom at 24 m) from September 1988 until November 1989.

The total volume of Lake Bled and its Eastern and Western basin were calculated corresponding to the depths of the water sampling (Table 7.15), on the basis of the areas of the Lake Bled isobaths (see Figure 7.41). Changes in water levels were not taken into account for the calculations.

During the start of the tracer experiment in August 1988, the lake showed a stable thermal stratification. The thermocline was at a depth of 8–12 m. The stratification declined quickly in November 1988 and the lake was homothermous in December 1988. On days with strong winds, the lake was probably circulating during the entire winter, apart from those days when the lake was ice covered. There is no information available for the months of January and February 1989. It was not possible to do any measurements because the ice on the lake was too thin to walk on. At the beginning of March, the lake was again homothermous. It started to become stratified again by the end of March. This stratification lasted until November 1989, with the thermocline changing its depth (4–14 m) and thickness (2–6 m).

Table 7.15 Volumina of entire Lake Bled and its Eastern and Western basin

| Depth [m] | Upper limit [m] | Lower limit [m] | Volume [m ³] | | |
|-----------|-----------------|-----------------|--------------------------|-------------------|-------------------|
| | | | Entire Lake Bled | Eastern Lake Bled | Western Lake Bled |
| 0 | 0.0 | 1.0 | 1 415 880 | 961 730 | 454 150 |
| 2 | 1.0 | 3.0 | 2 759 040 | 1 892 440 | 866 600 |
| 4 | 3.0 | 5.0 | 2 662 080 | 1 851 080 | 811 000 |
| 6 | 5.0 | 7.0 | 2 566 880 | 1 805 440 | 761 440 |
| 8 | 7.0 | 9.0 | 2 473 440 | 1 755 520 | 717 920 |
| 10 | 9.0 | 11.0 | 2 371 800 | 1 697 780 | 674 020 |
| 12 | 11.0 | 13.0 | 2 253 760 | 1 624 400 | 629 360 |
| 14 | 13.0 | 15.0 | 2 127 520 | 1 543 200 | 584 320 |
| 16 | 15.0 | 17.0 | 1 950 400 | 1 413 500 | 536 900 |
| 18 | 17.0 | 19.0 | 1 692 600 | 1 207 700 | 484 900 |
| 20 | 19.0 | 21.0 | 1 385 900 | 952 000 | 430 900 |
| 22 | 21.0 | 23.0 | 1 011 800 | 639 300 | 372 500 |
| 24 | 23.0 | 25.0 | 533 900 | 169 400 | 304 100 |
| 26 | 25.0 | 27.0 | 226 900 | | 226 900 |
| 28 | 27.0 | 29.0 | 113 600 | | 113 600 |
| 30 | 29.0 | 30.0 | 10 450 | | 10 450 |

Calculation of residence time from the tracer test The amount of Uranine within Lake Bled was determined for the separate sampling dates. The measured Uranine concentrations in the different depths were assumed to be consistent within the corresponding layers. The calculated volumes and concentrations of the layers were added up separately for the whole water mass of the Eastern and Western basin, and for the entire lake (Table 7.16).

Uranine concentration data for days without measurements of the Uranine concentration were obtained by linear interpolation. Only daily averages were taken into consideration. About 60% (12.3 kg) of the amount of injected tracer (20.6 kg) was found in the lake on 19th August, just nine days after the injection (see Table 7.16). The “loss” of Uranine (app. 40%) has probably to be attributed to incorporation by organisms, as just a very small amount of the ‘lost’ tracer was found in the outflows. It is known that Uranine attaches to algae, but no detailed information is yet available. The calculation of Uranine (kg per day) passing through the natural outflow Jezernica, and the hypolimnic outflow Natega, was done on a daily basis.

The Uranine content in Lake Bled was initially nearly stable, as it remained virtually constant during the first month after injection on the 10th of August. A first decrease from approximately 12 to 4 kg of total Uranine occurred between the end of August and 19th September, 1988. Between 21st November and 20th December, when the lake changed from stratification to a homothermous state, a sudden strong decrease was observed (see Table 7.16, Figure 7.55).

Whereas the first decrease was caused probably by bio-absorption, the second was due probably to photolytic decay. During lake circulation, the tracer Uranine was

distributed throughout the whole water column, and decay in the first metre could take place due to incoming radiation. The theoretical half-life of Uranine is 11 h under the influence of daylight (see Section 4.1.2.6). The decrease in quantity of Uranine within the lake can be estimated by an exponential function:

$$c(t) = c_0 \exp(-\lambda t) \quad (7.18)$$

with: c = Uranine concentration after time (t)

c_0 = Uranine initial concentration ($t = 0$)

t = days after start

whereby λ = is the decay constant equal to $\ln 2/t_{0.5}$ with $t_{0.5}$ being the actual half-life of Uranine in Lake Bled during the tracer experiment, expressed in days

The mean concentration of Uranine in Lake Bled on 21st November, was $c_0 = 0.15 \text{ mg/m}^3$. The actual half-life of Uranine during the experiment is different from the theoretical half-life of Uranine due to the fact that the Uranine was only partly

Table 7.16 Ascertained Uranine amounts in Lake Bled [g/basin] (values are rounded)

| Day | Entire Lake | Western Basin | Eastern Basin |
|-----------|-------------|---------------|---------------|
| 15.08.88 | — | — | 4434 |
| 19.08.88 | 12313 | 7493 | 4820 |
| 27.08.88 | 11830 | 8349 | 3481 |
| 19.09.88 | — | — | 1738 |
| +20.09.88 | 4192 | 2455 | — |
| 27.09.88 | 4691 | 2895 | 1797 |
| 10.10.88 | 4853 | 3038 | 1815 |
| 18.10.88 | 3792 | 2213 | 1579 |
| 26.10.8 | 3857 | 2304 | 1553 |
| 28.10.88 | — | 2577 | — |
| 21.11.88 | 3824 | 2437 | 1388 |
| 20.12.88 | 272 | 150 | 122 |
| 24.01.89 | — | — | 13 |
| 01.03.89 | 80 | 55 | 25 |
| 21.03.89 | 28 | 4 | 23 |
| 18.04.89 | 148 | 111 | 37 |
| 16.05.89 | 58 | 17 | 41 |
| 13.06.89 | 23 | 23 | 0 |
| 06.07.89 | 35 | 16 | 19 |
| 08.08.89 | 41 | 22 | 19 |
| 13.09.89 | — | — | 3 |
| +14.09.89 | 40 | 36 | — |
| 10.10.89 | — | 0 | — |
| 02.11.89 | 24 | 23 | 1 |
| 05.12.89 | — | — | 0 |
| +06.12.89 | 16 | 16 | — |

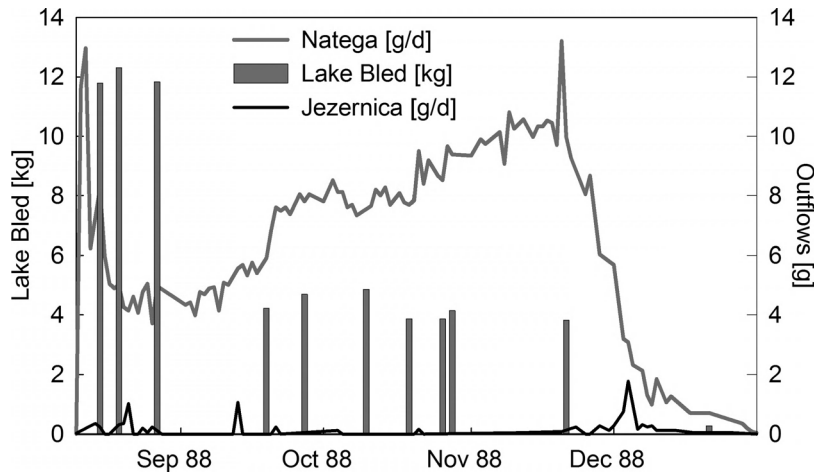


Figure 7.55 Contents of Uranine within Lake Bled, and losses through its outflows Natega and Jezernica.

Table 7.17 Measured and calculated Uranine concentrations

| Date | Measured Uranine | | Calculated Uranine | |
|----------|----------------------|-------|----------------------|-------|
| | [mg/m ³] | [kg] | [mg/m ³] | [kg] |
| 21.11.88 | 0.15 | 3.82 | | |
| 20.12.88 | 0.011 | 0.27 | 0.014 | 0.38 |
| 01.03.89 | 0.003 | 0.08 | 0.0034 | 0.09 |
| 21.03.89 | 0.001 | 0.027 | 0.007 | 0.018 |

exposed to the daylight. We assume that the decay of Uranine takes place only within the first metre of the water column, which has a volume of $1.42 \times 10^6 \text{ m}^3$. Under the further assumption of 12 h of daylight and a daily renewal of the exposed water volume during homothermal days, we can calculate an actual half-life of Uranine within Lake Bled of $t_{0.5} = 8.46$ days. For days with ice-cover (54 days in the winter 1988/1989), we assume that there is no decay through light. Table 7.17 shows the measured and calculated values of Uranine concentration and amounts of Uranine within Lake Bled for the homothermous phase from November 1988 until March 1989.

With the beginning of the stratification of the lake at the end of March 1989 and 1990, respectively, a sudden increase of Uranine within the lake occurred (Figure 7.56). It seems to be correlated to the known distribution of nutrients which are fixed in the sediment during the stagnation, and which will be redistributed in the lake water at the beginning of the circulation phase. The amount of Uranine decreased again by the end of 1989. A similar pattern was found in 1990. The high value in December 1990 might have been caused by a mistake in measurements, as there was no Uranine measured in the Western basin apart from the very high value of 2.6 mg/l in the sample at the depth of 24 m. The measurements at the same date in the Eastern basin detected Uranine

in only 8 and 24 m depth with values about 200 times lower (0.012 and 0.015 mg/l, respectively) than in the Western basin.

As expected only a very small amount of Uranine was measured in the natural outflow Jezernica. Daily losses in the range of a few milligrams, amounted to a few grams a month (see Figure 7.56). With the start of the circulation, the Uranine concentration increased suddenly, but went back to low values a few days later. On 28th November 1988, 120 days after the injection on 10th August 1988, Lake Bled had changed from stratification to a homothermic state. The amount of Uranine leaving the lake through the hypolimnic outflow Natega was higher, but did not coincide with the decrease of Uranine within the lake basin. It amounted to a few grams a day, or 100 to 300 g a month, in the months August, September, October and November 1988. After the start of circulation in Lake Bled in November 1988, Uranine concentration in the hypolimnic outflow decreased rapidly to a few grams per month (Table 7.18).

In the year 1990, the Uranine outflow through the natural effluent was distinctly higher than in the year 1989, immediately after the injection. Overall, it showed a kind of seasonal pattern (see Figure 7.56). During the lake's stagnation in the first three months of the tracer experiment, the decay of the fluorescence under daylight can be neglected. With the start of the circulation, 120 days after the injection on 28th November 1988, the Uranine concentration increased suddenly but went back to low values a few days later. The amount of Uranine leaving the lake through the hypolimnic outflow Natega was higher, but did not coincide with the decrease of Uranine within the lake basin. It amounted to a few grams a day, or 100 to 300 g a month, in the months August, September, October and November 1988. After the start of the circulation of Lake Bled in November 1988, Uranine concentration in the hypolimnic outflow decreased rapidly to a few grams per month (Table 7.18). Stored Uranine was probably set free during the circulation phase. Two years after the injection, Uranine was still

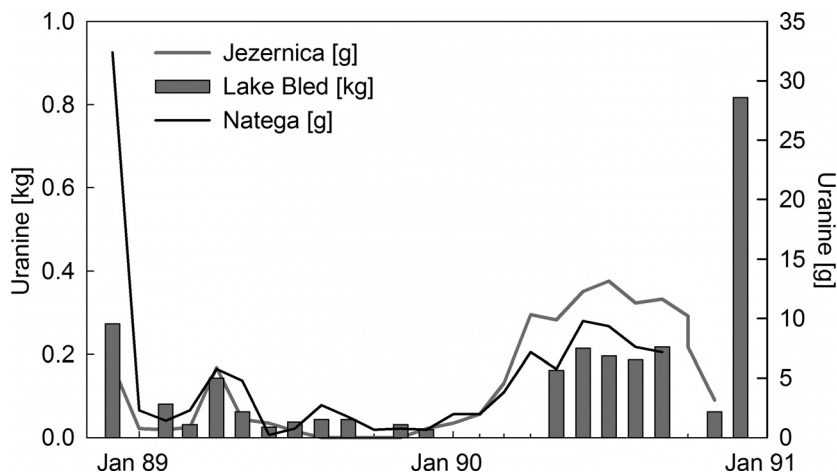


Figure 7.56 Uranine contents in Lake Bled and Uranine losses through the outflow Jezernica from December 1988 until February 1991.

Table 7.18 Monthly discharge and loss of Uranine through the hypolimnic effluent Natega and the effluent Jezernica

| Month | Discharge [m ³ /month] | | Uranine loss [kg/month] | |
|-------|-----------------------------------|-----------|-------------------------|-------------|
| | Natega | Jezernica | Natega | Jezernica |
| 08.88 | 607 392 | 1 508 544 | 0.119 793 6 | 0.003 182 2 |
| 09.88 | 648 000 | 8 84 736 | 0.178 113 6 | 0.002 230 0 |
| 10.88 | 669 600 | 5 28 768 | 0.258 357 6 | 0.000 327 5 |
| 11.88 | 648 000 | 270 432 | 0.281 772 0 | 0.002 327 6 |
| 12.88 | 626 832 | 305 166 | 0.032 231 1 | 0.006 034 8 |
| 01.89 | 267 840 | 559 089 | 0.002 073 6 | 0.000 826 1 |
| 02.89 | 241 920 | 855 265 | 0.001 252 7 | 0.000 406 0 |
| 03.89 | 475 200 | 673 312 | 0.002 099 4 | 0.000 612 8 |
| 04.89 | 872 640 | 665 537 | 0.005 620 4 | 0.005 835 8 |
| 05.89 | 751 680 | 374 370 | 0.004 635 2 | 0.001 333 7 |
| 06.89 | 756 000 | 759 538 | 0.000 937 5 | 0.001 019 1 |
| 07.89 | 846 720 | 487 467 | 0.000 574 7 | 0.000 375 8 |
| 08.89 | 937 440 | 622 682 | 0.002 600 6 | 0.000 000 0 |
| 09.89 | 665 280 | 567 732 | 0.001 633 2 | 0.000 000 0 |
| 10.89 | 937 440 | 364 434 | 0.000 514 1 | 0.000 000 0 |
| 11.89 | 907 200 | 798 851 | 0.000 604 9 | 0.000 000 0 |
| 12.89 | 846 720 | 922 320 | 0.000 634 4 | 0.000 713 8 |

Table 7.19 Residence time of water in Lake Bled

| | |
|--|----------------|
| Theoretical mean residence time (relation inflow/outflow) | App. 4 years |
| Experimental mean residence time (from true tracer concentration) | App. 7.5 years |
| Experimental mean residence time (from corrected tracer concentration) | App. 4.5 years |

found within the lake's basins and in the outflows. This can be explained by a 'storing' of the Uranine, safely away from decay due to light. Nevertheless, it also gives a hint that the real residence time of Lake Bled is very long. Since Lake Bled is situated in a karstified region it cannot be completely ruled out that a considerable part of the lake water is disappearing through an unknown sublacustric karst channel.

It is difficult to calculate the residence time from the tracer experiment because of the great difference of the amount of Uranine within the lake, and its outflow through the effluents. Therefore, the mean residence time can be calculated approximately solely on the basis of the Uranine loss through the outflows Natega and Jezernica. The following observations were made: On 28th November 1988, 120 days after tracer injection, when the lake started circulation, 853 and 8 g Uranine had left the lake via the hypolimnic outflow and the natural outflow, respectively. Thus, it would theoretically take 2760 days, or 7.5 years, to renew the water in the lake, or in other words, before all the Uranine would have left the lake. Taking the Uranine loss by bio-absorption into consideration (40%), the mean residence time is corrected to approximately 4.6 years, which corresponds well with the theoretical mean residence time of approximately 4 years, calculated from the relation of inflow and outflow in 1983 (Table 7.19).

The same model, although somewhat modified, used to evaluate the first tracer study was applied again (Rajar and Cetina, 1986). To model the mean residence time of water in Lake Bled, a function from previous recovery and residence time was developed. Including the consideration of losses due to bioabsorption, this function was applied to the entire injected tracer mass. However, the instability of the tracer in long-term tests was problematic.

7.3.7.6 General assessment

The tracer experiments in Lake Bled were carried out in order to prove the suitability of an artificial fluorescence tracer experiment for lake mixing investigation. To obtain more detailed information on the residence time was another objective. With Uranine being used for the first time as a tracer in a long-term investigation in such a big water basin ($25.56 \times 10^6 \text{ m}^3$), some problems occurred which made it difficult to get the appropriate results for the problem to be solved, especially because little is known about the incorporation of Uranine by, or the attachment to, organisms. For short periods of time, for example from tracer injection until the beginning of the circulation, some calculations are possible. Because of the Radovna water stratifying underneath the thermocline, these calculations only describe the replacement of the hypolimnion with Radovna water. The simulation of the decrease in Uranine concentration, based on the decay of Uranine through light, resulted in values comparable to the measured ones. Therefore, only a short time prediction of Uranine concentration was possible in Lake Bled. The measurements in the years after the injection showed that there had to be other processes involved as well. Due to political restrictions, it was not possible to investigate with environmental isotopes in Lake Bled. Also, the insufficient knowledge of the microbial uptake of Uranine, the karstic environment, and the fact that the water was only renewed in the hypolimnion added to the problems that were encountered.

7.3.8 Case study: 'Optimization of a sewage effluent into Lake Murten'

Within lake catchments the drainage of purified sewage into the lake is often not preventable. Frequently, expertise on this topic is required. The central problem is in each case the determination of the optimal positioning of the effluent pipeline's mouth. As far as possible it should be situated in the hypolimnion in order to avoid an eutrophication of the epilimnion during the summer stagnation (Nydegger, 1967, 1976; Leibundgut and Hirsig, 1977; Hirsig, Leibundgut and Nydegger, 1982; Hirsig, 1983; Leibundgut and Zupan, 1992).

Nowadays the issue is usually a matter of modelling. However, such models are rarely readily available and the effort to establish a reliable model is considerable. This is true in particular for the problem presented there since the local border conditions such as bottom and bank morphology have a strong impact on the advection and dispersion of local currents and are not well known in Lake Murten. Tracer experiments are a target oriented alternative as they can help to establish and to validate a model (see Section 7.3.4).

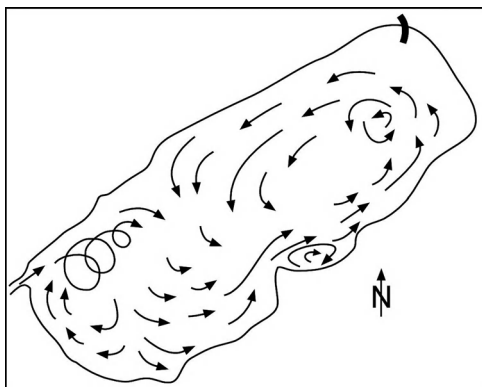


Figure 7.57 Principle inflow induced current patterns of a lake on the Northern hemisphere due to Coriolis forces exemplarily shown at Lake Murten, Switzerland (Nydegger, 1976).

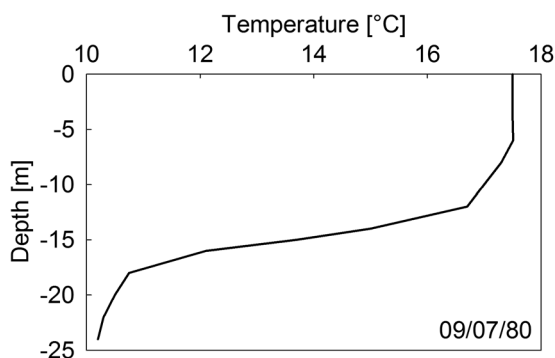


Figure 7.58 Vertical profile of water temperature in Lake Murten on 9 July 1980. The thermocline extends from 12 to 17 m below surface (from Hirsig, 1981, modified).

Information about the principle inflow induced patterns driven by the Coriolis forces of currents in lakes in the Northern hemisphere, according to Nydegger (1976), is provided in Figure 7.57 (cf. colour plate section, Plates 5–7). The current pattern of this phenomenon showing the characteristics of eddies to the right within the general left rotation is shown by way of example for Lake Murten (Nydegger 1976).

Lake Murten is a well-mixed Swiss alpine foreland lake. The goal of the investigation was to follow the subaquatic stratification and propagation of treated sewage effluent into the lake in order to determine the optimal site and depth of the effluent pipe (Hirsig, Leibundgut and Nydegger, 1982). The stratification and propagation of the effluent are affected by physical environmental parameters such as the water temperature (Figure 7.58) and the currents, which are driven the river water inflow and by the wind (Hirsig, Leibundgut and Nydegger, 1982; Leibundgut and Zupan, 1992).

To accomplish this task, 6 kg of Uranine were injected on ninth July 1980 over 3.5 h through the existing sewage effluent pipe at a depth of 8 m (Figure 7.59). The continuous

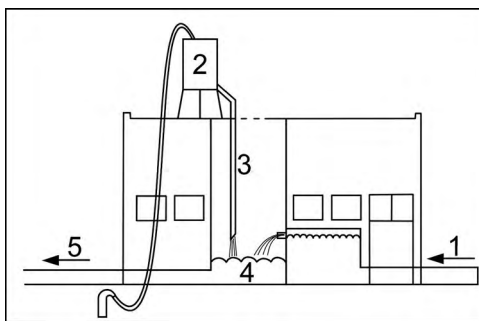


Figure 7.59 Tracer injection at sewage plant by means of a 'Mariotte bottle' (2) to ensure a constant inflow rate. (1) inlet sewage water, (3) injection hose, (4) traced sewage, (5) pipe to the lake (from Hirsig, 1981, modified).

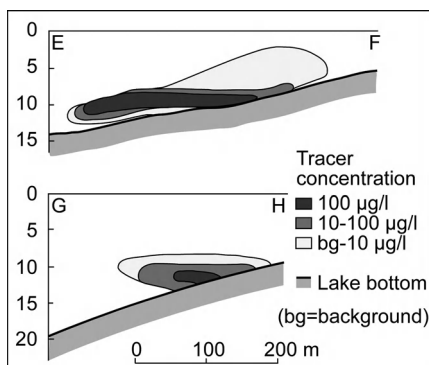


Figure 7.60 Profiles E-F and G-H of traced effluent water shortly after injection. Situation of cross sections see Figure 7.61.

injection ensured that possible short term variable conditions upon entering the lake would be smoothed. The experiment was carried out intentionally under potentially difficult environmental conditions caused by high inflow runoff and strong wind.

Over the following two days, the propagation of the tracer cloud in the lake was registered by means of six boat trips using an underwater in situ fluorometer (Variosens). The increased salt content and the heavy suspended solid material of the sewage water resulted in an increased density of the sewage water tracer mix. Therefore the traced effluent solution sank at first and formed an approximately 1 m thick layer above the lake slope. As expected, the tracer cloud subsequently stratified directly above the thermocline at a depth of 10 to 12 m (Figure 7.60).

Additionally, the propagation of the tracer cloud was governed by the inflow induced lake current as visualized in Figure 7.57 and, simultaneously, by a west wind induced current. The current induced by the inflow of the river 'La Broye' was very strong during the test as a result of the high runoff. However, the wind impact was also considerable. This westward current was especially prominent above the thermocline, thus in the layer

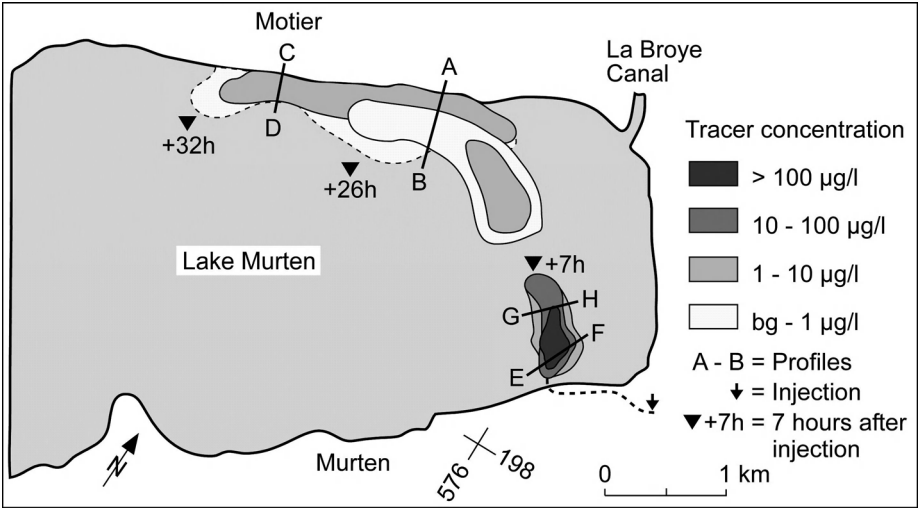


Figure 7.61 Transport stream of treated effluent in Lake Murten (July 1980) traced by Uranine. Location and horizontal dispersion.

where the stratification of the tracer cloud occurred. The track of the traced effluent water followed the general counter clockwise left rotation around the lake (Figure 7.61). Within this main stream eddies to the right, driven by Coriolis forces, caused a mixing of the tracer cloud with lake water and diluted the tracer concentration.

Due to the combination of the currents caused by inflow and wind, the sewage water rose partially to the surface at the opposite bank of the lake as shown in the profiles A–B and C–D in Figures 7.61 and 7.62. This effect is highly dangerous and should be avoided since it activates the eutrophication providing nutrients in the trophic layer of the lake.

However, a dilution by a factor of 1:200–4000 had occurred, which lowered the danger with respect to eutrophication. The superimposition of the currents, on the other hand, is a plausible explanation of the observed spreading of the tracer cloud. The maximum transport velocity was around 100–130 m/h. Based on the results of the tracing experiment, an optimal inflow depth of 9 m was recommended. During similar conditions in the summertime, the River ‘La Broye’ induces a strong current

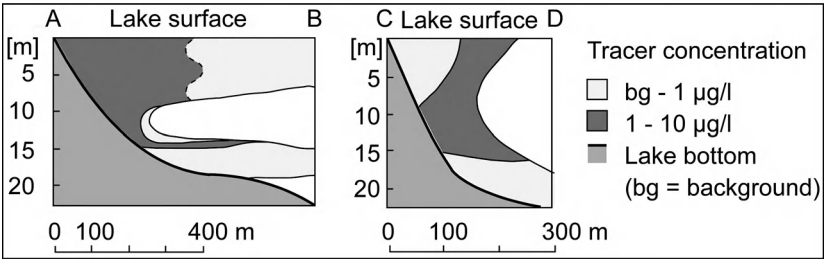


Figure 7.62 Vertical profiles A–B and C–D through the tracer cloud at the wet bank of the lake. Location see Figure 7.61.

over the thermocline in this depth. This ensures a dilution of the sewage and will thus prohibit an increased build-up of nutrients. During phases when the effluent water has a lower temperature, it will stratify deeper and consequently be less harmful regarding eutrophication.

7.4 Glaciers

Current global climate change is affecting glaciated areas especially. The meltwater runoff volumes coming from glaciers and the processes that form runoff are of increasing interest in planning for future water resources management in mountain and mountain foreland regions. The issue is to be found beneath the headline: 'Mountains as Water Towers.' The runoff from mountain areas is of considerable and increasing relevance as a source of water supply and irrigation, as well as for hydroelectric power generation (e.g. Weingartner, Viviroli and Schädler, 2007; Notter *et al.*, 2007; Viviroli *et al.*, 2007; Hagg *et al.*, 2006). Research and expert work on water balance and runoff generation in mountain regions, and glaciated areas in particular, uses tracer methods broadly, both artificial and natural. In the context of climate change, environmental tracers are widely used for paleoclimatological and paleohydrological studies. Stable isotopes and gaseous tracers (CO₂, noble gases) play an important role for the reconstruction of past climatic conditions. This issue, however, is not the subject of this book.

The issue of snowmelt and runoff components from glaciatic areas is investigated intensively by environmental tracers. Runoff from glaciated catchments is characterized by a high temporal and spatial variability. Variations are observed at the daily and seasonal time scale. The focus of the studies presented in the following is on internal drainage patterns and processes rather than on snow hydrology.

Hydrologically, glaciers have similarities to solid and unconsolidated rock aquifers. A glacier can be considered to be an aquifer, although with specific characteristics. Water itself forms the aquifer consisting of ice, firn and snow (water in solid phase), while rocks and other debris material are transported by the glaciers and finally deposited as moraines (Figure 7.63). This particular aquifer is highly dynamic due to temperature dependence, which causes rapidly alternating solid-liquid phase transitions. Storage, runoff and phase transitions show a high temporal variability.

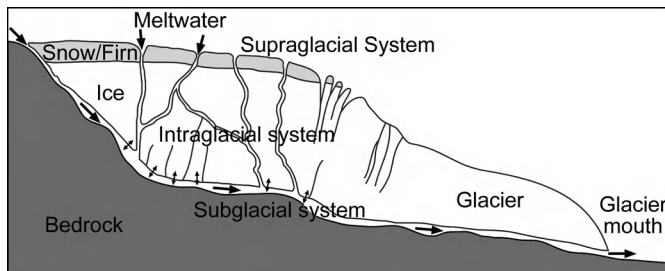


Figure 7.63 The glacier and its drainage system (from Aschwanden and Leibundgut 1982, generalized)

In hydrological terms the three subsystems of the drainage system in a glacier can be compared to groundwater aquifers (Shreve, 1972; Lang, Leibundgut and Festel, 1979; Oerter, 1981). These subsystems consist of the supraglacial system formed by partially saturated snow and firn, the intraglacial subsystem characterized by preferential flow paths and a subglacial flow system. Aschwanden and Leibundgut (1982) postulated and used a three-component model to explain the drainage of the Corner glacier during ablation. In this model, the intraglacial system was represented by a fissure-fracture system and the subglacial system was described as a channel network. The subglacial flow system is often characterized by large tunnels at the end of the ablation period. A certain similarity to fissured rock and karst aquifers is obvious.

The covering snow and firn layer has porous aquifer properties. During diagenesis, the hydraulic conductivity of the firn body decreases more and more, and reaches very low values in the glacier ice. The intra- and subglacial fissures and fractures are caused by pressure differences and shear stress. Meltwater can widen these fissures to channels. Finally, the flow concentrates in major subglacial drainage channels at the bottom of the glacier (Röthlisberger, 1972; Iken and Bindshäddler, 1986). The widening of these channels can be reversed when the water pressure in these ice channels drops beneath ice pressure. The seasonal development of the glacial drainage system as well as the daily variations of runoff results from the balance of these processes (Röthlisberger and Lang, 1987).

The water cycle of a glaciated catchment can be conceived as the total flow through a series of connected or parallel storage systems. This corresponds to a multiple component model with varying fractions of slow and fast components. While precipitation is the primary infiltration source in the snow covered parts of the catchment, ablation is the most important factor controlling discharge. Total discharge consists of surface, intra- and subglacial flow, while in some cases groundwater flow from the underlying aquifer can also be significant. In the upper snow-firn layers, models normally used for porous unconsolidated rock aquifers can be applied (Oerter and Moser, 1982).

Applying tracers in hydroglaciology is generally a case of inverse system identification. According to the system approach in tracerhydrology a known input (water, tracer, minerals) is transformed into a measurable output through a system that is to be determined (cf. Chapter 2). Tracers enable an identification of runoff components and the determination of flow and transport parameters.

By analogy to spring catchments, glacier catchments usually have a collected runoff in the form of a glacial stream rising at the glacier mouth. In studies investigating the glacial runoff, the water should be sampled as close as possible to the glacier mouth. Hydrological information about the glacial catchment is stored naturally in variations of runoff, mineralization and isotope signatures, or in the observed concentration of an injected tracer. In combination with techniques for runoff separation, this information can be deciphered and can provide conclusive information on the system itself, including storage and runoff (Leibundgut, Uhlenbrook and McDonnell, 2001). Since artificial tracer tests give insight into the internal processes of flow in the glacier system, they are helpful tools for establishing adequate, experimentally sound model conceptions about runoff from glaciated areas.

Tracer methods have manifold applications in hydroglaciological research. The characteristic scale of the problem under investigation is an important criterion for the application of natural or artificial tracers. The combined application of natural and artificial tracers is the best option, because one provides integrated information and the other provides the response to an exactly defined input function. Investigations on mass balance and integrated studies on runoff generation processes (experimental hydrograph separation) are the principal field in which isotopic and other natural tracers are applied (Moser and Ambach, 1977; Behrens, Oerter and Reinwarth, 1982; Oerter, 1981). Pure meltwater differs from groundwater by the almost complete absence of organic components and a much lower mineralization. Both components can be separated by means of geogenic tracers such as Na^+ , K^+ , Ca^{2+} , Mg^{2+} and electrical conductivity (Collins, 1977, 1979a, b, 1982; Brown and Fuge, 1998; Tranter *et al.*, 2002).

The primary aim of an artificial tracer experiment is to get a complete tracer breakthrough curve. The purpose is to gain as much information as possible about the water flow. Artificial tracers in hydroglaciology are applied mainly to investigate the drainage behaviour of glaciers and particularly the development of the glacial drainage system. Furthermore, they can be used to prove hydrological connections and separate catchment areas. Additionally, they allow the determination of flow parameters such as flow velocity and dispersion. Depending on the problems to be solved, most of the experiments are conducted during the ablation period (Shreve, 1972; Lang, Leibundgut and Festel, 1979; Aschwanden and Leibundgut, 1982; Leibundgut, 1986a, b; Moeri and Leibundgut, 1986; Seaberg *et al.*, 1988; Nienow, Sharp and Willis, 1998; Fountain and Walder, 1998; Hock and Hooke, 1993; Hock, Iken and Wangler, 1999; Schuler, 2002).

Alpine, temperate glaciers show a characteristic development of the glacial drainage system starting in spring and accelerating into summer. This process is reversed during the fall. The winter drainage is of less significance. To summarize the development, a characteristic picture can be drawn (Leibundgut, 1986b). The results of a systematic investigation of this issue in the Findelen Glacier in the Swiss Alps are given in Figure 7.64. The development of the drainage system is described by the parameter runoff (m^3/s).

The overall picture in Figure 7.64 shows the characteristic evolution during the ablation period. Except in July, the variability from year to year is moderate. In principle, the figure also shows the glacial runoff regime from glaciated areas. It is, amongst the different types of flow regimes, one with the smallest variability from year to year (Aschwanden, Weingartner and Leibundgut, 1986).

Performed successfully, artificial tracer tests provide a tracer breakthrough curve. On that basis, the flow and transport parameters (velocities and dispersion) are obtained (Brugman, 1986). The parameters obtained from tracer experiments in the Findelen Glacier depicted in Figure 7.65 together with the tracer recovery, confirm the picture shown in Figure 7.64, in principle. The effective start of the drainage system evolution is in June, which corresponds approximately to the long term mean average. The maximum is reached in July (Figure 7.64) or in August (Figure 7.65). In September/October a strong decline of the drainage system is evident. However, two distinct effects are recognizable. The flow velocities show asymmetries in development and backformation. In spite of the decline of the drainage system in fall, the velocities are higher than in the first evolution phase in spring. This can be attributed to the condition of pressure flow

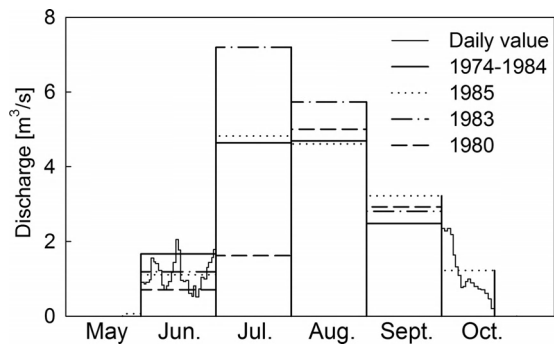


Figure 7.64 Variations of monthly mean of discharge as an indicator for the seasonal development of the glacial drainage system in an alpine glacier (Findelen) and its variability from year to year. Daily values in October 1983.

occurring preferentially in spring and early summer, while gravity flow dominates in fall (Röthlisberger, 1972; Iken and Bindenschädler, 1986).

The terms maximal flow velocity and intensive flow velocity do not conform completely to the theory given in Chapter 5. However, the terms and the determination of these parameters are common in hydroglaciology. They are defined as:

- v_{\max} maximal flow velocity calculated from x/t_{\max} where t_{\max} is the first appearance of tracer (above detection limit),
- v_{int} bulk flow velocity calculated from x/t_{int} where t_{int} (or t_{peak}) is the time when the concentration peak (maximal concentration) is observed
- v_{mean} mean flow velocity calculated from x/\bar{t} where \bar{t} is the centre of gravity of the tracer breakthrough (Equation (5.59), for the limits of the application of that method see Section 5.1.3).

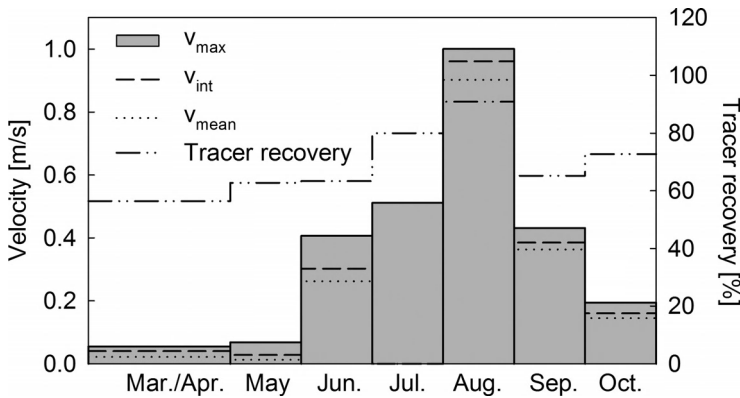


Figure 7.65 Flow velocities (v) and tracer recovery from wintertime to the end of ablation period yielded from several tracer experiments in the (Findelen) glacier during the 1970s and 1980s.

In publications (the English ones in particular) dealing with tracer experiments in glaciers, the expressions v_{\max} and v_{int} are not used. For both expressions, the term 'mean flow velocity' is often used.

Tracer recovery is an important means by which to judge and interpret the glacial drainage system. High recovery indicates open, large channels and, conversely, small recovery indicates water circulation in rather small fissures and channels. However, small recovery rates may also be caused by sorption on the sediments in the subglacial channels.

Generally, smaller tracer recovery is an indication for flow through a more complex intra and subglacial system. In order to investigate this hypothesis, a term calculated from the ratio of v_{\max}/v_{mean} was introduced in order to provide an initial insight into the glacial flow system (Leibundgut, 1986a). It also accommodated the fact that tracing tests in the past were usually not evaluated completely.

The ratio between the maximum and the mean flow velocity enables the preliminary judging of the flow path characteristics. It provides an idea whether the water flow passed mainly through a well-developed flow path system or through a poorly integrated one. A ratio value between 1 and 1.5 indicates well developed flow path characteristics while a ratio > 1.5 indicates poorly integrated ones (strongly heterogeneous).

The ratio between the maximum and the mean flow velocity in large and narrow channels is not proportional. The theoretical ratio for water flow in tubular flow paths with a constant diameter and with turbulent flow lies between 1.16–1.3 (Lehmann, 1932). If the water flow is laminar, the ratio increases to two. Laminar flow, however, is limited to pathways with very narrow diameters. Within rough and twisted flow paths, the change from laminar to turbulent flow already appears at a lower critical velocity. In the flow system of a glacier, the condition of a constant diameter is usually not met.

Under the conditions of a turbulent flow in large flow paths, the roughness is of less significance. The ratio $v_{\max} : v_{\text{mean}}$ will remain below 1.3; however, it increases with an increasing narrowness of the flow paths. To characterize the natural conditions, a threshold ratio between the maximum and the mean flow velocity obtained from field tests was set empirically to a value of $1.3 + 15\% \sim 1.5$ (Leibundgut, 1986a). A ratio value < 1.5 indicates well developed flow path characteristics and a ratio > 1.5 indicates those that are poorly integrated. The ratio value indicates whether the water flows mainly through a well-developed flow path system or through a poorly integrated one.

As mentioned above, the primary aim of a tracer test using artificial tracers is always to get a complete tracer breakthrough curve. Then, as much information about the water flow as possible is obtained from the curve. Nienow (1993) proposed a system of subglacial drainage systems based on the shapes of idealized tracer breakthrough curves. Grust and Hock (2004) provide a table summarizing the flow velocities of known tracer experiments in glaciated areas.

Only a few tracer experiments are known to have been executed during wintertime or in the accumulation area (Moeri and Leibundgut, 1986; Lang, Leibundgut and Festel, 1979). The experiment was interesting insofar as the injection took place in September, while the sampling was carried out over the winter at the tapping of the Aletsch glacier. It proved, for the first time, the through-flow of the meltwater generated during the ablation period through the glacial drainage system during wintertime. The obtained

flow velocities during winter are usually up to 100 times lower than the corresponding velocities of alpine glaciers in the ablation period. For Scandinavian glaciers, the figure is 10 times lower (Hooke, Miller and Kohler, 1988; Hock and Hooke, 1993). The drainage and runoff patterns at the glacier bed vary over short distances, and the large subglacial channels play an important role for the runoff in winter.

The use of artificial tracers in glacier studies is limited almost exclusively to temperate alpine valley glaciers. In Western Greenland, a large tracer experiment was carried out for the first time on the ice shield north-east of Jakobshavn (Leibundgut and Gees, 1989, cf. colour plate section, Plate 8a). Its goal was to investigate the state of the glacial drainage system to the ice edge and to separate subglacial catchments. Vatne *et al.* (1995) reported a tracing test in an investigation of a polythermic glacier in Spitsbergen. The evaluation of experiments carried out in cold glaciers is different from that of temperate glaciers (Menzies, 1995; Hodgkins, Tranter and Downswell, 1997; Hodgkins, 2001).

7.4.1 Specific techniques of tracer experiments in glaciers

Due to their highly dynamic components, investigations of the water flow in glaciers are interesting, but especially difficult. Such studies require special tracing techniques. The goal and the specific site conditions determine the choice of tracers. Due to transport problems in glaciated areas, the test material must be limited to those items that are absolutely necessary. Depending on the test goals, decisions concerning where, when, which and how much tracer is to be injected, and where and in which way the tracer passage is to be recorded, must be planned with special care. Usually, only highly concentrated tracers can be used. Among these, the fluorescent tracers are the best suited and have been applied almost exclusively. Uranine and Rhodamines in particular, and to a lesser extent others, have been used. Since backgrounds in glacial waters are normally very low, sodium chloride, lithium and strontium salts can also be considered for small scale tests.

In glaciers, the adsorption coefficient is generally low due to the absence of organic and cohesive mineral material. However, suspended load may affect the tracers anyhow. Also, the chemical stability and pH-dependence of some of the fluorescent dyes are usually unproblematic. In addition, the light sensitivity of the fluorescent dyes is uncritical in investigating intra- and subglacial flow systems. However, it plays an important and problematic role in tracing snow and firn, particularly in laminar injections of the tracer.

7.4.2 Injection

In order to avoid a contamination of the unprotected glacial aquifer with the fluorescent tracer due to wind drift, the tracer should be dissolved at home or in the base camp below the glacier under investigation. Usually, low water temperatures lower the solubility of the tracer substances. Thus there is always the risk of the solution precipitating at low temperatures in glaciated areas. Uranine reacts especially sensitively. The use of solubilizers is recommended. They enable the exploitation of the full physical solubility of the respective tracer. In general, injections should not be carried out with solutions

that have a concentration higher than 10%. Dilution of the highly concentrated solutions with meltwater is unproblematic. The estimation of the required tracer mass follows the instructions given in Section 6.2.

The most common injection of traced water into glaciers is performed through moulins. In investigations of the intra- and subglacial systems, naturally occurring moulins in the ablation area can be exploited for the injections (see colour plate section, Plate 8b). However, boreholes are being used increasingly to inject the tracer directly into the desired location within the intra- or subglacial system. Frequently, the water needed for the wetting and flushing of the injection hose must be melted from snow and firn. In accumulation areas, it may be necessary to bridge the unsaturated firn zone with a borehole (Lang, Leibundgut and Festel, 1979). The risk of the sinking of the traced water into stagnant water zones, due to its increased density, is low in well-developed drainage systems, but should still be considered (cf. Section 7.4.5.2).

With injections in moulins, approximated 'piston flow,' relatively low dispersivity and, thus, relatively low losses can generally be assumed. However, losses due to freezing and migration into unconnected cavities within the glacier can occur. These losses depend strongly upon the developmental stage of the flow system and its changes during the tracing test. When the flow of meltwater abates, the channel system can reconvert due to the ice pressure and the tracer is incorporated into the newly formed ice.

Due to the high temporal variability of the drainage system, the timing of the injection is important when investigating water flow in glaciers. Additional preliminary measurements of the meltwater levels, or, alternatively, the water pressure in the drainage system can provide information as to the development of the drainage system (Röthlisberger, 1972; Iken and Bindenschädler, 1986; Oerter, 1981). The end of the ablation period with a maximal meltwater level is best suited for investigations of completely developed flow systems.

7.4.3 Sampling

The sampling sites are determined by the objectives of the experiment and the expected flow paths. In glacial runoff tracing tests, spatial sampling is usually limited to the glacial mouth where all of the water exits. Sampling within the glacier itself can be conducted with boreholes, but this is often a difficult task (Leibundgut, 1986b).

A compromise between the practicability and quality of the measurements must often be sought in the correct planning and the duration of the sampling programme. The sampling intervals are determined by the characteristic breakthrough times in the investigated areas, on the one hand, and the strongly weather-dependent flow dynamic of the glacier on the other. Due to the high variability of the glacial runoff, a high temporal resolution in sampling is necessary in order to catch the tracer breakthrough with all its possible secondary peaks. Thus, to get an adequate determination of the breakthrough, automatic samplers are usually indispensable. Automatic samplers require an independent power supply and need to be heated in order to avoid freezing. Sampling intervals that are too long may have drastic effects on the registration of the tracer breakthrough curve, as described in Section 6.1.

In situ measurements, which are state of the art, are problematic in glaciated areas due firstly to logistic problems such as sensitivity of the electrical devices to low temperature, need of power supply and transport of heavy measurement arrangements, and secondly because the varying amounts of suspended solids cause problems with the calibration of the measurement of fluorescence tracers. The registration of the tracer passage can be completed by taking individual samples and analysing them later in the laboratory. In a case where the firn body itself is to be investigated, special sampling arrangements must be set up (Oerter and Moser, 1982).

Activated charcoal bags for sampling are a suitable technique for long-term surveying in poorly accessible glaciated areas, provided a semiquantitative or even qualitative detection of the tracer concentration is sufficient (Lang, Leibundgut and Festel, 1979).

7.4.4 Analyses

The detection limit of (fluorescence) tracers is usually low in pure glacial water. However, as mentioned above, glacial meltwater contains large amounts of suspended solids. Through sedimentation of the suspended solids in the sample bottles, and subsequent decanting, this problem can be solved. The suspended solids lead to an increase in the detection limit and to a higher error due to varying background caused by variations in suspended solid loads. The temperature dependence of the tracers does not present a methodological problem. It can be overcome by measuring the fluorescence of the calibration solutions and the samples at the same temperature in the laboratory, and in the case of in situ measurements, by applying a temperature correction within the software of the instrument or complete afterwards (see Section 4.1). In hydroglaciology, combining tracing tests with several injections is often needed in order to meet the research requirements. Because of the strong variations in the glacial runoff system, the desired identical hydrological boundary conditions can only be guaranteed through simultaneous injections of different tracers. In that case, the tracer mixture must be separable afterwards (cf. Section 4.1.3).

7.4.5 Case study: 'Tracer experiments in temperate alpine glaciers – Findelen'

For investigating the relationship between the development of the intra- and subglacial channel-flow system and runoff behaviour, artificial tracer tests are a powerful tool.³ These investigations have mainly been carried out during the ablation period, when meltwater generally passes without much delay and storage through main intra- and subglacial drainage channels. Peak tracer concentrations, cumulative tracer recovery and water flow velocities are high. The case study of Findelen is representative of numerous studies dealing with the drainage of temperate alpine glaciers. It is particularly

³Stenborg (1969), Behrens *et al.* (1971), Shreve (1972), Ambach *et al.* (1972), Röthlisberger (1972), Nye (1976), Lang, Leibundgut and Festel (1979), Moser and Ambach (1977), Collins (1979a, b, 1982), Spring (1980), Aschwanden and Leibundgut (1982), Leibundgut (1986b).

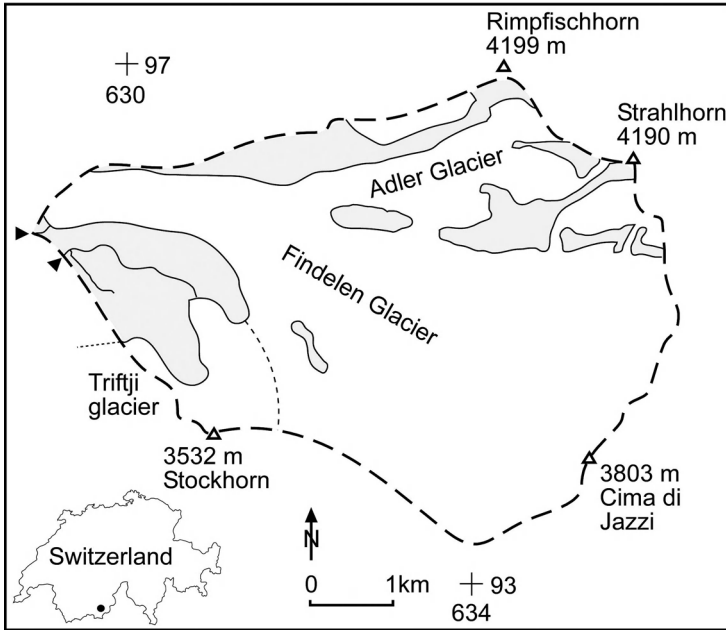


Figure 7.66 Investigation area with catchment of Findelen Glacier and adjacent glaciers. ▼ Intake of meltwater for water power plant.

interesting since experiments in summer (ablation) as well in wintertime (accumulation) were conducted. A first study was carried out during the 1982 ablation phase while the second was conducted during the accumulation phase in 1984. Both campaigns served to complete the picture of the formation and backformation of the glacial drainage system and of the seasonal development of the flow relationships (Moeri and Leibundgut, 1986).

The catchment of the Findelen Glacier in the Swiss Alps covers an area of over 24.5 km², 80% of which was glaciated during the experiments. The altitude ranges from 2474 m (glacier mouth) to 4190 m a.s.l (Figure 7.66). The ice depths around the injection sites amounted to 170 m in the lower part and 110 m in the upper plateau.

The mean runoff in the summer of 1982 developed from 0.28 m³/s in May to 2.10 m³/s in June, 6.80 m³/s in July, 5.71 m³/s in August to 3.10 m³/s in September (Figure 7.67). It reflects nicely the development of the intrasubglacial drainage system during the ablation phase, as described above (Leibundgut, 1986b). The observed high variability is typical for the day-night rhythm of glacier meltwater runoff during ablation. During the measuring period 1984 (from second March to fourteenth April), the discharge values of the winter runoff from the Findelen Glacier varied between 0.052 and 0.084 m³/s. To record the meltwater runoff during the tracer experiments a continuously recording stage-gauge had to be installed in the drainage tunnel (intake) of the captation of Grande Dixence S.A. (Figure 7.66).

Previous tracer experiments targeted the investigation of the interrelationships between subglacial water pressure, water flow, water storage and glacier movement (Iken,

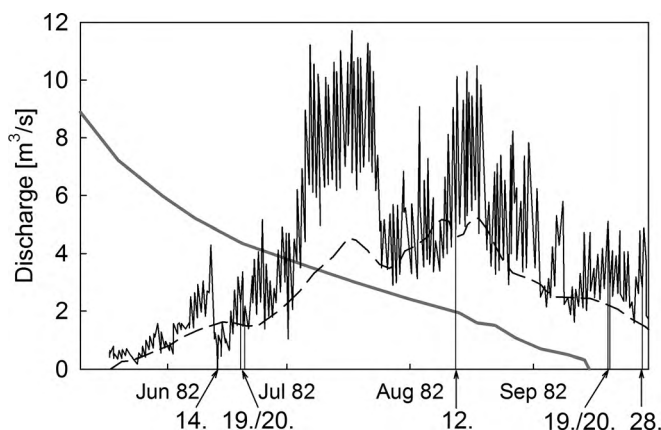


Figure 7.67 Runoff Findelen Glacier: Hydrograph 1982, hourly values (black line) and flow duration curve (dark grey line); Average hydrograph 1972–1982 (dashed line). 14. and so on: injection dates of the 5 experiments (source Grande Dixence S. A., from Moeri, 1983).

1977; Iken and Bindshaedler, 1986). To augment the knowledge thus gained, several tracer tests were conducted in order to investigate the intra- and subglacial flow behaviour and the development of the glacial drainage systems. Based on experience of the earlier studies, the experiments were prepared carefully. Out of the available fluorescent tracers Uranine, Eosine, Amidorhodamine G and Rhodamine B and Rhodamine B extra were chosen as potential tracers for the experiments. The combination of the tracers in the real experiments was affected due to the specific local conditions at the time of test. Tracers were injected at different sites in boreholes or moulins in order to take the spatial heterogeneity of the drainage system into account.

7.4.5.1 Summer experiments 1982

Five combined tracing tests were carried out between June and the end of September 1982 so as to characterize the drainage system during ablation at its initial, maximum and final states. The experiments were bound to the weather conditions since the tests were to be carried out under pure snow melt conditions. The relevant features of all of the experiments are listed in Table 7.20.

In the experiments only Uranine (B24) was injected on the upper plateau, whereas on the lower plateau Rhodamine B extra (B22) and Sulphorhodamine G were applied (Figures 7.68 and 7.69). Due to a failed injection in B 22, the tracer Tinopal ABP was injected during the second experiment (19th/20th June). Tinopal is an optical brightener tracer which is no longer in use.

Tracer breakthrough during ablation in glaciers is characterized by a quick response. Additionally, the day/night rhythm of runoff often causes secondary peaks in tracer breakthrough. Consequently, a tight sampling schedule at the glacier mouth, in the order of 15 min during the rising limb, is needed. This was ensured by means of

Table 7.20 Features of the injections of the summer experiments in Findelen Glacier 1982. The injection occurred as a concentrated solution. E: Experiment, I: Injection, L: Location, B: borehole, M: Moulin, RBe: Rhodamine B extra, UR: Uranine, SRG: Sulforhodamine G, T ABP: Tinopal ABP

| E [Date] | I [Time] | Tracer | Mass [kg] | L | Ice thickness [m] | Tube length [m] | Inflow [l/s] |
|----------|----------|--------|-----------|-----|-------------------|-----------------|--------------|
| 14.6.82 | 18.27 | RBe | 1.0 | B22 | 170 | 150 | — |
| | 17.10 | UR | 1.0 | B24 | 110 | 100 | — |
| 19.6.82 | 20.35 | RBe | 0.5 | B22 | 170 | 100 | — |
| 20.6.82 | 17.56 | TI ABP | 25.0 | B22 | 170 | 150 | — |
| | 17.56 | UR | 0.5 | B24 | 110 | 100 | — |
| 12.8.82 | 16.16 | RBe | 1.0 | M22 | 170 | — | 10 |
| | 16.16 | UR | 1.0 | M24 | 100 | — | 1 |
| 19.9.82 | 16.20 | SRG | 0.5 | M16 | 170 | — | 50 |
| 20.9.82 | 16.15 | RBe | 1.0 | M22 | 170 | — | 10 |
| | 16.15 | UR | 1.0 | M24 | 100 | — | 1 |
| 28.9.82 | 16.20* | RBe | 0.5 | M22 | 170 | — | 3 |
| | 15.30* | UR | 0.5 | M24 | 100 | — | 0.5 |

*For reasons of comparison time converted to summer time (CEST).

an automatic sampler of the type APEG. The samples were later analysed with a spectrofluorometer (Perkin Elmer 3000).

Out of the five total tests the breakthrough curves of the first two conducted at the beginning of ablation and in June and that of the last one conducted at the end of ablation period are presented by way of example (Figures 7.70 and 7.71). Additionally, the relevant data of all experiments are listed in Table 7.21 (Moeri, 1983). They enable a comprehensive discussion of the evolution of the glacial drainage system and the flow development during the ablation period.

After an unsteady start of the ablation early in June, a first experiment could be performed on the 14th of June. Late in the afternoon, taking advantage of the daily flow maximum, a parallel slug injection of the tracers Uranine and Rhodamine B was carried out in two boreholes by drilling hoses straight into the subglacial system (Figure 7.68). One kilogram Uranine was injected into borehole B 24 on the upper plateau while Rhodamine B was injected into borehole B 22 located on the lower plateau at a distance of 1712 m from the sampling site (Figure 7.69).

After 63 min, Rhodamine B from the lower plateau first appeared at the sampling site. Then, after 200 min, Uranine from the upper plateau first appeared. Obviously, the drainage system was better developed in the lower part of the glacier compared to the upper part at this time. Both tracer breakthroughs occurred relatively compactly within a few days with a mean flow velocity of 0.20 m/s (Rhodamine) and 0.13 m/s (Uranine). The tracer returns were 65% (Rhodamine) and 41% (Uranine), respectively (Figure 7.70). The long tailing of the breakthroughs contrasts somewhat with the assumed larger conduits, indicated by the way the flushing water disappeared in the borehole, as discussed below. However, it conforms to the expected situation soon after the onset



Figure 7.68 Injection at borehole B 22 on Findelen Glacier.

of the ablation period, which is a poorly developed drainage system (cf. introduction Section 7.4).

Water used to flush the tracers did not cause notable water level changes in the injection boreholes, which indicated large water channels (fissures, fractures) nearby. The flushing of the injection equipment was continued for another 10 min after the tracer concentration had dropped below the visual limit (approx. 30 mg/m³). The flow relationships in the glacial stream were used to determine suitable times for the injections. The later injections could be carried out without flushing.

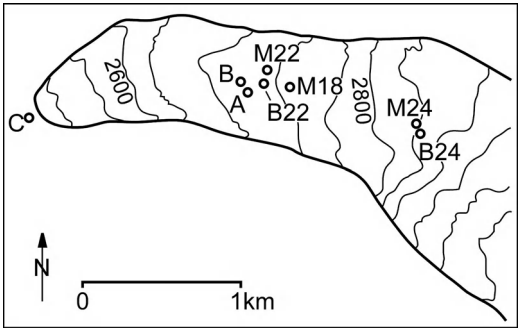


Figure 7.69 Injection sites on Findelen Glacier during the 1982 experiments. B24 (borehole) and M24 (moulin) are situated on the upper plateau of the glacier. C: sampling and gauging site.

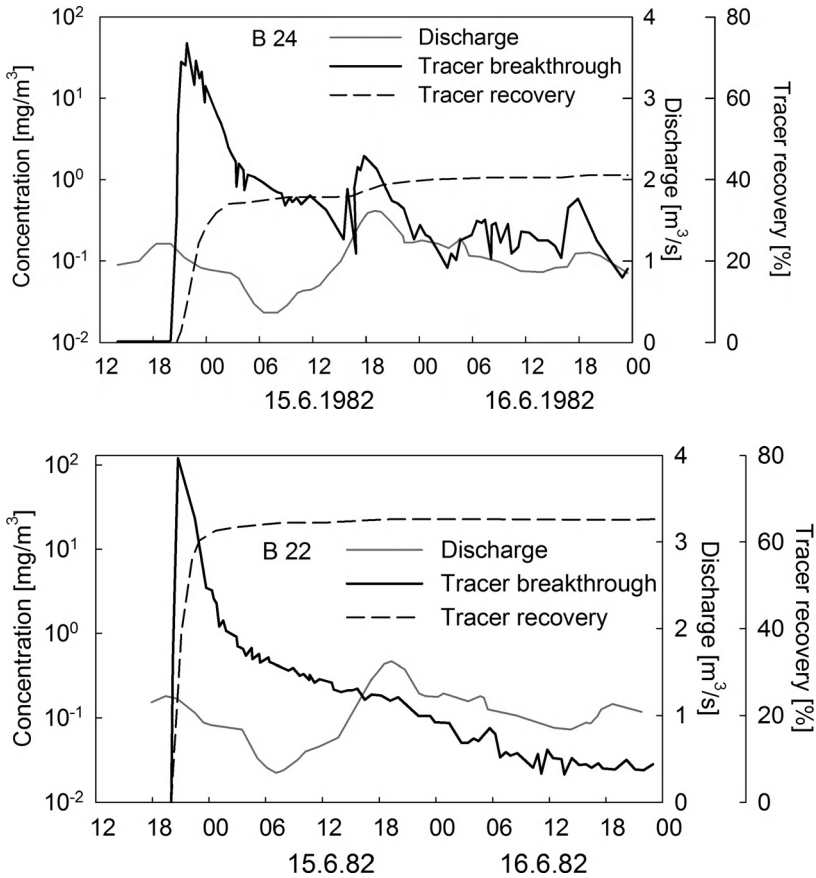


Figure 7.70 Tracer breakthroughs Findelen Glacier tracer experiments on 14 June 1982 at the beginning of ablation period. Top: Uranine injection at B 24, upper plateau; bottom: Rhodamine B extra injection at B 22, lower plateau.

The terms maximal flow velocity and intensive flow velocities do not conform completely to the theory given in Chapter 5. The definitions of the terms and their determination in hydroglaciology are presented in the introduction in Section 7.4.

On 28th/29th September, a few days before the winter started in the Alps, the last experiment was conducted. In two moulins, M 24, upper plateau 500 g of Uranine and in M22 on the lower plateau 500 g Rhodamine B extra, were injected. As is typical for the end of the ablation period, the supraglacial runoff to the moulins was considerably smaller than in the earlier experiments (Table 7.20).

In contrast to the summer experiments, which showed a constant runoff, the runoff decreased distinctly during the September autumn experiment. The tracer breakthrough from the injection on the upper plateau was still quite compact. However, the Rhodamine breakthrough from the lower plateau took more time to reach the glacier mouth. The concentration peak at the beginning of the breakthrough was highly

Table 7.21 Results of tracer experiments on Findelen Glacier summer 1982. E: Experiment, I: Injection, L: Location, TR: Tracer recovery, MB: Main Breakthrough, SB: Secondary Breakthrough, RBe: Rhodamine B extra, UR: Uranine, SRG: Sulfurhodamine G, T ABP: Tinopal ABP

| E [Date] | I [Time] | tracer | L | t _{max} [min] | t _{int} [min] | \bar{t} [min] | v _{max} [m/s] | v _{int} [m/s] | v _{mean} [m/s] | v _{max} /v _{min} | TR [%] | MB | SB |
|----------|----------|--------|-----|------------------------|------------------------|-----------------|------------------------|------------------------|-------------------------|------------------------------------|--------|-------|-----|
| 14.6.82 | 18.27 | RBe | B22 | 93 | 123 | 142 | 0.31 | 0.23 | 0.20 | 1.55 | 65 | 100 | — |
| | 17.10 | UR | B24 | 200 | 290 | 337 | 0.22 | 0.15 | 0.13 | 1.69 | 41 | 87 | 11 |
| 19.6.82 | 20.35 | RBe | B22 | 100 | 130 | 133 | 0.29 | 0.22 | 0.21 | 1.38 | 58 | 100 | — |
| 20.6.82 | 17.56 | T ABP | B22 | 49 | 49 | — | 0.58 | 0.58 | — | — | 8 | 100 | — |
| | 17.56 | UR | B24 | 184 | 274 | 342 | 0.24 | 0.16 | 0.13 | 1.85 | 52 | 52 | 48 |
| 12.8.82 | 16.16 | RBe | M22 | 59 | 59 | 74 | 0.49 | 0.49 | 0.39 | 1.26 | 78 | 97 | 3 |
| | 16.16 | UR | M24 | 44 | 59 | 63 | 0.97 | 0.73 | 0.69 | 1.41 | 91 | 100 | — |
| 19.9.82 | 16.20 | SRG | M16 | 40 | 70 | 69 | 0.77 | 0.44 | 0.45 | 1.71 | 79 | 73+26 | 1 |
| 20.9.82 | 16.15 | RBe | M22 | 135 | 240 | 216 | 0.21 | 0.12 | 0.13 | 1.62 | 18 | (97) | (3) |
| | 16.15 | UR | M24 | 75 | 90 | 101 | 0.58 | 0.48 | 0.43 | 1.35 | 93 | 100 | — |
| 28.9.82 | 15.20 | RBe | M22 | 250 | 1270 | 1257 | 0.11 | 0.02 | 0.02 | 5.50 | 15 | 42 | 58 |
| | 14.30 | UR | M24 | 105 | 120 | 121 | 0.41 | 0.36 | 0.36 | 1.14 | 77 | 100 | — |

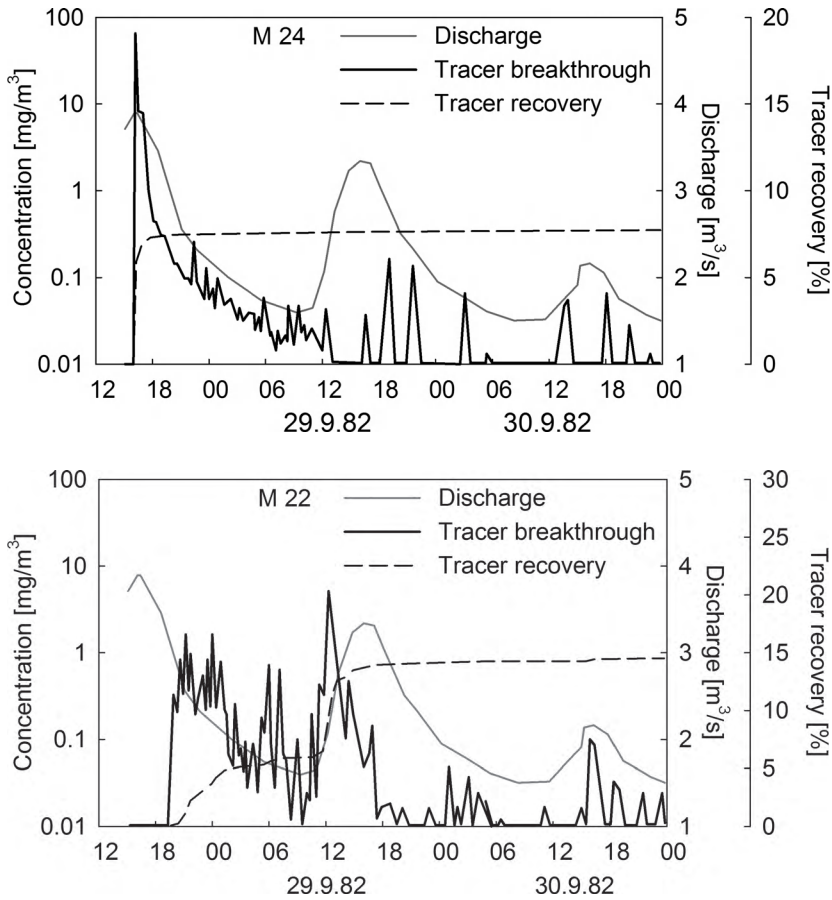


Figure 7.71 Findelen Glacier Rhodamine tracer experiment 28 September 1982 at the end of ablation period. Top: Uranine experiment; Bottom: Rhodamine experiment.

variable and there was no clear, recognizable concentration peak. The actual concentration peak did not occur before the second day, which was unique for all experiments. The tracer recovery of 15% was remarkably low. Out of the total recovered tracer mass 58% was provided by the peak breakthrough during the second day. The flow velocities as given in Table 7.21 were also low. The data clearly show the final state of the summer drainage system.

The overall assessment of the results from the first campaign during the ablation phase show that the time of the tracer injection is decisive for the tracer return and flow velocities. They are low at the beginning and at the end of the ablation period. The tracer return fluctuated between 15% and 93%, and the mean flow velocities reached values between 0.13 m/s and 0.69 m/s. The different injection sites also showed distance dependence upon the main subglacial drainage channels. The tracer breakthrough can be quite compact, or may exhibit definite secondary maxima and a longer tailing.

Even though the tracer substances were injected through boreholes and larger moulins, which were supposed to be well connected to the large drainage system, the recessions of the tracer concentration curves and secondary maxima were found to be very slow. However, the parameters obtained from injections through boreholes and small moulins, which were not supposed to be directly connected to the main subglacial drainage system, showed even more differentiated features: The measured flow velocities of the traced water as well as the cumulative tracer return are significantly lower from these locations than from the better connected ones described above. Obviously, runoff delay and water storage play an important role at these sites. The present results also indicate a delay in the runoff and water storage in the glacier depending on the weather and the daily course of the temperature. Over the summer, the subglacial drainage system first widens at the beginning of the ablation phase and then narrows again towards the end of the ablation phase.

Obviously, the characteristics of the applied tracer is another criterion for the interpretation of the tracer breakthroughs. In spite of the different sorption tendency of Uranine and Rhodamine, this factor can almost be ignored completely in large ice channels and quick breakthroughs. For smaller channels and fissures, on the other hand, one should consider the introduction given in Section 7.4.

7.4.5.2 Winter experiments 1984

The winter experiments started on 2nd March 1984. The injections of 1 kg each of Rhodamine B extra and Uranine were performed. Rhodamine B extra was injected in a borehole (A in Figure 7.69) and Uranine was injected in an inactive moulin (B in Figure 7.69) by means of drilling hoses (Iken and Binschädler, 1986). The distance to the sampling site at the glacial outlet was 1531 and 1495 m, respectively, and the horizontal distance between A and B was only 38 m (Figure 7.69). The injection of Rhodamine B extra took 21 min. One and half cubic metres of water were needed to rinse the hoses and to get the tracer into the subglacial water carrying system over 1 h. The water table in this borehole rose a little, but dropped to its previous level afterwards. On the following day, the subglacial water was marked with Uranine through the remains of a moulin of the previous year at site borehole B (Figure 7.69). In contrast to the previous day, the injection took only 4 min. Because of bad weather the tracer had to be pumped into the system through the pump of the drilling gear. During flushing with 95 m³ of water after the injection, the water table remained stationary.

The breakthrough curves from the accumulation phase differ greatly from those of the ablation period. The tracer reappeared with varying, generally decreasing concentrations over a total sampling time of six weeks (Figure 7.72).

The discharge curve shows a generally decreasing trend at the end of the measuring period (Figure 7.72). Short term variations are more frequent at the beginning of March. They may be attributable partly to the inaccuracy of the gauging station, but they also coincide with fluctuations of the Uranine tracer concentration curve. Thus, they likely represent actual short term variations in the basal winter runoff from the

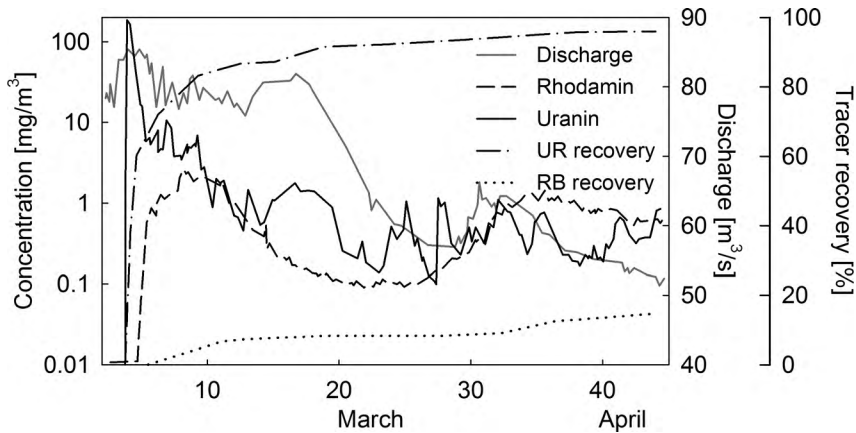


Figure 7.72 Tracer experiment Findelen Glacier under winter accumulation conditions with injection into a borehole (RB) and into an inactive moulin (UR).

Findelen Glacier. The fluctuations tend to decrease in amplitude as well as in frequency over the investigation period.

Figure 7.72 shows the tracer concentration and the cumulative tracer recovery for both injections in comparison to the discharge at the sampling site. After the injection in borehole A, Rhodamine reaches its maximum concentration four days later. A pronounced secondary concentration peak 26 days after the first coincides with an increase in runoff. Until the end of the test, 14.7% of the tracer input passed at the glacier terminus (Table 7.22).

Uranine, which was injected through borehole B, drained quite differently. Maximum tracer concentration (195 mg/m^3) was reached within a few hours after injection. A steep rise as well as a rapid fall of the concentration marks this peak. Subsequently, the values generally decrease very slowly and finally level off at about 3 mg/m^3 . While the fluctuations of Rhodamine are very smooth, those of Uranine are wild and erratic. When compared to runoff, only the lower Uranine concentrations from the 5th to the 13th of March generally coincide with higher discharge values. This indicates

Table 7.22 Results from tracer experiments on Findelen Glacier March/April 1984

| | Borehole A Rhodamine B extra | Borehole B Uranine |
|--------------------------|------------------------------|--------------------|
| Cumulative tracer return | 14.7% | 96.4% |
| Maximum velocity | 0.82 cm/s | 9.7 cm/s |
| Intensive velocity | 0.31 cm/s | 5.5 cm/s |
| Mean velocity | 0.16 cm/s | 2.5 cm/s |

Maximum, intensive and mean velocities correspond to the times of the first occurrence of tracer, the maximum tracer concentration and the centre of gravity of the TBC.

that during short term runoff variations (within a few hours) the fluctuations of the Uranine concentration curve are caused solely by a simple dilution effect. In contrast to the experiment with Rhodamine the cumulative tracer recovery amounts to 96.4% (Table 7.22). The tracer recovery rate of Uranine is comparable to that of the earlier summer tracer tests on the Findelen Glacier, while the Rhodamine value lies in the same range as in the previous late September tests (Moeri, 1983). In terms of flow velocities, the picture is quite different. In both tests the water was drained at a rate which was more than 100 times slower than in the corresponding experiments during the ablation period of 1982. The impacts of the aforementioned variations of the glacial water table (site B) are shown in the tracer concentration curves as well (Figure 7.67). Uranine which had been injected through the moulin itself, reacted to the first water level increase with increased and more constant concentration values from March 14th to 20th. Rhodamine did not seem to be affected by this change of water pressure. The dye tracers also behaved differently in regards to the second water level discontinuity (March 29th). The fluctuations in the Uranine concentration were not suppressed as they were after March 13th. Only the minimal concentration values seemed to be elevated. Rhodamine in contrast, reached its secondary maximum five days after the second runoff increase (April 4th).

In Figure 7.72, the Rhodamine and Uranine concentration curves are compared to the discharge values. The differences between the two tracers are evident but there are also some astonishing similarities: (1) the decrease in tracer concentration from 11th of March to fourteenth of March and (2) the increase from 29th of March to 2nd of April show nearly identical values. Whether this coincidence is mere chance, or an expression of the same runoff-affecting factors for both tests, is hard to tell. Equal amounts of both tracers had been injected and, assuming the same runoff conditions, similar concentration values should have resulted. Beside these two similarities the differences in peak tracer concentration and tracer recovery rate as well as flow velocities and variability of the tracer concentration are more distinguishing and conclusive.

The mean water velocities amounted to 0.16 cm/s (borehole) and 2.5 cm/s (moulin) confirming the generally known relation between the two values during the accumulation and ablation phase. The tracer return came to 15% for Rhodamine from the borehole and 97% for Uranine from the moulin (Table 7.22). The higher return and higher velocity from the experiment in the moulin show that the water drainage in winter also occurs in locally variable patterns in the subglacial system. Up to a certain degree, the main subglacial channels were still passable, although flow delays and water storage were considerably more significant than during the ablation phase. The occurrence of a second major peak after one month during the second test in the borehole shows that strong temporary water storage occurred there.

First of all, the winter dye tracer experiments show that water is still being drained in quite differing local patterns at the bottom of the Findelen Glacier. To a certain degree, the big subglacial channels formed during the ablation period are still capable of conducting water relatively efficiently down the glacier (Figure 7.72, Uranine test). The result confirms the findings of an experiment on the Aletsch Glacier 1977 (Lang, Leibundgut and Festel, 1979). Although peak tracer concentration and recovery rate are high in the test conducted through an inactive moulin, runoff delay, to a smaller extent,

still exists. Water storage is also indicated by the tracer experiment and is definitely more important than during the ablation period. Local water table variations at the same site show their effect on the total winter runoff at the terminus of the glacier and affect tracer concentration and tracer output as well. Concentration fluctuations are suppressed (10th to 13th March) during the first water level increase but not during the second event (29th March). The delayed and stored part of the dyed water volume at the glacier bed (injection site B) was drained at temporally varying rates. This could be due to quite rapidly changing flow conditions from a, rather flat and rectangular drainage channel to one that is more spacious, circular and braided. There even seems to be some regularity to this process, as secondary tracer concentration maxima tend to occur every two to three days.

The water flow velocities of the Rhodamine B extra tests are comparable to groundwater flow in coarse-grained aquifers, and much lower than in the Uranine test (Table 7.22). The same holds true for peak tracer concentration and cumulative tracer return. In relation to the water table increase of 29th March, a distinct and pronounced second tracer maximum occurred which yielded about 50% of the total Rhodamine output.

7.5 Catchment scale

Previous case studies dealt with the specific compartments of the water cycle. The case studies of this chapter cover the entire catchment scale and consequently have an integrated character incorporating several compartments. An integrated tracerhydrology considers the entire system as a whole, although the interactions between the subsystems are still relevant and of great importance. Integrated water resource management based on consolidated findings of the research follows a similar integrated approach.

Runoff generation forms the centre of all these interactions and processes. Runoff generation processes are among the most important processes in catchment hydrology. In recent years, tracer methods, combined with hydrometric measurements and advanced geophysical methods, have proven to be effective for identifying runoff generation mechanism in smaller catchments up to the mesoscale. In flood generation in particular, tracer studies have contributed substantially to the understanding of processes. Early tracer studies already led to a new understanding of the respective amounts of new and old water in runoff (Stichler and Herrmann, 1978; Sklash and Farvolden, 1979; Herrmann *et al.*, 1984; Buttle and Peters, 1997; Frederickson and Criss, 1999; Hangen *et al.*, 2001; Leibundgut *et al.*, 2007). The authors state the crucial role of the slow and fast groundwater components for runoff generation, even during stormflow events. Comprehensive discussions are to be found in Kendall and McDonnell (1998), Uhlenbrook, Leibundgut and Maloszewski (2000), Leibundgut, Uhlenbrook and McDonnell (2001), Uhlenbrook and Leibundgut (2002), Uhlenbrook, Leibundgut and Maloszewski (2002), Anderson, Peters and Walling (2003), Weiler *et al.* (2003) and Leibundgut and Uhlenbrook (2007). A critical review concerning the issue is provided by Burns (2002).

Natural and geochemical tracers often have distinctly different concentrations in precipitation, in vadose zone water and groundwater. The combination of measured data and the mass balance approach enables the distinction of the above mentioned runoff components. Oxygen and hydrogen isotopes are often used to separate event and pre-event water, that is the discharge component consisting of precipitation (direct runoff) and the component consisting of water that was present in the catchment before the event started (old water). The role of direct runoff was often overestimated until the hydrograph separation by environmental isotopes (Herrmann, Martinec and Stichler, 1978). The percentage of the contribution of pre-event water to total runoff ranges from 21 to 97% (Genereux and Hooper, 1998). Geochemical tracers such as silica, chloride, magnesium and many others are used to distinguish between groundwater and soil water (e.g. Sklash and Farvolden, 1979; Wels, Cornett and Lazerte, 1991; Bazemore, Eshleman and Hollenbeck, 1994; Armbruster and Leibundgut, 1997; Nimz, 1998; Rice and Hornberger, 1998; Kirchner, 2003). The fundamentals of small scale hydrology in the framework of isotope hydrology are presented in Buttle (1998). Genereux (1998) presented a method for quantifying the uncertainties in a multi component tracer-based hydrograph separation.

On the hill slope scale artificial tracers are used to investigate runoff generation processes such as macro pore and bypass flow (e.g. Turner and Barnes, 1998; Weiler, Naef and Leibundgut, 1998; Tsujimura, Tanaka and Onda, 1998; Sirin, Köhler and Bishop, 1998; Peters, Ratcliffe and Tranter, 1998; Uhlenbrook and Leibundgut, 1999; Herrmann *et al.*, 1999; Uhlenbrook and Leibundgut, 2002; Tilch *et al.*, 2004; Uhlenbrook *et al.*, 2004; Uhlenbrook, Roser and Tilch, 2004; Tromp-van Merveld and McDonnell, 2006; Weiler and McDonnell, 2007; Scherrer *et al.*, 2007; McGuire, Weiler and McDonnell, 2007).

Environmental and artificial tracers have also been applied to study the relations in the soil-plant-atmosphere system in a dry pine forest (Wenninger *et al.*, 2004). A comprehensive summary of the role of the soil-plant-atmosphere system in the catchments scale is presented by Dawson and Ehleringer (1998).

The methodology of using tracer studies to investigate the role of runoff components in the hydrology of larger basins is not as well developed as it is in headwater catchments. In a macroscale basin in Germany tritium and stable isotopes (^{18}O and ^2H) were used to improve a water balance modelling in a long term study. In particular, the impact of groundwater components on modelling the water balance could be defined using tritium data. The recession of bomb tritium in the river discharge of large basins indicates a contribution of direct runoff of 30–50% and varying amounts for fast and slow ground water components. Mean residence times of 8 to 14 years were found for the fast ground water component, 21 to 93 years for the slow ground water component. The overall mean residence time ranged from 14 to 50 years within these basins (Königer *et al.*, 2005, 2008).

Ingraham, Caldwell and Verhagen (1998) describe the principle of arid catchment hydrology. The runoff generation on a rocky, semiarid Mediterranean hillslope was investigated with sprinkler experiments. Significantly different concentrations of chloride, sulfate and nitrate ions in sprinkled water served as tracers (Lange *et al.*, 2003). The specific mechanism of runoff separation in tropical catchments characterized by high

rainfall amounts is discussed in Bonell *et al.* (1998) and that of snowmelt-dominated systems in Rodhe (1998).

Studies about the time water needs to flow through the catchment are in close connection to runoff generation investigations. The water or catchment transit time integrates many hydrological processes characteristic for the catchment. These are amongst others: different storages, flow pathways, catchment heterogeneity and different sources of water within the catchment. The transit time is also of great interest for gaining knowledge on the behaviour of contaminants or other solutes. A review of catchment transit time researches and investigations is provided by McGuire and McDonnell (2006). Due to their nature in being an integrating catchment parameter, natural tracers are well suited to evaluate catchment transit times. In particular, oxygen and hydrogen isotopes are often used for this purpose (e.g. ^3H , ^{18}O : Maloszewski *et al.*, 1992, 2002; ^{18}O : McGuire, DeWalle and Gburek, 2002; ^3H : McGlynn *et al.*, 2003; ^2H : Asano, Uchida and Ohte, 2002), although others such as ^{35}S or chloride are used as well. While the above mentioned studies estimated travel times using either the linear, dispersion, exponential or mixing model, Kirchner, Feng and Neal (2000) analysed the chloride time series of a head water stream (Plynlimon, Wales) using spectral methods. They showed that the concentration bears a fractal scaling over three orders of magnitude. Consequently, in regard to solutes or contaminants the catchment transit time cannot be described by a single characteristic flushing time but rather has to be expressed at least by a long lasting low level component combined with a fast, intense one.

Regarding the interactions between different hydrological compartments, groundwater-surface water interactions have been investigated intensively. They comprise several processes such as:

- groundwater exfiltration into rivers and lakes,
- sublacustric and submarine groundwater discharge in lakes and coastal sea,
- groundwater exchange between neighbouring aquifers,
- surface water infiltration into unsaturated zone and groundwater,
- hyporheic exchange of water in both directions.

An understanding of these often complex hydrological processes is crucial for the understanding of the system's function and the processes in catchment hydrology. Once again, tracer methods are appropriate tools and play an important role in catchment hydrology research and in applied water resources management.

Groundwater exfiltration into streams is a crucial component for low flow discharges. The role of tracers in low flow studies is not as extensively developed as for flood generation processes. However, an increasing amount of research on this issue has been conducted (Rank *et al.*, 1998; Kendall and Coplen, 2001; Gibson *et al.*, 2002; Königer, 2003, 2008; Königer *et al.*, 2001, 2008; Königer and Leibundgut, 2001; Königer, Leibundgut and Lohner, 2000; Aggarwal *et al.*, 2007; Ogrinc *et al.*, 2008). During a dry period river water consists often mainly of groundwater. This water component also plays an important role in water quality. The groundwater is often reflected in its isotope

signals. If the corresponding input signal of a system is given, information on recharge areas (altitude), the recharge season as well as residence times and influencing processes (e.g. evaporation and mixing) can be derived (Königer *et al.*, 2009).

Sublacustric and submarine groundwater discharges in lakes and coastal sea water are of regional significance in many places (Sanford *et al.*, 2007). However, only a few techniques are known to address the issue adequately. The identification and especially the quantification of these exchanges are very difficult. Tracer methods can make a substantial contribution to identification as well as quantification (Leibundgut and Attinger, 1986; Gospodaric and Leibundgut, 1986; Leibundgut and Attinger, 1988; Rieg and Leibundgut, 1992; Walker and Krabbenhoft, 1998; Ross, Rieg and Leibundgut, 2001).

Recently, radium isotopes have been used in order to determine the residence times of lakes and coastal areas. These isotopes are very useful in locations with saline inflows or fresh-salt-water interfaces, as the hydrochemical behaviour of Radium changes depending on the salinity of the aqueous solution. Residence times and mass balances are estimated based on the radioactive decay of different radium species. Moore (2000) used the ratio of the isotopes $^{223}\text{Ra} : ^{224}\text{Ra}$ for the age dating of coastal water. Burnett and Dulaiova (2003) estimated the dynamics of groundwater input into the coastal zone via continuous ^{222}Rn measurements. Kluge *et al.* (2007) quantified the groundwater inflow into lakes using ^{222}Rn . The groundwater inflow to a shallow, poorly-mixed wetland and in alpine lakes has been estimated from a mass balance of radon by Cook *et al.* (2008) and Gurrieri and Furniss (2004).

An equally complex issue is the *groundwater exchange between neighbouring aquifers*. It is an important process in karstified areas where exchange between different karst aquifers and between karst- and porous aquifers is common. Successful assessments of such processes and of the entire specific systems are reported in investigations in the Dinaric Karst, in the Swiss Alps and in the Central-Eastern Peloponnesus (Gospodaric and Habic, 1976; Bögli and Harum, 1981; Morfis and Zojer, 1986; Rieg *et al.*, 1993). Furthermore, tracer techniques can also be used for the detection and quantification of hydrological connections between lakes and the adjacent aquifers (Leibundgut and Adler, 1989).

Indirect groundwater recharge by *surface water infiltration* and river water infiltration into the unsaturated zone and groundwater aquifers is the dominant recharge process in many regions (Solomon, Cook and Sanford, 1998; McDonell *et al.*, 1998). An assessment of these processes by stable isotopes and geochemical components is an approved technique (Stichler, Maloszewski and Moser, 1986; Königer, 2003; Königer and Leibundgut, 2001; Königer, Leibundgut and Lohner, 2000; Königer *et al.*, 2001; Fette *et al.*, 2005; Hunt *et al.*, 2005). A transport of solutes, which can be used as tracers, is connected to the transfer of water from surface to groundwater (Hoehn, 1998).

The application of artificial tracers in order to investigate surface water infiltration is only promising in very small water courses due to the huge masses that would be needed for those experiments (see colour plate section, Plate 8c). However, the tracing of surface water infiltrating into moulins in karst areas is also an established method (Section 7.1).

The hyporheic zone is a zone characterized by a highly, spatially and temporally varying exchange between ground and surface water. The transition zone of the streambed is characterized by a potential for nutrient and solute retention and by an increase of

hydraulic residence time in streams (Morrice *et al.*, 1997; Bencala, 2000). Hyporheic zone investigations, focused on the hydraulic exchange patterns within the hyporheic zone, can be conducted with artificially applied tracers (e.g. NaBr: Morrice *et al.*, 1997; Ryan and Packman, 2006; $^{51}\text{Cr(III)}$ and ^3H : Wörman *et al.*, 2002; Rhodamine WT: Laenen and Bencala, 2001; Saenger and Zanke, 2009). In the case of an adequately large difference of surface water and groundwater temperature, profile measurements show hyporheic zones and their vertical extensions (e.g. White *et al.*, 1987). Constantz ascertained waterloss and gaining reaches of a stream and determined diurnal changes in infiltration rates by using only measured stream temperature changes (Constantz and Thomas, 1997; Constantz, 1998). The role of temperature in hyporheic water movement was investigated using fibre optic technique by Selker *et al.* (2006). Constantz *et al.* (2002), Hatch *et al.* (2006) analysed temperature profiles for investigating stream losses beneath ephemeral channels. Geist and Dauble (1998) used electrical conductivity measurements as a natural indicator for exchange reaches in a section of the Colombia River in order to characterize habitats. A combined application of tracers in assessing the water exchanges in hyporheic zone is presented by Doussan *et al.* (1994) and Hoehn and Cirpka (2006).

The techniques of tracer experiments in catchments are not described in detail here. Rather, the specific techniques for each of the compartments (groundwater) are explained in the respective chapters.

7.5.1 Case study: 'Surface-groundwater interaction'

7.5.1.1 Introduction and aim

This investigation was aimed at identifying the impact of the construction of a dam on the local aquifer and on groundwater levels in Northern Italy. The subject of the investigation was how two rivers were connected hydraulically to the shallow aquifer. An important aspect of dam construction is whether and to which degree a river is connected to the local aquifer. If the river and the local aquifer are separated by a layer of low conductivity, leakage and groundwater level response will be less pronounced. Natural and artificial tracers were used. In this case study the application of tracers for the investigation of these aspects is demonstrated. The study involved an artificial tracer experiment and the investigation of a time series of oxygen-18 and deuterium in groundwater and surface waters.

The study was conducted in the Italian Alps near Bolzano close to the rivers Adige and Isarco. Bolzano's mean annual temperature is around 12 °C and the mean annual precipitation is 780 mm per year. Both rivers have a nivo-glacial runoff regime, that is the annual runoff is dominated by meltwater from glaciers and seasonal snow covers located in the upper parts of the catchment. Accordingly, the highest discharge is observed during the early summer months. The valley floors are filled with highly permeable alluvial sediments. The aquifer is composed of alternating gravels and river-bank sediments. There is a layer of fine sediments at 5–10 m depth that could act as an aquitard.

7.5.1.2 Methodology

Stable isotopes were used to characterize general groundwater flow. A sampling campaign was carried out for which groundwater, samples of river water from both rivers and water from boreholes were analysed for the stable isotopes of water. Stable isotope analyses were carried out at with mass spectrometry.

A gas tracer (SF_6) experiment was carried out. SF_6 was injected into the Isarco River to detect a potential direct flow connection from the Isarco to local groundwater. The nontoxic and inert gas SF_6 was injected into the river water for one week (30th April to 6th May 2002) using special equipment which ensured a continuous input of gas into the river by diffusion. Three observation wells close to the River Isarco were monitored for this gas. In order to ensure that sufficient concentrations were attained in the river, the concentration of SF_6 in the downstream river water itself was controlled during the injection period. In addition, the fluorescent tracer Eosine was injected into the Isarco River on 28th May 2002. Measurements of this tracer were conducted by online spectrometry in a borehole close to the river in order to detect even short peaks of fluorescent tracer in the borehole. Further samples were taken at monitoring boreholes for backup analysis in the laboratory. In addition to the tracer experiments rainfall, river runoff and groundwater level were monitored.

7.5.1.3 Water level monitoring

Water level recorders were installed and were working successfully from 20th April 2002. At the same time the water level recorder of the Adige River was working. A major spring flood event and its effect on the water levels in the boreholes were recorded: all of the boreholes reacted to the increased water level in the Adige River within 12 to 24 h (Figure 7.73).

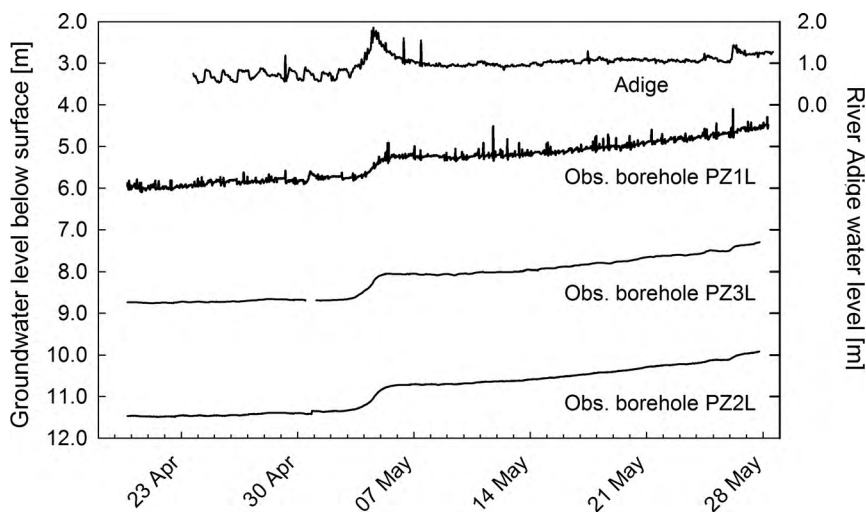


Figure 7.73 Water level of the Adige river and of the boreholes PZ1L, PZ2L, PZ3L.

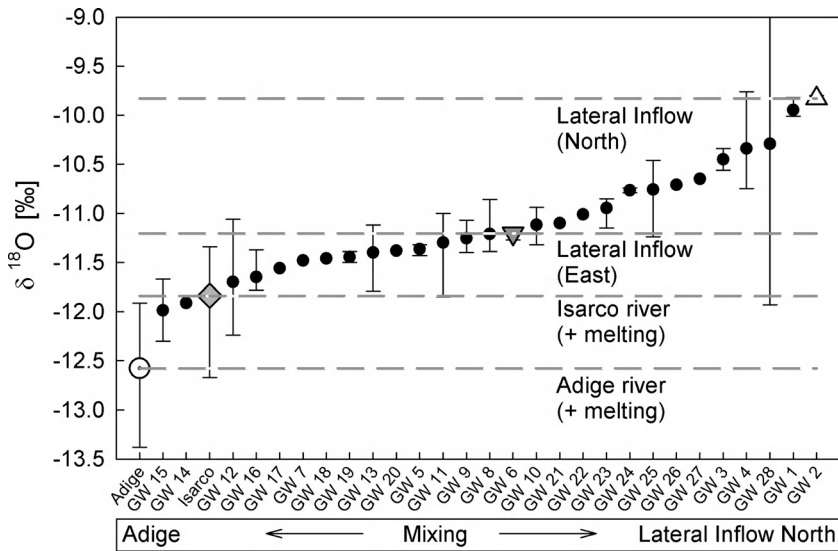


Figure 7.74 Temporal and spatial variability of stable isotopes in surface and groundwater.

7.5.1.4 Stable isotopes

The oxygen-18 versus deuterium plots obtained for the groundwater from the springs and boreholes followed the temporal variation of the river water from the Adige and Isarco rivers. No significant fractionation effects due to evaporation were observed. Within the limits of analytical error all samples plotted on the meteoric water line. Oxygen-18 and deuterium values correlated strongly with $\delta^2\text{H} = 8 \cdot \delta^{18}\text{O} + 10$. In the following, the results are plotted only for oxygen-18 due to the clear correlation with deuterium.

In Figure 7.74 the average values and the range of variation (minimum to maximum) are shown for all surface and groundwater samples. This graph summarizes the spatial and temporal variability in the study area. The source of the lightest water was the River Adige (open circle). It is characterized by the catchment with the highest elevations. The variability in oxygen-18 concentrations ranged from -13.5 to -11.9 ‰. The Isarco river (grey square) had an average oxygen-18 composition of -11.8 ‰ (-12.6 to -11.3 ‰). Local recharge from the eastern (triangle downwards) and the northern fringes of the study area (triangle upwards) represented the heaviest end members. The absolute averages of $\delta^{18}\text{O}$ and the temporal variability for the individual sampling points indicates from which sources groundwater can stem and how strong the direct influence of surface water with short residence times is. The influence of surface water on the groundwater in boreholes correlates strongly with the observed variability (the higher the variability the higher the permeability). For example, GW 28 has a very high variability and therefore a high permeability, while GW 1 is an example of the opposite.

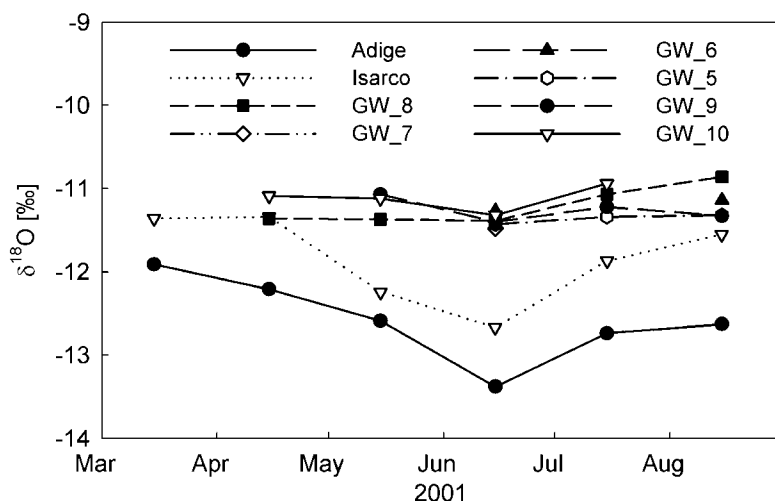


Figure 7.75 Temporal distribution of ^{18}O isotopes for different boreholes and river water.

In the northern part of the study area, boreholes have $\delta^{18}\text{O}$ values of about -9.8‰ . These values are the heaviest values in the study area and represent inflow from lower elevation tributaries. Boreholes with a relatively stable composition are more distant from recharge sources. The other samples indicate a mixture between these components and in some cases with river water. The temporal distribution was taken into account to identify the type of mixing. The temporal variability of stable isotopes in groundwater demonstrates which boreholes react to changes in the discharge of Adige and Isarco. Borehole 10, in particular, shows a direct response, that can only stem from the Adige River because of its light composition. All other boreholes have an isotopic composition corresponding to that of the River Isarco.

The isotopic compositions from different sampling campaigns have been combined in Figure 7.75. This figure gives an impression of the spatial and temporal variability. An isotopic composition well below -11.5‰ (GW 9 and GW 10) can only be explained by riverbed infiltration because no source other than river water has lower values. The spatial distribution of oxygen-18 was plotted along profiles cutting through the study area (Figure 7.76). The profiles were arranged to cut perpendicularly through the rivers Adige and Isarco. In order to emphasize this criterion a dashed threshold line has been drawn: groundwater samples below this line are most likely influenced by riverbed infiltration, at least temporarily.

According to profile 1 (Figure 7.76, top), borehole GW 12 contains significant amounts of riverbed infiltration in August and July 2001. In profile 2 (Figure 7.76, bottom), GW 11 is located slightly below the threshold in August 2001. This can point to a weak influence of riverbed infiltration. Along the profiles strong variations in the boreholes between the different campaigns point to a strong influence of inflows with smaller residence times. These inflows reflect the seasonal variability of the recharge sources (rainfall or river water). For the other boreholes the effects of seasonal variation are weak or not evident.

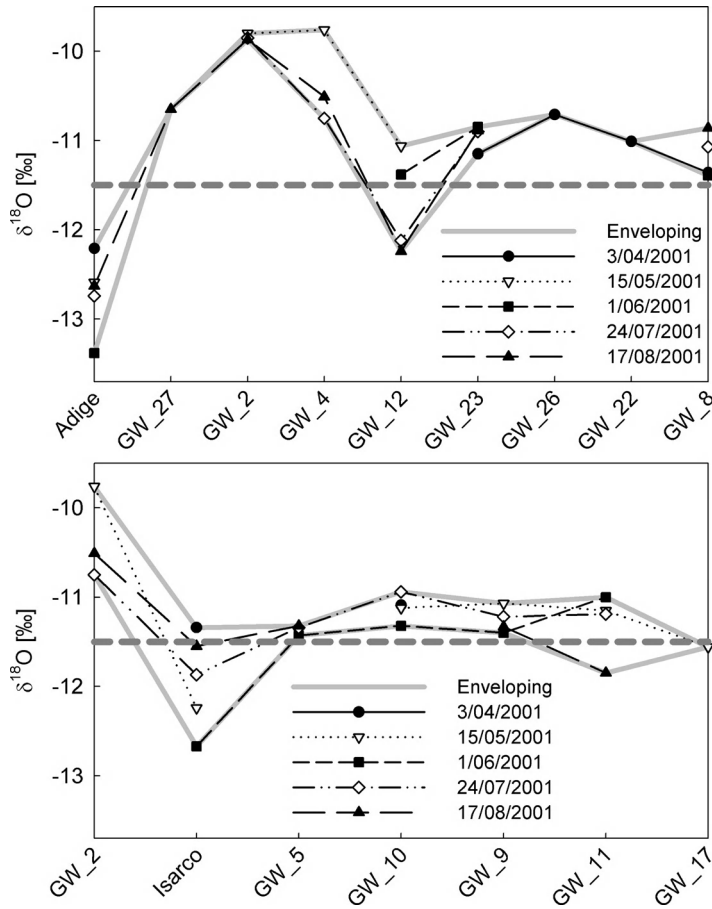


Figure 7.76 Spatial distribution of ^{18}O isotopes along two profiles at different times.

7.5.1.5 Artificial tracer, SF_6

The injection of SF_6 coincided with the major spring flood between 3rd and 6th May 2002. Before the experiment the river and groundwater were sampled and analysed for SF_6 . The tracer could not be detected (detection limit 10 fmol/l). The concentration in the river after the injection reached values greater than 10 000 fmol/l. A SF_6 concentration of less than 1‰ of river water can still be detected.

In samples taken until the end of May 2002 in all three wells, tracer gas could be clearly detected in all the wells with concentrations between 50 and 150 fmol/l (Figure 7.77). This is direct evidence that river water reached the three monitoring wells PZ1L, PZ2L and PZ3L within less than 10 days. The relative concentration in the boreholes also gives an indication of the percentage of riverbed infiltration water in the groundwater and had the order $\text{PZ3L} > \text{PZ1L} > \text{PZ2L}$. The percentage of river water mixed into the groundwater is in proportion to the measured SF_6 concentration. The

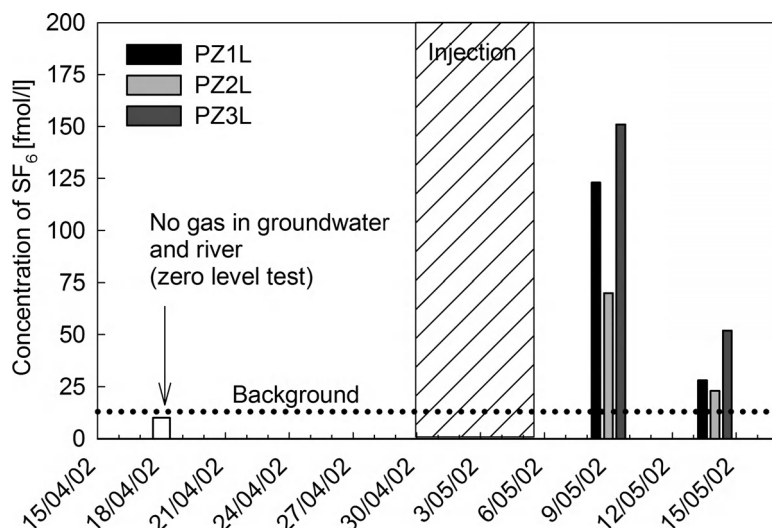


Figure 7.77 Reaction of the wells to the tracer injection into the river: all wells show a response.

contribution of infiltrated river water ranged from 1 to 2%. Taking the degassing of SF_6 into account the portion could be higher.

7.5.1.6 Fluorescent dyes

Eosine was injected into the Isarco River on twenty-eighth May 2002. The first appearance of the tracer in a borehole close to the River Isarco was detected on the 30th of May. The tracer breakthrough ended on the 3rd of June around 12:00 a.m. The maximum Eosine concentration was about $0.1 \mu\text{g/l}$. This indicates a contribution of about 3 to 5% of river water at the peak. The time lag between input and first appearance was about 1.5 days. The resulting maximum flow velocity is around 45 m/day, which is very high.

7.5.1.7 Conclusions

In this study environmental and artificial tracers were combined. Environmental tracers helped to identify boreholes, for which a detectable influence of surface water exists. These boreholes could be identified by monitoring the temporal variability of stable isotopes along cross sections near the observed rivers. However, environmental isotopes cannot provide an unambiguous proof of a flow connection. Therefore, additional artificial tracer tests were conducted. Sulfur hexafluoride (SF_6) provided a more sensitive tracer method and indicated fast flow connections and flow velocities. The amount of direct contribution of river water in an observation borehole could be quantified, and the maximum velocity could be determined. These

data provided the basis for a detailed hydraulic modelling of the surface-groundwater system.

7.5.2 Case study: 'Runoff generation processes investigated using tracers'

7.5.2.1 Introduction and aim

This study is presented in order to demonstrate the application of tracer methods to the investigation of hydrological processes in catchments. In particular runoff generation processes and runoff components of a mesoscale catchment are investigated. The research was conducted in the well investigated Brugga Catchment ($\sim 40 \text{ km}^2$), which is a subcatchment of the Dreisam Basin, located in the Black Forest Mountains in south-western Germany. This case study is based on the publications of Lindenlaub *et al.* (1997), Uhlenbrook (1999), Didszun (2004), Hoeg, Uhlenbrook and Leibundgut (2000), Uhlenbrook and Hoeg (2003), Uhlenbrook, Leibundgut and Maloszewski (2000), Uhlenbrook *et al.* (2002, 2004), Uhlenbrook, Didszun and Wenninger (2008), Uhlenbrook and Leibundgut (2002), Wenninger *et al.* (2004), Uhlenbrook and Sieber (2005), Didszun and Uhlenbrook (2008), Wissmeyer and Uhlenbrook (2008). Environmental tracers were used to characterize residence times in surface and different subsurface flow systems in the catchment. Hydrograph separation using naturally occurring tracers like geochemical and environmental isotope tracers provided information that helped to evaluate runoff generation processes and define source areas of different runoff components. On a longer time scale, residence times, reservoir volumes and the hydraulic characteristics of flow systems were estimated.

7.5.2.2 Description of test site

Elevations in the Brugga Basin range from 434 to 1493 m a.s.l. More than three quarters of the catchment is comprised of moderate to steep slopes, about 20% consists of hilltops and hilly upland and about 5% is comprised of valley floors (Figures 7.78 and 7.79). The average slope is 17.5° , with maximum steepness reaching 46° . Most of the catchment (75%) is forested, the remaining area is pasture. Urbanized areas comprise less than 2%.

Underlying bedrock consists of gneiss and anatectic gneisses, covered by soils and periglacial drift with depths ranging from 0 to 10 m. Most soils are highly permeable, Horton overland flow was only observed on sealed surfaces. About 6% of the catchment is saturated during most of the year. The extent of the saturated areas does not vary considerably over time (Güntner *et al.*, 1999). Most saturated areas are directly connected to the surface drainage system. Mean annual precipitation amounts to 1750 mm, generating a mean annual discharge of approximately 1220 mm. The observation of



Figure 7.78 Typical part of the Brugga catchment with steep forested slopes.

discharge, temperature, hydrochemical and isotopic variation at different springs in the headwater area shows that fast and slow subsurface flow components are contributing to runoff (Figure 7.80).

Based on these observations a perceptual model of the Brugga catchment including three major runoff components and associated storages with respective residence times was devised. The relative contribution from these runoff sources, the storage parameters and the residence times were investigated with environmental tracers.

7.5.2.3 Methodology

Separation of runoff components The separation of runoff components is based on the assumption of mass conservation and the continuity of tracer masses in the system. Theoretically, it is possible to separate n components from $(n - 1)$ tracers. In practice however, analytical errors and uncertainties and nonconservative behaviour of tracers limit the application of such approaches to a few end members. Furthermore, initial concentrations need to be sufficiently different and linearly independent.

There are only a few tracers to which these assumptions apply. Stable isotopes are commonly used. However, only either deuterium or ^{18}O can be used because of their

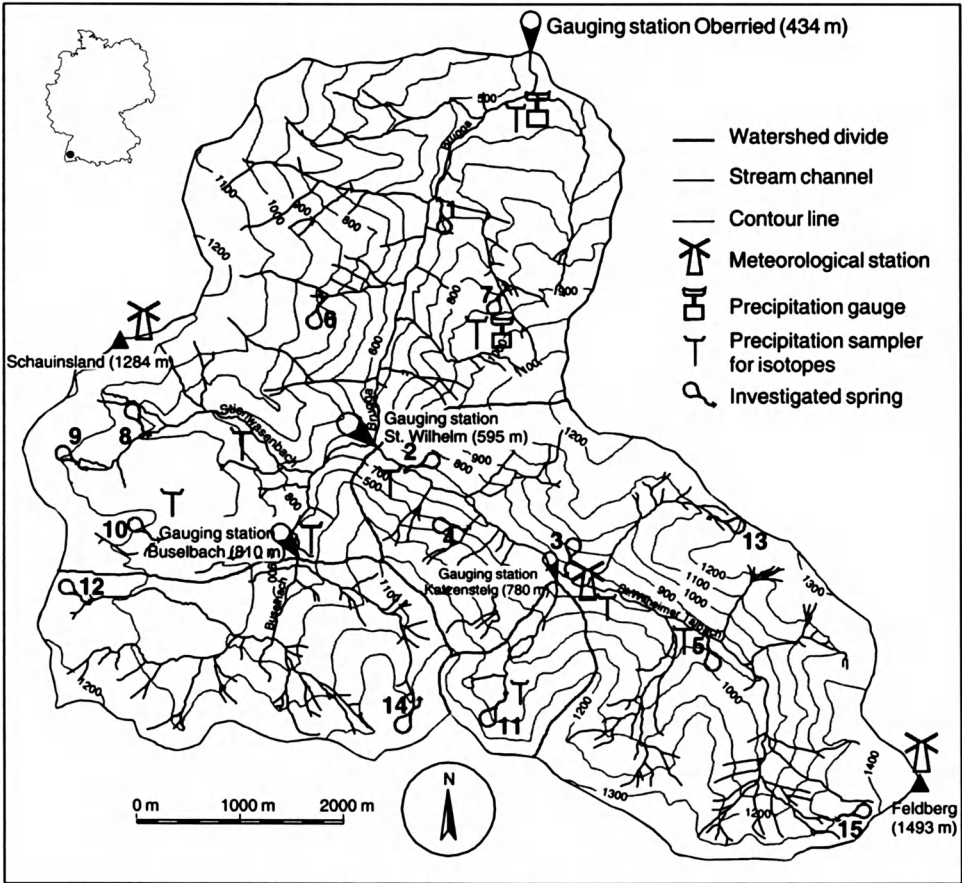


Figure 7.79 The Brugga catchment with hydrometric and isotope network (from Uhlenbrook and Leibundgut, 2002).

linear dependence: i.o.w. if one of these isotopes is used the other one does not provide additional independent information. Chloride and silica have been proposed as additional (largely) conservative tracers (Uhlenbrook *et al.*, 2002). In many cases chloride can be considered to be a quite conservative tracer, except for situations where additional sources may be relevant (e.g. pollution). Additionally, the low overall concentrations of chloride may not provide sufficient resolution to distinguish different end members which may be a limiting factor. Uhlenbrook *et al.* (2002) and Uhlenbrook and Hoeg (2003) have also used silica in order to distinguish groundwater with longer residence times and fast runoff components in the water of the Brugga and the Zastlerbach. For such a study, it needs to be assumed that silica equilibria are established prior to mixing and will be preserved. In the case of the Brugga and Zastler subcatchments these assumptions could be made.

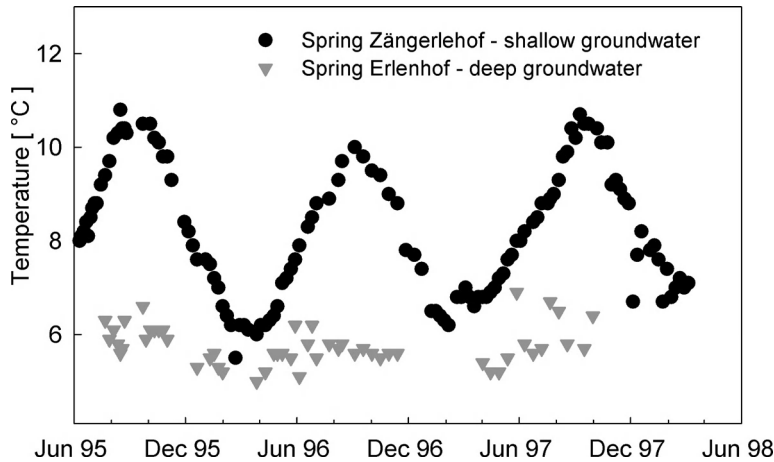


Figure 7.80 Temperature variation in two typical springs in the study area (adapted from Uhlenbrook *et al.*, 2002).

As an example of a two-component separation with ^{18}O to separate event (Q_E) and pre-event water (Q_P) from total runoff (Q_T), the proportion of event water in total runoff can be calculated by:

$$\frac{Q_E}{Q_T} = \frac{c_{T^{18}\text{O}} - c_{P^{18}\text{O}}}{c_{E^{18}\text{O}} - c_{P^{18}\text{O}}} \quad (7.19)$$

and in analogy, the proportion of pre-event water:

$$\frac{Q_P}{Q_T} = \frac{c_{T^{18}\text{O}} - c_{E^{18}\text{O}}}{c_{P^{18}\text{O}} - c_{E^{18}\text{O}}} \quad (7.20)$$

where $c_{x^{18}\text{O}}$ is the isotopic content of ^{18}O in the component x regarded (cf. Section 6.5).

To realize the hydrograph separation, the tracer concentration, in this case isotopic content, of each component must be known. In this study, the isotopic content of pre-event water was determined by analysing the hydrochemical and isotopic composition of base flow. To determine the isotopic content of the event water fraction, the measured isotopic ratio of precipitation was used. First, the overall mean in the rainfall of an event was taken to represent the isotopic ratio of event water (bulk mean). Second, only the incremental mean isotopic content of rain of the actual time step was used to separate the fraction of event water (according to McDonnell, Stewart and Owens, 1991). ^{18}O was used for separating event and pre-event water. In addition silica was used to identify and separate the water from different source areas and flow mechanisms. The highest concentrations of silica are expected to be in the water from the deepest aquifers, wherein many fractures occur and contact time is long. Therefore, silica can also be used to estimate transit time of water and characteristics of the aquifer matrix.

The silica concentration in overland flow was approximated to be zero due to short contact time.

Residence times and system functions of representative spring catchments For representative springs an estimation of overall residence time was made based on ^3H , ^{18}O and CFCs. The input function of ^{18}O was measured during the sampling period of 3 years at a weekly interval inside the basin in several rain gauges and was extended back in time to 1971 using regression methods linking ^{18}O with temperature and the data of three stations located in the region (Stuttgart/Bad Cannstatt, Karlsruhe and Weil am Rhein). The input function of ^3H on an annual basis from 1962 to 1998 was derived from Hohenpeissenberg, Bavaria, Germany. The backward extension until 1950 was carried out with data from Ottawa, Canada. However, the input functions of precipitation do not represent the input to the groundwater system. Runoff coefficients can be used as weighting factors to determine the monthly weight of the input function and derive the real system input function. Monthly infiltration coefficients were derived based on a hydrological model (HBV, Bergström, 2001).

The background atmospheric mixing ratios of CFCs were derived from a dataset measured in Northern Ireland (Atmospheric Life Time Experiment/Global Atmospheric Gases Experiment (ALE/GAGE)). Small gaps in the data were filled with linear regression. Within the Brugga Basin, ground truth samples were taken in order to verify the input function (Chapter 3).

The following lumped parameter models (see Chapter 5) were used to derive the residence times in the investigated spring systems: the exponential model (EM), Equation (5.115), the combined exponential-piston flow model (EPM), Equation (5.116), and the dispersion model (DM), Equation (5.117).

Long term multi component runoff separation in the catchment scale In order to quantify long term runoff components a modelling approach was applied. The observed dynamics of ^{18}O at the gauging station were modelled by summation of three separate systems according to the conceptual catchment model (Figure 7.81). For the first component, direct runoff, the monthly ^{18}O content of rainfall was taken, as it could be assumed that event water left the basin within hours or days. Both subsurface flow systems were represented by system functions, which were determined for springs in the preceding step. The runoff proportions (α) of the three components were determined by fitting of observed and modelled ^{18}O values.

7.5.2.4 Data

The monitoring period began in July 1995 and is still on-going in 2009. Several intensive monitoring periods were carried out during several weeks. In the following, the results from the summer 1998 campaign are reported. Precipitation was collected at nine rain gauges located at different altitudes and exposures. Sampling for isotopic composition

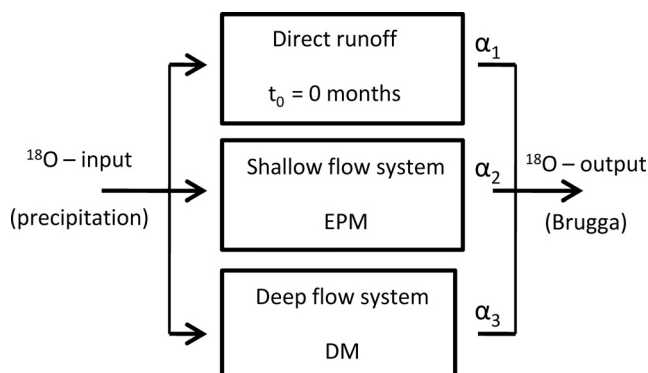


Figure 7.81 Scheme of model approach for the quantification of long term runoff components in the Brugga catchment (adapted from Uhlenbrook *et al.*, 2002).

was done weekly or twice a week, while meteorological parameters were measured continuously at 10 and 30 min intervals at three climate stations. During the intensive sampling period in summer 1998, a rain sampler, which sampled all the rain, was installed in the centre of the catchment in order to investigate intrastorm variability of the isotope composition in precipitation.

To investigate saturated zone water, up to 15 springs were sampled on a weekly to bi-weekly basis for temperature, pH, electrical conductivity, silica concentration and isotopic composition. Streamflow was measured with pressure probes at the outlet of the Brugga Basin in Oberried. Water samples were taken weekly or biweekly and were analysed for ^{18}O , silica and major anions and cations for a check of ion balances. During the intensive sampling period in summer 1998, samples were taken by automatic sampling systems in up to 30 min intervals. To improve the determination of residence times, additional samples for tritium and CFCs analysis were taken in June of 1998.

7.5.2.5 Results and discussion

Runoff components (event-based) In order to determine the contributions of the individual flood runoff components, to derive the ratio of event/pre-event water and to investigate from which sources the runoff originated, several single events were analysed using the environmental tracer ^{18}O as well as the geogenic tracers silica and chloride. Figure 7.82 shows the results of the two component hydrograph separations. Whereas ^{18}O separates the water into contributions of event and pre-event water, silica and chloride are tracers indicating the source area. It can be seen that in the first event up to 50% of runoff was comprised of event water, while in the second event the portion of pre-event water rose significantly by up to about 85%. Here, the difference between the usage of incremental and bulk mean for the event water portion was negligible (<3% of

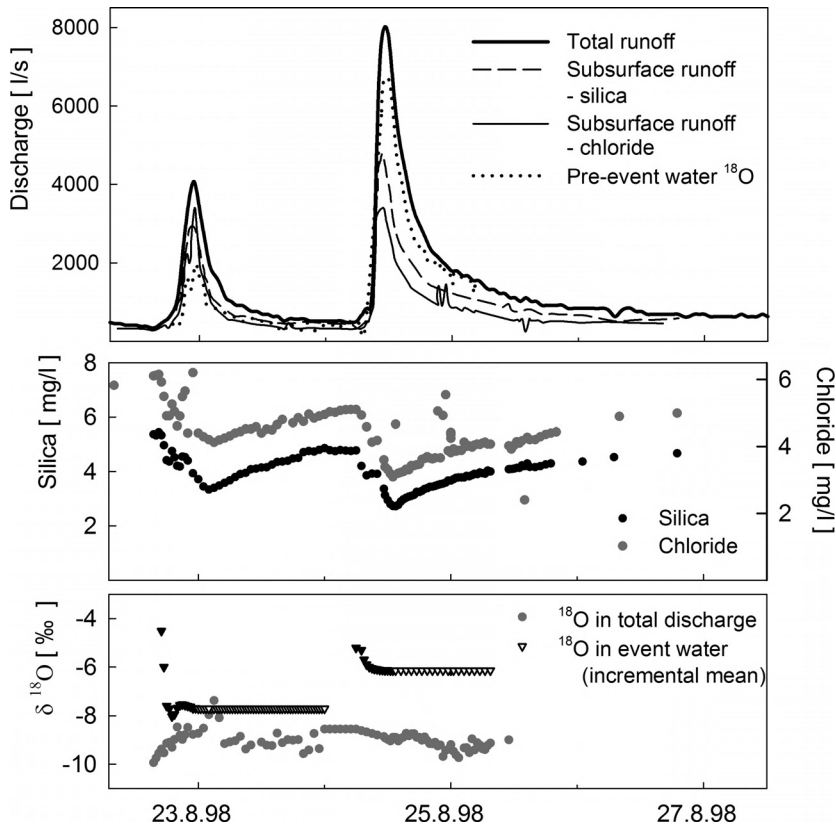


Figure 7.82 Runoff component separation with ^{18}O , silica and chloride (from Uhlenbrook *et al.*, 2002).

total runoff volume). The contribution of event surface water, derived from geogenic tracers, is smaller compared to the portion of event water in the first event. In the second event, the ratio of event water is smaller. This can be explained by the contribution of subsurface water stored and activated during the second event. Basically, the results confirmed that the major part of the runoff volume is pre-event water.

Residence times and system functions of spring catchments Residence times have been estimated at five springs in the upper part of the Brugga catchment. Regarding the analysis of ^{18}O , the measured data of the two springs Zipfeldobel and Zängerlehof show a distinct dampening and temporal lagging of minima and maxima compared to the measured data of precipitation. Mean residence times t_0 were estimated at 28 and 36 months, derived from application of the EPM (5.116) and EM (5.115), respectively. These springs are considered to be representative of the shallow groundwater flow system in the area (Figure 7.83).

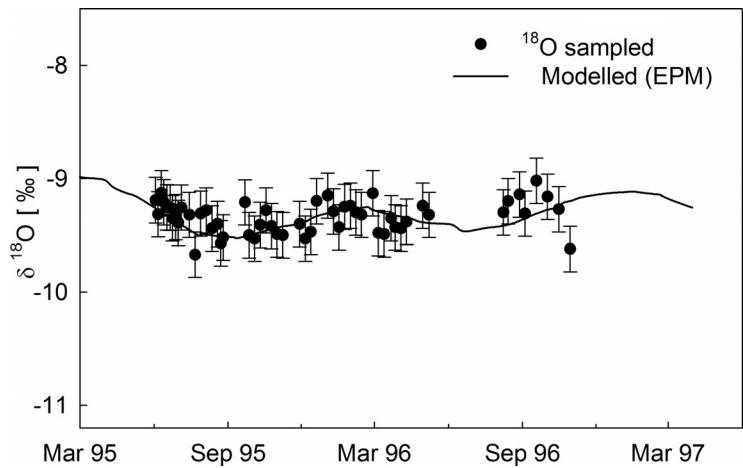


Figure 7.83 Modelled and observed $\delta^{18}\text{O}$ for the spring Zängerlehof. The analytical error for stable isotope measurements is $\pm 0.2\text{‰}$ (from Uhlenbrook *et al.*, 2002).

Three other springs, Stollen, Mooshof and Erlenhof, are considered to be representative of the deeper groundwater system. Here the ^{18}O –method was not applicable due to a lack of seasonal variation in the data, which suggests residence times longer than 5 years. Based on ^3H data, derived from application of the DM (5.117), the mean residence times of these springs are between 6.2 and 8.6 years (Figure 7.84). Due to the low tritium input a high degree of uncertainty is associated with residence time estimation for the slow component. Due to low concentrations of ^3H in the water, residence time could also be much higher (>60 years with recharge before the bomb peak

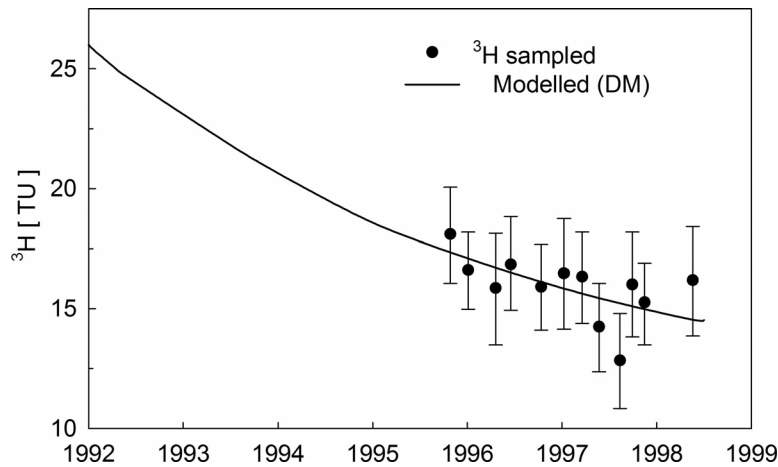


Figure 7.84 Modelled and observed ^3H for the spring ‘Stollen’. For the measurements an analytical error of $\pm 1.5 \text{ TU}$ is given (from Uhlenbrook *et al.*, 2002).

in the 1950s). However, as CFCs were detected and their concentrations corresponded to those typical for recent recharge (<10 years) the mathematically possible case of residence times >60 years could be rejected.

Quantification of runoff components in the long term Three different runoff components and their specific variations in ^{18}O were summarized in order to model the run of the ^{18}O signature at the basin outlet over the monitoring period of 3 years with a monthly resolution. An averaged mean residence time of the two representative springs (Zipfeldobel and Zängerlehof) of 32 months was applied as the mean residence time of the shallow flow system in the EPM (5.116). The DM (5.117) with an average mean residence time of 7.1 years taken from analyses of the springs 'Stollen, Mooshof and Erlenhof' was applied in the calculations to describe the third component (deep groundwater flow system).

For event water, a proportion of 11.1% was used based on the event analysis. For the deeper flow system, a contribution of 19.5% was derived. The experiment showed that the dominant runoff component in the Brugga Basin with a proportion of 69.4% was the shallow flow system. For some months during spring and autumn, the ^{18}O signatures were too similar. In these cases no real solution could be found and these months were excluded from the analysis. This observation may also indicate that during these months the solutions found are not representative and different system states prevail.

To check the plausibility of the long term multi-component analysis and to interpret the results, some simple calculations were made: Based on a mean runoff of $1.54 \text{ m}^3/\text{s}$, specific runoff proportions multiplied with their respective residence time, the mean stored volumes of water are $8.8 \times 10^7 \text{ m}^3$ in the shallow flow system and $6.6 \times 10^7 \text{ m}^3$ in the deeper flow system, respectively. If the shallow flow system is related to a saturated catchment, high altitude areas and areas of block debris (approx. 75% of the entire catchment) and assuming a porosity of $n = 0.3$, the average thickness of the aquifer has to be about 8.5 m. The same estimation was carried out for the deeper flow system. Here the estimation of porosity is more difficult due to the great spatial variability. However, a mean groundwater storage volume in the upslope area was estimated from calculations using the mean discharge of two investigated springs to about $2.5 \times 10^7 \text{ m}^3$. Subtracting that from the total water storage volume of the deep flow system, a mean volume of $4.1 \times 10^7 \text{ m}^3$ is attributed to the remaining areas.

The total volume of the fissured rock aquifer was estimated to be $2.0 \times 10^9 \text{ m}^3$ based on geometric calculations. Related to the estimated water volume this implies an overall mean porosity of 2%. Taking into account the fact that the basin is located close to the major fault zone of the Upper Rhine Graben and that some clayey weathering occurs close to the surface and near shear faults, this value appears plausible. The mean contributions to runoff of each of the three runoff components and the main characteristics of corresponding subsurface flow systems are shown in Table 7.23.

Uncertainties in runoff separation have several, different sources. To begin with, the analytical error in tracer analysis has to be mentioned and, if the quantitative flow contribution of the components is taken into account, the error in runoff measurement. Regarding the tracers used in the study described above, the intrastorm variability of

Table 7.23 Mean proportion of runoff components and main characteristics of the different flow systems (Uhlenbrook *et al.*, 2002)

| | Mean proportion within sampling period, % | Mean residence time, years | | | Stored mean volume, m ³ | Mean storage height, m |
|---------------------|---|----------------------------|---------------------|----------|--|---|
| | | ¹⁸ O Data | ³ H Data | CFC-Data | | |
| Event water | 11.1 | hours to days | — | — | | |
| Shallow groundwater | 69.4 | 2–3 | <5 | — | 8.6×10^7 | 2.55 |
| Deep groundwater | 19.5 | >5 | 6–9; ~60 | <10 | 2.5×10^7 ^{a,b} 4.1×10^7 ^c | 4.2 ^{a,b} 1.03 ^c |

^aRelated to the hilly uplands, approx. 14.8% of catchment.

^bCalculated from the springs Erlenhof and Mooshof (uplands), which are representative for this source area.

^cRelated to the mean storage volume of the hard rock aquifer of the whole basin.

¹⁸O as well as the elevation and temperature effect have to be considered. In case of silica, there again is a dependence on temperature and incomplete equilibria. In general, when using natural tracers, their spatial heterogeneity has to be kept in mind. It is evident that the choice of the number of runoff components in the preceding conceptual model can also cause an error, if one or more components were missed or added erroneously. Uhlenbrook and Hoeg (2003) showed the uncertainty in estimating the different runoff components of the basin described above with the application of the classical Gaussian error estimation to the data of two- and multi-component hydrograph separations, derived from experiments in a subcatchment. In particular, if the investigated runoff component represents a small proportion of the total runoff (e.g. event water, surface component), the relative error may be significant and may reach the absolute value of the estimated component contribution. Regarding the two component hydrograph separation, they detected the analytical error in tracer analysis and discharge measurement and the spatial heterogeneity of tracer concentrations are the most likely source of uncertainty. In the three component separation, again the spatial heterogeneity has the greatest impact, while analytical errors in measurement have minor impacts. The elevation and temperature effect of ¹⁸O and silica and the solution of minerals during the event were ranked as intermediate. It has to be mentioned that the presented results were site and event specific. Transferred to other terrains, the importance of error sources may vary.

7.5.2.6 Application of tracer results for model design and model validation

Beside other validation techniques like, for example, split sample test (Klemeš, 1986), tracer data can be used as part of multi-response validation. Uhlenbrook and Leibundgut (2002) showed the application of tracer data for validating of the tracer-aided-catchment model (TAC) in the Brugga Basin, described above. The calibration

parameter of the TAC model was basin runoff; fitting was carried out through calibration supported by Monte Carlo Simulations. In their study, besides basin runoff, spring discharge, snow cover and snowmelt, simulated silica concentrations in basin runoff and in discharge of the mentioned spring were compared with measurements from inside the basin. After calibrating the model in the way described above, the simulated and measured silica concentrations in the basin outlet and in spring discharge were compared in order to validate the model.

Overall, the silica simulation in basin runoff over the whole simulation period of 3.2 years was less accurate than the runoff simulation (R_{eff} according to Nash and Sutcliffe (1970): 0.36 to 0.77). But, if individual simulation periods were analysed, a dependence of the silica simulation accuracy to the accuracy of the runoff simulation could be detected. In periods with poor runoff simulation, the silica concentration was also not well simulated, whereas during periods when runoff was predicted accurately, the silica concentrations in the runoff were also reproduced well (see Figure 7.85). The investigation showed that model validation with tracer data can provide a more realistic description of the basin and its specific processes. Here, especially a more realistic conceptualization of the runoff generation processes in the model was achieved.

In addition, Uhlenbrook and Sieber (2005) also demonstrated the potential of tracer data for a reduction of the model uncertainty. They showed that including silica data into the model calibration helped to reduce the uncertainty of predicting flood

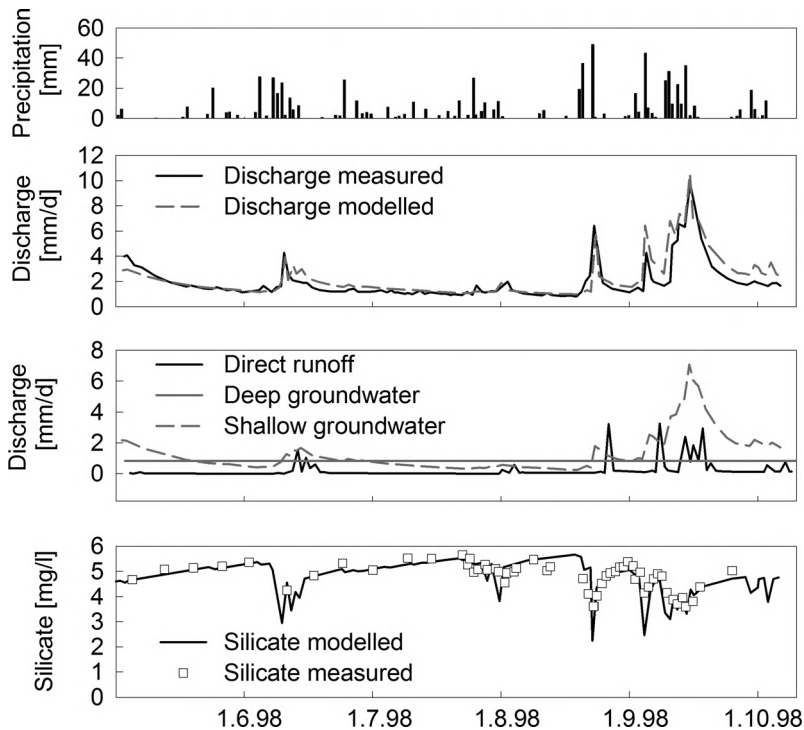


Figure 7.85 Silica in runoff, measured and simulated (from Uhlenbrook and Leibundgut, 2002).



Figure 7.86 Left: Spring area Zipfeldobel. Right: Slope of the spring catchment Zängerlehof.

discharge significantly in the Brugga Catchment. They also demonstrated that including an additional gauging station from a subcatchment reduced the model uncertainty even more. However, as setting up a gauging station is quite costly, the use of tracer data sampled during short targeted field campaigns can be very valuable for improving hydrological model predictions.

7.5.2.7 Multi tracer experiments at hillslopes

The hydrograph separation based on environmental tracers, as presented in the previous section, shows the dominant role of the shallow groundwater system for runoff generation in the Brugga Catchment. This result was confirmed by many other studies and experiments in this research catchment (e.g. Wenninger *et al.*, 2004; Uhlenbrook and Hoeg, 2003).

Just one of several additional artificial tracer experiments carried out in spring catchments in the Dreisam River Basin is presented here. In this case, the application of artificial and environmental tracers yielded results that seemed inconsistent at first sight. These results are reported here for several reasons. It is very likely that tracer studies leading to inconsistent results are published less often, although a lot can be learned from such cases. The study is a representative example of how the simultaneous use of several methods on the same topic can lead to different results (cf. Chapter 2) and what they might tell us about tracers and the hydrological system.

The experiment was conducted in order to investigate flow processes within the subsurface layers of slopes (Didszun, 2000; Uhlenbrook *et al.*, 2008). The multi tracer test was supposed to improve the understanding of near surface runoff processes in the drift cover of slopes. Furthermore, the tracer experiment was carried out to provide direct information on flow paths and travel times. Two fluorescent dyes (Uranine and Naphthionate) and a salt tracer (bromide) were injected in October 1999 at nonsteady conditions during naturally occurring rainfall events. The experiment was performed uphill of the spring ‘Zipfeldobel’ (Figure 7.86).

The spring Zipfeldobel (Figure 7.87) is characterized by a comparatively slow and delayed response of spring discharge to precipitation. Although the time lag between

rainfall and initial increase in spring discharge is only a few hours, the peak discharge is not reached until several days after the beginning of a rainfall event. The response also depends on the intensity of rainfall events. The flow behaviour of spring B (Zänglerhof) is different and will not be described further here (Figure 7.87). The runoff generation mechanism of these springs is discussed in Leibundgut (2004), Uhlenbrook, Didszun and Leibundgut (2005) and Uhlenbrook, Didszun and Wenninger (2008).

The role of different runoff generation mechanisms can also be investigated based on hydrochemical end members and an end-member-based hydrograph separation (Section 6.5). A two-component hydrograph separation using dissolved silica was carried out accounting for the fact that only small variations of hydrochemistry could be found (Figure 7.88). However, an alternative tracer was not available.

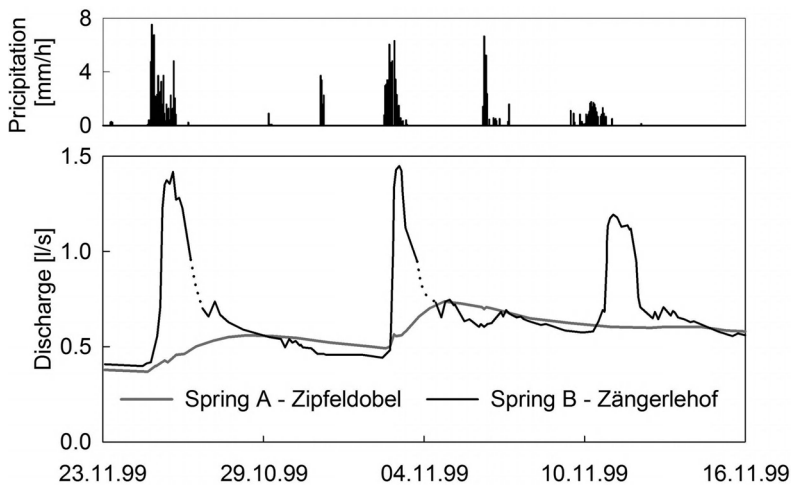


Figure 7.87 Flow behaviour of the springs A and B depending on precipitation. Dotted lines: interpolated data due to loss of data.

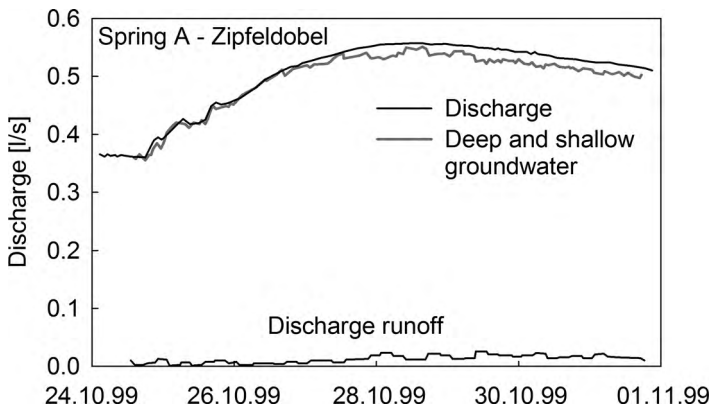


Figure 7.88 Hydrograph separation using dissolved silica (spring A – Zipfeldobel).

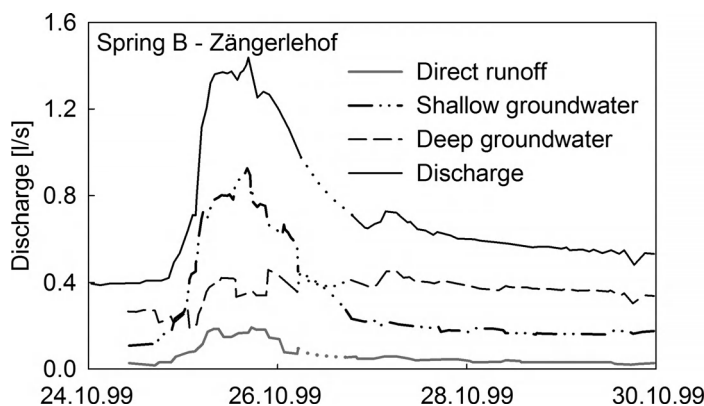


Figure 7.89 Hydrograph separation using Deuterium and silica (spring B – Zängerlehof).

The hydrograph separation suggests that shallow and deep groundwater contributions are the dominant runoff components. Only a small fraction of runoff is produced by direct runoff. Direct runoff could reach the springs during the event by water flowing along preferential pathways (Figures 7.88 and 7.89).

A detailed description of the hydrograph separation is given in Uhlenbrook, Didszun and Wenninger (2008). According to the results of the electrical resistivity tomography (ERT) measurements (Uhlenbrook, Didszun and Wenninger, 2008), the different hydrological and hydrochemical responses could be attributed primarily to different structures of the debris and drift cover as well as to the land use at the hill slopes above each spring.

Artificial tracer experiment The artificial tracer experiment was aimed at investigating the direct runoff component in more detail and at clarifying the role of shallow groundwater for spring discharge and runoff generation. In a multi tracer experiment the three tracers Naphthionate, Uranine and Sodium bromide were injected (Figure 7.90):

1. Sodium bromide (5 kg) was injected 10 m uphill as a line injection in a small trench (0.3×1.5 m, about 0.2 m deep).
2. Naphthionate (2 kg) was injected about 19 m uphill in a similar small trench (Figure 7.91).
3. Uranine (0.15 kg) was injected at the same distance in a hand-drilled well at depths of about 1 m in order to avoid the possible retention of the tracer by sorption in the upper soil horizons.

The objective was the tracing of the flow paths of the infiltrating water in the spring catchment with the first two injections. The third injection occurred underneath the

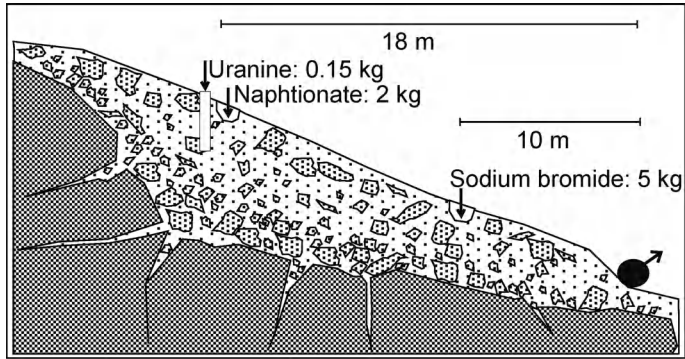


Figure 7.90 Cross section of the spring catchment Zipfeldobel. The injection sites are located in the periglacial cover above the bedrock.



Figure 7.91 Injection of Naphtionate in a trench 18 m uphill the spring Zipfeldobel.

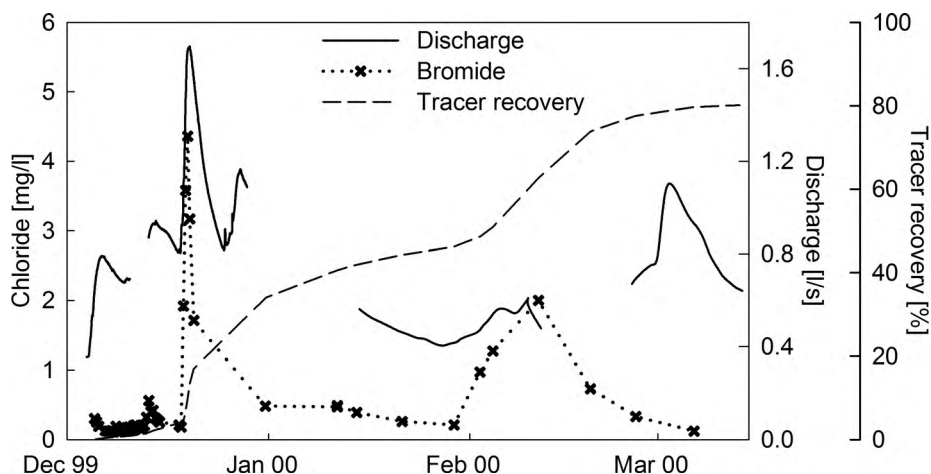


Figure 7.92 Breakthrough of bromide in the spring 'Zipfeldobel.' Injection in the unsaturated zone in October 1999 (adapted from Didzun, 2000).

upper soil layer (A horizon, large porosity) to avoid a possible sorptive retention of the tracer. This tracer was supposed to trace the lateral flow paths below the root zone.

In order to create conditions similar to the natural flow driving infiltration, percolation and lateral flow, only limited amounts of water were added before (a few litres) and after the injection (a few tens of litres). The breakthrough of the tracers did not match expectations. None of the fluorescent tracers could be detected in spring water for the following 2 months. Only bromide eventually yielded a useable tracer breakthrough as it was detected 8 weeks after the injection (Figure 7.92).

The main hypotheses explaining the missing tracer breakthrough of fluorescent tracers are:

- The tracer was immobilized in the unsaturated zone as a result of dry weather conditions and a high water deficit at the end of the summer-autumn seasons.
- The lateral flow in the subsurface layer was delayed by the low connectivity of lateral subsurface flow paths.
- The tracer Uranine was affected by sorption due to low pH, high organic content originating of the upper soil.
- The injected tracer mass of Naphtionate was probably too small considering the recommended ratio 20:1 for Naphtionate; Uranine (Section 4.1).

As described in Section 4.1 the application of Uranine in substrates having a low pH-value is difficult due to the change of the electrical charge of the Uranine molecule and the consecutive loss of the tracer by sorption. It should additionally be noted that

Uranine develops to a cation at pH values of below 5 and, consequently, can be lost to sorption more easily. This can be a reason why Uranine could not be found in spring discharge.

The bromide tracer breakthrough shows some correlation with discharge. Small rainfall events seem to have flushed the tracer. Due to rather dry general weather conditions during the first weeks after injection, the bromide tracer was obviously also retarded along its flow path. The tracer recovery of bromide calculated with a mean discharge of 0.7 l/s reached 80% in total after a monitoring period of approximately 5 months. This high recovery rate confirms the suitability of bromide for tracer tests under difficult conditions.

The overall assessment of the tracer experiment shows an underestimation of tracer travel times in the planning of the experiment. Since the tracer breakthrough was expected to occur much faster, samples were taken every 4 h at the beginning of the experiment.

The results of the electrical resistivity tomography (ERT) measurements (Uhlenbrook, Didszun and Wenninger, 2008) showed that the tracers were injected in a local anomaly which blocked the flow of the traced water. This may be another explanation for the inconsistency of the results obtained by artificial and environmental tracers. In addition, it highlights the problem of local microstructures that may disturb an artificial tracer experiment.

These additional hydrological factors may have led to different results compared to those obtained from environmental tracers. Nevertheless, the tracer test results added to the knowledge of hill slope hydrology and can help in characterizing runoff generation. From the comparison of both methods more can also be learned about the transport characteristics of artificial tracers, especially during unusual or extreme conditions.

According to the axiom of tracerhydrology, described in Chapter 2 – combine several techniques in order to have a comprehensive idea of the processes – the tracer test presented here enables at least a qualitative instructive interpretation. It is an example of a multi-technical approach of using tracers in Hydrology (Uhlenbrook, Didszun and Wenninger 2008).

The lessons learnt from this experiment have been used during subsequent studies in several catchments. Furthermore, the efforts made to find the reason for the inconsistencies and the repetition of the experiments using the knowledge that is now available lead to acceptable and probable solutions in most of the cases.

A collection of tracer related studies in the test site Dreisam, Black Forest, Germany is given in the note below.⁴

⁴Uhlenbrook, Didszun and Wenninger (2008), Didszun and Uhlenbrook (2008), Wissmeier and Uhlenbrook (2007), Uhlenbrook, Didszun and Leibundgut (2005), Uhlenbrook *et al.* (2005), Didszun (2004), Uhlenbrook *et al.* (2004), Uhlenbrook, Roser and Tilch (2004), Wenninger *et al.* (2004), Uhlenbrook and Hoeg (2003), Uhlenbrook *et al.* (2002), Uhlenbrook and Leibundgut (2002a, 2002b), Eisele and Leibundgut (2002), Hangen *et al.* (2001), Uhlenbrook and Leibundgut (2000), Uhlenbrook *et al.* (2000a, b), Brodersen *et al.* (2000), Hoeg, Uhlenbrook and Leibundgut (2000), Mehlhorn, Lindenlaub and Leibundgut (1999), Mehlhorn and Leibundgut (1999a, b), Mehlhorn (1999), Uhlenbrook and Leibundgut (1999), Mehlhorn *et al.* (1998), Cui (1997), Cui, Demuth and Leibundgut (1995).

References

- Adams, S., Titus, R., Xu, Y. (2004): Groundwater Recharge Assessment of the Basement Aquifers of Central Namaqualand. *WRC Report 1093/1/04*, Water Research Commission, Pretoria.
- Adar, E.M., Dody, A., Geyh, M.A., Yair, A., Yakirevich, A., Issar, A.S. (1998): Distribution of stable isotopes in arid storms. *Hydrogeology Journal*, **6** (19), 1431–2174.
- Adar, E.M. (1996): Quantitative evaluation of flow systems, groundwater recharge and transmissivities using environmental tracers. Manual on Mathematical Models in Isotope Hydrology. *IAEA-TECDOC-910*, 113–154. IAEA, Vienna.
- Adar, E.M., Leibundgut, Ch. (eds.) (1995): Application of Tracers in Arid Zone Hydrology. *IAHS Publication*, **232**.
- Adar, E., Sorek, S. (1989): Multi-compartmental modeling for aquifer parameter estimation using natural tracers in non-steady flow. *Advances in Water Resources*, **12**, 84–89.
- Adar, E.M., Neuman, S.P., Woolhiser, D.A. (1988): Estimation of spatial recharge distribution using environmental isotopes and hydrochemical data. I. Mathematical model and application to synthetic data. *Journal of Hydrology*, **97**, 251–277.
- Adar, E.M. and Neuman, S.P. (1988): Estimation of spatial recharge distribution using environmental isotopes and hydrochemical data. II. Application to Aravaipa Valley in Southern Arizona, USA. *Journal of Hydrology*, **97**, 297–302.
- Aeschbach-Hertig, W., Peters, F., Beyerte, U., Kipfer, R. (2000): Palaeotemperature reconstruction from noble gases in ground water taking into account equilibration with entrapped air. *Nature*, **405** (6790), 1040–1044.
- Aggarwal, P.K., Alduchov, O., Araguas Araguas, L., Dogramaci, S., Katzelberger, G., Kriz, K., Kulkari, K.M., Kurtas, T., Newman, B.D., Pucherm, A. (2007): New Capabilities for Studies Using Isotopes in the Water Cycle. *Eos Transactions, American Geophysical Union*, **88** (49), 357–538.
- Albrecht, A., Goudsmit, G., Zeh, M. (1999): Importance of lacustrine physical factors for the distribution of anthropogenic ^{60}Co in Lake Biel. *Limnology and Oceanography*, **44** (1), 196–206.
- Alexander, E.C. Jr., Quinlan, J.F. (1992): *Practical tracing of groundwater with emphasis on karst terranes, 2nd edition*. Short course manual. Geological Society of America, Boulder.
- Aley, T.J., Fletcher, M.W. (1976): The water tracer's cookbook. *Missouri Speleology*, **16** (3), 1–32.
- Allaire-Leung, S.E., Gupta, S.C., Moncrief, J.F. (1999): Dye adsorption in a loamy soil as influenced by potassium bromide. *Journal of Environmental Quality*, **28**, 1831–1837.

- Allison, G.B., Stone, W.J., Hughes, M.W. (1985): Recharge in karst and dune elements of a semi-arid landscape as indicated by natural isotopes and chloride. *Journal of Hydrology*, **76**, 1–25.
- Allison, G.B., Barnes, C.J. (1983): Estimation of evaporation from non-vegetated surfaces. *Nature*, **301**, 143–145.
- Allison, G.B., Hughes, M.W. (1978): The use of environmental chloride and tritium to estimate total local recharge to an unconfined aquifer. *Australian Journal of Soil Research*, **16**, 181–195.
- Ambach, W., Behrens, H., Bergamnn, H., Moser, H. (1972): Markierversuche am inneren Abflusssystem des Hintereisferners (Ötztaler Alpen). *Zeitschrift für Gletscherkunde und Glazialgeologie*, **8**, 137–145.
- Amin, I.E., Campana, M.E. (1996): A general lumped parameter model for the interpretation of tracer data and transit time calculations in hydrologic systems. *Journal of Hydrology*, **179**, 1–21.
- André, J.C., Baudot, Ph., Bouchy, M., Niclaude, M. (1977): Quantitative studies of the synchronous excitation method in spectrofluorimetry: Application to tracer concentration measurements in hydrology. *Analytica Chimica Acta*, **92**, 369.
- André, J.C., Molinari, J. (1976): Mises au point sur les différents facteurs physico-chimiques influant sur la mesure de concentration de traceurs fluorescents et leurs conséquences pratiques en hydrologie. *Journal of Hydrology*, **30**, 257–285.
- Andreini, M.S., Steenhuis, T.S. (1990): Preferential Paths of Flow under Conventional and Conservation Tillage. *Geoderma*, **46**, 85–102.
- Aoki, P.E., Bombonato, C., Maloszewski, P. (1996): Determination of hydrodynamic parameters in the Paiva Castro reservoir using artificial tritium. In: *Isotopes in water resources management*, 1, IAEA-STI/PUB/970, 157–166, IAEA, Vienna.
- Appelo, C.A.J., Postma, D. (2007): *Geochemistry, Groundwater and Pollution*. 2nd edition, CRC Press, Boca Raton, 649 p.
- Aragno, M., Müller, I. (1982): Premières expériences de tracage des eaux souterraines dans le karst du jura neuchâtelois (Suisse) à l'aide de bactériophages. *Bulletin d'Hydrogéologie*, **4**, 59–81. Neuchâtel.
- Armbruster, V. and Leibundgut, C. (1997): The use of silica to characterise the allogenic flysch component in Vipava springs during the observation of single events, in Karst hydrogeological investigations in south-western Slovenia, Ljubljana (A. Kranjc, ed.) *Acta Carsologica*, **26** (1), pp. 206–12.
- Armbruster, H., Mors, K., Eiswirth, M., Hötzl, H., Merkler, G.P., Nägelsbach, E. (1992): Leakage detection of sewing pipes by combined geophysical and tracer techniques. In: *Tracer Hydrology 92. Proceedings of the 6th International Symposium on Water Tracing, September 21–26, 1992, Karlsruhe*, Hötzl, H., Werner, A. (eds.), 97–100. Balkema, Rotterdam.
- Asano, Y., Uchida, T., Ohte, N. (2002): Residence times and flow paths of water in steep unchannelled catchments, Tanakami, Japan. *Journal of Hydrology*, **261** (1–4), 173–192.
- Aschwanden, H., Weingartner, R., Leibundgut, Ch. (1986): Zur regionalen Übertragung von Mittelwerten des Abflusses. *Deutsche Gewässerkundliche Mitteilungen*, Part I: **30** (2/3), 52–61, Part II: **30** (4), 93–99.
- Aschwanden, H., Leibundgut, Ch. (1982): Die Markierung des Wassers des Gonerseeausbruches mit drei Fluoreszenztracern. *Beiträge zur Geologie der Schweiz – Hydrologie*, **28** (II), 535–549. Berne.
- ATH (ed) (1992): Transport Phenomena in Different Aquifers (Investigations 1987–1992). *Steirische Beiträge zur Hydrogeologie*, **43**, 3–283. Graz.

- Attinger, R. (1988): Tracerhydrologische Untersuchungen im Alpstein. Methodik des kombinierten Tracereinsatzes für die hydrologische Grundlagenerarbeitung in einem Karstgebiet. *Geographica Bernensia*, **G 29**. Berne.
- Attinger, R., Leibundgut, Ch. (1986): Coastal Region between Argos and Astros (Peloponnesus), in *Karst Hydrogeology of the Central and Eastern Peloponnesus (Greece)*, (eds Morfis, A., Zojer, H.). *Steirische Beiträge zur Hydrogeologie*, **37/38**, 198–215. Graz.
- Auckenthaler, A., Raso, G., Huggenberger, P. (2002): Particle transport in a karst aquifer: natural and artificial tracer experiments with bacteria, bacteriophages and microspheres. *Water Science and Technology*, **46** (3), 131–138.
- Avisar, D., Clark, J.F. (2005): Evaluating Travel Times Beneath an Artificial Recharge Pond Using Sulfur Hexafluoride. *Environmental and Engineering Geoscience*, **11** (4), 309–317.
- Baertschi, P. (1976): Absolute ^{18}O content of Standard Mean Ocean Water. *Earth and Planetary Science Letters*, **31**, 341–344.
- Bailey, G., White, J.L. (1970): Factors influencing the adsorption, and movement of pesticides in soil. *Residue Reviews*, **32**, 29–92.
- Bandow, F. (1950): *Lumineszenz. Ergebnisse und Anwendung in Physik, Chemie und Biologie*. Wissenschaftliche Verlagsgesellschaft m.b.H., Stuttgart, 255 p.
- Barber, W. (1965): Pressure water in the Chad Formation of Bornu and Dikwa emirates, north-eastern Nigeria. *Geol Surv Niger Bull*, **35**, 1–138.
- Barber, W., Jones, D.C. (1965): The geology and hydrogeology of the Maiduguri, Borno Province. *Geol Surv Niger Bull*, **35**, 520–521.
- Barczewski, B., Flachowsky, J. (2003): Strategies and technologies for in-situ site assessment. In: *ConSoil 2003, Proceedings of the 8th International FZK/TNO Conference on Contaminated Soil, ICC Gent, Belgium, 12–16 May 2003*, Annokkée G.J., Arendt F., Uhlmann, O. (eds.), Forschungszentrum Karlsruhe GmbH, Karlsruhe, 3860–2863.
- Barczewski, B., Marschall, P. (1992): Development and application of lightfibre fluorometer for tracer tests. In: *Tracer Hydrology 92. Proceedings of the 6th International Symposium on Water Tracing, September 21–26 1992, Karlsruhe*, Hötzl, H., Werner, A. (eds.), 33–39. Balkema, Rotterdam.
- Bard, E., Hamlin, M., Fairbanks, R.G., Zindler, A. (1990): Calibration of the ^{14}C time scale over the past 30,000 years using mass spectrometry on corals. *Radiocarbon*, **35**, 191–199.
- Barnes, C.J., Turner, J.V. (1998): Isotopic Exchange in Soil Water. In: *Isotope Tracers in Catchment Hydrology*, Kendall, C., McDonnell, J. (eds.), 137–162. Elsevier, Amsterdam.
- Batsche, H., Bauer, F., Behrens, H., Buchtela, K., Dombrowski, H.J., Geisler, R., Geyh, M.A., Hötzl, H., Hribar, F., Küss, W., Mairhofer, J., Maurin, V., Moser, H., Neumaier, F., Schmitz, J., Schnitzer, W.A., Schreiner, A., Vogg, H., Zötl, J. (1970): Kombinierte Karstwasseruntersuchungen in Gebiet der Donauversickerung (Baden-Württemberg) in den Jahren 1967–1969. *Steirische Beiträge zur Hydrogeologie*, **22**, 5–16. Graz.
- Batsche, H., Bauer, F., Behrens, H., Buchtela, K., Hribar, F., Käss, W., Knutsson, G., Mairhofer, J., Maurin, V., Moser, H., Neumaier, F., Ostanelk, L., Rajner, W., Rauert, W., Sagl, H., Schnitzer, W.A., Zötl, J. (1967): Vergleichende Markierversuche im Mittelsteirischen Karst. *Steirische Beiträge zur Hydrogeologie*, **18/19**, 331–404. Graz.
- Bauer, S., Fulda, C., Schäfer, W. (2001): A multi-tracer study in a shallow aquifer using age dating tracers ^3H , ^{85}Kr , CFC-113 and SF_6 – indication for retarded transport of CFC-113. *Journal of Hydrology*, **248**, 14–34.
- Bauer, F. (1972): Weitere Erfahrungen beim Uraninnachweis mit Aktivkohle. *Geologisches Jahrbuch*, **C2**, 19–27. Bundesanstalt für Bodenforschung (by now BGR – Federal Institute for Geosciences and Natural Resources), Hanover.

- Bauer, F. (1969): Karsthydrologische Untersuchungen im Schneealpenstollen in den steirisch-niederösterreichischen Kalkalpen. *Steirische Beiträge zur Hydrogeologie*, **21**, 193–213. Graz.
- Bauer, F. (1967): Die Durchführung und Auswertung von Sporentriftversuchen, in Fachtagung über die Anwendung von Markierstoffen zur Verfolgung unterirdischer Wässer in Graz vom 28. März bis 1. April 1966, (eds Maurin V., Zötl J.). *Steirische Beiträge zur Hydrogeologie*, **18/19**, 249–266. Graz.
- Bäumle, R., Einsiedel, F., Hötzl, H., Käss, W., Witthüser, K. (2001): Comparative tracer studies in a highly permeable fault zone at the Lindau fractured rock test site, SW Germany. *Steirische Beiträge zur Hydrogeologie*, **52**, 136–145. Graz.
- Bazemore, D.E., Eshleman K.N., Hollenbeck, K.J. (1994): The role of soil water in stormflow generation in a forested headwater catchment: synthesis of natural tracer and hydrometric evidence. *Journal of Hydrology*, **162**, 47–75.
- Bear, J. (1972): *Dynamics of Fluids in Porous Media*. American Elsevier, New York, 764 pp.
- Bear, J. (1961): On the tensor form of dispersion in porous media. *Journal of Geophysical Research*, **66**, 1185–1197.
- Becker, M.W., Coplen, T.B. (2001): Use of deuterated water as a conservative artificial ground-water tracer. *Hydrogeology Journal*, **9**, 512–516.
- Becker, A., Sosnowski, P. (1969): Eine Impulsantwort für Flußabschnitte zur Durchflussvorherbestimmung. *Wasserwirtschaft-Wassertechnik*, **19** (12), 73–85.
- Beffa, C., Rutschmann, P., Trösch, J. (1990): Stofftransportmodelle für Fließgewässer., unpublished report (German) VAW, Swiss Federal Institute of Technology, Zurich.
- Behrens, H., Beims, U., Dieter, H., Dietze, G., Eikmann, T., Grummt, T., Hanisch, H., Henseling, H., Käss, W., Kerndorff, H., Leibundgut, Ch., Müller-Wegener, U., Rönnefahrt, I., Scharenberg, B., Schleyer, R., Schloz, W., Tilkes, F. (2001): Toxicological and ecotoxicological assessment of water tracers. *Hydrogeology Journal*, **9**, 321–325.
- Behrens, H., Benischke, R., Bricelj, M., Harum, T., Käss, W., Kosi, G., Leditzky, H.P., Leibundgut, Ch., Maloszewski, P., Maurin, V., Rajner, V., Rank, D., Reichert, B., Stadler, H., Stichler, W., Trimborn, P., Zojer, H., Zupan, M. (1992): Investigations with Natural and Artificial Tracers in the Karst System of the Lurbach System (Peggau-Tanneben-Semriach, Austria, in Transport Phenomena in Different Aquifers (Investigations 1987–1992), (ed ATH). *Steirische Beiträge zur Hydrogeologie*, **43**, 9–158. Graz.
- Behrens, H., Leibundgut, Ch. (1992): Results with Naphtionate, in Transport Phenomena in Different Aquifers (Investigations 1987–1992), (ed ATH). *Steirische Beiträge zur Hydrogeologie*, **43**, 3–283. Graz.
- Behrens, H., Demuth, N. (1992): Measurements of light into surface waters by photolysis of fluorescent dye tracers. In: *Tracer Hydrology 92. Proceedings of the 6th International Symposium on Water Tracing, September 21–26 1992, Karlsruhe*, Hötzl, H., Werner, A. (eds.), 49–56. Balkema, Rotterdam.
- Behrens, H., Demuth, N. (1990): Lichtmessung in Gewässern über die Photolyse von Fluoreszenztracern. *GSF-Jahresbericht 1989, GSF-HY 1/90*, 216–233. Munich-Neuherberg.
- Behrens, H., Leibundgut, Ch., Theodoratos, P., Vitoriu-Georgouli, A. (1986): Tracing with fluorescent tracers, in 5th international Symposium on Underground Water Tracing, Athens 1986: Karst Hydrogeology of the Central and Eastern Peloponnesus (Greece), (eds Morfis, A., Zojer, H.). *Steirische Beiträge zur Hydrogeologie*, **37**, 235–247. Graz.
- Behrens, H. (1986): Water Tracer chemistry – a Factor Determining Performance and Analytics of Tracers. In: *Proceedings of the 5th International Symposium on Underground Water Tracing, Athens, Greece*, Morfis, A., Paraskevopoulou, P. (eds.), 121–133. Institute of Geology and Mineral Exploration, Athens.

- Behrens, H., Oerter, H., Reinwarth, O. (1982): Results of tracer experiments with fluorescent dyes on Vernagtferner (Oetztal Alps, Austria) from 1974 to 1982. *Zeitschrift für Gletscherkunde und Glazialgeologie*, **18** (1), 65–83.
- Behrens, H., Teichmann, G. (1982): Neue Ergebnisse über den Lichteinfluss auf Fluoreszenztracer. In: Tracermethoden in der Hydrologie. Proceedings Internationale Fachtagung über die Anwendung von Tracermethoden in der Hydrologie, Leibundgut, Ch., Weingartner, R. (eds.), *Beiträge zur Geologie der Schweiz, Hydrologie* **28** I, 69–77. Berne.
- Behrens, H. (1982): Verfahren zum qualitativen und quantitativen Nachweis von nebeneinander vorliegenden Fluoreszenztracern. In: Tracermethoden in der Hydrologie. Proceedings Internationale Fachtagung über die Anwendung von Tracermethoden in der Hydrologie, Leibundgut, Ch., Weingartner, R. (eds.), *Beiträge zur Geologie der Schweiz, Hydrologie* **28** I, 39–50. Berne.
- Behrens, H., Hötzl, H., Maurin, V. (1981): Die Markierung mit Fluoreszenztracern, Nachweismethoden und Ergebnisse, in Hydrogeologische Untersuchungen im Karst des hinteren Muotatales (Schweiz), (eds Behrens, H., Bögli, A., Hötzl, H., Käss, W., Kraus, W., Leibundgut, Ch., Maurin, V., Moser, H., Rajner, V., Rank, D., Stichler, W., Zojer, H., Zötl, J.G.). *Steirische Beiträge zur Hydrogeologie*, **33**, 198–220. Graz.
- Behrens, H. (1981): Die Markierung mit Salzen – Lithiumchlorid, in Hydrogeologische Untersuchungen im Karst des hinteren Muotatales (Schweiz), (eds Behrens, H., Bögli, A., Hötzl, H., Käss, W., Kraus, W., Leibundgut, Ch., Maurin, V., Moser, H., Rajner, V., Rank, D., Stichler, W., Zojer, H., Zötl, J.G.). *Steirische Beiträge zur Hydrogeologie*, **33**, 220–223. Graz.
- Behrens, H. (1973): Eine Verbesserte Nachweismethode für Fluoreszenzindikatoren und ihre Anwendung zur Feststellung von Fließwegen im Grundwasser. *Zeitschrift der Deutschen Geologischen Gesellschaft*, **124**, 535–544.
- Behrens, H., Bergmann, H., Moser, H., Rauert, W., Stichler, W., Ambach, W., Eisner, H., Pessi, K. (1971): Study of the discharge of an alpine glacier by means of environmental isotopes and dye tracers. *Zeitschrift für Gletscherkunde und Glazialgeologie*, **7**, 79–102.
- Behrens, H. (1971): Untersuchungen zum quantitativen Nachweis von Fluoreszenzfarbstoffen bei ihrer Anwendung als hydrologische Markierungsstoffe. *Geologica Bavarica*, **64**, 120–121.
- Belmans, C., Wesseling J.G., Feddes, R.A. (1983): Simulation model of the water balance of a cropped soil: SWATRE. *Journal of Hydrology*, **63**, 271–286.
- Bencala, K.E. (2000): Hyporheic zone hydrological processes. *Hydrological Processes*, **14**, 2797–2798 (invited commentary).
- Bencala, K.E., McKnight, D.M., Zellweger, G.W. (1990): Characterization of transport in an acidic and metal-rich mountain stream based on a lithium tracer injection and simulations of transient storage. *Water Resources Research*, **26**, 989–1000.
- Bencala, K., Walters, R. (1983): Simulation of Solute Transport in a Mountain Pool-and-Riffle Stream: A Transient Storage Model. *Water Resources Research*, **19**, 718–724.
- Bendel, L. (1948): *Ingenieurgeologie, Vol. II*. Springer, Berlin, Heidelberg, New York.
- Benischke, R., Goldscheider, N., Smart, Ch. (2007): Tracer techniques. In: *Methods in Karst Hydrogeology* (Goldscheider, N., Drew, D. eds.), *International Contributions To Hydrogeology* Vol. 26, 147–170. Taylor & Francis, London.
- Benischke, R., Leis, A., Stadler, H. (2004): Deuterium as a reference in a multi-tracing experiment in a karst system – a comparative study. In: *International Symposium of Isotope Hydrology and Integrated Water Resources Management*, IAEA Conference & Symposium Papers, IAEA-CSP-23, p. 206. IAEA, Vienna.
- Benischke, R., Leitner, A. (1992): Fiberoptic fluorescence sensors. An advanced concept for tracer hydrology. In: *Tracer Hydrology 92. Proceedings of the 6th International Symposium on Water*

- Tracing, September 21–26 1992, Karlsruhe*, Hötzl, H., Werner, A. (eds.), 41–48. Balkema, Rotterdam.
- Benischke, R., Schmerlaib, H. (1986): Pyranin: A Fluorescent dye for Tracer Hydrology. Review of physico-chemical properties, the toxicity and applicability. In: *Proceedings of the 5th International Symposium on Underground Water Tracing, Athens, Greece*, Morfis, A., Paraskevopoulou, P. (eds.), 135–148. Institute of Geology and Mineral Exploration, Athens.
- Benischke, R., Harum, T. (1984): Computergesteuerte Abflussmessung in offenen Gerinnen nach der Tracerverdünnungsmethode (Integrationsverfahren). *Steirische Beiträge zur Hydrogeologie*, **36**, 127–127. Graz.
- Benischke, R., Hötzl, H., Leditzky, H.P., Maurin, V., Ramsbacher, P., Zojer, H., Zötl, J.G. (1980): Der Einsatz von Triftstoffen, in *Karsthydrologische Untersuchungen mit natürlichen und künstlichen Tracern im Neuenburger Jura (Schweiz)*, (eds Müller, I., Zötl, J.G.). *Steirische Beiträge zur Hydrogeologie*, **32**, 81–86. Graz.
- Benson, C.F., Bowman, R.S. (1994): Tri- and Tetrafluorobenzoates as Nonreactive Tracers in Soil and Groundwater. *Soil Science Society of America Journal*, **58**, 1123–1129.
- Bergström, S. (2001): *The HBV model – Its structure and applications*. SMHI Rep. RH. 4, Swedish Meteorol. Hydrol. Inst., Norrköping.
- Beyerle, U., Aeschbach-Hertig, W., Hofer, M., Imboden, D.M., Baur, H. & Kipfer, R. (1999): Infiltration of river water to a shallow aquifer investigated with $^3\text{H}/^3\text{He}$, noble gases and CFCs. *Journal of Hydrology*, **220**, 169–185.
- Binley, A., Cassiani, G., Middleton, R., Winship, P. (2002): Vadose zone flow model parameterisation using cross-borehole radar and resistivity imaging. *Journal of Hydrology*, **267**, 147–159.
- Birks, S., Gibson, J., Gourcy, L., Aggarwal, P. (2002): Maps and animations offer new opportunities for studying the global water cycle, *Eos Transactions, American Geophysical Union Electronic Supplement.*, **83** (37), available at http://www.agu.org/eos_elec/020082e.html (accessed 21 April 2009).
- Bloss, S., Euler, G., Engel, H., Grubert, G., Hanisch, H., Krahé, P., Pfaud, A., Teuber, W., Wegner (1987): Eignung und Anwendung von Vorhersagemodellen für einen “Warn- und Alarmplan Rhein”. Bericht des DWVK-Arbeitskreises “Warn- und Alarmplan Rhein”, report (German), DVWK, Koblenz.
- Boehrer, B., Matzinger, A., Schimmele, M. (2000): Similarities and differences in the annual temperature cycles of East German mining lakes. *Limnologia*, **30**, 271–279.
- Bögli, A., Leibundgut, Ch., Zojer, H. (1981): Die Markierung mit Salzen – Natriumchloride, in *Hydrogeologische Untersuchungen im Karst des hinteren Muotatales (Schweiz)*, (eds Behrens, H., Bögli, A., Hötzl, H., Käss, W., Kraus, W., Leibundgut, Ch., Maurin, V., Moser, H., Rajner, V., Rank, D., Stichler, W., Zojer, H., Zötl, J.G.). *Steirische Beiträge zur Hydrogeologie*, **33**, 223–225. Graz.
- Bögli, A., Harum, T. (1981): Hydrogeologische Untersuchungen im Karst des hinteren Muotatales (CH). *Steirische Beiträge zur Hydrogeologie*, **33**, 125–264. Graz.
- Bögli, A. (1980): *Karst hydrology and physical speleology*. Springer, Berlin Heidelberg New York.
- Bogner, C., Wolf, B., Schlather, M., Huwe, B. (2008): Analysing flow patterns from dye tracer experiments in a forest soil using extreme value statistics. *European Journal of Soil Science*, **59**, 103–113. DOI: 10.1111/j.1365-2389.2007.00974.x
- Bonell, M., Barnes, D.J., Grant, C.R., Howard, A., Burns, J. (1998): High Rainfall, Response-Dominated catchments: A comparative study in tropical northeast Queensland with temperate New Zealand. In: *Isotope Tracers in Catchment Hydrology* (Kendall, C., McDonnell, J.J., eds.), 347–390. Elsevier, Amsterdam.

- Bouma, J., Dekker, L.W. (1978): A case study on infiltration into a dry clay soil: 1. Morphological observations. *Geoderma*, **20**, 27–40.
- Bowen, J., Wilkinson, B. (2002): Spatial distribution of ^{18}O in meteoric precipitation. *Geology*, **30**, 315–318.
- Bowman, R.S., Gibbens, J.F. (1992): Difluorobenzoates as Nonreactive tracers in Soil and Ground Water. *Ground Water*, **30** (1), 8–14.
- Bowman, R.S. (1984a): Evaluation of Some New Tracers for Soil Water Studies. *Soil Science Society of America Journal*, **48**, 987–993.
- Bowman, R.S. (1984b): Analysis of soil extracts for inorganic and organic tracer anions via high performance liquid chromatography. *Journal of Chromatography*, **285**, 467–477.
- Brandi-Dohrn, F.M., Dick, R.P., Hess, M., Selker, J.S. (1996): Field evaluation of passive capillary samplers. *Soil Science Society of America Journal*, **60**, 1705–1713.
- Brandi-Dohrn, F.M., Leibundgut, Ch., Dick, R.P., Selkers, J.S. (1995): Collecting tracers in the vadose zone In: Tracer technologies for Hydrological Systems (Leibundgut, Ch., ed.). *IAHS Publication*, **229**, 173–181.
- Bredenkamp, D.B., Botha, L.J., Van Tonder, G.J., Van Rensburg, H.J. (1995): *Manual on quantitative estimation of groundwater recharge and aquifer storativity*. Water Research Commission, Pretoria, 326 p.
- Bremicker, M. (1989): Verfahren zur Analyse und Simulation der Stoffausbreitung in Fließgewässern. Diplom thesis, Institute of Physical Geography, Chair in Hydrology, University of Freiburg.
- Bricelj, M., Sisko, M. (1992): Inactivation of phage tracers by exposure to liquid-air interfaces. In: *Tracer Hydrology 92. Proceedings of the 6th International Symposium on Water Tracing, September 21–26 1992*, Karlsruhe, Hötzel, H., Werner, A. (eds.), 71–75. Balkema, Rotterdam.
- Brodersen, Ch., Pohl, S., Lindenlaub, M., Leibundgut, Ch., von Wilpert, K. (2000): Influence of vegetation structure on isotope content of throughfall and soil water. *Hydrological Processes*, **14**, 1439–1448.
- Broer, G., Wijnstock, N. (1990): Determination of Rhodamine WT by HPCL, unpublished report, Ministry of Transport and Public Works, Lelystad.
- Brooks, R.H., Corey, A.T. (1964): Hydraulic properties of porous media. Hydrol. Paper 3, Colorado State University, Fort Collins, Colorado, USA.
- Brown, G.H., Fuge, R. (1998): Trace element chemistry of glacial meltwaters in an Alpine headwater catchment. *IAHS Publication*, **248**, 435–442.
- Brown, M.C., Ford, D.C. (1973): Caves and groundwater patterns in a tropical karst environment: Jamaica, West Indies. *American Journal of Science*, **273**, 622–633.
- Brumley, W.C., Farley, J.W. (2003): Determining Eosine as a groundwater migration tracer by capillary electrophoresis/laser-induced fluorescence using a multiwavelength laser. *Electrophoresis*, **24**, 2335–2339.
- Brüschweiler, B. (2007): Markierstoffe im Bereich von Trinkwasserfassungen. *Gas, Wasser, Abwasser*, **87** (5), 355–359.
- Buchanan, T.J., Somers, W.P. (1969): Discharge measurements at gauging stations. *Techniques of Water-Resources Investigations of the United States Geological Survey*, Book 3, Chapter A8. U.S. Geological Survey, Denver.
- Brugman, M.M. (1986): Water flow at the base of a surging glacier. Dissertation, California Institute of Technology, Pasadena, 267 p.
- Burnett, W.C., Dulaiova, H. (2003): Estimating the dynamics of groundwater input into the coastal zone via continuous radon-222 measurements. *Journal of Environmental Radioactivity*, **69** (1–2), 21–35.

- Burns, D.A. (2002): Stormflow-hydrograph separation based on isotopes: the thrill is gone – what's next? *Hydrological Processes*, **16**, 1515–1517.
- Busenberg, E., Plummer, L.N. (2000): Dating young groundwater with sulfur hexafluoride: Natural and anthropogenic sources of sulfur hexafluoride. *Water Resources Research*, **36** (10), 3011–3030.
- Busenberg, E., Plummer, L.N. (1992): Use of chlorofluoro methanes (CCl₃F and CCl₂F₂) as hydrological tracers and age-dating tools: Example – The alluvium and terrace system of Central Oklahoma. *Water Resources Research*, **28**, 2257–2283.
- Buttle, J.M. (1998): Fundamentals of Small Catchment Hydrology. In: *Isotope Tracers in Hydrology* (Kendall, C., McDonnell, J.J., eds.), 1–43. Elsevier, Amsterdam.
- Buttle, J.M., Peters, D.L. (1997): Inferring hydrological processes in a temperate basin using isotopic and geochemical hydrograph separation: a re-evaluation. *Hydrological Processes*, **11** (6), 557–573.
- Buttle, J.M. (1994): Isotope hydrograph separations and rapid delivery of pre-event water from drainage basins. *Progress in Physical Geography*, **18**, 16–41.
- Calder, I.R. (1992): Deuterium tracing for the estimation of transpiration from trees Part 2 Estimation of transpiration rates and transpiration parameters using a time-averaged deuterium tracing method. *Journal of Hydrology*, **130**, 27–35.
- Calder, I.R., Narayanswamy, M.N., Srinivasalu, N.V., Darling, W.G., Lardner, A.J. (1986): Investigation into the use of deuterium as a tracer for measuring transpiration of eucalypts. *Journal of Hydrology*, **84**, 345–351.
- Caldiga, C.U., Greibrokk, T. (1998): Ultra-trace determination of fluorinated aromatic carboxylic acids in aqueous reservoir fluids using solid-phase extraction in combination with gas chromatography-mass spectrometry. *Journal of Chromatography*, **793**, 297–306.
- Cameron, D.R., Klute, A. (1977): Convective-dispersive solute transport with a combined equilibrium and kinetic adsorption model. *Water Resources Research*, **13**, 183–189.
- Campana, M.E., Harrington, G.A., Tezcan, L. (2001): Compartmental model approaches to groundwater flow simulation, in *Environmental isotopes in the hydrological cycle, Principles and application, Vol. 6 Modelling*, (ed W.G. Mook), IHP-V, Technical Documents in Hydrology 39, Vol. 6, 39–74, UNESCO, Paris.
- Campana, M.E. (1987): Generation of ground-water age distributions. *Ground Water*, **25**, 51–58.
- Campana, M.E., Mahin, D.A. (1985): Model-derived estimates of groundwater mean ages, recharge rates, effective porosities and storage in a limestone aquifer. *Journal of Hydrology*, **76**, 247–264.
- Campana, M.E., Simpson, E.S. (1984): Groundwater residence times and recharge rates using a discrete state compartment model and C-14 data. *Journal of Hydrology*, **72**, 171–185.
- Campana, M.E. (1975): Finite-state models of transport phenomena in hydrologic systems. Dissertation, University of Arizona, Tucson, 252 p.
- Capel, P., Giger, W., Reichert, P., Wanner, O. (1988): Accidental input of pesticides into the Rhine River. *Environmental Science & Technology*, **22**, 992–996.
- Carnahan, C.L., Remer, J.S. (1984): Nonequilibrium and equilibrium sorption with a linear sorption isotherm during mass transport through an infinite porous medium: Some analytical solutions. *Journal of Hydrology*, **73**, 227–258.
- Carpenter, J.H. (1968): *Tracer for circulation and mixing in natural waters*. Turner, Palo Alto.
- Carter, R.C., Kaufman, W.J., Orlob, G.T., Todd, D.K. (1959): Helium as a ground-water tracer. *Journal of Geophysical Research*, **64**, 2433–2439.
- Cencur Curk, B., Bricelj, M., Stichler, W. (2006): Experimental Study of Flow and Solute Transport in the Unsaturated Zone of Karst Rock in Slovenia. *Geophysical Research Abstracts*, **8**, 06920. SRef-ID: 1607-7962/gra/EGU06-A-06920.

- Choi, J.J., Harvey, W., Conklin, M.H. (2000): Characterizing multiple timescales of stream and storage zone interaction that affect solute fate and transport in streams. *Water Resources Research*, **36**, 1511–1518.
- Chrysikopoulos, C.V. (1993): Artificial tracers for geothermal reservoir studies. *Environmental Geology*, **22**, 60–70.
- Cirpka, O.A., Kitanidis, P.K. (2001): Transport of volatile compounds in porous media in the presence of a trapped gas phase. *Journal of Contaminant Hydrology*, **49**, 263–285.
- Clark, I., Fritz, P. (1997): *Environmental Isotopes in Hydrogeology*. Lewis Publishers, Boca Raton, New York.
- Clark, J., Schlosser, P., Stute, M., Simpson, J. (1996): SF₆ – ³He Tracer Release Experiment: A New Method of Determining Longitudinal Dispersion Coefficients in Large Rivers. *Environmental Science and Technology*, **30**, 1527–15332.
- Coats, K., Smith, B. (1964): Dead-end pore volume and dispersion in porous media. *Society of Petroleum Engineers Journal*, **4**, 73–84.
- Collins, D. N., (1982): Flow-routing of meltwater in an alpine glacier as indicated by dye tracer tests. *Beiträge zur Geologie der Schweiz – Hydrologie*, **28** (II): 523–534. Berne.
- Collins, D.N., (1979a): Hydrochemistry of meltwaters draining from an Alpine Glacier. *Arctic and Alpine Research*, **11** (3), 307–324.
- Collins, D.N. (1979b): Qualitative determination of the subglacial hydrology of two alpine glaciers. *Journal of Glaciology*, **23** (81), 347–362.
- Collins D.N. (1977): Hydrology of an alpine glacier as indicated by the chemical composition of meltwater. *Zeitschrift für Gletscherkunde und Glaziologie*, **12** (1–2), 219–238.
- Constantz, J., Stewart, A.E., Niswonger, R., Sarma, L. (2002): Analysis of temperature profiles for investigating stream losses beneath ephemeral channels. *Water Resources Research*, **38** (12). DOI: 10.1029/2001WR001221.
- Constantz, J. (1998): Interaction between stream temperature, streamflow, and groundwater exchanges in alpine streams. *Water Resources Research*, **34** (7), 1609–1615.
- Constantz, J., and Thomas, C. L. (1997), Streambed temperature profiles as indicators of percolation characteristics beneath arroyos in the Middle Rio Grande Basin, USA, *Hydrological Processes*, **11** (12), 1621–1634.
- Cook, P.G., Wood, C., White, T., Simmons, C.T., Fass, T., Brunner, P. (2008): Groundwater inflow to a shallow, poorly-mixed wetland estimated from a mass balance of radon. *Journal of Hydrology*, **354** (1–4), 213–226.
- Cook, P.G., Herczeg, A.L. (2000): *Environmental Tracers in Subsurface Hydrology*. Kluwer Academic Publishers, Boston, Dordrecht, London, 529 p.
- Cook, P.G., Solomon, D.K. (1997): Recent advances in dating young groundwater: chlorofluorocarbons, ³H/³He and ⁸⁵Kr. *Journal of Hydrology*, **191**, 245–265.
- Corey, J.C. (1968): Evaluation of dyes for tracing water movement in acid soils. *Soil Science*, **106** (3), 182–187.
- Costin, D., Davis, P., Gerald, R. and Katz, B. (1963): Dye diffusion experiments in the New York Bight. Technical Report Lamont, Geol. Obs. No Cu-2-63 to AEC.
- Couture, R.A., Seitz, M.G. (1983): Sorption of anions of iodine by iron oxides and kaolinite. *Nuclear and Chemical Waste Management*, **4** (4), 301–306.
- Craig, H., Hom, B. (1968): Relationship between deuterium, oxygen-18 and chlorinity in the formation of sea ice. *Eos Transactions, American Geophysical Union*, **49**, 216–217.
- Craig, H., Gordon, L.I. (1965): Deuterium and Oxygen-18 variations in the Ocean and the Marine Atmosphere. *Proceedings of Isotopes in Oceanographic Studies and Paleotemperatures, Spoleto, Italy*, (ed E. Tongioli). Sischi and Figli, Pisa, pp. 161–182.

- Craig, H., Gordon, L.I., Horibe, Y. (1963): Isotopic exchange effects in the evaporation of water, 1. low – temperature experimental results. *Journal of Geophysical Research*, **68**, 5079–87.
- Craig, H. (1961): Isotopic variations in meteoric waters. *Science*, **133**, 1702–1703.
- Criss, R., Davisson, L., Surbeck, H. and Winston, W. (2007): Isotopic methods, in *Methods in Karst Hydrogeology* (eds N. Goldscheider and D. Drew.), International Contributions to Hydrogeology Vol. 26. Taylor & Francis, London, pp. 123–45).
- Cui, Y.F. (1997): Different approaches towards an understanding of runoff generation. *Freiburger Schriften zur Hydrologie*, **7**, 164 pp. Freiburg.
- Cui, Y.F., Demuth, S., Leibundgut, Ch. (1995): Runoff separation using tracer. In: *Solutions '95. Proceedings of the XXVI Congress of the International Association of Hydrogeologists, June 4–10, Edmonton, Alberta, Canada*.
- Cunnold, D.M., Weiss, R.F., Prinn, R.G., Hartley, P.G., Simmonds, P.G., Fraser, P.J., Miller, B., Alyea, F.N., Porter, L. (1997): GAGE/AGAGE measurements indicating reductions in global emissions of CCl₃F and CCl₂F₂ in 1992–1994. *Journal of Geophysical Research*, **102**, 1259–1269.
- Dahan, O., Ronen, Z. (2001): Analytical Procedure for Simultaneous Use of Seven Fluorobenzoates in Multitracer Tests. *Ground Water*, **39** (3), 366–370.
- Dansgaard, W. (2004): *Frozen Annals – Greenland Ice Sheet Research*. The Niels Bohr Institute, University of Copenhagen, Denmark, 122 p.
- Dansgaard, W. (1964): Stable isotopes in precipitation. *Tellus*, **16** (4), 436–468.
- Dansgaard, W. (1961): *The isotopic Composition of natural waters: with special reference to the Greenland Ice Cap*. Lunos, Copenhagen, 120 p.
- Dassargues, A. (ed.) (2000): Tracers and Modelling in Hydrogeology. *IAHS Publication*, **262**, 572 p.
- Davis, S.N., Campbell, D.J., Bentley, H.W., Flynn, T.J. (1985): *Ground Water Tracers*. National Water Well Association, Worthington, Ohio, 200 p.
- Dawson, T.E., Ehleringer, J.R. (1998): Plants, Isotopes and Water Use: a Catchment-Scale Perspective. In: *Isotope Tracers in Catchment Hydrology* (Kendall, C., McDonnell, J.J., eds.), 165–194. Elsevier, Amsterdam.
- De Carvalho-Dill, A., Gerlinger, K., Hahn, T., Hötzl, H., Käss, W., Leibundgut, Ch., Maloszewski, P., Müller, I., Oetzel, S., Rank, D., Teutsch, G., Werner, A. (1992): Porous Aquifer – Test Site Merdingen (Germany) in Transport Phenomena in Different Aquifers (Investigations 1987–1992), (ed ATH). *Steirische Beiträge zur Hydrogeologie*, **43**, 251–282. Graz.
- Dechant, M., Hacker, P. (1986): Neue Entwicklungen in der Methode des Sporennachweises. In: *Proceedings of the 5th International Symposium on Underground Water Tracing, Athens, Greece*, Morfis, A., Paraskevopoulou, P. (eds.), 149–155. Institute of Geology and Mineral Exploration, Athens.
- Dechant, M. (1967): Die Färbung der Lycopodiumsporen, in Fachtagung über die Anwendung von Markierungsstoffen zur Verfolgung unterirdischer Wässer in Graz vom 28. März bis 1. April 1966. Specialists' Conference on the Tracing of Subterranean Waters in Graz, March 28–April 1, 1966, (Maurin, V., Zötl, J., eds). *Steirische Beiträge zur Hydrogeologie*, **18/19**, 241–247. Graz.
- Deeks, L.K., Bengough, A.G., Stutter, M.I., Young, I.M., Zhang, X.X. (2008): Characterisation of flow paths and saturated conductivity in a soil block in relation to chloride breakthrough. *Journal of Hydrology*, **348**, 431–441.
- Dent, M.C., Lynch, S.D., Schulze, R.E. (1989): Mapping Mean Annual and other Rainfall Statistics over Southern Africa. Department of Agricultural Engineering, University of Natal. WRC-ACRU Report 109/1/89, **27**. Water Research Commission, Pretoria.

- Derby, N.E., Knighton, R.E. (2001): Vadose Zone Processes and Chemical Transport. Field-Scale Preferential Transport of Water and Chloride Tracer by Depression-Focused Recharge. *Journal of Environmental Quality*, **30**, 194–199.
- Dervey, A. (1985): Beitrag zum Sorptionsverhalten von Fluoreszenztracern. *Publikation Gewässerkunde*, **63**. Diplom thesis, Institute of Geography, University of Berne, 80 p.
- De Smedt, F., Wauters, F., Sevilla, J. (1986): Study of tracer movement through unsaturated sand. *Journal of Hydrology*, **85**, 169–181.
- De Smedt, F., Wierenga, P.J. (1979): A generalised solution for solute flow in soils with mobile and immobile water. *Water Resources Research*, **15**, 1137–1141.
- DeWalle, D., Edwards, P., Swistock, B., Aravena, R., Drimmie, R. (1997): Seasonal isotope hydrology of three Appalachian forest catchments. *Hydrological Processes*, **11**, 1895–1906.
- Didzun, J., Uhlenbrook, S. (2008): Scaling of dominant runoff generation processes: Nested catchments approach using multiple tracers. *Water Resources Research*, **44**, W02410, doi:10.1029/2006WR005242.
- Didszun, J. (2004): Experimentelle Untersuchungen zur Skalenabhängigkeit der Abflussbildung. *Freiburger Schriften zur Hydrologie*, **19**, 221 p. Freiburg.
- Didszun, J. (2000): Abflussbildung an Hängen. Diplom thesis, Institute of Hydrology, University of Freiburg.
- Dienert, F. (1913): Remarques au sujet des expériences avec la fluoréscence. *CR Acad Sci* **157**, 660–661.
- Dinçer, T., al-Mugrin, A., Zimmermann, U. (1974): Study of the infiltration and recharge through sand dunes in arid zones with special reference to the stable isotopes and thermonuclear tritium. *Journal of Hydrology*, **23**, 259–274.
- Dinçer, T., Payne, B.R., Florkowski, T., Martinec, J., Tongiorgi, E. (1970): Snowmelt runoff from measurements of tritium and oxygen-18. *Water Resources Research*, **6**, 110–124.
- Divine, C.E., Sanford, W.E., McCray, J.E. (2003): Helium and Neon Groundwater Tracers to Measure Residual DNAPL: Laboratory Investigation. *Vadose Zone Journal*, **2**, 382–388.
- Dody, A., Adar, E.M., Yakirevich, A., Geyh, M.A., Yair, A. (1995): Evaluation of depression storage in an arid rocky basin using stable isotopes of oxygen and hydrogen. *IAHS Publication*, **232**, 417–427.
- Dounas, A., Kallergis, C., Morfis, A., Pagounis, M., Zojer, H. (1982): Die Ergebnisse eines Markierversuch im östlichen Kopais Becken Griechenland. *Beiträge zur Geologie der Schweiz, Hydrologie* **28 I**, 161–168. Berne.
- Doussan, C., Toma, A., Paris, B., Poitevin, G., Ledoux, E., Detay, M. (1994): Coupled use of thermal and hydraulic head data to characterize river-groundwater exchanges. *Journal of Hydrology*, **153** (1–4), 215–229.
- Drew, D.I., Smith, D.I. (1969): Techniques for the tracing of subterranean drainage. *British Geomorphological Research Group Technical Bulletin*, **2**, 1–36.
- Drew, B.P. (1968): A review of the available methods for tracing underground waters. *Proceedings of the British Speleologic Association*, **6**, 1–19.
- Droogers, P., Stein, A., Bouma, J., de Boer, G. (1998): Parameters for describing soil macroporosity derived from staining patterns. *Geoderma*, **83**, 293–308.
- Drost, W., Hoehn, E. (1989): Macrodispersivity in Granular Aquifers Determined with Single-well Techniques Using ^{82}Br as a Tracer. *Radiochimica Acta*, **47**, 13–20.
- Drost, W. (1983): Single well technique. In: Tracer Methods in Isotope Hydrology, IAEA-TECDOC-291, 7–16. IAEA, Vienna.
- Drost, W., Neumaier, F. (1974): Application of single borehole methods in groundwater research. *Isotope Techniques in Groundwater Hydrology 1974*, **2**, IAEA-STI/PUB/373, IAEA, Vienna, 241–254.

- Drost, W., Klotz, D., Koch, A. (1968): Point dilution methods of investigation groundwater flow by means of radioisotopes. *Water Resources Research*, **4** (1), 125–146
- Dunn, B. (1968): Nomographs for determining amount of Rhodamine B dye for time-of-travel studies. In: Selected techniques in water resources investigations 1966–67. *U.S. Geological Survey Water-Supply Paper* **1892**, 9–14.
- Durka, W., Schulze, E.-D., Gebauer, G., Voerkelius, S. (1994): Effects of forest decline on uptake and leaching of deposited nitrate determined from ^{15}N and ^{18}O measurements. *Nature*, **372** (6508), 765–767.
- Dyck, S., Peschke, G. (1995): *Grundlagen der Hydrologie*. 3rd Edition, Verlag für Bauwesen, Berlin, 536 p.
- Edmunds, W.M., Fellman, E., Goni, I.B., McNeill, G., Harkness, D.D. (1998): Groundwater, palaeoclimate and palaeorecharge in the southwest Chad Basin, Borno state, Nigeria. In: *International Symposium on isotope techniques in the study of past and current environmental changes in the hydrosphere and the atmosphere*. Vienna, 14–18 April 1997, IAEA-SM-349. IAEA, Vienna, pp. 693–797.
- Edmunds, W.M., Fellman, E., Goni, I.B. (1999): Lakes, groundwater and palaeohydrology in the Sahel of NE Nigeria: evidence from hydrogeochemistry. *Journal of the Geological Society*, **156**, 345–355.
- Ehnes, T. (2006): Der Einfluss der Schneeschmelze auf die Abflussbildung und die Grundwasserneubildung im Einzugsgebiet der Dreisam. Diplom thesis, Institute of Hydrology, University of Freiburg.
- Eichinger, L., Merkel, B., Nemeth, G., Salvamoser, J., Stichler, W. (1984): Seepage and velocity determinations in unsaturated quaternary gravel. In: *Recent investigations in the Zone of Acretion*, *Proc. Munich*, Oct. 1984, 303–313.
- Einsiedl, F. (2005): Flow system dynamics and water storage of a fissured-porous karst aquifer characterized by artificial and environmental tracers. *Journal of Hydrology*, **312** (1–4), 312–321.
- Einsiedl, F., Maloszewski, P. (2005): Tracer tests in fractured rocks with a new fluorescent dye-pyrene-1,3,6,8-tetra sulphonic acid (PTS). *Hydrological Sciences Journal*, **50**, 543–554.
- Einsiedl, F., Maloszewski, P., Stichler, W. (2005): Estimation of denitrification potential in a karst spring using the isotopes of ^{15}N and ^{18}O . *Biogeochemistry*, **72** (1), 67–86.
- Eisele, M., Leibundgut, Ch. (2002): Modelling nitrogen dynamics for a mesoscale catchment using a minimum information requirement (MIR) concept. *Hydrological Sciences Journal*, **47** (5), 753–768.
- Eisenbrand, J. (1966): *Fluorometrie. Eine Anleitung zu quantitativen, fluorometrischen und spektrofluorimetrischen Messungen*. Wissenschaftliche Verlagsgesellschaft, Stuttgart, 155 p.
- Eissele, K. (1963): Zur Deutung und Auswertung von Salzversuchen. *Gas und Wasserfach (Wasser und Abwasser)*, **104** (49), 1158–1160.
- Engblom, J.N., Sanford, W.E., Stednick, J.D. (2004): Tracing the Hydrologic Connection between Turquoise Lake and Local Mine Dewatering Tunnels with Dissolved Sulphur Hexafluoride. In: *Hydrology Days 2004, Proceedings of the 24th American Geophysical Union Annual Hydrology Days, March 10–12 2004, Fort Collins, Colorado*, J.A. Ramirez (ed.), 84–94. American Geophysical Union, Washington.
- Engel, H., Menzel, T., Wander, K. (1988): Fliesszeiten im Rhein aus Wasserspiegelberechnungen, unpublished report (German), German Federal Institute of Hydrology (BfG), Koblenz.
- Englert, A. (2003): Measurement, Estimation and Modelling of Groundwater Flow Velocity at Krauthausen Test Site. Dissertation, RWTH Aachen University.
- Eriksson, E., Khunakasem, V. (1969): Chloride concentration in groundwater, recharge rate and rate of deposition of chloride in the Israel Coastal Plain. *Journal of Hydrology*, **7**, 178–197.

- Environment Canada (1993): *Effluent dispersion in the Fraser River from the Glenbrook combined Sewer Overflow at New Westminster, BC*, report Environment Canada, North Vancouver.
- Feddes, R.A., Kabat, P., van Bakel, P.J.T., Bronswijk, J.J.B., Halbertsma, J. (1988): Modelling soil water dynamics in the unsaturated zone – State of the art. *Journal of Hydrology*, **100**, 69–111.
- Feddes, R.A., Kowalik, P.J. and Zaradny, H., 1978. *Simulation of field water use and crop yield*. John Wiley & Sons, New York, 189 p.
- FEFLOW: Finite Element Subsurface Flow & Transport Simulation System. WASY Institute for Water Resources Planning and Systems research Ltd., Berlin.
- Fette, M., Kipfer, R., Schubert, C.J., Hoehn, E., Wehrli, B. (2005): Assessing river–groundwater exchange in the regulated Rhone River (Switzerland) using stable isotopes and geochemical tracers. *Applied Geochemistry*, **20** (4), 701–712.
- Feuerstein, D.L., Selleck, R.E. (1963): Fluorescent tracers for dispersion measurements. *Journal of the Sanitary Engineering Division of the American Society of Civil Engineers*, **89**, 1–21.
- Feyen, H., Wunderli, H., Wydler, H., Papritz, A. (1999): A tracer experiment to study flow paths of water in a forest soil. *Journal of Hydrology*, **225**, 155–167.
- Field, M.S. (2003): A review of some tracer-test design equations for tracer-mass estimation and sample-collection frequency. *Environmental Geology*, **43**, 867–881.
- Figuera-Johnson, M.A., Tindall, J.A., Friedel, M. (2007): A Comparison of ^{18}O Composition of Water Extracted from Suction Lysimeters, Centrifugation, and Azeotropic Distillation. *Water Air and Soil Pollution*, **184**, 63–75. doi 10.1007/s11270-007-9399-8.
- Fischer, M. (1982): Abflussmessungen mit Tracern nach dem Verdünnungsverfahren. *Beiträge zur Geologie der Schweiz, Hydrologie* **28** (II), 447–458. Berne.
- Flachowsky, J., Batereau, K., Klaas, N., Müller, M. and B. Barczewski (2005): Aktuelle Ergebnisse und Entwicklungen beim Einsatz von Vor-Ort-Analytik. In: *Ressource Untergrund. 10 Jahre VEGAS: Forschung und Technologieentwicklung zum Schutz von Grundwasser und Boden (28–29 September 2005, Universität Stuttgart)*, Braun, J., Koschitzky, H.P., Müller, M. (eds.), 182–194. Institute of Hydraulic Engineering, University of Stuttgart in cooperation with UFZ-Helmholtz Center for Environmental Research, Leipzig.
- Florkowski, T. (1991): Tritium in river flow-rate gauging – theory and experience. In: *Use of artificial tracers in hydrology, IAEA-TECDOC-601*, 35–44. IAEA, Vienna.
- Flury, M., Wai, N.N. (2003): Dyes as tracers for vadose zone hydrology. *Reviews of Geophysics*, **41** (1). 1002. doi:10.1029/2001RG000109.
- Flury, M., Flühler, H. (1995): Tracer Characteristics of Brilliant Blue FCF. *Soil Science Society of America Journal*, **59**, 22–27.
- Flury, M., Flühler, H. (1994): Brilliant blue FCF as a dye tracer for solute transport studies – a toxicological overview. *Journal of Environmental Quality*, **23**, 1108–1112.
- Flury, M., Flühler, H., Jury, W.A., Leuenberger, J. (1994): Susceptibility of soils to preferential flow of water: a field study. *Water Resources Research*, **30** (7), 1945–1954.
- Flynn, R.M., Hacini, Y., Schnegg, P.A., Costa, R., Diomande, K.A. (2006): Use of Tracer Tests and Geophysical Logging to Understand Solute and Microorganism Tracer Responses in Monitoring Wells with Long Screen Intervals in a Gravel Aquifer. *Beiträge zur Hydrogeologie*, **55**, 5–20. Graz.
- Flynn, R.M., Schnegg, P.A., Costa, R., Mallen, G., Zwahlen, F. (2005): Identification of zones of preferential groundwater tracer transport using a mobile downhole fluorometer. *Hydrogeology Journal*, **13** (2), 366–377.
- Fontes, J.Ch., Andrews, J.N., Edmunds, W.M., Guerre, A., Travi, Y. (1991): Palaeorecharge by the Niger River (Mali) deduced from groundwater geochemistry. *Water Resources Research*, **27**, 199–214.

- Fontes, J.Ch., Coque, R., Dever, L., Filly, A., Mamou, A. (1983): Paleohydrologie isotopique de l'Oued el Akarit (sud tunise) au Pleistocene superieur et a l'Holocene. *Palaeogeography, Palaeoclimatology, Palaeoecology*, **43** (1–2), 41–62.
- Fontes, J.Ch., Garnier, J.M. (1979): Determination of the initial ^{14}C activity of total dissolved carbon: A review of existing models and a new approach. *Water Resources Research*, **15**, 399–413.
- Forrer, I., Papritz, A., Kasteel, R., Flühler, H., Luca, D. (2000): Quantifying dye tracers in soil profiles by image processing. *European Journal of Soil Sciences*, **51**, 313–322.
- Förster, T. (1982): *Fluoreszenz organischer Verbindungen*. Reprint of 1st edition (1952), 315 p. Vandenhoeck and Ruprecht, Göttingen.
- Forster, M., Moser, H., Loosli, H.H. (1984): Isotope hydrological study with carbon-14 and argon-39 in the Bunter Sandstones of the Saar Region. In: *Isotope Hydrology 1983*, IAEA-STI/PUB/650, 515–533. IAEA, Vienna.
- Forster, M. (1983): C-14- und Ar-39-Gehalte in einem Grundwasserleiter des Saarlandes: Vergleich zweier Grundwasserdatierungsmethoden. Dissertation, Faculty of Physics, University of Munich.
- Foster, J. (ed.) (2000): *Tracers in Geomorphology*. John Wiley & Sons Ltd, Chichester, 560 p.
- Fountain, A.G., Walder, J.S. (1998): Water Flow Through Temperate Glaciers. *Reviews of Geophysics*, **36** (3), 299–328.
- Franke, C., Westerholm, H., Niessner, R. (1997): Solid-Phase extraction (SPE) of the fluorescent tracers Uranine and Sulphorhodamine B. *Water Resources Research*, **31** (10), 2633–2637.
- Frederickson, G.C., Criss, R.E. (1999): Isotope hydrology and residence times of the unimpounded Meramec River basin, Missouri. *Chemical Geology*, **157**, 303–317.
- Fried, J.J., Combarnous, M.A. (1971): Dispersion in porous media. In: *Advances in Hydrosciences*, Chow, V.T. (ed.), **7**, 169–282. Academic Press, New York.
- Fritz, P., Fontes, J.Ch. (eds.) (1986): *Handbook of Environmental Isotope Geochemistry*. Elsevier, Amsterdam.
- Früngel, F. (1989): In-situ-Fluorometrie. Anwendung in der geophysikalischen und biologischen Gewässerkunde. *Die Geowissenschaften*, **7** (7), 196–202.
- Früngel, F., Koch, C. (1974): Practical experience with the Variosens equipment in measuring chlorophyll concentrations and fluorescent tracer substances, like rhodamine, fluorescein and some new substances. *Oceans*, **6**, 241–247.
- Früngel, F. (1972): The VARIOSENS, a new in situ instrumentation for the fluorescent tracer technology and sand-caused turbidity. In: *Environment '73 Conference*, Total Concept Exhibitions Pty., Balgowlah.
- Gamlin, J.D., Clark, J.F., Woodside, G., Herndorn, R. (2001): Large-Scale Tracing of Ground Water with Sulfur Hexafluoride. *Journal of Environmental Engineering*, February, **127** (2), 171–174.
- Garcia Gutiérrez, M.G., Guimerà, J., Illera de Llano, A., Benitez, A.H., Humm, J., Saltino, M. (1997): Tracer Test at El Berocal Site. *Journal of Contaminant Hydrology*, **26**, 179–188.
- Gaspar, E. (ed.) (1987): *Modern trends in tracer hydrology*, Vol. 2. CRC Press, Boca Raton, 137 p.
- Gaspar, E., Onescu, M. (1972): *Radioactive Tracers in Hydrology, Developments in Hydrology I*. Elsevier, Amsterdam, London, New York, 342 p.
- Gat, J., Mook, W., Meijer H. (2000): *Environmental isotopes in the hydrological cycle, Principles and Application, Vol. 2 Atmospheric Water*, (ed W.G. Mook), IHP-V, Technical Documents in Hydrology No. 39 Vol. 2. UNESCO, Paris, 113 p.
- Gat, J.R. (1995): The relationship between the isotopic composition of precipitation, surface runoff and groundwater for semiarid and arid zones. *IAHS Publication*, **232**, 406–416.

- Gat, J.R., Gonfiantini, R. (1981): Stable Isotope Hydrology. Deuterium and Oxygen-18 in the Water Cycle. Technical Report Series IAEA, 210, 391 p. STI/DOC/10/210. IAEA, Vienna.
- Gat, J.R. (1981): Lakes. In: Stable Isotope Hydrology – Deuterium and Oxygen-18 in the Water Cycle, Gat, J.R., Gonfiantini, R. (eds.), IAEA Technical Report Series, 210, 203–221. IAEA, Vienna.
- Gat, J.R. (1980): The isotopes of hydrogen and oxygen in precipitation in *Handbook of Environmental Isotope Geochemistry, 1. The Terrestrial Environment* (eds A.P. Fritz and J.Ch. Fontes), Elsevier, Amsterdam, pp. 21–47.
- Gat, J.R. (1970): Environmental isotope balance of Lake Tiberias. In: *Isotope Hydrology 1970*, IAEA-STI/PUB/255, 151–162. IAEA, Vienna.
- Gaudet, J.P., Jegat, H., Vachaud, G., Wierenga, P.J. (1977): Solute transfer with exchange between mobile and stagnant water through unsaturated sand. *Soil Science Society of America Journal*, **41**, 665–671.
- Gee, G.W., Ward, A.L., Caldwell, T.G., Ritter, J.C. (2002): A vadose-zone water fluxmeter with divergence control. *Water Resources Research*, **38**, doi:10.1029/2001WR00816.
- Geist, D.R., Dauble, D.D. (1998): Redd Site Selection and Spawning Habitat Use by Fall Chinook Salmon: The Importance of Geomorphic Features in Large Rivers. *Environmental Management*, **22** (5), 655–699.
- Genereux, D.P., Hooper, R.P. (1998): Oxygen and Hydrogen Isotopes in rainfall-Runoff Studies. In: *Isotope Tracers in Hydrology* (Kendall, C., McDonnell, J.J., eds.), 319–338. Elsevier, Amsterdam.
- Genereux, D.P. (1998): Quantifying uncertainty in tracer-based hydrograph separations. *Water Resources Research*, **34** (4), 915–919.
- Genereux, D.P., Hemond, H.F., Mulholland, P.J. (1993): Use of radon-222 and calcium as tracers in a three-end-member mixing model for streamflow generation on the West Fork of the Walker Branch Watershed. *Journal of Hydrology*, **142**, 167–211.
- German-Heins, J., Flury, M. (2000): Sorption of brilliant blue FCF in soils affected by pH and ionic strength. *Geoderma*, **97**, 87–101.
- Germann, P., Beven, K. (1981): Water flow in soil macropores I. An experimental approach. *Journal of Soil Science*, **32**, 1–13.
- Geyh, M.A., Ploethner, D. (1997): *Isotope Hydrological Study in Eastern Owambo, Etosha Pan, Otavi Mountain Land and Central Omatako catchment including Waterberg Plateau. German-Namibian Groundwater Exploration Project*. Technical Cooperation Project No. 89. 2034. 0., Follow-up report, 2, 34 p. Federal Institute for Geosciences and Natural Resources, Hanover.
- Geyh, M.A. (1995): Geochronologische Aspekte Paläohydrologischer und Paläoklimatischer Befunde in Namibia. *Geomethodica*, **20**, 75–99.
- Geyh, M.A., Schleicher, H. (1990): *Absolute age determination: physical and chemical dating methods and their application*. Springer, Berlin, 503 p.
- Ghodrati, M., Jury, W.A. (1990): A field study using dyes to characterize preferential flow of water. *Soil Science Society of America Journal*, **54** (6), 1558–1563.
- Giardino, C., Gomasasca, M. (2006): Derivation of chlorophyll-a concentrations and bottom properties of Lake Garda from remote sensing. *EARSeL Newsletter*, **66**, 17–19.
- Giauque, W.F., Johnston, H.L. (1929): The Isotopes of Oxygen. *Nature*, **124**, 13–14. doi: 10.1038/124013c0.
- Gibson, J.J., Edwards, T.W.D., Birks, S.J., St Amour, N.A., Buhay, W.M., McEachern, P., Wolfe, B.B., Peters, D.L. (2005): Progress in isotope tracer hydrology in Canada. *Hydrological Processes*, **19**, 303–327.
- Gibson, J.J. (2002a): Short-term evaporation and water budget comparisons in shallow arctic lakes using non-steady isotope mass balance. *Journal of Hydrology*, **264**, 247–266.

- Gibson, J.J. (2002b): A new conceptual model for predicting isotope enrichment of lakes in seasonal climates. *International Geosphere Biosphere Programme News*, **10**, 10–11.
- Gibson, J.J., Prepas, E.E., McEachern, P. (2002): Quantitative comparison of lake throughflow, residency, and catchment runoff using stable isotopes: modelling and results from a regional survey of Boreal lakes. *Journal of Hydrology*, **262** (1–4), 128–144.
- Gibson, J.J., Aggarwal, P.K., Hogan, J., Kendall, C., Martinelli, L.A., Stichler, W., Rank, D., Groni, R., Choudhry, C., Gat, J.R., Bhattacharya, S., Sugimoto, A., Fekete, B., Pietroni, A., Maurer, T., Panalello, H., Stone, D., Seyler, P., Maurice-Bourgin, L., Herczeg, A. (2002): Isotope studies in large river basins: A new global research focus. *Eos Transactions American Geophysical Union*, **83** (52), 613–617.
- Gibson, J.J., Edwards, T.W., Bursey, G.G., Prowse, T.D. (1993): Estimating evaporation using stable isotopes: quantitative results and sensitivity analysis for two catchments in northern Canada. *Nordic Hydrology*, **24**, 79–94.
- Ginn, T.R., Wood, B.D., Nelson, K.E., Scheibe, T.D., Murphy, E.M., Clement, T.P. (2002): Processes in microbial transport in the natural subsurface. *Advances in Water Resources*, **25**, 1017–1042.
- Gish, T.J., Kung, K.-J.S., Perry, D.C., Posner, J., Bubenzer, G., Helling, C.S., Kladvko, E.J., Steenhuis, T.S. (2004): Vadose Zone Processes and Chemical Transport – Impact of Preferential Flow at Varying Irrigation Rates by Quantifying Mass Fluxes. *Journal of Environmental Quality*, **33**, 1033–1040.
- Goldscheider, N., Hötzl, H., Kottke, K. (2001): Microbiological decay of Naphtionate in water samples as a source of misinterpretation of tracer tests, in *New Approaches Characterizing Groundwater Flow. Proceedings of the 31st International Association of Hydrogeologists Congress 10–14, September 2001, Munich, Germany* (eds K.P. Seiler and S. Wöhllich), Swets & Zeitlinger, Lisse, 77–81.
- Gonfiantini, R., Fröhlich, K., Araguas-Araguas, L., Rozanski, K. (1998): Isotopes in Groundwater Hydrology. In: *Isotope Tracers in Catchment Hydrology* (Kendall, C., McDonnell, J.J., eds.), 203–238. Elsevier, Amsterdam.
- Gonfiantini, R. (1986): Environmental isotopes in lake studies, in *Handbook of environmental isotope geochemistry, Vol. 2, The Terrestrial Environment*, (eds A.P. Fritz and J.Ch. Fontes), Elsevier, Amsterdam, pp. 113–168.
- Goni, I.B., Fellman, E. and Edmunds, W.M. (2001): Rainfall geochemistry in the Sahel region of northern Nigeria. *Atmospheric Environment*, **35**, 4331–39.
- Göppert, N., Goldscheider, N. (2008): Solute and Colloid Transport in Karst Conduits under Low- High-Flow Conditions. *Groundwater*, **46** (1), 61–68.
- Gospodaric, R., Leibundgut, Ch. (1986): Evaluation and Interpretation of the Tracing Data. In: *Karst Hydrology of the Central and Eastern Peloponnesus (Greece)*, Morfis, A., Zojer, H. (eds.). *Steirische Beiträge zur Hydrogeologie*, **37/38**, 276–287. Graz.
- Gospodaric, R., Habić, P. (eds.) (1977): *3rd International Symposium of Underground Water Tracing, Ljubljana-Bled, Yugoslavia*. Institute for Karst Research, Ljubljana, 188 p.
- Gospodaric, R., Zötl, J. (eds) (1976): Markierung unterirdischer Wässer – Untersuchungen in Slowenien 1972–1975. *Steirische Beiträge zur Hydrogeologie*, **28**, 7–257. Graz.
- Goudsmit, G.H., Peeters, F., Gloor, M., Wüest, A. (1997): Boundary versus internal diapycnal mixing in stratified natural waters. *Journal of Geophysical Research*, **102**, 27903–27914.
- Grabczak, J., Maloszewski, P., Rozanski, K., Zuber, A. (1984): Estimation of the tritium input function with the aid of stable isotopes. *Catena*, **11**, 105–114.
- Griffioen (1989): *Alarmmodell für den Rhein*, report (German), KHR-Bericht Nr. II-2, International Commission for the Hydrology of the Rhine basin (CHR), Lelystad.

- Grisak, G.E., Pickens, J.F. (1980): Solute transport through fractured media 1. The effects of matrix diffusion. *Water Resources Research*, **16**, 719–730.
- Grossmann, J., Bredemeier, M., Udluft, P. (1990): Sorption of trace elements by suction cups of aluminum-oxide, ceramic, and plastics. *Zeitschrift für Pflanzenernährung und Bodenkunde*, **153**, 359–364.
- Grust, K., Hock, R. (2004): Gletscherabfluss. In: *Geohydrologische Markierungstechnik*, W. Käss (ed.). Gebrüder Borntraeger, Berlin, Stuttgart, 428–445.
- Gunn, J., Tranter, J., Perkins, J., Hunter, C. (1998): Sanitary bacterial dynamics in a mixed karst aquifer. *Karst Hydrology, IAHS Publication*, **248**, 61–70.
- Günneberg, F. (1990): Tracer-Versuch im Rhein 24.04.-03.05.1989. In-situ Verfolgung des Rhodamin WT mit Laser-angeregten Fluoreszenzen, unpublished report (German), German Federal Institute of Hydrology (BfG), Koblenz.
- Günthert, W., Behrens, H. (1982): Messungen des physikalischen Sauerstoffeintrags in Fließgewässern mit Tracern – Verfahren und Anwendungsbeispiele. *Beiträge zur Geologie der Schweiz, Hydrologie* **28** (II), 471–482. Berne.
- Güntner, A., Uhlenbrook, S., Seibert, J., Leibundgut, Ch. (1999): Multi-criterial validation of TOPMODEL in a mountainous catchment. *Hydrological Processes*, **13**, 1603–1620.
- Gupta, S.K., Moravcik, P.S., Lau, L.S. (1994): Use of injected helium as a hydrological Tracer. *Hydrological Sciences*, **39**, 109–119.
- Gurrieri, J.T., Furniss, G. (2004): Estimation of groundwater exchange in alpine lakes using non-steady mass-balance methods. *Journal of Hydrology*, **297** (1–4), 187–208.
- Gvirtzman, H., Gorelick, S.M. (1991): Dispersion and advection in unsaturated porous media enhanced by anion exclusion. *Nature*, **352**, 793–795.
- Gygax, F., Schwab, W. (1969): Neue Wege in der Markierung von Grundwasser. *Geographica Helvetica*, **24** (3), 125–130.
- Haas, J.L. (1959): Evaluation of ground water tracing methods used in speleology. *Bulletin of the National Speleological Society*, **21** (2), 67–76.
- Haase, P., Pugnaire, F.I., Fernández, E.M., Puigdefàbregas, J., Clark, S.C., Incoll, L.D. (1996): An investigation of rooting depth of the semiarid shrub *Retama sphaerocarpa* (L.) Boiss. by labelling of ground water with a chemical tracer. *Journal of Hydrology*, **177** (1–2), 23–31.
- Hacker, P., Zojer, H., Zötl, J.G. (1983): Ergebnisse eines kombinierten Markierungsversuches im Basaltgebiet von Kibwezi (Kenya). *Steirische Beiträge zur Hydrogeologie*, **34/35**, 107–125. Graz.
- Hadi, S., Leibundgut, Ch., Friedrich, K., Maloszewski, P. (1997): New fluorescent tracers. In: *Tracer Hydrology 97. Proceedings of the 7th International Symposium on Water Tracing 26–31 May 1997, Portoroz, Slovenia*, Kranjc, A. (ed.), 55–62. Balkema, Rotterdam.
- Hadi, S. (1997): New hydrological tracer synthesis and investigation. Dissertation, Institute of Hydrology, University of Freiburg.
- Hageman, R., Nief, G., Roth, E. (1970): Absolute isotopic scale for deuterium analysis of natural waters. Absolute D/H ratio for SMO. *Tellus*, **22**, 712–715.
- Hagg, W., Braun, L.N., Weber, M., Becht, M. (2006): Runoff modelling in glacierized Central Asian catchments for present-day and future climate. *Nordic Hydrology*, **37** (2), 93–105.
- Hangen, E., Gerke, H.H., Schaaf, W., Hüttl, R.F. (2005): Assessment of preferential flow processes in a forest-reclaimed lignitic mine soil by multicell sampling of drainage water and three tracers. *Journal of Hydrology*, **303**, 16–37.
- Hangen, E., Lindenlaub, M., Leibundgut, Ch., von Wilpert, K. (2001): Investigating mechanisms of stormflow generation by natural tracers and hydrometric data: a small catchment study in the Black Forest, Germany. *Hydrological Processes*, **15**, 183–199.

- Harden, H.S., Roeder, E., Hooks, M., Chanton, J.P. (2008): Evaluation of onsite sewage treatment and disposal systems in shallow karst terrain. *Water Research*, **42** (10–11), 2585–2597.
- Harrington, G.A., Walker, G.R., Love, A.J., Narayan, K.A. (1999): A compartmental mixing-cell approach for quantitative assessment of groundwater dynamics in the Otway Basin, South Australia. *Journal of Hydrology*, **214**, 49–63.
- Harris, D.C., Bertolucci, M.D. (1989): *Symmetry and Spectroscopy. An Introduction to Vibrational and Electronic Spectroscopy*. Dover Publications, New York, 550 p.
- Harvey, R.W., George, L.W., Smith, R.L., LeBlanc, D.R. (1989): Transport of microspheres and indigenous bacteria through a sandy aquifer: results of natural and forced gradient tracer experiments. *Environmental Science and Technology*, **23**, 51–56.
- Hassan, M.A., Ergenzinger, P. (2003): Tracers in fluvial geomorphology. In: *Tools in Fluvial Morphology*, Piegay, G.M.K. (ed.), 397–423. John Wiley, New York.
- Hatano, R., Booltink, H.W.G. (1992): Using fractal dimensions of stained flow patterns a clay soil to predict bypass flow. *Journal of Hydrology*, **135**, 121–131.
- Hatano, R., Kawamura, N., Ikeda, J., Sakuma, T. (1992): Evaluation of the effect of morphological features of flow paths on solute transport by using fractal dimensions of methylene blue staining pattern. *Geoderma*, **53**, 31–44.
- Hatch, C.E., Fisher, A.T., Revenaugh, J.S., Constantz, J., Ruehl, C. (2006): Quantifying surface water-groundwater interactions using time series analysis of streambed thermal records: Method development. *Water Resources Research*, **42**. W10410, doi:10.1029/2005WR004787.
- Haws, N.W., Das, B.S., Rao, P.S.C. (2004): Dual-domain solute transfer and transport processes: evaluation in batch and transport experiments. *Journal of Contaminant Hydrology*, **75**, 257–280.
- Hendry, M.J., Lawrence, J.R., Maloszewski, P. (1999): Effects of velocity on the transport of two bacteria through saturated sand. *Ground Water*, **37**, 103–112.
- Hendry, M.J., Lawrence, J.R., Maloszewski, P. (1997): The role of sorption in the transport of *Klebsiella oxytoca* through saturated silica sand. *Ground Water*, **35**, 574–584.
- Herrmann, A., Schöninger, M., Schumann, S., Trimborn, P., Stichler, W., Groth, P. (2001): Multilateral approach of fissured rock aquifer systems in the Harz Mts., Germany to assess risk potentials of drinking water reservoirs, in *New Approaches Characterizing Groundwater Flow. Proceedings of the 31st International Association of Hydrogeologists Congress 10–14, September 2001, Munich, Germany* (eds K.P. Seiler and S. Wöhrlich.), Swets & Zeitlinger, Lisse, 951–956.
- Herrmann, A., Bahls, S., Stichler, W., Gallart, F., Latron, J. (1999): Isotope hydrological study of mean transit times and related hydrological conditions in Pyrenean experimental basins (Vallcebre, Catalonia). *IAHS Publication*, **259**, 101–110.
- Herrmann, A., Maloszewski, P., Stichler, W. (1987): Changes of ^{18}O contents of precipitation water during seepage in the unsaturated zone. In: *Proceedings of International Symposium on Groundwater Monitoring and Management, Dresden, GDR, 23–28 March 1987*.
- Herrmann, A., Koll, J., Leibundgut, Ch., Maloszewski, P., Rau, R., Rauert, W., Stichler, W. (1984): Anwendung von Tracertechniken zur Erfassung des Wasserumsatzes in kleinen Einzugsgebieten. *Deutsche Gewässerkundliche Mitteilungen*, **28**, 65–74.
- Herrmann, A., Martinec, J., Stichler, W. (1978): Study of Snowmelt-Runoff Components using Isotope Measurements. *Proceedings Modelling of Snow cover runoff*, U. S. Army cold Regions Research and Engineering Laboratory, Hanover.
- Herrmann, A. (1977): In situ chlorophyll and plankton measurements with the batfish vehicle. *Oceans*, **9**, 541–545.
- Heys, B. (1968): Closing address. *Trans Cave Research Group of Great Britain*, **10** (2), 121.
- Himmelblau, D.M., Bischoff, K.B. (1968): *Process Analysis and Simulation: Deterministic Systems*. Wiley, New York.

- Himmelsbach, T., Hötzl, P., Maloszewski, P. (1998): Solute Transport Processes in a Highly Permeable Fault Zone of Lindau Fractured Rock Test Site (Germany). *Ground Water*, **36** (5), 792–800.
- Hirsig, P., Petermann, J. (1984): Markierversuch im Sempachersee zur Ermittlung der Ausbreitungsvorgänge am Diffusor L2, unpublished report, 53 p. Kirchlindach.
- Hirsig, P. (1983): Wind – und zuflussbedingte Strömung im Murtensee (CH). Dissertation, University of Berne.
- Hirsig, P., Leibundgut, Ch., Nydegger, P. (1982): The present situation regarding the use of fluorescent tracers in limnology. *Beiträge zur Geologie der Schweiz – Hydrologie*, **28**, 495–510. Berne.
- Hirsig, P. (1981): Markierung von gereinigtem Abwasser und dessen Verfolgung im See mittels fluoreszierender Tracer, am Beispiel der ARA der Region Murten, unpublished report (German), Institute of Geography, University of Berne.
- Ho, D.T., Schlosser, P., Caplow, T. (2002): Determination of longitudinal dispersion coefficient and net advection in the tidal Hudson River with a large-scale, high resolution SF₆ tracer release experiment. *Environmental Science and Technology*, **36** (15), 3234–3241.
- Hock, R., Iken, A., Wangler, A. (1999): Tracer experiments and Borehole observations in the overdeepening of Aletschgletscher, Switzerland. *Annals of Glaciology*, **29**, 253–260.
- Hock, R., Hooke, R. (1993): Evolution of the internal drainage system in the lower part of ablation area of Storglaciären, Sweden. *Geological Society of America Bulletin*, **105**, 537–546.
- Hodel, H.P. (2009): Hydrometrie – Messung gewässerkundlicher Grössen. In: *Taschenbuch der Wasserwirtschaft*, Lecher, K., Lühr, H.P., Zahnke, U.C.E. (eds.) in print. Vieweg & Teubner Verlag, Wiesbaden.
- Hodel, H.P., Stoller, F., Diem, M. (2004): Tracermessungen mit Lichtleiter-Fluorometer in Wildbächen und Gebirgsflüssen. In: *Proceedings of “Neuere Entwicklungen in der Durchflussmessung in natürlichen und künstlichen Gerinnen”, March 2004, Munich*. TU München, Munich.
- Hodel, H.P., Stoller, F. (2000): Messkampagne mit Lichtleiter-Fluorometer LLF-1 und LLF-M – Sept. '99, Ziele, Erfahrungen, Messungen, Ausblick und offene Fragen, technical report (unpublished, German), Landeshydrologie und -geologie (by now Federal Office for Water and Geology), Berne.
- Hodel, H.P. (1993): Untersuchung zur Geomorphologie, der Rauheit, des Strömungswiderstandes und des Fliessvorganges in Bergbächen. Dissertation, Swiss Federal Institute of Technology Zurich, 289 p.
- Hodel, H.P. (1992): Anwendung von Tracerverfahren zur Durchflussermittlung, 17. DVWK-Fortbildungslehrgang Hydrologie, Durchflusserfassung in offenen Gerinnen – klassisches Verfahren und neue Entwicklungen, Sept. 1992, Essen.
- Hodgkins, R. (2001): Seasonal evolution of meltwater generation, storage and discharge at a non-temperate glacier in Svalbard. *Hydrological Processes*, **15** (3), 441–460.
- Hodgkins, R., Tranter, M., Downswell, J.A. (1997): Solute provenance, transport and denudation in a high arctic glacierized catchment. *Hydrological Processes*, **11**, 1813–1832.
- Hoefs, J. (1997): *Stable Isotope Geochemistry*. 4th edition, Springer, Berlin, 201 p.
- Hoeg, S., Uhlenbrook, S., Leibundgut, Ch. (2000): Hydrograph separation in a mountainous catchment – combining hydrochemical and isotopic tracers. *Hydrological Processes*, **14** (7), 1199–1216.
- Hoehn, E., Cirpka, O.A. (2006): Assessing hyporheic zone dynamics in two alluvial flood plains of the Southern Alps using water temperature and tracers. *Hydrology and Earth System Sciences Discussion*, **3**, 335–364.

- Hoehn E. (1998): Solute exchange between river water and groundwater in headwater environments. *IAHS Publication*, **248**, 165–172.
- Hoffmann, R. and Dietrich, P. (2004): Geoelektrische Messungen zur Bestimmung von Grundwasserflussrichtungen und -geschwindigkeiten. *Grundwasser*, **3** (24), 194–203.
- Hofstraal, J.W., Steendijk, M., Vriezakkolk, G., Schreurs, W., Broer, G.J.A.A., Wijnstok, N. (1991): Determination of Rhodamine WT in surface water by solid-phase extraction and HPLC with fluorescence detection. *Water Research*, **25** (7), 883–890.
- Högberg, P. (1997): Tansley Review No. 95: ^{15}N natural abundance in soil-plant systems. *New Phytologist*, **137** (2), 179–203.
- Höhener, P., Werner, D., Balsiger, C., Pasteris, G. (2003): Worldwide Occurrence and Fate of Chlorofluorocarbons in Groundwater. *Critical Reviews in Environmental Science and Technology*, **33** (1), 1–29.
- Holden, J. (2004): Hydrological Connectivity of Soil Pipes Determined by Ground-Penetrating Radar Tracer Detection. *Earth Surface Processes and Landforms*, **29**, 437–442.
- Holden, N.M., Scholefield, D., Williams, A.G., Dowd, J.F. (1995): The simultaneous use of three common hydrological tracers for fine spatial and temporal resolution investigation of preferential flow in a large soil block. *Tracers in Hydrology*, Ch. Leibundgut (ed.). *IAHS Publication*, **229**, 77–86.
- Holtkamp, J. (2008): Modelling isotope fractionation in precipitation. Diplom thesis, Institute of Hydrology, University of Freiburg.
- Hooke, R.L., Miller, S.B., Kohler, J. (1988): Character of the englacial and subglacial drainage system in the upper part of ablation areas of Storglaciären, Sweden. *Journal of Glaciology*, **34** (117), 228–231.
- Hornberger, G.M., Mills, A.L., Herman, J.S. (1992): Bacterial transport in porous media: evaluation of a model using laboratory observations. *Water Resources Research*, **28**, 915–938.
- Hötzl, H. (1996): Grundwasserschutz in Karstgebieten. *Grundwasser*, **1**, 5–11.
- Hötzl, H., Werner, A. (eds.) (1992): *Tracer Hydrology 92. Proceedings of the 6th International Symposium on Water Tracing, September 21–26 1992, Karlsruhe*. Balkema, Rotterdam, 452 p.
- Hötzl, H. (1991): Advantages and limitations in the use of artificial tracers in the study of complex aquifers. *International Association of Hydrogeologists (IAH) Memoires*, **22** (1), 183–193. Lausanne.
- Hötzl, H., Käss, W., Reichert, B. (1991): Application of microbial tracers in groundwater studies. *Water Science and Technology*, **24** (2), 295–300.
- Hötzl, H., Maurin, V., Zötl, J. (1977): Results of the Injection of Lycopodium Spores. In: *3rd International Symposium of Underground Water Tracing, Ljubljana-Bled, Yugoslavia*, Gospodarc, R., Habic, P. (eds.), 167–181. Institute for Karst Research, Ljubljana.
- Hötzl, H., Maurin, V., Zötl, J. (1976): Die Markierung mit Sporen. *Steirische Beiträge zur Hydrogeologie*, **28**, 153–166. Graz.
- Hötzl, H. (ed) (1973): Die Hydrogeologie und Hydrochemie des Einzugsgebietes der obersten Donau. *Steirische Beiträge zur Hydrogeologie*, **25**, 5–102. Graz.
- Hu, Q., Moran, J.E. (2005): Simultaneous analyses and applications of multiple fluorobenzoate and halide tracers in hydrologic studies. *Hydrological Processes*, **19**, 2671–2687.
- Hubbard, E.F., Kilpatrick, F.A., Martens, L.A. and Wildon, J.F. Jr. (1982): Measurement of time of travel and dispersion in streams by dye tracing, in *Techniques of Water-Resources Investigations of the USGS, Book 3*, available at <http://pubs.usgs.gov/twri/twri3-a9/> (accessed 21 April 2009).
- Hunt, R.J., Coplen, T.B., Haas, N.L., Saad, D.A., Borchardt, M.A. (2005): Investigating surface water–well interaction using stable isotope ratios of water. *Journal of Hydrology*, **302** (1–4), 154–172.

- IAEA/WMO (2006): Global Network of Isotopes in Precipitation. The GNIP Database. Accessible at: <http://isohis.iaea.org> (accessed 21 April 2009).
- IAEA (2006): *Use of Chlorofluorocarbons in Hydrology: A Guidebook*, IAEA-STI/PUB/1238, 277 p. IAEA, Vienna.
- IAEA (2002): *Use of Isotopes for Analyses of Flow and Transport Dynamics in Groundwater Systems*, CD-ROM, IAEA-UIAGS/CD, 02-00131, IAEA, Vienna.
- IAEA (2001): Isotope techniques in water resource investigations in arid and semi-arid regions. *IAEA-TECDOC-1207*, 99 p. IAEA, Vienna.
- IAEA (1985): Stable and radioactive isotopes in the study of the unsaturated soil zone. *IAEA-TECDOC-357*, 183 p. IAEA, Vienna.
- Iken, A., Bindschädler, R. (1986): Combined measurement of subglacial waterpressure and surface velocity of the Findelengletscher, Switzerland: conclusions about drainage system and sliding mechanism. *Journal of Glaciology*, **32**, 101–119.
- Iken, A. (1977): Variations of surface velocities on some alpine glaciers at intervals of a few hours. Comparison with arctic glaciers. *Zeitschrift für Gletscherkunde und Glazialgeologie*, **13**, 23–35.
- Imboden, D., Lemmin, U., Joller, T., Schurter, M. (1983): Mixing processes in lakes: mechanism and ecological relevance. *Schweizerische Zeitschrift für Hydrologie*, **48**, 196–229.
- Imboden, D. (1973): Limnologische Transport- und Nährstoffmodelle. *Schweizerische Zeitschrift für Hydrologie*, **35**, 29–68.
- Ingerson, E., Pearson, F.J. Jr. (1964): Estimation of age and rate motion of groundwater by the ^{14}C -method, in *Recent researches in the fields of hydrosphere, atmosphere and nuclear chemistry*, 263–283. Atmosphere and Nuclear Geochemistry, Sugarawa Festival Volume Maruzen, Tokyo.
- Ingraham, N.L., Caldwell, E.A., Verhagen, B.T. (1998): Arid catchments. In: *Isotope Tracers in Catchment Hydrology* (Kendall, C., McDonnell, J.J., eds.), Elsevier Science, Amsterdam, 435–460.
- Ingraham, N.L. and Criss, R.E. 1993: The effects of surface area and volume on the rate of isotopic exchange between water and vapour. *Journal of Geophysical Research*, **98**, 20547–20553.
- Jäggi, M., Paris, U. (1978): Ein Färbversuch zur Abklärung des Ausbreitungsvorgangs des gereinigten Abwassers der Kläranlage Bibertal-Hegau im Rhein. *Wasser, Energie, Luft*, **70** (8/9), 243–249.
- Jaynes, D.B., Ahmed, S.I., Kung, K.-J.S., Kanwar, R.S. (2001): Temporal Dynamics of Preferential Flow to a Subsurface Drain. *Soil Science Society of America Journal*, **65**, 1368–1376.
- Jaynes, D.B. (1994): Evaluation of Fluorobenzoate Tracers in Surface Soils. *Ground Water*, **32** (4), 532–538.
- Jonsson, K., Johansson, H., Wörman, A. (2004): Sorption Behavior and Long-Term Retention of Reactive Solutes in the Hyporheic Zone of Streams. *Journal of Environmental Engineering*, **130** (5), 573–584.
- Joseph, A., Frangi, J.P., Aranyossy, J.F. (1992): Isotope characteristics of meteoric water and groundwater in the Sahelo-Sudanese Zone. *Journal of Geophysical Research*, **97**, 7543–7551.
- Joseph, D., Sendner, M., Weidemann, F. (1964): Untersuchungen über die horizontale Diffusion in der Nordsee. *Ocean Dynamics*, **17** (2), 57–75.
- Jouzel, J., Merlivat, L. (1984): Deuterium and oxygen-18 in precipitation: modeling of the isotopic effects during snow formation. *Journal of Geophysical Research*, **89**, 11749–11757.
- Juhler, R.K., Mortensen, A.P. (2002): Analysing fluorobenzoate tracers in groundwater samples using liquid chromatography-tandem mass spectrometry. A tool for leaching studies and hydrology. *Journal of Chromatography*, **957**, 11–16.
- Kalma, S.J., Thornburn, P.J., Dunn, G.M. (1998): A comparison of heat pulse and deuterium tracing techniques for estimating sap flow in Eucalyptus grandis trees. *Tree Physiology*, **18**, 697–705.

- Kasnavia, T., Vu, D., Sabatini, D.A. (1999): Fluorescent dye and media properties affecting sorption and tracer selection. *Ground Water*, **37**, 376–381.
- Käss, W. (2004): *Geohydrologische Markierungstechnik*, 2nd edition, Lehrbuch der Hydrogeologie 9. Gebrueder Borntraeger, Berlin, Stuttgart, 557 p.
- Käss, W. (1998): *Tracing technique in geohydrology*. Balkema, Rotterdam, 581 p.
- Käss, W. (1994): Hydrological tracing practice on underground contaminations. *Environmental Geology*, **23**, 23–29.
- Käss, W., Reichert, B. (1986): Tracing of karst water with fluorescent spores. In: *Proceedings of the 5th International Symposium on Underground Water Tracing, Athens, Greece* (Morfi, A., Paraskevopoulou, P., eds.), 157–165. Institute of Geology and Mineral Exploration, Athens.
- Käss, W., Morfi, A., Paraskevopoulou, P., Stylianou, A. (1986): Tracing with salts, in 5th International Symposium on Underground Water Tracing, Athens 1986: Karst Hydrogeology of the Central and Eastern Peloponnesus (Greece) (eds Morfi, A., Zojer, H.). *Steirische Beiträge zur Hydrogeologie*, **37/38**, 248–252. Graz.
- Käss, W. (1982): Fluoreszierende Sporen als Markierungsmittel. *Beiträge zur Geologie der Schweiz, Hydrologie* **28** II, 131–134. Berne.
- Käss, W. (ed.) (1972): Internationale Fachtagung zur Untersuchung unterirdischer Wasserwege mittels künstlicher und natürlicher Markierungsmittel, Freiburg/Br. *Geologisches Jahrbuch*, **C 2**, Bundesanstalt für Bodenforschung (by now BGR – Federal Institute for Geosciences and Natural Resources), Hanover.
- Käss, W. (1967a): Erfahrungen mit Uranin bei Färbversuchen, in Fachtagung über die Anwendung von Markierungsstoffen zur Verfolgung unterirdischer Wässer in Graz vom 28. März bis 1. April 1966. Specialists' Conference on the Tracing of Subterranean Waters in Graz, March 28–April 1, 1966 (eds Maurin, V., Zötl, J.). *Steirische Beiträge zur Hydrogeologie*, **18/19**, 123–134. Graz.
- Käss, W. (1967b): Salzungsversuche mit Kalisalz, in Fachtagung über die Anwendung von Markierungsstoffen zur Verfolgung unterirdischer Wässer in Graz vom 28. März bis 1. April 1966. Specialists' Conference on the Tracing of Subterranean Waters in Graz, March 28–April 1, 1966, (eds Maurin, V., Zötl, J.). *Steirische Beiträge zur Hydrogeologie*, **18/11**, 275–279. Graz.
- Käss, W. (1964): Die unmittelbare Bestimmung von Uranin-Spuren bei Färbversuchen. *Steirische Beiträge zur Hydrogeologie*, **15/16**, 37–65. Graz.
- Kasteel, R., Burkhardt, M., Giesa, S., Vereecken, H. (2005): Characterization of Field Tracer Transport Using High-Resolution Images. *Vadose Zone Journal*, **4**, 101–111.
- Kasteel, R., Vogel, H.-J., Roth, K. (2002): Effect of non-linear adsorption on the transport behaviour of brilliant blue in a field soil. *European Journal of Soil Sciences*, **53**, 231–240.
- Katz, B.G., Plummer, L.N., Busenberg, E., Revsz, K.M., Jones, B.F., Lee, T.M. (1995): Chemical evolution of groundwater near a sinkhole lake, Northern Florida 2. Chemical Patterns, Mass Transfer Modeling, and rates of Mass Transfer Reactions. *Water Resources Research*, **36**, 1565–1584.
- Kaufmann, S., Libby, W.F. (1954): The natural distribution of tritium. *Physical Review*, **93**, 1337–1344.
- Kazezyilmaz-Alhan, C.M. (2008): Analytical solutions for contaminant transport in streams. *Journal of Hydrology*, **348**, 524–534.
- Kendall, C., Coplen, T. (2001): Distribution of oxygen-18 and deuterium in river water across the United States. *Hydrological Processes*, **15**, 1363–1393.
- Kendall, C., McDonnell, J.J. (eds.) (1998): *Isotope Tracers in Catchment Hydrology*. Elsevier, New York, 839 p.

- Kern, J.S. (1995): Evaluation of soil water retention models based on basic soil physical properties. *Soil Science Society of America Journal*, **59**, 1134–1141.
- Ketelsen, H., Meyer-Windel, S. (1999): Adsorption of brilliant blue FCF by soils. *Geoderma*, **90**, 131–145.
- Kilpatrick, F.A. (1993): Simulation of soluble waste transport and buildup in surface waters using tracers. *Techniques of Water-Resources Investigations of the U.S. Geological Survey, Book 3, Chapter A20*. U.S. Geological Survey, Denver.
- Kilpatrick, F.A., Wilson, J. (1989): Determination of stream reaeration coefficients by the use of tracers. *Techniques of Water-Resources Investigations of the United States Geological Survey, Applications of Hydraulics, Book 3*. U.S. Geological Survey, Denver.
- Kilpatrick, F.A., Wilson, J.F. Jr. (1989): Measurement of time of travel and dispersion in streams by dye tracing. *Techniques of Water-Resources Investigations of the United States Geological Survey, Book 3, Chapter A9*. U.S. Geological Survey, Denver.
- Kilpatrick, F.A., Cobb, E.D. (1985): Measurement of discharge using tracers. *Techniques of Water-Resources Investigations of the United States Geological Survey, Book 3, Chapter A16*. U.S. Geological Survey, Denver.
- Kinnunen, K. (1978): Tracing water movements by means of *Escherichia coli* bacteriophages. *Publications of the Water Research Institute, National Board of Waters, Finland*, **25**.
- Kirchner, J.W. (2003): A double paradox in catchment hydrology and geochemistry. *Hydrological Processes*, **17**, 871–874.
- Kirchner J.W., Feng, X., Neal, C. (2000): Fractal stream chemistry and its implications for contaminant transport in catchments. *Nature*, **403** (6769), 524–527.
- Kirk, S.T., Campana, M.E. (1990): A deuterium-calibrated groundwater flow model of a regional carbonate-alluvial system. *Journal of Hydrology*, **119**, 357–388.
- Klemeš, V. (1986): Operational testing of hydrological simulation models. *Hydrological Sciences Journal*, **31** (1), 13–24.
- Klotz, D., Maloszewski, P., Moser, H. (1988): Mathematical modeling of radioactive tracer migration in water flowing through saturated porous media. *Radiochimica Acta*, **44/45**, 373–973.
- Klotz, D. (1982a): Verhalten hydrologischer Tracer in ausgewählten Fluvio-glazialen Kiesen, Hangschutt-Kiesen und tertiären Kies-Sanden aus Bayern. In: Tracermethoden in der Hydrologie. Proceedings Internationale Fachtagung über die Anwendung von Tracermethoden in der Hydrologie, Leibundgut, Ch., Weingartner, R. (eds.), Beiträge zur Geologie der Schweiz, Hydrologie **28**, 245–256. Berne.
- Klotz, D. (1982b): Verhalten hydrologischer Tracer in ausgewählten Sanden und Kiesen. *GSF-Bericht R 290*, 17–29. Munich-Neuherberg.
- Kluge, T., Ilmberger, J., Rohden, C. von, Aeschbach-Hertig, W. (2007): Tracing and quantifying groundwater inflow into lakes using radon-222. *Hydrology and Earth System Sciences Discussion*, **4**, 1519–1548.
- Kollmann, W.F.H., Meyer, J.W., Supper, R. (1992): Geoelectric surveys in determining the direction and velocity of groundwater flow, using introduced salt tracer. In: *Tracer Hydrology 92. Proceedings of the 6th International Symposium on Water Tracing, September 21–26 1992, Karlsruhe*, Hötzl, H., Werner, A. (eds.), 109–113. Balkema, Rotterdam.
- Königer, P., Leibundgut, Ch., Link, T.J., Marshall, J.D. (2009): Stable isotopes used as applied water tracers in column and field studies. *Organic Geochemistry*, Special issue ‘Stable Isotopes in Biogeosciences’, submitted.
- Königer, P., Schwientek, M., Uhlenbrook, S., Leibundgut, Ch., Krause, W.J. (2008): Tritium balance in macro-scale river basins analysed through distributed hydrological modeling. *Hydrological Processes*, **22**, 567–576.

- Königer, P., Marshall, J.D. (2008): Stable isotopes used as artificial tracers of snow melt infiltration and plant water uptake. *Geophysical Research Abstracts*, **10**, EGU2008-A-06346, 2008. SRef-ID: 1607-7962/gra/EGU2008-A-06346.
- Königer, P., Wittmann, S., Krause, W.J., Leibundgut, Ch. (2005): Tritium based water balance modeling in a macroscale catchment. *Hydrological Processes*, **19**, 3313–3320.
- Königer, P. (2003): Tracerhydrologische Ansätze zur Bestimmung der Grundwasser-Neubildung. *Freiburger Schriften zur Hydrologie*, **16**, 89 p. Freiburg.
- Königer, P., Leibundgut, Ch. (2001): Study of River Water Impacts on Groundwater during Flood Events in a Dry Flood Plain of the Upper Rhine Valley. Groundwater Ecology – A tool for management of water resources. *EU Report EUR 1987*, 369–374
- Königer, P., Uhlenbrook, S., Jäger, L., Mayer, H. (2001): Isotope hydrological investigations on groundwater origin in the flood plain of the Upper Rhine Valley, in *New Approaches Characterizing Groundwater Flow: Proceedings of the Xxi International Association of Hydrogeologists Congress Munich/Germany/10-14 September 2001*, (Seiler, K.P., Wohnlich, S., eds.), pp. 363–6. Swets & Zeitlinger, Lisse.
- Königer, P., Leibundgut, Ch., Lohner, R.D. (2000): Isotope study of surface water seepage during a flood event in the Upper Rhine Valley. *IAHS Publication*, **262**, 122–127.
- Kool, J.B., Parker, J.C. (1988): Analysis of the inverse problem for transient unsaturated flow. *Water Resources Research*, **24**, 817–830.
- Kool, J.B., Parker, J.C., van Genuchten, M.Th. (1987): Parameter estimation for unsaturated flow and transport models – a review. *Journal of Hydrology*, **91**, 255–293.
- Kool, J.B., Parker, J.C., van Genuchten, M.Th. (1985): Determining soil hydraulic properties from one-step outflow experiments by parameter estimation. I. Theory and numerical studies. *Soil Science Society of America Journal*, **49**, 1348–1354.
- Kosakowski, G., Berkowitz, B., Scher, H. (2000): Analysis of field observations of tracer transport in a fractured till. *Journal of Contaminant Hydrology*, **47**, 29–51.
- Kovar, K., Tappeiner, U., Peters, N.E., Craig, R.G. (eds.) (1998): Hydrology, Water Resources and Ecology in Headwaters. *IAHS Publication*, **248**, 576 + vxi p. ISBN 978-1-901502-45-9.
- Kranjc, A. (ed.) (1997a): *Tracer Hydrology 97. Proceedings of the 7th International Symposium on Water Tracing 26–31 May 1997, Portoroz, Slovenia*. Balkema, Rotterdam, 468 p.
- Kranjc, A. (ed.) (1997b): Karst Hydrogeological Investigations in South-Western Slovenia. *Acta Carsologica*, **26** (1). Ljubljana.
- Kreft, A., Zuber, A. (1979): Determination of aquifer parameters by a two-well pulsed method using radioactive tracers – comments. *Journal of Hydrology*, **41**, 171–176.
- Kreft, A., Zuber, A. (1978): On the physical meaning of the dispersion equation and its solutions for different initial and boundary conditions. *Chemical Engineering Science*, **33**, 1471–1480.
- Kuhn, W., Thurkauf, M. (1958): Isotope separation in the freezing of water and diffusion of the possibility of a multiplication of the isotope separation appearing during freezing in hairpin counter current device. *Helvetica Chimica Acta*, **41**, 938–971.
- Kühne, A., Leibundgut, Ch., Petermann, J., Schädler, B., Schudel, B., Schneider, G., Spreafico, M. (1991): Fließzeitenbestimmung und Stofftransportuntersuchungen im Rhein, Mitteilung Nr. 13, Swiss Agency for the Environment, Forests and Landscape (by now Federal Office for the Environment), Berne.
- Kühne, A. (1988): Berechnung von mittleren Abflussgeschwindigkeiten im Rhein mit Hilfe des Modells FLORIS, unpublished report (German), Laboratory of Hydraulics, Hydrology and Glaciology, Swiss Federal Institute of Technology Zurich.
- Kuik, C.A. van (1994): Analysis of pollutant transport in the Upper Rhine, unpublished report, Faculty of Civil Engineering, Department of Sanitary and Environmental Engineering, Delft University of Technology.

- Kuik, C.A. van, Mazijk, A. van (1994): Analysis of the transport of a pollution cloud in the Upper-Rhine River between Lake of Constance and Basel. Communications on hydraulic and geotechnical engineering, unpublished report, Faculty of Civil Engineering, Delft University of Technology.
- Kulli, B., Stamm, C., Papritz, A., Flühler, H. (2003): Discrimination of Flow Regions on the Basis of Stained Infiltration Patterns in Soil Profiles. *Vadose Zone Journal*, **2**, 238–248.
- Külls, Ch., Schwartz, U., Leibundgut, Ch., Schick, A. (1995): Channel infiltration study using dye tracers. *IAHS Publication*, **232**, 429–436.
- Kung, S., Klavdivko, E.J., Gish, T.J., Steenhuis, T.S., Bubenzer, G., Helling, C.S. (2000): Quantifying Preferential Flow by Breakthrough of Sequentially Applied Tracers: Silt Loam Soil. *Soil Science Society of America Journal*, **64**, 1296–1304.
- Laenen, A., Bencala, K.E. (2001): Transient storage assessments of dye-tracer injections in rivers of the Willamette Basin, Oregon. *Journal of the American Water Resources Association*, **37** (2), 3676–377.
- Laitinen, H.A. (1960): *Chemical Analysis*. McGraw-Hill, New York, 611 p.
- Landeshydrologie und -geologie (1991): Fliesszeitbestimmung und Stofftransportuntersuchungen im Rhein, Mitteilung Nr. 13, Swiss Agency for the Environment, Forests and Landscape (by now Federal Office for the Environment), Berne.
- Lang, H., Leibundgut, Ch., Festel, E. (1979): Results from tracer experiments on the water flow through the Aletschglacier. *Zeitschrift für Gletscherkunde und Glazialgeologie*, **15** (2), 209–218.
- Lange, J., Greenbaum, N., Husary, S., Ghanem, M., Leibundgut, Ch., Schick, A.P. (2003): Runoff generation from successive simulated rainfalls on a rocky, semi-arid, Mediterranean hillslope. *Hydrological Processes*, **17**, 279–296.
- Lange, J., Leibundgut, Ch. (2003): Surface Runoff and Sediment Dynamics in Arid and Semi-Arid Regions. In: *Understanding Water in a Dry Environment*, Simmers, I. (ed.), 115–146. Balkema, Rotterdam.
- Lange, J., Leibundgut, Ch., Grodek, T., Lekach, J., Schick, A. (1998): Using artificial tracers to study water losses of ephemeral floods in small arid streams. *IAHS Publication*, **247**, 31–40.
- Launay, M., Tripier, M., Guizerix, J., Viriot, M.L., André, J.C. (1980): Pyranine used as a Fluorescent Tracer in Hydrology: pH effects in determination of its concentration. *Journal of Hydrology*, **46**, 377–383.
- Law, C.S., Watson, A.J., Liddicoat, M.I. (1994): Automated vacuum analysis of sulphur hexafluoride in seawater: derivation of the atmospheric trend (1970–1993) and potential as a transient tracer. *Marine Chemistry*, **48**, 57–69.
- Leditzky, H.P. (1978): Interpretation von Ionenaustauschvorgängen beim Einsatz von Salzen zur Verfolgung unterirdischer Wasserwege durch Sedimentuntersuchungen. *Steirische Beiträge zur Hydrogeologie*, **30**, 169–174. Graz.
- Lehmann, O. (1932): *Die Hydrographie des Karstes: auf einfach entwickelter, physikalischer und hydraulischer Grundlage*. Enzyklopädie der Erdkunde, 6 b. Deuticke, Leipzig, Vienna, 212 p.
- Leibundgut, Ch., Uhlenbrook, S. (eds.), Chiffard, P., Didzun, J., Kirnbauer, R., Leibundgut, Ch., Merta, M., Merz, B., Peschke, G., Rezzoug, A., Schumann, A., Seidler, C., Tilch, N., Uhlenbrook, S., Zepp, H., Zillgens, B. (2007): Abflussbildung und Einzugsgebietsmodellierung. *Freiburger Schriften zur Hydrologie*, **24**, 203 p. Freiburg.
- Leibundgut, Ch. (2004): Wasser- und Stoffhaushalt sind Zwillinge, in *Alpenwelt – Gebirgswelten. Inseln, Brücken, Grenzen. Tagungsbericht und wissenschaftliche Abhandlungen des 54. Deutschen Geographentags Bern 2003, 28. September bis 4. Oktober 2003*. Heidelberg, Bern, (eds W. Gämmerli, P. Messerli, P. Meusbürger and H. Wanner.), 171–180. Heidelberg, Berne.
- Leibundgut, Ch., Uhlenbrook, S., McDonnell, J.J. (2001): Runoff generation and implications for river basin modelling. *Freiburger Schriften zur Hydrologie*, **13**. Freiburg.

- Leibundgut, Ch., McDonnell, J.J., Schultz, G. (eds.) (1999): *Integrated Methods in Catchment Hydrology – Tracer, Remote Sensing and New Hydrometric Techniques*. IAHS Publication, **258**, 284 p.
- Leibundgut, Ch. (1998a): Vulnerability of karst aquifers, in *Karst Hydrology*, IAHS Publication, **247**, 45–60.
- Leibundgut, Ch. (1998b): Tracer-based assessment of vulnerability in mountainous headwaters, in *Hydrology, Water Resources and Ecology in Headwaters*, IAHS Publication, **248**, 317–325.
- Leibundgut, Ch., Gunn, J., Dassargues, A. (eds.) (1998): *Karst Hydrology*. IAHS Publication, **247**, 146 p.
- Leibundgut, Ch., Hadi, S. (1997): A contribution to toxicity of fluorescent tracers, in *Tracer Hydrology 97. Proceedings of the 7th International Symposium on Water Tracing 26–31 May 1997, Portoroz, Slovenia*, (ed A. Kranjc), 69–76. Balkema, Rotterdam.
- Leibundgut, Ch., Mazijk, A. van (1996a): Kalibrierung des Rhein-Alarm-Modells für die Mosel anhand der Markierversuche 05/92 und 11/92, unpublished report (German), Institute of Physical Geography, chair in Hydrology, University of Freiburg.
- Leibundgut, Ch., Mazijk, A. van (1996b): Kalibrierung des Rhein-Alarm-Modells für die Aare anhand des Markierversuchs 03/94, unpublished report (German), Institute of Physical Geography, chair in Hydrology, University of Freiburg.
- Leibundgut, Ch., Vonderstrass, I. (red.), Bergkvist, S., Abramowski, C., Paul, H. (1995): *Karstwasseruntersuchungen im Gebiet Churfürsten/Alvier – Kurzbericht*, report (German), Amt für Umweltschutz des Kantons St. Gallen, St. Gallen.
- Leibundgut, Ch. (ed.) (1995): *Tracer Technologies for Hydrological Systems*. IAHS Publication, **229**.
- Leibundgut, Ch., Speidel, U., Wiesner, H. (1993): Transport processes in rivers investigated by tracer experiments. IAHS Publication, **215**, 211–217.
- Leibundgut, Ch., Zupan, M. (1992): Determination of residence time in Lake Bled, in *Tracer Hydrology 92. Proceedings of the 6th International Symposium on Water Tracing, September 21–26 1992, Karlsruhe*, (eds H. Hötzeland, A. Werner.), 3–10. Balkema, Rotterdam.
- Leibundgut, Ch., Wiesner, H. (1992): Markierversuch Rhein 06/91, Abschlußbericht, unpublished report (German), Institute of Physical Geography, chair in Hydrology, University of Freiburg.
- Leibundgut, Ch., De Carvalho-Dill, A., Malozewski, P., Müller, I., Schneider, J. (1992): Investigation of Solute Transport in the Porous Aquifer of the Test Site Wilerwald (Switzerland), in *Transport Phenomena in Different Aquifers (Investigations 1987–1992)*, (ed ATH). *Steirische Beiträge zur Hydrogeologie*, **43**, 229–250. Graz.
- Leibundgut, Ch. (1991): Eichung und Verbesserung eines Alarmmodells für den Rhein, in *Vorträge Wasserbau-Seminar, Wintersemester 1990/91: Schadstofftransport in Grund- und Oberflächengewässern*, (ed G. Rouvé) *Mitteilungen des Instituts für Wasserbau und Wasserwirtschaft der Rheinisch-Westfälischen Technischen Hochschule Aachen*, **81**, 29–46, Aachen.
- Leibundgut, Ch., Bremicker, M. (1989): Abschnittsweise Auswertung des Markierversuches Albbruck-Basel mit dem Dispersions-Transportansatz, unpublished report (German) to Landeshydrologie und -geologie (by now Federal Office for Water and Geology), Berne.
- Leibundgut, Ch., Bremicker, M., Wiesner, H. (1989): Markierversuch Rhein 04/89, unpublished report (German), Institute of Hydrology, University of Freiburg.
- Leibundgut, Ch., Gees, A. (1989): Dye tracer experiments at Pakitsoq – Greenland 1988, unpublished report to the Geological Survey of Greenland.
- Leibundgut, Ch., Adler, O. (1989): Einfluss der Wassernutzung auf Weiherbiotope, unpublished report (German), Institute of Hydrology, University of Freiburg.

- Leibundgut, Ch., Attinger, R. (1988): Grundzüge der Karsthydrologie des Alpsteins. Tracerhydrologische Untersuchungen im Hinblick auf Gewässerschutzmassnahmen. *Publikation Gewässerkunde*, **101**. Berne.
- Leibundgut, Ch., Petermann, J., Schudel, P. (1988): Markierversuch Rhein Albruck-Basel, unpublished report (German), Institute of Geography, University of Berne.
- Leibundgut, Ch. (1987): Hydroökologische Untersuchungen in einem alpinen Einzugsgebiet – Grindelwald, Schlussbericht zum Schweizerischen MAB-Programm Nr. 30, unpublished report (German), Institute of Geography, University of Berne.
- Leibundgut, Ch., Wernli, H.R. (1986): Naphthionate – Another Fluorescent Dye, in *Proceedings of the 5th International Symposium on Underground Water Tracing, Athens, Greece* (eds A. Morfias, P. Paraskevopoulou), 167–177. Institute of Geology and Mineral Exploration, Athens.
- Leibundgut, Ch., Attinger, R. (1986): Karst Hydrogeology of the Central and Eastern Peloponnesus. Coastal region between Argos and Astros. *Steirische Beiträge zur Hydrogeologie*, **37/38**, 198–214. Graz.
- Leibundgut, Ch., Luder, B. (1986): Ein Messgerät zur Bestimmung des Abflusses nach dem Verdünnungsverfahren, unpublished report (German), Institute of Geography, University of Berne.
- Leibundgut, Ch. (1986a): Characteristics of Flow Path Conditions by Evaluating Artificial Tracer Techniques. In: *Proceedings of the 5th International Symposium on Underground Water Tracing, Athens, Greece*, Morfias, A., Paraskevopoulou, P. (eds.), 311–319. Institute of Geology and Mineral Exploration, Athens.
- Leibundgut, Ch. (1986b): Zur Anwendung künstlicher Tracer in Gletschern. *Publikation Gewässerkunde*, **85**. Institute of Geography, University of Berne.
- Leibundgut, Ch. (1984): Hydrologic Potential – changes and Stresses, in *The Transformation of Swiss Mountain Regions* (Brugger, E.A., Furrer, G., Messerli, B., Messerli, P., eds.), 167–194. Paul Haupt, Berne, Stuttgart.
- Leibundgut, Ch., Moeri, Th., Peschel, H., Petermann, J., Stampfli, M., Wälti, R. (1983): Strömungsuntersuchungen mittels Tracerversuchen im Bledsee. *Publikation Gewässerkunde*, **39**, Institute of Geography, University of Berne.
- Leibundgut, Ch., Weingartner, R. (eds.) (1982): Tracermethoden in der Hydrologie, Tagungsbericht des 4. SUWT – Internationale Fachtagung über die Anwendung von Tracermethoden in der Hydrologie, Bern. In: *Beiträge zur Geologie der Schweiz – Hydrologie*, **28 I + 28 II**, Berne.
- Leibundgut, Ch. (1982): Stand und Entwicklung der Tracerhydrologie. In: Tracermethoden in der Hydrologie Tagungsbericht des 4. SUWT – Internationale Fachtagung über die Anwendung von Tracermethoden in der Hydrologie, Bern, Leibundgut, Ch., Weingartner, R. (eds.). *Beiträge zur Geologie der Schweiz – Hydrologie*, **28 I + 28 II**, 23–35. Berne.
- Leibundgut, Ch., Wernli, H.R. (1982): Zur Frage der Einspeisemengenberechnung für Fluoreszenztracer. In: Tracermethoden in der Hydrologie Tagungsbericht des 4. SUWT – Internationale Fachtagung über die Anwendung von Tracermethoden in der Hydrologie, Bern, Leibundgut, Ch., Weingartner, R. (eds.). *Beiträge zur Geologie der Schweiz – Hydrologie*, **28 (I)**, 119–131. Berne.
- Leibundgut, Ch. (1981a): Methodik und Ergebnisse der Tracerversuche, in Tracerhydrologische Untersuchungen im Langetental, Leibundgut, Ch., Harum, T. (eds). *Steirische Beiträge zur Hydrogeologie*, **33**, 5–123. Graz.
- Leibundgut, Ch. (1981b): Zum Adsorptionverhalten von Fluoreszenztracern. Festschrift Josef G. Zötl, Forschungszentrum Graz.
- Leibundgut, Ch., Harum, T. (eds) (1981): Tracerhydrologische Untersuchungen im Langetental. *Steirische Beiträge zur Hydrogeologie*, **33**, 5–123. Graz.

- Leibundgut, Ch. (1978): Beiträge zur Anwendung von künstlichen Tracern in der Hydrologie. Including contributions by R. Fässler, E. Festel, B. Werthemann, Ch. Klinkenbergh, J. Kövesdi, I. Krummenacher, M. Schüpbach, M. Stampfli, R. Weingartner and H.R. Wernli, unpublished report (German), Institute of Geography, University of Berne.
- Leibundgut, Ch., Hirsig, P. (1977): Zur Anwendung fluoreszierender Tracer in der Limnologie. *Gas, Wasser, Abwasser*, **12**, 833–841.
- Leibundgut, Ch., Lüthi, B. (1977): Bestimmung des Seihvermögens von Grundwasserleitern mittels Tracer. In: *3rd International Symposium of Underground Water Tracing, Ljubljana-Bled, Yugoslavia*, Gospodaric, R., Habic, P. (eds.), 141–148. Institute for Karst Research, Ljubljana.
- Leibundgut, Ch. (1975): Färbversuche im Grundwasser des Oberaargaus. *Jahrbuch des Oberaargaus*, **18**, 143–171. Herzogenbuchsee, available at: http://www.digibern.ch/jahrbuch_oberaargau/jahrbuch.1975/JBOAG.1975.143.171_faerbversuch-grundwasser.pdf, verified 19 July 2009.
- Leibundgut, Ch. (1974): Fluoreszierende Markierfarbstoffe in der Hydrologie. *Mitteilungen der Naturforschenden Gesellschaft Bern*, **31**, 63–84. Berne.
- Leibundgut, Ch. (1973): Anwendung von Markierfarbstoffen in der Hydrologie. Award as the best of the Faculty of Philosophy and Natural Sciences, University of Berne.
- Leis, A., Benischke, R. (2004): Comparison of different stable hydrogen isotope-ratio measurement techniques for tracer studies with deuterated water in the unsaturated zone and in groundwater. In: 7th Workshop of the European Society for Isotope Research, Bojar, A.-V., Fritz, H., Bojar, H.-P. (eds.), *Berichte des Institutes für Erdwissenschaften, Geologie und Paläontologie, der Karl-Franzens-Universität Graz*, **8**, 85–87. Graz.
- Lenda, A., Zuber, A. (1970): Tracer dispersion in groundwater experiments. In: *Isotope Hydrology 1970*, IAEA-STI/PUB/255, IAEA, Vienna, 619–641.
- Lennartz, B., Kamra, S.K. (1998): Temporal variability of solute transport under vadose zone conditions. *Hydrological Processes*, **12**, 1939–1949.
- Levin, M., Gat, J.R., Issar, A. (1980): Precipitation, flood and groundwaters of the Negev Highlands: an isotopic study of desert hydrology. In: *Arid Zone Hydrology: Investigations with isotope techniques*. IAEA-STI/PUB/547, 3–22. IAEA, Vienna.
- Lindenlaub, M., Leibundgut, Ch., Mehlhorn, J., Uhlenbrook, S. (1997): Interactions of hard rock aquifers and debris cover for runoff generation. *IAHS Publication*, **241**, 63–74.
- Lindqvist, L. (1960): A flash photolysis study of Fluorescein. *Arkiv För Kemi*, **16**, 79–38.
- Little, L.W., Lamb, J.C. (1973): Acute toxicity of 46 selected dyes to Fathead minnow (*Pimephales promelas*). In: *Dyes and the Environment- Reports on Selected Dyes and Their Effects, Vol. 1*, 1–26. American dye manufacturers institute, New York.
- Lloyd, J.B.F. (1971): Synchronized excitation of fluorescence emission spectra. *Nature*, **231**, 64–65.
- Loosli, H.H., Lehmann, B.E., Balderer, W. (1989): Argon-39, Argon-37 and Krypton-85 isotopes in Stripa ground waters. *Geochimica et Cosmochimica Acta*, **53** (8), 1825–1829.
- Loosli, H.H. (1983): A dating method with ^{39}Ar . *Earth and Planetary Science Letters*, **63**, 51–62.
- Loosli, H.H., Oeschger, H. (1968): Erstmaliger Nachweis von ^{39}Ar im atmosphärischen Argon und Grundlagen zu einer Datierungsmethode mittels dieses Isotops. *Zeitschrift für angewandte Mathematik und Physik*, **19** (3), 528–528.
- Love, A.J., Herczeg, A.L., Leaney, F.W., Stadter, M.F., Dighton, J.C., Armstrong, D. (1994): Groundwater residence time and palaeohydrology in the Otway Basin, South Australia: ^2H , ^{18}O and ^{14}C data. *Journal of Hydrology*, **153**, 157–187.
- Lu, J., Wu, L. (2003): Visualizing bromide and iodide water tracer in soil profiles by spray methods. *Journal of Environmental Quality*, **32**, 363–367.

- Luder, B., Fritschi, B. (1990): Abflussmessung in offenen Gerinnen – Renaissance der Salzverdünnung. *Wasser, Energie, Luft*, **82** (3/4), 48–50.
- Maciejewski, S., Małoszewski, P., Stumpp, C., Klotz, D. (2006): Modelling of water flow through typical Bavarian Soils based on lysimeter experiments: 1. Estimation of hydraulic characteristics of the unsaturated zone. *Hydrological Sciences Journal*, **51**, 285–297.
- Maciejewski, S. (1993): Numerical and experimental study of solute transport in unsaturated soils. *Journal of Contaminant Hydrology*, **14**, 193–206.
- Maciejewski, S., Zaradny, H., Klotz, D. (1992): Application of SWATREZ-UNDYS model for simulation of water and tracer movement in unsaturated soil. In: *Tracer Hydrology 92. Proceedings of the 6th International Symposium on Water Tracing, September 21–26 1992, Karlsruhe*, (Hötzl, H., Werner, A., eds.), p. 439–443. Balkema, Rotterdam.
- Maduabuchi, C., Faye, S., Maloszewski, P. (2006): Isotope evidence of palaeorecharge and palaeoclimate in the deep confined aquifers of the Chad Basin, NE Nigeria. *Science of the Total Environment*, **370**, 467–479.
- Magal, E., Weisbrod, N., Yakirevicha, A., Yechieli, Y. (2008): The use of fluorescent dyes as tracers in highly saline groundwater. *Journal of Hydrology*, **358** (1–2), 124–133.
- Mägdessell, J. (1990): Zum Fliessverhalten von Tracern und Schadstoffen im Porengrundwasser. Diplom thesis, Institute of Hydrology, University of Freiburg.
- Mairhofer, J. (1996): Die Bestimmung der Fliessrichtung in einem einzigen Bohrloch mittels radioaktivem Tracer. *Steirische Beiträge zu Hydrogeologie*, **48**, 69–79.
- Maiss, M., Ilmberger, J., Zenger, A., Münnich, K.O. (1994): A SF₆ tracer study of horizontal mixing in Lake Constance. *Aquatic Sciences*, **56** (4), 307–328.
- Maiss, M., Ilmberger, J., Münnich, K.O. (1994): Vertical mixing in Überlingersee (Lake Constance) traced by SF₆ and heat. *Aquatic Sciences*, **56** (4), 329–347.
- Majoube, M. (1971): Fractionnement en Oxygène 18 et en Deutérium entre l'eau et sa vapeur. *Journal de Chimie Physique et de Physico-Chimie Biologique*, **68** (10), 1423–1436.
- Malcolm, R.L., Aiken, G.R., Thurman, E.M., Avery, P.A. (1980): Hydrophilic organic solutes as tracers in groundwater recharge studies. In: *Contaminants and Sediments*, Baker, R.A. (ed.), 71–88. Butterworth-Heinemann, Woburn.
- Mali, N., Urbanc, J., Leis, A. (2007): Tracing of water movement through the unsaturated zone of a coarse gravel aquifer by means of dye and deuterated water. *Environmental Geology*, **51** (8), 1401–1412.
- Mallen, G., Malozewski, P., Flynn, R., Rossi, P., Engel, M., Seiler, K.P. (2005): Determination of bacterial and viral transport parameters in a gravel aquifer assuming linear kinetic sorption and desorption. *Journal of Hydrology*, **306** (1–3), 21–36.
- Maloszewski, P., Maciejewski, S., Stumpp, C., Stichler, W., Trimborn, P., Klotz, D. (2006): Modelling of water flow through typical Bavarian Soils (Germany): 2. Environmental deuterium transport. *Hydrological Sciences Journal*, **51** (2), 298–313.
- Maloszewski, P., Wachniew, P., Czaprynski, P. (2006): Study of hydraulic parameters in heterogeneous gravel beds: Constructed wetland in Nowa Słupia (Poland). *Journal of Hydrology*, **331**, 630–642.
- Malozewski, P., Büttner, G., Apel, R., Krafft, H., Scholz, M., Wagner, B. (2005): Quantitative evaluation of tracer experiments in alpine karst and porous aquifers in the Berchtesgader National Park. *Landschaftsökologie und Umweltforschung*, **48**, 11–18. Braunschweig.
- Maloszewski, P., Stichler, W., Zuber, A. (2004): Interpretation of environmental tracers in groundwater systems with stagnant water zones. *Isotopes in Environmental and Health Studies*, **40** (1), 21–33.
- Maloszewski, P., Zuber, A., Bedbur, E., Matthess, G. (2003): Transport of three herbicides in ground water at Twin Lake test site, Chalk River, Ontario, Canada. *Ground Water*, **41**, 376–386.

- Maloszewski, P., Stichler, W., Zuber, A., Rank, D. (2002): Identifying the flow systems in a karstic-fissured-porous aquifer, the Schneetalpe, Austria, by modelling of environmental ^{18}O and ^3H isotopes. *Journal of Hydrology*, **256**, 48–59.
- Maloszewski, P., Herrmann, A., Zuber, A. (1999): Interpretation of tracer tests performed in fractured rock of the Lange Bramke basin, Germany. *Hydrogeology Journal*, **7**, 209–218.
- Maloszewski, P., Benischke, R., Harum, T., Zojer, H. (1998): Estimation of solute transport parameters in a karstic aquifer using artificial tracer experiments. In: “Shallow Groundwater Systems”, *IAHS Publication*, **18**, Dillon, P., Simmers, I. (eds.), 177–191.
- Maloszewski, P., Zuber, A. (1996): Lumped parameter models for the interpretation of environmental tracer data. In: Manual on Mathematical Models in Isotope Hydrology, *IAEA-TECDOC-910*, 9–58. IAEA, Vienna.
- Maloszewski, P. (1994): Mathematical Modelling of Tracer Experiments in Fissured Aquifers. *Freiburger Schriften zur Hydrologie*, **2**, 107 p. Freiburg.
- Maloszewski, P., Zuber, A. (1993): Principles and practice of calibration and validation of mathematical models for the interpretation of environmental tracer data in aquifers. *Advances in Water Resources*, **16**, 173–190.
- Maloszewski, P., Zuber, A. (1992): On the calibration and validation of mathematical models for the interpretation of tracer experiments in groundwater. *Advances in Water Resources*, **15**, 47–62.
- Maloszewski, P., Rauert, W., Trimborn, P., Herrmann, A., Rau, R. (1992): Isotope hydrologic study of mean transit times in an alpine basin (Wimbachtal, Germany). *Journal of Hydrology*, **140**, 343–360.
- Maloszewski, P., Harum, T., Benischke, R. (1992): Mathematical modelling of tracer experiments in the karst of Lurbach system. *Steirische Beiträge zur Hydrogeologie*, **43**, 116–136. Graz.
- Maloszewski, P., Zuber, A. (1991): Influence of matrix diffusion and exchange reactions on radiocarbon ages in fissured carbonate rocks. *Water Resources Research*, **27**, 1937–1945.
- Maloszewski, P., Zuber, A. (1990): Mathematical modeling of tracer behavior in short-term experiments in fissured rocks. *Water Resources Research*, **26**, 1517–1528.
- Maloszewski, P., Zuber, A. (1985): On the theory of tracer experiments in fissured rocks with a porous matrix. *Journal of Hydrology*, **79**, 333–358.
- Maloszewski, P., Rauert, W., Stichler, W., Herrmann, A. (1983): Application of flow models in an alpine catchment area using tritium and deuterium data. *Journal of Hydrology*, **57**, 207–231.
- Maloszewski, P., Zuber, A. (1982): Determining the turnover time of groundwater systems with the aid of environmental tracers, I. Models and their applicability. *Journal of Hydrology*, **57**, 207–231.
- Maloszewski, P. (1981): Computerprogramm für die Berechnung der Dispersion und der effektiven Porosität in geschichteten porösen Medien. *GSF-Bericht R* **269**, 33 p. Munich-Neuherberg.
- Mandel, S. (1991): Use of tracers in well tests. In: Use of artificial tracers in hydrology, *IAEA-TECDOC-601*, 145–156. IAEA, Vienna.
- Margrita, R., Gaillard, B. (1991): Use of artificial tracers for the determination of aquifer parameters. In: Use of artificial tracers in hydrology, *IAEA-TECDOC-601*, 131–144. IAEA, Vienna.
- Markofsky, M. (1980): Strömungsmechanische Aspekte der Wasserqualität. *Gas und Wasserfach (Wasser und Abwasser)*, **18**.
- Marti, F., Della Valle, G., Krech, U., Gees, R.A., Baumgartner, E. (1979): Markierungsversuche in Grundwasser mit Farbe Bakterien und Viren. *Trinkwasserhygiene, Alimanta*, **18**, 135–145.
- Maurin, V., Zötl, J. (eds) (1967): Fachtagung über die Anwendung von Markierungsstoffen zur Verfolgung unterirdischer Wässer in Graz vom 28. März bis 1. April 1966. Specialists'

- Conference on the Tracing of Subterranean Waters in Graz, March 28–April 1, 1966. *Steirische Beiträge zur Hydrogeologie*, **18/19**, 413 p., Graz.
- Mazijk, A. van, Gils, J.A.G. van, Weitbrecht, V. (2000): *Analyse und Evaluierung der 2-D-Module zur Berechnung des Stofftransportes in der Windows-Version des Rheinalarmmodells in Theorie und Praxis*, report (German), KHR- Bericht Nr. II-16, International Commission for the Hydrology of the Rhine basin (CHR), Lelystad.
- Mazijk, A. van, Leibundgut, Ch. (1999): *Rhein-Alarm-Modell Version 2.1, Erweiterung um die Kalibrierung von Aare und Mosel*, report (german), KHR-Bericht Nr. II-14, International Commission for the Hydrology of the Rhine basin (CHR), Lelystad.
- Mazijk, A. van (1996): One-dimensional approach of transport phenomena of dissolved matter in rivers. Dissertation, Delft University of Technology.
- Mazijk, A. van, Wiesner, H., Leibundgut, Ch. (1992): Das Alarmmodell für den Rhein – Theorie und Kalibrierung der Version 2.0. *Deutsche Gewässerkundliche Mitteilungen*, **36** (2) 42–47.
- Mazijk, A. van, Mierlo, J. van, Wiesner, H. (1991): Verifikation des Rheinalarmmodelles Version 2.0 anhand der Markierversuche Basel-Strassburg 11/88, Basel-Niederlande 05/90, Village Neuf-Niederlande 09/90, unpublished report (German), Institute of Physical Geography, University of Freiburg and Delft University of Technology
- Mazijk A. van, Verwoerd, P., Mierlo, J. van, Bremicker, M., Wiesner, H. (1991): *Rheinalarmmodell Version 2.0. Kalibrierung und Verifikation*, report (german) KHR-Bericht Nr. II-4, International Commission for the Hydrology of the Rhine basin (CHR), Lelystad.
- Mazijk A. van, Verwoerd, P. (1989): Eichung eines stationären Stillwasserzonenmodells anhand des Markierversuchs “Albbruck – Basel”, unpublished report (German) Delft University of Technology and Rijkswaterstaat.
- Mazor, E. (2004): *Chemical and Isotopic Groundwater Hydrology*. CRC Press, Boca Raton, 453 p.
- Mbonu, M. Travi, Y. (1994): Labelling of precipitation by stable isotopes (^{18}O and ^2H) over the Jos plateau and the surrounding plains (northcentral Nigeria). *Journal of African Earth Sciences*, **19**, 91–98.
- McBratney, A.B., Moran, C.J., Stewart, J.B., Cattle, S.R., Koppi, A.J. (1992): Modifications to a method of rapid assessment of soil macropore structure by image analysis. *Geoderma*, **53**, 255–274.
- McCarthy, J.F., Howard, K.M., McKay, L.D. (2000): Effect of pH on Sorption and Transport of Fluorobenzoic Acid Ground Water Tracers. *Journal of Environmental Quality*, **29**, 1806–1813.
- McDonnell, J.J., Rowe, L., Stewart, M. (1999): A combined tracer-hydrometric approach to assess the effect of catchment scale on water flow path, source and age, in Integrated Methods in Catchment Hydrology, *IAHS Publication* **258**, 265–273.
- McDonnell, J.J., McGlynn, B.L., Kendall, K., Shanley, J., Kendall, C. (1998): the role of near stream riparian zones in the hydrology of steep upland catchments. *IAHS Publication*, **248**, 173–180.
- McDonnell, J.J., Stewart, M., Owens, I. (1991): Effect of Catchment-Scale Subsurface Mixing on Stream Isotopic Response, *Water Resources Research*, **27** (12), 3065–3073.
- McDonnell, J.J., Bonell, M., Stewart, M.K., Pearce, A.J. (1990): Deuterium variations in storm rainfall: implications for stream hydrograph separation. *Water Resources Research*, **26** (3), 455–458.
- McGlynn, B., McDonnell, J.J., Stewart, M., Seibert, J. (2003): On the relationships between catchment scale and streamwater mean residence time. *Hydrological Processes*, **17** (1), 175–181.
- McGuire, K.J., Weiler, M., McDonnell, J.J. (2007): Integrating tracer experiments with modeling to assess runoff processes and water transit times. *Advances in Water Resources*, **30**, 824–837.
- McGuire, K.J., McDonnell J.J. (2006): A review and evaluation of catchment transit time modelling. *Journal of Hydrology*, **330**, 543–563.

- McGuire, K.J., DeWalle, D.R., Gburek, W.J. (2002): Evaluation of mean residence time in subsurface waters using oxygen-18 fluctuations during drought conditions in the mid-Appalachians. *Journal of Hydrology*, **261**, 132–149.
- McGuire, P.E., Lowery, B. (1994): Monitoring drainage solution concentrations and solute flux in unsaturated soil with a porous cup sampler and soil moisture sensors. *Ground Water*, **32**, 356–362.
- McKinney, C.R., McCrea, J.M., Epstein, S., Allen, H.A., Urey, H.C. (1950): Improvement in mass spectrometers for the measurement of small differences in isotope abundance ratios. *Review of Scientific Instruments*, **21**, 724.
- Mehlhorn, J. (1999): Tracerhydrologische Ansätze in der Niederschlags-Abfluss-Modellierung. *Freiburger Schriften zu Hydrologie*, **8**, 150 p. Freiburg.
- Mehlhorn, J., Leibundgut, Ch. (1999a): Die Modellierung des Abflussprozesses mit tracerhydrologisch ermittelten Verweilzeiten und Abflusskomponenten. *Hydrologie und Wasserbewirtschaftung*, **43** (4), 164–174.
- Mehlhorn, J., Leibundgut, Ch. (1999b): The use of tracer hydrological time parameters to calibrate baseflow in rainfall-runoff-modelling. *IAHS Publication*, **258**, 93–100.
- Mehlhorn, J., Lindenlaub, M., Leibundgut, Ch. (1999): Improving hydrological process modelling by coupling a rainfall-runoff model with tracer techniques. *IAHS Publication*, **254**, 157–163.
- Mehlhorn, J., Armbruster, V., Uhlenbrook, S., Leibundgut, Ch. (1998): Determination of the geomorphological instantaneous unit hydrograph using tracer experiments in headwater basin. *IAHS Publication*, **248**, 327–335.
- Mehlhorn, J., Leibundgut, Ch., Rogg, H. (1995): Determination of the flow and transport parameters of the unsaturated zone using dye tracers. In: Tracer Technologies for Hydrological Systems. *IAHS Publication*, **229**, 183–190.
- Mendel, H.G. (1988): *Beschreibung hydrologischer Vorhersagemodelle im Rheineinzugsgebiet*, report (German), KHR-Bericht Nr. I-7, International Commission for the Hydrology of the Rhine basin (CHR), Lelystad.
- Menzies, J. (1995). Glaciers and ice sheets. In: Menzies, J. (ed.): *Modern Glacial Environments: Processes, Dynamics and Sediments*, 101–138. Butterworth-Heinemann, Oxford.
- Merlivat, L., Jouzel, J. (1979): Global climatic interpretation of the deuterium – oxygen-18 relationship for precipitation. *Journal of Geophysical Research*, **84**, 5029–5033.
- Merlivat, L. (1978): Molecular diffusivities of H_2^{16}O , HD^{16}O and H_2^{18}O in gases. *Journal of Chemical Physics*, **69** (6), 2864–2871.
- Mierlo, J.M.C. van (1993): Kontrollanalyse der Kalibrierung des Rheinalarmmodells. Diplom thesis, Institute of Physical Geography, Chair in Hydrology, University of Freiburg.
- Mikovari, A., Peter, C., Leibundgut, Ch. (1995): Investigation of preferential flow using tracer techniques. Tracers in Hydrology, Ch. Leibundgut (ed.), *IAHS Publication*, **229**, 87–98.
- Milanovi, P. (1981): *Karst hydrology*. Water Resources Publications, Littleton, Colorado, 276 p.
- MODFLOW: MODular three-dimensional finite-difference ground-water FLOW model. USGS Ground-Water Software. United States Geological Survey, National Center, Reston.
- Moeri, Th., Leibundgut, Ch. (1986): Winter Dye Tracer Experiments on the Findelengletscher. *Zeitschrift für Gletscherkunde und Glaziologie*, **22** (1), 33–41.
- Moeri, Th. (1983): Beitrag zum Abflussgeschehen des Findelengletschers. Diplom thesis, Institute of Geography, University of Berne.
- Mon, J., Flury, M., Harsh, J.B. (2006): Sorption of four triarylmethane dyes in a sandy soil determined by batch and column experiments. *Geoderma*, **133**, 217–224.

- Mook, W.G. (2001): *Environmental isotopes in the hydrological cycle, Principles and applications*. IHP-V, Technical Documents in Hydrology No. 39, UNESCO, Paris.
- Mook, W.G., Bommerson, J.C., Staverman, W.H. (1974): Carbon fractionation between dissolved bicarbonate and gaseous carbon dioxide. *Earth and Planetary Sciences Letters*, **22**, 169–176.
- Mooney, S.J., Morris, C. (2008): A morphological approach to understanding preferential flow using image analysis with dye tracers and X-ray Computed Tomography. *Catena*, **73** (2), 204–211.
- Moore, R.D. (2005a): Introduction to salt dilution gauging for streamflow measurement. Part 3: Slug injection. *Streamline Watershed Management Bulletin*, **8** (2), 1–6.
- Moore, R.D. (2005b): Introduction to Salt Dilution Gauging for Streamflow Measurement. Part IV: The Mass Balance (or Dry Injection Method). *Streamline Watershed Management Bulletin*, **9** (1), 6–12.
- Moore, R.D. (2004a): Introduction to Salt Dilution Gauging for Streamflow Measurement: Part 1. *Streamline Watershed Management Bulletin*, **7** (4), 20–23.
- Moore, R.D. (2004b): Introduction to salt dilution gauging for streamflow measurement. Part 2: Constant-rate injection. *Streamline Watershed Management Bulletin*, **8** (1), 11–15.
- Moore, W.S. (2000): Ages of continental shelf waters determined from 223Ra and 224Ra. *Journal of Geophysical Research*, **105** (C9), 22117–23894.
- Morfis, A., Paraskevopoulou, P. (eds.) (1986): *Proceedings of the 5th International Symposium on Underground Water Tracing, Athens, Greece*. Institute of Geology and Mineral Exploration, Athens, 473 p.
- Morfis, A., Zojer, H. (eds) (1986): Karst Hydrogeology of the Central and Eastern Peloponnesus (Greece), in 5th International Symposium on Underground Water Tracing, Athens 1986: Karst Hydrogeology of the Central and Eastern Peloponnesus (Greece) (Morfis, A., Zojer, H. eds). *Steirische Beiträge zur Hydrogeologie*, **37/38**, 1–301. Graz.
- Mori, K. (1978): A Mean residence time of the Deep Water of Two Meromictic Lakes in Japan. Report for the Environmental Science, Mie Univ. No. 3, 133–142.
- Morrice, J.A., Valett, H.M., Dahm, C.N., Camapan, M.E. (1997): Alluvial characteristics, groundwater-surface water exchange and hydrological retention in headwater streams. *Hydrological Processes*, **11**, 253–267.
- Morris, C., Mooney, S.J. (2004): A high-resolution system for the quantification of preferential flow in undisturbed soil using observations of tracers. *Geoderma*, **118**, 133–143.
- Mortensen, A.P., Jensen, K.H., Nilsson, B., Juhler, R.K. (2004): Multiple Tracing Experiments in Unsaturated Fractured Clayey Till. *Vadose Zone Journal*, **4**, 634–644.
- Moser, H., Rauert, W. (eds.) (1980): *Isotopenmethoden in der Hydrologie. Lehrbuch der Hydrogeologie*, **8**, 400 p. Gebrüder Borntraeger, Berlin/Stuttgart.
- Moser, H., Ambach, W. (1977): Glacial-hydrological investigations in the Oetztal alps made between 1968 and 1975. *Zeitschrift für Gletscherkunde und Glazialgeologie*, **13**, 167–179.
- Moser, H., Sagl, H. (1967): Die Direktmessung hydrologischer Farbtracer im Gelände, in Fachtagung über die Anwendung von Markierungsstoffen zur Verfolgung unterirdischer Wässer in Graz vom 28. März bis 1. April 1966. Specialists' Conference on the Tracing of Subterranean Waters in Graz, March 28–April 1, 1966, (eds Maurin, V., Zötl, J.). *Steirische Beiträge zur Hydrogeologie*, **18/19**, 179–183. Graz.
- Mossman, D., Schnoor, J., Stumm, W. (1988): Predicting the effects of a pesticide release to the Rhine River. *Journal of the Water Pollution Control Federation*, **60** (10), 1806–1812.
- Mualem, Y. (1976): A new model for predicting the hydraulic conductivity of unsaturated porous media. *Water Resources Research*, **12**, 513–522.

- Mugie, A.L. (1990): Oberflächengeschwindigkeit des Rheins in Zusammenhang mit dem Alarmmodell, unpublished report (Nr. 90.085X), Rijkswaterstaat DBW/RIZA, Leystad.
- Mull, D.S., Liebermann, T.D., Smoot, J.L., Woosley, L.H. (1988): *Application of dye-tracing techniques for determining solute transport characteristics of ground water in karst terranes*. Report, EPA904/688-001, U.S. Environmental Protection Agency, Atlanta, Georgia, 103 p.
- Müller, I., Zötl, J.G. (eds) (1980): Karsthydrologische Untersuchungen mit natürlichen und künstlichen Tracern im Neuenburger Jura (Schweiz). *Steirische Beiträge zur Hydrogeologie*, 32, 5-100. Graz.
- Münnich, K.O. (1968): Isotopendatierung von Grundwasser. *Naturwissenschaften*, 55, 158–163.
- Nash, J.E., Sutcliffe, J.V. (1970): River flow forecasting through conceptual models: part I – a discussion of principles. *Journal of Hydrology*, 10, 282–290.
- Nativ, R., Adar, M. E., Dahan, O., Geyh, M., (1995a): Water recharge and solute transport through the vadose zone of fractured chalk under desert conditions. *Water Resources Research*, 31, 253–261.
- Nativ, R., Adar, M.E., Dahan, O., Nissim, I., Geyh, M.A. (1995b): Questions pertaining to isotopic and hydrochemical evidence of fracture-controlled water flow and solute transport in a chalk aquitard. In: *Tracers in Arid Zone Hydrology, Proceedings of IAHS Symposium*, 317–327. IAHS, Vienna.
- Nativ, R., Adar, M.E., Nissim, I., Dahan, O. (1992): Groundwater recharge and solute migration into a desert Aquitard. In: *Tracer Hydrology 92. Proceedings of the 6th International Symposium on Water Tracing, September 21–26 1992, Karlsruhe*, Hötzel, H., Werner, A. (eds.), 339–344. Balkema, Rotterdam.
- Naturaqua PBK AG (1994): Markierversuch Aare 03/1994. Experimentelle Bestimmung von Stofftransportparametern, unpublished report (German) to Landeshydrologie und -geologie (by now Federal Office for Water and Geology), Berne.
- Naturaqua (1990): Markierversuche Rhein-Basel, Alarmstation Weil am Rhein. Markierversuche mit Querschnittsaufnahmen zur Festlegung der Probenahmestellen im Rheinquerschnitt bei km 171.35 (Palmrainbrücke), unpublished report (German) to Landeshydrologie und -geologie (by now Federal Office for Water and Geology), Berne.
- Naturaqua & GIUB (Institute of Geography, University of Berne) (1989): Markierversuch Rheinau-Basel. Beschaffung von Eingabedaten für ein Alarm- und Stofftransportmodell mittels Traceruntersuchungen, unpublished report (German) to Landeshydrologie und -geologie (by now Federal Office for Water and Geology), Berne.
- Naturaqua & GIUB (Institute of Geography, University of Berne) (1988): Markierversuch Rhein Basel. Verteilung des gereinigten Abwassers der “Pro Rheno Betriebs AG” im Rhein unter spezieller Berücksichtigung des Flussquerschnittes Km 171 (NADUF), unpublished report (German) to Landeshydrologie und -geologie (by now Federal Office for Water and Geology), Berne.
- Navada, S.V. (1991): Safety aspects of the use of artificial radioactive tracers in hydrology. In: *Use of artificial tracers in hydrology, IAEA-TECDOC-601*, 179–200. IAEA, Vienna.
- Neal, C., Christophersen, N., Neale, R., Smith, C.J., Whitehead, P.G., Reynolds, B. (1988): Chloride in precipitation and streamwater for the upland catchment of the River Severn, mid-Wales: some consequences for hydrochemical models. *Hydrological Processes*, 2, 155–165.
- Nebel, Ch. (1992): Limno-hydrologische Untersuchungen im Bledsee 1992. Diplom thesis, Institute of Hydrology, University of Freiburg.
- Neff, H.-P. (1995): Kalibrierung der Aare und der Mosel im Rhein-Alarm-Modell. Diplom thesis, Institute of Physical Geography, Chair in Hydrology, University of Freiburg.
- Neretnieks, I. (1980): Diffusion in the rock matrix. An important factor in radionuclide retardation. *Journal of Geophysical Research*, 85 (B8), 4379–4397.

- Nestmann, E.R., Kowbel, D.J., Ellenton, J. (1980): Mutagenicity in Salmonella of fluorescent dye tablets used in water tracing. *Water Research*, **14** (7), 901–902.
- Netter, R., Behrens, H. (1992): Application of different water tracers for investigation of constructed wetlands hydraulics. In: *Tracer Hydrology 92. Proceedings of the 6th International Symposium on Water Tracing, September 21–26 1992, Karlsruhe* (Hötzl, H., Werner, A., eds.), 125–130. Balkema, Rotterdam.
- Niehn, S., Kinzelbach, W. (1998): Artificial colloid tracer tests: development of a compact on-line microsphere counter and application to soil column experiments. *Journal of Contaminant Hydrology*, **35**, 249–259.
- Nienow, P., Sharp, M., Willis, I. (1998): Seasonal Changes in the Morphology of the Subglacial Drainage System, Haut Glacier D'arolla, Switzerland. *Earth Surface Processes and Landforms*, **23**, 825–843.
- Nienow, P. (1993): Dye tracer investigations of glacier hydrological systems. Dissertation, St. Johns College, Cambridge, 337 p.
- Nier, A.O. (1957): *Nuclear Masses and their Determination*. Pergamon Press, London, 158 p.
- Nimz, G.J. (1998): Lithogenic and Cosmogenic Tracers in Catchment Hydrology. In: *Isotope Tracers in Hydrology*, Kendall, C., McDonnell, J.J. (eds.), 319–338. Elsevier, Amsterdam.
- Nolte, E., Krauthan, P., Korschinek, G., Maloszewski, P., Fritz, P., Wolf, M. (1991): Measurements and interpretation of ^{36}Cl in groundwater, Milk River, Alberta, Canada, *Applied Geochemistry*, **6**, 435–445.
- Notter, B., MacMillan, L., Viviroli, D., Weingartner, R., Liniger, H.P. (2007): Impacts of environmental change on water resources in the Mt. Kenya region. *Journal of Hydrology*, **343**: 266–278.
- Nützmann, G., Thiele, M., Maciejewski, S., Joswig, K. (1998): Inverse modelling techniques for determining hydraulic properties of coarse-textured porous media by transient outflow methods. *Advances in Water Resources*, **3**, 273–284.
- Nydegger, P. (1976): Strömungen in Seen. Untersuchungen in situ und an nachgebildeten Modellseen. *Beiträge zur Geologie der Schweiz, Kleine Mitteilungen*, **66**. Berne.
- Nydegger, P. (1967): Untersuchungen über Feinstofftransport in Flüssen und Seen: über Entstehung von Trübungshorizonten und zuflußbedingten Strömungen im Brienzersee und einigen Vergleichseen. *Beiträge zur Geologie der Schweiz – Hydrologie*, **16**, 92 p. Berne.
- Nye, J.F. (1976): Water flow in glaciers: Jökulhlaups, tunnels and veins. *Journal of Glaciology*, **17**, 181–207.
- Oerter, H., Moser, H. (1982): Water storage and drainage within the firn of a temperate glacier (Verhagtferner, Ötztaler Alps, Austria). Hydrological Aspects of Alpine and High Mountain Areas. *IAHS Publication*, **138**, 71–81.
- Oerter, H. (1981): Untersuchungen über den Abfluss aus dem Vernagtferner unter besonderer Berücksichtigung des Schmelzwasserabflusses im Firnkörper. *GSF-Bericht R 267*. Munich-Neuherberg.
- Ogawa, S., Baveye, P., Boast, C.W., Parlange, J.-Y., Steenhuis, T. (1999): Surface fractal characteristics of preferential flow patterns in field soils: evaluation and effect of image processing. *Geoderma*, **88** (3), 109–137.
- Ogrinc, N., Kanduc, T., Stichler, W., Vrec, P. (2008): Spatial and seasonal variations in $\delta^{18}\text{O}$ and δD values in the river Sava in Slovenia. *Journal of Hydrology*, **359**, 303–312.
- Öhrström, P., Hamed, Y., Persson, M., Berndtsson, R. (2004): Characterizing unsaturated solute transport by simultaneous use of dye and bromide. *Journal of Hydrology*, **289**, 23–35.
- Öhrström, P., Persson, M., Albergel, J., Zante, P., Nasri, S., Berndtsson, R., Olsson, J. (2002): Field-scale variation of preferential flow as indicated from dye coverage. *Journal of Hydrology*, **257**, 164–173.

- O'Neil, J.R. (1968): Hydrogen and oxygen isotope fractionation between ice and water. *Journal of Physical Chemistry*, **72**, 3683–3684.
- Onodera, S., Kobayashi, M. (1995): Evaluation of seasonal variation in bypass flow and matrix flow in a forest soil layer using bromide ion. In: *Tracers in Hydrology*, Leibundgut, Ch. (ed.). IAHS Publication, **229**, 99–108.
- Ossman, D.J., Schnoor, J.L. and Stumm, W. (1988): Predicting the effects of a pesticide release to the Rhine river. *Journal of Water Pollution Control Federation*, **60** (10) 1806–1812.
- Oster, H., Sonntag, C., Münnich, K.O. (1996): Groundwater age dating with chlorofluorocarbons. *Water Resources Research*, **32**, 2989–3001.
- Oteze, G.E., Foyose, E.A. (1998): Regional developments in the hydrogeology of the Chad Basin. *Water Resources*, **1** (1), 9–29.
- Ozima, M., Podozek, F.A. (1983): *Noble Gases Geochemistry*. Cambridge University Press, Cambridge, 366 p.
- Ozretisch, R.J. (1975): Mechanism for deep water renewal in Lake Nitinat. *Estuary and Coastal Marine Sciences*, **3**, 189–200.
- Palancar, M.C., Aragon, J.M., Sanchez, F., Gil, R. (2003): The determination of longitudinal dispersion coefficients in rivers. *Water Environment Research*, **75** (4), 324–335.
- Pang, L., Close, M., Goltz, M., Noonan, M., Sinton, L. (2005): Filtration and transport of *Bacillus subtilis* spores and the F-RNA phage MS2 in a coarse alluvial gravel aquifer: Implications in the estimation of setback distances. *Journal of Contaminant Hydrology*, **77** (3), 165–194.
- Parriaux, A., Liskay, M., Mueller, I., della Valle, G. (1988): *Guide Pratique Pour L'usage des Tracers artificiels en Hydrogéologie*. Swiss Geological Society, Hydrogeological Group, GEOLEP-Report-1988-001, 48 p. GEOLEP EPFL, Lausanne.
- Parsons, D.F., Hayashi, M., van der Kamp, G. (2004): Infiltration and solute transport under a seasonal wetland: bromide tracer experiments in Saskatoon, Canada. *Hydrological Processes*, **18**, 2011–2027.
- Patankar, S.V. (1980): *Numerical Heat Transfer and Fluid Flow*. McGraw-Hill Book Company, New York.
- Pearce, A.J., Stewart, M.K., Sklash, M.G. (1986): Storm runoff generation in humid headwater catchments. *Water Resources Research*, **22**, 1263–1272.
- Pearson, R.J., Comfort, S.D., Inskeep, W.P. (1992): Analysis of fluorobenzoate tracers by ion chromatography. *Soil Science Society of America Journal*, **56**, 1794–1796.
- Pearson, F.J. (1965): *Use of 13-C/12-C ratios to correct radiocarbon ages of material initially diluted by limestone*. In: Proc. 6th Intern. Conf. Radiocarbon and Tritium, Pulman, Washington, 357.
- Peeters, F., Wüest, A., Piepke, G., Imboden, D.M. (1996): Horizontal mixing in lakes. *Journal of Geophysical Research*, **101** (C8), 18361–18375.
- Peeters, F., Wüest, A., Imboden, D.M. (1993): Comparison of the results of tracer experiments in lakes with predictions based on horizontal mixing models. *Verhandlungen der Internationalen Vereinigung für Limnologie*, **25**, 69–74.
- Peeters, F., Wüest, A. (1992): Mess-System zur Erfassung dreidimensionaler Tracerverteilungen in Seen. *Gas, Wasser, Abwasser*, **72**, 456–61.
- Perillo, C.A., Gupta, S.C., Nater, E.A., Moncrief, J.F. (1999): Prevalence and initiation of preferential flow paths in a sandy loam with argillic horizon. *Geoderma*, **89**, 307–331.
- Perillo, C.A., Gupta, S.C., Nater, E.A., Moncrief, J.F. (1998): Flow velocity effects on the retardation of FD&C Blue no. 1 food dye in soil. *Soil Science Society of America Journal*, **62**, 39–45.

- Perlega, W. (1977): Der Nachweis von Fluoreszenzfarbstoffen mittel Aktivkohle. In: *3rd International Symposium of Underground Water Tracing, Ljubljana-Bled, Yugoslavia*, Gospodaric, R., Habic, P. (eds.), 195–201. Institute for Karst Research, Lubljana.
- Persson, M. (2005): Accurate Dye Tracer Concentration Estimations Using Image Analysis. *Soil Science Society of America Journal*, **69** (4), 968–975.
- Petermann, J., Leibundgut, Ch., Gossauer, M., Morgenthaler, D. Schudel, B. (1989): Markierversuch Rhein Rheinau-Basel, unpublished report (German), Institute of Geography, University of Berne.
- Peters, N.E., Ratcliffe, E.B., Tranter, M. (1998): Traceing solute mobility at the Panola Research Watershed, Georgia, USA: variations in Na^+ , Cl^- , H_4SiO_4 concentrations. *IAHS Publication*, **248**, 483–490.
- Peters, N.E., Coudrain-Ribstein, A. (eds.) (1997): *Hydrochemistry*. IAHS Publication, **244**, 344 + xii p.
- Peters, N.E., Hoehn, E., Leibundgut, Ch., Tase, N., Walling, D.E. (eds.) (1993): *Tracers in Hydrology*. IAHS Publication, **215**, 350 p.
- Petersen, C.T., Hansen, S., Jensen, H.E. (1997): Depth distribution of preferential flow patterns in a sandy soil as affected by tillage. *Hydrology and Earth System Sciences*, **4**, 769–776.
- Pike, E.B., Bufton, A.W.J., Gould D.J. (1969): The use of *Serratia indica* and *Bacillus subtilis* var. *niger* spores for tracing sewage dispersion in the sea. *Journal of Applied Bacteriology*, **32**, 206–216. London.
- Plata, A. (1991): Detection of leaks from reservoirs and lakes. In: *Use of artificial tracers in hydrology*, IAEA-TECDOC-601, 71–130. IAEA, Vienna.
- Plata, A. (1983): Single well techniques using radioactive tracers. In: *Tracer Methods in Isotope Hydrology*, IAEA-TECDOC-291, 17–46. IAEA, Vienna.
- Plummer, L.N., Busenberg, E. (2000): Chlorofluorocarbons. In: *Environmental tracers in subsurface hydrology* (Cook, P.G., Herczeg, A.L., eds.), Kluwer, Dordrecht, Netherlands, 441–478.
- Pointet, T. (1997): Hard Rock Hydrosystems. *IAHS Publication*, **241**, 168 p.
- Pollack, H.A., Stipp, J.J. (1967): Improved synthesis for methane and benzene radiocarbon dating. *International Journal of Applied Radio Isotopes*, **18**, 359–364.
- Poreda, R.J., Cerling, T.E., Solomon, D.K. (1988): Tritium and helium isotopes as hydrologic tracers in a shallow unconfined aquifer. *Journal of Hydrology*, **103**, 1–9.
- Przewłocki, K., Yurtsever, Y. (1974): Some conceptual mathematical models and digital simulation approach in the use of tracers in hydrological systems, in *Isotope Techniques in Groundwater Hydrology 1974*, Vol. 2, IAEA STI/PUB/373, 425–450, IAEA, Vienna.
- Ptak, T., Piepenbrink, M., Martac, E. (2004): Tracer tests for the investigation of heterogeneous porous media and stochastic modelling of flow and transport – a review of some recent developments. *Journal of Hydrology*, **294**, 122–163.
- Ptak, T., Schmid, G. (1996): Dual-tracer transport experiments in a physically and chemically heterogeneous porous aquifer: Effective transport parameters and spatial variability. *Journal of Hydrology*, **183** (1–2), 117–138.
- Quay, P.D., Broecker, W.S., Hesslein, R.H., Schindler, D.W. (1980): Vertical diffusion rates determined by tritium tracer experiments in the thermocline and hypolimnion of two lakes. *Limnology and Oceanography*, **25**, 201–218.
- Quinlan, J.F. (1986): Discussion of Groundwater Tracers. *Ground Water*, **24** (2), 253–259.
- Quinlan, J.F., Smart, P.L. (1977): Identification of dyes used in water-tracing: A suggestion to improve communication. In: *3rd International Symposium of Underground Water Tracing, Ljubljana-Bled, Yugoslavia*, Vol. 2, Gospodaric, R., Habic, P. (eds.), 263–267. Institute for Karst Research, Lubljana.

- Rainey, M.P., Tyler, A.N., Gilvear, D.J., Bryant, R.G., McDonald, P. (2003): Mapping intertidal estuarine sediment grain size distributions through airborne remote sensing. *Remote Sensing of Environment*, **86**, 480–490.
- Rajar, R., Četina, M., Širca, A. (1997): Hydrodynamic and water quality modelling: Case studies. *Ecological Modelling*, **101**, 209–228.
- Rajar, R. (1989): Numerical and Experimental simulation of two-dimensional turbulent flow. *Hydrosoft 1989, Proceedings of the International Conference on Hydraulic Engineering Software*, Portoroz, Yugoslavia, 1989.
- Rajar, R. and Cetina, M. (1986): Mathematical simulation of Two-Dimensional Lake Circulation. *Hydrosoft 1986, Proceedings of the International Conference on Hydraulic Engineering Software*, Southampton, UK: Springer, Berlin, New York, 315–324.
- Ramspacher, P., Zojer, H., Herzog, U., Gospodaric, R., Strucl, I., Stichler, W. (1986): Karsthydrologische Untersuchungen des Petzenmassivs unter Verwendung natürlicher und künstlicher Tracer. In: *Proceedings of the 5th International Symposium on Underground Water Tracing, Athens, Greece*, Morfis, A., Paraskevopoulou, P. (eds.), 377–388. Institute of Geology and Mineral Exploration, Athens.
- Rank, D., Adler, A., Araguas Araguas, L., Fröhlich, K., Rozanski, K., Stichler, W. (1998): Hydrological parameters and climatic signals derived from long-term tritium and stable Isotope teme series of the River Danube. In: *International Symposium on isotope techniques in the study of past and current environmental changes in the hydrosphere and the atmosphere*. Vienna, 14 – 18 April 1997 (IAEA-SM-349), 191–205. IAEA, Vienna.
- Rantz, S.E. (1982): Measurement and computation of streamflow: vol 1. Measurement of stage and discharge. *U.S. Geological Survey Water-Supply Paper* **2175**.
- Rao, B., Hathaway, D. (1989): A three-dimensional mixing-cell solute transport model and its application. *Ground Water*, **27**, 509–516.
- Rao, S.M. (1983): Use of radioactive tracers in studies on infiltration through unsaturated zone. In: *Tracer Methods in Isotope Hydrology*, IAEA-TECDOC-291, 47–66. IAEA, Vienna.
- Rathbun, R.E. (1979): Estimating the gas and dye quantities for modified tracer technique measurements of stream re-aeration coefficients. *U.S. Geological Water-Resources Investigations* 79–27, 42 p.
- Reber, U., Weingartner, R. (1986): Ökologische und tracerhydrologische Untersuchungen zum Einfluss der Kläranlage Orpund auf ein überdüngtes Naturschutzgebiet. *Gas, Wasser, Abwasser*, **66** (3), 146–149.
- Reeves, A.D., Henderson, D.E., Beven, K.J. (1998): Flow separation in undisturbed soils using multiple anionic tracers. Part 1. Analytical methods and unsteady rainfall and return flow experiments. *Hydrological Processes*, **10** (11), 1435–1450.
- Rekar, S., Hindak, F. (2002): *Aphanizomenon slovenicum* sp. nov.: Morphological and ecological characters of a new cyanophyte/cyanobacterial species from Lake Bled, Slovenia. *Annales de Limnologie*, **38** (4), 271–285.
- Renaud, J.-P., Cloke, H.L., Weiler, M. (2007): Comment on “An assessment of the tracer-based approach to quantifying groundwater contributions to streamflow” by J.P. Jones, Sudicky, E.A., Brookfield, A.E., Park, Y.J., *Water Resources Research*, **43**, W02407, doi:10.1029/2005WR004130.
- Rice, K.C., Hornberger, G.M. (1998): Comparison of hydrochemical tracers to estimate source contributions to peak flow in a small forested catchment. *Water Resources Research*, **34**, 1755–1766.
- Richards, L.A. (1931): Capillary conduction of liquids through porous media. *Physics*, **1**, 318–333.
- Rieg, A. (1995): Karte IV Konfliktbereiche 1:50000. In: *Karstwasseruntersuchungen im Gebiet Churfürsten/Alvier – Kurzbericht*, Leibundgut, Ch., Vonderstrass, I. (red.), Bergkvist, S.,

- Abramowski, C., Paul, H., report (German), Amt für Umweltschutz des Kantons St. Gallen., St. Gallen St. Gallen.
- Rieg, A. (1994): Zur Hydrologie im Karstgebiet Churfisten / Alvier. Dissertation, Institute of Hydrology, University of Freiburg.
- Rieg A., Leibundgut, Ch., Brand, M., Ries, Th. (1993): Interactions between Karst and porous groundwater investigated by tracer experiments. *IAHS Publication*, **215**, 253–261.
- Rieg, A., Leibundgut, Ch. (1992): Gauging of high variable discharge using tracer dilution method. In: *Tracer Hydrology 92. Proceedings of the 6th International Symposium on Water Tracing, September 21–26 1992, Karlsruhe*, Hötzl, H., Werner, A. (eds.), 287–289. Balkema, Rotterdam.
- Rijtema, P.E. (1969): Soil moisture forecasting. *Nota* **513**, Institute for Land and Water Management Research, Wageningen, 28 p.
- Rismal, M. (1980): Presoja posameznih metod za sanacijo Blejskega jezera. [The judgement of individual methods for sanitation the Lake of Bled]. *Gradbeni vestnik* **29**, 34–46. Ljubljana.
- Robson, J.E. (1956): A bacterial method for tracing sewage pollution. *Journal of Applied Bacteriology*, **19** (2), 243–246.
- Rodhe, A. (1998): Snowmelt-dominated systems. In: *Isotopes in Catchment Hydrology*, (Kendall, C., Mc Donnell, J.J. eds.), 391–434. Elsevier, Amsterdam.
- Rohden, C. von, Ilmberger, J. (2001): Tracer experiment with sulfur hexafluoride to quantify the vertical transport in a meromictic pit lake. *Aquatic Sciences*, **63**, 417–431.
- Roldao, J., Pegly, J., Leal, G. (1997): In situ determination of the dilution efficiency of submarine sewage outfall's with the help of fluorescent dye tracers. In: *Tracer Hydrology 97. Proceedings of the 7th International Symposium on Water Tracing 26–31 May 1997, Portoroz, Slovenia*, Kranjc, A. (ed.), 143–149. Balkema, Rotterdam.
- Roldao, J.S.F. (1991): Appraisal of the ^{85}Kr and propane methods to determine reaeration rate coefficients in large rivers. In: *Use of artificial tracers in hydrology. IAEA-TECDOC-601*, 45–60. IAEA, Vienna.
- Ross, J.H., Rieg, A., Leibundgut, Ch. (2001): Tracer study on the tectonic control of the drainage system in the the contact karst zone of Lake Voralp (Swiss Alps). *Acta Carsologica*, **30** (2), 203–213. Ljubljana.
- Rossi, P., De Carvalho-Dill, A., Müller, I., Aragno, M. (1994): Comparative tracing experiments in a porous aquifer using bacteriophages and fluorescent dye on a test field located at Wilerwald (Switzerland) and simultaneously surveyed in detail on a local scale by radio-magneto-tellury (12–240 kHz). *Environmental Geology*, **23**, 192–200.
- Rossi, P. (1994): Advances in biological tracer techniques for hydrology and hydrogeology using bacteriophages. Dissertation, University of Neuchâtel, 200p.
- Rossi, P. (1992): Use of bacteriophages as groundwater tracers: Decay rate and adsorption. In: *Tracer Hydrology 92. Proceedings of the 6th International Symposium on Water Tracing, September 21–26 1992, Karlsruhe*, Hötzl, H., Werner, A. (eds.), 65–70. Balkema, Rotterdam.
- Rost, F.W.D. (1991): *Quantitative Fluorescence Microscopy*. Cambridge University Press, Cambridge, 250 p.
- Röthlisberger, H., Lang, H. (1987): Glacial Hydrology. In: *Glacial-fluvial Sediment Transfer*, Furnell, A.M., Clark, M.J. (eds.), 207–284. Wiley, Chichester.
- Röthlisberger, H., (1972): Water pressure in intra- and subglacial channels. *Journal of Glaciology*, **11** (62), 117–203.
- Rozanski, K., Araguás-Araguás, L., Gionfinatini, R. (1993): Isotopic patterns in modern global precipitation. In: *Climate Change in Continental Isotopic Records*, Swart, P., Lohmann, K., McKenzie, J., Savin, S. (eds.), *Geophysical Monograph Series*, **78**, American Geophysical Union, Washington.

- Ryan, R.J., Packman, A.I. (2006): Changes in streambed sediment characteristics and solute transport in the headwaters of Valley Creek, an urbanizing watershed. *Journal of Hydrology*, **323**, 74–91.
- Sabatini, D.A., Austin, T.A. (1991): Characteristics of Rhodamine WT and Fluorescein as adsorbing ground-water tracers. *Ground Water*, **29**, 341–349.
- Sabir, I.H., Torgersen, J., Haldorson, S. and Aleström, P. (1999): DNA tracers with information capacity and high detection sensitivity tested in groundwater studies. *Hydrogeology Journal*, **7**, 264–272.
- Saenger, N., Zanke, U.C.E. (2009): A depth – oriented view of hydraulic exchange patterns between surface water and the hyporheic zone: analysis of field experiments at the River Lahn, Germany. *Fundamental and Applied Limnology*, **61** (Special Issue: Advances in Limnology), 9–27.
- Salomons, W., Mook, W.G. (1986): Isotope geochemistry of carbonates in the weathering zone. In: *Handbook of environmental isotope geochemistry: The terrestrial environment*, Fritz, P., Fontes, J.C. (eds), 239–269. Elsevier, Amsterdam.
- Salvamoser, J. (1981): Vergleich der Altersbestimmung von Grundwasser mit Hilfe des Tritium- und Krypton-85-Gehalts. *Naturwissenschaften*, **68** (6), 328–329.
- Sambale, Ch., Peschke, G., Uhlenbrook, S., Leibundgut, Ch., Markert, B. (2000): Simulation of vertical water flow and bromide transport under temporarily very dry conditions. *IAHS Publication*, **262**, 339–345.
- Sanford, W., Langevin, C., Polemio, M., Povinec, P. (eds.) (2007): A New Focus on Groundwater–Seawater Interactions, Proceedings of Symposium HS1001 at IUGG2007, Perugia, July 2007, *IAHS Publication* **312**.
- Sanford, W.E., Solomon, D.K. (1998): Site Characterization and Containment Assessment with Dissolved Gases. *Journal of Environmental Engineering*, **122** (6), 572–574.
- Sanford, W.E., Shropshire, R.G., Solomon, D.K. (1996): Dissolved gas tracers in groundwater: Simplified injection, sampling, and analysis. *Water Resources Research*, **32** (6), 1635–1642.
- Sansoni, M., Schudel, P., Wagner, T., Leibundgut, Ch. (1988): Aquiferparameterermittlung im Porengrundwasser mittels fluoreszierender Tracer. *Gas, Wasser, Abwasser*, **129** (3), 141–48.
- Scanlon, B.R. (2000): Uncertainties in estimating water fluxes and residence times using environmental tracers in an arid unsaturated zone. *Water Resources Research*, **36** (2), 395–409.
- Scanlon, B.R. (1991): Evaluation of moisture flux from chloride data in desert soils. *Journal of Hydrology*, **128**, 137–156.
- Scheffer, F., Schachtschabel, P. (2008): *Lehrbuch der Bodenkunde*. 15th revised and extended edition. Springer, Heidelberg.
- Scheidegger, A.E. (1961): General theory of dispersion in porous media. *Journal of Geophysical Research*, **66**, 3273–3278.
- Scherrer, S., Naef, F., Fach, A.O., Cordery, I. (2007): Formation of runoff at the hillslope scale during intense precipitation. *Hydrology and Earth System Sciences*, **11** (2), 907–922.
- Schlather, M., Huwe, B. (2005a): A risk index for characterizing flow pattern in soils using dye tracer distributions. *Journal of Contaminant Hydrology*, **79**, 25–44.
- Schlather, M., Huwe, B. (2005b): A stochastic model for 3-dimensional flow patterns in infiltration experiments. *Journal of Hydrology*, **310**, 17–27.
- Schlatter, J.W., Wüst, A., Imboden, D.M. (1997): Hypolimnetic density currents traced by sulphur hexafluoride (SF₆). *Aquatic Sciences*, **59** (3), 225–242.
- Schlosser, P., Stute, M., Sonntag, C., Münnich, K.O. (1988): Tritium/3-Helium dating of shallow groundwater. *Earth and Planetary Science Letters*, **89** (3/4), 353–362.

- Schlotter, D. (2007): The spatio-temporal distribution of ^{18}O and ^2H of precipitation in Germany – an evaluation of regionalization methods. Diplom thesis, Institute of Hydrology, University of Freiburg.
- Schmid, G., Barczewski, B. (1995): Development and application of a fibre optic fluorimeter for in situ tracer concentration measurements in groundwater and soil. *IAHS Publication*, **229**, 13–20.
- Schnegg P.-A., Le Doucen O. (2006): Multispectral field fluorometer for tracer tests in waters of high natural fluorescence. In: Durán, J.J., Andreo, B. y carrasco, F. (Eds). Karst, climate change and groundwater. *Hidrogeología y Aguas Subterráneas*, **18**, 65–75. Madrid.
- Schnegg, P.A. (2002): An inexpensive field fluorometer for hydrogeological tracer tests with three tracers and turbidity measurement. *Groundwater and Human Development*, **3**, 1484–1488.
- Schnegg, P.A., Bossy, F. (2001): Sonde for Downhole Measurement of Water Turbidity and Dye Tracer Concentration. In: *New Approaches Characterizing Groundwater Flow. Proceedings of the 31st International Association of Hydrogeologists Congress 10–14 September 2001, Munich, Germany*, (eds Seiler, K.P., Wöhnlich, S.), 795–798. Swets & Zeitlinger, Lisse.
- Schnegg, P.A., Kennedy, K. (1998): A new borehole fluorometer for double tracer tests. In: *Mass transport in fractured aquifers and aquitards, May 14–16 1998*, Copenhagen. Geoscience Center Copenhagen.
- Schofield, S., Jankowski, J. (2004): Hydrochemistry and isotopic composition of NaHCO_3 -rich groundwaters from the Ballimore region, central New South Wales, Australia. *Chemical Geology*, **52**, 111–134.
- Schudel, P., Leibundgut, Ch. (1988): Untersuchungen über hydraulische Eigenschaften und Reinigungsleistung einer Sankfilterkläranlage. *Gas, Wasser, Abwasser*, **68** (8), 450–459.
- Schuler, T. (2002): Investigation of water drainage through an alpine glacier by tracer experiments and numericall modelling. Dissertation, Swiss Federal Institute of Technology Zurich.
- Schwarzenbach, R.P., Gschwend, P.M., Imboden, D.M. (1993): *Environmental Organic Chemistry*. VCH-Wiley, New York, 696 p.
- Schwerdtfeger, J. (2009): Assessment of water quality and hydrological functioning in the Pantanal wetland, Brazil. Diplom thesis, Institute of Hydrology, University of Freiburg.
- Schwinning, S., Davis, K., Richardson, L., Ehleringer, J.R. (2002): Deuterium enriched irrigation indicates different forms of rain use in shrub/grass species of the Colorado Plateau. *Oecologia*, **130**, 345–355.
- Seaberg, S., Seaberg, Z., Hooke, R. Leb, R., Wiberg, D. (1988): Character of engacial and subglacial drainage system in the lower part of Storglaciären, Seden. *Journal of Glaciology*, **34**, 557–572.
- Seaman, J.C. (1998): Retardation of fluorobenzoates tracers in highly weathered soil and groundwater systems. *Soil Science Society of America Journal*, **62**, 354–361.
- Seifert, O. (1996): Modellierungsansätz in der Karsthydrologie. Diplom thesis, Institute of Hydrology, University of Freiburg.
- Seiler, K.P., Wöhnlich, S. (eds.) (2001): *New Approaches Characterizing Groundwater Flow. Proceedings of the 31st International Association of Hydrogeologists Congress 10–14 September 2001, Munich, Germany*. Swets & Zeitlinger, Lisse, 1800 p.
- Selker, J.S., Thévenaz, L., Huwald, H., Mallet, A., Luxemburg, W., van de Giesen, N., Stejskal, M., Zeman, J., Westhoff, M., Parlange, M.B. (2006): Distributed fiber-optic temperature sensing for hydrologic systems. *Water Resources Research*, **42**, W12202. doi:10.1029/2006WR005326.
- Seo, I.W., Baek, K.O., Jeon, T.M. (2006): Analysis of transverse mixing in natural streams under slug tests. *Journal of Hydraulic Research*, **44** (3), 350–362.

- Shapiro, A.M., Renken, R.A., Harvey, R.W., Zygnerski, M.R., Metge, D.W. (2008): Pathogen and chemical transport in the karst limestone of the Biscayne aquifer: 2. Chemical retention from diffusion and slow advection. *Water Resources Research*, **44**, W08430. doi: 10.1029/2007WR006059.
- Shiau, B.J., Sabatini, D.A., Harwell, J.H. (1992): Sorption of Rhodamine WT as Affected by Molecular Properties. In: *Tracer Hydrology 92. Proceedings of the 6th International Symposium on Water Tracing, September 21–26 1992, Karlsruhe*, Hötzl, H., Werner, A. (eds.), 57–64. Balkema, Rotterdam.
- Shreve, R.L. (1972): Movement of waters in glaciers. *Journal of Glaciology*, **11** (61), 204–214.
- Siegenthaler, U. (1982): Bestimmung der Verweildauer von Grundwasser im Boden mit radioaktiven Umweltisotopen. *Gas, Wasser, Abwasser*, **52**, 283–290.
- Siline-Bekthourine, A.I. (1951): Hydrogéologie Spéciale, 1. Gossendarctvennoe Izdatelctvo Geologicheshoi Litertouri, Moscow
- Silliman, S.E., Dunlap, R., Fletcher, M., Schneegurt, M.A. (2001): Bacterial transport in heterogeneous porous media: Observations from laboratory experiments. *Water Resources Research*, **37**, 2699–2708.
- Simmers, I. (ed.) (1987): Estimation of Natural Groundwater Recharge. *Proceedings of the NATO Advanced Research Workshop on Estimation of Natural Recharge of Groundwater*. Springer, 1987, 510 p.
- Simpson, E.S., Duckstein, L. (1976): Finite state mixing-cell models. *Karst Hydrology and Water Resources*, Vol. 2, 489–508, Water Resources Publications, Fort Collins, Colorado.
- Simunek, J., Sejna, M., Saito, H., Sakai, M., van Genuchten, M.T. (2008): The HYDRUS-1D software package for simulating the one-dimensional movement of water, heat and multiple solutes in variably-saturated media. Version 4.0. Report Document, Riverside, California.
- Singha, K., Gorelick, S.M. (2005): Saline tracer visualized with three-dimensional electrical resistivity tomography. *Water Resources Research*, **41**, W05023, doi: 10.1029/2004WR003460.
- Sinreich, S., Goldscheider, N., Hötzl, H. (2002): Hydrogeologie einer alpinen Bergsturzmasse (Schwarzwassertal, Vorarlberg). *Beiträge zur Hydrogeologie*, **53**, 5–20.
- Sinton, L.W., Ching, S.B. (1987): An Evaluation of two Bacteriophages as Sewage Tracers. *Water, Air, and Soil Pollution*, **35**, 347–356.
- Sirin, A., Köhler, S., Bishop, K. (1998): Resolving flow pathways and geochemistry in a headwater forested wetland with multiple tracers. *IAHS Publication*, **248**, 337–342.
- Sklash, M., Farvolden, R. (1979): The role of Groundwater in Storm runoff. *Journal of Hydrology*, **43**, 45–65.
- Smart, P.L., Wilson, C.M. (1984): Two Methods for the Tracing of Pipeflow on Hillslopes. *Catena*, **11**, 159–168.
- Smart, P.L. (1982): A review of the toxicity of 12 fluorescent dyes used for water tracing. *Beiträge zur Geologie der Schweiz, Hydrologie* **28** I, 101–112. Berne.
- Smart, P.L., Laidlaw, I.M.S. (1977): Evaluation of some fluorescent dyes for water tracing. *Water Resources Research*, **13**, 15–33.
- Smart, P.L., Smith, D.I. (1976): Water tracing in tropical regions, the use of fluorometric techniques in Jamaica. *Journal of Hydrology*, **30**, 179–195.
- Smart, P.L. (1976): The Use of Optical Brighteners for Water Tracing. *Transactions of the British Cave Research Association*, **3** (2), 62–76.
- Smethie, W.M., Solomon, D.K., Shiff, S.L., Mathieu, G.G. (1992): Tracing groundwater flow in the Borden aquifer using krypton-85. *Journal of Hydrology*, **130**, 279–297.
- Smettem, K.R.J., Collis-George, N. (1985): Statistical characterization of soil biopores using a soil peels method. *Geoderma*, **36**, 27–36.

- Smettem, K.R.J., Trudgill, S.T. (1983): An evaluation of some fluorescent and non-fluorescent dyes in the identification of water transmission routes in soils. *Journal of Soil Science*, **34**, 45–56.
- Solomon, D.K., Cook, P.G. (2000): ^3H and ^3He . In Cook, P.G., Herczeg, A.L. (eds.): *Environmental Tracers in Subsurface Hydrology*, 397–424. Kluwer Academic Publishers, Boston, Dordrecht, London.
- Solomon, D.K., Cook, P.G., Sanford, W.E. (1998): Dissolved Gases in subsurface Hydrology. In: *Isotope Tracers in Catchment Hydrology*, Kendall, C., McDonnell, J.J. (eds.), 291–318. Elsevier, Amsterdam.
- Speidel, U. (1991): Untersuchungen des Stofftransports in Fließgewässern mit der in-situ-Fluorometrie am Beispiel Rhein. Diplom thesis, Institute of Physical Geography, Chair in Hydrology, University of Freiburg.
- Spreafico, M., Gees, A. (1997): Manual “Determination of discharge in open channels using the LHG-dilution Method”, Landeshydrologie und-geologie (by now Federal Office of Water and Geology), Berne.
- Spreafico, M., Mazijk, A. van (1993): *Alarmmodell Rhein – Ein Modell für die operationelle Vorhersage des Transports von Schadstoffen im Rhein*, report (german), KHR-Bericht Nr. I-12, International Commission for the Hydrology of the Rhine basin (CHR), Lelystad.
- Spreafico, M., Leibundgut, Ch., Kühne, A. (1989): Abschätzung der Fließzeiten und Konzentrationen von mitgeführten Stoffen im Rhein. *Gas, Wasser, Abwasser*, **96** (9), 559–564.
- Spring, U. (1980): Intraglazialer Wasserabfluss: Theorie und Modellrechnungen. Mitteilungen VAW, 48, 197 p. Versuchsanstalt für Wasserbau, Hydrologie und Glaziologie, Swiss Federal Institute of Technology Zurich.
- Stamm, Ch., Sermet, R., Leuenberger, L., Wunderli, H., Wydler, H., Flühler, H., Gehre, M. (2002): Multiple tracing of fast solute transport in a drained grassland soil. *Geoderma*, **109**, 245–268.
- Steinebach, G. (1995): Das Alarmmodell Rhein und weitergehende Methoden zur Stofftransportberechnung. *Wasser & Boden*, **47** (10), 21–27.
- Stenborg, T. (1969): Studies of the internal drainage of glaciers. *Geografiska Annaler*, **51A**, 13–41.
- Stern, O., Volmer, M. (1919): Über die Abklingungszeit der Fluoreszenz. *Physikalische Zeitschrift*, **20**, 183–188.
- Stetzenbach, K.J., Jensen, S.L., Thompson, G.M. (1982): Trace enrichment of fluorinated organic acids used as groundwater tracers by liquid chromatography. *Environmental Science and Technology*, **16**, 250–254.
- Stevens, C.L., Lawrence, G.A., Hamblin, P. (2004): Horizontal dispersion in the surface layer of a long narrow lake. *Journal of Environmental Engineering Sciences*, **3** (5), 413–417.
- Stewart, M.K., McDonnell, J.J. (1991): Modeling baseflow soil water residence times from deuterium concentrations. *Water Resources Research*, **27**, 2682–2693.
- Stichler, W., Maloszewski, P., Moser, H. (1986): Modelling of river water infiltration using oxygen-18 data. *Journal of Hydrology*, **83**, 355–365.
- Stichler, W., Herrmann, A. (1978): Verwendung von Sauerstoff-18-Messungen für hydrologische Bilanzierungen. *Deutsche Gewässerkundliche Mitteilungen*, **22** (1), 9–13.
- Stuiver, M., Reimer, J. (1993): Extended ^{14}C data base and revised CALIB 3.0 ^{14}C age calibration program. *Radiocarbon*, **35** (1), 215–230.
- Stuiver, M., Kra, R. (eds.) (1986): Calibration issue. *Radiocarbon*, **28** (2B), 805–1030.
- Stumpp, C. (2008): Quantification of Heterogeneity in the unsaturated flow using environmental isotopes. *Freiburger Schriften zur Hydrologie*, **26**, 112 p. Freiburg.
- Stumpp, C., Maloszewski, P., Stichler, W., Maciejewski, S. (2007): Quantification of heterogeneity of the unsaturated zone based on environmental deuterium observed in lysimeter experiments. *Hydrological Sciences Journal*, **52**, 748–762.

- Sturm, K., Hoffmann, G., Langmann, B., Stichler, W. (2005): Simulation of ^{18}O in precipitation by the regional circulation model REMOiso. *Hydrological Processes*, **19**, 3425–3444.
- Sudicky, E.A., Jones, J.P., Brookfield, A.E. and Park, Y.J. (2007): Reply to comment by J.-P. Renaud et al. on “An assessment of the tracer-based approach to quantifying groundwater contributions to streamflow”. *Water Resources Research*, **43**, W09602, doi:10.1029/2006WR005416.
- Sudicky, E.A., Frind, E.O. (1982): Contaminant transport in fractured porous media: analytical solution for a system of parallel fractures. *Water Resources Research*, **18**, 1634–1642.
- Sugisaki, R., Aoki, T. (1993): Application of inert Gases as Tracers in a Multi Well System. *The Journal of Earth and Planetary Sciences, Nagoya University*, **40**, 17–26.
- Sutton, D.J., Kabala, Z.J. Francisco, A., Vasudevan, D. (2001): Limitations and potential of commercially available Rhodamine WT as a groundwater tracer. *Water Resources Research*, **37** (6), 1641–1656.
- Suzuoki, T., Kumura, T. (1973): D/H and $^{18}\text{O}/^{16}\text{O}$ fractionation in the ice-water system. *Mass Spectroscopy*, **21**, 229–233.
- Sweeting, M.M. (1973): *Karst landforms*. Columbia University Press, New York.
- Szapiro, S., Steckel, F. (1967): Physical properties of heavy oxygen water. 2 Vapour pressure. *Transactions of the Faraday Society*, **63**, 883.
- Taupin, J.D., Gallaire, R., Arnaud, Y. (1997): Analyses isotopiques et chimiques des précipitations sahéliennes de la région de Niamey au Niger: implications climatologiques. In: *Hydrochemistry*, Peters, N.E., Coudrain-Ribstein, A. (eds). *IAHS Publication*, **244**, 151–162.
- Taupin, J.D., Coudrain-Ribstein, A., Gallaire, R., Zuppi, G.M., Filly, A. (2000): Rainfall characteristics (^{18}O , ^2H , ΔT and ΔH_r) in western Africa, regional scale and influence of irrigated areas. *Journal of Geophysical Research*, **105**, 11911–11924.
- Taylor, G.I. (1954): The dispersion of Matter in Turbulent Flow through a Pipe. *Proceedings of the Royal Society*, **223**, 446–468.
- Teuber, W., Wander, K. (1987): *Fliesszeiten im Rhein aus Flügelmessungen*, report German Federal Institute of Hydrology (BfG), BfG-0392, Koblenz.
- Thatcher, L.L., Janzer, V.J., Edwards, R.W. (1977): Methods for determination of radioactive substances in water and fluvial sediments. *Techniques of Water- Resources Investigations of the U.S. Geological Survey*, Book 5, Chapter A5, 79–81. U.S. Geological Survey, Denver.
- Tilch, N., Uhlenbrook, S., Diidzun, J., Zilgens, B., Kirnbauer, R., Markart, G. (2004): Hochwasser-relevante Wasserumsatzräume und hydrologische Prozesse im Löhnersbacheinzugsgebiet (Kitzbüheler Alpen, Österreich). In: *Tagungsband zum Tag der Hydrologie 2004*, Potsdam.
- Timeus, G. (1926): Le indagini sull’origini delle acque sotterranee. In: *Duemila Grotte*, Bertarelli, I.V., Timeus, E. (eds.), 153–166. Touring Club Italiano, Milano.
- Tolstikhin, I. & Kamensky, I (1969): Determination of groundwater ages by the $^3\text{H} - ^3\text{He}$ method. Translation from *Geokhimiya*, No 8, 1027–1029. *Geochemistry international*, 1969, **7–8**, 810–811.
- Tranter, M., Sharp, M.J., Lamb, H.R., Brown, G.H., Hubbard, B.P., Willis, C.I. (2002): Geochemical weathering at the bed of Haut Glacier d’Arolla, Switzerland – a new model. *Hydrological Processes*, **16** (5), 959–993.
- Tromp-van Meerveld, H.J., McDonnell, J.J. (2006): Threshold relations in subsurface storm flow: 2. The fill and spill hypothesis. *Water Resources Research*, **42**, W02411, doi:10.1029/2004WR003800.
- Tsujimura, M., Tanaka, T., Onda, Y. (1998): Effet of subsurface flow on the isotopic composition of soil water in headwater basins. *IAHS Publication*, **248**, 343–352.
- Turin, H.J., Groffman, A.R., Wolfsberg, L.E., Roach, J.L., Strietelmeier, B.A. (2002): Tracer and radionuclide sorption to vitric tuffs of Busted Butte, Nevada. *Applied Geochemistry*, **17**, 825–836.

- Turner, J.V., Barnes, D.J. (1998): Modeling of Isotopes and Hydrogeochemical Responses in Catchment Hydrology. In: *Isotope Tracers in Catchment Hydrology*, Kendall, C., McDonnell, J.J. (eds.), 723–755. Elsevier, Amsterdam.
- Turner, J., Macpherson, D., Stokes, R. (1987): Mechanism of catchment flow processes using natural variations in deuterium and oxygen-18. *Journal of Hydrology*, **94**, 143–162.
- UBA (Umweltbundesamt) (1996): Toxicological tests for fluorescent tracers, unpublished report, Federal Environment Agency, Germany.
- Uddin, M.K., Dowd, J.F., Wenner, D.B. (1999): Krypton Tracer Test to characterize the Recharge of Highly Fractured Aquifer in Lawrenceville, Georgia. In: *Proceedings of the 1999 Georgia Water Resources Conference, held March 30-31, at the University of Georgia*, Hatcher, K.J. (ed.), 516–519. Institute of Ecology, University of Georgia, Athens.
- Uhlenbrook, S., Didszun, J., Wenninger, J. (2008): Source areas and mixing of runoff components at the hillslope scale – a multi-technical approach. *Hydrological Sciences Journal*, **53** (4), 741–753.
- Uhlenbrook, S., Didszun, J., Leibundgut, Ch. (2005): Runoff Generation Processes at Hillslopes and Their Susceptibility to Global Change. In: *Mountain Research Initiative – Global Change and Mountain Regions*, Huber, U. (ed.), Springer, Dordrecht.
- Uhlenbrook, S., Wenninger, J., Didszun, J., Tilch, N. (2005): Use of electrical resistivity tomography (ERT) and tracers to explore flow pathways and residence times at the hillslope scale. *Geophysical Research Abstracts*, **7**, 2nd GA, EGU-A-04948.
- Uhlenbrook, S., Sieber, A. (2005): On the value of experimental data to reduce the prediction uncertainty of a process-oriented catchment model. *Environmental Modelling & Software*, **20** (1), 19–32.
- Uhlenbrook, S., Tilch, N., Johst, M., Kirnbauer, R. (2004): Hochwasserrelevante Hangaquifere im Löhnersbachgebiet (Kitzbüheler Alpen) – tracerhydrologische Prozessforschung und N/A-Modellierung. In: *Hydrogeologie regionaler Aquifere, FH-DGG Tagung, Darmstadt*.
- Uhlenbrook, S., Roser, S., Tilch, N. (2004): Development of a distributed, but conceptual catchment model to represent hydrological processes adequately at the meso scale. *Journal of Hydrology*, **291**, 278–296.
- Uhlenbrook, S., McDonnell, J., Leibundgut, Ch. (guest. eds) (2003): Runoff Generation and Implications for River Basin Modelling, Special issue of *Hydrological Processes*, **17** (2), 197–512.
- Uhlenbrook, S., Hoeg, S. (2003): Quantifying uncertainties in tracer-based hydrograph separations: a case study for two-, three- and five-component hydrograph separations in a mountainous catchment. *Hydrological Processes*, **17** (2), 431–453.
- Uhlenbrook, S., Leibundgut, Ch. (2002): Process-oriented catchment modelling and multiple-response validation. *Hydrological Processes*, **16**, 423–440.
- Uhlenbrook, S., Frey, M., Leibundgut, Ch., Maloszewski, P. (2002): Hydrograph separations in a mesoscale mountainous basin at event and seasonal timescales. *Water Resources Research*, **38** (6), 1096. doi:10.1029/2001WR000938.
- Uhlenbrook, S., Leibundgut, Ch., Maloszewski, P. (2000): Natural tracers for investigating residence times, runoff components and validation of a rainfall-runoff model. *IAHS Publication*, **262**, 465–472.
- Uhlenbrook, S., Leibundgut, Ch. (2000a): Development and validation of a process oriented catchment model based on dominating runoff processes. *Physics and Chemistry of the Earth (B)*, **25** (7–8), 653–657.
- Uhlenbrook, S., Leibundgut, Ch. (2000b): Process-oriented catchment modelling and multiple-response validation. In: *On the Future of distributed hydrological modelling in Hydrology, Intern. Franqui Chair Workshop, Leuven, Belgium, 12–15 April 2000*, Leuven, Beven, K. (ed).

- Uhlenbrook, S., Leibundgut, Ch. (1999): Integration of tracer information into the development of a rainfall-runoff-model. *IAHS Publication*, **258**, 93–100.
- Uhlenbrook, S. (1999): Untersuchung und Modellierung der Abflußbildung in einem mesoskali-gen Einzugsgebiet. *Freiburger Schriften zur Hydrologie*, **10**, 201 p. Freiburg.
- UNESCO (1973 with Supplements 1975, 1977 and 1983): Groundwater studies: an international guide for research and practice. UNESCO, Paris.
- Upstill-Goddard, R.C., Wilkins, C.S. (1995): The potential of SF₆ as a geothermal tracer. *Water Research*, **29** (4), 1065–1068.
- Urey, H.C. (1947): The thermodynamic properties of isotopic substances. *Journal of the Chemical Society*, May 1947, 562–581.
- USGS (2008): *The Reston Chlorofluorocarbon Laboratory*. <http://water.usgs.gov/lab> (accessed 21 April 2009).
- Vanderborght, J., Gähwiler, P., Wydler, H., Schultze, U., Flühler, H. (2002): Imaging Fluorescent Dye Concentrations on Soil Surfaces: Uncertainty of Concentration Estimates. *Soil Science Society of America Journal*, **66**, 760–773.
- Van Der Meer, B.W., Coker, G., Chen, S.S.-Y. (1994): *Resonance energy transfer: theory and data*. Wiley VCH, New York.
- Van Genuchten, M.T. (1980): A closed-form equation for predicting the hydraulic conductivity of unsaturated soils. *Soil Science Society of America Journal*, **44**, 892–898.
- Van Genuchten, M.T., Wierenga, P.J. (1977): Mass transfer studies in sorbing porous media: 2. Experimental evaluation with tritium (³H₂O). *Soil Science Society of America Journal*, **4**, 272–278.
- Van Ommen, H.C., Dekker, L.W., Dijsma, R., Hulsof, J., van der Molen, W.H. (1988): A new technique for evaluating the presence of preferential flow paths in nonstructured soils. *Soil Science Society of America Journal*, **52**, 1192–1193.
- Van Ommen, H.C. 1985. The “mixing-cell” concept applied to transport of non-reactive and reactive components in soils and groundwater. *Journal of Hydrology*, **78**, 201–213.
- Van Stiphout, T.P.J., van Lanen, H.A.J., Boersma, O.H., Bouma, J. (1987): The effect of bypass flow and internal catchment of rain on the water regime in a clay loam grassland soil. *Journal of Hydrology*, **95**, 1–11.
- Vatne, G., Etzelmiiller, B., Sollid, J.L., Strand Odegrd, R. (1995): Hydrology of a polythermal glacier, Erikbreen, Northern Spitsberge. *Nordic Hydrology*, **26**, 169–190.
- Verboeket-Klavers, H., Sprokkereef, E. (1994): Alarmmodell Rhein. Systemdokumentation, International Commission for the Hydrology of the Rhine basin (CHR), Lelystad.
- Vereecken, H., Döring, U., Hardelauf, H., Jaekel, U., Hashagen, U., Neuendorf, O., Schwarze, H., Seidemann, R. (2000): Analysis of solute transport in a heterogeneous aquifer: the Krauthausen field experiment. *Journal of Contaminant Hydrology*, **45**, 329–358.
- Vereecken, H., Maes, J., Feyen, J. (1990): Estimating unsaturated hydraulic conductivity from easily measured soil properties. *Soil Science*, **149**, 1–12.
- Verga, G., Zuppi, G. (1986): Groundwater Tracing in Landfill and Garbage Deposits Studies in Piedmont Region. In: *Proceedings of the 5th International Symposium on Underground Water Tracing, Athens, Greece*, Morfis, A., Paraskevopoulou, P. (eds.), 331–339. Institute of Geology and Mineral Exploration, Athens.
- Verwoerd, P. (1990): Alarmmodell “Rhein”, Systemdokumentation, report (German), Institute for Inland Water Management and Waste Water Treatment, DBW-RIZA – 90.085X, Lelystad.
- Vilks, P., Bachinski, D.B. (1996): Colloid and suspended particle migration experiments in a granite fracture. *Journal of Contaminant Hydrology*, **21**, 269–279.
- Viriot, M.L., André, J.C. (1989): Fluorescent dyes: A search for new tracer for hydrology. *Analisis*, **17**, 97–111.

- Vitvar, T., Balderer, W. (1997): Estimation of mean water residence times and runoff generation by ^{18}O measurements in pre-Alpine catchment. *Applied Geochemistry*, **12**, 787–796.
- Viviroli, D., Dürri, H.H., Messerli, B., Meybeck, M., Weingartner, R. (2007): Mountains of the world, – water towers for humanity: Typology, mapping, and global significance. *Water Resources Research*, **43**, W07447, doi:10.1029/2006WR005653.
- Vogel, J.C. (1993): Variability of carbon isotope fractionation during photosynthesis. In: *Stable Isotopes and Plant Carbon – Water Relations*, Ehleringer, A.E., Farquhar, G.D. (eds.), Academic Press, San Diego, California, 29–38.
- Vogel, J.C., Lerman J.C., Mook W.G. (1975): Natural isotopes in surface and groundwater from Argentina. *Hydrological Sciences Bulletin*, **20**, No. 2, 203–221.
- Vogel, J.C. (1970): Carbon-14 dating of groundwater. In: *Isotope Hydrology 1970*, 225–239. IAEA, Vienna.
- Vogt, H.J. (1976): Isotopentrennung bei der Verdunstung von Wasser. Dissertation, Institute of Environmental Physics, University of Heidelberg.
- Volk, C.M., Elkins, J.W., Fahey, D.W., Dutton, G.S., Gilligan, J.M., Loewenstein, M., Podolske, J.R., Chan, K.R., Gunson, M.R. (1997): Evaluation of source gas lifetimes from stratospheric observations. *Journal of Geophysical Research*, **102** (D21), 25543–25564.
- Vrhovsek, D., Kosi, G., Zupan, M. (1981): Ocena stanja Blejskega jezera v obdobju od septembra 1979 do decembra 1980 na podlagi fitoplanktona in fizikalnekemičnih parametrov. [The condition of Lake Bled from September 1979 to December 1980 evaluated with phytoplankton and physico-chemical parameters]. *Biološki Vestnik* **29**: 157–180. Ljubljana.
- Wachtler, A. (2006): Groundwater Recharge from the Alluvium of an Ephemeral Stream: the Buffelsrivier, South Africa. Investigation of Direct and Indirect Recharge Processes Using Environmental Tracer and Modeling Approaches. Diplom thesis, Institute of Hydrology, University of Freiburg.
- Walker, J.F., Krabbenhoft, D.P. (1998): Groundwater and Surface Water Interactions in Riparian and Lake-Dominated Systems. In: *Isotope Tracers in Catchment Hydrology*, Kendall, C., McDonnell, J.J. (eds.), 467–486. Elsevier, Amsterdam.
- Wang, Z., Lu, J., Wu, L., Jury, W.A. (2002): Visualizing Preferential Flow Paths using Ammonium Carbonate and a pH Indicator. *Soil Science Society of America Journal*, **66**, 347–351.
- Wanninkhoff, R., Ledwell J.R., Broecker, W.S. (1985): Gas exchange – wind speed relation measured with sulfur hexafluoride on a lake. *Science*, **227**, 1224–1226.
- Ward, R.S., Harrison, I., Leader, R.U., Williams, A.T. (1997): Fluorescent polystyrene microspheres of colloidal and particulate materials: Examples of their use and developments in analytical technique. In: *Tracer Hydrology 97. Proceedings of the 7th International Symposium on Water Tracing 26–31 May 1997, Portoroz, Slovenia*, Kranjc, A. (ed.), 99–103. Balkema, Rotterdam.
- Watson, A.J., Ledwell, J.R. (2000): Oceanographic tracer release experiments using sulfur hexafluoride. *Journal of Geophysical Research*, **105** (C6), 14325–14337.
- Watson, A.J., Upstill-Goddard, R.C., Liss, P.S. (1991): Air-Sea gas exchange in rough and stormy seas measured by a dual tracer technique. *Nature*, **349**, 145–147.
- Watson, A.J., Liddicott, M.I., Ledwell, J.R. (1987): Perfluorodecalin and sulphur hexafluoride as purposeful marine tracers: some development and analysis techniques. *Deep-Sea Research*, **34**, 19–31. Oxford, Great Britain.
- Weihermüller, L., Siemens, J., Deurer, M., Knoblauch, S., Rupp, H., Göttlein, A., Pütz, T. (2007): In Situ Soil Water Extraction: A Review. *Journal of Environmental Quality*, **36**, 1735–1748. doi: 10.2134/jeq2007.0218.
- Weihermüller, L. (2005): Comparison of different soil water extraction systems for the prognoses of solute transport at the field scale using numerical simulations, field, and lysimeter

- experiments. *Schriften des Forschungszentrum Jülich, Umwelt/Environment* **55**. Forschungszentrum Jülich, Jülich.
- Weiler, M., McDonnell, J.J. (2007): Conceptualizing lateral preferential flow and flow networks and simulating the effects on gauged and ungauged hillslopes. *Water Resource Research*, **43**, W03403, doi:10.1029/2006WR004867.
- Weiler, M., Flühler, H. (2004): Inferring flow types from dye patterns in macroporous soils. *Geoderma*, **120**, 137–153.
- Weiler, M., McGlynn, B.L., McGuire, K.J., McDonnell, J.J. (2003): How does rainfall become runoff? A combined tracer and runoff transfer function approach. *Water Resources Research*, **39** (11), 1315. doi:10.1029/2003WR002331.
- Weiler, M., Naef, F. (2003): An experimental tracer study of the role of macropores in infiltration in grassland soils. *Hydrological Processes*, **17** (2), 477–493.
- Weiler, M. (2001): Mechanisms Controlling Macropore Flow During Infiltration-Dye Tracer Experiments and Simulations. Dissertation, Swiss Federal Institute of Technology Zurich, 151 p.
- Weiler, M., Naef, F., Leibundgut, Ch. (1998): Study of runoff generation on hillslopes using tracer experiments and a physically based numerical hillslope model. *IAHS Publication*, **248**, 353–362.
- Weingartner, R., Viviroli, D., Schädler, B. (2007): Water Resources in mountain regions: A methodological approach to assess the water balance in a highland-lowland-system. *Hydrological Processes*, **21** (5), 578–585.
- Weise, S., Moser, H. (1987): Groundwater dating with helium isotopes, in *Isotope Techniques in Water Resources Evaluation*, IAEA-STI/PUB/757. IAEA, Vienna, 105–126.
- Weiss, S., Müller, A., Schulz, W., Weber, W.H. (2008): Identifizierung von Farbstoff-Tracern und deren Metaboliten nach HPTLC/AMD und Nano-Chip-LC/QTOF-MS. Poster presentation Zweckverband Landeswasserversorgung, Stuttgart, 2008.
- Wels C., Cornett R.J., Lazerte, B.D. (1991): Hydrograph Separation: A Comparison of Geochemical and Isotopic Tracers. *Journal of Hydrology*, **122**, 253–274.
- Wenninger, J. (2007): Prozesshydrologische Untersuchung im System Boden-Vegetation-Atmosphäre. *Freiburger Schriften zur Hydrologie*, **25**, 151 p. Freiburg.
- Wenninger, J., Uhlenbrook, S., Tilch, N., Leibundgut, Ch. (2004): Experimental evidence of fast groundwater responses on a hillslope / floodplain area in the Black Forest Mountains, Germany. *Hydrological Processes*, **18** (17), 3315–3322.
- Wernli, H.R. (2007): Abflussmessung mittels Tracerverdünnung – Pumpmethode mit Pocket-fluorimeter. *Hydrologie und Wasserbewirtschaftung*, **51** (1), 2–8.
- Wernli, H.R. (2003): Einführung in die Tracerhydrologie, Sommersemester 2003. Lecture Notes, Institute of Geography, University of Berne.
- Wernli, H.R. (1996): Weiterentwicklung der Abflussmessung nach dem Tracerverdünnungsverfahren, unpublished report, Institute of Geography, University of Berne, Switzerland.
- Wernli, H.R., Leibundgut, Ch. (1993): Der Einsatz von Tracermethoden in komplexen Molasseaquiferen. *Steirische Beiträge zur Hydrogeologie*, **44**, 173–191. Graz.
- Wernli, H.R. (1986): Naphtionat – ein neuer Fluoreszenztracer zur Wassermarkierung. *Deutsche Gewässerkundliche Mitteilungen*, **30**, 16–19.
- Werthemann, B. (1980a): Experimente mit fluoreszierenden Tracern zur Erforschung der Diffusionsverhältnisse im Zürichsee. *Vierteljahrsschrift der Naturforschenden Gesellschaft Zürich*, **125** (3), 249–258.
- Werthemann, B. (1980b): Physikalisch-limnologische Untersuchungen mittels fluoreszierender Tracer. Diplom thesis, Institute of Geography, University of Berne.

- White, D.S., Elzinga, C.H., Hendricks, S.P. (1987): Temperature Patterns within the Hyporheic Zone of a Northern Michigan River. *Journal of the North American Benthological Society*, **6** (2), 85–91.
- White, W.B. (1967): Modifications of fluorescein dye groundwater tracing techniques, in Fachtagung über die Anwendung von Markierungsstoffen zur Verfolgung unterirdischer Wässer in Graz vom 28. März bis 1. April 1966. Specialists' Conference on the Tracing of Subterranean Waters in Graz, March 28–April 1, 1966 (Maurin, V., Zötl, J., eds). *Steirische Beiträge Hydrogeologie*, **18/19**, 151–158. Graz.
- Wiesner, H. (1989): Untersuchungen zur Stoffausbreitung im Oberrhein mit Hilfe von Tracerversuchen. Diplom thesis, Institute of Physical Geography, Chair in Hydrology, University of Freiburg.
- Williams, R.T., Bridges, J.W. (1964): Fluorescence of solutions: A review. *Journal of Clinical Pathology*, **17**, 371–394.
- Wilson, J.F. (1968): *Fluorometric procedures for dye tracing*. In: *Techniques of Water-Resources Investigations of the USGS, Book 3, Chapter. A 12*. (updated version 1986 available at <http://pubs.usgs.gov/twri/twri3-a12/> accessed 21 April 2009).
- Wilson, R.D., McKay, D.M. (1996): SF₆ as Conservative Tracer in Saturated Media with High Intragranular Porosity or High Organic Carbon Content. *Ground Water*, **34** (2), 241–249.
- Wilson, R.D., McKay, D.M. (1995): Direct Detection of Residual Nonaqueous Phase Liquid in the Saturated Zone Using SF₆ as a Partitioning Tracer. *Environmental Science and Technology*, **29**, 1255–1258.
- Wilson, R.D., McKay, D.M. (1993): The Use of Sulphur Hexafluoride as a Conservative Tracer in Saturated Sandy Media. *Ground Water*, **31** (5), 719–724.
- Wissmeier, L., Uhlenbrook, S. (2007): Distributed, high-resolution modelling of ¹⁸O signals in a mesoscale catchment. *Journal of Hydrology*, **332**, 497–510.
- Woessner, W.W., Ball, P.N., DeBorde, D.C., Troy, T.L. (2001): Viral Transport in a Sand and Gravel Aquifer Under Field Pumping Conditions. *Ground Water*, **39** (6), 886–894.
- Wolfbeis, O.S., Furlinger, E., Kroneis, H., Marsoner, H. (1983): Fluorometric Analysis. *Fresenius Zeitschrift für Analytische Chemie*, **320**, 271–273.
- Wolkersdorfer, Ch. (2001): Tracer Tests in Flooded Underground Mines. In: *New Approaches Characterizing Groundwater Flow. Proceedings of the 31st International Association of Hydrogeologists Congress 10–14 September 2001, Munich, Germany*, Seiler, K.P., Wohnlich, S. (eds.), 229–233. Swets & Zeitlinger, Lisse.
- Wood, W.W. (1999): Use and Misuse of the Chloride-Mass Balance Method in Estimating Ground Water Recharge. *Ground Water*, **37** (1), 2–3.
- Wood, W.W., Sanford, W.E. (1995): Chemical and isotopic methods for quantifying groundwater recharge in a regional, semiarid environment. *Ground Water*, **33** (3), 458–468.
- Wörman, A., Packman, A.I., Johansson, H., Jonsson, K. (2002): Effect of flow-induced exchange in hyporheic zones on longitudinal transport of solutes in streams and rivers. *Water Resources Research*, **38** (1), 1001, doi:10.1029/2001WR000769.
- Wright, K.E., Hull, L.C. (2004): An Evaluation of Tracers for Use in Vadose Zone Investigations at the Idaho National Engineering and Environmental Laboratory. Idaho Completion Project, Project No. 23378. Prepared for the U.S. Department of Energy Assistant Secretary for Environmental Management under DOE Idaho Operations Office Contract DE-AC07-99ID13727.
- Yoshida, S., Muramatsu, Y., Uchida, S. (1992): Studies on the sorption of I[−] (iodide) and IO₃[−] (iodate) onto Andosols. *Water, Air and Soil Pollution*, **63** (3–4), 321–329.

- Yurtsever, Y., Payne, B.R. (1985): Time-variant linear compartmental model approach to study flow dynamics of a karstic groundwater system by the aid of environmental tritium (a case study of south-eastern karst area in Turkey). *IAHS Publication*, **161**, 545–561.
- Yurtsever, Y., Gat, J. (1981): Atmospheric waters. In: *Stable Isotope Hydrology – Deuterium and Oxygen-18 in the Water Cycle*, Gat, J., Gonfiantini, R. (eds.), 103–142. IAEA, Vienna.
- Zaradny, H. (1993): *Groundwater Flow in Saturated and Unsaturated Soil*. Balkema, Rotterdam, 279 p.
- Zellweger, G.W. (1994): Testing and comparison of four ionic tracers to measure stream flow loss by multiple tracer injection. *Hydrological Processes*, **8** (2), 155–165.
- Zimmermann, U., Münnich, K.O., Roether, W. (1967): Downward movement of soil moisture traced by means of hydrogen isotopes. In: *Isotope techniques in the Hydrological Cycle*, Geophysical Monograph Series, 11 (G.E. Stout, ed.), American Geophysical Union, Washington, DC.
- Zoellmann, K., Kinzelbach, W., Fulda, C. (2001): Environmental tracer transport (^3H and SF_6) in the saturated and unsaturated zones and its use in nitrate pollution management. *Journal of Hydrology*, **240**, 187–205.
- Zollinger, H. (1991): *Color chemistry: syntheses, properties and applications of organic dyes and pigments*. VCH-Wiley, Weinheim, second, revised edition, 485 p.
- Zötl, J. (1974): *Karsthydrogeologie*. Springer, Vienna, 291 p.
- Zötl, J. (1967): Entwicklung und Anwendung der Sporentrift, in Fachtagung über die Anwendung von Markierungsstoffen zur Verfolgung unterirdischer Wässer in Graz vom 28. März bis 1. April 1966. Specialists' Conference on the Tracing of Subterranean Waters in Graz, March 28–April 1, 1966, (Maurin, V., Zötl, J., eds). *Steirische Beiträge Hydrogeologie*, **18/19**, 235–240. Graz.
- Zuber, A., Maloszewski, P. (2001): Lumped parameter models, in *Environmental isotopes in hydrological cycle, Principles and applications, Vol. 6 Modelling*, (W.G. Mook, ed.), IHP-V, Technical Documents in Hydrology No. 39, Vol. 6, 5–36. UNESCO, Paris.
- Zuber, A. (1983): On the environmental isotope method for determining the water balance of some lakes. *Journal of Hydrology*, **61**, 409–427.
- Zuber, A. (1974): Theoretical possibilities of the two-well pulse method. In: *Isotopes Techniques in Groundwater Hydrology*, IAEA-STI/PUB/373 IAEA, Vienna, 277–294.
- Zuber, A. (1970): Dispersion of tracer in flow through porous media and its aspects in application to hydrology. Sc. Biul. S. Staszic Academy of Mining and Metallurgy, No. 302; Mathematics-Physics-Chemistry, Biul. 7, AGH Kraków, 89 p.
- Zupan, M. (1989): The influence of ecosystem to fluorescent dyes. *Acta Carsologica*, **18**, 297–309. Ljubljana.
- Zupan, M. (1982): Einfluss der Wasserverschmutzung an der Zerstörung der Fluoreszenztracer. *Beiträge zur Geologie der Schweiz, Hydrologie* **28 I**, 79–89. Berne.
- Zvikelsky, O., Weisbrod, N. (2006): Impact of particle size on colloid transport in discrete fractures. *Water Resources Research*, **42** (12), W12S08. doi:10.1029/2006WR004873.

Index

References appearing in figures set in *italic*, references appearing in tables set in **bold**, references appearing in boxes B, references appearing in colour plates P

A

- α -Radiation 112, 113
- Aare, River 247
- AAS (Atomic Absorption Spectroscopy) **103**
- Ablation 304
- Advanced tracers 57
- AES (Atom Emission Spectroscopy) **103**
- Aerial photos 247
- Accident 8, 10, 252
 - accidental leaks, spills 248, 252
- Acid Red **60**
- Acid Yellow **60**
- Acid Blue 9 *see* Brilliant Blue
- Acid dissociation constant 115
- Acidic media, acidic environments 72, 83
- Actinometer (fluorescence actionmeter) 75
- Activatable tracers 58
- Active charcoal 100–2, 310
- Adiabatic cooling 26, 28–9, 29
- Advection-dispersion model 253
- Age dating
 - Argon-39 50
 - Carbon-14 13, 51
 - Krypton-85 13, 50, 51
 - CFCs, *see* Chlorofluorocarbons 13
 - SF₆ 13
 - Tritium 43
- Alberta, Canada 247
- Alert model 254–7, 273
- Aletsch glacier 307–8
- Alpine glaciers experiments 305, 306, 310–21
- Amidorhodamine G **60**, **67**, **73–4**, 74, 76, **82–3**, 86, **87**, 90, 91, 185, 192, 312
 - experiment in glacier 239–46
- Ammonium 42–3, 121, 293
- Ammonium carbonate 121
- Amphiphilic 76
- Analysis
 - active charcoal 101
 - FBA tracers 117
 - fluorescent tracers 89–95
 - gas tracers 119–120
 - isotopes 13–6
 - lycopodium spores 109
 - microspheres (fluorescent) 111
- Andarax catchment 53–6B
- Anion 76, 102–104, 106–7, 114–7, **114**, 214, 336
 - exclusion 76, 104
- Anthraquinones **60**, 66
- Aperture *see* Fissure aperture
- Apparent parameter 164
- Aqueous diffusion coefficient *see* (molecular) Diffusion coefficient
- Aquatic ecosystem 246
- Aquiclude 105
- Aquifer 1, 3–6, 10, 30, 39, 42, 44, 46–8, 53B, 57, 61, 76, 79, 82–5, 100, *101*, 105–111, 116, 119–20, 126–7, 130, 131, 140, *141*, 143–6, 149, 153, *154*, 161–3, 164–67, *165*, *166*, 172, 181–2, 185–86, 198–99, 202–04, 210–23, 224, **225**, 229, 239–52, 303, 304, 321, 323–5, 334, 339, 350, 352

Aquifer (*Continued*)

- black box 10, 12
 - dispersion model (DM) 162, 166, 167
 - estimation of tracer injection mass 185
 - exponential model 162
 - filtration capacity of aquifers 108, 239–46
 - Piston-Flow model 162–3, 163, 165–6, 166, 166, 167
 - vulnerability 203, 205–09
 - see also* Double-porosity aquifer
 - see also* Fissured aquifer
 - see also* Fractured aquifer
 - see also* Karst aquifer
 - see also* Porous aquifer
- Aquitard 165
- Argon-39 50, 119
- Arid regions 203
- Arid stream 190
- Artificial tracer 5, 8, 57–122, 58, 187, 204, 240, 248
 - column experiment 148–9
 - combined pumping-tracer test 149–50, 151
 - definition 8
 - double-porosity (fissured) medium
 - experiment 153, 154
 - ideal artificial tracer 123–54
 - modelling streams and rivers 158–160
 - modelling under saturated flow conditions 123–154
 - modelling under unsaturated flow conditions 154–158
 - assessment of vulnerability 208B, 209B
 - fields of application 57
 - required properties 66
 - main groups 57, 58
 - multi-flow systems 140–4, 141, 151, 152, 152
 - tritiated water (^3H) as 117
 - use in surface waters 250–1
 - western Greenland test 308
 - see also* deuterium ^2H ; dissolved gas tracers; drifting particles; fluorescent tracers; fluorobenzoic acids; nonfluorescent dyes; radioactive tracers; salt tracers
- Arrival time (of pollutant plume) 252
- ATH *see* International Association of Tracer Hydrology
- Attenuation 35
- Authorities, environmental 179
- Automatic fitting procedure 133, 174
- Automatic samplers 309

B

- β -emission 43
 - β -radiation 112, 113
- Background 10, 5, 188–94 192, 216, 274, 278, 308, 310, 335
 - fluorescence 67, 68, 88–9, 94–5, 101
 - electrical conductivity 194
 - natural background 94–5, 177, 188
 - salts 104–07
 - gas 116, 118–19
- Back-up chlorination 179
- Bacteria (as tracers) 9, 58, 79, 107, 108, 109–11, 218, 221
 - bacterial tracing tests 248
 - case study filtration 239–46
 - pathogenic bacteria 111
- Bacteriophages *see* Phages
- Bank infiltration 168–70
- Barometric formula 47
- Basel 254, 258
- Basic Violet 60
- Batch tests (fluorescent tracers) 81, 82
 - distribution coefficients from batch experiments 82
 - instruction 81
- Bavaria 35, 156, 219, 335
- Becquerel definition 112, 117
- Bessel function, modified 159
- Bias 38
- Biel, Lake 247
- Bio-absorption 294
- Biochemical decay 251
- Black-box models *see* lumped-parameter models
- Bled, Lake tracer experiments 282–99, 282, 284, 287, 288, 289, 290, 292, 294, 295, 296, 298
 - isobathic pattern 283
 - stratification 285
 - pattern of currents 290
- Bohinska, Lake (Slovenia) 355 P7
- Boltzmann constant 19
- Borax (sodium borate) 103
- Borehole 27, 48, 53B, 98, 101–2, 117, 181–2, 196–7, 204, 211, 216–21, 226, 227–28, 309, 312, 313, 314, 318, 319, 320, 326, 326–8, 328, 328–30
- Boron 9
- Boundary conditions 128, 130
- Breakthrough (curve) 188, 191, 209B, 24, 261, 263, 268
- Brilliant Blue 122, 230
- Brine 105

- Bromide-84, **103**, 105–6, 151, 118
 as tracer for visualization 121
 interference with Eosine 106
 Bromide-82, 223
 Brugga catchment *see* Dreisam
 Buffelsriver catchment, (South Africa) 196–8
 Buffering fluorescent tracer solutions 70
 Bypass outlet 243, **244**
- C**
¹⁴C-dating 13, 50–2
 C3 plants 52
 C4 plants 52
 Calibration (instruments, devices) 193
 Calibration of models *see* Model calibration
 Canada 18, 247, 238, 335
 Canadian lakes 247
 Carbocylfluorescein trisodium salt 60, 65
 Carbon isotopes 216–17
 Carbon-13 13
 Carbon-14 13
 Catchment, Catchment hydrology 170–2,
 321–47, 202
 delineation of catchments 208B
 subcatchments 207B
 arid catchment hydrology 322
 artificial tracers (case studies) 202–03, 207,
 218, 229, 230, 240, 246, 247–51, 305, 307,
 308, 322–25, 330, 347, 350
 flood generation 321
 groundwater exchange between aquifers 323,
 324
 groundwater exfiltration 323–4
 groundwater-surface water interactions 323
 hyporheic zone 324–5
 runoff generation processes 321
 geochemical tracers 322
 soil-plant-atmosphere system 322
 sublacustric and submarine discharges 323,
 324
 surface water infiltration, 323–4
 transit times 323
 water balance modelling 322
 Cation 102–104
 Caustic potash 101, 109
 Centre of gravity 136
 CFCs (Chlorofluorocarbons) 13, 48, 53B,
 118–19
 CFC-11 48
 CFC-12 48, 53B
 CFC-113 48, 53B
 Chad aquifers Nigeria 210–18, 21, 215
 Chad, Lake 212
 Charcoal bags 319, 100–2
 Chemical (in)stability 59, 105, 106, 107, **114**,
 117, 308
 fluorescent tracers 84–86
 Chloride 41, 105, 192, 193
 mass-balance (CMB) method 195–8
 Chlorine-36 9
 Chlorofluorocarbons *see* CFC
 Chlorophyll 291
 Choice of tracer 177
 CHR (International Commission for the
 Hydrology of the Rhine) 252
 Chromatography effect 76–77, 77, 85
 Chrom-51, chromium-51 115
 Churfirten-Alvier massif 207B–9B, 208B
 C.I. (Colour Index) 61
 Circulation lake *see* Flow dynamics in lakes
 Clogging 112, 190
 Clubmoss spores *see* Lycopodium spores
 CMB - Chemical Mass Balance Correction 52
 Cobalt-60 **114**, 247
 Colour Index *see* C.I.
 Column (experiment) 41, 78–9, 130–1, 131,
 148–9, 148, 149, **149**, 185
 column axis 127
 retardation coefficients from column
 experiments **83**
 Combined pumping-tracer test 130–2, 131, 146,
 149–50, 149, **151**, 160, 185, 186
 Combined Exponential Piston Flow Model
 (EPM) 162, 163, 166
 Combined Least Squares Method (LSQM)
 133–6, 148, 149, 150
 Combined Piston Flow Diffusion Model
 (SPFM) 165–166, 166, 166
 Compartmental model 162–3
 Coliphag Sm 2 108
 Concentration curve *see* tracer breakthrough
 curve
 multi-peak concentration curve 140
 peak concentration curve 132–33
 plateau concentration 190, 191
 Conceptual model 6, 7, 28, 140, 202
 definition 9
 conceptual system modelling 207
 complex hydrological systems *P3b–d*
 lumped-parameter approach in groundwater
 systems 161
 spring system 205B

- Conceptual model (*Continued*)
 tracer transport in multi-flow systems 141
 tracer transport in a fissured aquifer 145
- Confined aquifers 217–18
- Constant rate injection 190–1, 191, **192**
- Contamination, contaminants 8, 45, 86, 106, 108, 116, 179–80, 229, 246, 253, 308
 fluorescence tracers 67, 86, 97, 116
 flow/transport 106
 decontamination 291 *see also* Remediation
 point sources 246
- Continuity equation 154–5
- Continuous injection 274
- Conservative (or nonreactive) tracer **66**, 69–70, 106, 116
- Conservativity 59, 66, 118
- Convection 36, 57, 78, 125, 140, 144, 156–7, 163
- Convergence approach 6–7, 7, 207B
- Convolution integral 162
- Continental effect 27–9
- Coriolis forces 285, 288, 290, 292
- Correction methods, Carbon-14 52
 Carbon stable isotope correction, definition 52
 Chemical mass balance, definition 52
 Reservoir correction 52
- Costs (tracer studies) 178
- Counter vortexes 285, 354
- Counting method 111
- Cultivation (of bacteria and bacteriophages) 111
- Cumulative curve method (CCM) 137–40, 138, 148, 150, 152, 154
- Current dynamics in lakes *see* Flow dynamics in lakes
- Current velocity 286
- Curie, definition 112, 117
- Cuxhaven 24
- Cyprus 25
- D**
- δ notation 15–7, 52, 118
- D & C Green 8 *see* Pyranine
- D & C Red 22 *see* Eosine
- D & C Yellow 7 *see* Uranine
- Danube, River 168–9
- Darcy-Buckingham equation 154–5
- Darcy's Law 144, 221–3
- Data collection 176–7
- Dating *see* age dating
- Dead pond zones 266, 267, 268, 268, 269
- Dealkylation (of fluorescent tracers) 85
- Decay constant, tritium 44
- Degradation (of FBAs) 116
- Delta notation 16
- Denitrification 43
- Detection limit 67–69, 100–1, 104–6, 110–1, 114, 117, 185, 191–2, 213, 216–7, 219, 247, 306, 310, 329
 bacteriophages 110
 FBAs 117
 fluorescent tracers 67–69, **67**, **87**
 radioactive tracers 114
 salt tracer 104
- Detergent 109
- Detritus 109
- Deuterated water 117–8
- Deuterium ^2H 13, 38, 170, 84, 117–8, 232–9
- Deuterium excess
- Difluoro-Benzoic Acids (DFBAs) 115
- Diffuse inflow 274, 276
- Diffusion coefficient 116, 124, 145, 147, 157, 160, 247
 deuterium 118
 FBAs 116
 molecular 124, 126, 157, 160
 effective 145, 147
 gas 247
 isotopic, 20
- Diffusion parameter, definition 145, 146, 147, 159
- Dilution factor 51, **52**
- Dilution gauging, dilution method *see* discharge gauging
- Diodes (LED) 96–7
- Discharge gauging, discharge measurement 75, 186, 187–95, **192**, 193–4, 194
 constant rate injection 190–1, 191, **192**
 evaluation of methods **192**
 slug injection (integration method, gulp injection) 158, 188–90, 188, **192**, 194–5
- Dirac function $\delta(t)$ 127–8
- Dirac impulse 79, 148, 188
- Direction log 222
- Dispersion 249, 255, 263
- Dispersion tensor 124
- Dispersion equation 123–132, 142
- Dispersion coefficient 253, 256, 262, 263
 longitudinal 124, 142, 249, 254, 261, **265**, 270
 transverse 124, 126, 272
- Dispersion-convection (equation) 140, 156
 definition 162

- Dispersion model (DM) 117, 162, 163, 166, 167, 236–9, 166, 253
- Dispersion model, Dispersion parameter P_D 127, 130, 131, 132, 134, 142, 143, 145, 147, 162
- definition 127
- Dispersion, vertical, lateral and longitudinal 187
- Dispersive transport 78, 159
- Dispersivity 123
- longitudinal 124, 157, 158, 269
- transverse 124
- Dissolution constant 47
- Distribution coefficient K_d 79–81
- batch experiments (fluorescent tracers) 82
- definition 80
- Dissolved gas tracers *see* Gas tracer
- DM *see* Dispersion model
- DNA 9, 58, 108
- Double-labelled water 117
- Double-porosity aquifers 144–7
- Double-porosity system 123, 144, 145, 153–4, 153, 154, 156, 157, 158, 161, 164–6, 165, 203
- Drainage system 246, 331, 356
- glacier 303–18
- Dreisam river catchment (Brugga) 22, 44, 200, 331, 332, 333, 335, 336–42, 347
- Drifting particle tracers (drift substances) 57, 58, 107–12, 108
- case study 239–46
- particle size 108, 108, 111
- measurement techniques 111–2
- sampling 112, 244
- tracer studies 246
- in karst system studies 107
- measurement techniques 111–12
- sampling techniques 112
- special applications potential 107
- Dye tracers *see* Fluorescent tracers, Nonfluorescent dye tracers
- E**
- ε *see* Enrichment factor
- Eco-toxicological 86, 117, 251
- Eddies (lake) 288, 290
- EDTA-complex 115
- Effective water porosity *see* Porosity
- Effective diffusion coefficient *see* Diffusion coefficient
- Electrical conductivity 102–3, 194, 194, 212–3, 247, 247, 251, 335, 336
- Electron capture detector (ECD) 119
- EM *see* Exponential model
- Emission fluorescence 60–4, 67–8, 85, 88–93, 96–99, 193
- β -emission 43
- tritium 44
- End member mixing analysis (EMMA) 40–1, 198–200
- Enrichment factor isotopic 17
- Environmental effects (of tracer application) 86
- Environmental isotopes *see* Environmental tracers
- Environmental risks (tracer experiments) 177
- Environmental tracer data 123, 160–72
- modelling of environmental tracer data 160–173
- Environmental tracers 8, 13–56, 203
- age dating 43–56
- Carbon-13, 9, 52
- common tracers ($^{18}\text{O}/^{16}\text{O}$, $^2\text{H}/\text{H}$, $^{13}\text{C}/^{12}\text{C}$, $^{15}\text{N}/^{14}\text{N}$) 13
- Deuterium 13
- input function 14
- Nitrogen-15 13, 42–3
- Noble gases 13
- Oxygen-18 13
- residence times 14
- stable isotopes in groundwater 38–40
- stable isotopes in soil 35–8
- stable isotopes of water 15–35
- EPM *see* Combined Exponential Piston Flow Model
- Eosine (Eosine Yellow) 60, 64, 67, 69, 85, 85, 87, 185
- detection limit of 67, 87
- potential interference with Bromide 106
- solubility of 67, 87
- toxicological aspects 86
- photolytic decay 74, 74
- Epifluorescence microscopy 111
- Epilimnion 21, 285, 286, 291, 299
- Equilibrium fractionation 20–1, 34–5
- Escherichia Coli 108, 109, 240
- Estimation tracer injection mass *see* Injection mass
- Ethyl alcohol 109
- Evaporative enrichment 30–2
- Evaporation 20–1, 30, 32–5, 202
- from lakes 33–5
- Excess air 47

- Experimental data, modelling of 123–174
 exponential model (EM) 162, 163
 Exponential Piston Flow Model (EPM) 162, 163, 165–166, 166
 Experiment, tracer
 experimental setup 204
 lake 284–91, 285
 rivers or streams 158–60, 258–273
 study planning and execution 175–82
 establishment of a sampling process 178, 178
 measurements to monitor tracer
 breakthroughs 178
 depth-dependent sampling 182
 effects on sorption of all the bottles 181
 risk management 176, 179
 Excitation 61–64, 64, 67, 67, 67–69, 68, 74, 84, 88–93, 90, 96–97, 193
 Execution tracer study, experiment 175–82, 176
 Extinction coefficient 62, 67
- F**
 FD&C Blue-1 *see* Brilliant Blue
 Fibre optic fluorometer (FOF) 96–7, 96, 97–8
 for dilution gauging 193
 single well 224
 unsaturated zone 232
 hyporeic zone 325
 FIELD 136
 Field computer 194
 Field fluorometer 97–9
 Filter fluorometer 88–9
 Filters, depth of 181
 Filtration capacity (filtration potential) 108, 239–46, 245
 definition 240, 242, 245
 field test arrangement 242
 filtration coefficient 240–4
 mechanical filtration 240
 laboratory test arrangement 241
 multi tracer experiments 239–46
 definition 240
 water supply installation 242
 well 243, 243, 244, 245
 sampling 243, 244
 soil surface 242, 243, 243, 244
 laboratory experiments 240–2
 soils tested 240, 241
 test arrangement 240, 241
 Filtration pool 243, 245
 Filtration test 232–9, 239–46
 Findelen Glacier 305, 306, 310–21
 Finite differences methods 125, 292
 Finite elements methods 125
 Fissure aperture 144, 145, 146
 Fissured rock aquifer 123, 144, 145, 153, 154, 203 *see also* Double-porosity aquifer
 Fissure spacing 144
 Fissure 144
 fissure porosity *see* Porosity
 Single Fissure Dispersion Model (SFDm)
 146–7, 147, 153, 153, 154, 159–60
 Fitting procedure 133, 174
 Flash flood 190
 Flow direction 57, 125, 126, 127, 128, 129, 207, 222, 224
 Flow dynamics in lakes 289
 circulation pattern 292
 current dynamics, lake currents 248
 current velocity 286
 current pattern 284, 290, 300
 inflow-induced currents 300
 wind-induced currents 284
 internal flow dynamics (lake) 285, 288
 Flow path 11, 33, 57, 140–3, 323, 342, 344, 346–7
 soil 107, 121, 230, 243
 groundwater 110, 140–43, 151–2, 165, 169, 203–04, 220–1
 preferential 207, 230
 lake 277, 279
 glacier 304, 307
 Flow parameters rivers 252
 FLOWPC 167
 Flow-through fluorometer 98
 Flow velocity 123, 126, 159, 242, 253, 269
 see also Mean water velocity
 Fluocapteurs *see* Charcoal bags
 Fluorescein *see* Uranine
 Fluorescence 61–64
 actinometer 75
 intensity 62–69, 67, 65
 photolysis of 72–5, 74, 74, 84–5, 87, 186, 250–1, 250, 192, 250, 250, 251, 294, 295
 quenching 68, 73, 84
 salinity (affecting fluorescence) 84
 spectrum 63–64, 64
 Fluorescent tracers 57, 58, 59–102, 189, 190, 191, 192, 250
 amphiphilic nature 76
 case study 239–46
 commercial names 60, 61
 detection limit 67–69, 67, 87
 distribution coefficients batch experiments 82

- fluorescence intensity (fluorescence yield) 65, **67, 87**
- lycopodium spore 109
- measurement techniques 88–102
- metabolism, microbiological degradation, decay of 70, 85–86, 240, 299
- methodological basics of 59
- photolysis (light sensitivity) 72–75, **74, 74, 87**
- properties, characteristics **66, 87**
- oxidative processes (affecting fluorescent tracers) 84
- quantum yield 62
- retardation coefficients column experiments **83**
- separation 89–95, 90–95
- solubility 65, 66–67, **87**
- sorption 76–84, 77, **83, 87**
- structural formulae 67
- sulfonic acid functional groups 65
- temperature dependence 72, **73**
- toxicity 86, **87**
- Fluorine atom 115
- Fluorinated compounds 118
- Fluorometry, Fluorometer 68–9, 88, 88–9, 98, 94, 94–100
 - measurement techniques 88–102
 - future techniques 95, 99–100
 - light scattering problems 95, 95
 - fibre optic fluorometer (FOF) 96–7, 96, 97–8
 - field fluorometer *in situ* measurements 97–9
 - filter fluorometer 88–9
 - flow-through fluorometer 98
 - in situ* fluorometer 258, 268, 269
 - pocket fluorometer 98
 - spectral fluorometer 89–9, 93, 98, 275
 - Variosens fluorometer 99
 - separation ratio calculation 93–4
 - separation synchronous technique 89, 92, 92–3, 94
 - synchronous scan technique 63–64, 64, 70–1, 71, 89–94, 90, 9, 94
 - Stokes shift 63, 64, 65, 89, 90
 - types 96–100
 - underwater fluorometer 263
- Fluorescent microspheres *see* Microspheres
- Fluorobenzoates *see* Fluorobenzoic acids (FBAs)
- Fluorobenzoic acids (FBAs) 115–17
- Fluorometer *see* Fluorometry
- Flushing injection 245, 287
- Fluvial sediment 249
- Fluvioglacial aquifer 242–6
- Förster resonance 84
- Fractionation 17–22
 - diffusive fractionation, definition 18, 19
 - equilibrium fractionation 17, 18
 - fractionation factor 17, 18
 - humidity effect, definition 19
 - kinetic fractionation 20
 - Rayleigh fractionation 18, 21
 - definition, 28
 - non-isothermal 28
 - definition, 29
- Fraction of water flux 143
- Fractured aquifer *see* Fissured aquifer
- France 252
- Fringe 286
- Front line 269, 284, 286–87
- Fully penetrating well *see* Injection well
- G**
- γ -Radiation 112, 113
- Garmisch 24
- Gas chromatography 47
- Gas diffusion coefficients 247
- Gas tracers, dissolved 118–20, 202
- GC-ECD 47, 119
- GC-MS 117
- Geiger counters 113, 114
- Germany catchments, stations 22, 24, 30, 31, 35, 153, 168, 200, 252, 273, 322, 331, 335, 347, 349P1
- Germs (as tracers) 109, 230
 - case study 239–6
- Glaciers 303–21
 - ablation, discharge 304
 - Aletsch Glacier 307–8
 - analyses 310
 - artificial tracer tests
 - automatic samplers 309
 - boreholes 309–20
 - internal flow processes 247, 304
 - in situ* measurements 310
 - injection 308–9
 - laminar flow 307
 - ratio max./mean flow velocity 307
 - runoff 304
 - sampling 309–10
 - seasonal development of drainage system 304, 305, 306 *see also* Findelen Glacier
 - snowmelt and runoff 303
 - solid and unconsolidated rock aquifers 303, 303
 - specific techniques 308
 - tracer breakthrough 305–7, 312–13, 315

- Glaciers (*Continued*)
 tracer recovery 307
 turbulent flow 307
 winter test, Aletsch Glacier 307–8
 water cycle 304, 305, 306
- Glas bottles (sampling) 85, 181
- Global Meteoric Water Line (GMWL) 22, 32–3
 215, 216
- Global Network of Isotopes in Precipitation *see*
 GNIP
- GNIP (IAEA Global Network of Isotopes in
 Precipitation) 22, 26, 29–30, 349 P1
- Goodness-of-fit 174
- Gorner Glacier 304, 356, P8
- Graham's Law of Effusion 19
- Grand Canal d'Alsace 259
- Greece 23
- Greenhouse gas effect (SF₆) 119
- Groundwater 202–29, *see also* Aquifer
 aquifer vulnerability 203
 below dunes 30
 Buffelsriver catchment (South Africa) 196–8
 case studies 210–29
 carbon isotopes ($\delta^{13}\text{C}$) 216–17
 Chad aquifers (Nigeria) 210–18, 21, 215
 chloride mass-balance method 195–8
 confined aquifers 217–18
 environmental tracers 203–4
 experiments 202
 groundwater age 217–18
 hydrochemistry 204, 213–14
 isotope composition 215–16
 karst areas 202–3
 multi-well tracer tests 204
 nitrate isotope analysis 42
 palaeo-recharge water 216
 protection zones 245 *see also* Protection zones
 radiocarbon analysis 213
 recharge 27, 195–8
 sampling 181–2, 196, 197, 197–8, **197**
 systems 202–3, 205B–209B
 Sahara-Sahel, sources of precipitation 214
 $\delta^{18}\text{O}$ and $\delta^2\text{H}$ 213
 tracer applications 202–4
 velocity 242
 well network 211, 212
 vulnerability *see* Vulnerability
- Groundwater recharge 2–3, **11**, 11–2, 14, 26–7,
 30, 36–40, 44, 47–8, **52**, 52–4, 56, 160–61,
 165, 165–66, 171–72, 181, 195–8, 202–04,
207, 210–11, 215–218, 229, 233, 236, 324,
 327–28, 338–39, 352, P4
- Groynes 258
- Gulp injection *see* Injection
- H**
- Haber-Bosch process 43
- Half-life
 Carbon-14 51, 217
 Krypton-85 50
 Tritium 43
- Half-life (radioactive decay) 43, 50, 113–15,
 223
- Half-life, fluorescence (photolytic decay) 74–5,
 74, 276, 295–6
- Halides 107, 116
- Headwater 71, 187, 210, 247, 322, 332
- Helium 9, 44–5, 119
- Health risks 114, 177, 179
- Henry's Law 19, 46–7, 53B
- Henry Coefficient 47, 53B
- Hinged double-board 243
- Homothermic (lake) 293
- HPLC 117, 258
- HPTL/AMD 85, 95, 100
- Humins 104
- Hydraulic characteristics (of unsaturated soil)
 155–6, 156
- Hydraulic conductivity 123, 144
- Hydraulic gradient 144
- Hydraulic model 272
- Hydraulic modelling 253
- Hydrochemistry 204, 213–14
- Hydrodynamics
 lakes 251
 rivers 248
- Hydroglaciology *see* Glacier
- Hydrograph separation 11, 14, 40–1, 198–200,
 305, 322, 331, 334, 336, 340, 343–44
- Hydrological connection between lakes, ponds
 or pools and the adjacent aquifers 248
- Hydrological data 175
- Hydrological system 5–6, 6, 7, 8, **8**, 10, 13–14,
 18–9, 24, 27, 40, 41, 57, 86, 102, 119, 179,
 198, 201, 204, 206, 208, 246, 342, 351
 system characteristics 206B
 subsystems 202
 system function 208B
- Hydrophobic 66, 76, 109, 111
- HYDRUS-1D 155, 157
- Hygiene 107, 108, 110
- Hypolimnion 283, 285–6, 285, 286, 288, 290
 hypolimnic outflow 293, 294, 297
- Hyporheic interstitial 11, 98, 115, 323–25

I

- IAEA *see* International Atomic Energy Agency
 IAHS *see* International Association on Hydrological Sciences
 IC (Ion Chromatography) **103**, 117, 213
 ICP-MS (Inductively Coupled Plasma Mass Spectrometry) 13, 107
 ICP-EOS I (Induced Coupled Plasma-Optic Emission Spectroscopy) **103**
 Ideal tracer 57, **66**, 76–78, 76, 78, 79, 115
 Immobile water 144, 145, 159
 Indium 58, 115
 Infiltration **11**, 51, 57, 108, 121, 155, 161, 170–1, 155, 218–9, 221, 224, 230, 232, 242, 304, 323, 325, 328–9, 335, 346
 Inflow-induced currents 300
 Initial activity 51, **52**
 Initial conditions 128, 130
 Injection 181, 187, 190, **243**, 259, 287, 287, 294
 constant rate injection 190–1, 190, 191, **192**
 injection equipment 119, 243
 internal injection (lake) 251
 slug injection, gulp injection 188–90, 188, **192**, 190, **192**, 194–5
 unsaturated zone, filtration experiment 245
 injection mass estimation 104, 177–8, 182–6, **183–4**, 243
 Injection site 253, 263
 Injection well 127
 fully penetrating 126, 126, 128
 partially penetrating 127
 Inlet 15, 16, 2.62, 274, 284, 286, 290, 301
 Input function 7, 8, 14, 24, 29, 35, 37–9, 44, 46, 46–50, 55, 105, 168, 170–71, 171, 198, 235, 266, 305, 335
 CFCs 46, 48
 Tritium 46
In situ measurement, technique 250, 258, 268, 269, 273, 284
 Instantaneous injection *see* Injection
 Integrated tracerhydrological approach 202
 Integration method *see* Discharge gauging
 Internal flow dynamics (lake) 285, 288
 Interaction 1, 11, 38, 49, 67, 76, 100, 121, 141, 160, 201, 203, **207**, 214, 246, 321, 323, 325
 International Association of Tracer Hydrology (ATH) 3, 59, 202
 International Association on Hydrological Sciences (IAHS) 3, 59
 International Atomic Energy Agency (IAEA) 3, 15, 22, 26, 29–30, 59, 112, 167
 International Commission on Tracers (ICT) of the IAHS 59
 Intraglacial 303–4, 356
 Inverse modelling (IM) (or deconvolution) 10, 40, 133–6, 155, 232
 Iodide **103**, 106–107, 121
 Iodate anion 106–7
 Ion exchange 76, 104–07, 117, 213, 217, 231, 240
 Ion selective electrode 76, **103**, 105–06
 Irradiation 73, 75, 93, 96, 249, 248–51
 Isar 275
 Isarco 325–30
 Isobathic pattern 283
 Isotherm 24, 28–9, 77–81
 Isothermal fractionation 28
 Isotopes 53B *see also* Stable isotopes
 Isotope effects 18
 altitude effect 18, 25, 26
 amount effect 18
 continental effect 18, 27
 definition 28
 latitude effect 18
 seasonal effect 18, 24
 temperature effect 23
 Isotope exchange 21
 Isotope mass balance 33, 40
 Isotope measurements
 double inlet spectrometer 15
 ICP-MS 13
 mass spectrometry 15
 precision 16
 tunable diode laser spectroscopy (TDLAS) 13, 16
 Isotope thermometer 24
 Isotopic abundance ratio **15**, 16
 Isotopic composition (regional)
 Dreisam basin, Germany 22
 Germany 31
 Cyprus 25
 Kalahari, Namibia 32
 Negev Desert 33
 Pantanal, Brazil 34
 Isotopic composition (compartmental)
 floods (flash) 38
 groundwater 38–40
 lakes 33, 34
 springs 40
 rainfall 22, 23
 runoff 38, 41
 soil 35–38
 unsaturated zone 35, 36
 Isotopic residence time 37

- Italy 252, 325
 Iteration (procedure) 136
- K**
 Kalahari 32
 Karst 107, 202, 207B
 karst aquifers, catchments 140, 141, 171, 143, 202–3, 206B, 208B
 karst massif, porous-fissured 171, 172
 karst system 205B
 Krypton-85, 7, 9, 13, 50–1, 119, 249, 13, 50
 Kinetic reaction 77–9, 78, 81
- L**
 Lag coefficient 267, 273
 Lakes 2, 8, 11, 16, 30, 33, 247–51
 alpine lake 282
 bacterial tracing tests 248
 Bled, Lake 75, 97, 284, 284, 285, 286, 287, 287–88, 289–90, 289–305
 Chad, Lake 212
 dynamics 288 *see also* Current dynamics
 evaporation 33–4
 hydrodynamics of lakes 251 *see also* Stratification, Mixing
 eutrophic 291
 lake remediation *see* Remediation
 lake research 247
 lake topography 290
 lake ventilation 248
 lake water balance 247
 mesotrophic 282, 291
 mixing and internal flow processes 33–4, 247
 outlet 284
 profiles (tracer concentration) 284, 286, 287, 287
 Rhodamine B test 248
 rotation (lakes) 285–6, 288, 290
 SF₆ 247
 stratification 21
 temperature-depth profiles during tracer experiments indispensable 251
 ⁶⁰Co 247
 Laminar flow 307
 Laser techniques (fluorescence) 99
 Layer 186, 210, 212, 214, 216, 219, 222, 228, 240, 243, 245, 247, 325, 342, 344, 346
 isotopic 20–1, 33–5
 fluorescence tracer 62, 69, 75, 95, 100
 glacier 304, 325
 lake 284, 286, 287–8, 289, 292, 294, 301–2
 multi-layered 140–44, 152, 182
 LC–MS–MS 117
 LD50 116
 Least squares method 134
 LED diodes 96–7
 Legislation (tracer experiment) 179
 Lethal dose 116
 Light scattering 95, 95
 Liquid scintillation counting 43
 Lindau Rock Laboratory, Germany 153
 Lithium 103, 106
 Lithium chloride 106
 Lithium hydroxide 106
 Longitudinal dispersion *see* Dispersion
 Longitudinal Dispersivity *see* Dispersivity
 Loss of tracer 294, 296, 297, 298, 298
 Luminescence 62
 Lumped-parameter models, approach 6, 10, 12, 123, 145, 160–7, 161–63, 161, 163, 163–5, 165–66, 166–67, 173, 181, 233
 Lycopodium spores 58, 108, 109, 111
 case study 239–46
 lycopodium clavatum 108
 Lysimeter 37, 115, 117, 155, 170, 230–38, 234
- M**
 Macropores 35, 83, 241, 243
 Mapping 176–7
 Mariotte bottle 190, 190, 191
 Matrix 77–8, 78, 83, 102, 104, 106, 11, 124, 144–47, 145, 153, 163–64, 202, 207, 217, 229, 334
 Mass numbers 112
 Mathematical model, definition 9 *see also* Model
 Mathematical Modelling *see* Modelling
 Mean residence time *see* Residence time
 Mean transit time 130, 142, 143, 146, 147, 159, 161, 162, 172, 291
 Mean water velocity 125, 142, 145, 265
 Measurement techniques
 advanced 13, 68, 100
 fluorescent tracers 88–111
 salt tracers 100
 Methylene Blue 121
 MFDm *see* Multi-Flow Dispersion Model
 Micro organism 107
 Microbial degradation 85
 Microspheres 9, 107, 108, 108, 111
 Migration 286

- Minimum flow distances (discharge gauging) 188
- Mitigation velocity **291**
- Mixing cell model *see* Multi-cell model
- Mixing
 in aquifers 181
 lake mixing 247
 mixing process after tracer injection (stream) 187, 193
- Mobile water 123, 142, 144, 159, 268
- Mobility (of tracer) 81, 105, 116, 121, 244
- Model 123–174
 calibration 9, 143, 174, 248, 253, 257, 258, 263, 279, 342 *see also* Fitting procedure
 efficiency 174
 parameter 254
 validation 10, 248, 253, 258, 264, 292, 340
- Modelling 9–12, 123–174, 253, 255
 environmental tracer 6, 10, 12
- Mole fraction **15**
- Molecular diffusion *see* Diffusion
- Molecular velocity 19
- Moments, method (MM) 136–7, 148, **149**, 150, 152, 154, 178
- Monopole test *see* Combined pumping tracer experiment
- Multi-cell approach, multi-cell model 172–3
- Multi-flow systems 140–4, 141, 151–2, 152, **152**
- Multi-Flow Dispersion Model (MFDM) 143, 152
- Multi-layered aquifer 140, 141, 144–5, 152, **152**, 182
- Multilateral approach 7, 206B
- Multi-tracer experiment 7, 89, 102, 105–6, 109, 112, 116, 118, 229, 239–46, 342, 344
- Multi-well tracer test 204
- Munich 35, 232, 235, 273
- Murten, Lake 299–303
- N**
- Nano-Chip-LC/QTOF-MS 85, 95, 100
- Naphthionate **60**, 66, 67, **67**, 69, **87**, 76, 74, 185
 detection limit of **67**, **87**
 microbial degradation of 85
 solubility of **67**, **87**
 toxicological aspects 86
- NAPLs (detection by gas tracers) 120
- Natural components 209B
- Natural tracers *see* Environmental tracers
- Negev 33
- Neon **9**, 44, 119
- Netherlands 252–3, 258, 264
- Neutrons 112
- Nigeria 210–218
- Nitrate 42–3, 196, 226, 228, 230, 332
- Nitrification 42
- Nitrogen-15 13, 42–3
- Noble gases 44, 50, 51, 118–9
- Nonfluorescent dye tracers 120–2
- Nonideal tracer 57, 77, 79
 breakthrough of 77, 78
 reaction 77
 nonreactive tracer 123
- North Sea 248, 252, 254
- Nowa Slupia, Poland 151
- Nuclear bomb tests 43
- Nuclear power plant 248
- Nuclide 112–15, 113, **114**, 249
- O**
- Olsewski tube 283
- One-well test *see* Single well technique
- Origin assignment 14
- Oscillatoria rubescens 282
- Overlay spatial information 205B, 206B
- Oxygen-18 9, 13, 325–28
- P**
- Packer 182, 182
- Paiva Castro reservoir 277–81
- Paleohydrological studies 247
- Palaeo-recharge water 216
- Parameter estimation 127, 136, 143, 150, 153–54, 253–54
- Partial pressure 47
- Particle tracers 57, **58**, 107–12, 108
- Partitioning tracer 120
- Passau 168–69
- Peak concentration 132–33
- Penetration tracer 244
- Percent modern Carbon (pmC) 51, definition 215
- Percolation pool 243, 245
- Perfluorohydrocarbons 248
- PFCs 118
- PFM *see* Piston Flow Model
- Phages **9**, **58**, 107, 108, 109–11
- pH dependence (fluorescent tracers) **66**, 70–2, 71, 91, 92, 308
- Phosphate **9**
- Phosphorus 249

- Phosphorus-32 248
 Photobleaching *see* Photolysis
 Photo-densitometry 247
 Photolysis, photochemical decay (fluorescent tracers) 72–5, 74, **74**, 84–5, **87**, 186, 250–1, **250**, 192, 250, **250**, 251, 294, 295
 Physio-chemical parameter **9**, 208B
 Phytoplankton **9**, 107, 282, 291
 Piston Flow Model (PFM) 162, 163, 165–6, 166, 166, 167
 Planktothrix rubescens (*oscillatoria rubescens*) 282
 Plankton net 112, 243, 244
 Planning tracer study, experiment 6, 15, 70, 74–5, 86, 175–82, 176, 191, 289, 303, 309, 347
 pmC 51, definition 215
 Pocket fluorometer 98, 189–90
 Point source 203
 Pollutant 10, 13, 42, 78, 228–29, 248, 252, 255, 265, 280
 Pollutant dilution 249
 Pollutant transport, migration, propagation 86, 106, 108, 180, 239 246, 249, 253, 272
 Pollutant plume 252
 Pollution tracer 8, **9**, 10, 13, 107, 247
 Pollution 109, 263
 point source 203
 rivers 252
 Poliomyelitis virus 108, 108
 Polyethylene bottles 86, 181
 Polystyrene latex particles 111
 Polysulfone bottle 86, 181
 Pore size substrate 108
 Porosity 10, 12, 82, 123–24, 131–32, 144–56, 156–66, 181, 185–86, 202, 219–22, 236, 339, 344
 effective porosity 128, 131
 fissure porosity, definition 144
 Porous aquifer 105–6, 203, 324
 fluvioglacial aquifer 242–6
 sandy aquifer 186
 single well 224
 sorption 79
 tracer mass estimation 85
 Porous-fissured karst massif 172
 Potassium Chloride (KCl) **103**
 Preferential flow 203, 207, **207**, 221, 230
 glacier 304
 soils, unsaturated zone 120, 229–30
 Process studies 14, 202
 Propagation tracer in surface water 257, 287, 289, 290
 horizontal 247
 pollutant plume 252
 Proportion (of river water) 168
 Protection zones 2, 11, 111, 176, 203, 207, 247
 delineation 207B, 240
 porous groundwater 240, 245
 karst aquifer 207
 Protocol forms 178
 Proton 65, 70, 112
 Pseudomonas fluorescens 109
 Pyranine **60**, 61, 66, 67, **67**, **87**
 detection limit of **67**, **87**
 solubility of 67, **87**
 toxicological aspects 86
 pH value and wavelength shift 70, 71
 process of photolytic decay 74, 74
 Pumping station 243
 Pumping tracer test 130–2, 131, 146, 149–50, 149, **151**, 160, 185, 186
- Q**
 Quantum yield fluorescent tracers 62, 67
 Quenching *see* Fluorescence quenching
- R**
 Radiation 43, 50, 112–113, **11**
 irradiation 73, 75, 93, 96, 249, 248–51
 Radioactive isotopes 112
 Radioactive tracers **58**, 112–18, 114–15, **114**, 117
 Chrom-51 115
 decay constant/half-life relationship 113
 environmental risks 114, 228
 health risks 114
 Indium-114, 115
 single-well techniques 115, 223
 Tritium (^3H), main uses 115
 Radioactivity, decay 112–13, 113
 Radionuclide 113, 112–15, 113, **114**, 249
 Radon-222 199, 324
 Radovna, River 283, 287, 293
 Radial (convergent) flow conditions 127, 146, 153
 Radium-226 324
 Rainfall 14, 22–43, 24, 31, 31–3, 34, 35–42, 95, 175, 196–98, 208, 210–11, 214–21, 323, 326, 328, 334–35, 342–43, 347, 349
 rainfall distribution 22, 22, 29–30, 31, 36
 Raman effect 64, 93–4
 Rainfall, stable isotopes in *see* Isotopes

- Rayleigh distillation 18, 21–2, 28–9, 29
 Rayleigh equation 34
 Reaction isotherm *see* Isotherm
 Reactive tracer 77–78, 77, 116
 Reaeration 249
 Recharge 14, 27, 37, 195
 Recovery *see* Tracer mass recovery
 Regional Meteoric Water Line 22
 Regionalization of isotopes in rainfall 29
 Reference tracer 106, 118, 244–5
 Real-time-predictions 252
 Regulations, national 86
 Relative tracer mass recovery 79, *see also* Tracer mass recovery
 Remediation 1, 3, 43
 lake remediation 230, 248, 282–3, 291
 Reservoir effect 51
 Residence time 8, 11, 14–5, 25, 27, 37–39, 44, 48–50, 55–7, 203, 206–10, 230, 241, **298**
 catchment 322–38
 definition 37
 lake 247, 282, 287, 292–9
 soil 37
 Retardation coefficient, factor 77, 79, 81–4, 164–5
 Reticula 109
 Rheinfelden 258
 Rhine Alert Model 254–7, 273
 Rhine, River experiment 252–73
 1D Rhine model 267
 adjacent aquifers 252
 dead pond zones 266, 267, 268, 268, 269
 high flow conditions 264
 flow velocities 263
 fluorescence tracers 258, 273
 hydraulic parameters 252
 injection 259, 259
 low flow conditions 263–4, 269
 meander section 261, 262
 mean runoff 258–9
 measured and modelled breakthrough curves 263, 264
 pollutant transport/distribution 269–70, 270
 river sections (parameter) 256–7, 259, **260**, 261–3, 261, 262–3, **265**
 samplers automatic 253, **259**, 259
 sampling sites 253, 258, 264
 stagnant water zone effects 266–8
 variation coefficients 257, **260**, 263, 265, **265**, 266
 transverse dispersion 271–2, 271
 travel times deviations 266–7, **267**, 269, 272, 323, 342, 272
 rhodamines 64, 69, 84, 86, **87**, 98, 186, 192
 case study 258, 259, 263, 264, 273, 284–7, 285, 287, 288
 detection limit of **67**, **87**
 photolytic decay process 74, 74
 Rhodamine B **60**, **67**, **87**, 248, 284–7, 285, 287, 288, 291
 Rhodamine WT **60**, **67**, 76, **87**, 258, 259, 263, 264, 273
 solubility of **67**, **87**
 Richards equation 154–5
 Rin-Quelle 188
 Risk management (experiments) 176, 179
 River 246, 248–9
 case studies 249
 estimation tracer injection mass 186
 hydrodynamics 248–9
 river basin 246
 tracer experiment in rivers or streams 158–60, 158, 252–273
 tracer transport in rivers 158–60, 252–273
 turbulent river 187, 249
 dispersion of sewage 249
 River sections 254, 256, 264, 270, 271
 Rock aquifers 98, 154, 203, 303–4, 303, 339, **340**
 Runoff 304
 Runoff generation 11–4, 39–40, 57, 195, 198, 202, 207B, 229, 331–47
 Runoff component 202, 209B, 322
 Runoff separation 57, 304, 322, 335, 339 *see also* End member mixing analysis
 Runoff regime 305
 Rocks attenuation 35
 Rotation (lakes) 285–6, 288, 290
 Routing approach 266
- S**
 SAFM (1D A-D transport model) 254
 Sahara-Sahel 214
 Salt tracers **58**, 102–7, **103**, 191, **192**, 193
 measurement techniques, analysis **103**, 107
 Salt dilution technique 193–4, 194
 Salt measurement sets 193, 194
 Salinity 47, 84
 Sampling 167, 177, 178–9, 204, 258, 259, 293
 gas tracer 118, 119
 groundwater 181–2, 182
 particle tracers 112, 244
 sampling interval, frequency 178, 178

- Sampling (*Continued*)
 sampling bottles 178
 sampling concept 178, 180
 sampling multi layer 182
 Sandoz chemical plant 252
- Sanitary measure, lake 283
- Saturated flow conditions 123–154, 239
- Sava River (Slovenia) 355 P7
- SAX (strong anion exchange column) 117
- Schneealpe (Austria) 171
- Scintillation counter/counting (liquid) 43, 51, 113, 213
- Seasonal effect 24–5
- Sediment tracing methods 249
- Semi-arid regions 203
- Semiconductor counter 113
- Sempach, Lake 248
- Sensitivity tracers 101, 105, 118–9, 214, 229
 fluorescent tracers 59, **87**, 101, 250, 273, 308, 310
- Separation fluorescent tracers 89–95, 90–95
- Serratia marcescens 108
- Sewage 43, 86, 102, 108, 230, 248–9, 252, 273–6, 282, 291, 299–303
- Sewage effluent 248–9, 273–76, 291, 299–303
- Sewage system 291
- SF₆ (sulfur hexafluoride) 13, 49, 50, 118, 119, 247, 248, 249
- SFDM *see* Single Fissure Dispersion Model
- Silicium-32, **9**, 41
- Silica 41, 322, 333–37, 337, 340–44, 343–4
- Simulation 258
- Single well, borehole technique 115, 204, 221–9
- Single fissure (single fracture) 144, 146
- Single Fissure Dispersion Model (SFDM) 146–7, 147, 153, **153**, 154, 159–60
- Single-porosity medium 161
 by fibre optic 221, 222, 223, 224, 226, 226
 by online fluorometer 226–9, 227–8, 227, 228
 by radioactive isotope ⁸²Br 223–4, 224, **225**
 filter velocity estimation 222–3
 tracer dilution logs and direction logs 221, 222, 223
- Siphon 283, 291
- Slovenia 75, 282, 293, 355
- Slug injection (integration method, gulp injection) 158, 188–90, 188, **192**, 194
- SMOW standard 15–6, 22, 31, **43**, **199**, 213, 349
- Sodium chloride (NaCl) **9**, **103**, 105–7, 191–93
- Sodium-fluorescein *see* Uranine
- Soil 35, **232**, 233, 235
- Soil hydraulic parameters
 characteristics 156, 235, 239
 deuterium transport 232–9
 filtration capacity of soils 239–46
 hydraulic characteristics unsaturated soil 155–6, 156
 modelling 233–9, **237**, 238
 soil-aquifer system 239–46
 van Genuchten model 232
 visualization 121
- Solubility 66–67
 fluorescent tracers 67, **87**
 salt tracers **103**
- Solvent Green **60**
- Solution 79, 81, 82, **82**, 119, 180, 180, 190–1, 243, 251, 259, 274
- Sorption 49, 71–2, 76–84, **87**, 116, 120, 186, 192, 316, 347
 anion exclusion 104
 bacteria and bacteriophages 110
 Brilliant Blue 122
 chloride 105
 FBAs 116
 fluorescent tracers **66**, 66–87, 77, 78, 80, **83**, **87**, 97–100, 102
 ion exchange 103, **103**
 nonfluorescent (dye) tracers 120
 non-ideal tracers 77–8, 78
 particle tracer 108–10
 pH-induced absorption 72
 reversible sorption 76–78, 77, 78
 radioactive tracers 114–16, **116**
 salt tracers 102–6
 sorption isotherm 78
 sorption tests 81
- Distribution 10, 12, 37, 39–40, 44, 56, 99, 120, 125, 125, 129, 129, 133, 181, 198, 203–4
 coefficient 79–82
 concentration borehole 221–30
 function 161–67
 rainfall 22, 29–30, 36
 surface water, river lakes 269–329, 353–56 P5, P6, P7, P8
 tracer concentration 129, 129
- Spatial information overlay 205B, 206B
- SPE (solid-phase extraction) 100
- SPFM *see* Combined Piston Flow Diffusion Model
- Spectral 100, 275
 fluorescence analyses 65, 68, 88–90, 90, 93–4, 94–5, 94–95, 96, 98, 100

- Spectral fluorometer 89–9, 93, 98, 275
 Spectrum fluorescent tracers 63–64, 64
 Spores 107, 109, 111, 112, 240–6 *see also*
 Lycopodium spores
 multi-coloured spores 112
 Spring 6, 38–9, 98–102, 140, 146, 161, 171–73,
 177, 181, 188, 304–06, 326–7, 329, 332
 experiment vulnerability 218–21
 experiment hillslope 332–346, 332, 334, 338,
 342–43, 345–46
 system 205B
 vulnerability 205–209B, 205B, 209B, 209B,
 218–21
 Solute transport 12, 116, 117, 229, 2254, 258
 Stable isotopes 160, 202
 Stagnant water 10, 123, 129, 144, 166, 158–60,
 232 *see also* immobile water
 river zones 254–58, 266–8, 267, 268
 Stagnation (lakes) 283, 291, 296, 297, 299 *see*
 also Stratification
 Staphylococcus *crus* 109
 Starch-iodide-complex 107
 Stationary discharge relationships 254
 Stern-Volmer equation 84
 Stokes shift ($\Delta\lambda$) 63, 64, 65, 89, 90
 Staining techniques 120
 Stratification, lakes 247, 283, 284, 285, 286, 287,
 289, 291, 293, 297
see also Stagnation
 Stream
 stream erosion 249
 stream line 268
 tracer transport 158–60
Streptococcus faecalis ATTC 109, 240–6
 Structural formulae dyes 63, 67
 Structure model 7, 351, P3
 St. Venant equation 256
 Subglacial (drainage system) 303–20
 Sublacustric water exchange 248
 Submarine water exchange 248
 Succinylfluorescein disodium salt 59, 65
 Sulfonic acid functional groups 65
 Sulforhodamine B **60**, **67**, 86, **87**
 dealkylation of 85, 85
 process of photolytic decay 74, 74
 Sulforhodamine G (extra) *see*
 Amidorhodamine G
 Sulfur hexafluoride *see* SF₆
 Sulphur-34, **9**
 Super saturation 282
 Supra glacial 303
 Surface water 246–99 *see also* Lakes *see also*
 Rivers
 ecotoxicological harmlessness 251
 tracer losses due to photolytic decay 250–1,
 250
 in situ measurements 250
 transport process in 250
 surface-groundwater interaction experiment
 325–31, 273–76
 artificial tracer SF₆ 326, 329–30, 330
 tracer gas 329–30, 330
 stable isotopes 126, 327–8, 329
 effluent inflow 273–6
 continuous injection 274
 diffuse inflow 274, 276
 maximum concentration 275, 276
 Suspension 109, 111
 Synchronous scan 63–64, 64, 70–1, 71, 89–94,
 90, 91
 System approach, system hydrology 5–7, 40, 304
 see also Hydrological system
 System function 208B
 Switzerland, catchments, stations 23, 188, 247,
 252, 253, 258, 300, 353–6 P5, P6, P7, P8

T
 Tailing (effect) 156, 158, 158, 189, 262, 313, 317
 Target concentration 182, 243
 Taylor series 133, 134–5
 TBC (Tracer Breakthrough Curve) 188, 191,
 209B, 24, 261, 263, 268
 TDLAS (Tunable Diode Laser Spectrography) 13
 TDI (Tolerable Daily Intake) approach 186
 Techniques, tracerhydrology 175–200, 201
 Temperature
 as tracer **9**, 247
 dependence fluorescent tracers 72
 effect (isotopes) 23–30, 23
 isotope fractionation 18–23
 Temperature-depth profiles 251
 Temperature, lake water 285
 Tensor form 123
 Test field 128, 128, 185
 Time distribution tracer concentration 129, 129
 Tinopal (Tinopal ABP) 312, **313**, **316**
 Thermic, lake 287, 297, 308
 Terminal lakes, 16
 Thermocline 284–5, 285, 286, 289, 293
 Through-flow fluorometer 243
 Through-flow measurement 240, 241, 244
 Tortuosity factor 124

- Toxicity 86, 105, 115, 116, 122
 Brilliant Blue 122
 Ceriodaphnia96-h 116
 FBA tracers 116
 fluorescent tracers 59, **66**, 86, **87**
- Toxicological (eco-) 86, 117, 192, 251
- Tracer 3, 8, **9**
 definition of tracers 7–9
 classification of 8
 available hydrological **9**
 characteristics **240**
- Tracer breakthrough (curve) 188, *191*, *209B*, *24*, *261*, 263, 268
- Tracer cloud 189, 192, 247, 262, 269, 271, 285, **287**, **291**
- Tracer distribution (lake) 287
- Tracer tests 15, 61, 62, 71, 75, 79, 83, 90, 102, 106, 111, 114, 116–20, 149, *154*, 174, 204, 208, 228, **260**, 264, **265**, 266, 273, *290*, **294**, 304–307, 310, 312, 320, 330, 342, 347
 modelling experiments in streams and rivers 158–60
- Tracer front (velocity) 284, 286–87
- Tracer injection mass *see* Injection mass
- Tracerhydrology 1–2, *2 see also* Techniques of tracerhydrology
 approach, integrated 3
 approach (vulnerability assessment) 207B–09B
 fields of application **11**, 12
 tracers in hydrology, integrated concept of 5–12, 201
- Tracer mass recovery 77, 78, 79, 79–80, *80*, *117*, *133*, *134*, 137–8, 240, 307
- Tracer methods 1, 3, 7, 12, 14, 57, 203, 205, 207, 208, 208, 229, 246, 253–4, 282, 303, 305, 321, 323–4, 331, *351P3*
- Tracer transport *see* Transport of tracer
- Transit time 123, 143, 172, 293
 distribution function 161–2, *163*, *166*
- Transport equations 123–33, *125*, *131*, *132*, *134*, 157
- Transport model
 lake 283
 river 252–73, 272
- Transport processes 246
 transport process in surface water 250
- Transport of tracer 127, 140, 269
 horizontal transport 128
 in a fissured aquifer *145*
 in rivers 158–60
- Transfer coefficient 157
- Transit time 130, 142, 143, 146, *147*, 159, 161–63, *172*, 291
- Transport parameter 139, 143, **265**
 estimation 133–140
 parameter in rivers 252
 transport velocity 261, 267
- Transverse dispersion 271–2, *271*
- Transverse dispersion coefficient *see* Dispersion
- Transverse dispersivity *see* Dispersivity
- Transverse (or space) distribution 129, *129*
- Travel time 15, 120, 182, 228, 230, 266–7, **267**, 269, 272, 323, 342, 272
- Trial-and-error procedure 133
- Tritiated water 115
- Tritium (^3H) 37, 43–45, 77, 115, 160, 214–15, 170–2, 247
 application of measurements in catchment areas 170–2
 decline of activity with decay time *113*
 input function *171*
 peak 37, *44*
- TU, tritium unit. definition 43
- Tunable diode laser spectroscopy (TDLAS) 13
- Turbulent flow 187, 232, 307
- Turnover 289–90
- U**
- Uncertainty 14, 16, 27, 58, 69, 152, 200, 253, 338, 340, 342
- Underwater fluorometer 263
- Unsaturated flow conditions 154–8, 239
- Unsaturated soil 156
- Unsaturated zone (or vadose zone) 83, 106, 116, 122, 123, 148
 Brilliant Blue, FCF 122, 230
 case studies in 229–46
 double-porosity model 156–7
 filtration capacity 108, 242–46
 immobile water 156, 157
 hydraulic functions 155
 HYDRUS-1D 157
 lysimeter methods 155
 mobile water 155–6, 157
 Richards equation 154–5
 steady-state methods 155
 tracers specific aspects 83, 230–2
 visualization experiments 120–122
- Upper Rhine *see* Rhine

- Uranine 9, 58–9, **60**, 60–64, 64, 66, **67**, 67–70, 69, **73**, **74**, 74, 75, 79, 80, **82–3**, 83, 85, **87**, 91, 91–2, 93, 94–5, 96, 98, 100–02, 105–6, 149, 185–6, 19–94, 220, 221–26, **240**, 243, 243–45, 245, 246–7, **247**, 273, 315–21, **319**, 344, 346–7, 355P7, 356P8
 breakthrough curves 79, 80
 case study 239–46, 258, 269, 273
 case study Lake Bled 287–90, 288, 289, 290, **291**, 293, 294–8, **295**, **296**, **296–7**, 296, **296**, 297, **298**, 298–300, 302
 case study glacier 308, 321–5, **316**, 317
 case study catchment 342, 344, 346–7
 chemical structure 66
 column experiments 79–80, 80
 effects of pH 66, 70
 detection limit of **67**, **87**
 microbial degradation of 85
 photochemical decay of 73–4, 74, **74**
 solubility of **67**, **87**
 spectra of 63, 64, 64, 94
 synchronous scan spectrum of 64
 toxicological aspects 86
 Uranine loss 297, **298**, 298
 Uranine/Eosine 91–2, 92
- V**
 Vadose zone *see* Unsaturated zone
 Validation 1, 3, 10, 123, 178, **192**, 193, 203, 248, 253–4, 258, 263, 264, 292, 340–41
 Validation of mathematical models *see* Model validation
 Van Genuchten model 232
 Variance of the tracer concentration curve 137
 Variation coefficient 257, **260**, 263, **265**, 266
 Variosens 254, 269, 284
 Vector form 123
 Velocity vector 124, 125
 Velocity 19, 76, 81, 104, 115, 120, 123–26, 142–45, **149**, **151**, 204, 206, **207**, 221–27, 242, 253, 255–57, **260**, 262–69, 277–81, 288, **290**
 Viable tracer 110
 Vienna 171
 Vienna Standard Mean Ocean Water (VSMOW) 15, 22
 Viruses **9**, **58**, 107, 108
 Visualization experiments 120–122
- VPDB (Vienna Pee Dee Belemnite) 52
 VSMOW 15, 22
 Volatility (salt tracers) 102
 Volatility (gas tracers) 120
 Volcanic 49
 Volume of water (lake) **294**
 Volumetric flow rate 143, 161
 Vortexes 285, 354
 Vulnerability 203
 anthropogenic components 209B
 aquifer vulnerability 203
 assessment 205B–209B
 ecohydrological approach 205–6B
 intrinsic vulnerability 203, 205B, 206B–9B, **207B**, 209B
 map 203, 208B
 specific vulnerability 206B, 209B
 vulnerability zones, delineation of 207B, 208B
 spring 218–21
 rocks attenuation in 35
 tracerhydrological approach 207–8B, 209B
- W**
 Warning system 252
 Wasseralmquelle 171, 172
 Waste water 43, 86, 102, 108, 230, 248–9, 252, 273–6, 282, 291, 299–303
 Water content 156, **164**
 Water suction 156
 Water supply (installations) 108, 240, 242
 Water protection zone 108
 Water (flow) velocity 123, 126, 159, 242, 253, 269 *see also* Mean water velocity
 Weighted isotopic average 38
 Weighing function 39 definition
 Well, filter depth 181
 Wetland 34, 40, 151, 324
- X**
 Xanthene dyes **60**, 64–65, 65, 83
 Xenon (gas) 119
 Xenon lamp 88, 95, 99
 Xylem flow 117
- Y**
 Yeast fungus 108
 Yield 62, 67, 86, **87**, 114, 134